RECENT ADVANCES in MATHEMATICS, STATISTICS and ECONOMICS

Proceedings of the 2014 International Conference on Pure Mathematics - Applied Mathematics (PM-AM '14)

Proceedings of the 2014 International Conference on Economics and Statistics (ES '14)

Venice, Italy
March 15-17, 2014

RECENT ADVANCES in MATHEMATICS, STATISTICS and ECONOMICS

Proceedings of the 2014 International Conference on Pure Mathematics - Applied Mathematics (PM-AM '14)
Proceedings of the 2014 International Conference on Economics and Statistics (ES '14)

Venice, Italy
March 15-17, 2014

All papers of the present volume were peer reviewed by no less than two independent reviewers. Acceptance was granted when both reviewers' recommendations were positive.

ISBN: 978-1-61804-225-5

RECENT ADVANCES in MATHEMATICS, STATISTICS and ECONOMICS

Proceedings of the 2014 International Conference on Pure Mathematics - Applied Mathematics (PM-AM '14)

Proceedings of the 2014 International Conference on Economics and Statistics (ES '14)

Venice, Italy
March 15-17, 2014

Organizing Committee

General Chairs (EDITORS)

- Prof. Panos M. Pardalos,
  Distinguished Prof. of Industrial and
  Systems Engineering,
  University of Florida, USA
- Professor Ravi P. Agarwal
  Department of Mathematics
  Texas A&M University - Kingsville
  700 University Blvd.
  Kingsville, TX 78363-8202, USA
- Prof. Ljubiša Kočinac, University of Nis,
  Nis, Serbia
- Prof. Reinhard Neck
  Department of Economics
  Klagenfurt University
  Klagenfurt, Austria
- Prof. Nikos Mastorakis
  Industrial Engineering Department
  Technical University of Sofia
  Bulgaria
- Prof. Klimis Ntalianis,
  Tech. Educ. Inst. of Athens (TEI),
  Department of Marketing and Advertizement
  Athens, Greece

Senior Program Chair

- Professor Philippe Dondon
  ENSEIRB
  Rue A Schweitzer 33400 Talence
  France
- Prof. Valery Y. Glizer,
  Ort Braude College, Karmiel, Israel

Program Chairs

- Prof. Filippo Neri
  Dipartimento di Informatica e Sistemistica
  University of Naples "Federico II"
  Naples, Italy
- Prof. Constantin Udriste,
  University Politehnica of Bucharest,
  Bucharest, Romania
- Prof. Marcia Cristina A. B. Federson,
  Universidade de São Paulo,
  São Paulo, Brazil
- Prof. Sandra Sendra
  Instituto de Inv. para la Gestión Integrada de Zonas Costeras (IGIC)
  Universidad Politécnica de Valencia
  Spain

Tutorials Chair

- Professor Pradip Majumdar
  Department of Mechanical Engineering
  Northern Illinois University
  Dekalb, Illinois, USA

Special Session Chair

- Prof. Pavel Varacha
  Tomas Bata University in Zlin
  Faculty of Applied Informatics
  Department of Informatics and Artificial Intelligence
  Zlin, Czech Republic

Workshops Chair

- Prof. Sehie Park,
  The National Academy of Sciences,
  Republic of Korea
- Prof. Panos Pardalos,
  Department of University of Florida,
  USA

Local Organizing Chair

- Assistant Prof. Klimis Ntalianis,
  Tech. Educ. Inst. of Athens (TEI),
  Athens, Greece
- Prof. Vincenzo Niola
  Departement of Mechanical Engineering for Energetics
  University of Naples "Federico II"
  Naples, Italy
- Prof. Ryszard S. Choras
  Institute of Telecommunications
  University of Technology & Life Sciences
  Bydgoszcz, Poland

Publication Chair

- Prof. Gen Qi Xu
  Department of Mathematics
  Tianjin University
  Tianjin, China
- Prof. Panos Pardalos,
  Department of University of Florida,
  USA

Publicity Committee

- Prof. Vjacheslav Yurko,
  Saratov State University,
  Astrakhanskaya, Russia
- Prof. Myriam Lazard
  Institut Superieur d' Ingenierie de la Conception
  Saint Die, France

International Liaisons

- Professor Jinhu Lu, IEEE Fellow
  Institute of Systems Science
  Academy of Mathematics and Systems Science
  Chinese Academy of Sciences
  Beijing 100190, P. R. China
- Prof. Olga Martin
  Applied Sciences Faculty
  Politehnica University of Bucharest
  Romania
- Prof. Vincenzo Niola
  Departement of Mechanical Engineering for Energetics
  University of Naples "Federico II"
  Naples, Italy
- Prof. Eduardo Mario Dias
  Electrical Energy and Automation
  Engineering Department
  Escola Politecnica da Universidade de Sao Paulo
  Brazil
- Prof. Nikos Mastorakis
  Industrial Engineering Department
  Technical University of Sofia
  Bulgaria

Steering Committee

- Prof. Stefan Siegmund, Technische Universitaet Dresden, Germany
- Prof. Aida Bulucea, University of Craiova, Romania
- Prof. Zoran Bojkovic, Univ. of Belgrade, Serbia
- Prof. Metin Demiralp, Istanbul Technical University, Turkey
- Prof. Imre Rudas, Obuda University, Budapest, Hungary

Program Committee for PURE MATHEMATICS

Prof. Ferhan M. Atici, Western KentuckyUniversity, Bowling Green, KY 42101, USA
Prof. Ravi P. Agarwal, Texas A&M University - Kingsville, Kingsville, TX, USA
Prof. Martin Bohner, Missouri University of Science and Technology, Rolla, Missouri, USA
Prof. Dashan Fan, University of Wisconsin-Milwaukee, Milwaukee, WI, USA
Prof. Paolo Marcellini. University of Firenze, Firenze, Italy
Prof. Xiaodong Yan, University of Connecticut, Connecticut, USA
Prof. Ming Mei, McGill University, Montreal, Quebec, Canada
Prof. Enrique Llorens, University of Valencia, Valencia, Spain
Prof. Yuriy V. Rogovchenko, University of Agder, Kristiansand, Norway
Prof. Yong Hong Wu, Curtin University of Technology, Perth, WA, Australia
Prof. Angelo Favini, University of Bologna, Bologna, Italy
Prof. Andrew Pickering, Universidad Rey Juan Carlos, Mostoles, Madrid, Spain
Prof. Guozhen Lu, Wayne state university, Detroit, MI 48202, USA
Prof. Gerd Teschke, Hochschule Neubrandenburg - University of Applied Sciences, Germany
Prof. Michel Chipot, University of Zurich, Switzerland
Prof. Juan Carlos Cortes Lopez, Universidad Politecnica de Valencia, Spain
Prof. Julian Lopez-Gomez, Universitad Complutense de Madrid, Madrid, Spain
Prof. Jozef Banas, Rzeszow University of Technology, Rzeszow, Poland
Prof. Ivan G. Avramidi, New Mexico Tech, Socorro, New Mexico, USA
Prof. Kevin R. Payne, Universita' degli Studi di Milano, Milan, Italy
Prof. Juan Pablo Rincon-Zapatero, Universidad Carlos III De Madrid, Madrid, Spain
Prof. Valery Y. Glizer, ORT Braude College, Karmiel, Israel
Prof. Norio Yoshida, University of Toyama, Toyama, Japan
Prof. Feliz Minhos, Universidade de Evora, Evora, Portugal
Prof. Mihai Mihailescu, University of Craiova, Craiova, Romania
Prof. Lucas Jodar, Universitat Politecnica de Valencia, Valencia, Spain
Prof. Dumitru Baleanu, Cankaya University, Ankara, Turkey
Prof. Jianming Zhan, Hubei University for Nationalities, Enshi, Hubei Province, China
Prof. Zhenya Yan, Institute of Systems Science, AMSS, Chinese Academy of Sciences, Beijing, China
Prof. Nasser-Eddine Mohamed Ali Tatar, King Fahd University of Petroleum and Mineral, Dhahran, Saudi Arabia
Prof. Jianqing Chen, Fujian Normal University, Cangshan, Fuzhou, Fujian, China
Prof. Josef Diblik, Brno University of Technology, Brno, Czech Republic
Prof. Stanislaw Migorski, Jagiellonian University in Krakow, Krakow, Poland
Prof. Qing-Wen Wang, Shanghai University, Shanghai, China
Prof. Luis Castro, University of Aveiro, Aveiro, Portugal
Prof. Alberto Fiorenza, Universita' di Napoli "Federico II", Napoli (Naples), Italy
Prof. Patricia J. Y. Wong, Nanyang Technological University, Singapore
Prof. Salvatore A. Marano, Universita degli Studi di Catania, Catania, Italy
Prof. Sung Guen Kim, Kyungpook National University, Daegu, South Korea
Prof. Maria Alessandra Ragusa, Universita di Catania, Catania, Italy
Prof. Gerassimos Barbatis, University of Athens, Athens, Greece
Prof. Jinde Cao, Distinguished Prof., Southeast University, Nanjing 210096, China
Prof. Kailash C. Patidar, University of the Western Cape, 7535 Bellville, South Africa
Prof. Mitsuharu Otani, Waseda University, Japan
Prof. Luigi Rodino, University of Torino, Torino, Italy
Prof. Carlos Lizama, Universidad de Santiago de Chile, Santiago, Chile
Prof. Jinhu Lu, Chinese Academy of Sciences, Beijing, China
Prof. Narcisa C. Apreutesei, Technical University of Iasi, Iasi, Romania
Prof. Sining Zheng, Dalian University of Technology, Dalian, China
Prof. Daoyi Xu, Sichuan University, Chengdu, China
Prof. Zili Wu, Xi'an Jiaotong-Liverpool University, Suzhou, Jiangsu, China
Prof. Wei-Shih Du, National Kaohsiung Normal University, Kaohsiung City, Taiwan

Prof. Khalil Ezzinbi, Universite Cadi Ayyad, Marrakesh, Morocco
Prof. Youyu Wang, Tianjin University of Finance and Economics, Tianjin, China
Prof. Satit Saejung, Khon Kaen University, Thailand
Prof. Chun-Gang Zhu, Dalian University of Technology, Dalian, China
Prof. Mohamed Kamal Aouf, Mansoura University, Mansoura City, Egypt
Prof. Yansheng Liu, Shandong Normal University, Jinan, Shandong, China
Prof. Naseer Shahzad, King Abdulaziz University, Jeddah, Saudi Arabia
Prof. Janusz Brzdek, Pedagogical University of Cracow, Poland
Prof. Mohammad T. Darvishi, Razi University, Kermanshah, Iran
Prof. Ahmed El-Sayed, Alexandria University, Alexandria, Egypt

Program Committee for APPLIED MATHEMATICS

Prof. Martin Bohner, Missouri University of Science and Technology, Rolla, Missouri, USA
Prof. Martin Schechter, University of California, Irvine, USA
Prof. Ivan G. Avramidi, New Mexico Tech, Socorro, New Mexico, USA
Prof. Michel Chipot, University of Zurich, Zurich, Switzerland
Prof. Xiaodong Yan, University of Connecticut, Connecticut USA
Prof. Ravi P. Agarwal, Texas A&M University - Kingsville, Kingsville, TX, USA
Prof. Yushun Wang, Nanjing Normal university, Nanjing, China
Prof. Detlev Buchholz, Universitaet Goettingen, Goettingen, Germany
Prof. Patricia J. Y. Wong, Nanyang Technological University, Singapore
Prof. Andrei Korobeinikov, Centre de Recerca Matematica, Barcelona, Spain
Prof. Jim Zhu, Western Michigan University, Kalamazoo, MI, USA
Prof. Ferhan M. Atici, Department of Mathematics, Western Kentucky University, USA
Prof. Gerd Teschke, Institute for Computational Mathematics in Science and Technology, Neubrandenburg, Berlin-Dahlem, Germany
Prof. Meirong Zhang, Tsinghua University, Beijing, China
Prof. Lucio Boccardo, Universita degli Studi di Roma "La Sapienza", Roma, Italy
Prof. Shanhe Wu, Longyan University, Longyan, Fujian, China
Prof. Natig M. Atakishiyev, National Autonomous University of Mexico, Mexico
Prof. Jianming Zhan, Hubei University for Nationalities, Enshi, Hubei Province, China
Prof. Narcisa C. Apreutesei, Technical University of Iasi, Iasi, Romania
Prof. Chun-Gang Zhu, Dalian University of Technology, Dalian, China
Prof. Abdelghani Bellouquid, University Cadi Ayyad, Morocco
Prof. Jinde Cao, Southeast University/ King Abdulaziz University, China
Prof. Josef Diblik, Brno University of Technology, Brno, Czech Republic
Prof. Jianqing Chen, Fujian Normal University, Fuzhou, Fujian, China
Prof. Naseer Shahzad, King Abdulaziz University, Jeddah, Saudi Arabia
Prof. Sining Zheng, Dalian University of Technology, Dalian, China
Prof. Leszek Gasinski, Uniwersytet Jagielloński, Krakowie, Poland
Prof. Satit Saejung, Khon Kaen University, Muang District, Khon Kaen, Thailand
Prof. Juan J. Trujillo, Universidad de La Laguna, La Laguna, Tenerife, Spain
Prof. Tiecheng Xia, Department of Mathematics, Shanghai University, China
Prof. Stevo Stevic, Mathematical Institute Serbian Academy of Sciences and Arts, Beograd, Serbia
Prof. Lucas Jodar, Universitat Politecnica de Valencia, Valencia, Spain
Prof. Noemi Wolanski, Universidad de Buenos Aires, Buenos Aires, Argentina
Prof. Zhenya Yan, Chinese Academy of Sciences, Beijing, China
Prof. Juan Carlos Cortes Lopez, Universidad Politecnica de Valencia, Spain
Prof. Wei-Shih Du, National Kaohsiung Normal University, Kaohsiung City, Taiwan
Prof. Kailash C. Patidar, University of the Western Cape, Cape Town, South Africa
Prof. Hossein Jafari, University of Mazandaran, Babolsar, Iran
Prof. Abdel-Maksoud A Soliman, Suez Canal University, Egypt
Prof. Janusz Brzdek, Pedagogical University of Cracow, Cracow, Poland
Dr. Fasma Diele, Italian National Research Council (C.N.R.), Bari, Italy

Program Committee for ECONOMICS & STATISTICS

Prof. Panos Pardalos, Department of University of Florida, USA
Prof. Shuliang Li, The University of Westminster, London, UK
Prof. Jiri Strouhal, University of Economics Prague, Czech Republic
Prof. Morris Adelman, Prof. of Economics, Emeritus, MIT, USA
Prof. Robert L. Bishop, Prof. of Economics, Emeritus, MIT, USA
Prof. Glenn Loury, Prof. of Economics, Brown University, USA
Prof. Fernando Alvarez, Prof. of Economics, University of Chicago, USA
Prof. Mark J. Perry, Prof. of Finance and Business Economics, University of Michigan-Flit, USA
Prof. Biswa Nath Datta, IEEE Fellow, Distinguished Research Prof., Northern Illinois University, USA
Prof. Gamal Elnagar, University of South Carolina Upstate, Spartanburg, SC, USA
Prof. Jiri Klima, Technical faculty of CZU in Prague, Czech Republic
Prof. Goricanec Darko, University of Maribor, Maribor, Slovenia
Prof. Ze Santos, Rua A, 119. Conj. Jardim Costa do Sol, Brazil
Prof. Ehab Bayoumi, Chalmers University of Technology,Goteborg, Sweden
Prof. Luis Tavares Rua, Cmte Guyubricht, 119. Conj. Jardim Costa do Sol. Atalaia, Brazil
Prof. Igor Kuzle, Faculty of electrical engineering and computing, Zagreb, Croatia
Prof. Maria do Rosario Alves Calado, University of Beira Interior, Portugal
Prof. Gheorghe-Daniel Andreescu, "Politehnica" University of Timisoara, Romania
Prof. Reinhard Neck, Department of Economics, Klagenfurt University, Klagenfurt, Austria
Prof. Aida Bulucea, University of Craiova, Romania
Prof. Zhuo Li, Beijing University Of Technology, Beijing, China
Prof. Pradip Majumdar, Northern Illinois University, Dekalb, Illinois, USA
Prof. Ricardo Gouveia Rodrigues, University of Beira Interior, Portugal

Additional Reviewers

Angel F. Tenorio	Universidad Pablo de Olavide, Spain
Ole Christian Boe	Norwegian Military Academy, Norway
Abelha Antonio	Universidade do Minho, Portugal
Xiang Bai	Huazhong University of Science and Technology, China
Genqi Xu	Tianjin University, China
Moran Wang	Tsinghua University, China
Minhui Yan	Shanghai Maritime University, China
Jon Burley	Michigan State University, MI, USA
Shinji Osada	Gifu University School of Medicine, Japan
Bazil Taha Ahmed	Universidad Autonoma de Madrid, Spain
Konstantin Volkov	Kingston University London, UK
Tetsuya Shimamura	Saitama University, Japan
George Barreto	Pontificia Universidad Javeriana, Colombia
Tetsuya Yoshida	Hokkaido University, Japan
Deolinda Rasteiro	Coimbra Institute of Engineering, Portugal
Matthias Buyle	Artesis Hogeschool Antwerpen, Belgium
Dmitrijs Serdjuks	Riga Technical University, Latvia
Kei Eguchi	Fukuoka Institute of Technology, Japan
Imre Rudas	Obuda University, Budapest, Hungary
Francesco Rotondo	Polytechnic of Bari University, Italy
Valeri Mladenov	Technical University of Sofia, Bulgaria
Andrey Dmitriev	Russian Academy of Sciences, Russia
James Vance	The University of Virginia's College at Wise, VA, USA
Masaji Tanaka	Okayama University of Science, Japan
Sorinel Oprisan	College of Charleston, CA, USA
Hessam Ghasemnejad	Kingston University London, UK
Santoso Wibowo	CQ University, Australia
M. Javed Khan	Tuskegee University, AL, USA
Manoj K. Jha	Morgan State University in Baltimore, USA
Miguel Carriegos	Universidad de Leon, Spain
Philippe Dondon	Institut polytechnique de Bordeaux, France
Kazuhiko Natori	Toho University, Japan
Jose Flores	The University of South Dakota, SD, USA
Takuya Yamano	Kanagawa University, Japan
Frederic Kuznik	National Institute of Applied Sciences, Lyon, France
Lesley Farmer	California State University Long Beach, CA, USA
João Bastos	Instituto Superior de Engenharia do Porto, Portugal
Zhong-Jie Han	Tianjin University, China
Francesco Zirilli	Sapienza Universita di Roma, Italy
Yamagishi Hiromitsu	Ehime University, Japan
Eleazar Jimenez Serrano	Kyushu University, Japan
Alejandro Fuentes-Penna	Universidad Autónoma del Estado de Hidalgo, Mexico
José Carlos Metrôlho	Instituto Politecnico de Castelo Branco, Portugal
Stavros Ponis	National Technical University of Athens, Greece

Table of Contents

ISBN: 978-1-61804-225-5

ISBN: 978-1-61804-225-5

ISBN: 978-1-61804-225-5

Keynote Lecture 1

On the Distinguished Role of the Mittag-Leffler and Wright Functions in Fractional Calculus

Professor Francesco Mainardi
Department of Physics, University of Bologna, and INFN
Via Irnerio 46, I-40126 Bologna, Italy
E-mail: francesco.mainardi@bo.infn.it.it

Abstract: Fractional calculus, in allowing integrals and derivatives of any positive real order (the term "fractional" is kept only for historical reasons), can be considered a branch of mathematical analysis which deals with integro-di erential equations where the integrals are of convolution type and exhibit (weakly singular) kernels of power-law type. As a matter of fact fractional calculus can be considered a laboratory for special functions and integral transforms. Indeed many problems dealt with fractional calculus can be solved by using Laplace and Fourier transforms and lead to analytical solutions expressed in terms of transcendental functions of Mittag-Leffler and Wright type. In this plenary lecture we discuss some interesting problems in order to single out the role of these functions. The problems include anomalous relaxation and diffusion and also intermediate phenomena.

Brief Biography of the Speaker: For a full biography, list of references on author's papers and books see:
Home Page: http://www.fracalmo.org/mainardi/index.htm
and http://scholar.google.com/citations?user=UYxWyEEAAAAJ&hl=en&oi=ao

ISBN: 978-1-61804-225-5

Keynote Lecture 2

Latest Advances in Neuroinformatics and Fuzzy Systems

Yingxu Wang, PhD, Prof., PEng, FWIF, FICIC, SMIEEE, SMACM
President, International Institute of Cognitive Informatics and Cognitive Computing (ICIC)
Director, Laboratory for Cognitive Informatics and Cognitive Computing
Dept. of Electrical and Computer Engineering
Schulich School of Engineering
University of Calgary
2500 University Drive NW,
Calgary, Alberta, Canada T2N 1N4
E-mail: yingxu@ucalgary.ca

Abstract: Investigations into the neurophysiological foundations of neural networks in neuroinformatics [Wang, 2013] have led to a set of rigorous mathematical models of neurons and neural networks in the brain using contemporary denotational mathematics [Wang, 2008, 2012]. A theory of neuroinformatics is recently developed for explaining the roles of neurons in internal information representation, transmission, and manipulation [Wang & Fariello, 2012]. The formal neural models reveal the differences of structures and functions of the association, sensory and motor neurons. The pulse frequency modulation (PFM) theory of neural networks [Wang & Fariello, 2012] is established for rigorously analyzing the neurosignal systems in complex neural networks. It is noteworthy that the Hopfield model of artificial neural networks [Hopfield, 1982] is merely a prototype closer to the sensory neurons, though the majority of human neurons are association neurons that function significantly different as the sensory neurons. It is found that neural networks can be formally modeled and manipulated by the neural circuit theory [Wang, 2013]. Based on it, the basic structures of neural networks such as the serial, convergence, divergence, parallel, feedback circuits can be rigorously analyzed. Complex neural clusters for memory and internal knowledge representation can be deduced by compositions of the basic structures.

Fuzzy inferences and fuzzy semantics for human and machine reasoning in fuzzy systems [Zadeh, 1965, 2008], cognitive computers [Wang, 2009, 2012], and cognitive robots [Wang, 2010] are a frontier of cognitive informatics and computational intelligence. Fuzzy inference is rigorously modeled in inference algebra [Wang, 2011], which recognizes that humans and fuzzy cognitive systems are not reasoning on the basis of probability of causations rather than formal algebraic rules. Therefore, a set of fundamental fuzzy operators, such as those of fuzzy causality as well as fuzzy deductive, inductive, abductive, and analogy rules, is formally elicited. Fuzzy semantics is quantitatively modeled in semantic algebra [Wang, 2013], which formalizes the qualitative semantics of natural languages in the categories of nouns, verbs, and modifiers (adjectives and adverbs). Fuzzy semantics formalizes nouns by concept algebra [Wang, 2010],

verbs by behavioral process algebra [Wang, 2002, 2007], and modifiers by fuzzy semantic algebra [Wang, 2013]. A wide range of applications of fuzzy inference, fuzzy semantics, neuroinformatics, and denotational mathematics have been implemented in cognitive computing, computational intelligence, fuzzy systems, cognitive robotics, neural networks, neurocomputing, cognitive learning systems, and artificial intelligence.

Brief Biography of the Speaker: Yingxu Wang is professor of cognitive informatics and denotational mathematics, President of International Institute of Cognitive Informatics and Cognitive Computing (ICIC, http://www.ucalgary.ca/icic/) at the University of Calgary. He is a Fellow of ICIC, a Fellow of WIF (UK), a P.Eng of Canada, and a Senior Member of IEEE and ACM. He received a PhD in software engineering from the Nottingham Trent University, UK, and a BSc in Electrical Engineering from Shanghai Tiedao University. He was a visiting professor on sabbatical leaves at Oxford University (1995), Stanford University (2008), University of California, Berkeley (2008), and MIT (2012), respectively. He is the founder and steering committee chair of the annual IEEE International Conference on Cognitive Informatics and Cognitive Computing (ICCI*CC) since 2002. He is founding Editor-in-Chief of International Journal of Cognitive Informatics and Natural Intelligence (IJCINI), founding Editor-in-Chief of International Journal of Software Science and Computational Intelligence (IJSSCI), Associate Editor of IEEE Trans. on SMC (Systems), and Editor-in-Chief of Journal of Advanced Mathematics and Applications (JAMA). Dr. Wang is the initiator of a few cutting-edge research fields or subject areas such as denotational mathematics, cognitive informatics, abstract intelligence (□I), cognitive computing, software science, and basic studies in cognitive linguistics. He has published over 160 peer reviewed journal papers, 230+ peer reviewed conference papers, and 25 books in denotational mathematics, cognitive informatics, cognitive computing, software science, and computational intelligence. He is the recipient of dozens international awards on academic leadership, outstanding contributions, best papers, and teaching in the last three decades.

http://www.ucalgary.ca/icic/

http://scholar.google.ca/citations?user=gRVQjskAAAAJ&hl=en

Editor-in-Chief, International Journal of Cognitive Informatics and Natural Intelligence
Editor-in-Chief, International Journal of Software Science and Computational Intelligence
Associate Editor, IEEE Transactions on System, Man, and Cybernetics - Systems
Editor-in-Chief, Journal of Advanced Mathematics and Applications
Chair, The Steering Committee of IEEE ICCI*CC Conference Series

Keynote Lecture 3

Recent Advances and Future Trends on Atomic Engineering of III-V Semiconductor for Quantum Devices from Deep UV (200nm) up to THZ (300 microns)

Professor Manijeh Razeghi
Center for Quantum Devices
Department of Electrical Engineering and Computer Science
Northwestern University
Evanston, Illinois 60208
USA
E-mail: razeghi@eecs.northwestern.edu

Abstract: Nature offers us different kinds of atoms, but it takes human intelligence to put them together in an elegant way in order to realize functional structures not found in nature. The so-called III-V semiconductors are made of atoms from columns III (B, Al, Ga, In. Tl) and columns V(N, As, P, Sb,Bi) of the periodic table, and constitute a particularly rich variety of compounds with many useful optical and electronic properties. Guided by highly accurate simulations of the electronic structure, modern semiconductor optoelectronic devices are literally made atom by atom using advanced growth technology such as Molecular Beam Epitaxy (MBE) and Metal Organic Chemical Vapor Deposition (MOCVD). Recent breakthroughs have brought quantum engineering to an unprecedented level, creating light detectors and emitters over an extremely wide spectral range from 0.2 mm to 300 mm. Nitrogen serves as the best column V element for the short wavelength side of the electromagnetic spectrum, where we have demonstrated III-nitride light emitting diodes and photo detectors in the deep ultraviolet to visible wavelengths. In the infrared, III-V compounds using phosphorus ,arsenic and antimony from column V ,and indium, gallium, aluminum, ,and thallium from column III elements can create interband and intrsuband lasers and detectors based on quantum-dot (QD) or type-II superlattice (T2SL). These are fast becoming the choice of technology in crucial applications such as environmental monitoring and space exploration. Last but not the least, on the far-infrared end of the electromagnetic spectrum, also known as the terahertz (THz) region, III-V semiconductors offer a unique solution of generating THz waves in a compact device at room temperature. Continued effort is being devoted to all of the above mentioned areas with the intention to develop smart technologies that meet the current challenges in environment, health, security, and energy. This talk will highlight my contributions to the world of III-V semiconductor Nano scale optoelectronics. Devices from deep UV-to THz.

Brief Biography of the Speaker: Manijeh Razeghi received the Doctorat d'État es Sciences Physiques from the Université de Paris, France, in 1980.
After heading the Exploratory Materials Lab at Thomson-CSF (France), she joined Northwestern University, Evanston, IL, as a Walter P. Murphy Professor and Director of the Center for

ISBN: 978-1-61804-225-5

Quantum Devices in Fall 1991, where she created the undergraduate and graduate program in solid-state engineering. She is one of the leading scientists in the field of semiconductor science and technology, pioneering in the development and implementation of major modern epitaxial techniques such as MOCVD, VPE, gas MBE, and MOMBE for the growth of entire compositional ranges of III-V compound semiconductors. She is on the editorial board of many journals such as Journal of Nanotechnology, and Journal of Nanoscience and Nanotechnology, an Associate Editor of Opto-Electronics Review. She is on the International Advisory Board for the Polish Committee of Science, and is an Adjunct Professor at the College of Optical Sciences of the University of Arizona, Tucson, AZ. She has authored or co-authored more than 1000 papers, more than 30 book chapters, and fifteen books, including the textbooks Technology of Quantum Devices (Springer Science+Business Media, Inc., New York, NY U.S.A. 2010) and Fundamentals of Solid State Engineering, 3rd Edition (Springer Science+Business Media, Inc., New York, NY U.S.A. 2009). Two of her books, MOCVD Challenge Vol. 1 (IOP Publishing Ltd., Bristol, U.K., 1989) and MOCVD Challenge Vol. 2 (IOP Publishing Ltd., Bristol, U.K., 1995), discuss some of her pioneering work in InP-GaInAsP and GaAs-GaInAsP based systems. The MOCVD Challenge, 2nd Edition (Taylor & Francis/CRC Press, 2010) represents the combined updated version of Volumes 1 and 2. She holds 50 U.S. patents and has given more than 1000 invited and plenary talks. Her current research interest is in nanoscale optoelectronic quantum devices.

Dr. Razeghi is a Fellow of MRS, IOP, IEEE, APS, SPIE, OSA, Fellow and Life Member of Society of Women Engineers (SWE), Fellow of the International Engineering Consortium (IEC), and a member of the Electrochemical Society, ACS, AAAS, and the French Academy of Sciences and Technology. She received the IBM Europe Science and Technology Prize in 1987, the Achievement Award from the SWE in 1995, the R.F. Bunshah Award in 2004, and many best paper awards.

ISBN: 978-1-61804-225-5

A Wave Diffraction Problem with Higher Order Impedance Boundary Conditions

A. M. Simões
Center of Mathematics - University of Beira Interior (CM-UBI),
Department of Mathematics of University of Beira Interior,
6200-001 Covilhã, Portugal,
Email: asimoes@ubi.pt

***Abstract*—**In this paper, we consider an impedance boundary transmission problem for the Helmholtz equation originated by a problem of wave diffraction by an infinite strip with higher order imperfect boundary conditions. Operator theoretical methods and relations between operators are built to deal with the problem and, as consequence, a transparent interpretation of the problem in an operator theory framework are associated to the problem. In particular, different types of operator relations are exhibited for different types of operators acting between Lebesgue and Sobolev spaces on a finite interval and the positive half-line. All this has consequences in the understanding of the structure of this type of problems. At the end, we describe when the operators associated with the problem enjoy the Fredholm property in terms of the initial space order parameters.

***Keywords*—**Helmholtz equation, higher order impedance boundary condition, Bessel potential space, convolution type operator, Fredholm operator, Wiener-Hopf operator, wave diffraction.

I. Introduction

By using methods from operator theory, in this paper, inspired by the work [14], we will consider a boundary-transmission problem for the Helmholtz equation which arises within the context of wave diffraction theory [3]–[5], [7]–[19], [20], [21] and [24]–[28] on a finite strip [9], [10] and [15] with impedance boundary conditions [7] and [9].

Was A. Sommerfeld the first one to consider canonical boundary value problems for time-harmonic waves governed by the Helmholtz equation in the famous work entitled *Mathematische Theorie der Diffraction*, [29]. Since then, a great number of researchers have made such a study their priority and a great number of different approaches have been presented and developed in the applied mathematics literature for studying canonical problems of plane wave diffraction. The most known and efficient methods and procedures to study such kind of problems are based on the classical Wiener-Hopf technique and the Maliushinets method [21], [28].

In the present work we will consider a Sommerfeld type problem where the geometry comprises a strip facing higher order imperfect boundary conditions. We want to understand better what are the operators behind such a problem. Thus, one of the main goals of the present work is the use of an operator theoretical machinery that will translate the problem into the study of properties of certain known types of operators associated to the problem.

To be more concrete, we will consider Wiener-Hopf operators and convolution type operators on finite intervals with semi-almost periodic Fourier symbol matrices. Convolution type operators $\mathcal{W}$ on finite intervals $\mathcal{I}$,

$$\mathcal{W}\varphi(x) = c\varphi(x) + \int_{\mathcal{I}} K(x-y)\varphi(y)\,dy, \qquad x \in \mathcal{I}.$$

are one-dimensional linear integral operators where the integration kernels K depend on the difference of the arguments and the domain of integration as well as the range of the independent variable are given by the same interval. In a constructive way, we will obtain this type of operators in Sobolev and Lebesgue spaces. This is because we will consider the problem formulated between Bessel potential spaces and defined with a complex wave number k which also allows a certain freedom in the corresponding smoothness orders.

II. Preliminaries and Formulation of the problem

In this section we establish the notation and some preliminary concepts in view of presenting the mathematical formulation of the problem.

We denote by $\mathcal{S}(\mathbb{R}^n)$ the Schwartz space of all rapidly decreasing functions and by $\mathcal{S}'(\mathbb{R}^n)$ the dual space of tempered distributions on $\mathbb{R}^n$. As mentioned in the previous section, we will develop our study in a framework of Bessel potential spaces $\mathcal{H}^s$ defined by the elements $\varphi \in \mathcal{S}'(\mathbb{R}^n)$ such that

$$\|\varphi\|_{\mathcal{H}^s(\mathbb{R}^n)} := \left\| \mathcal{F}^{-1}(1+|\xi|^2)^{s/2} \cdot \mathcal{F}\varphi \right\|_{L^2(\mathbb{R}^n)} < +\infty,$$

with $s \in \mathbb{R}$ and where $\mathcal{F} = \mathcal{F}_{x\mapsto\xi}$ is the Fourier transformation in $\mathbb{R}^n$ defined by

$$(\mathcal{F}\phi)(\xi) = \int_{\mathbb{R}^n} e^{i\xi\cdot x}\phi(x)dx, \qquad \xi \in \mathbb{R}^n.$$

For a given Lipschitz domain $\mathcal{D}$, on $\mathbb{R}^n$, by $\widetilde{\mathcal{H}}^s(\mathcal{D})$ we mean the closed subspace of $\mathcal{H}^s(\mathbb{R}^n)$ whose elements have supports in $\overline{\mathcal{D}}$, and by $\mathcal{H}^s(\mathcal{D})$ the space of distributions on $\mathcal{D}$ which have extensions into $\mathbb{R}^n$ belonging to $\mathcal{H}^s(\mathbb{R}^n)$. The space $\widetilde{\mathcal{H}}^s(\mathcal{D})$ is endowed with the subspace topology, and on $\mathcal{H}^s(\mathcal{D})$ we introduce the norm of the quotient space $\mathcal{H}^s(\mathbb{R}^n)/\widetilde{\mathcal{H}}^s(\mathbb{R}^n\backslash\overline{\mathcal{D}})$. Throughout the paper we will use the notation

$$\mathbb{R}^n_{\pm} := \{x = (x_1, \ldots, x_{n-1}, x_n) \in \mathbb{R}^n : \pm x_n > 0\}.$$

Adopting cartesian axes $Oxyz$ with the y-axis vertically upwards, we will consider a perpendicular time-harmonic

electromagnetic plane wave incident on a strip Σ in $\mathbb{R}^3$ where the material is considered to be invariant under the z-axis direction. Thus, the geometry of the problem is two dimensional and the strip will be therefore represented by

$$\Sigma :=]0, a[\quad \text{for} \quad 0 < a < \infty.$$

We are now in position to formulate our impedance boundary conditions problem.

For $\Omega := \mathbb{R}^2 \backslash \overline{\Sigma}$ and given $n \in \mathbb{N}_0$, we are interested in studying the properties of an element $u \in \mathcal{H}^{1+\varepsilon}(\Omega)$, for some $\varepsilon \geq 0$, which satisfies the Helmholtz equation

$$\left(\frac{\partial^2}{\partial x^2} + \frac{\partial^2}{\partial y^2} + k^2 \right) u = 0 \qquad \text{in} \quad \Omega,$$

together with the impedance boundary condition

$$\left\{ \begin{array}{l} p^+ u_{n+1}^+ + q^+ u_n^+ = h^+ \\ p^- u_{n+1}^- + q^- u_n^- = h^- \end{array} \right. \qquad \text{on} \quad \Sigma, \tag{1}$$

where the wave number $k \in \mathbb{C}$ is given, as well as the impedance parameters $p^{\pm}, q^{\pm} \in \mathbb{C}$,

$$u_n^{\pm} := \left(\frac{\partial^n u}{\partial y^n} \right)_{|y=\pm 0}$$

denote the traces of u on the upper and lower banks of Σ, respectively, and $h^{\pm} \in \mathcal{H}^{-\frac{1}{2}-n+\varepsilon}(\Sigma)$ are arbitrarily given elements. For instance, is well known that for $n = 0$ and $n = 1$ we have $u_n^{\pm}$ as the traditional Dirichlet and Neumann traces, respectively.

III. Reduction of the Problem to a System of Convolution type Operators

In this section we will use operator techniques in view of a characterization of the problem by means of finite interval convolution type operators. In the next section, such characterization of the problem, will be used to present certain extension methods in view to obtain corresponding operator relations, between the operator related to the problem and new Wiener-Hopf operators.

We will consider the densities ϑ and φ defined by

$$\left[\begin{array}{c} \vartheta \\ \varphi \end{array} \right] = \left[\begin{array}{c} u_1^+ - u_1^- \\ u_0^+ - u_0^- \end{array} \right] \in \widetilde{\mathcal{H}}^{-\frac{1}{2}+\varepsilon}(\Sigma) \times \widetilde{\mathcal{H}}^{\frac{1}{2}+\varepsilon}(\Sigma).$$

For an integer j, it follows

$$u_j^+ = (-1)^j \mathcal{F}^{-1} t^j \cdot \mathcal{F} u_0^+$$

and

$$u_j^- = \mathcal{F}^{-1} t^j \cdot \mathcal{F} u_0^-,$$

where

$$t(\xi) = (\xi^2 - k^2)^{\frac{1}{2}} = t_+(\xi) t_-(\xi)$$

with $t_{\pm}$ the squareroot functions

$$t_{\pm}(\xi) = (\xi \pm k)^{\frac{1}{2}} = |\xi \pm k|^{\frac{1}{2}} \, e^{\frac{1}{2} i \arg(\xi \pm k)},$$

$\xi \in \mathbb{R}$, with branch cuts $\Gamma_{\mp} = \{\pm k \pm it, \, t \geq 0\}$, respectively,

$$\arg(\xi - k) \in \left] -\frac{3\pi}{2}, \frac{\pi}{2} \right[$$

and

$$\arg(\xi + k) \in \left] -\frac{\pi}{2}, \frac{3\pi}{2} \right[.$$

Using these formulas, we can define an invertible convolution operator

$$B_{\Phi_B, \Sigma} := \mathcal{F}^{-1} \Phi_B \cdot \mathcal{F}$$

which maps $\widetilde{\mathcal{H}}^{-\frac{1}{2}+\varepsilon}(\Sigma) \times \widetilde{\mathcal{H}}^{\frac{1}{2}+\varepsilon}(\Sigma)$ into $\widetilde{\mathcal{H}}^{-\frac{1}{2}-n+\varepsilon}(\Sigma) \times \widetilde{\mathcal{H}}^{\frac{1}{2}-n+\varepsilon}(\Sigma)$ as

$$B_{\Phi_B, \Sigma} \left[\begin{array}{c} \vartheta \\ \varphi \end{array} \right] = \left[\begin{array}{c} u_{n+1}^+ - u_{n+1}^- \\ u_n^+ - u_n^- \end{array} \right], \tag{2}$$

with Fourier symbol

$$\Phi_B = \frac{1}{2} \left[\begin{array}{cc} (1 + (-1)^n) t^n & (1 - (-1)^n) t^{n+1} \\ (1 - (-1)^n) t^{n-1} & (1 + (-1)^n) t^n \end{array} \right].$$

Now, by the use of (2), it is possible to rewrite the boundary condition (1) as

$$C_{\Phi_C, \Sigma} \left[\begin{array}{c} u_{n+1}^+ - u_{n+1}^- \\ u_n^+ - u_n^- \end{array} \right] = \left[\begin{array}{c} h^+ \\ h^- \end{array} \right] \tag{3}$$

where we define a convolution type operator

$$C_{\Phi_C, \Sigma} := r_{\Sigma} \mathcal{F}^{-1} \Phi_C \cdot \mathcal{F}$$

which maps the spaces $\widetilde{\mathcal{H}}^{-\frac{1}{2}-n+\varepsilon}(\Sigma) \times \widetilde{\mathcal{H}}^{\frac{1}{2}-n+\varepsilon}(\Sigma)$ into the spaces $\mathcal{H}^{-\frac{1}{2}-n+\varepsilon}(\Sigma) \times \mathcal{H}^{-\frac{1}{2}-n+\varepsilon}(\Sigma)$ with Fourier symbol

$$\Phi_C = \frac{1}{2} \left[\begin{array}{cc} p^+ - q^+ t^{-1} & -p^+ t + q^+ \\ -p^- - q^- t^{-1} & -p^- t - q^- \end{array} \right]. \tag{4}$$

Throughout the paper, we are using r_{Σ} to denote the restriction operator to $\Sigma \subset \mathbb{R}$ and in the particular case of $r_{\mathbb{R}_+}$ we will simply write r_+ for this restriction.

From (2) and (3), we obtain

$$C_{\Phi_C, \Sigma} B_{\Phi_B, \Sigma} \left[\begin{array}{c} \vartheta \\ \varphi \end{array} \right] = \left[\begin{array}{c} h^+ \\ h^- \end{array} \right].$$

Our immediate goal will be to extend this last convolution type operator on a finite interval into a convolution type operator on the half-line. In view of this, we will need to consider some extension operator relations.

IV. Extension Methods and Relations Between Operators

We will now perform some operator extension procedures in view of obtaining corresponding operator relations between the operators presented in the last section and new Wiener-Hopf operators. These operator relations will be used in the last section to study the Fredholm property of the operators associated with the problem.

Definition 4.1: [15] Let us consider two operators

$$A : X_1 \to Y_1$$

and

$$B : X_2 \to Y_2,$$

acting between Banach spaces.

(i) The operators A and B are said to be algebraically equivalent after extension if there exist additional Banach spaces Z_1 and Z_2 and invertible linear operators

$$E : Y_2 \times Z_2 \to Y_1 \times Z_1$$

and

$$F : X_1 \times Z_1 \to X_2 \times Z_2$$

such that

$$\left[\begin{array}{cc} A & 0 \\ 0 & I_{Z_1} \end{array} \right] = E \left[\begin{array}{cc} B & 0 \\ 0 & I_{Z_2} \end{array} \right] F. \tag{5}$$

(ii) If, in addition to (i), the invertible and linear operators E and F in (5) are bounded, then we will say that A and B are topologically equivalent after extension operators, or simply say that A and B are equivalent after extension operators, [1].

(iii) A and B are said to be equivalent operators in the particular case when

$$A = E\, B\, F,$$

for some bounded invertible linear operators

$$E : Y_2 \to Y_1$$

and

$$F : X_1 \to X_2.$$

The above notion of topological equivalence after extension relation is equivalente to the concept of *matricial coupling* [1]. We refer to [4], [6] and [15] for a discussion on the differences between algebraic and topological equivalence after extension relations between convolution type operators.

We will now apply some results of [6] to our convolution type operator $C_{\Phi_C,\Sigma}$.

Theorem 4.1: The convolution type operator $C_{\Phi_C,\Sigma}$ with Fourier symbol (4) is algebraically equivalent after extension to the Wiener-Hopf operator $\mathcal{C}_{\Phi_\mathcal{C},\mathbb{R}_+}$ which maps $\widetilde{\mathcal{H}}^{-\frac{1}{2}-n+\varepsilon}(\mathbb{R}_+) \times \widetilde{\mathcal{H}}^{\frac{1}{2}-n+\varepsilon}(\mathbb{R}_+) \times \widetilde{\mathcal{H}}^{-\frac{1}{2}-n+\varepsilon}(\mathbb{R}_+) \times \widetilde{\mathcal{H}}^{-\frac{1}{2}-n+\varepsilon}(\mathbb{R}_+)$ into $\mathcal{H}^{-\frac{1}{2}-n+\varepsilon}(\mathbb{R}_+) \times \mathcal{H}^{\frac{1}{2}-n+\varepsilon}(\mathbb{R}_+) \times \mathcal{H}^{-\frac{1}{2}-n+\varepsilon}(\mathbb{R}_+) \times \mathcal{H}^{-\frac{1}{2}-n+\varepsilon}(\mathbb{R}_+)$ given by

$$\mathcal{C}_{\Phi_\mathcal{C},\mathbb{R}_+} := r_+ \mathcal{F}^{-1} \Phi_\mathcal{C} \cdot \mathcal{F},$$

and with $\Phi_\mathcal{C}$ being the Fourier symbol defined by

$$\Phi_\mathcal{C}(\xi) = \begin{bmatrix} e^{-i\xi a} & 0 & 0 & 0 \\ 0 & e^{-i\xi a} & 0 & 0 \\ \frac{1}{2}(p^+ - q^+ t^{-1}(\xi)) & \frac{1}{2}(-p^+ t(\xi) + q^+) & e^{i\xi a} & 0 \\ \frac{1}{2}(-p^- - q^- t^{-1}(\xi)) & \frac{1}{2}(-p^- t(\xi) - q^-) & 0 & e^{i\xi a} \end{bmatrix}.$$

So, there are Banach spaces X_1 and Y_1 and linear homeomorphisms E_1 and F_1 such that

$$\left[\begin{array}{cc} C_{\Phi_C,\Sigma} & 0 \\ 0 & I_{Z_1} \end{array} \right] = E_1 \left[\begin{array}{cc} \mathcal{C}_{\Phi_\mathcal{C},\mathbb{R}_+} & 0 \\ 0 & I_{Z_2} \end{array} \right] F_1.$$

The proof is omitted in here because is a well-known result addressed in [22]. For some generalizations see [6], [23].

Due to the use of the lifting procedure, and choosing convenient auxiliary bounded invertible operators, we now obtain a new operator relation for an operator acting between Lebesgue spaces – which is presented in the next result.

We will use the notation $L^2_+(\mathbb{R}) := \widetilde{\mathcal{H}}^0(\mathbb{R}_+)$.

Theorem 4.2: The Wiener-Hopf operator $\mathcal{C}_{\Phi_\mathcal{C},\mathbb{R}_+}$ defined above between Bessel potential spaces is equivalent to the Wiener-Hopf operator

$$\widehat{\mathcal{C}}_{\Phi_{\widehat{\mathcal{C}}},\mathbb{R}_+} := r_+ \mathcal{F}^{-1} \Phi_{\widehat{\mathcal{C}}} \cdot \mathcal{F} : \left[L^2_+(\mathbb{R})\right]^4 \to \left[L^2(\mathbb{R}_+)\right]^4,$$

where $\Phi_{\widehat{\mathcal{C}}}$ has the block matricial representation

$$\Phi_{\widehat{\mathcal{C}}}(\xi) = \left[\begin{array}{c:c} \mathfrak{A}(\xi) & 0_2 \\ \hdashline \mathfrak{C}(\xi) & \mathfrak{B}(\xi) \end{array} \right] \tag{6}$$

where

$$\mathfrak{A}(\xi) = \left[\begin{array}{cc} \zeta^{-\frac{1}{2}-n+\varepsilon}(\xi) e^{-i\xi a} & 0 \\ 0 & \zeta^{\frac{1}{2}-n+\varepsilon}(\xi) e^{-i\xi a} \end{array} \right],$$

$$\mathfrak{B}(\xi) = \left[\begin{array}{cc} \zeta^{-\frac{1}{2}-n+\varepsilon}(\xi) e^{i\xi a} & 0 \\ 0 & \zeta^{-\frac{1}{2}-n+\varepsilon}(\xi) e^{i\xi a} \end{array} \right],$$

$$\mathfrak{C}(\xi) = \left[\begin{array}{cc} \mathfrak{C}_{11}(\xi) & \mathfrak{C}_{12}(\xi) \\ \mathfrak{C}_{21}(\xi) & \mathfrak{C}_{22}(\xi) \end{array} \right],$$

with

$$\mathfrak{C}_{11}(\xi) = \frac{1}{2}(p^+ \zeta^{-\frac{1}{2}-n+\varepsilon}(\xi) - q^+ \zeta^{-n+\varepsilon}(\xi)(\xi - k)^{-1}),$$

$$\mathfrak{C}_{12}(\xi) = \frac{1}{2}(-p^+ \zeta^{-n+\varepsilon}(\xi) + q^+ \zeta^{-\frac{1}{2}-n+\varepsilon}(\xi)(\xi + k)^{-1}),$$

$$\mathfrak{C}_{21}(\xi) = \frac{1}{2}(-p^- \zeta^{-\frac{1}{2}-n+\varepsilon}(\xi) - q^- \zeta^{-n+\varepsilon}(\xi)(\xi - k)^{-1}),$$

$$\mathfrak{C}_{22}(\xi) = \frac{1}{2}(-p^- \zeta^{-n+\varepsilon}(\xi) - q^- \zeta^{-\frac{1}{2}-n+\varepsilon}(\xi)(\xi + k)^{-1}),$$

$\zeta(\xi) = \frac{\xi - k}{\xi + k} = \frac{\lambda_-}{\lambda_+}$, $\xi \in \mathbb{R}$ and 0_2 denotes the 2×2 zero matrix.

Proof: The equivalence relation can be directly obtained by computing the following operator composition

$$\mathcal{C}_{\Phi_\mathcal{C},\mathbb{R}_+} = \mathrm{W}_{\Phi_E,\mathbb{R}_+}\, l_0\, \widehat{\mathcal{C}}_{\Phi_{\widehat{\mathcal{C}}},\mathbb{R}_+} l_0 \mathrm{W}_{\Phi_F,\mathbb{R}_+},$$

where

$$l_0 : \left[L^2(\mathbb{R}_+)\right]^4 \to \left[L^2_+(\mathbb{R})\right]^4$$

denotes de zero extension operator and where $\mathrm{W}_{\Phi_E,\mathbb{R}_+} l_0$ is defined between the spaces $\left[L^2(\mathbb{R}_+)\right]^4$ and $\mathcal{H}^{-\frac{1}{2}-n+\varepsilon}(\mathbb{R}_+) \times \mathcal{H}^{\frac{1}{2}-n+\varepsilon}(\mathbb{R}_+) \times \mathcal{H}^{-\frac{1}{2}-n+\varepsilon}(\mathbb{R}_+) \times \mathcal{H}^{-\frac{1}{2}-n+\varepsilon}(\mathbb{R}_+)$ by

$$\mathrm{W}_{\Phi_E,\mathbb{R}_+} l_0 := r_+ \mathcal{F}^{-1} \Phi_E \cdot \mathcal{F} l_0$$

with

$$\Phi_E(\xi) = \begin{bmatrix} \lambda_-^{\frac{1}{2}+n-\varepsilon} & 0 & 0 & 0 \\ 0 & \lambda_-^{-\frac{1}{2}+n-\varepsilon} & 0 & 0 \\ 0 & 0 & \lambda_-^{\frac{1}{2}+n-\varepsilon} & 0 \\ 0 & 0 & 0 & \lambda_-^{\frac{1}{2}+n-\varepsilon} \end{bmatrix}$$

and $l_0 \mathrm{W}_{\Phi_F,\mathbb{R}_+}$ is defined between $\widetilde{\mathcal{H}}^{-\frac{1}{2}-n+\varepsilon}(\mathbb{R}_+) \times \widetilde{\mathcal{H}}^{\frac{1}{2}-n+\varepsilon}(\mathbb{R}_+) \times \widetilde{\mathcal{H}}^{-\frac{1}{2}-n+\varepsilon}(\mathbb{R}_+) \times \widetilde{\mathcal{H}}^{-\frac{1}{2}-n+\varepsilon}(\mathbb{R}_+)$ and $\left[L^2_+(\mathbb{R})\right]^4$ by

$$l_0 \mathrm{W}_{\Phi_F,\mathbb{R}_+} := l_0 r_+ \mathcal{F}^{-1} \Phi_F \cdot \mathcal{F}$$

with

$$\Phi_F(\xi)=\begin{bmatrix} \lambda_+^{-\frac{1}{2}-n+\varepsilon} & 0 & 0 & 0 \\ 0 & \lambda_+^{\frac{1}{2}-n+\varepsilon} & 0 & 0 \\ 0 & 0 & \lambda_+^{-\frac{1}{2}-n+\varepsilon} & 0 \\ 0 & 0 & 0 & \lambda_+^{-\frac{1}{2}-n+\varepsilon} \end{bmatrix}.$$

Notice that the bounded operators $\mathrm{W}_{\Phi_E,\mathbb{R}_+}l_0$ and $l_0\mathrm{W}_{\Phi_F,\mathbb{R}_+}$ are invertible as pointed out in [30, §2.10.3]. ■

V. Fredholm Analysis

Our main goal is to study and characterize the Fredholm property of the finite interval convolution type operator $C_{\Phi_C,\Sigma}$ for general ε. We will use different factorization procedures applied to the operators introduced in the last section. We start by recalling the definition of Fredholm operator.

Definition 5.1: Let X, Y be two Banach spaces and $A : X \to Y$ a bounded linear operator with closed image. The operator A is called a Fredholm operator if

$$n(A) := \dim\, Ker\, A < \infty$$

and

$$d(A) := \dim\, Y/Im\, A < \infty.$$

If A is a Fredholm operator, then the Fredholm index of A is the integer defined by

$$Ind\, A = n(A) - d(A).$$

Theorem 5.1: Let $\Phi_{\widehat{\mathcal{C}}}$ be defined by (6) and

$$\det \mathfrak{C}(\pm\infty) \neq 0.$$

The operator $\widehat{\mathcal{C}}_{\Phi_{\widehat{\mathcal{C}}},\mathbb{R}_+}$ presented in the last theorem admits the factorization

$$\widehat{\mathcal{C}}_{\Phi_{\widehat{\mathcal{C}},\mathbb{R}_+}} = \widehat{\mathrm{W}}_{\widehat{\Phi}_-,\mathbb{R}_+}\widetilde{\mathcal{C}}_{\Phi_{\tilde{\mathcal{C}},\mathbb{R}_+}}\widehat{\mathrm{W}}_{\widehat{\Phi}_+,\mathbb{R}_+}$$

where $\widehat{\mathrm{W}}_{\widehat{\Phi}_-,\mathbb{R}_+}$ and $\widehat{\mathrm{W}}_{\widehat{\Phi}_+,\mathbb{R}_+}$ are invertible operators having Fourier symbols

$$\widehat{\Phi}_-(\xi) = \left[\begin{array}{cc:cc} -1 & 0 & -e^{-ia\xi}\tau^-(\xi) & \\ 0 & -1 & & \\ \hdashline 0 & 0 & -1 & 0 \\ 0 & 0 & 0 & -1 \end{array}\right]$$

and

$$\widehat{\Phi}_+(\xi) = \left[\begin{array}{cc:cc} 0 & 0 & 1 & 0 \\ 0 & 0 & 0 & 1 \\ \hdashline 1 & 0 & e^{ia\xi}\tau^+(\xi) & \\ 0 & 1 & & \end{array}\right],$$

which admit bounded analytic extensions in $\Im m\, \xi < 0$ and $\Im m\, \xi > 0$, respectively, and with

$$\tau^-(\xi) = \frac{1-S(\xi)}{2}\mathfrak{C}^{-1}(-\infty) + \frac{1+S(\xi)}{2}\begin{bmatrix} e^{i\pi(-1-2n+2\varepsilon)} & 0 \\ 0 & e^{i\pi(1-2n+2\varepsilon)} \end{bmatrix}\mathfrak{C}^{-1}(+\infty)$$

and

$$\tau^+(\xi) = \frac{1-S(\xi)}{2}\mathfrak{C}^{-1}(-\infty) + \frac{1+S(\xi)}{2}\begin{bmatrix} e^{i\pi(-1-2n+2\varepsilon)} & 0 \\ 0 & e^{i\pi(-1-2n+2\varepsilon)} \end{bmatrix}\mathfrak{C}^{-1}(+\infty)$$

where $S : \mathbb{C} \to \mathbb{C}$ is the normalized sine-integral function given by

$$S(\xi) = \frac{2}{\pi}\int_0^\xi \frac{\sin x}{x}dx$$

and where $\mathfrak{C}^{-1}(-\infty)$ and $\mathfrak{C}^{-1}(+\infty)$ are defined by

$$\mathfrak{C}^{-1}(-\infty) = \begin{bmatrix} \frac{1}{p^+} & -\frac{1}{p^-} \\ -\frac{1}{p^+} & -\frac{1}{p^-} \end{bmatrix}$$

and

$$\mathfrak{C}^{-1}(+\infty) = \begin{bmatrix} \frac{1}{p^+}e^{i\pi(1+2n-2\varepsilon)} & -\frac{1}{p^-}e^{i\pi(1+2n-2\varepsilon)} \\ -\frac{1}{p^+}e^{i\pi(2n-2\varepsilon)} & -\frac{1}{p^-}e^{i\pi(2n-2\varepsilon)} \end{bmatrix}$$

if

$$\det \mathfrak{C}(-\infty) = -\frac{p^+p^-}{2} \neq 0$$

and

$$\det \mathfrak{C}(+\infty) = -\frac{p^+p^-}{2}e^{i\pi(-1-4n+4\varepsilon)} \neq 0,$$

respectively.

The Fourier symbol $\Phi_{\widetilde{\mathcal{C}}}$ belongs to $PC^{4\times4}(\dot{\mathbb{R}})$, the space of four by four matrix-valued functions with piecewise continuous entries on $\dot{\mathbb{R}} = \mathbb{R} \cup \{\infty\}$, and is given by

$$\Phi_{\widetilde{\mathcal{C}}}(\xi) = \left[\begin{array}{c:c} \mathfrak{A}(\xi) & \mathfrak{B}(\xi) \\ \hdashline \mathfrak{D}(\xi) & -\mathfrak{C}(\xi) \end{array}\right] \tag{7}$$

where

$$\mathfrak{A}(\xi) = \left(\begin{bmatrix} \zeta^{-\frac{1}{2}-n+\varepsilon}(\xi) & 0 \\ 0 & \zeta^{\frac{1}{2}-n+\varepsilon}(\xi) \end{bmatrix} - \tau^-(\xi)\mathfrak{C}(\xi)\right)\tau^+(\xi) + \tau^-(\xi)\begin{bmatrix} \zeta^{-\frac{1}{2}-n+\varepsilon}(\xi) & 0 \\ 0 & \zeta^{-\frac{1}{2}-n+\varepsilon}(\xi) \end{bmatrix},$$

$$\mathfrak{B}(\xi) = e^{-ia\xi}\left(\tau^-(\xi)\mathfrak{C}(\xi) - \begin{bmatrix} \zeta^{-\frac{1}{2}-n+\varepsilon}(\xi) & 0 \\ 0 & \zeta^{\frac{1}{2}-n+\varepsilon}(\xi) \end{bmatrix}\right),$$

$$\mathfrak{D}(\xi) = e^{ia\xi}\left(\mathfrak{C}(\xi)\tau^+(\xi) - \begin{bmatrix} \zeta^{-\frac{1}{2}-n+\varepsilon}(\xi) & 0 \\ 0 & \zeta^{-\frac{1}{2}-n+\varepsilon}(\xi) \end{bmatrix}\right).$$

The proof of the last result can be done by direct computation and therefore is here omitted. Anyway, we have,

$$\lim_{\xi\to\pm\infty}\left(\tau^-(\xi)\mathfrak{C}(\xi) - \begin{bmatrix} \zeta^{-\frac{1}{2}-n+\varepsilon}(\xi) & 0 \\ 0 & \zeta^{\frac{1}{2}-n+\varepsilon}(\xi) \end{bmatrix}\right) = 0, \tag{8}$$

$$\lim_{\xi\to\pm\infty}\left(\mathfrak{C}(\xi)\tau^+(\xi) - \begin{bmatrix} \zeta^{-\frac{1}{2}-n+\varepsilon}(\xi) & 0 \\ 0 & \zeta^{-\frac{1}{2}-n+\varepsilon}(\xi) \end{bmatrix}\right) = 0. \tag{9}$$

These last two results are a consequence of the fact that we agree that

$$\lim_{\xi\to-\infty}\zeta^\sigma(\xi) = 1$$

and

$$\lim_{\xi\to+\infty}\zeta^\sigma(\xi) = e^{i2\pi\sigma},$$

for $\sigma \in \mathbb{R}$.

In order to continue, let us consider, for $\Phi \in PC^{n\times n}(\dot{\mathbb{R}})$, the function

$$\overline{\Phi} : \dot{\mathbb{R}} \times [0,1] \to \mathbb{C}^{n\times n}$$

defined by

$$\overline{\Phi}(\xi,\mu) := (1-\mu)\Phi(\xi-0) + \mu\Phi(\xi+0),$$

$(\xi,\mu) \in \dot{\mathbb{R}} \times [0,1]$, where

$$\Phi(\infty - 0) := \Phi(+\infty)$$

and

$$\Phi(\infty + 0) := \Phi(-\infty).$$

The following result [2, Theorem 5.9] helps us to study the Fredholm property for the operator $C_{\Phi_C,\Sigma}$.

Theorem 5.2: For $\Phi \in PC^{n\times n}(\dot{\mathbb{R}})$, it follows that

$$\det \overline{\Phi}(\xi,\mu) \neq 0$$

for all $(\xi,\mu) \in \dot{\mathbb{R}} \times [0,1]$ if and only if

$$\mathcal{W}_{\Phi,\mathbb{R}_+} := r_+\mathcal{F}^{-1}\Phi \cdot \mathcal{F} : \left[L^2_+(\mathbb{R})\right]^n \to \left[L^2(\mathbb{R}_+)\right]^n$$

is a Fredholm operator.

In case of having the Fredholm property, the Fredholm index of $\mathcal{W}_{\Phi,\mathbb{R}_+}$ is given by

$$Ind\,\mathcal{W}_{\Phi,\mathbb{R}_+} = -wind(\det \overline{\Phi}),$$

where $wind$ denotes the winding number.

Finally, we are able to present the Fredholm characterization to our operator $C_{\Phi_C,\Sigma}$ and, consequently, to our initial problem.

Theorem 5.3: The finite interval convolution type operator $C_{\Phi_C,\Sigma}$ is a Fredholm operator with zero Fredholm index if and only if

$$\varepsilon \neq \frac{q}{2} \quad \text{for} \quad q \in \mathbb{Z}. \tag{10}$$

Proof: First of all, we notice that from Theorems 4.1–5.1 we conclude that the operator $C_{\Phi_C,\Sigma}$ is algebraically equivalent after extension to the operator

$$\widetilde{\mathcal{C}}_{\Phi_{\widetilde{c}},\mathbb{R}_+} := r_+\mathcal{F}^{-1}\Phi_{\widetilde{\mathcal{C}}} \cdot \mathcal{F} : \left[L^2_+(\mathbb{R})\right]^4 \to \left[L^2(\mathbb{R}_+)\right]^4$$

where $\Phi_{\widetilde{\mathcal{C}}}$ is given by (7). Therefore, in view to obtain the desired conclusion, that $C_{\Phi_C,\Sigma}$ is a Fredholm operator, we start by deducing the conditions which characterize the Fredholm property of $\widetilde{\mathcal{C}}_{\Phi_{\widetilde{c}},\mathbb{R}_+}$.

Letting

$$\overline{\Phi}_{\widetilde{\mathcal{C}}}(\xi,\mu) = (1-\mu)\Phi_{\widetilde{\mathcal{C}}}(\xi-0) + \mu\Phi_{\widetilde{\mathcal{C}}}(\xi+0)$$

and

$$\Phi_{\widetilde{\mathcal{C}}}(\infty \pm 0) := \Phi_{\widetilde{\mathcal{C}}}(\mp\infty),$$

by Theorem 5.2, we have that

$$\det \overline{\Phi}_{\widetilde{\mathcal{C}}}(\xi,\mu) \neq 0$$

for $(\xi,\mu) \in \dot{\mathbb{R}} \times [0,1]$ if and only if the operator $\widetilde{\mathcal{C}}_{\Phi_{\widetilde{c}},\mathbb{R}_+}$ has the Fredholm property. Additionally, from Theorem 5.1, we already know that the Fourier symbol $\Phi_{\widetilde{\mathcal{C}}}$ can be written as

$$\Phi_{\widetilde{\mathcal{C}}}(\xi) = \widehat{\Phi}_-^{-1}(\xi)\Phi_{\widehat{\mathcal{C}}}(\xi)\widehat{\Phi}_+^{-1}(\xi).$$

Thus, for any $\xi \in \mathbb{R}$ we have

$$\det \Phi_{\widetilde{\mathcal{C}}}(\xi \pm 0) = \det \Phi_{\widehat{\mathcal{C}}}(\xi)$$

because $\Phi_{\widehat{\mathcal{C}}}(\xi)$ has no discontinuities on the real line, $\det \widehat{\Phi}_\pm^{-1}$ also have no discontinuities on the real line and, moreover, $\det \widehat{\Phi}_\pm^{-1} \equiv 1$. Therefore,

$$\begin{aligned} \det \overline{\Phi}_{\widetilde{\mathcal{C}}}(\xi,\mu) &= \det\left[(1-\mu)\Phi_{\widehat{\mathcal{C}}}(\xi) + \mu\Phi_{\widehat{\mathcal{C}}}(\xi)\right] \\ &= \det \Phi_{\widehat{\mathcal{C}}}(\xi) \\ &= \zeta^{-1-4n+4\varepsilon}(\xi) \\ &\neq 0, \end{aligned}$$

in the case of $\xi \in \mathbb{R}$.

For $\xi = \infty$, we have,

$$\det \overline{\Phi}_{\widetilde{\mathcal{C}}}(\infty,\mu) = \det\left[(1-\mu)\Phi_{\widetilde{\mathcal{C}}}(+\infty) + \mu\Phi_{\widetilde{\mathcal{C}}}(-\infty)\right].$$

Appealing to the limits (8)–(9), we obtain

$$\Phi_{\widetilde{\mathcal{C}}}(-\infty) = \left[\begin{array}{c|c} \mathfrak{C}^{-1}(-\infty) & 0_2 \\ \hline 0_2 & -\mathfrak{C}(-\infty) \end{array}\right]$$

and

$$\Phi_{\widetilde{\mathcal{C}}}(+\infty) = \left[\begin{array}{c|c} \mathfrak{A}\mathfrak{C}^{-1}(+\infty)\mathfrak{B} & 0_2 \\ \hline 0_2 & -\mathfrak{C}(+\infty) \end{array}\right],$$

with

$$\mathfrak{A} = \begin{bmatrix} e^{i\pi(-1-2n+2\varepsilon)} & 0 \\ 0 & e^{i\pi(1-2n+2\varepsilon)} \end{bmatrix},$$

and

$$\mathfrak{B} = \begin{bmatrix} e^{i\pi(-1-2n+2\varepsilon)} & 0 \\ 0 & e^{i\pi(-1-2n+2\varepsilon)} \end{bmatrix}.$$

Thus, by direct computation, we have

$$\Phi_{\widetilde{\mathcal{C}}}(-\infty) = \begin{bmatrix} \frac{1}{p^+} & -\frac{1}{p^-} & 0 & 0 \\ -\frac{1}{p^+} & -\frac{1}{p^-} & 0 & 0 \\ 0 & 0 & -\frac{1}{2}p^+ & \frac{1}{2}p^+ \\ 0 & 0 & \frac{1}{2}p^- & \frac{1}{2}p^- \end{bmatrix}$$

and

$$\Phi_{\widetilde{\mathcal{C}}}(+\infty) = \begin{bmatrix} a_{11} & a_{12} & 0 & 0 \\ a_{21} & a_{22} & 0 & 0 \\ 0 & 0 & a_{33} & a_{34} \\ 0 & 0 & a_{43} & a_{44} \end{bmatrix},$$

with

$$a_{11} = \frac{1}{p^+} e^{i\pi(-1-2n+2\varepsilon)},$$
$$a_{12} = -\frac{1}{p^-} e^{i\pi(-1-2n+2\varepsilon)},$$
$$a_{21} = -\frac{1}{p^+} e^{i\pi(-2n+2\varepsilon)},$$
$$a_{22} = -\frac{1}{p^-} e^{i\pi(-2n+2\varepsilon)},$$
$$a_{33} = -\frac{p^+}{2} e^{i\pi(-1-2n+2\varepsilon)},$$
$$a_{34} = \frac{p^+}{2} e^{i\pi(-2n+2\varepsilon)},$$
$$a_{43} = \frac{p^-}{2} e^{i\pi(-1-2n+2\varepsilon)},$$
$$a_{44} = \frac{p^-}{2} e^{i\pi(-2n+2\varepsilon)}.$$

Finally, the last results, tell us that

$$\det \overline{\Phi}_{\widetilde{\mathcal{C}}}(\infty,\mu) = \begin{vmatrix} b_{11} & b_{12} & 0 & 0 \\ b_{21} & b_{22} & 0 & 0 \\ 0 & 0 & b_{33} & b_{34} \\ 0 & 0 & b_{43} & b_{44} \end{vmatrix},$$

where

$$b_{11} = \frac{1-\mu}{p^+} e^{i\pi(-1-2n+2\varepsilon)} + \frac{\mu}{p^+},$$
$$b_{12} = -\frac{1-\mu}{p^-} e^{i\pi(-1-2n+2\varepsilon)} - \frac{\mu}{p^-},$$
$$b_{21} = -\frac{1-\mu}{p^+} e^{i\pi(-2n+2\varepsilon)} - \frac{\mu}{p^+},$$
$$b_{22} = -\frac{1-\mu}{p^-} e^{i\pi(-2n+2\varepsilon)} - \frac{\mu}{p^-},$$
$$b_{33} = -\frac{(1-\mu)p^+}{2} e^{i\pi(-1-2n+2\varepsilon)} - \frac{\mu p^+}{2},$$
$$b_{34} = \frac{(1-\mu)p^+}{2} e^{i\pi(-2n+2\varepsilon)} + \frac{\mu p^+}{2},$$
$$b_{43} = \frac{(1-\mu)p^-}{2} e^{i\pi(-1-2n+2\varepsilon)} + \frac{\mu p^-}{2},$$
$$b_{44} = \frac{(1-\mu)p^-}{2} e^{i\pi(-2n+2\varepsilon)} + \frac{\mu p^-}{2}.$$

So,

$$\det \overline{\Phi}_{\widetilde{\mathcal{C}}}(\infty,\mu) = \left[(1-\mu)e^{i\pi(-1-2n+2\varepsilon)} + \mu\right]^2 \left[(1-\mu)e^{i\pi(-2n+2\varepsilon)} + \mu\right]^2.$$

As a consequence, $\widetilde{\mathcal{C}}_{\Phi_{\tilde{\mathcal{C}}},\mathbb{R}_+}$ is a Fredholm operator if and only if

$$(1-\mu)e^{i\pi(-1-2n+2\varepsilon)} + \mu \neq 0 \tag{11}$$

and

$$(1-\mu)e^{i\pi(-2n+2\varepsilon)} + \mu \neq 0, \tag{12}$$

$\mu \in [0,1]$.

Since the sets

$$\mathcal{S}_1 = \left\{(1-\mu)e^{i\pi(-1-2n+2\varepsilon)} + \mu \ : \ \mu \in [0,1]\right\}$$

and

$$\mathcal{S}_2 = \left\{(1-\mu)e^{i\pi(-2n+2\varepsilon)} + \mu \ : \ \mu \in [0,1]\right\}$$

define the line segments joining 1 to $e^{i\pi(-1-2n+2\varepsilon)}$ and 1 to $e^{i\pi(-2n+2\varepsilon)}$, respectively, for holding the inequalities in (11) and (12), we need that

$$e^{i\pi(-1-2n+2\varepsilon)} \notin \mathbb{R}_-$$

and

$$e^{i\pi(-2n+2\varepsilon)} \notin \mathbb{R}_-.$$

Thus

$$\pi(-1-2n+2\varepsilon) \neq \pi + 2\pi q$$

and

$$\pi(-2n+2\varepsilon) \neq \pi + 2\pi q,$$

$q \in \mathbb{Z}$, i.e.,

$$\varepsilon \neq 1+n+q \quad \text{and} \quad \varepsilon \neq \frac{1}{2}+n+q, \qquad q \in \mathbb{Z}.$$

So, we have $\varepsilon \neq \frac{q}{2}$, $q \in \mathbb{Z}$.

Therefore, from the operator identities provided by both the above mentioned algebraic and topological equivalence relations, given in Theorems 4.1–5.1, we conclude that $\widetilde{\mathcal{C}}_{\Phi_{\tilde{\mathcal{C}}},\mathbb{R}_+}$ and $C_{\Phi_C,\Sigma}$ are Fredholm operators if and only if condition (10) holds, and that the corresponding defect spaces of these operators have the same dimensions. From this, and since by [1, Theorem 3] Fredholm operators in Banach spaces are equivalent after extension if and only if their corresponding defect spaces have equal dimensions, we even arrive at the conclusion that $\widetilde{\mathcal{C}}_{\Phi_{\tilde{\mathcal{C}}},\mathbb{R}_+}$ and $C_{\Phi_C,\Sigma}$ are not only algebraically equivalent after extension but also topologically equivalent after extension.

Finally, jointing the last conclusion with Theorem 5.2, we obtain the following result for the Fredholm index of $C_{\Phi_C,\Sigma}$,

$$\begin{aligned} Ind\, C_{\Phi_C,\Sigma} &= Ind\, \widetilde{\mathcal{C}}_{\Phi_{\tilde{\mathcal{C}}},\mathbb{R}_+} \\ &= -wind\left(\det \overline{\Phi}_{\widetilde{\mathcal{C}}}(\xi,\mu)\right) \\ &= -\frac{1}{2\pi}\left(\left[\arg\det \overline{\Phi}_{\widetilde{\mathcal{C}}}(\xi,\mu)\right]_{\mathbb{R}} + \left[\arg\det \overline{\Phi}_{\widetilde{\mathcal{C}}}(\infty,\mu)\right]_{[0,1]}\right) \\ &= -\frac{1}{2\pi}\left(\left[\arg\det \Phi_{\widetilde{\mathcal{C}}}(\xi)\right]_{\mathbb{R}} + \left[\arg\det \overline{\Phi}_{\widetilde{\mathcal{C}}}(\infty,\mu)\right]_{[0,1]}\right), \end{aligned}$$

where $[f(\xi)]_{\mathbb{R}}$ denotes the increment of $f(\xi)$ when ξ varies through $\mathbb{R}$ from $-\infty$ to $+\infty$ and $[f(\infty,\mu)]_{[0,1]}$ is the increment of $f(\infty,\mu)$ when μ varies through $\mathbb{R}$ from 0 to 1. Directly, we obtain

$$\left[\arg\det \Phi_{\widetilde{\mathcal{C}}}(\xi)\right]_{\mathbb{R}} = \pi(-2-8n+8\varepsilon)$$

and

$$\left[\arg\det \overline{\Phi}_{\widetilde{\mathcal{C}}}(\infty,\mu)\right]_{[0,1]} = \pi(2+8n-8\varepsilon).$$

So, we have the desired result $Ind\, C_{\Phi_C,\Sigma} = 0$. ■

ISBN: 978-1-61804-225-5

VI. Conclusion

In the present paper we were able to characterize the Fredholm property of particular operators associated with an impedance boundary problem which are a generalization of the results presented in [14]. For practical and theoretical reasons, with the Fredholm property we are able to answer further questions about this kind of diffraction problems in particular the invertibility and the image normalization of the operators related with the problem. We plan to do this in future works.

Acknowledgment

This work was partially supported by the Center of Mathematics of University of Beira Interior (CM-UBI) through the project PEst-OE/MAT/UI0212/2014.

References

[1] H. Bart and V. E. Tsekanovskii, Matricial coupling and equivalence after extension, *Oper. Theory Adv. Appl.* **59**, 143–160, 1992.

[2] A. Böttcher, Yu. I. Karlovich, and I. M. Spitkovsky, *Convolution Operators and Factorization of Almost Periodic Matrix Functions*, Birkhäuser Verlag, Basel, 2002.

[3] A. Büyükaksoy and G. Çýnar, Solution of a matrix Wiener-Hopf equation connected with the plane wave diffraction by an impedance loaded parallel plate waveguide, *Math. Methods Appl. Sci.* **28**, 1633–1645, 2005.

[4] L. P. Castro, Regularity of convolution type operators with PC symbols in Bessel potential spaces over two finite intervals, *Mathematische Nachrichten* **261**-**262**(1), 23–36, 2003.

[5] L. P. Castro, Solution of a Sommerfeld diffraction problem with a real wave number, in: C. Constanda, M. Ahues, A. Largillier (eds.), *Integral Methods in Science and Engineering*, Birkhäuser, Boston, MA, 25–30, 2004.

[6] L. P. Castro, Wiener-Hopf operators on unions of finite intervals: relations and generalized inversion, in: F. J. Cobos (ed.) et al., *Proceedings of the Meeting on Matrix Analysis and Applications*, University of Sevilha, Sevilha, 148–155, 1997.

[7] L. P. Castro and D. Kapanadze, The impedance boundary-value problem of diffraction by a strip, *Journal of Mathematical Analysis and Applications* **337**(2), 1031–1040, 2008.

[8] L. P. Castro and D. Kapanadze, Wave diffraction by a half-plane with an obstacle perpendicular to the boundary, *J. Differential Equations*, **254**, 493–510, 2013.

[9] L. P. Castro and D. Kapanadze, Wave diffraction by a strip with first and second kind boundary conditions: the real wave number case, *Mathematische Nachrichten*, **281**, 1400–1411, 2008.

[10] L. P. Castro and A. Moura Santos, An operator approach for an oblique derivative boundary-transmission problem, *Math. Meth. Appl. Sci.*, **27**, 1469–1491, 2004.

[11] L. P. Castro and D. Natroshvili, The potential method for the reactance wave diffraction problem in a scale of spaces, *Georgian Math. J.* **13**, 251–260, 2006.

[12] L. P. Castro and A. M. Simões, Fredholm analysis for a wave diffraction problem with higher order boundary conditions on a strip, in: *Mathematical Problems in Engineering and Aerospace Sciences*, Cambridge Scientific Publishers, Cambridge, 535–542, 2009.

[13] L. P. Castro and A. M. Simões, Mathematical treatment of a wave diffraction problem with higher order boundary conditions, in: *Trends and Challenges in Applied Mathematics*, Matrix Rom Publishers, Bucharest, 44–49, 2007.

[14] L. P. Castro and A. M. Simões, The impedance problem of wave diffraction by a strip with higher order boundary conditions, *AIP Conference Proceedings*, **1561**(1), 184–193, 2013.

[15] L. P. Castro and F.-O. Speck, Relations between convolution type operators on intervals and on the half-line, *Integral Equations Operator Theory* **37**, 169–207, 2000.

[16] L. P. Castro, F.-O. Speck, and F.S. Teixeira, Explicit solution of a Dirichlet-Neumann wedge diffraction problem with a strip, *J. Integral Equations Appl.* **5**, 359–383, 2003.

[17] L. P. Castro, F.-O. Speck, and F.S. Teixeira, On a class of wedge diffraction problems posted by Erhard Meister, *Oper. Theory Adv. Appl.* **147**, 213–240, 2004.

[18] S. N. Chandler-Wilde, The impedance boundary value problem for the Helmholtz equation in a half-plane, *Math. Methods Appl. Sci.* **20**, 813–840, 1997.

[19] D. Colton and R. Kress, *Inverse Acoustic and Electromagnetic Scattering Theory*, Springer-Verlag, Berlin, 1998.

[20] A. K. Gautesen, Diffraction of plane waves by a wedge with impedance boundary conditions, *Wave Motion* **41**, 239–246, 2005.

[21] D. S. Jones, *Methods in Electromagnetic Wave Propagation. Volume 1: Theory and Guided Waves. Volume 2: Radiating Waves*, Clarendon Press, Oxford, 1987.

[22] A. B. Kuijper, A note on first kind convolution equations on a finite interval, *Integral Equations Operator Theory* **14**, 146–152, 1991.

[23] A. B. Kuijper and I. M. Spitkovskij, On convolution equations with semi-almost periodic symbols on a finite interval, *Integral Equations Operator Theory* **16**, 530–538, 1993.

[24] W. McLean, *Strongly Elliptic Systems and Boundary Integral Equations*, Cambridge Univ. Press, Cambridge, UK, 2000.

[25] E. Meister, Some multiple-part Wiener-Hopf problems in mathematical physics, in: *Mathematical Models and Methods in Mechanics*, Banach Center Publ., vol. 15, PWN, Polish Scientific Publishers, Warsaw, 359–407, 1985.

[26] E. Meister and F.-O. Speck, Modern Wiener-Hopf methods in diffraction theory, in: *Ordinary and Partial Differential Equations, vol. II*, Pitman Res. Notes Math. Ser., vol. 216, Longman Sci. Tech., Harlow, 130–171, 1989.

[27] A. Moura Santos, F.-O. Speck, and F. S. Teixeira, Compatibility conditions in some diffraction problems, in: *Direct and Inverse Electromagnetic Scattering*, Pitman Res. Notes Math. Ser., vol. 361, Longman, Harlow, 25–38, 1996.

[28] B. Noble, *Methods based on the Wiener-Hopf Technique for the Solution of Partial Differential Equations*, Pergamon Press, London, 1958; Chelsea Publishing Company, New York, 1988.

[29] A. Sommerfeld, Mathematische Theorie der Diffraction, *Math. Ann.* **47**, 317–374, 1896.

[30] H. Triebel, *Interpolation Theory, Function Spaces, Differential Operators*, second ed., Barth, Leipzig, 1995.

Humbert polynomials and functions in terms of Hemite polynomials

Clemente Cesarano

***Abstract*—** By starting from the standard definitions of the incomplete two-variable Hermite polynomials, we propose non-trivial generalizations and we show some applications to the Bessel-type functions as the Humbert functions. We also present a generalization of the Laguerre polynomials in the same context of the incomplete-type and we use these to obtain relevant operational techniques for the Humbert-type functions.

***Keywords*—** Hermite Polynomials, Laguerre polynomials, Generating Functions, Orthogonal Polynomials, Humbert polynomials, Humbert Functions, Bessel Functions.

I. INTRODUCTION

IT is possible to introduce a generalization of the Hermite polynomials which are a vectorial extension of the ordinary Kampé de Feriét one-variable Hermite polynomials [1]. We have indicated this class of the Hermite polynomials, of two-index and two-variable, by the symbol $He_{m,n}(x,y)$, and we stated their definition through the following generating function:

$$e^{\underline{h}^t \hat{M} \underline{z} - \frac{1}{2}\underline{h}^t \hat{M} \underline{h}} = \sum_{m=0}^{+\infty}\sum_{n=0}^{+\infty} \frac{t^m}{m!}\frac{u^n}{n!} He_{m,n}(x,y), \tag{1}$$

where:

$$\underline{z} = \begin{pmatrix} x \\ y \end{pmatrix} \text{ and } \underline{h} = \begin{pmatrix} t \\ u \end{pmatrix}$$

are two vectors of the space $\mathbb{R}^2$ such that: $t \neq u$, $(|t|,|u|) < +\infty$, and the superscript "t" denotes transpose.

A different generalization of the Hermite polynomials could be obtained by using the slight similar procedure onto the two-variable generalized Hermite polynomials [1,2]:

$$H_n(x,y) = n! \sum_{r=0}^{\left[\frac{n}{2}\right]} \frac{y^r x^{n-2r}}{r!(n-2r)!}, \tag{2}$$

C. Cesarano and Dario Assante are with the Faculty of Engineering, International Telematic University UNINETTUNO, Rome, Italy (phone: +39 0669207675; e-mail: c.cesarano@uninettunouniversity.net).

defined by the generating function of the form:

$$\exp(xt + yt^2) = \sum_{n=0}^{+\infty} \frac{t^n}{n!} H_n(x,y). \tag{3}$$

Let u and v continuous variables, such that $u \neq v$ and $(|u|,|v|) < +\infty$, $\tau \in \mathbb{R}$, we will say incomplete 2-dimensional Hermite polynomials, the polynomials defined by following generating function:

$$\exp(xu + yv + \tau uv) = \sum_{m=0}^{+\infty}\sum_{n=0}^{+\infty} \frac{u^m}{m!}\frac{v^n}{n!} h_{m,n}(x,y \mid \tau). \tag{4}$$

This class of Hermite polynomials has been deeply studied for its importance in applications, as quantum mechanical problems, harmonic oscillator functions and also to investigate the statistical properties of chaotic light [3].

By using the techniques of the generating function method [4,5], it is easy to obtain the explicit form of the above polynomials:

$$h_{m,n}(x,y \mid \tau) = m!n! \sum_{r=0}^{[m,n]} \frac{\tau^r x^{m-r} y^{n-r}}{r!(m-r)!(n-r)!}, \tag{5}$$

where $[m,n] = \min(m,n)$.

An interesting particular case of this class of Hermite polynomials is presented when $x = y = 1$ and $\tau = x$:

$$h_{m,n}(1,1 \mid x) = g_{m,n}(x). \tag{6}$$

It is significant to study the polynomials $g_{m,n}(x)$ since they can be used to define other forms of the incomplete 2-dimensional Hermite polynomials of the type $h_{m,n}(.,.|.)$ themselves and since they often appear in the description of the applications in quantum optics. From the relation (6) and by using the definitions (4) and (5), we can immediately write the following general relation:

$$h_{m,n}(x,y \mid \tau) = x^m y^n g_{m,n}\left(\frac{\tau}{xy}\right). \tag{7}$$

ISBN: 978-1-61804-225-5

The incomplete 2-dimensional Hermite polynomials can be used to obtain different forms of the multi-index Bessel functions, in particular for the case of the Humbert functions. We remind that the ordinary cylindrical Bessel functions [6] are specified by the generating function:

$$\exp\left[\frac{x}{2}\left(t-\frac{1}{t}\right)\right]=\sum_{n=-\infty}^{+\infty}t^n J_n(x), \tag{8}$$

and a generalization of them, it is represented by the case of two-index, one-variable type [7,8]:

$$J_{m,n}(x)=\sum_{s=-\infty}^{+\infty}J_{m-s}(x)J_{n-s}(x)J_s(x), \tag{9}$$

with the following generating function:

$$\exp\left[\frac{x}{2}\left(u-\frac{1}{u}\right)+\left(v-\frac{1}{v}\right)\left(uv-\frac{1}{uv}\right)\right]= \\ =\sum_{m=-\infty}^{+\infty}\sum_{n=-\infty}^{+\infty}u^m v^n J_{m,n}(x), \tag{10}$$

where $x\in\mathbb{R}$ and $u,v\in\mathbb{R}$, such that $0<|u|\neq|v|<+\infty$.

This class of Bessel functions satisfied analogous interesting relations as the ordinary Bessel functions. For instance, by deriving in the equation (10) with respect to *x*, we have:

$$\frac{1}{2}\left(u-\frac{1}{u}\right)+\left(v-\frac{1}{v}\right)\left(uv-\frac{1}{uv}\right)\sum_{m=-\infty}^{+\infty}\sum_{n=-\infty}^{+\infty}u^m v^n J_{n,m}(x)= \\ =\sum_{m=-\infty}^{+\infty}\sum_{n=-\infty}^{+\infty}u^m v^n\frac{d}{dx}J_{m,n}(x), \tag{11}$$

which allows us to state the following recurrence relation:

$$\frac{d}{dx}J_{m,n}(x)=\frac{1}{2}\left\{\left[J_{m-1,n}(x)-J_{m+1,n}(x)\right]+\left[J_{m,n-1}(x)-J_{m,n+1}(x)\right]+ \\ +\left[J_{m-1,n-1}(x)-J_{m+1,n+1}(x)\right]\right\}. \tag{12}$$

By using the same procedure, it is easy to obtain the other two recurrence relations for this class of Bessel functions:

$$\frac{2m}{x}J_{m,n}(x)=\left[J_{m,n-1}(x)-J_{m,n+1}(x)\right]+ \\ +\left[J_{m-1,n-1}(x)-J_{m+1,n+1}(x)\right], \tag{13}$$

and:

$$\frac{2n}{x}J_{m,n}(x)=\left[J_{m,n-1}(x)-J_{m,n+1}(x)\right]+ \\ +\left[J_{m-1,n-1}(x)-J_{m+1,n+1}(x)\right]. \tag{14}$$

It is interesting to note that, for $x=0$, from the explicit form of the generalized two-index Bessel function (eq. (9)), we get:

$$J_{m,n}(0)=\sum_{s=-\infty}^{+\infty}J_{m-s}(0)J_{n-s}(0)J_s(0), \tag{15}$$

and, since:

$$J_s(0)\neq 0 \text{ , when } s=0, \tag{16}$$

we, finally, obtain:

$$J_{m,n}(0)=\delta_{m,0}\delta_{n,0}. \tag{17}$$

As a particular case of the two-index, one-variable Bessel functions, we can introduce the Humbert functions [9], by setting:

$$b_{m,n}(x,y\,|\,\tau)=\sum_{r=0}^{+\infty}\frac{\tau^r x^{m+r}y^{n+r}}{r!(m+r)!(n+r)!}, \tag{18}$$

defined through the following generating function:

$$\exp(xu+yv+\tau uv)=\sum_{m=0}^{+\infty}\sum_{n=0}^{+\infty}u^m v^n b_{m,n}(x,y\,|\,\tau). \tag{19}$$

It is evident the similar structure between these functions and the incomplete 2-dimensional Hermite polynomials presented previously (see eqs. (4,5)). For this reason, the Humbert functions are usual exploited in connection with the Hermite polynomials of the type $h_{m,n}(x,y\,|\,\tau)$.

We can immediately note, for instance, that the Humbert functions could be expressed in terms of the incomplete Hermite polynomials. By rewriting, in fact, the expression in equation (19), we have:

$$\exp\left[xu+yv+\tau uv-\tau\left(uv-\frac{1}{uv}\right)\right]=\sum_{m=0}^{+\infty}\sum_{n=0}^{+\infty}u^m v^n b_{m,n}(x,y\,|\,\tau), \tag{20}$$

and, from the generating function of the ordinary Bessel function (eq. (8)), we find:

$$b_{m,n}(x,y\,|\,\tau)=\sum_{r=0}^{[m,n]}\frac{(-1)^r h_{m-r,n-r}(x,y\,|\,\tau)J_r(2\tau)}{r!(m-r)!(n-r)!}. \tag{21}$$

In the following, we will indicate with:

$g_{m,n}(x)$ and $b_{m,n}(x)$,

the Humbert polynomials and the Humbert functions respectively. In the next sections we will study the properties of these particular polynomials and functions and we will see some their non trivial generalizations along with the analysis of the related applications to facilitate some operational computation.

II. Relevant Properties for Humbert Polynomials and Functions

In the previous section we have introduced the incomplete 2-dimensional Hermite polynomials through the relations (4,5). By using the equivalences stated in equations (6,7), we can now state the expression of the generating function for the Humbert polynomials $g_{m,n}(x)$. We have:

$$\exp(u+v+xuv)=\sum_{m=0}^{+\infty}\sum_{n=0}^{+\infty}\frac{u^m}{m!}\frac{v^n}{n!}g_{m,n}(x) \tag{22}$$

where, again, $u\neq v$ and $(|u|,|v|)<+\infty$, $\tau\in\mathbb{R}$.

By following the same procedure used to derive the recurrence relations related to the two-index, one-variable Bessel function in the previous section, we can find similar expressions for this class of Humbert polynomials. In fact, by deriving, respectively, with respect to *x*, *u* and *v*, we obtain:

$$\begin{aligned}&\frac{d}{dx}g_{m,n}(x)=mng_{m-1,n-1}(x),\\&g_{m+1,n}(x)=g_{m,n}(x)+mxg_{m-1,n}(x),\\&g_{m,n+1}(x)=g_{m,n}(x)+nxg_{m,n-1}(x).\end{aligned} \tag{23}$$

By using the above relations, it is possible to state the differential equation satisfied by the polynomials $g_{m,n}(x)$. After an easy manipulation of the equations in the (23), we get:

$$mg_{m-1,n}(x)=\left(m-x\frac{d}{dx}\right)g_{m,n}(x), \tag{24}$$

$$ng_{m,n-1}(x)=\left(n-x\frac{d}{dx}\right)g_{m,n}(x) \tag{25}$$

and also:

$$mng_{m-1,n-1}(x)=\left(m-x\frac{d}{dx}\right)\left(n-x\frac{d}{dx}\right)g_{m,n}(x). \tag{26}$$

After equating equation (24) with the first of the relations obtained in (23), we can state the following differential equation solved by the Humbert polynomials:

$$x^2y''-\left[(m+n-1)x+1\right]y'+mny=0. \tag{27}$$

We note that, from the equation (25), it also follows:

$$\begin{aligned}&g_{m,+1n}(x)=g_{m,n}(x)+nxg_{m,n}(x)-x^2\frac{d}{dx}g_{m,n}(x),\\&g_{m,n+1}(x)=g_{m,n}(x)+mxg_{m,n}(x)-x^2\frac{d}{dx}g_{m,n}(x)\end{aligned} \tag{28}$$

Which suggest the introduction of the following operators:

$$\begin{aligned}&\hat{S}_m^{+}=1+\hat{n}x-x^2\frac{d}{dx},\\&\hat{S}_n^{+}=1+\hat{m}x-x^2\frac{d}{dx},\end{aligned} \tag{29}$$

where we have denoted with the symbols:

$\hat{m}$ and $\hat{n}$

a kind of number operators, in the sense that their action read as following:

$\hat{m}\hat{n}g_{s,r}(x)=srg_{s,r}(x)$.

It is now evident, by using the relations stated in the equations (23-28) and by the definition of the operators expressed in equation (29), that the following expressions hold:

$$\begin{aligned}&\hat{S}_m^{+}g_{m,n}(x)=g_{m+1,n}(x),\\&\hat{S}_n^{+}g_{m,n}(x)=g_{m,n+1}(x).\end{aligned} \tag{30}$$

The above relations, combined with the first in the equation (23), allow us to state the following relevant differential equation:

$$\begin{aligned}&\frac{d}{dx}\left[1+(n+1)x-x^2\frac{d}{dx}\right]\left[1+mx-x^2\frac{d}{dx}\right]g_{m,n}(x)=\\&=(m+1)(n+1)g_{m,n}(x).\end{aligned} \tag{31}$$

It is possible to derive similar relations regarding the Humbert functions. Before to proceed, we remind that, the function defined by the following generating function:

$$\exp\left(t-\frac{x}{t}\right)=\sum_{n=-\infty}^{+\infty}t^nC_n(x) \tag{32}$$

is known as the Tricomi function [10], which its explicit form is:

$$C_n(x)=\sum_{r=0}^{+\infty}\frac{(-1)^rx^r}{r!(n+r)!}. \tag{33}$$

It is possible to introduce a generalization of the above function in the sense of the Humbert functions. In fact, from the equation (18) it is immediately recognized that we can call generalized Tricomi function, the function expressed by the following relation:

$$C_{m,n}(x) = b_{m,n}(1,1 \mid x). \tag{34}$$

By using the same procedure outlined above, we can derive, for the Humbert functions the analogous recurrence relations stated for the polynomials $g_{m,n}(x)$. In fact, by considering the relation (34), we have:

$$\begin{aligned} &\frac{d}{dx}C_{m,n}(x) = C_{m+1,n+1}(x), \\ &mC_{m,n}(x) = C_{m-1,n}(x) - xC_{m+1,n+1}(x), \\ &nC_{m,n}(x) = C_{m,n-1}(x) - xC_{m+1,n+1}(x). \end{aligned} \tag{35}$$

We can combine the above relations, to get:

$$\begin{aligned} &C_{m-1,n}(x) = \left(m + x\frac{d}{dx}\right)C_{m,n}(x), \\ &C_{m,n-1}(x) = \left(n + x\frac{d}{dx}\right)C_{m,n}(x). \end{aligned} \tag{36}$$

These last relations suggest to introduce similar operators acting on these generalized Tricomi function as well as we have done for the Humbert polynomials. We have indeed:

$$\begin{aligned} &\hat{E}_m^- = \hat{m} + x\frac{d}{dx}, \\ &\hat{E}_n^- = \hat{n} + x\frac{d}{dx}, \\ &\hat{E}_{m,n}^{+,+} = \frac{d}{dx}. \end{aligned} \tag{37}$$

We have used, again, the same notation as expressed for the operators in equation (29). By following the same procedure used for the Humbert polynomials, we can easily to state the following differential equation:

$$x^2 y''' - (m+n+3)xy'' + (mn+m+n+1)y' = y. \tag{38}$$

III. Further Generalizations for Humbert Polynomials and Functions and Incomplete Laguerre Polynomials

In the paper [10], we have showed some relations linked the cylindrical Bessel function and the Tricomi function; in particular, we have seen that:

$$x^{-\frac{n}{2}} J_0(2\sqrt{x}) = C_n(x) = \sum_{r=0}^{+\infty} \frac{(-1)^r x^r}{r!(n+r)!}. \tag{39}$$

The relations stated in the previous sections and the structure of the 0^{th} order Tricomi function, allow us to introduce a generalization of the Laguerre polynomials.
We will say incomplete 2-dimensional Laguerre polynomials, the polynomials defined by the following generating function:

$$\exp(u+v)C_0(xuv) = \sum_{m=0}^{+\infty}\sum_{n=0}^{+\infty} \frac{u^m}{m!}\frac{v^n}{n!} l_{m,n}(x), \tag{40}$$

where their explicit form reads:

$$l_{m,n}(x) = m!n! \sum_{r=0}^{[m,n]} \frac{(-1)^r x^r}{(r!)^2 (m-r)!(n-r)!}. \tag{41}$$

It is evident the similar structure with the Humbert polynomials discussed in the previous sections.
We remind that the ordinary Laguerre polynomials [10] have the following operational expression:

$$L_n(x) = \left(1 - \hat{D}^{-1}\right)^n, \tag{42}$$

where $\hat{D}_x^{-1}$ denotes the inverse of the derivative operator [11-14], being essentially an integral operator, it will be specified by the operational rule:

$$\hat{D}_x^{-1}(1) = \frac{x^n}{n!}. \tag{43}$$

From the above considerations, we can firstly write the following expression for the 0^{th} Tricomi function:

$$C_0(x) = \sum_{r=0}^{+\infty} \frac{(-1)^r \hat{D}_x^{-r}}{r!} = \exp\left(-\hat{D}_x^{-1}\right), \tag{44}$$

and then we can state the important equivalence between the Humbert polynomials and the incomplete 2-dimensional Laguerre polynomials, that is:

$$l_{m,n}(x) = g_{m,n}\left(-\hat{D}_x^{-1}\right). \tag{45}$$

By recalling the explicit forms of the generalized two-variable Laguerre polynomials:

$$L_n(x,y)=\left(y-\hat{D}_x^{-1}\right)^n=n!\sum_{r=0}^{n}\frac{(-1)^r y^{n-r}x^r}{(r!)^2(n-r)!} \tag{46}$$

and from the particular expression of their generating function, in terms of the Tricomi function:

$$\sum_{n=0}^{+\infty}\frac{t^n}{n!}L_n(x,y)=\exp(yt)C_0(xt)\,, \tag{47}$$

we can finally establish a link between the incomplete 2-dimensional laguerre polynomials and the generalized Laguerre of the form $L_n(x,y)$. We have:

$$l_{m,n}(x)=m!n!\sum_{r=0}^{[m,n]}\frac{g_{m-r,n-r}(-y)L_r(x,y)}{r!(m-r)!(n-r)!}\,. \tag{48}$$

The considerations and the following results obtained to define the incomplete 2-dimensional polynomials, can be used to introduce a similar generalization for the Humbert functions. By considering indeed the following generating function:

$$\exp(u+v)C_0\left(\frac{x}{uv}\right)=\sum_{m=0}^{+\infty}\sum_{n=0}^{+\infty}u^m v^n A_{m,n}(x)\,, \tag{49}$$

we easily obtain the explicit form of the function $A_{m,n}(x)$:

$$A_{m,n}(x)=\sum_{r=0}^{+\infty}\frac{(-1)^r x^r}{(r!)^2(m+r)!(n+r)!}\,. \tag{50}$$

It is easy to note the analogy between the above expression and the generalized Tricomi function presented in the previous section. We find in fact:

$$A_{m,n}(x)=C_{m,n}\left(-\hat{D}_x^{-1}\right). \tag{51}$$

In the same way, it is possible obtain an expression of the functions $A_{m,n}(x)$ involving the generalized two-variable Laguerre polynomials. From the relation stated in equation (48) and form the (50), we have:

$$A_{m,n}(x)=\sum_{r=0}^{+\infty}\frac{g_{m+r,n+r}(-y)L_r(x,y)}{r!(m+r)!(n+r)!}\,. \tag{52}$$

IV. Concluding Remarks

Before closing the paper, we want just to mention how the concepts and the formalism discussed in the previous sections allows also the generalizations of other simple distribution functions like the Poisson distribution.

By using the Tricomi function of order *m:*

$$C_m(-x)=\sum_{r=0}^{+\infty}\frac{x^r}{r!(m+r)!}\,, \tag{53}$$

we can indeed define the following two-index distribution:

$$P_n(x;m)=\frac{x^n}{n!(m+n)!C_m(-x)}\,, \tag{54}$$

where the generating function is given by the relation:

$$\frac{C_m(-xt)}{C_m(-x)}=\sum_{n=0}^{+\infty}\frac{t^n}{n!}P_n(x;m)\,. \tag{55}$$

The evaluation of the associated momenta can be easily simplified with the use of the well known property, satisfied by the Tricomi functions:

$$(-1)^r\left(\frac{d}{dx}\right)^r C_n(x)=C_{n+r}(x)\,. \tag{58}$$

Accordingly, we calculate the following average values:

$$\begin{aligned}\langle n\rangle&=\frac{C_{m+1}(-x)}{C_m(-x)},\\ \langle n^2\rangle&=\frac{C_{m+2}(-x)}{C_m(-x)}+\langle n\rangle.\end{aligned} \tag{59}$$

The higher order moments are also given by similar closed relations.

It is remarkable about this probability distribution that, unlike the Poisson distribution, the variance:

$$\sigma=\sqrt{\bar{n^2}-\bar{n}^2}\,,\ \text{where}\ \bar{a}=\langle a\rangle \tag{60}$$

is smaller than $\sqrt{\bar{n}}$.

This type of distribution can be exploited in quatum mechanics within the context of bunching phenomena. This example show that the use of multi-index polynomials and Bessel-type functions with their associated formalism offers wide possibilities in the applications of pure and applied mathematics.

References

[1] Appell, P., Kampé de Fériet, J., "Fonctions hypergéométriques et hypersphériques. Polinomes d'Hermite", *Gauthier-Villars*, Paris, 1926.

[2] Dattoli, G., "Incomplete 2-D Hermite polynomials: Propeties and applications", *Journal of Mathematical Analysis and Applications*, 284 (2), pp 447-454, 2003.

[3] Dodonov, V.V., Man'ko, V.I.,"New relations for two-dimensional Hermite polynomials", *Journal of mathematical Physics*, 35 (8), pp. 4277-4294, 1994.

[4] Gould, H.W., Hopper, A.T., "Operational formulas connected with two generalizations of Hermite polynomials", *Duke Math. J.*, 29, pp. 51-62, 1962.
[5] Srivastava, H.M., Manocha, H.L., "A treatise on generating functions", Wiley, New York, 1984.
[6] Watson, J.H., "A treatise on Bessel functions", *Cambridge University press*, 1958.
[7] Dattoli, G., Torre, A. "Theory and applications of generalized Bessel functions", *Aracne, Rome*, 1996.
[8] Cesarano, C., Assante, D., "A note on generalized Bessel functions", *Int. J. of Math. Models and Methods in Appl. Sci.*, 7 (6), pp 625-629, 2013.
[9] Aktas, R., Sahin, R., Altin, A., "On a multivariable extension of the Humbert polynomials", *Applied Mathematics and Computation*, 218 (3), pp. 662-666, 2011.
[10] Cesarano, C., "Monomiality Principle and related operational techniques for Orthogonal Polynomials and Special Functions", *Int. J. of Math. Models and Methods in Appl. Sci.*, to appear, 2013.
[11] Dattoli, G., Lorenzutta, S., Ricci, P.E., Cesarano, C., "On a family of hybrid polynomials", *Integral Transforms and Special Functions*, 15 (6), pp. 485-490, (2004).
[12] Dattoli, G., Lorenzutta, Cesarano, C., "Bernestein polynomials and operational methods", *Journal of Computational Analysis and Applications*, 8 (4), pp. 369-377, 2006.
[13] Dattoli, G., Srivastava, H.M., Cesarano, C., "The Laguerre and Legendre polynomials from an operational point of view", *Applied Mathematics and Computation*, 124 (1), pp. 117-127 (2001).
[14] Dattoli, G., Cesarano, C., "On a new family of Hermite polynomials associated to parabolic cylinder functions", *applied Mathematics and Computation*, 141 (1), pp. 143-149, 2003.

Clemente Cesarano is assistant professor of Mathematical Analysis at Faculty of Engineering- International Telematic University UNINETTUNO-Rome, ITALY. He is coordinator of didactic planning of the Faculty and he also is coordinator of research activities of the University. Clemente Cesarano is Honorary Research Associates of the Australian Institute of High Energetic Materials His research activity focuses on the area of Special Functions, Numerical Analysis and Differential Equations.
He has work in many international institutions as ENEA (Italy), Ulm University (Germany), Complutense University (Spain) and University of Rome La Sapienza (Italy). He has been visiting researcher at Research Institute for Symbolic Computation (RISC), Johannes Kepler University of Linz (Austrian). He is Editorial Board member of the Research Bulletin of the Australian Institute of High Energetic Materials, the Global Journal of Pure and Applied Mathematics (GJPAM), the Global Journal of Applied Mathematics and Mathematical Sciences (GJ-AMMS), the Pacific-Asian Journal of Mathematics, the International Journal of Mathematical Sciences (IJMS), the Advances in Theoretical and Applied Mathematics (ATAM), the International Journal of Mathematics and Computing Applications (IJMCA).
Clemente Cesarano has published two books and over than fifty papers on international journals in the field of Special Functions, Orthogonal Polynomials and Differential Equations.

Some results via de la Vallée-Poussin mean in probabilistic 2-normed spaces

U. Yamancı, M. Gürdal, and S. Aytar

***Abstract*—**In this article we introduce some new type of summability methods for double sequences involving the ideas of de la Vallée-Poussin mean in probabilistic 2-normed space and examine some important results.

***Keywords*—** t-norm, probabilistic 2-normed space, double sequence, statistical completeness, de la Vallé e-Poussin mean.

I. Introduction

PROBABILISTIC normed space is significant as a generalization of deterministic results of linear normed spaces. In a PN space, the norms of the vectors are represented by probability distribution functions instead of nonnegative real numbers. If x is an element of a PN space, then its norm is denoted by F_x, and the value $F_x(t)$ is interpreted as the probability that the norm of x is smaller than t. In [24], probabilistic normed spaces were first introduced by Śerstnev and then by it was extended to random/probabilistic 2-normed spaces by Golet [5] using the notion of 2-norm which is defined by Gähler [3,4] and since then, many researchers have studied these subjects and obtained various results [6-8,23,27,28]. Afterwards, Alsina et al. [1] presented a new definition of a PN space which includes the definition of Śerstnev [25] as a special case. This new definition rapidly became the standard one and it has been adopted by many authors (for instance, [9-16,19,20]).

The concepts of statistical convergence for sequences of real numbers was introduced (independently) by Steinhaus [26] and Fast [2]. The concept of statistical convergence was further discussed and developed by many authors in more general abstract spaces [6,9-11,13,20].

Some new type of summability methods for double sequences involving the ideas of de la Vallée-Poussin mean has not been studied previously in the setting of probabilistic 2-normed (PTN) spaces. Motivated by this fact, in this paper, the notion of (λ,μ)-summable, statistically (λ,μ)-summable, statistically (λ,μ)-Cauchy and statistically (λ,μ)-complete for double sequence with respect to PTN-space and establish some interesting results.

U. Yamancı is with the Suleyman Demirel University, Department of Mathematics, 32260, Isparta, TURKEY (corresponding author to provide phone: +90-246-2114310; fax: +90-246-2371106; e-mail: ulasyamanci@sdu.edu.tr).

M. Gürdal, is with the Suleyman Demirel University, Department of Mathematics, 32260, Isparta, TURKEY (corresponding author to provide phone: +90-246-2114101; fax: +90-246-2371106; e-mail: gurdalmehmet@sdu.edu.tr).

S. Aytar is with the Suleyman Demirel University, Department of Mathematics, 32260, Isparta, TURKEY (corresponding author to provide phone: +90-246-2114120; fax: +90-246-2371106; e-mail: salihaytar@sdu.edu.tr).

II. Definitions and Notations

First we recall some of the basic concepts, which will be used in this paper.

The notion of convergence for double sequence was introduced by Pringsheim [18]: We say that a double sequence $x=(x_{j,k})_{j,k\in\mathbb{N}}$ of reals is convergent to L in Pringsheim's sense (shortly, (P) convergent) provided that $\varepsilon>0$ there exists a positive integer N such that $|x_{j,k}-L|<\varepsilon$ whenever $j,k\geq N$.

Statistical convergence for double sequences $x=(x_{jk})$ of real numbers was introduced and studied by Mursaleen and Edely [17] as follows: Let $K\subseteq\mathbb{N}\times\mathbb{N}$ and $K(h,l)=\{j\leq h,k\leq l:(j,k)\in A\}$, where $h,l\in\mathbb{N}$. Then we define upper and lower asymptotic density of a two-dimensional set K, respectively

$$\overline{\delta}_2(K):=(P)\limsup_{h,l\to\infty}\frac{|K(h,l)|}{hl};\ \underline{\delta}_2(K):=(P)\liminf_{h,l\to\infty}\frac{|K(h,l)|}{hl}.$$

If $\overline{\delta}_2(K)=\underline{\delta}_2(K)$, then the common value $\delta_2(K)$ is called the double asymptotic density of the set K and

$$\delta_2(K)=(P)\lim_{h,l\to\infty}\frac{|K(h,l)|}{hl}.$$

The double sequence $x=(x_{j,k})$ statistically converges to a point L if for each $\varepsilon>0$ we have $\delta_2(K(\varepsilon))=0$, where $K(\varepsilon)=\{(j,k),j\leq h,k\leq l:|x_{j,k}-L|\geq\varepsilon\}$ and in such situation we will write $L=st\text{-}\lim x$ (or $x_{j,k}\to L(st)$)

Let $\lambda=(\lambda_m)$ and $\mu=(\mu_n)$ are two non-decreasing sequences of positive numbers tending to ∞ such that

$$\lambda_{m+1}\leq\lambda_m+1,\ \lambda_1=0 \text{ and } \mu_{n+1}\leq\mu_n+1,\ \mu_1=0.$$

ISBN: 978-1-61804-225-5

Recall that (λ,μ)-density of the set $K\subseteq \mathbb{N}\times\mathbb{N}$ is given by

$$\delta_{\lambda,\mu}(K)=(P)\lim_{m,n}\frac{1}{\lambda_m\mu_n}\left|\{m-\lambda_m+1\le j\le m,\ n-\mu_n+1\le k\le n\ :\ (j,k)\in K\}\right|$$

provided that the limit exists. If $\lambda_m=m$ for all m, and $\mu_n=n$ for all n, the (λ,μ)-density is reduced to the double natural density.

The generalized double de la Valée-Pousin mean is defined by

$$t_{m,n}(x)=\frac{1}{\lambda_m\mu_n}\sum_{(j,k)\in J_m\times I_n}x_{jk},$$

where $J_m=[m-\lambda_m+1,m]$ and $I_n=[n-\mu_n+1,n]$.

We say that $x=(x_{jk})$ is (λ,μ)-statistically convergent to the number L if for every $\varepsilon>0$,

$$(P)\lim_{m,n}\frac{1}{\lambda_m\mu_n}\left|\{j\in J_m,k\in I_n\ :\ |x_{jk}-L|\ge\varepsilon\}\right|=0.$$

and in such situation we will write $st_{\lambda,\mu}\text{-}\lim x=L$.

Definition 1. *([3,4]) Let X be a real vector space of dimension d, where $2\le d<\infty$. A 2-norm on X is a function $\|\cdot,\cdot\|:X\times X\to\mathbb{R}$ which satisfies* (**i**) $\|x,y\|=0$ *if and only if x and y are linearly dependent;* (**ii**) $\|x,y\|=\|y,x\|$; (**iii**) $\|\alpha x,y\|=|\alpha|\|x,y\|$, $\alpha\in\mathbb{R}$; (**iv**) $\|x,y+z\|\le\|x,y\|+\|x,z\|$. *The pair $(X,\|\cdot,\cdot\|)$ is then called a 2-normed space.*

As an example of a 2-normed space we may take $X=\mathbb{R}^2$ being equipped with the 2-norm $\|x,y\|:=$ the area of the parallelogram spanned by the vectors x and y, which may be given explicitly by the formula

$$\|x,y\|=|x_1y_2-x_2y_1|,\quad x=(x_1,x_2),\quad y=(y_1,y_2).$$

Observe that in any 2-normed space $(X,\|\cdot,\cdot\|)$ we have $\|x,y\|\ge0$ and $\|x,y+\alpha x\|=\|x,y\|$ for all $x,y\in X$ and $\alpha\in\mathbb{R}$. Also, if x,y and z are linearly dependent, then $\|x,y+z\|=\|x,y\|+\|x,z\|$ or $\|x,y-z\|=\|x,y\|+\|x,z\|$. Given a 2-normed space $(X,\|\cdot,\cdot\|)$, one can derive a topology for it via the following definition of the limit of a sequence: a sequence (x_n) in X is said to be convergent to x in X if $\lim_{n\to\infty}\|x_n-x,y\|=0$ for every $y\in X$.

All the concepts listed below are studied in depth in the fundamental book by Schweizer and Sklar [22].

Definition 2. *Let $\mathbb{R}$ denotes the set of real numbers, $\mathbb{R}_+=\{x\in\mathbb{R}\ :\ x\ge0\}$ and $S=[0,1]$ the closed unit interval. A mapping $f:\mathbb{R}\to S$ is called a distribution function if it is nondecreasing and left continuous with $\inf_{t\in\mathbb{R}}f(t)=0$ and $\sup_{t\in\mathbb{R}}f(t)=1$.*

We denote the set of all distribution functions by D^+ such that $f(0)=0$. If $a\in\mathbb{R}_+$, then $H_a\in D^+$, where

$$H_a(t)=\begin{cases}1, & \text{if } t>a,\\ 0, & \text{if } t\le a.\end{cases}$$

It is obvious that $H_0\ge f$ for all $f\in D^+$.

Definition 3. *A triangular norm (t-norm) is a continuous mapping $*:S\times S\to S$ such that $(S,*)$ is an abelian monoid with unit one and $c*d\le a*b$ if $c\le a$ and $d\le b$ for all $a,b,c,d\in S$. A triangle function τ is a binary operation on D^+ which is commutive, associative and $\tau(f,H_0)=f$ for every $f\in D^+$.*

Definition 4. *Let X be a linear space of dimension greater than one, τ is a triangle, and $\mathbf{F}:X\times X\to D^+$. Then $\mathbf{F}$ is called a probabilistic 2-norm and $(X,\mathbf{F},\tau)$ a probabilistic 2-normed space if the following conditions are satisfied:*

(2.2.1) $\mathbf{F}(x,y;t)=H_0(t)$ *if x and y are linearly dependent, where $\mathbf{F}(x,y;t)$ denotes the value of $\mathbf{F}(x,y)$ at $t\in\mathbb{R}$,*

(2.2.2) $\mathbf{F}(x,y;t)\ne H_0(t)$ *if x and y are linearly independent,*

(2.2.3) $\mathbf{F}(x,y;t)=\mathbf{F}(y,x;t)$ *for all $x,y\in X$,*

(2.2.4) $\mathbf{F}(\alpha x,y;t)=\mathbf{F}(x,y;\frac{t}{|\alpha|})$ *for every $t>0,\alpha\ne0$ and $x,y\in X$,*

(2.2.5) $\mathbf{F}(x+y,z;t)\ge\tau(\mathbf{F}(x,z;t),\mathbf{F}(y,z;t))$ *whenever $x,y,z\in X$.*

III. Main results

In this section, our aim is to define some concepts of (λ,μ)-summable, statistically (λ,μ)-summable, statistically (λ,μ)-Cauchy and statistically (λ,μ)-complete for double with respect to PTN-space and obtain some interesting results.

Definition 5. *Let $(X,\mathbf{F},\tau)$ be a PTN space. The double sequence $x=(x_{jk})$ in X is said to be (λ,μ)-summable (or briefly, $\mathbf{F}(\lambda,\mu)$-summable) to L if for each $\varepsilon>0$, $q\in(0,1)$ and each nonzero $z\in X$ there exists $N\in\mathbb{N}$ such that $\mathbf{F}(t_{m,n}(x)-L,z;\varepsilon)>1-q$ for all $m,n>N$. In this case, we write $\mathbf{F}(\lambda,\mu)\text{-}\lim x,z=L$.*

ISBN: 978-1-61804-225-5

Definition 6. *Let* $(X,\mathbf{F},\tau)$ *be a PTN space. The double sequence* $x=(x_{jk})$ *in* X *is said to be statistically* (λ,μ)*-summable (or briefly,* $\mathbf{F}(st_{\lambda,\mu})$*-summable) to* L *if* $\delta_2(K_{\lambda,\mu})=0$*, where*

$$K_{\lambda,\mu}=\{(m,n)\in \mathbb{N}\times\mathbb{N} : \mathbf{F}(t_{m,n}(x)-L,z;\varepsilon)\le 1-q\},$$

i.e. if for each $\varepsilon>0,\ q\in(0,1)$ *and each nonzero* $z\in X$

$$(P)\lim_{h,l}\frac{1}{hl}\left|\{m\le h,n\le l : \mathbf{F}(t_{m,n}(x)-L,z;\varepsilon)\le 1-\lambda\}\right|=0$$

or, equivalently

$$(P)\lim_{h,l}\frac{1}{hl}\left|\{m\le h,n\le l : \mathbf{F}(t_{m,n}(x)-L,z;\varepsilon)>1-\lambda\}\right|=1.$$

In this case, we write $\mathbf{F}(st_{\lambda,\mu})\text{-}\lim x,z=L,$ *and* L *is called* $\mathbf{F}(st_{\lambda,\mu})$*-limit of* x*.*

Definition 7. *Let* $(X,\mathbf{F},\tau)$ *be a PTN space. The double sequence* $x=(x_{jk})$ *in* X *is said to be statistically* (λ,μ)*-Cauchy (or briefly,* $\mathbf{F}(st_{\lambda,\mu})$*-Cauchy) if for each* $\varepsilon>0,$ $q\in(0,1)$ *and each nonzero* $z\in X$ *there exists* $M,N\in\mathbb{N}$ *such that for all* $m,p\ge M,$ $n,q\ge N,$ *the set* $S_\varepsilon(\lambda,\mu)=\{(m,n)\in\mathbb{N}\times\mathbb{N} : \mathbf{F}(t_{m,n}(x)-t_{p,q}(x),z;\varepsilon)\le 1-q\}$ *has double natural density zero, i.e.*

$$(P)\lim_{h,l}\frac{1}{hl}\left|\{m\le h,n\le l : \mathbf{F}(t_{m,n}(x)-t_{p,q}(x),z;\varepsilon)\le 1-q\}\right|=0.$$

Theorem 1. *Let* $(X,\mathbf{F},\tau)$ *be a PTN space. If a double sequence* $x=(x_{jk})$ *in* X *is statistically* (λ,μ)*-summable, that is,* $\mathbf{F}(st_{\lambda,\mu})\text{-}\lim x,z=L$ *exists, then* $\mathbf{F}(st_{\lambda,\mu})\text{-}\lim x,z$ *is unique.*

Proof. Suppose that $\mathbf{F}(st_{\lambda,\mu})\text{-}\lim x,z=L_1$ and $\mathbf{F}(st_{\lambda,\mu})\text{-}\lim x,z=L_2,$ where $L_1\ne L_2.$ For given $\varepsilon>0$ and each nonzero $z\in X,$ select $q>0$ such that $\tau((1-q),(1-q))>1-\varepsilon.$ Then, for any $t>0$, we define

$$A_q(\lambda,\mu)=\{(m,n)\in\mathbb{N}\times\mathbb{N} : \mathbf{F}(t_{m,n}(x)-L_1,z;t)\le 1-q\}$$

and

$$B_q(\lambda,\mu)=\{(m,n)\in\mathbb{N}\times\mathbb{N} : \mathbf{F}(t_{m,n}(x)-L_2,z;t)\le 1-q\}.$$

Since, $\mathbf{F}(st_{\lambda,\mu})\text{-}\lim x,z=L_1$ implies $\delta_2(A_\lambda(\lambda,\mu))=0$ and similarly, we have $\delta_2(B_\lambda(\lambda,\mu))=0.$ Now, let $C_q(\lambda,\mu)=A_q(\lambda,\mu)\cap B_q(\lambda,\mu).$ It follows that $\delta_2(C_q(\lambda,\mu))=0$ and hence the complement $C_q^c(\lambda,\mu)$ is nonempty set and $\delta_2(C_q^c(\lambda,\mu))=1.$ Now, if $(m,n)\in\mathbb{N}\times\mathbb{N}\setminus C_q(\lambda,\mu),$ then

$$\mathbf{F}(L_1-L_2,z;t)\ge\tau\left(\mathbf{F}\left(t_{m,n}(x)-L_1,z;\frac{t}{2}\right),\mathbf{F}\left(t_{m,n}(x)-L_2,z;\frac{t}{2}\right)\right)$$
$$>\tau((1-q),(1-q))>1-\varepsilon.$$

Since $\varepsilon>0$ is arbitrary, we get $\mathbf{F}(L_1-L_2,z;t)=1$ for all $t>0$ and each nonzero $z\in X.$ Hence $L_1=L_2,$ which proves theorem.

Theorem 2. *Let* $(X,\mathbf{F},\tau)$ *be a PTN space. If a double sequence* $x=(x_{jk})$ *in* X *is* $\mathbf{F}(\lambda,\mu)$*-summable to* L*, then it is* $\mathbf{F}(st_{\lambda,\mu})$*-summable to the same limit.*

Proof. Let us consider that $\mathbf{F}(\lambda,\mu)\text{-}\lim x,z=L.$ For every $\varepsilon>0,t>0$ and nonzero $z\in X,$ there exists positive integer N such that

$$\mathbf{F}(t_{m,n}(x)-L,z;t)>1-\varepsilon$$

holds for all $m,n\ge N.$ Since

$$M_\varepsilon(\lambda,\mu)=\{(m,n)\in\mathbb{N}\times\mathbb{N} : \mathbf{F}(t_{m,n}(x)-L,z;t)\le 1-\varepsilon\}$$

is contained in $\mathbb{N}\times\mathbb{N}$. Therefore $\delta_2(M_\varepsilon(\lambda,\mu))=0,$ that is, $x=(x_{jk})$ is $\mathbf{F}(st_{\lambda,\mu})$-summable to $L.$

The following example shows that the converse of Theorem 2 need not be true.

Example 1. *Consider* $X=\mathbb{R}^2$ *with* $\|x,y\|:=|x_1y_2-x_2y_1|$ *where* $x=(x_1,x_2),$ $y=(y_1,y_2)\in\mathbb{R}^2$ *and let* $\tau(a,b)=ab$ *for all* $a,b\in S.$ *For all* $(x,y)\in\mathbb{R}^2$ *and* $t>0,$ *consider*

$$\mathbf{F}_{x,y}(t)=\frac{t}{t+\|x,y\|}.$$

Then $(\mathbb{R}^2,\mathbf{F},\tau)$ *is a PTN space. The double sequence* $x=(x_{jk})$ *is defined by*

$$t_{m,n}(x)=\begin{cases}mn, & \text{if } m,n=w^2,\ w\in\mathbb{N}\\ 0, & \text{otherwise.}\end{cases}$$

For $\varepsilon>0,t>0$ *and nonzero* $z\in X,$ *write*

$$M_\varepsilon(\lambda,\mu)=\{(m,n)\in\mathbb{N}\times\mathbb{N} : \mathbf{F}(t_{m,n}(x),z;t)\le 1-\varepsilon\}.$$

It is easy to see that

$$\mathbf{F}(t_{m,n}(x),z;t)=\frac{t}{t+\|t_{m,n}(x),y\|}=\begin{cases}\frac{t}{t+mnz}, & \text{for } m,n=w^2,\ w\in\mathbb{N}\\ 1, & \text{otherwise;}\end{cases}$$

and hence

$$\lim\mathbf{F}(t_{m,n}(x),z;t)=\begin{cases}0, & \text{if } m,n=w^2,\ w\in\mathbb{N}\\ 1, & \text{otherwise.}\end{cases}.$$

ISBN: 978-1-61804-225-5

We see that the sequence $x=(x_{jk})$ *is not* $\mathbf{F}(\lambda,\mu)$*-summable in* $(\mathbb{R}^2,\mathbf{F},\tau)$*. But the set* $M_\varepsilon(\lambda,\mu)$ *has double natural density zero since* $M_\varepsilon(\lambda,\mu)\subset\{(1,1),(4,4),(9,9),...\}$*. From here, we obtain that the converse of Theorem 2 need not be true.*

Theorem 3. *Let* $(X,\mathbf{F},\tau)$ *be a PTN space. If a double sequence* $x=(x_{jk})$ *in* X *is statistically* $\mathbf{F}(st_{\lambda,\mu})$*-summable to* L *if and only if there exists a subset*

$$M=\{(j_m,k_n):\ j_1<j_2<...;\ k_1<k_2<...\}\subseteq\mathbb{N}\times\mathbb{N}$$

such that $\delta_2(K)=1$ *and* $\mathbf{F}(\lambda,\mu)\text{-}\lim x_{j_m,k_n},z=L.$

Proof. Suppose that there exists a subset

$$M=\{(j_m,k_n):\ j_1<j_2<...;\ k_1<k_2<...\}\subseteq\mathbb{N}\times\mathbb{N}$$

such that $\delta_2(M)=1$ and $\mathbf{F}(\lambda,\mu)\text{-}\lim x_{j_m,k_n},z=L.$ Then there exists $N\in\mathbb{N}$ such that $\mathbf{F}(t_{m,n}(x)-L,z;t)>1-\varepsilon$ holds for all $m,n>N.$ Put

$$M_\varepsilon(\lambda,\mu)=\{(m,n)\in\mathbb{N}\times\mathbb{N}:\ \mathbf{F}(t_{j_m,k_n}(x)-L,z;t)\le 1-\varepsilon\}$$

and $M'=\{(j_{N+1},k_{N+1}),(j_{N+2},k_{N+2}),...\}.$ Then $\delta_2(M')=1$ and $M_\varepsilon(\lambda,\mu)\subseteq\mathbb{N}-K'$ which implies that $\delta_2(M_\varepsilon(\lambda,\mu))=0.$ Hence $x=(x_{jk})$ is statistically (λ,μ)-summable to L in PTN space.

Conversely, suppose that $x=(x_{jk})$ is $\mathbf{F}(st_{\lambda,\mu})$-summable to $L.$ For $q=1,2,...$ and $t>0,$ write

$$M_q(\lambda,\mu)=\left\{(m,n)\in\mathbb{N}\times\mathbb{N}:\ \mathbf{F}(t_{j_m,k_n}(x)-L,z;t)\le 1-\frac{1}{q}\right\},$$

and

$$K_q(\lambda,\mu)=\left\{(m,n)\in\mathbb{N}\times\mathbb{N}:\ \mathbf{F}(t_{j_m,k_n}(x)-L,z;t)>\frac{1}{q}\right\}.$$

Then $\delta_2(M_q(\lambda,\mu))=0$ and

$$K_1(\lambda,\mu)\supset K_2(\lambda,\mu)\supset ...K_i(\lambda,\mu)\supset K_{i+1}(\lambda,\mu)\supset ... \quad (1)$$

and

$$\delta_2(K_q(\lambda,\mu))=1,\ q=1,2,.... \quad (2)$$

Now, we have to show that $(m,n)\in K_q(\lambda,\mu),$ $x=(x_{j_m,k_n})$ is $\mathbf{F}(\lambda,\mu)$-summable to $L.$ Assume that $x=(x_{j_m,k_n})$ is not $\mathbf{F}(\lambda,\mu)$-summable to $L.$ Hence, there exists $\varepsilon>0$ such that $\mathbf{F}(t_{j_m,k_n}(x)-L,z;t)\le\varepsilon$ for infinitely many terms. Let

$$K_\varepsilon(\lambda,\mu)=\{(m,n)\in\mathbb{N}\times\mathbb{N}:\ \mathbf{F}(t_{j_m,k_n}(x)-L,z;t)>\varepsilon\},$$

and $\varepsilon>\frac{1}{q}$ with $q=1,2,3,....$ Then

$$\delta_2(K_\varepsilon(\lambda,\mu))=0,$$

and by (1), $K_q(\lambda,\mu)\subset K_\varepsilon(\lambda,\mu).$ Hence $\delta_2(K_q(\lambda,\mu))=0,$ which contradicts (2) and therefore $x=(x_{j_m,k_n})$ is $\mathbf{F}(\lambda,\mu)$-summable to $L.$

Theorem 4. *Let* $(X,\mathbf{F},\tau)$ *be a PTN space. If a double sequence* $x=(x_{jk})$ *in* X *is* (λ,μ)*-summable, then it is statistically* (λ,μ)*-Cauchy.*

Proof. Assume that $\mathbf{F}(st_{\lambda,\mu})\text{-}\lim x,z=L.$ Let $\varepsilon>0$ be a given number so that choose $q>0$ such that

$$\tau((1-q),(1-q))>1-\varepsilon.$$

Then, for $t>0$ and nonzero $z\in X$, we have

$$\delta_2(A_q(\lambda,\mu))=0, \quad (3)$$

where $A_q(\lambda,\mu)=\{(m,n)\in\mathbb{N}\times\mathbb{N}:\ \mathbf{F}(t_{m,n}(x)-L,z;\frac{t}{2})\le 1-q\}$ which implies that

$$\delta_2(A_q^c(\lambda,\mu))=\delta_2\left(\left\{(m,n)\in\mathbb{N}\times\mathbb{N}:\ \mathbf{F}\left(t_{m,n}(x)-L,z;\frac{t}{2}\right)>1-q\right\}\right)=1.$$

Let $(f,g)\in A_q^c(\lambda,\mu).$ Then $\mathbf{F}(t_{f,g}(x)-L,z;\frac{t}{2})>1-q.$ Now, let

$$B_\varepsilon(\lambda,\mu)=\left\{(m,n)\in\mathbb{N}\times\mathbb{N}:\ \mathbf{F}\left(t_{m,n}(x)-t_{f,g}(x),z;\frac{t}{2}\right)\le 1-\varepsilon\right\}.$$

We need to show that $B_\varepsilon(\lambda,\mu)\subset A_q(\lambda,\mu).$ Let $(m,n)\in B_\varepsilon(\lambda,\mu)\setminus A_q(\lambda,\mu).$ Then

$\mathbf{F}(t_{m,n}(x)-t_{f,g}(x),z;t)\le 1-\varepsilon$ and $\mathbf{F}(t_{m,n}(x)-L,z;\frac{t}{2})>1-q,$ in particular $\mathbf{F}(t_{f,g}(x)-L,z;\frac{t}{2})>1-q.$ Then

$$\begin{aligned}1-\varepsilon&\ge\mathbf{F}(t_{m,n}(x)-t_{f,g}(x),z;t)\\&\ge\tau\left(\mathbf{F}\left(t_{m,n}(x)-L,z;\frac{t}{2}\right),\mathbf{F}\left(t_{f,g}(x)-L,z;\frac{t}{2}\right)\right)\\&>\tau((1-q),(1-q))>1-\varepsilon,\end{aligned}$$

which is imposible. Therefore $B_\varepsilon(\lambda,\mu)\subset A_q(\lambda,\mu).$ Hence, by (3) $\delta_2(B_\varepsilon(\lambda,\mu))=0.$ Therefore, x is statistically (λ,μ)-Cauchy in PTN-space.

Definition 8. *Let* $(X,\mathbf{F},\tau)$ *be a PTN space. Then,*

(a) *PTN-space is said to be complete if every Cauchy double sequence is* P*-convergent in* $(X,\mathbf{F},\tau).$

(b) *PTN-space is said to be statistically* (λ,μ)*-complete (or briefly,* $\mathbf{F}(st_{\lambda,\mu})$*-complete) if every statistically* (λ,μ)*-Cauchy sequence in PTN space is statistically* (λ,μ)*-summable.*

ISBN: 978-1-61804-225-5

Theorem 5. *Every probabilistic 2-normed space* $(X,\mathbf{F},\tau)$ *is* $\mathbf{F}(st_{\lambda,\mu})$*-complete but not complete in general.*

Proof. Assume that $x=(x_{jk})$ is $\mathbf{F}(st_{\lambda,\mu})$-Cauchy but not $\mathbf{F}(st_{\lambda,\mu})$-summable. Then there exists $M,N\in\mathbb{N}$ such that for all $m,p\geq M$, $n,q\geq M$, the set

$$D_{\varepsilon}(\lambda,\mu)=\left\{(m,n)\in\mathbb{N}\times\mathbb{N}:\mathbf{F}(t_{m,n}(x)-t_{p,q}(x),z;t)\leq 1-\varepsilon\right\}=0$$

has double natural density zero, i.e. $\delta_2(E_{\varepsilon}(\lambda,\mu))=0$ and

$$\delta_2(E_{\varepsilon}(\lambda,\mu))=\delta_2\left(\left\{(m,n)\in\mathbb{N}\times\mathbb{N}:\mathbf{F}\left(t_{m,n}(x)-L,z;\frac{t}{2}\right)>1-\varepsilon\right\}\right)=0.$$

It follows that $\delta_2(E_{\varepsilon}^{c}(\lambda,\mu))=1$. Since

$$\mathbf{F}(t_{m,n}(x)-t_{p,q}(x),z;t)\geq 2\mathbf{F}\left(t_{m,n}(x)-L,z;\frac{t}{2}\right)>1-\varepsilon,$$

if $\mathbf{F}(t_{m,n}(x)-L,z;\frac{t}{2})>\frac{1-\varepsilon}{2}$. Hence $\delta_2(E_{\varepsilon}^{c}(\lambda,\mu))=0$, which give rise to a contradiction, since $x=(x_{jk})$ is $\mathbf{F}(st_{\lambda,\mu})$-Cauchy. Consequently, $x=(x_{jk})$ must be $\mathbf{F}(st_{\lambda,\mu})$-summable.

To see that a probabilistic 2-normed space is not complete in general, for this, we have the following example:

Example 2. $X=(0,1]\times(0,1]$ *and* $\mathbf{F}(x,z;t)=\frac{t}{t+\|x,z\|}$ *for* $t>0$ *and nonzero* $z\in X$. *Then* $(X,\mathbf{F},\tau)$ *is a probabilistic 2-normed space but not complete, since the double sequence* $\left(\frac{1}{mn}\right)$ *is Cauchy with respect to* $(X,\mathbf{F},\tau)$ *but not P-convergent with respect to the present PTN-space.*

IV. Conclusion

This study indeed presents a relationship between two various disciplines: the theory of probabilistic normed spaces and summability theory. Some new type of summability methods for double sequences involving the ideas of de la Vallée-Poussin mean has not been studied previously in the setting of probabilistic 2-normed (PTN) spaces. Motivated by this fact, in this paper, the notion of (λ,μ)-summable, statistically (λ,μ)-summable, statistically (λ,μ)-Cauchy and statistically (λ,μ)-complete for double sequence with respect to PTN-space and establish some interesting results. These results can be utilized to study the convergence problems of double sequences having chaotic pattern in probabilistic 2-normed spaces.

References

[1] C. Alsina, B. Schweizer, and A. Sklar, "On the definition of a probabilistic normed space", *Aequationes Math.*, vol. 46, pp. 91-98, 1993.

[2] H. Fast, "Sur la convergence statistique", *Colloq. Math.*, 2(1951), 241-244.

[3] S. Gähler, "2-metrische räume und ihre topologische struktur", *Math. Nachr.*, vol. 26, no 1-4, pp. 115-148, 1963.

[4] S. Gähler, "Lineare 2-normietre räume", *Math. Nachr.*, vol. 28, no. 1-2, pp. 1-43, 1964.

[5] I. Golet, "On probabilistic 2-normed spaces", *Novi Sad. J. Math.*, vol. 35, no. 1, pp. 95-102, 2005.

[6] M. Gürdal, and S. Pehlivan, "The statistical convergence in 2-Banach spaces", *Thai. J. Math.*, vol. 2, no. 1, pp. 107-113, 2004.

[7] M. Gürdal, and I. Açık, "On **I**-cauchy sequences in 2-normed spaces", *Math. Inequal. Appl.*, vol. 11, no. 2, pp. 349-354, 2008.

[8] M. Gürdal, A. Şahiner, and I. Açık, "Approximation theory in 2-Banach spaces", *Nonlinear Analysis*, vol. 71, no. 5-6, pp. 1654-1661, 2009.

[9] S. Karakus, "Statistical convergence on probabilistic normed spaces", *Math. Comm.*, vol. 12, no. 1, pp. 11-23, 2007.

[10] S.A. Mohiuddine, and E. Şavaş, "Lacunary statistically convergent double sequences in probabilistic normed spaces", *Ann. Univ. Ferrara*, vol. 58, pp. 331-339, 2012.

[11] S.A. Mohiuddine, and M. Aiyub, "Lacunary statistical convergence in random 2-normed spaces", *Appl. Math. Inf. Sci.*, vol. 6, no. 3, pp. 581-585, 2012.

[12] S.A. Mohiuddine, and E. Şavaş, "Lacunary statistically convergent double sequences in probabilistic normed spaces", *Abstract and Applied Analysis*, vol. 2013, 5 pages, 2013.

[13] M. Mursaleen, "On statistical convergence in random 2-normed spaces", *Acta Sci. Math. (Szeged)*, vol. 76, no. 1-2, pp. 101-109, 2010.

[14] M. Mursaleen, and A. Alotaibi, "On **I**-convergence in random 2-normed spaces", *Math. Slovaca*, vol. 61, no. 6, pp. 933-940, 2011.

[15] M. Mursaleen, and S.A. Mohiuddine, "On ideal convergence of double sequences in probabilistic normed spaces", *Math. Reports*, vol. 12, no. 62, pp. 359-371, 2010.

[16] M. Mursaleen, and S.A. Mohiuddine, "On ideal convergence in probabilistic normed spaces", *Math. Slovaca*, vol. 62, no. 1, pp. 49-62, 2012.

[17] M. Mursaleen, and O.H. Edely, "Statistical convergence of double sequences", *J. Math. Anal. Appl.*, vol. 288, pp. 223-231, 2003.

[18] A. Pringsheim, "Zur theorie der zweifach unendlichen Zahlenfolgen", *Math. Ann.*, vol. 53, pp. 289-321, 1900.

[19] E. Şavaş, and S.A. Mohiuddine, "λ-statistically convergent double sequences in probabilistic normed spaces", *Math. Slovaca*, vol. 62, no. 1, pp. 99-108, 2012.

[20] E. Şavaş, "On generalized statistical convergence in random 2-normed space", *Iranian Journal of Science and Technology*, vol. A4, pp. 417-423, 2012.

[21] B. Schweizer, and A. Sklar, "Statistical metric spaces", *Pacific J. Math.*, vol. 10, pp. 313-334, 1960.

[22] B. Schweizer, and A. Sklar, "Probabilistic metric spaces", North Holland, New York-Amsterdam-Oxford, 1983.

[23] A.H. Siddiqi, "2-normed spaces", *Aligarh Bull. Math.*, pp. 53-70, 1980.

[24] A.N. Serstnev, "Random normed space: Questions of completeness", *Kazan Gos. Univ. Uchen. Zap.*, vol. 122, no. 4, pp. 3-20, 1962.

[25] A.N. Serstnev, "On the notion of a Random normed space", *Dokl. Akad. nouk. SSR.*, vol. 149, pp. 280-283, 1963.

[26] H. Steinhaus, "Sur la convergence ordinaire et la convergence asymptotique", *Colloq. Math.*, vol. 2, pp. 73-74, 1951.

[27] A. Şahiner, M. Gürdal, S. Saltan, and H. Gunawan, "Ideal Convergence in 2-normed Spaces", *Taiwanese J. Math.*, vol. 11, no. 4, pp. 1477-1484, 2007.

[28] U. Yamancı, and M. Gürdal, "**I**-statistical convergence in 2-normed space", *Arab Journal of Mathematical Sciences*, vol. 20, no. 1, pp. 41-47, 2014.

Ulaş¸ Yamancı received the MSc at Graduate School of Natural and Applied Sciences at Süleyman Demirel University of Isparta in Turkey. His research interests are: Toeplitz operator, Berezin symbols, Reproducing Kernels, Statistical convergence, Ideal convergence.

M. Gürdal received the PhD degree in Mathematics for Graduate School of Natural and Applied Sciences at Süleyman Demirel University of Isparta in Turkey. His research interests are in the areas of functional analysis and operator theory including statistical convergence, Berezin sembols, Banach algebras, Toeplitz Operators. He has published research articles in reputed international journals of mathematical science. He is referee and editor of mathematical journals.

S. Aytar received the PhD degree in Mathematics for Graduate School of Natural and Applied Sciences at Süleyman Demirel University of Isparta in Turkey. His research interests are in the areas of functional analysis, convex analysis, applied mathematics including statistical convergence, fuzzy sets, Rough convergence. He has published research articles in reputed international journals of mathematical science. He is referee of mathematical journals.

Subordination formulae for space-time fractional diffusion processes via Mellin convolution

Gianni Pagnini
BCAM – Basque Center for Applied Mathematics
Alameda de Mazarredo 14, E–48009 Bilbao
and
IKERBASQUE, Basque Foundation for Science
Alameda Urquijo 36–5, Plaza Bizkaia, E–48011 Bilbao
Basque Country – Spain
Email: gpagnini@bcamath.org

***Abstract*—Fundamental solutions of space-time fractional diffusion equations can be interpret as probability density functions. This fact creates a strong link with stochastic processes. Recasting probability density functions in terms of subordination laws has emerged to be important to built up stochastic processes. In particular, for diffusion processes, subordination can be understood as a diffusive process in space, which is called parent process, that depends on a parameter which is also random and depends on time, which is called directing process. Stochastic processes related to fractional diffusion are self-similar processes. The integral representation of the resulting probability density function for self-similar stochastic processes can be related to the convolution integral within the Mellin transform theory. Here, subordination formulae for space-time fractional diffusion are provided. In particular, a noteworthy new formula is derived in the diffusive symmetric case that is spatially driven by the Gaussian density. Future developments of the research on the basis of this new subordination law are discussed.**

I. Introduction

Fractional diffusion processes are processes governed by diffusion-type equations including fractional differential operators [1], [2]. In particular, Fractional Calculus has emerged to be a useful mathematical tool for modelling non-local effects and then, for what concerns diffusion, to model those phenomena for which the classical local flux-gradient relationship does not hold and a non-local relationship is required. Since these difference from classical/*normal* diffusion, such processes are referred to as *anomalous* diffusion processes.

The resulting diffusion process differs from classical diffusion because the probability density function (PDF) of particle distribution is not Gaussian and because the variance of particle spreading does not grow linearly in time. Anomalous diffusion has been experimentally established in nature in several phenomena, see e.g. [3], [4], [5], [6], [7].

Mellin transform theory has an important role in the study of space-time fractional diffusion equations especially to derive solution in terms of the Mellin–Barnes integral representation [8], [9], [10]. Furthermore, Mellin transform is also intrinsically related to probability theory. In fact, the PDF of the product of two independent random variables is determined by the Mellin convolution of the two corresponding densities [9], [11]. The resulting integral formula can be seen also as a subordination law. The relationship between them is reported.

Hence certain integral formulae for fundamental solutions of space-time fractional diffusion equation can be read as subordination laws. Here manipulation of such formulae is performed with the final aim to obtain a new formula, for the spatial symmetric case, with the valuable property to be based on the Gaussian density. And backing to Mellin convolution, suggestions for future research development to generate stochastic processes by the product of two independent random variables are addressed.

The paper is organized as follows. In Section II the space-time fractional diffusion equation is reviewed in detail discussing the probability density interpretation of the Green functions and showing solutions and special cases. In Section III the essential notions and notations concerning Mellin transform are reported and the relationship with subordination laws highlighted. In Section IV subordination laws for fundamental solution of space-time fractional diffusion are given and a new formula for symmetric diffusion is derived whose parent process is the Gaussian density. Finally, Section V contains summary, conclusions and future developments.

II. The space-time fractional diffusion equation

Space-time fractional diffusion equation is obtained from the ordinary diffusion equation by replacing the first order time derivative with the *Caputo* time-fractional derivative of order β, i.e. ${}_tD^{\beta}_*$, and the second order space derivative with the *Riesz–Feller* space-fractional derivative of order α and asymmetry parameter θ, i.e. ${}_xD^{\alpha}_{\theta}$, [8]

$$ {}_tD^{\beta}_* \, u(x;t) = {}_xD^{\alpha}_{\theta} \, u(x;t) \,, \quad x \in R \,, \quad t \in R^+_0 \,. \qquad (1) $$

ISBN: 978-1-61804-225-5

The real parameters α, θ and β are restricted as follows

$$\begin{cases} 0 < \alpha \leq 2\,, \\ |\theta| \leq \min\{\alpha, 2-\alpha\}\,, \\ 0 < \beta \leq 1 \quad \text{or} \quad 1 < \beta \leq \alpha \leq 2\,. \end{cases} \tag{2}$$

The *Caputo* time-fractional derivative ${}_tD^{\beta}_{*}$ is defined by its Laplace transform as

$$\int_0^{+\infty} \mathrm{e}^{-st} \left\{ {}_tD^{\beta}_{*}\, u(x;t) \right\} dt = s^{\beta}\, \widetilde{u}(x;s) - \sum_{n=0}^{m-1} s^{\beta-1-n}\, u^{(n)}(x;0^+)\,, \tag{3}$$

with $m-1 < \beta \leq m$ and $m \in I\!N$.

The *Riesz–Feller* space-fractional derivative ${}_xD^{\theta}_{\theta}$ is defined by its Fourier transform according to

$$\int_{-\infty}^{+\infty} \mathrm{e}^{+i\kappa x} \left\{ {}_xD^{\alpha}_{\theta}\, u(x;t) \right\} dx = -|\kappa|^{\alpha}\, \mathrm{e}^{i(\operatorname{sign}\kappa)\theta\pi/2}\, \widehat{u}(\kappa;t)\,, \tag{4}$$

with α and θ as stated in (2).

In literature the time-fractional derivative is sometimes considered in the Riemann–Liouville sense, here denoted by ${}_tD^{\beta}$. Its relationship with the time-fractional derivative in the Caputo sense is [12]

$${}_tD^{\beta}_{*}\, u(x;t) = {}_tD^{\beta}\, u(x;t) - \frac{t^{-\beta}}{\Gamma(1-\beta)}\, u(x;0)\,, \tag{5}$$

and equation (1) becomes

$${}_tD^{\beta}\, u(x;t) = {}_xD^{\alpha}_{\theta}\, u(x;t) + \frac{t^{-\beta}}{\Gamma(1-\beta)}\, u(x;0)\,, \tag{6}$$

with $x \in R$ and $t \in R_0^+$. Equation (1) is stated also as

$$\frac{\partial u}{\partial t} = {}_tD^{1-\beta} \left[{}_xD^{\alpha}_{\theta}\, u(x;t) \right]\,. \tag{7}$$

However, it is possible to show that the fundamental solutions of (1), (6) and (7) are equal [12].

Solution of (1) can be determined in terms of the fundamental solution, or Green function, $K^{\theta}_{\alpha,\beta}(x;t)$ as follows

$$u(x;t) = \int_{-\infty}^{+\infty} K^{\theta}_{\alpha,\beta}(x-\xi;t)\, u(\xi;0)\, d\xi\,, \tag{8}$$

with the initial and boundary conditions $\{u(x;0) = \delta(x)\,, u_t(x;0) = 0\}$ when $0 < \beta \leq 1$ and when $1 < \beta \leq 2$ a second initial condition corresponding to $u_t(x;0) = \left.\dfrac{\partial u}{\partial t}\right|_{t=0}$ is needed such that two Green functions follow according to the conditions $\{u(x;0) = \delta(x)\,, u_t(x;0) = 0\}$ and $\{u(x;0) = 0\,, u_t(x;0) = \delta(x)\}$, respectively.

By taking into account the Laplace transform for the *Caputo* time fractional derivative (3) and the Fourier transform for the *Riesz–Feller* space fractional derivative (4), the composite Fourier–Laplace transform of the *first* Green function results to be

$$\widehat{\widetilde{K^{\theta}_{\alpha,\beta}}}(\kappa;s) = \frac{s^{\beta-1}}{s^{\beta} + |\kappa|^{\alpha}\, \mathrm{e}^{i(\operatorname{sign}\kappa)\theta\pi/2}}\,, \tag{9}$$

and of the *second* Green function

$$\widehat{\widetilde{K^{\theta}_{\alpha,\beta}}}(\kappa;s) = \frac{s^{\beta-2}}{s^{\beta} + |\kappa|^{\alpha}\, \mathrm{e}^{i(\operatorname{sign}\kappa)\theta\pi/2}}\,. \tag{10}$$

From (9), for the first Green function it holds

$$\widehat{\widetilde{K^{\theta}_{\alpha,\beta}}}(0;s) = 1/s \quad \text{and then} \quad \widehat{K^{\theta}_{\alpha,\beta}}(0;t) = 1\,, \tag{11}$$

so that the *normalization property* follows

$$\int_{-\infty}^{+\infty} K^{\theta}_{\alpha,\beta}(x;t)\, dx = 1\,. \tag{12}$$

Hence it can be interpret as a PDF for particle distribution in x and evolving in time t. Differently, from (10), for the second Green function it holds

$$\widehat{\widetilde{K^{\theta}_{\alpha,\beta}}}(0;s) = 1/s^2 \quad \text{and then} \quad \widehat{K^{\theta}_{\alpha,\beta}}(0;t) = t\,, \tag{13}$$

so that it follows

$$\int_{-\infty}^{+\infty} K^{\theta}_{\alpha,\beta}(x;t)\, dx = t\,, \tag{14}$$

and the *normalization property* is not met. The second Green function (10) emerges to be a primitive (with respect to the variable t) of the first Green function (9), so that it cannot be interpreted as a PDF of x evolving in t because it is no longer normalized [13]. Finally, solely the first Green function can be considered for diffusion problems.

In general, fundamental solution $K^{\theta}_{\alpha,\beta}(x;t)$ algebraically decreases as $|x|^{-(\alpha+1)}$, thus it belongs to the domain of attraction of the Lévy stable densities of index α. Moreover, $K^{\theta}_{\alpha,\beta}(x;t)$ self-similarly scales as

$$K^{\theta}_{\alpha,\beta}(x;t) = t^{-\beta/\alpha}\, K^{\theta}_{\alpha,\beta}\left(\frac{x}{t^{\beta/\alpha}}\right)\,, \tag{15}$$

and it meets the following *symmetry relation*

$$K^{\theta}_{\alpha,\beta}(-x;t) = K^{-\theta}_{\alpha,\beta}(x;t)\,, \tag{16}$$

which allows the restriction of the analysis to $x \in R_0^+$. In this x-range, i.e. $x \in R_0^+$, the analytical solution of (1) can be expressed by the following Mellin–Barnes integral representation [14], [8],

$$K^{\theta}_{\alpha,\beta}(x;t) = \frac{1}{\alpha x} \times \frac{1}{2\pi i} \int_{\omega-i\infty}^{\omega+i\infty} \frac{\Gamma\left(\frac{s}{\alpha}\right) \Gamma\left(1-\frac{s}{\alpha}\right) \Gamma(1-s)}{\Gamma\left(1-\frac{\beta}{\alpha}s\right) \Gamma(\rho\, s) \Gamma(1-\rho\, s)} \left(\frac{x}{t^{\beta/\alpha}}\right)^{s} ds\,, \tag{17}$$

where $\rho = \dfrac{\alpha-\theta}{2\,\alpha}$ and ω is a suitable real constant. Solution (17) can be also expressed in terms of H-Fox function [14], [15].

ISBN: 978-1-61804-225-5

The special cases of space-time fractional diffusion equation (1) are the following.

The *space-fractional diffusion* equation, i.e. $0 < \alpha < 2$ and $\beta = 1$, so that when $x \in R_0^+$

$$K_{\alpha,1}^{\theta}(x;t) = L_{\alpha}^{\theta}(x;t) = t^{-1/\alpha} L_{\alpha}^{\theta}\left(\frac{x}{t^{1/\alpha}}\right), \qquad (18)$$

where $L_{\alpha}^{\theta}(x)$ is the class of strictly stable densities with algebraic tail decaying as $|x|^{-(\alpha+1)}$ and infinite variance. Moreover, a stable PDF with $0 < \alpha < 1$ and extremal value of the asymmetry parameter θ are one-sided with support R_0^+ if $\theta = -\alpha$ and R_0^- if $\theta = +\alpha$.

The *time-fractional diffusion* equation, i.e. $\alpha = 2$ and $0 < \beta < 2$, so that when $x \in R_0^+$

$$K_{2,\beta}^{0}(x;t) = \frac{1}{2} M_{\beta/2}(x;t) = \frac{1}{2} t^{-\beta/2} M_{\beta/2}\left(\frac{x}{t^{\beta/2}}\right), \qquad (19)$$

where $M_{\nu}(x)$, $0 < \nu < 1$, is the M-Wright/Mainardi density [16], [17], [18], [19], [20], [21], [18], which has stretched exponential tails and finite variance proportional to t^{β}. Since $\alpha = 2$, according to (2), it holds $\theta = 0$, then the PDF is symmetric and the extension to $x \in R$ is obtained by replacing x with $|x|$ in (19).

The *neutral fractional diffusion* equation, i.e. $0 < \alpha = \beta < 2$, whose solution can be expressed in explicit form by non-negative simple elementary functions [22], [8], so that when $x \in R_0^+$

$$\begin{aligned} K_{\alpha,\alpha}^{\theta}(x;t) &= N_{\alpha}^{\theta}(x;t) \\ &= \frac{t^{-1}}{\pi} \frac{(x/t)^{\alpha-1} \sin[\frac{\pi}{2}(\alpha-\theta)]}{1 + 2(x/t)^{\alpha} \cos[\frac{\pi}{2}(\alpha-\theta)] + (x/t)^{2\alpha}}. \end{aligned} \qquad (20)$$

Recently Luchko [23] has considered and analyzed the case $1 < \alpha < 2$ and $\theta = 0$ of (20). Moreover, PDF (20) with $0 < \alpha < 1$ is emerged in the study of finite Larmor radius effects on non-diffusive tracer transport in a zonal flow [24] as well as numerically evidenced in non-diffusive chaotic transport by Rossby waves in zonal flow [25].

The *classical diffusion* equation, i.e. $\alpha = 2$ and $\beta = 1$, whose Gaussian solution is recovered as limiting case from both the space-fractional ($\alpha = 2$) and the time-fractional ($\beta = 1$) diffusion equation, so that when $x \in R_0^+$

$$\begin{aligned} K_{2,1}^{0}(x;t) = L_{2}^{0}(x;t) &= \frac{1}{2} M_{1/2}(x;t) \\ &= \mathcal{G}(x;t) = \frac{\mathrm{e}^{-x^2/(4t)}}{\sqrt{4\pi t}}. \end{aligned} \qquad (21)$$

The last special case is the limit case of the *D'Alembert wave equation*, i.e. $\alpha = \beta = 2$, such that when $x \in R_0^+$ it holds

$$K_{2,2}^{0}(x;t) = \frac{1}{2} M_{1}(x;t) = \frac{1}{2} \delta(x-t). \qquad (22)$$

III. Mellin convolution and subordination law in stochastic processes

A. The Mellin transform

Main definitions and formulae of Mellin transform are here reminded for completeness with what follows. The interest reader can find exhaustive presentation of the Mellin transform theory, for example, in the book by Marichev [26] where connections with Fourier and Laplace transforms are also reported. However, the theory of Mellin transform independently of Laplace or Fourier transforms was introduced by Butzer and Jansche [27], [28].

Let $f(x) \in L_{loc}(\mathbb{R}^+)$, then the Mellin transform $f^*(s)$, $s \in \mathbb{C}$, of a sufficiently well-behaved function $f(x)$, $x \in \mathbb{R}^+$, is defined as

$$f^*(s) = \int_0^{+\infty} f(x)\, x^{s-1}\, dx, \quad s \in \mathbb{C}. \qquad (23)$$

Formula (23) defines the Mellin transform in a vertical strip in the s-plane whose boundaries are determined by the analytic structure of $f(x)$ as $x \to 0^+$ and $x \to +\infty$. When

$$f(x) = \begin{cases} O\left(x^{-\omega_1-\epsilon}\right) & \text{as} \quad x \to 0^+, \\ \\ O\left(x^{-\omega_2-\epsilon}\right) & \text{as} \quad x \to +\infty, \end{cases} \qquad (24)$$

then, for every (small) $\epsilon > 0$ and $\omega_1 < \omega_2$, integral (23) converges absolutely and defines an analytic function in the strip $\omega_1 < \mathrm{Re}\{s\} < \omega_2$, i.e. the *strip of analyticity* of $f^*(s)$.

The inversion formula follows directly from the inversion formula for the bilateral Laplace transform, i.e.

$$f(x) = \frac{1}{2\pi i} \int_{\omega-i\infty}^{\omega+i\infty} f^*(s)\, x^{-s}\, ds, \quad \omega_1 < \omega < \omega_2, \qquad (25)$$

when $f(x)$ is continuous.

Denoting by $\overset{\mathcal{M}}{\longleftrightarrow}$ the juxtaposition of a function $f(x)$, $x \in \mathbb{R}^+$, with its Mellin transform $f^*(s)$, $s \in \mathbb{C}$, some important properties of Mellin transform are

$$x^a\, f(x) \overset{\mathcal{M}}{\longleftrightarrow} f^*(s+a), \quad a \in \mathbb{C}, \qquad (26)$$

$$f(x^b) \overset{\mathcal{M}}{\longleftrightarrow} \frac{1}{|b|} f^*(s/b), \quad b \in \mathbb{C}, \quad b \neq 0, \qquad (27)$$

$$f(cx) \overset{\mathcal{M}}{\longleftrightarrow} c^{-s}\, f^*(s), \quad c \in \mathbb{R}^+, \qquad (28)$$

from which it follows

$$x^a\, f(cx^b) \overset{\mathcal{M}}{\longleftrightarrow} \frac{1}{|b|}\, c^{-(s+a)/b}\, f^*\left(\frac{s+a}{b}\right). \qquad (29)$$

Differently from Fourier and Laplace transforms, *Mellin convolution* formula does not concern variable shifting but scaling and it emerges to be

$$h(x) = \int_0^{\infty} f\left(\frac{x}{\xi}\right) g(\xi)\, \frac{d\xi}{\xi} \overset{\mathcal{M}}{\longleftrightarrow} f^*(s)\, g^*(s) = h^*(s). \qquad (30)$$

In general, formula (30) can be rewritten for $\gamma > 0$ as

$$\begin{aligned} h(x) &= \int_0^{\infty} f\left(\frac{x}{\xi^{\gamma}}\right) g(\xi)\, \frac{d\xi}{\xi^{\gamma}} \\ &\overset{\mathcal{M}}{\longleftrightarrow} f^*(s)\, g^*[\gamma(s-1)+1] = h^*(s). \end{aligned} \qquad (31)$$

Formula (31) embodies the operative tool of the following analysis.

B. Subordination law

A stochastic process $X(t)$ is called *subordinated process* if it is obtained by a stochastic process $Y(\tau)$, $\tau \in I\!R_0^+$, by the randomization of the parameter τ according to a process $T(t)$ with non-negative independent increments [29]. The resulting process $X(t) = Y(T(t))$ is said to be subordinated to $Y(t)$, that is called the *parent process*, and to be directed by $T(t)$, that is called the *directing process*.

The subordinated process $X(t) = Y(T(t))$ emerges to be governed by a spatial PDF of x evolving in time t, i.e. $\psi(x;t)$, determined by the subordination law

$$\psi(x;t) = \int_0^\infty q(x;\tau)\,\varphi(\tau;t)\,d\tau\,, \tag{32}$$

where $q(x;\tau)$ is the spatial PDF of x depending on the parameter τ and corresponding to the process $Y(\tau)$, $\varphi(\tau;t)$ is the PDF underlying the process $T(\tau)$ with non-negative independent increments and depending on the parameter t.

Assuming self-similarity for the parent process $Y(\tau)$ then it holds

$$q(x;\tau) = \tau^{-\gamma}\,q\Big(\frac{x}{\tau^\gamma}\Big)\,, \quad \gamma > 0\,, \tag{33}$$

and formula (32) reads

$$\psi(x;t) = \int_0^\infty q\Big(\frac{x}{\tau^\gamma}\Big)\,\varphi(\tau;t)\,\frac{d\tau}{\tau^\gamma}\,, \quad \gamma > 0\,. \tag{34}$$

Moreover, let Z_1 and Z_2 be two real *independent* random variables with PDFs $p_1(z_1)$, $z_1 \in I\!R$, and $p_2(z_2)$, $z_2 \in I\!R_0^+$, respectively. From theory of probability it follows that the joint probability $p(z_1, z_2)$ is

$$p(z_1, z_2) = p_1(z_1)\,p_2(z_2)\,. \tag{35}$$

Introducing the change of variables

$$\begin{cases} z_1 = z/\lambda^\gamma\,, \\ \\ z_2 = \lambda\,, \end{cases} \tag{36}$$

whose Jacobian equals $1/\lambda^\gamma$, it follows that

$$p(z,\lambda)\,dz\,d\lambda = p_1\left(\frac{z_1}{\lambda^\gamma}\right)\,p_2(\lambda)\frac{d\lambda}{\lambda^\gamma}\,dz\,, \tag{37}$$

and integrating in $d\lambda$ the PDF of $Z = Z_1 Z_2^\gamma$ finally turns out to be

$$p(z) = \int_{-\infty}^{+\infty} p_1\left(\frac{z}{\lambda^\gamma}\right)\,p_2(\lambda)\,\frac{d\lambda}{\lambda^\gamma}\,. \tag{38}$$

When $\gamma = 1$ formula (38) corresponds to Mellin convolution integral (30) and in general, when $\gamma \neq 1$, it is equal to (31) proving the fact that Mellin convolution is related to the PDF resulting from the product of two independent random variables.

Clearly, by making the change of variables $z = x\,t^{-\gamma\Omega}$ and $\lambda = \tau\,t^{-\Omega}$ and by setting $\tau^{-\gamma}p_1(x/\tau^\gamma) \equiv \tau^{-\gamma}q(x/\tau^\gamma)$ and $t^{-\Omega}p_2(\tau/t^\Omega) \equiv \varphi(\tau;t)$, from (38) formula (34) is recovered and it holds $t^{-\gamma\Omega}p(x/t^{\gamma\Omega}) \equiv \psi(x;t)$.

Hence, the stochastic process $X(t) = Y(T(t))$ follows the same one-point one-time PDF of the process $X = X_1 X_2^\gamma$. Then for a given diffusion equation, a stochastic process corresponding to the Green function can be generated by the product of two independent random variables distributed according to the PDFs involved in the subordination law.

This approach to provide stochastic processes has been recently discussed by the author and collaborators [30]. In particular this method has been introduced to develop self-similar stochastic processes with stationary increments following a method proposed by Mura [31] to derive the so-called generalized grey Brownian motion [32], [33]. Actually, the generalized grey Brownian motion has been shown to be related to the Green function of the Erdélyi–Kober fractional diffusion [34], [35], [36].

IV. Subordination laws for the space-time fractional diffusion

A first valuable subordination-type formula for $K^\theta_{\alpha,\beta}(x;t)$ was derived by Uchaikin & Zolotarev [37], [38], i.e.

$$K^\theta_{\alpha,\beta}(x;t) = \int_0^\infty L^\theta_\alpha(x;(t/y)^\beta)\,L^{-\beta}_\beta(y)\,dy\,, \tag{39}$$

and, by putting $t/y = \xi^{1/\beta}$, it becomes [8]

$$K^\theta_{\alpha,\beta}(x;t) = \int_0^\infty L^\theta_\alpha(x;\xi)\,L^{-\beta}_\beta(t;\xi)\,\frac{t}{\beta\,\xi}\,d\xi\,. \tag{40}$$

Further important subordination formulae were derived in literature. A practical method is the following. Noting the close relationship between Mellin–Barnes integral representation of fundamental solutions (17) and Mellin inversion formula (25), by splitting Mellin transform of Green functions in two known Mellin transforms then subordination laws can be derived by using Mellin convolution formula (30, 31) [8], [9], [11]. The same method was used also to obtain a Gaussianization of Lévy noise in signal filtering [39].

In particular, it is reported that when $0 < \beta \leq 1$ it holds [8, equation (6.16)]

$$K^\theta_{\alpha,\beta}(z) = \alpha\,\int_0^\infty \xi^{\alpha-1}\,M_\beta\left(\xi^\alpha\right)\,L^\theta_\alpha(z/\xi)\,\frac{d\xi}{\xi}\,, \tag{41}$$

and when $0 < \beta/\alpha \leq 1$

$$K^\theta_{\alpha,\beta}(z) = \int_0^\infty M_{\beta/\alpha}(\xi)\,N^\theta_\alpha(z/\xi)\,\frac{d\xi}{\xi}\,. \tag{42}$$

Applying the changes of variable $\xi = \tau^{1/\alpha}/t^{\beta/\alpha}$ and $\xi = \tau/t^{\beta/\alpha}$ in (41) and (42), respectively, and replacing z with $x/t^{\beta/\alpha}$, when $0 < \beta \leq 1$ it follows [8], [9],

$$t^{-\beta/\alpha}K^\theta_{\alpha,\beta}\left(\frac{x}{t^{\beta/\alpha}}\right) = \int_0^\infty \tau^{-1/\alpha}L^\theta_\alpha\left(\frac{x}{\tau^{1/\alpha}}\right)t^{-\beta}M_\beta\left(\frac{\tau}{\beta}\right)d\tau\,, \tag{43}$$

and when $0 < \beta/\alpha \leq 1$

$$t^{-\beta/\alpha}K^\theta_{\alpha,\beta}\left(\frac{x}{t^{\beta/\alpha}}\right) = \int_0^\infty \tau^{-1}N^\theta_\alpha\left(\frac{x}{\tau}\right)t^{-\beta/\alpha}M_{\beta/\alpha}\left(\frac{\tau}{t^{\beta/\alpha}}\right)d\tau\,, \tag{44}$$

or analogously when $0 < \beta \leq 1$ [8], [9],

$$K^{\theta}_{\alpha,\beta}(x;t) = \int_0^{\infty} L^{\theta}_{\alpha}(x;\tau)\, M_{\beta}(\tau;t)\, d\tau\,, \qquad (45)$$

and when $0 < \beta/\alpha \leq 1$

$$K^{\theta}_{\alpha,\beta}(x;t) = \int_0^{\infty} N^{\theta}_{\alpha}(x;\tau)\, M_{\beta/\alpha}(\tau;t)\, d\tau\,. \qquad (46)$$

The symmetric case, i.e. $\theta = 0$, of formula (45) was previously derived by Saichev & Zavlasky [22]. Moreover, combining (40) and (45) for $0 < \beta \leq 1$, with $\tau\,, t \in I\!R^{+}_{0}$, it follows the identity [8]

$$L^{-\beta}_{\beta}(t;\tau)\, \frac{t}{\beta\,\tau} = M_{\beta}(\tau;t)\,, \qquad (47)$$

and by using self-similarity properties

$$L^{-\beta}_{\beta}\left(\frac{t}{\tau^{1/\beta}}\right)\, \frac{t}{\beta\,\tau^{1/\beta+1}} = \frac{1}{t^{\beta}}\, M_{\beta}\left(\frac{\tau}{t^{\beta}}\right)\,, \qquad (48)$$

with $0 < \beta \leq 1$ and $\tau\,, t \in I\!R^{+}_{0}$.

Since L^{θ}_{α}, M_{ν} and N^{θ}_{α} are special cases of $K^{\theta}_{\alpha,\beta}$, see Section II, subordination formulae (45) and (46) can be restated also in terms of $K^{\theta}_{\alpha,\beta}(x;t)$ only, after the opportune choice of parameters [8], [9]. In fact when $0 < \beta \leq 1$

$$K^{\theta}_{\alpha,\beta}(x;t) = 2\int_0^{\infty} K^{\theta}_{\alpha,1}(x;\tau)\, K^{0}_{2,2\beta}(\tau;t)\, d\tau\,, \qquad (49)$$

and when $0 < \beta/\alpha \leq 1$

$$K^{\theta}_{\alpha,\beta}(x;t) = 2\int_0^{\infty} K^{\theta}_{\alpha,\alpha}(x;\tau)\, K^{0}_{2,2\beta/\alpha}(\tau;t)\, d\tau\,. \qquad (50)$$

Formula (45), or the analog ones, shows that the solution of the space-time fractional diffusion equation (1) can be expressed in terms of the solution of the space-fractional diffusion equation of order α, i.e. $K^{\theta}_{\alpha,1}(x;t) = L^{\theta}_{\alpha}(x;t)$, and of the solution of the time-fractional diffusion equation of order 2β, i.e. $K^{0}_{2,2\beta}(\tau;t) = M_{\beta}(\tau;t)/2$, $\tau \in R^{+}_{0}$. Moreover, formulae (45) and (46), or the analog ones, by involving non-negative functions allow the PDF interpretation of $K^{\theta}_{\alpha,\beta}(x;t)$. Furthermore, it is worth-noting to remark that formula (46), or the analog ones, is fundamental to extend such probability interpretation to the range $1 < \beta \leq \alpha \leq 2$.

By using (45) a new subordination law for the space-time fractional diffusion can be derived. In fact, it is well known that the following subordination formula for Lévy stable density holds [29], [9], [11],

$$L^{\theta}_{\alpha}(x;t) = \int_0^{\infty} L^{\gamma}_{\eta}(x;\xi)\, L^{-\nu}_{\nu}(\xi;t)\, d\xi\,, \qquad (51)$$

where $\alpha = \eta\nu$, $\theta = \gamma\nu$ and

$$0 < \alpha \leq 2\,, \quad |\theta| \leq \min\{\alpha, 2-\alpha\}\,, \qquad (52)$$

$$0 < \eta \leq 2\,, \quad |\gamma| \leq \min\{\eta, 2-\eta\}\,, \quad 0 < \nu \leq 1\,. \qquad (53)$$

Hence, inserting (51) into (45) gives

$$\begin{aligned} K^{\theta}_{\alpha,\beta}(x;t) &= \int_0^{\infty}\left\{\int_0^{\infty} L^{\gamma}_{\eta}(x;\xi) L^{-\nu}_{\nu}(\xi;\tau) d\xi\right\} M_{\beta}(\tau;t) d\tau\,, \\ &= \int_0^{\infty} L^{\gamma}_{\eta}(x,\xi)\left\{\int_0^{\infty} L^{-\nu}_{\nu}(\xi;\tau) M_{\beta}(\tau;t)\, d\tau\right\} d\xi\,, \qquad (54) \end{aligned}$$

where the exchange of integration is allowed by the fact that the involved functions are normalized PDFs. Finally, using again (45) to compute the integral into braces in (54), when $0 < \beta \leq 1$, the following *new* subordination law is obtained

$$K^{\theta}_{\alpha,\beta}(x;t) = \int_0^{\infty} L^{\gamma}_{\eta}(x;\xi)\, K^{-\nu}_{\nu,\beta}(\xi,t)\, d\xi\,, \qquad (55)$$

with $\alpha = \eta\nu$, $\theta = \gamma\nu$ and the same restrictions stated in (52) and (53) for the values of parameters.

In the particular case $\eta = 2$ and $\gamma = 0$, so that $\nu = \alpha/2$ and $\theta = 0$, a Gaussian subordination follows. In fact $L^{0}_{2}(x;t) = \mathcal{G}(x;t) = \dfrac{\mathrm{e}^{-x^2/(4\,t)}}{\sqrt{4\,\pi\,t}}$ so that formula (55) becomes

$$K^{0}_{\alpha,\beta}(x;t) = \int_0^{\infty} \mathcal{G}(x;\xi)\, K^{-\alpha/2}_{\alpha/2,\beta}(\xi;t)\, d\xi\,, \qquad (56)$$

with $0 < \alpha \leq 2$ and $0 < \beta \leq 1$.

V. Conclusion

In the present paper fundamental solutions of space-time fractional diffusion equations have been analysed. In particular, by using Mellin–Barnes integral representation and Mellin convolution, integral formulae can be derived that may be understood as subordination laws. It is well known that Mellin convolution gives the integral representation of the PDF resulting from the product of two independent random variables. Then subordination laws suggest how to built up stochastic processes by using the product of two independent variables that follows a desired one-point one-time PDF.

Manipulation of literature formulae has been performed with the aim to obtain a new subordination-type formula for space-time fractional diffusion. The derived new formula, when reduced to the case of spatial symmetric diffusion, has emerged to be based on the Gaussian density. That is a valuable property.

In fact, the derived formula proves that stochastic processes, whose one-point one-time PDF is solution of the symmetric space-time fractional diffusion equation, can be generated by the product of a Gaussian distributed motion and an independent positive random variable with specified PDF. The leading role of the Gaussian motion is remarkable even because it is a very well studied process and largely suitable for the simulation of trajectories. In particular because self-similar with stationary increments and characterized by solely the first and the second moments.

To conclude, the derived subordination formula is the basis for future development of a self-similar stochastic process with stationary increments to model space-time fractional diffusion in the spatial symmetric case.

Acknowledgment

The author would like to thank Prof. Francesco Mainardi for continuous useful discussions, advice and encouragement.

REFERENCES

[1] I. Podlubny, *Fractional Differential Equations*. San Diego: Academic Press, 1999.

[2] D. Baleanu, K. Diethelm, E. Scalas, and J. J. Trujillo, *Fractional Calculus: Models and Numerical Methods*. New Jersey: World Scientific Publishers, 2012, series on Complexity, Nonlinearity and Chaos, volume 3.

[3] R. Metzler and J. Klafter, "The restaurant at the end of the random walk: recent developments in fractional dynamics descriptions of anomalous dynamical processes," *J. Phys. A: Math. Theor.*, vol. 37, no. 31, pp. R161–R208, 2004.

[4] S. Ratynskaia, K. Rypdal, C. Knapek, S. Khrapak, A. V. Milovanov, A. Ivlev, J. J. Rasmussen, and G. E. Morfill, "Superdiffusion and viscoelastic vortex flows in a two-dimensional complex plasma," *Phys. Rev. Lett.*, vol. 96, no. 10, p. 105010, 2006.

[5] P. Dieterich, R. Klages, R. Preuss, and A. Schwab, "Anomalous dynamics of cell migration," *Proc. Nat. Acad. Sci.*, vol. 105, no. 2, pp. 459–463, 2008.

[6] G. Dif-Pradalier, P. H. Diamond, V. Grandgirard, Y. Sarazin, J. Abiteboul, X. Garbet, P. Ghendrih, A. Strugarek, S. Ku, and C. S. Chang, "On the validity of the local diffusive paradigm in turbulent plasma transport," *Phys. Rev. E*, vol. 82, p. 025401(R), 2010.

[7] M. Chevrollier, N. Mercadier, W. Guerin, and R. Kaiser, "Anomalous photon diffusion in atomic vapors," *Eur. Phys. J. D*, vol. 58, pp. 161–165, 2010.

[8] F. Mainardi, Y. Luchko, and G. Pagnini, "The fundamental solution of the space-time fractional diffusion equation," *Fract. Calc. Appl. Anal.*, vol. 4, no. 2, pp. 153–192, 2001.

[9] F. Mainardi, G. Pagnini, and R. Gorenflo, "Mellin transform and subordination laws in fractional diffusion processes," *Fract. Calc. Appl. Anal.*, vol. 6, no. 4, pp. 441–459, 2003.

[10] F. Mainardi and G. Pagnini, "Mellin–Barnes integrals for stable distributions and their convolutions," *Fract. Calc. Appl. Anal.*, vol. 11, pp. 443–456, 2008.

[11] F. Mainardi, G. Pagnini, and R. Gorenflo, "Mellin convolution for subordinated stable processes," *J. Math. Sci.*, vol. 132, no. 5, pp. 637–642, 2006.

[12] R. Gorenflo and F. Mainardi, "Parametric subordination in fractional diffusion processes," in *Fractional Dynamics. Recent Advances*, J. Klafter, S. C. Lim, and R. Metzler, Eds. Singapore: World Scientific, 2012, pp. 227–261.

[13] F. Mainardi and G. Pagnini, "The Wright functions as solutions of the time-fractional diffusion equations," *Appl. Math. Comput.*, vol. 141, pp. 51–62, 2003.

[14] G. Pagnini, *Generalized Equations for Anomalous Diffusion and their Fundamental Solutions*. Thesis for Degree in Physics, University of Bologna, October 2000, in Italian.

[15] F. Mainardi, G. Pagnini, and R. K. Saxena, "Fox H functions in fractional diffusion," *J. Comput. Appl. Math.*, vol. 178, pp. 321–331, 2005.

[16] F. Mainardi, A. Mura, and G. Pagnini, "The M-Wright function in time-fractional diffusion processes: A tutorial survey," *Int. J. Differ. Equations*, vol. 2010, p. 104505, 2010.

[17] ——, "The functions of the Wright type in fractional calculus," *Lecture Notes of Seminario Interdisciplinare di Matematica*, vol. 9, pp. 111–128, 2010.

[18] G. Pagnini, "The M-Wright function as a generalization of the Gaussian density for fractional diffusion processes," *Fract. Calc. Appl. Anal.*, vol. 16, no. 2, pp. 436–453, 2013.

[19] D. O. Cahoy, "On the parametrization of the M-Wright function," *Far East J. Theor. Stat.*, vol. 34, no. 2, pp. 155–164, 2011.

[20] ——, "Estimation and simulation for the M-Wright function," *Commun. Stat.-Theor. M.*, vol. 41, no. 8, pp. 1466–1477, 2012.

[21] ——, "Moment estimators for the two-parameter M-Wright distribution," *Computation. Stat.*, vol. 27, no. 3, pp. 487–497, 2012.

[22] A. Saichev and G. Zaslavsky, "Fractional kinetic equations: solutions and applications," *Chaos*, vol. 7, pp. 753–764, 1997.

[23] Y. Luchko, "Fractional wave equation and damped waves," *J. Math. Phys.*, vol. 54, p. 031505, 2013.

[24] K. Gustafson, D. del Castillo-Negrete, and W. Dorland, "Finite Larmor radius effects on nondiffusive tracer transport in zonal flows," *Phys. Plasmas*, vol. 15, p. 102309, 2008.

[25] D. del Castillo-Negrete, "Non-diffusive, non-local transport in fluids and plasmas," *Nonlin. Processes Geophys.*, vol. 17, pp. 795–807, 2010.

[26] O. I. Marichev, *Handbook of Integral Transforms of Higher Trascendental Functions, Theory and Algorithmic Tables*. Ellis Horwood, Chichester, 1983.

[27] P. Butzer and S. Jansche, "A direct approach to Mellin transform," *J. Fourier Anal. Appl.*, vol. 3, pp. 325–276, 1997.

[28] ——, "Mellin transform theory and the role of its differential and integral operators," in *Transform Methods & Special Functions, Varna '96*, P. Rusev, I. Dimovski, and V. Kiryakova, Eds., Proc. Second Int. Conference, Varna (Bulgaria) 23–30 August 1996. Sofia: Bulgarian Academy of Sciences, 1998, pp. 63–83, ISBN 954-8986-05-1.

[29] W. Feller, *An Introduction to Probability Theory and its Applications*, 2nd ed. New York: Wiley, 1971, vol. 2.

[30] G. Pagnini, A. Mura, and F. Mainardi, "Two-particle anomalous diffusion: Probability density functions and self-similar stochastic processes," *Phil. Trans. R. Soc. A*, vol. 371, p. 20120154, 2013.

[31] A. Mura, *Non-Markovian Stochastic Processes and Their Applications: From Anomalous Diffusion to Time Series Analysis*. Lambert Academic Publishing, 2011, ph.D. Thesis, Physics Department, University of Bologna, 2008.

[32] A. Mura and G. Pagnini, "Characterizations and simulations of a class of stochastic processes to model anomalous diffusion," *J. Phys. A: Math. Theor.*, vol. 41, p. 285003, 2008.

[33] A. Mura and F. Mainardi, "A class of self-similar stochastic processes with stationary increments to model anomalous diffusion in physics," *Integr. Transf. Spec. F.*, vol. 20, no. 3–4, pp. 185–198, 2009.

[34] G. Pagnini, "The evolution equation for the radius of a premixed flame ball in fractional diffusive media," *Eur. Phys. J. Special Topics*, vol. 193, pp. 105–117, 2011.

[35] ——, "Erdélyi–Kober fractional diffusion," *Fract. Calc. Appl. Anal.*, vol. 15, no. 1, pp. 117–127, 2012.

[36] G. Pagnini, A. Mura, and F. Mainardi, "Generalized fractional master equation for self-similar stochastic processes modelling anomalous diffusion," *Int. J. Stoch. Anal.*, vol. 2012, p. 427383, 2012.

[37] V. V. Uchaikin and V. M. Zolotarev, *Chance and Stability. Stable Distributions and their Applications*. Utrecht: VSP, 1999.

[38] V. V. Uchaikin, "Montroll–Weiss problem, fractional equations and stable distributions," *Int. J. Theor. Phys.*, vol. 39, pp. 2087–2105, 2000.

[39] G. Pagnini and Y. Chen, "Mellin convolution for signal filtering and its application to the Gaussianization of Lévy noise," in *Proceedings of the ASME Design Engineering Technical Conference*, vol. 3. ASME 2011 International Design Engineering Technical Conferences and Computers and Information in Engineering Conference, IDETC/CIE 2011. Washington D.C., USA, August 28–31, 2011, pp. 149–154.

Derivation of a numerical method with free second-order derivatives

Young Hee Geum

Abstract—We have proposed the second-derivative-free numerical method and determined the control parameters to converge cubically. In addition, we have developed the order of convergence and the asymptotic error constant. Applying this iterative scheme to a variety of examples, numerical results have shown a successful asymptotic error constants with cubic convergence.

Keywords—second-derivative-free, order of convergence, asymptotic error constant, iterative method , multiple root, root-finding

1.. INTRODUCTION

MANY researchers[4,5,6,7,8] have been iterested in developping the iteration methods and deriving the asymptotic error constant to find the roots of nonlinear equations. The Newton's method is one of the most well-known iteration method and is applied.

Suppose that a function $f : \mathbb{C} \to \mathbb{C}$ has a multiple zero α with integer multiplicity $m \geq 1$ and is analytic[1,2,3] in a small neighborhood of α. We find an approximated α by a scheme

$$x_{n+1} = g(x_n),\ n = 0,\ 1,\ 2, \cdots, \tag{1}$$

where $g : \mathbb{C} \to \mathbb{C}$ is an iteration function and $x_0 \in \mathbb{C}$ is given. Then we find an approximated α using an iterative method. To solve the equation, we develoop the following scheme:

$$g(x) = x - \lambda f(x - \mu h(x))/f'(x) \tag{2}$$

where

$$h(x) = \begin{cases} f(x)/f'(x), & if\ x \neq \alpha \\ \lim_{x\to\alpha} f(x)/f'(x), & if\ x = \alpha. \end{cases} \tag{3}$$

Let $p \in \boldsymbol{N}$ be given and $g(x)$ satisfy the following relation

$$\begin{cases} \left|\frac{d^p}{dx^p} g(x)\right|_{x=\alpha} = |g^{(p)}(\alpha)| < 1, & \text{if } p = 1. \\ g^{(i)}(\alpha) = 0 \text{ for } 1 \leq i \leq p-1 \text{ and } g^{(p)}(\alpha) \neq 0, & \text{if } p \geq 2. \end{cases} \tag{4}$$

Since $g(x)$ is continuous at $x = \alpha$, $g(x)$ is represented by

$$g(x) = \begin{cases} x - \lambda F(x), & if\ x \neq \alpha \\ x - \lambda \lim_{x\to\alpha} F(x), & if\ x = \alpha. \end{cases} \tag{5}$$

where $z(x) = x - \mu h(x)$ and $F(x) = \frac{f(x-\mu h(x))}{f'(x)}$.

Young Hee Geum was supported by the National Research Foundation of Korea funded by the Ministry of Education, Science and Technology (Project No. 2011-0014638). Young Hee Geum is with the Department of Applied Mathematics, Dankook University, Cheonan, Korea 330-714. e-mail: conpana@empal.com.

By Corollary 1 and Corollary 2, we have $[f(z)]^{(k)}_{x=\alpha} = 0,\ 0 \leq k \leq m-1$ and $f(\alpha) = f'(\alpha) = \cdots = f^{(m-1)}(\alpha) = 0,\ f^{(m)} \neq 0$. Using L'Hospital's rule repeatedly, we obtain

$$\lim_{x\to\alpha} F(x) = \frac{[f(z)]^{(m-1)}_{x=\alpha}}{[f'(x)]^{(m-1)}} = 0 \tag{6}$$

The next corollary is useful to calculate $g'(\alpha)$, $g''(\alpha)$ and $g'''(\alpha)$.

Corollary 1: Suppose $f : \mathbb{C} \to \mathbb{C}$ has a multiple root α with a given integer multiplicity $m \geq 1$ and is analytic in a small neighborhood of α. Then the function $h(x)$ and its derivatives up to order 3 evaluated at α has the following properties with $\theta_j = \frac{f^{(m+j)}(\alpha)}{f^{(m)}(\alpha)}, j \in \mathbb{N}$:

(i) $h(\alpha) = 0$

(ii) $h'(\alpha) = \frac{1}{m}$

(iii) $h''(\alpha) = -\frac{2}{m^2(m+1)}\theta_1$

(iv) $h^{(3)}(\alpha) = \frac{6}{m^3(m+1)}\left\{{\theta_1}^2 - \frac{2m}{m+2}\theta_2\right\}$

Corollary 2: Let f stated in Corollary 1 have a multiple root α with a given multiplicity $m \geq 1$. Let $z(x) = x - \mu h(x)$ and $h(x)$ be defined by Eq.(3). Then the following hold:

$$\left.\frac{d^k}{dx^k} f(z)\right|_{x=\alpha} = [f(z)]^{(k)}|_{x=\alpha}$$

$$= \begin{cases} 0, & if\ 0 \leq k \leq m-1 \\ f^{(m)}(\alpha)\cdot z'(\alpha)^m, & if\ k = m \\ f^{(m+1)}(\alpha)\cdot z'(\alpha)^{m+1} + f^{(m)}(\alpha)\frac{m(m+1)}{2}\cdot z'(\alpha)^{m-1} z''(\alpha), & if\ k = m+1 \\ f^{(m+2)}(\alpha)\cdot z'(\alpha)^{m+2} + f^{(m+1)}(\alpha)\frac{(m+1)(m+2)}{2}\cdot z'(\alpha)^m z''(\alpha) & \\ \quad + f^{(m)}(\alpha)\cdot L_{m+2}(\alpha), & if\ k = m+2 \end{cases}$$

where $L_k = \binom{k}{3} t^{k-4}\{t\cdot(-\mu h''') + \frac{3}{4}(k-3)\mu^2 h''(\alpha)^2\}$.

2.. CONVERGENCE ANALYSIS

We establish some relationships between $\lambda, m, g'(\alpha)$, $g''(\alpha)$ and $g'''(\alpha)$, for maximum order of convergence[9,10,11].

We rewrite Eq.(2) into

$$(g - x)\cdot f'(x) = -\lambda f(z). \tag{7}$$

where $f = f(x), f' = f'(x)$ and $z = x - \mu h(x)$ are used for concise and the symbol $'$ denotes the derivative with respect to x.

Differentiating both sides of Eq(7) with respect to x, we obtain

$$(g' - 1)\cdot f' + (g - x)\cdot f''(x) = -\lambda[f(z)]^{(1)} \tag{8}$$

ISBN: 978-1-61804-225-5

Since g' is continuous at α, we have

$$g'(x)-1=\begin{cases} F_1(x), & if\ x\neq\alpha \\ \lim_{x\to\alpha}F_1(x), & if\ x=\alpha, \end{cases} \quad (9)$$

where $F_1(x)=-(g-x)f''(x)-\lambda[f(z)]^{(1)}/f'$.
Using Corollary 2 and $g(\alpha)=\alpha$, we have the following:

$$(g-x)f''(x)]_{x=\alpha}^{(k)} = \begin{cases} 0, & if\ 0\le k\le m-2, m\ge 2 \\ (m-1)(g'-1)f^{(m)}(\alpha), & if\ k=m-1, \end{cases} \quad (10)$$

$$[f(z)]^{(1)}\Big]_{x=\alpha}^{(k)} = \begin{cases} 0, & if\ 0\le k\le m-2,\ m\ge 2 \\ f^{(m)}(\alpha)(1-\frac{\mu}{m})^m, & if\ k=m-1, \end{cases} \quad (11)$$

Substituting Eq.(10) and Eq.(11) into Eq.(9), we have

$$g'(\alpha)-1=-(m-1)(g'(\alpha)-1)-\lambda(1-\frac{\mu}{m})^m$$

To obtain $g'(\alpha)=0$, we get

$$m=\lambda\left(1-\frac{\mu}{m}\right)^m=\lambda t^m \quad (12)$$

where $t^m=1-\frac{\mu}{m}$.
Differentiate both sides of Eq(8) with respect to x, we get

$$g''+2(g\prime-1)\cdot f''+(g-x)\cdot f^{(3)}=-\lambda[f(z)]^{(2)} \quad (13)$$

We rewrite

$$g''(x)=\begin{cases} F_2(x), & if\ x\neq\alpha \\ \lim_{x\to\alpha}F_2(x), & if\ x=\alpha, \end{cases} \quad (14)$$

where

$$F_2(x)=-2(g'-1)\cdot f''-(g-x)\cdot f^{(3)}-\lambda[f(z)]^{(2)}/f'.$$

We can get the numerator of $F_2(x)$ by computition similar to that done in $F_1(x)$

$$-2(g'-1)f''-(g-x)f^{(3)}-\lambda[f(z)]^{(2)} = \begin{cases} 0, & if\ 0\le k\le m-3 \\ f^{(m)}(\alpha)(m-\lambda t^m), & if\ k=m-2 \\ f^{(m+1)}(\alpha)[(m+1)-\lambda(t^{m+1}-t^m+t^{m-1})] & \\ -g''f^{(m)}(\alpha)\frac{(m+2)(m-1)}{2} & if\ k=m-1, \end{cases} \quad (15)$$

From Eq.(14) and Eq.(15), we get

$$g''=\frac{2\theta_1}{m(m+1)}\{(m+1)-\lambda(t^{m+1}-t^m+t^{m-1})\} \quad (16)$$

From Eq.(16), to have $g''(\alpha)=0$ we get the following relation,

$$m+1=\lambda(t^{m+1}-t^m+t^{m-1}) \quad (17)$$

Differentiate both sides of Eq.(13) with respect to x to obtain

$$g^{(3)}\cdot f'+3g''\cdot f''+3(g'-1)\cdot f^{(3)}+(g-x)\cdot f^{(4)}=-\lambda[f(z)]^{(3)}. \quad (18)$$

We rewrite

$$g^{(3)}(x)=\begin{cases} F_3(x), & if\quad x\neq\alpha \\ \lim_{x\to\alpha}F_3(x), & if\quad x=\alpha, \end{cases} \quad (19)$$

where

$$F_3(x)=-3g''f''-3(g'-1)f^{(3)}-(g-x)f^{(4)}-\lambda[f(z)]^{(3)}/f'\alpha=1.40449164821534$$

Hence, we have

$$-3g''f'']_{x=\alpha}^{(k)}-3(g'-1)f^{(3)}]_{x=\alpha}^{(k)}$$
$$-(g-x)f^{(4)}]_{x=\alpha}^{(k)}-\lambda[f(z)]^{(3)}]_{x=\alpha}^{(k)}$$

$$= \begin{cases} 0, & if\ 0\le k\le m-4 \\ f^{(m)}(\alpha)(m-\lambda t^m), & if\ k=m-3 \\ f^{(m+1)}(\alpha)\{m+1-\lambda(t^{m+1}-t^m+t^{m-1})\}, & if\ k=m-2 \\ -\frac{(m-1)(m^2+4m+6)}{6}g^{(3)}f^{(3)}+f^{(m+2)}(\alpha)(m+2) & \\ -\lambda\{f^{(m+2)}(\alpha)t^{m+2}-f^{(m+1)}(\alpha)\theta_1\frac{m+2}{m}(t^m-t^{m+1}) & \\ -f^{(m)}(\alpha)L_{m+2}(\alpha)\}, & if\ k=m-1, \end{cases} \quad (20)$$

Consequently, we have

$$g^{(3)}(\alpha)=\frac{6}{m(m+1)(m+2)}$$
$$\left[\theta_2(m+2)-\lambda\{\theta_2 t^{m+2}+{\theta_1}^2(t^m-t^{m+1})\frac{m+2}{m}+L_{m+2}(\alpha)\}\right]. \quad (21)$$

where $L_k=\binom{k}{3}t^{k-4}\{t\cdot(-\mu h''(\alpha))+\frac{3}{4}(k-3)\mu^2 h''(\alpha)^2\}$

Theorem 1: Let $f:\mathbb{C}\to\mathbb{C}$ have a zero α with integer multiplicity $m\ge 1$ and be analytic in a small neighborhood of α. Let θ_1,θ_2 be defined as in Corollary 1. Let t be a root of $\rho(t)$ defined in (20). Let x_0 be an initial guess chosen in a sufficiently small neighborhood of α. Then iteration method (2) with $\mu=m(1-t)$ has order 3 and its asymptotic error constant η as follows:

$$\eta=\frac{1}{6}|g^{(3)}(\alpha)|=\frac{1}{m(m+1)(m+2)}|\phi_1\theta_1^2+\phi_2\theta_2|,$$

where $\phi_1=-t^{m-2}\lambda q_1(t), \phi_2=m+2-\lambda t^{m-2}q_2(t)$, $q_1(t)=-\frac{(m+2)(t-1)^2\{2(m+1)t-m+1\}}{2m(m+1)}$ and $q_2(t)=t(t^3-2t+2)$.

3.. Numerical Results

In these experiments, we choose 300 as the minimum number of digits of precision by assigning *$MinPrecision=250* in Mathematica to obtain the specified nominal accuracy. We set the error bound ϵ to 0.5×10^{-235} for $\mid x_n-\alpha\mid<\epsilon$ and evaluate the n^{th} order derivative of the complicated nonlinear functions using the Mathematica[12] command ***D***[f, $\{x,n\}$].

As an example for the convergence, we investigate the order of convergence and the asymptotic error constant with a function $f(x)=\left\{x^{10}-\sqrt{3}x^3\cos(\pi x/6)+1/(x^2+1)\right\}(x-1)$ having a real zero $\alpha=1.0$ of multiplicity 2. We choose $x_0=0.92$ as an initial guess. Table 1 verifies cubic convergence. The computed asymptotic error constants are in sucessful agreement with theoretical asymptotic error constants η up to 10 significant digits. The computed root is rounded to be accurate up to the 235 significant digits.

Our analysis has been further confirmed through more test functions that are listed below:

$$f_1(x)=\cos x-x, \alpha=0.739085133215161$$
$$f_2(x)=(\sin^2 x-x^2+1)(\cos 2x+2x^2-3),$$

TABLE I
CONVERGENCE FOR

$$f(x) = \left\{x^{10} - \sqrt{3}x^3\cos(\pi x/6) + 1/(x^2+1)\right\}(x-1)$$

n	x_n	$\mid x_n - \alpha \mid$	$e_{n+1}/{e_n}^2$	η
0	0.920000000000000	0.800000		
1	0.991249484161490	0.0121355	1.367268100	3.033
2	0.999794338683744	0.000360502	2.685871931	54251
3	0.999999872081448	$3.35582 \times 1-^{-7}$	3.024323988	
4	0.999999999999950	2.91278×10^{-14}	3.033536758	
5	1.00000000000000	2.19446×10^{-27}	3.033542510	
6	1.00000000000000	1.24557×10^{-52}	3.033542510	
7	1.00000000000000	4.01279×10^{-104}	3.033542510	
8	1.00000000000000	4.16489×10^{-207}	3.033542510	
9	1.00000000000000	$-2.89905 \times 10^{-400}$		

TABLE II
CONVERGENCE FOR VARIOUS TEST FUNCTIONS.

$f(x)$	m	x_0	e_n	ν	η
$f_1(x)$	1	0.490	6.13024×10^{-293}	5	0.04875502284
$f_2(x)$	2	1.290	4.51173×10^{-253}	8	0.7835709502
$f_3(x)$	3	1.080	$0. \times 10^{-249}$	10	5.119146433
$f_4(x)$	4	2.190	1.18904×10^{-261}	8	0.5369302217
$f_5(x)$	5	2.270	2.41280×10^{-398}	9	1.11
$f_6(x)$	6	2.790	2.52653×10^{-359}	9	1.096153846
$f_7(x)$	7	2.590	1.92369×10^{-587}	10	3.591527519
$f_8(x)$	8	1.590	1.90760×10^{-308}	8	0.08249684013

$f_3(x) = (\sin(\pi x/2\sqrt{2}) - x^4 + 3)(x^2-2)^2$, $\alpha = \sqrt{2}$

$f_4(x) = (x^8 - 14x^4\sin(\pi x/4) - 32)(x^2 - 4x + 4)\log(x-1), \alpha = 2.00000000000000$

$f_5(x) = (3x^7 - 37x^4 + 208)\sin(\pi x/2)\log[x-1]^3$, $\alpha = 2.00000000000000$

$f_6(x) = (e^{(x^2+7x-30)} - 1)(x-3)\sin^4 \pi x/3$, $\alpha = 3.00000000000001$

$f_7(x) = (e^{-x}\sin x + \log[1 + (x-\pi)^2])(x-\pi)\sin^3 x(\log[x-\pi+1])^2, \alpha = \pi$

$f_8(x) = (x^2\sin(\pi x/8) + e^{(x-2)^2} - 1 - 2\sqrt{2})(x-2)^3\sin^4(\pi x/2), \alpha = 2.00000000000000$

Table 2 shows convergence behavior for the above test functions with the multiplicity m, the initial guess x_0, the least iteration number ν and the asymptotic error constant η. In the future study, we develop extended optimal iteration methods of higher order.

ACKNOWLEDGMENT

Young Hee Geum was supported by the National Research Foundation of Korea funded by the Ministry of Education, Science and Technology (Project No. 2011-0014638).

REFERENCES

[1] R. G. Bartle, *The Elements of Real Analysis*, 2nd ed., John Wiley & Sons., New York, 1976.
[2] Ward Cheney and David Kincaid, *Numerical Mathematics and Computing*, Brooks/Cole Publishing Company, Monterey, California 1980
[3] S. D. Conte and Carl de Boor, *Elementary Numerical Analysis*, McGraw-Hill Inc., 1980
[4] Qiang Du, Ming Jin, T. Y. Li and Z. Zeng, *"The Quasi-Laguerre Iteration"*, Mathematics of Computation, Vol. 66, No. 217(1997), pp.345-361.
[5] Y. H. Geum, *"The asymptotic error constant of leap-frogging Newtons method locating a simple real zero"*, Applied Mathematics of Computation, Vol. 66, No. 217(2007), pp.345-361.
[6] Y. K. Kim and Y. H. Geum, *" A cubic-order variant of Newton's method for finding multiple roots of nonlinear equations"*, Computer and Mathematics with Applications, Vol. 62(2011), pp.1634-1640
[7] A. Bathi Kasturiarachi, *"Leap-frogging Newton's Method"*, INT. J. MATH. EDUC. SCI. TECHNOL., Vol. 33, No. 4(2002), pp.521-527.
[8] L. D. Petkovic, M. S. Petkovic and D. Zivkovic, *"Hansen-Patrick's Family Is of Laguerre's Type"* , Novi Sad J. Math., Vol. 33, No. 1(2003), pp.109-115.
[9] Kenneth A. Ross, *Elementary Analysis*, Springer-Verlag New York Inc., 1980.
[10] J. Stoer and R. Bulirsh, *Introduction to Numerical Analysis*, pp.244-313, Springer-Verlag New York Inc., 1980.
[11] J. F. Traub, *Iterative Methods for the Solution of Equations*, Chelsea Publishing Company, 1982.
[12] Stephen Wolfram, *The Mathematica Book, 4th ed.*, Cambridge University Press, 1999.

Mathematical modeling of the evolution of the exterior boundary in spheroidal tumour growth

Foteini Kariotou, Panayiotis Vafeas, and Polycarpos K. Papadopoulos

***Abstract*—** The present paper concerns the formulation and the evolution of the non symmetrical growth of an avascular cancerous cell colony in an analytical mathematical fashion. Although most of the existing research considers spherical tumours, here we work in the frame of a more general case of the prolate spheroidal geometry. The tumour lies inside a host spheroidal shell which provides vital nutrients, receives the debris of the dead cells and also transmittes to the tumour the pressure imposed by the surrounding on its exterior boundary. Under the aim of studying the evolution of the exterior tumour boundary, we focus on the exterior conditions under which such a geometrical structure can be sustained. To that purpose, the corresponding nutrient concentration, the inhibitor concentration and the pressure field are calculated analytically providing the necessary data for the evolution equation to be solvable. It turns out that an avascular tumour can exhibit a prolate spheroidal growth only if the external conditions for the nutrient supply and the transversally isotropic pressure field have a specific form, which is consistent with the tumour evolution. Additionally, our model exhibits a geometrical reduction to special cases and, mainly, to the spherical geometry in order to recover the existing results for the sphere.

***Keywords*—**Mathematical modeling, boundary value problems, avascular tumour growth, prolate spheroidal geometry.

I. Introduction

CANCER tumour development inside a healthy tissue is an extremely complicated phenomenon that has drawn great multidiscipline scientific interest over the last century. A cancer tumour is a cell colony that grows, invading a healthy host tissue. Roughly speaking, it consists of cells that consume nutrients and proliferate many times before they die out of programmed death, called apoptosis or out of lack of nutrients, called necrosis. As a tumour grows, many different interrelated procedures take place, such as nutrient diffusion from the surrounding into the tumour, cell proliferation when the nutrient is enough and growth inhibition when either the nutrient is insufficient or an inhibitory substance is present. Supplementary, we may refer to several other processes such as cell death or disintegration, elastic interactions between the tumour tissue and the healthy tissue, as well as inner pressure effects. As the tumour develops it enjoys an avascular phase that corresponds to the stages right after tumorigenesis and ends with a steady state, where the tumour's volume gain, due to the new cancerous cells birth, balance the volume loss from the cells' death and disintegration. As the tumour's evolution proceeds, new phenomena, as angiogenesis, take place and the vascular phase begins, where the tumour develops a vascular net around it that provides the tumour cells with limitless nutrient supply and also it permits metastasis. As the present work focuses on the avascular phase on tumour evolution, we avoid presenting details on the proceeding phases, which can be found in the literature [1,2].

Mathematical modeling of avascular tumours has offered a great contribution in understanding the mechanisms involved with tumour growth. Since the initial construction of the basic analytical formulation [3,4], many mathematical models have been developed that investigate several aspects of tumour growth [1,5]. During the steady state, the avascular tumour is bounded in a sphere with an approximate diameter of 2mm. This feature justifies the consideration of spherical tumours in most of the related works, since in such small lengths, scale deviations from a spherical symmetry are not considered quantitatively significant. Moreover, tumours grown in vitro form spherical aggregates [3–7]. However, the theoretical and experimental analysis viewed in [8,9] has revealed that non–symmetric tumours may occur in a confined surrounding as a result of the pressure effects on the growing tissue. Such qualitative features that need to be addressed when the non symmetrical tumour growth is introduced, are reported in the [8–12] for several interesting cases of different geometries.

In this work, we study the evolution of the exterior tumour boundary, where the cancer colony is assumed to follow a prolate spheroidal structure. Within this frame, we search for the exact exterior conditions that can support such a model and secure its compatibility with both the physics and the geometry. In addition to most of the relative works that consider homogeneous exterior conditions in an infinite environment, we investigate the impact, on the tumour's evolution, of a transversally isotropic pressure field imposed from the immediate surrounding tissue on the growing tumour. It turns out that the nutrient field should be inhomogeneous and that only a special type of inhomogeneity is compatible with the particular evolution, under such pressure assumption. Since the evolution of the tumour depends on the balance between the enhancement and the inhibition of the cell proliferation which depends mainly on the available nutrient, on the present inhibitors and on the pressure impact, it is important to have an accurate mathematical model for the

Foteini Kariotou is with the School of Science and Technology, Hellenic Open University, 262 22, Patras, Greece (e-mail: kariotou@eap.gr).

Panayiotis Vafeas is with the Department of Chemical Engineering, University of Patras, 265 04 Patras, Greece (corresponding author to provide phone and fax: +30 2610 996872; e-mail: vafeas@chemeng.upatras.gr).

Polycarpos K. Papadopoulos is with the Department of Mechanical Engineering and Aeronautics, University of Patras, 265 04 Patras, Greece (e-mail: p.papadopoulos@des.upatras.gr).

ISBN: 978-1-61804-225-5

determination of those parameters in the interior of the tumour structure.

To this purpose–we consider a prolate spheroidal tumour that grows under the basic principles assumed in [4]. The tumour and the surrounding behave as incompressible fluids of different densities. The tumour receives nutrients by diffusion from its surrounding according to Fick's law, while the motility of the tumour cells is governed by a modification of Darcy's law. Our model concerns a fully developed tumour consisted of four regions, formed with respect to the nutrient and the inhibitor concentration levels. The dead cell debris form a necrotic core covered by a layer occupied by quiescent cells that do not have enough nutrient to proliferate. In the next layer the cells are also quiescent, but this is due to high inhibitor levels, even though the nutrient present is adequate to support proliferation. In the exterior tumour layer the nutrient concentration is high enough and the inhibitor concentration is low enough so that the cells there proliferate. All parts of the fully developed tumour are characterized by the same diffusion constant, while a physical interpretation detailed described in [11] allows us to work in the steady state conditions, since the diffusion time scale is significantly shorter than the growth time scale.

When the cancer tumour is avascular, the nutrient concentration, denoted by σ, is the primary parameter. The other two basic parameters of physical growth are the inhibitor concentration β and the pressure field P. To this end, we denote by σ_∞ the nutrient supply provided by the surrounding tissue and by P_∞ the pressure field imposed, in a form that attributes the characteristics of a transversally isotropic medium. Therein, cell life is sustained if $\sigma > \sigma_n^*$, while cell proliferation is possible if both $\sigma > \sigma_p^*$ and $\beta < \beta^*$ hold, where σ_n^*, σ_p^* and β^* are critical concentration values, which are characteristic of the host tissue. Then, the mathematical formulation of the nutrient, the inhibitor and the pressure field consists of boundary value problems joint together in a non–linear ordinary differential equation, which describes the tumour evolution. The analytical manipulation of the Poisson's and the Laplace's partial differential equations in combination with the application of appropriate boundary conditions at every compartment's interface, in order to obtain all the aforementioned fields, is mostly based on classical analytical techniques mainly drawn from references [13,14].

In section II the prolate spheroidal geometry of our model is postulated and the avascular tumour's domains with their boundaries are strictly defined. The corresponding boundary value problems in the prolate spheroidal coordinate system are stated in sections III and IV along with their implementation. In details, the analytical solution to obtain the nutrient and the inhibitor concentration is included in section III, while in section IV we derive the pressure field. In section V the evolution equation of the tumour's exterior boundary is provided and the conditions, which secure self–consistency of the mathematical problem, are obtained. These conditions provide one of the paper's main results on supporting a prolate spheroidal avascular growth. In addition, section VI is devoted to a geometrical reduction of the results drawn in this work into special cases and the corresponding spherical model in order to obtain the already known results for the spherical case. Finally, in section VII there is an outline of our work, which recapitulates the main points as a brief conclusion.

II. Statement of the Problem

Let us consider a fully developed avascular tumour that grows maintaining all its boundary surfaces as confocal prolate spheroids. Therefore, given the fixed positive number $c > 0$, which denotes the semifocal distance of the prolate spheroidal system, we set the transformed prolate spheroidal coordinates (τ, ζ, ϕ) with semi–axes $a_1 = a_2 = c\sqrt{\tau^2 - 1}$ and $a_3 = c\tau$, which are connected to the Cartesian coordinates $\mathbf{r} = (x_1, x_2, x_3)$ via the relations [13]

$$x_1 = c\sqrt{\tau^2 - 1}\sqrt{1 - \zeta^2}\cos\phi, \tag{1}$$

$$x_2 = c\sqrt{\tau^2 - 1}\sqrt{1 - \zeta^2}\sin\phi \tag{2}$$

and

$$x_3 = c\tau\zeta, \tag{3}$$

where the corresponding variables run within the intervals $\tau \geq 1$, $\zeta \in [-1,1]$ and $\phi \in [0, 2\pi)$.

For such ζ and ϕ, the tumour's compartments are defined so as to correspond to successive intervals of the prolate variable τ. In such terms, the tumour consists of a necrotic core Ω_n, defined for every $\tau \in [1, \tau_n)$, where $0 < \sigma < \sigma_n^*$, surrounded by a quiescent layer Ω_q, where $\tau \in (\tau_n, \tau_q)$ that is occupied by hypoxic cells, which are alive, but are not able to proliferate, since $0 < \sigma_n^* < \sigma < \sigma_p^*$. In the subsequent layer there is enough nutrient to support proliferation but there is too much inhibitor concentration present to allow division, namely Ω_{p_-}, for $\tau \in (\tau_q, \tau_{p_-})$. In the next confocal layer denoted as Ω_{p_+}, for $\tau \in (\tau_{p_-}, \tau_{p_+})$ cell proliferation takes place, since $\sigma > \sigma_p^*$ and $\beta < \beta^*$. Finally, the compartment of the normal host tissue Ω_e with $\tau \in (\tau_{p_+}, \tau_e)$ is strongly affected by the cancerous mass growth. The interfaces between the successive compartments are denoted by S_j for $j = n, q, p-, p+$. On the exterior surface S_e, the surrounding provides nutrient in the general form

$$\sigma_\infty(\mathbf{r}_e) = \sum_{l=0}^{\infty} \sigma_{\infty,l}(\tau_e) P_l(\zeta) \text{ for every } \zeta \in [-1,1] \tag{4}$$

and impose a pressure field

$$\mathrm{P}_\infty(\mathbf{r}_e) = \mathrm{p}_\infty(\tau_e)\left[1 + a\left(1 - \zeta^2\right)\right] \text{ for every } \zeta \in [-1,1], \tag{5}$$

where the nutrient parameters $\sigma_{\infty,l}(\tau_e)$ for $l \geq 0$ and the pressure parameter $\mathrm{p}_\infty(\tau_e)$ are subject to the exterior conditions. The constant $a > 0$ adapts the exterior pressure in a form that attributes the special characteristics of the prolate spheroidal tumour. Here, the functions P_l for $l \geq 0$, stand for the Legendre functions of the first kind [14].

Our goal is the solution of proper boundary value problems within the aforementioned domains, in order to obtain the basic fields, i.e. the nutrient and the inhibitor concentration, as well as the pressure field in a closed analytical form in terms of the data (4) and (5). Once done, we proceed to the evolution equation of the tumour's exterior boundary.

III. Nutrient and Inhibitor Concentration

As both the nutrient and the inhibitor diffuse inward to or outward from the tumour, respectively, their distribution is described by standard parabolic partial differential equations, as it is shown in details in [11]. Though, it is a common assumption [3,4] that as the diffusion time scale is significantly shorter than the growth time scale, the chemicals maintain a diffusive equilibrium state. Therein, the partial differential equations for the nutrient and for the inhibitor concentration, become

$$\Delta\sigma(\mathbf{r}) = \gamma_j \text{ for every } \mathbf{r} \in \Omega_j,\ j = n, q, p_-, p_+, e \qquad (6)$$

and

$$\Delta\beta(\mathbf{r}) = p_j \text{ for every } \mathbf{r} \in \Omega_j,\ j = n, q, p_-, p_+, e, \qquad (7)$$

respectively, where each physical constant γ_j and p_j denotes the consumption rate, or production rate, as the case may be, normalized by the well–known diffusion constants k_σ and k_β, respectively, at the corresponding region.

Here, we have assumed that as long as the cell remains in a certain phase of its cycle, its needs in nutrients are unaltered, no matter the availability on them. Therefore, we may suggest that all cells occupying the same tumour region have the same constant consumption rate, while the transmission from one region to another results to a discontinuous and instant change in the consumption rate, modeled by means of a step function. The same argumentation is followed for the inhibitor. In particular, the nutrient diffuses inward to the tumour and it is consumed at a rate γ_j that depends on the vital state of the cells and reflects the corresponding phase of the cell cycle, while, on the contrary, the inhibitor diffuses outward to the tumour and it is produced at a rate p_j. Obviously, $\gamma_n = 0$ as Ω_n is occupied by necrotic debris and $\gamma_q \neq 0$, since the cells in Ω_q are quiescent but alive. On the other hand, it is valid that $\gamma_{p_-} = \gamma_{p_+} := \gamma_p \geq \gamma_q$, since the cells in both Ω_{p_-} and Ω_{p_+} are in a more active state and, finally, $\gamma_e \geq \gamma_q$ but γ_e can be either grater or lower than γ_p depending on the kind of the healthy tissue in which the tumour grows. Probably, the suggestion of $\gamma_e \leq \gamma_p$ has a physical reasoning due to the greater demands of the much longer proliferation phase of the cancerous cell cycle compared to the normal cell cycle. However, without loss of generality and in order to make our calculations simpler, we assume that $\gamma_e = 0$. Under similar physical considerations as previously stated, we may refer to the inhibitor's physical constants and claim that $p_n \neq 0$ and $p_q = p_{p_-} = p_{p_+} := p_L$, while $p_e = 0$. Here, we complete with the position of the partial differential equations.

Both the nutrient and the inhibitor fields are regular at zero and continuous on each S_j for $j = n, q, p_-, p_+, e$ as well. Their normal derivatives must be also continuous on each boundary [11]. In terms of the outward unit normal vector $\hat{\boldsymbol{\tau}}$ and by definition [13] of the $\hat{\boldsymbol{\tau}}$–directional derivative in the prolate spheroidal coordinates, which reads as

$$\hat{\boldsymbol{\tau}} \cdot \nabla = \frac{\sqrt{\tau^2 - 1}}{c\sqrt{\tau^2 - \zeta^2}} \frac{\partial}{\partial \tau} \text{ for } \tau \in [1, \tau_e] \text{ and } \zeta \in [-1,1], \qquad (8)$$

it is readily seen that the boundary conditions to be satisfied for every $\zeta \in [-1,1]$ and $\phi \in [0, 2\pi)$ yield

$$\sigma(\tau_i, \zeta, \phi) = \sigma(\tau_j, \zeta, \phi) \text{ with } i, j = n, q, p_-, p_+, e \qquad (9)$$

and

$$\frac{\partial\sigma(\tau_i, \zeta, \phi)}{\partial\tau} = \frac{\partial\sigma(\tau_j, \zeta, \phi)}{\partial\tau} \text{ with } i, j = n, q, p_-, p_+, e \qquad (10)$$

for the nutrient concentration, while

$$\beta(\tau_i, \zeta, \phi) = \beta(\tau_j, \zeta, \phi) \text{ with } i, j = n, q, p_-, p_+, e \qquad (11)$$

and

$$\frac{\partial\beta(\tau_i, \zeta, \phi)}{\partial\tau} = \frac{\partial\beta(\tau_j, \zeta, \phi)}{\partial\tau} \text{ with } i, j = n, q, p_-, p_+, e \qquad (12)$$

for the inhibitor concentration, provided that always $\tau_j > \tau_i$. Conditions (9) and (10) are supplemented by the nutrient supply (4), i.e.,

$$\sigma(\tau_e, \zeta, \phi) = \sum_{l=0}^{\infty} \sigma_{\infty,l}(\tau_e) P_l(\zeta) \text{ for every } \zeta \in [-1,1]. \qquad (13)$$

Moreover, on the boundaries S_n and S_q the critical values are met, a fact that will be especially useful in Section V.

Applying the standard method of separation of variables in every compartment Ω_j for $j = n, q, p-, p+, e$, we solve the Laplace's and the Poisson's equations (6)–(7) and we perform some tedious but straightforward calculations, which are based on the proper application of the aforementioned boundary conditions (9)–(13 The results are obtained in a closed compact fashion in terms of the Heaviside function

$$H(\tau - \tau_j) = \begin{cases} 1, & \tau \geq \tau_j \\ 0, & \tau < \tau_j \end{cases} \text{ with } j = n, q, p_-, p_+ \qquad (14)$$

and accordingly to the notation for $j, k = n, q, p_-, p_+, e$ and $l, m = 0, 1, 2, \ldots$, provided by

$$E_{0,k}^{l,m} := E_{0,k}^{l,m}(\tau) = P_l(\tau) Q_m'(\tau_k) - Q_l(\tau) P_m'(\tau_k) \qquad (15)$$

and

$$W_{0,k}^{l,m} := W_{0,k}^{l,m}(\tau) = P_l(\tau) Q_m'(\tau_k) - P_l'(\tau) Q_m(\tau_k), \qquad (16)$$

where

$$E_{j,k}^{l,m} := E_{0,k}^{l,m}(\tau_j) \text{ and } W_{j,k}^{l,m} := W_{0,k}^{l,m}(\tau_j), \qquad (17)$$

written in view of the Legendre functions of the first P_l and of the second Q_l kind [14]. Let us notice that the prime denotes derivation with respect to the argument, while all the fields are taken at $\mathbf{r} = (\tau, \zeta, \phi)$ with $\tau \in [1, \tau_e)$, $\zeta \in [-1,1]$ and $\phi \in [0, 2\pi)$.

Then, the nutrient concentration yields

$$\sigma(\mathbf{r})=\frac{c^2}{9}\left\{\gamma_q\left[\frac{W^{2,0}_{n,n}}{Q_0'(\tau_n)}-\frac{W^{2,0}_{q,q}}{Q_0'(\tau_q)}+Q_0(\tau_e)\left(\frac{P_2'(\tau_n)}{Q_0'(\tau_n)}-\frac{P_2'(\tau_q)}{Q_0'(\tau_q)}\right)\right]\right.$$
$$\left.+\gamma_p\left[\frac{W^{2,0}_{q,q}}{Q_0'(\tau_q)}-\frac{W^{2,0}_{p_+,p_+}}{Q_0'(\tau_{p_+})}+Q_0(\tau_e)\left(\frac{P_2'(\tau_q)}{Q_0'(\tau_q)}-\frac{P_2'(\tau_{p_+})}{Q_0'(\tau_{p_+})}\right)\right]\right\}$$
$$-\frac{c^2}{9}\left[-\gamma_q\frac{E^{2,2}_{e,n}}{W^{2,2}_{n,n}}+(\gamma_q-\gamma_p)\frac{E^{2,2}_{e,q}}{W^{2,2}_{q,q}}+\gamma_p\frac{E^{2,2}_{e,p_+}}{W^{2,2}_{p_+,p_+}}\right]\frac{P_2(\tau)}{P_2(\tau_e)}P_2(\zeta)$$
$$+\sum_{l=0}^{\infty}\sigma_{\infty,l}(\tau_e)\frac{P_l(\tau)}{P_l(\tau_e)}P_l(\zeta)$$
$$+H(\tau-\tau_n)\frac{c^2}{9}\gamma_q\left[P_2(\tau)-P_2(\tau_n)-\frac{P_2'(\tau_n)}{Q_0'(\tau_n)}\big(Q_0(\tau)-Q_0(\tau_n)\big)\right.$$
$$\left.+\left(1-\frac{E^{2,2}_{0,n}}{W^{2,2}_{n,n}}\right)P_2(\zeta)\right]$$
$$-H(\tau-\tau_q)\frac{c^2}{9}(\gamma_q-\gamma_p)\left[P_2(\tau)-P_2(\tau_q)-\frac{P_2'(\tau_q)}{Q_0'(\tau_q)}\big(Q_0(\tau)-Q_0(\tau_q)\big)\right.$$
$$\left.+\left(1-\frac{E^{2,2}_{0,q}}{W^{2,2}_{q,q}}\right)P_2(\zeta)\right]$$
$$-H(\tau-\tau_{p_+})\frac{c^2}{9}\gamma_p\left[P_2(\tau)-P_2(\tau_{p_+})-\frac{P_2'(\tau_{p_+})}{Q_0'(\tau_{p_+})}\big(Q_0(\tau)-Q_0(\tau_{p_+})\big)\right.$$
$$\left.+\left(1-\frac{E^{2,2}_{0,p_+}}{W^{2,2}_{p_+,p_+}}\right)P_2(\zeta)\right]. \quad (18)$$

Similarly, for the inhibitor concentration we derive

$$\beta(\mathbf{r})=\frac{c^2}{9}\left[(p_L-p_n)\frac{W^{2,0}_{n,n}}{Q_0'(\tau_n)}-p_L\frac{W^{2,0}_{p_+,p_+}}{Q_0'(\tau_{p_+})}+p_nP_2(\tau)\right]$$
$$+\frac{c^2}{9}\left\{\left[(p_L-p_n)\frac{Q_2'(\tau_n)}{W^{2,2}_{n,n}}-p_L\frac{Q_2'(\tau_{p_+})}{W^{2,2}_{p_+,p_+}}\right]P_2(\tau)+p_n\right\}P_2(\zeta)$$
$$+H(\tau-\tau_n)\frac{c^2}{9}(p_L-p_n)\left[P_2(\tau)-P_2(\tau_n)-\frac{P_2'(\tau_n)}{Q_0'(\tau_n)}\big(Q_0(\tau)-Q_0(\tau_n)\big)\right.$$
$$\left.+\left(1-\frac{E^{2,2}_{0,n}}{W^{2,2}_{n,n}}\right)P_2(\zeta)\right]$$
$$-H(\tau-\tau_{p_+})\frac{c^2}{9}p_L\left[P_2(\tau)-P_2(\tau_{p_+})-\frac{P_2'(\tau_{p_+})}{Q_0'(\tau_{p_+})}\big(Q_0(\tau)-Q_0(\tau_{p_+})\big)\right.$$
$$\left.+\left(1-\frac{E^{2,2}_{0,p_+}}{W^{2,2}_{p_+,p_+}}\right)P_2(\zeta)\right], \quad (19)$$

where it is verified that both (18) and (19), satisfy (6) and (7), respectively and boundary conditions (9)–(13), as well.

IV. Pressure Field

The pressure field is imposed by the host boundary, along with the net cell gain. By combination of previous assumptions [4,5], which attribute the cells to the pressure gradient, as it is dictated by the Darcy law, we further assume that cells exhibit an active chemotactic movement [11] and move towards the direction of the nutrient gradient and opposite to the direction of the pressure and of the inhibitor gradients. In other words, we assume that the velocity of the tumour cells inside Ω_j with $j=n,q,p-,p+,e$ is given by

$$\mathbf{v}_j(\mathbf{r})=-\mu_P\nabla \mathrm{P}(\mathbf{r})+\mu_\sigma\nabla\sigma(\mathbf{r})-\mu_\beta\nabla\beta(\mathbf{r}) \text{ for } \mathbf{r}\in\Omega_j, \quad (20)$$

where μ_P, μ_σ and μ_β are proportionality constants, which characterize the motility of the cell. Applying the divergence operator on both sides of (20) and implying (6) and (7) we obtain

$$\Delta \mathrm{P}(\mathbf{r})=F_j \text{ for } \mathbf{r}\in\Omega_j \text{ with } j=n,q,p-,p+,e, \quad (21)$$

where

$$F_j := -G_j/\mu_P+\mu_\sigma\gamma_j/\mu_P-\mu_\beta p_j/\mu_P, \quad (22)$$

and $G_j := \nabla\cdot\mathbf{v}_j$ denote the mass per unit volume, per unit time that is produced or lost in the region Ω_j, normalized by the tissue's density [11]. Easy physical argumentations allow us to consider $F_q=F_{p_-}$, $F_{p_+}:=F_p$ and $F_e=0$.

The boundary conditions that will complement the partial differential equations (21) with (22) and provide uniqueness to the corresponding Boundary Value Problems–follow from the consideration that the pressure and its normal derivative must be regular at the origin and, moreover, they definitely should be continuous on the boundaries S_j for $j=n,q,p_-$, that is for $\zeta\in[-1,1]$ and $\phi\in[0,2\pi)$

$$\mathrm{P}(\tau_i,\zeta,\phi)=\mathrm{P}(\tau_j,\zeta,\phi) \text{ with } i,j=n,q,p_- \quad (23)$$

and

$$\frac{\partial \mathrm{P}(\tau_i,\zeta,\phi)}{\partial\tau}=\frac{\partial \mathrm{P}(\tau_j,\zeta,\phi)}{\partial\tau} \text{ with } i,j=n,q,p_-, \quad (24)$$

provided that $\tau_j>\tau_i$. On the other hand, since the tumour, the affected compartment and the host tissue are considered to be fluids of different phase, then the corresponding boundary conditions on S_{p_+} and S_e follow the Young–Laplace law for the case of two–face incompressible fluids. Thus,

$$\lim_{\tau\to\tau_j^-}\mathrm{P}(\mathbf{r})-\lim_{\tau\to\tau_j^+}\mathrm{P}(\mathbf{r})=\alpha_jJ(\mathbf{r}_j) \text{ with } j=p_+,e, \quad (25)$$

where J stands for the prolate spheroid's mean curvature and $\alpha_{p_+},\alpha_e\in\mathbb{R}$, while the pressure field's trace on the exterior surface at S_e is provided via (5), in the form

$$\lim_{\tau\to\tau_e^+}\mathrm{P}(\tau,\zeta,\phi)=\mathrm{P}_\infty(\tau_e,\zeta,\phi)=\mathrm{p}_\infty(\tau_e)\left[1+a\left(1-\zeta^2\right)\right] \quad (26)$$

for every $\zeta\in[-1,1]$ and $\phi\in[0,2\pi)$. In order to apply the boundary conditions (25), we expand function J in Legendre series. Hence, by virtue of a geometrical analysis of our system, the definition of the mean curvature in the prolate geometry results to

$$J(\tau,\zeta,\phi)=-\frac{\tau}{2c\sqrt{\tau^2-1}}\frac{1-2\tau^2+\zeta^2}{\sqrt{\left(\tau^2-\zeta^2\right)^3}}=\sum_{l=0}^{\infty}j_l(\tau)P_l(\zeta), \quad (27)$$

evaluated at $\tau=\tau_{p_+},\tau_e$ for every $\zeta\in[-1,1]$ and $\phi\in[0,2\pi)$. It can be easily verified that for $l\geq 0$,

$$j_{2l}(\tau)=\frac{\tau}{2c\sqrt{\tau^2-1}}\left[\left(2\tau^2-1\right)a_{2l}(\tau)-b_{2l}(\tau)\right], \tag{28}$$

corresponding to the even part and

$$j_{2l+1}(\tau)=0, \tag{29}$$

for the odd part, in terms of the complicated but practical notations

$$a_{2l}(\tau)=\frac{4l+1}{2^l\sqrt{\tau^2-1}}\sum_{k=0}^{l}\frac{(-1)^k(2l-2k-1)!!}{k!(l-k)!(2l-2k-2)!!}\times\left[\sqrt{\tau^{2l-2k}}+\sum_{m=0}^{l-k-2}\tau^{2m}\frac{(2l-2k-2m)!!}{(2l-2k-2m-1)!!}\right] \tag{30}$$

and

$$b_{2l}(\tau)=\frac{4l+1}{2^l\sqrt{\tau^2-1}}\sum_{k=0}^{l}\frac{(-1)^k(2l-2k+1)!!}{k!(l-k)!(2l-2k)!!}\times\left[\sqrt{\tau^{2l-2k}}+\sum_{m=0}^{l-k-1}\tau^{2m}\frac{(2l-2k-2m)!!}{(2l-2k-2m+3)!!}\right]. \tag{31}$$

Therefore, the pressure field that solves the boundary value problem (21)–(26) with the aid of definitions (26)–(31) at $\mathbf{r}=(\tau,\zeta,\phi)$ with $\tau\in[1,\tau_e)$, $\zeta\in[-1,1]$ and $\phi\in[0,2\pi)$, assumes the form

$$\begin{aligned}\mathrm{P}(\mathbf{r})=\frac{2}{3}\mathrm{p}_\infty(\tau_e)&\left[\left(a+\frac{3}{2}\right)-a\frac{P_2(\tau)}{P_2(\tau_e)}P_2(\zeta)\right]+\frac{c^2}{9}\left\{F_n\left(P_2(\tau)+P_2(\zeta)\right)\right.\\&-\left(F_n-F_q\right)\frac{E^{2,0}_{n,n}+P_2'(\tau_n)\left(Q_0(\tau_e)-Q_0(\tau_n)\right)}{Q_0'(\tau_n)}\\&-\left(F_q-F_p\right)\frac{E^{2,0}_{p_-,p_-}+P_2'(\tau_{p_-})\left(Q_0(\tau_e)-Q_0(\tau_{p_-})\right)}{Q_0'(\tau_{p_-})}\\&\left.-F_p\frac{E^{2,0}_{p_+,p_+}+P_2'(\tau_{p_+})\left(Q_0(\tau_e)-Q_0(\tau_{p_+})\right)}{Q_0'(\tau_{p_+})}\right\}\\&-\frac{c^2}{9}\left[\left(F_n-F_q\right)\frac{E^{2,2}_{e,n}}{W^{2,2}_{n,n}}+\left(F_q-F_p\right)\frac{E^{2,2}_{e,p_-}}{W^{2,2}_{p_-,p_-}}+F_p\frac{E^{2,2}_{e,p_+}}{W^{2,2}_{p_+,p_+}}\right]\frac{P_2(\tau)}{P_2(\tau_e)}P_2(\zeta)\\&+\sum_{l=0}^{\infty}\left[\alpha_e j_l(\tau_e)+\alpha_{p_+}j_l(\tau_{p_+})\frac{E^{l,l}_{e,p_+}}{W^{l,l}_{p_+,p_+}}\right]\frac{P_l(\tau)}{P_l(\tau_e)}P_l(\zeta)\\&-H(\tau-\tau_n)\frac{c^2}{9}\left(F_n-F_q\right)\left[P_2(\tau)-P_2(\tau_n)-\frac{P_2'(\tau_n)}{Q_0'(\tau_n)}\left(Q_0(\tau)-Q_0(\tau_n)\right)\right.\\&\left.+\left(1-\frac{E^{2,2}_{0,n}}{W^{2,2}_{n,n}}\right)P_2(\zeta)\right]\\&-H(\tau-\tau_{p_-})\frac{c^2}{9}\left(F_q-F_p\right)\left[P_2(\tau)-P_2(\tau_{p_-})-\frac{P_2'(\tau_{p_-})}{Q_0'(\tau_{p_-})}\left(Q_0(\tau)-Q_0(\tau_{p_-})\right)\right.\\&\left.+\left(1-\frac{E^{2,2}_{0,p_-}}{W^{2,2}_{p_-,p_-}}\right)P_2(\zeta)\right]\end{aligned}$$

$$\begin{aligned}&-H(\tau-\tau_{p_+})\left\{\frac{c^2}{9}F_p\left[P_2(\tau)-P_2(\tau_{p_+})-\frac{P_2'(\tau_{p_+})}{Q_0'(\tau_{p_+})}\left(Q_0(\tau)-Q_0(\tau_{p_+})\right)\right.\right.\\&\left.\left.+\left(1-\frac{E^{2,2}_{0,p_+}}{W^{2,2}_{p_+,p_+}}\right)P_2(\zeta)\right]\right.\\&\left.+\alpha_{p_+}\sum_{l=0}^{\infty}j_l(\tau_{p_+})\frac{E^{l,l}_{0,p_+}}{W^{l,l}_{p_+,p_+}}P_l(\zeta)\right\}.\end{aligned} \tag{32}$$

It is easily verified that, after some trivial calculations, expression (32), satisfies (21) and the boundary conditions (23)–(26), as well.

V. Evolution Equation

The aim of this work is to determine the evolution of the tumour's exterior boundary S_{p_+} under the assumption that it evolves normally to itself, so as to remain a confocal prolate spheroid throughout the tumour's development. Considering that the velocity of the cells on the exterior boundary is set to be

$$\mathbf{v}_{p_+}(\mathbf{r}_{p_+})=\frac{d\mathbf{r}_{p_+}}{dt}, \tag{33}$$

then equation (20) results to the following relationship in terms of $\hat{\boldsymbol{\tau}}$ [14], i.e.,

$$\hat{\boldsymbol{\tau}}\cdot\frac{d\mathbf{r}_{p_+}}{dt}=\hat{\boldsymbol{\tau}}\cdot\left[-\mu_P\nabla\mathrm{P}(\mathbf{r}_{p_+})+\mu_\sigma\nabla\sigma(\mathbf{r}_{p_+})-\mu_\beta\nabla\beta(\mathbf{r}_{p_+})\right]. \tag{34}$$

Then, since $\mathbf{r}_{p_+}=(\tau_{p_+},\zeta,\phi)$ for $\zeta\in[-1,1]$, $\phi\in[0,2\pi)$ and in view of (8), we obtain

$$c^2\frac{\tau_{p_+}^2-\zeta^2}{\tau_{p_+}^2-1}\frac{d\tau_{p_+}}{dt}=\frac{\partial}{\partial\tau}\left(-\mu_P\mathrm{P}(\mathbf{r}_{p_+})+\mu_\sigma\sigma(\mathbf{r}_{p_+})-\mu_\beta\beta(\mathbf{r}_{p_+})\right). \tag{35}$$

We, now, proceed by substituting the results (18), (19) and (32) evaluated on $S_{p_+}:\tau=\tau_{p_+}$, in (35) and we expand both its sides in Legendre series. Next, we use standard orthogonality properties of Legendre functions [14] to arrive at a system of equations with two outcomes.

Firstly, the system is self–consistent for every $\zeta\in[-1,1]$ and $\phi\in[0,2\pi)$ if the externally supplied nutrient has the particular form

$$\begin{aligned}\sigma(\tau_e,\zeta,\phi)=\sigma_{\infty,0}(\tau_e)&+\sigma_{\infty,2}(\tau_e)P_2(\zeta)\\&+\sum_{\substack{l=1\\l\neq 2}}^{\infty}\frac{\mu_P}{\mu_\sigma}\left(\alpha_e j_l(\tau_e)+\alpha_{p_+}j_l(\tau_{p_+})\frac{E^{l,l}_{e,p_+}}{W^{l,l}_{p_+,p_+}}\right)P_l(\zeta),\end{aligned} \tag{36}$$

where the term $\sigma_{\infty,0}(\tau_e)$ is arbitrary and it is conveniently chosen accordingly to the particular physical requirements of every problem, while

$$\begin{aligned}\sigma_{\infty,2}(\tau_e)=\frac{\mu_P}{\mu_\sigma}\frac{2a}{3}\mathrm{p}_\infty(\tau_e)&-\frac{\mu_P}{\mu_\sigma}\left(\alpha_e j_2(\tau_e)+\alpha_{p_+}j_2(\tau_{p_+})\frac{E^{2,2}_{e,p_+}}{W^{2,2}_{p_+,p_+}}\right)\\&+\frac{c^2}{9}f(\tau_n,\tau_q,\tau_{p_-},\tau_{p_+},\tau_e),\end{aligned} \tag{37}$$

while by definition

$$f\left(\tau_n,\tau_q,\tau_{p_-},\tau_{p_+},\tau_e\right)=\Bigg(\mu_P\left(F_n-F_q\right)+\mu_\sigma\gamma_q$$
$$-\mu_\beta\left(p_L-p_n\right)\Bigg)\left[\frac{E^{2,2}_{e,p_+}}{E^{2,2}_{n,n}}-\frac{E^{2,0}_{e,p_+}}{E^{2,0}_{p_+,n}}\right]\frac{P_2'\left(\tau_n\right)}{P_2'\left(\tau_{p_+}\right)}$$
$$-\mu_\sigma\left(\gamma_q-\gamma_p\right)\left[\frac{E^{2,2}_{e,p_+}}{E^{2,2}_{q,q}}-\frac{E^{2,0}_{e,p_+}}{E^{2,0}_{p_+,q}}\right]\frac{P_2'\left(\tau_q\right)}{P_2'\left(\tau_{p_+}\right)}$$
$$+\mu_P\left(F_q-F_p\right)\left[\frac{E^{2,2}_{e,p_+}}{E^{2,2}_{p_-,p_-}}-\frac{E^{2,0}_{e,p_+}}{E^{2,0}_{p_+,p_-}}\right]\frac{P_2'\left(\tau_{p_-}\right)}{P_2'\left(\tau_{p_+}\right)}$$
$$+\left(\mu_PF_p-\mu_\sigma\gamma_p+\mu_\beta p_L\right)\left[\frac{E^{2,2}_{e,p_+}}{E^{2,2}_{p_+,p_+}}-\frac{E^{2,0}_{e,p_+}}{E^{2,0}_{p_+,p_+}}\right]$$
$$-\mu_\beta\left[\left(p_L-p_n\right)\frac{P_2'\left(\tau_n\right)}{P_2'\left(\tau_{p_+}\right)}-p_L\frac{E^{2,2}_{n,n}}{E^{2,2}_{p_+,p_+}}\right]\frac{Q_2\left(\tau_e\right)P_2'\left(\tau_{p_+}\right)}{E^{2,2}_{n,n}}\Bigg\}.\quad(38)$$

Secondly, we derive the evolution equation of the exterior tumour boundary S_{p_+} at $\tau=\tau_{p_+}$, that is

$$\frac{d\tau_{p_+}}{dt}=\frac{1}{\left(3\tau^2_{p_+}-1\right)}\Bigg[\left(-\mu_P\left(F_n-F_q\right)-\mu_\sigma\gamma_q+\mu_\beta\left(p_L-p_n\right)\right)\tau_n\left(\tau_n^2-1\right)$$
$$+\mu_\sigma\left(\gamma_q-\gamma_p\right)\tau_q\left(\tau_q^2-1\right)-\mu_P\left(F_q-F_p\right)\tau_{p_-}\left(\tau^2_{p_-}-1\right)$$
$$+\left(-\mu_PF_p+\mu_\sigma\gamma_p-\mu_\beta p_L\right)\tau_{p_+}\left(\tau^2_{p_+}-1\right)\Bigg].\quad(39)$$

It is obvious that relationship (39) is an ordinary differential equation with respect to the function $\tau_{p_+}=\tau_{p_+}(t)$, where the uniqueness of its solution is secured by the initial condition $\tau_{p_+}(0)=T_{p_+}$, T_{p_+} being the initial radial prolate spheroidal variable of the S_{p_+} boundary. Moreover, the right hand–side of (39) depends on the time dependent boundaries at $\tau_n(t)$, $\tau_q(t)$, $\tau_{p_-}(t)$ and $\tau_{p_+}(t)$. Hence, equation (39) is solvable under constraints, which interrelate these boundaries and secure that (39) is dependent only on $\tau_{p_+}(t)$.

These constraints are provided by the critical values of the nutrient and inhibitor concentrations. In particular, the critical nutrient value σ_n^* determines if a cell dies out of starvation or not, so this value is met on the surface S_n, that is

$$\sigma_q\left(\mathbf{r}_n\right)=\sigma_n\left(\mathbf{r}_n\right)=\sigma_n^*\ \text{with}\ \mathbf{r}_n=\left(\tau_n,\zeta,\phi\right)\quad(40)$$

for every $\zeta\in[-1,1]$ and $\phi\in[0,2\pi)$. The nutrient σ_p^* and the inhibitor β^* value determine if a cell proliferates or not, so these critical values are met on surfaces S_q and S_{p_-} i.e.,

$$\sigma_q\left(\mathbf{r}_q\right)=\sigma_{p_-}\left(\mathbf{r}_q\right)=\sigma_p^*\ \text{with}\ \mathbf{r}_q=\left(\tau_q,\zeta,\phi\right)\quad(41)$$

and

$$\beta_q\left(\mathbf{r}_{p_-}\right)=\beta_{p_-}\left(\mathbf{r}_{p_-}\right)=\beta^*\ \text{with}\ \mathbf{r}_{p_-}=\left(\tau_{p_-},\zeta,\phi\right),\quad(42)$$

whereas $\zeta\in[-1,1]$ and $\phi\in[0,2\pi)$. Such kind of formulae can be obtained by integration of σ and β, given by (18)–(19), on the boundary surfaces $S_n:\tau=\tau_n$, $S_q:\tau=\tau_q$ and $S_{p_-}:\tau=\tau_{p_-}$, respectively, providing the critical values σ_n^*, σ_p^* and β^* as average values on these boundaries. This procedure implies

$$\sigma_n^*-\sigma_p^*=\frac{c^2}{9}\gamma_q\Bigg[P_2\left(\tau_n\right)-P_2\left(\tau_q\right)$$
$$-\frac{P_2'\left(\tau_n\right)}{Q_0'\left(\tau_n\right)}\left(Q_0\left(\tau_n\right)-Q_0\left(\tau_q\right)\right)\Bigg],\quad(43)$$

while

$$\sigma_{\infty,0}\left(\tau_e\right)=\sigma_n^*-\frac{c^2}{9}\gamma_q\Bigg[\frac{W^{2,0}_{n,n}}{Q_0'\left(\tau_n\right)}-\frac{W^{2,0}_{q,q}}{Q_0'\left(\tau_q\right)}$$
$$+Q_0\left(\tau_e\right)\left(\frac{P_2'\left(\tau_n\right)}{Q_0'\left(\tau_n\right)}-\frac{P_2'\left(\tau_q\right)}{Q_0'\left(\tau_q\right)}\right)\Bigg]$$
$$-\frac{c^2}{9}\gamma_p\Bigg[\frac{W^{2,0}_{q,q}}{Q_0'\left(\tau_q\right)}-\frac{W^{2,0}_{p_+,p_+}}{Q_0'\left(\tau_{p_+}\right)}$$
$$+Q_0\left(\tau_e\right)\left(\frac{P_2'\left(\tau_q\right)}{Q_0'\left(\tau_q\right)}-\frac{P_2'\left(\tau_{p_+}\right)}{Q_0'\left(\tau_{p_+}\right)}\right)\Bigg]\quad(44)$$

and

$$\beta^*=-\frac{c^2}{9}\Bigg[p_L\left(P_2\left(\tau_{p_+}\right)-P_2\left(\tau_{p_-}\right)-\frac{P_2'\left(\tau_{p_+}\right)}{Q_0'\left(\tau_{p_+}\right)}Q_0\left(\tau_{p_+}\right)\right)$$
$$+\left(p_L-p_n\right)\frac{P_2'\left(\tau_n\right)}{Q_0'\left(\tau_n\right)}Q_0\left(\tau_{p_-}\right)\Bigg].\quad(45)$$

Expressions (43)–(45) form a non–linear system of three equations with three unknowns τ_n, τ_q and τ_{p_-}, which can be solved to provide them as a function of τ_{p_+}. Therein, this set of solutions is substituted to the evolution equation (39) and, finally, the last one is solved with respect to $\tau_{p_+}=\tau_{p_+}(t)$ in order to obtain the outer boundary's evolution.

Concluding, a transversally isotropic pressure field alone cannot result to a prolate spheroidal tumour growth, but a specific nutrient supply given via (36) is also needed. This result could be interpreted in terms of the specific energy needed for the adhesion bonds between cells to preserve the lack of symmetry.

VI. Special Cases – Spherical Model

In this section, we are initially involved with the recovering of special geometrical cases. Consequently, the corresponding results for the oblate spheroidal geometry are obtained through the simple transformation [14]

$$\tau\to i\lambda\ \text{and}\ c\to-i\bar{c},\quad(46)$$

where $0\le\lambda<+\infty$ and $\bar{c}>0$ are the new characteristic variables. Hence, all the corresponding fields described during our previous analysis, are readily obtained in oblate spheroidal coordinates, providing us with the results drawn in [12]. The asymptotic case of the needle can be reached by a prolate spheroid, where $0<a_1=a_2<<a_3<+\infty$, while in the case where

$0 < a_2 << a_3 = a_1 < +\infty$ the oblate spheroid takes the shape of a circular disk. Those comprise some interesting limiting cases with physical importance.

On the other hand, the spheroidal geometry degenerates to the spherical one [14] in the limit, as the semifocal distance tends to zero, that is $c \to 0$. For the corresponding analytical reduction, the limiting process is complicated and involves an appropriate combination of c with the coordinate variables such as $r \equiv \|\mathbf{r}\| = c\sqrt{\tau^2 + \zeta^2 - 1}$ for $\tau \geq 1$ and $|\zeta| \leq 1$, as well as the following limits,

$$\lim_{c\to 0}(c\tau) = r \text{ and } \lim_{c\to 0}\left(\frac{1}{2c}\ln\frac{\tau+1}{\tau-1}\right) = \frac{1}{r}. \quad (47)$$

That way we recover the radial component r (as well as $\frac{1}{r}$) of the spherical coordinate system (r,ζ,ϕ) for $r \in [0,+\infty)$ (here $0 \leq r < r_e$) and the variables ζ, ϕ as usual [14], yielding

$$\mathbf{r} = \sum_{i=1}^{3} x_i \hat{\mathbf{x}}_i = r\sqrt{1-\zeta^2}\cos\varphi\hat{\mathbf{x}}_1 + r\sqrt{1-\zeta^2}\sin\varphi\hat{\mathbf{x}}_2 + r\zeta\hat{\mathbf{x}}_3, \quad (48)$$

where it is obvious that the spherical normal unit vector on the surface of every sphere is given by [14]

$$\lim_{c\to 0}\hat{\boldsymbol{\tau}} = \hat{\boldsymbol{r}} = \frac{\mathbf{r}}{r}. \quad (49)$$

In order to obtain the corresponding mathematical forms for the spherical case, we need the definitions of the associated Legendre functions of the first P_l^m and of the second Q_l^m kind [14] of degree $l = 0,1,2,...$ and of order $m = 0,1,2,...,l$, which lead to

$$\lim_{c\to 0}\left[c^l P_l^m(\tau)\right] = d_l \frac{l!}{(l-m)!}r^l \quad (50)$$

and

$$\lim_{c\to 0}\left[c^{-(l+1)}Q_l^m(\tau)\right] = q_l(-1)^m\frac{(l+m)!}{l!}r^{-(l+1)} \quad (51)$$

for every $\tau \geq 1$ and $r \in [0,+\infty)$ with the aim of the reduction formulas (47). Moreover,

$$d_l = \frac{(2l)!}{2^l(l!)^2} \quad (52)$$

and

$$q_l = \frac{1}{2^l}\sum_{k=0}^{[l/2]}\frac{(-1)^k(2l-2k)!}{k!(l-k)!(l-2k)!(2l-2k+1)} \quad (53)$$

with $(2l+1)d_l q_l = 1$, while the relationships (50) and (51) are utilized for the zero order ($m = 0$) in our case.

On the other hand, the spheroidal geometry degenerates to the spherical one in the limit as $c \to 0$, where a mathematical treatment upon our final results (18), (19), (32) and (39), leads to the recovering of the corresponding expressions for the sphere problem. Hence, using the standard reduction relations, described earlier, i.e., expressions (47)–(53), we proceed to the mathematical treatment for the calculation of the spherical fields in terms of the spherical position vector (48). To that end, the nutrient concentration (18) reduces to

$$\begin{aligned}\sigma_s(\mathbf{r}) = {} & \gamma_q\left[-\frac{r_q^2-r_n^2}{2}+\frac{1}{3r_e}\left(r_q^3-r_n^3\right)\right]+\gamma_p\left[-\frac{r_{p_+}^2-r_q^2}{2}+\frac{1}{3r_e}\left(r_{p_+}^3-r_q^3\right)\right]\\ & +H(r-r_n)\frac{\gamma_q}{3}\left[\frac{r^2-r_n^2}{2}+r_n^3\left(\frac{1}{r}-\frac{1}{r_n}\right)\right]\\ & -H(r-r_q)\frac{\gamma_q-\gamma_p}{3}\left[\frac{r^2-r_q^2}{2}+r_q^3\left(\frac{1}{r}-\frac{1}{r_q}\right)\right]\\ & -H(r-r_{p_+})\frac{\gamma_p}{3}\left[\frac{r^2-r_{p_+}^2}{2}+r_{p_+}^3\left(\frac{1}{r}-\frac{1}{r_{p_+}}\right)\right]\\ & +\sum_{l=0}^{\infty}\sigma_{\infty,l}(r_e)\left(\frac{r}{r_e}\right)^l P_l(\zeta) \text{ for every } \mathbf{r} = (r,\zeta,\phi), \end{aligned} \quad (54)$$

where the corresponding boundaries of the spherical tumour's structure, as well as the physical spherical quantities appearing within (54), represent the prolate spheroidal analogous. Under the same consideration the inhibitor concentration (19) has the spherical limiting expression

$$\begin{aligned}\beta_s(\mathbf{r}) = {} & \frac{p_L-p_n}{2}r_n^2-\frac{p_L}{2}r_{p_+}^2+\frac{p_n}{6}r^2\\ & +H(r-r_n)\frac{p_L-p_n}{3}\left[\frac{r^2-r_n^2}{2}+r_n^3\left(\frac{1}{r}-\frac{1}{r_n}\right)\right]\\ & -H(r-r_{p_+})\frac{p_L}{3}\left[\frac{r^2-r_{p_+}^2}{2}+r_{p_+}^3\left(\frac{1}{r}-\frac{1}{r_{p_+}}\right)\right], \ \mathbf{r} = (r,\zeta,\phi) \end{aligned} \quad (55)$$

with this form being less complicated compared to (54). In a similar way, the pressure field in spherical coordinates is taken from the appropriate limiting procedure via (32) as

$$\begin{aligned}\mathrm{P}_s(\mathbf{r}) = {} & \mathrm{p}_\infty(r_e)\left[1+\frac{2a}{3}\left(1-P_2(\zeta)\right)\right]+\frac{\alpha_e}{r_e}+\frac{\alpha_{p_+}}{r_{p_+}}\left(1-H(r-r_{p_+})\right)\\ & +\frac{1}{6}\left\{F_n r^2+\left(F_n-F_q\right)r_n^2\left[1+2r_n\left(\frac{1}{r_e}-\frac{1}{r_n}\right)\right]\right.\\ & \quad +\left(F_q-F_p\right)r_{p_-}^2\left[1+2r_{p_-}\left(\frac{1}{r_e}-\frac{1}{r_{p_-}}\right)\right]\\ & \quad \left.+F_p r_{p_+}^2\left[1+2r_{p_+}\left(\frac{1}{r_e}-\frac{1}{r_{p_+}}\right)\right]\right\}\\ & -H(r-r_n)\frac{F_n-F_q}{3}\left[\frac{r^2-r_n^2}{2}+r_n^3\left(\frac{1}{r}-\frac{1}{r_n}\right)\right]\\ & -H(r-r_{p_-})\frac{F_q-F_p}{3}\left[\frac{r^2-r_{p_-}^2}{2}+r_{p_-}^3\left(\frac{1}{r}-\frac{1}{r_{p_-}}\right)\right]\\ & -H(r-r_{p_+})\frac{F_p}{3}\left[\frac{r^2-r_{p_+}^2}{2}+r_{p_+}^3\left(\frac{1}{r}-\frac{1}{r_{p_+}}\right)\right] \end{aligned} \quad (56)$$

for every $\mathbf{r} = (r,\zeta,\phi)$, whereas relations (54)–(56) hold true when the spherical variables run within the intervals $r \in [0,r_e)$, $\zeta \in [-1,1]$ and $\phi \in [0,2\pi)$, while those expressions comprise part of the results of [11].

Finally, the evolution equation (39), after some trivial and straightforward manipulation, assumes the spherical form

$$\frac{dr_{p_+}}{dt}=\frac{1}{3r_{p_+}^2}\Big[\Big(-\mu_P\left(F_n-F_q\right)-\mu_\sigma\gamma_q+\mu_\beta\left(p_L-p_n\right)\Big)r_n^3 +\mu_\sigma\left(\gamma_q-\gamma_p\right)r_q^3-\mu_P\left(F_q-F_p\right)r_{p_-}^3 +\left(-\mu_P F_p+\mu_\sigma\gamma_p-\mu_\beta p_L\right)r_{p_+}^3\Big], \tag{57}$$

which is the corresponding spherical form of a fully non–linear ordinary differential equation with respect to the tumour outer boundary r_{p_+} and initial condition $r_{p_+}(0)=R_{p_+}$, since, in view of the critical values (43)–(45), we obtain

$$\sigma_n^*-\sigma_p^*=\frac{\gamma_q}{3}\left[\frac{r_n^2-r_q^2}{2}+r_n^3\left(\frac{1}{r_n}-\frac{1}{r_q}\right)\right], \tag{58}$$

while

$$\sigma_{\infty,0}\left(r_e\right)=\sigma_n^*-\gamma_q\left[-\frac{r_q^2-r_n^2}{2}+\frac{1}{3r_e}\left(r_q^3-r_n^3\right)\right] -\gamma_p\left[-\frac{r_{p_+}^2-r_q^2}{2}+\frac{1}{3r_e}\left(r_{p_+}^3-r_q^3\right)\right] \tag{59}$$

and

$$\beta^*=\frac{1}{3}\left[-p_L\frac{3r_{p_+}^2-r_{p_-}^2}{2}+\left(p_L-p_n\right)\frac{r_n^3}{r_{p_-}}\right]. \tag{60}$$

Once (58)–(60) are readily solved to obtain r_n, r_q and r_{p_-} as a function of r_{p_+}, then relationship (57) can be uniquely solved to evaluate r_{p_+} as a function of time and therefore to predict the evolution of the spherical tumour's exterior boundary, which is our final goal.

VII. Conclusion

In the present work we analyzed a continuous non symmetrical model of avascular tumour growth that evolves maintaining a prolate spheroidal multilayer structure, lying inside a finite confocal prolate spheroidal host medium. Its evolution is regulated by the diffusion of an inhomogeneous nutrient field, and of an internally produced inhibitory agent. Moreover the evolution is affected by a pressure field, generated from the compensation of cell proliferation and disintegration and the transversally isotropic pressure imposed from the surrounding medium.

Hence, the model is formulated in three boundary value problems that hold true as the tumour evolves and provide the nutrient field, the internally produced inhibitor field and the pressure field throughout the spheroidal tumour, as well as the host surrounding. The model includes an assumption for the evolution of the tumour's compartments, which is modeled as a non–linear ordinary differential equation with respect to the tumour's exterior boundary and it also includes the three aforementioned main fields, calculated on the exterior prolate spheroidal boundary. Connection formulae between all the other boundaries with respect to the tumour's exterior one are provided in analytical expressions.

It turns out that a concentric prolate spheroidal multilayer development under an externally imposed transversally isotropic pressure field could be secured only under a particular type of nutrient supply that in the same time specifies the way the exterior boundary evolves.

Our future step involves a numerical implementation of the derived analytical forms and of the non–linear evolution equation. Moreover, alternative evolution approaches for the same spheroidal structure in avascular tumour development, as well as alternative geometrical structure of the development, which is much more applicable to cancer growing in humans, is under our current investigation.

References

[1] T. Roose, S.J. Chapman and P.K. Maini, "Mathematical models of avascular tumor growth", *SIAM Journal on Applied Mathematics*, vol. 49, pp. 179–208, 2007.

[2] R.P. Araujo and D.L.S. McElwain, "A history of the study of solid tumour growth: the contribution of mathematical modeling", *Bulletin of Mathematical Biology*, vol. 66, pp. 1039–1091, 2004.

[3] H.P. Greenspan, "Models for the growth of a solid tumor by diffusion", *Studies in Applied Mathematics*, vol. 52, pp. 317–240, 1972.

[4] H.P. Greenspan, "On the growth and stability of cell cultures and solid tumors", *Journal of Theoretical Biology*, vol. 56, pp. 229–242, 1976.

[5] D.S. Jones and B.D. Sleeman, "Mathematical modeling of avascular and vascular tumor growth", *Advanced Topics in Scattering and Biomedical Engineering*, *World Scientific*, 305–331, 2008.

[6] J.A. Adam, "A mathematical model of tumour growth. II. Effects of geometry and spatial nonuniformity on stability", *Mathematical Biosciences*, vol. 86, pp. 183–211, 1987.

[7] H.M. Byrne and M.A.J. Chaplain, "Growth of necrotic tumors in the presence and absence of inhibitors", *Mathematical Biosciences*, vol. 135, pp. 187–216, 1996.

[8] G. Helmlinger, P.A. Netti, H.D. Lichtenbeld, R.J. Melder and R.K. Jain, "Solid stress inhibits the growth of multicellular tumour spheroids", *Nature Biotechnology*, vol. 15, pp. 778–783, 1997.

[9] G. Dassios, F. Kariotou, B.D. Sleeman, and M.N. Tsampas, "Mathematical modeling of the avascular ellipsoidal tumour growth", *Quarterly of Applied Mathematics*, vol. 70, pp. 1–24, 2012.

[10] M. Hadjinicolaou and F. Kariotou, "On the effect of 3D anisotropic tumour growth on modelling the nutrient distribution in the interior of the tumour", *Bulletin of the Greek Mathematical Society*, vol. 57, pp. 189–197, 2010.

[11] F. Kariotou and P. Vafeas, "The avascular tumour growth in the presence of inhomogeneous physical parameters imposed from a finite spherical nutritive environment", *International Journal of Differential Equations*, vol. 2012, Article ID 175434, pp. 1–25, 2012.

[12] F. Kariotou and P. Vafeas, "On the transversally isotropic pressure effect on avascular tumour growth", *Mathematical Methods in the Applied Sciences*, vol. 37, 277–282, 2014.

[13] P. Moon and D.E. Spencer, *Field theory Handbook*, Springer, Berlin, 1988.

[14] E.W. Hobson, *The Theory of Spherical and Ellipsoidal Harmonics*, Chelsea Publishing Company, New York, 1965.

Operational methods for Hermite polynomials

Clemente Cesarano

***Abstract*—** We exploit methods of operational nature to derive a set of new identities involving families of polynomials associated with operators providing different realizations of the Weyl group.

The identities, we will deal with, extend the Nielsen formulae, valid for ordinary Hermite to families of Hermite-like polynomials. It will also be shown that the underlying formalism yields the possibility of obtaining further identities relevant to multi-variable and multi-index polynomials.

***Keywords*—** Orthogonal Polynomials, Hermite, Weyl group, monomiality principle, generating functions.

I. Introduction

THE use of the *monomiality principle* [1], a by product of the Lie group treatment of special functions [2,3], has offered a powerful tool for studying the properties of families of special functions and polynomials. Within the context of such a treatment, a polynomial $p_n(x)$ is said *quasi-monomial* (*q.m.*), if two operators exist and act on the polynomial as a derivative and multiplicative operators respectively, namely:

$$\begin{aligned}&\hat{M}\, p_n(x) = p_{n+1}(x)\\ &\hat{P}\, p_n(x) = n p_{n-1}(x).\end{aligned} \tag{1}$$

In the case of two-variable Kampé de Fériet polynomials [1,4,5], we have:

$$H_n(x,y) = n!\sum_{r=0}^{\left[\frac{n}{2}\right]}\frac{y^r x^{n-2r}}{r!(n-2r)!} = (-i\sqrt{y})^n H_n\left(\frac{ix}{2\sqrt{y}}\right), \tag{2}$$

where the associated multiplication and derivative operators, are identified as:

$$\begin{aligned}&\hat{M} = x + 2y\frac{\partial}{\partial x}\\ &\hat{P} = \frac{\partial}{\partial x}.\end{aligned} \tag{3}$$

According to what has been discussed in reference [1], if $p_0(x) = 1$, then $p_n(x)$ can be explicitly constructed as:

$$\hat{M}^n\,(1) = p_n(x), \tag{4}$$

thus, in the case of Hermite, we obtain:

$$\left(x + 2y\frac{\partial}{\partial x}\right)^n (1) = \sum_{r=0}^{n}\binom{n}{r}(2y)^r H_{n-r}(x,y)\left(\frac{\partial}{\partial x}\right)^r (1) = \\ = H_n(x,y). \tag{5}$$

The above identity is essentially the Burchnall operational formula, whose proof can be found in the papers [6,7]; in the next section, where the problem is treated in a wider context, we will see a generalization of this identity.

By using the above relations, we can immediately state the following identity:

$$H_{2n}(x,y) = \left(x + 2y\frac{\partial}{\partial x}\right)^n \left(x + 2y\frac{\partial}{\partial x}\right)^n (1). \tag{6}$$

It is easy, in fact to note that the r.h.s. of the equation (6) could be written as:

$$\sum_{r=0}^{n}\binom{n}{r}(2y)^r H_{n-r}(x,y)\left(\frac{\partial}{\partial x}\right)^r H_n(x,y).$$

In the paper [1], we have stated many relevant relations regarding the two-variable Hermite polynomials, in particular it is also possible to obtain the following statement:

$$\frac{\partial^r}{\partial x^r}H_n(x,y) = \frac{n!}{(n-r)!}H_{n-r}(x,y), \tag{7}$$

which is useful to rewrite the relation (6) in the form:

$$H_{2n}(x,y) = (n!)^2\sum_{r=0}^{n}\frac{(2y)^{n-r}\left[H_r(x,y)\right]^2}{(r!)^2(n-r)!}. \tag{8}$$

By following an analogous procedure it is possible to derive these relevant relations satisfied by the two-variable Hermite polynomials:

C. Cesarano is with the Faculty of Engineering, International Telematic University UNINETTUNO, Rome, Italy (phone: +39 0669207675; e-mail: c.cesarano@uninettunouniversity.net).

$$H_{n+m}(x,y)=\sum_{r=0}^{[n,m]}\binom{n}{r}\binom{m}{r}r!(2y)^{n-r}H_{n-r}(x,y)H_{m-r}(x,y),$$

$$\left[H_n(x,y)\right]^2=(n!)^2\sum_{r=0}^{n}\frac{(-2y)^{n-r}H_{2r}(x,y)}{(r!)^2(n-r)!},\qquad(9)$$

$$H_n(x,y)H_m(x,y)=n!m!\sum_{r=0}^{[n,m]}\frac{(-2y)^{n-r}H_{n+m-2r}(x,y)}{r!(n-r)!(m-r)!},$$

where we have indicated with $[n,m]$ the minimum of (n,m).

These identities can be viewed as an extension of those derived by Nielsen [2], for the ordinary case.

The paper consists of three sections. In section II we will discuss higher order Kampé de Fériet Hermite polynomials and the associated identities; section III is devoted to final remarks and comments on the possible extension of the method presented to other families recognized as Hermite polynomials.

II. Operational rules and higher order Hermite polynomials

In the paper [4], we have seen the two-variable Hermite polynomials of order $m\in\mathbb{N}$, $m\geq 2$, defined by the series:

$$H_n^{(m)}(x,y)=n!\sum_{r=0}^{[n/m]}\frac{y^r x^{n-mr}}{r!(n-mr)!}.\qquad(10)$$

It is immediately easy to observe that these polynomials could be recognized as *quasi-monomial* under the action of the following operators:

$$\hat{M}=x+my\frac{\partial^{m-1}}{\partial x^{m-1}}$$
$$\hat{P}=\frac{\partial}{\partial x}.\qquad(11)$$

Moreover, it is possible to introduce a further generalization, by considering the case of *m*-variable Hermite polynomials of order *m*, by setting:

$$H_n^{(m)}(x_1,...,x_m)=n!\sum_{r=0}^{[n/m]}\frac{H_{n-mr}^{(m-1)}(x_1,...,x_m)x_m^r}{r!(n-mr)!}.\qquad(12)$$

This family of Hermite polynomials is also *quasi-monomial* with the related operators:

$$\hat{M}=x_1+\sum_{s=2}^{m}sx_s\frac{\partial^{s-1}}{\partial x_1^{s-1}}$$
$$\hat{P}=\frac{\partial}{\partial x}.\qquad(13)$$

In the paper [1], presenting the concepts and the related formalism of the *monomiality principle*, we stated the following identity:

$$\hat{M}\hat{P}\,p_n(x)=p_n(x),\qquad(14)$$

which implies that the present families of polynomials satisfy the differential equations:

$$\left(my\frac{\partial^m}{\partial x^m}+x\frac{\partial}{\partial x}\right)H_n^{(m)}(x,y)=nH_n^{(m)}(x,y),\qquad(15)$$

$$\left(\sum_{s=2}^{m}sx_s\frac{\partial^s}{\partial x_1^s}+x_1\frac{\partial^s}{\partial x_1}\right)H_n^{(m)}(x_1,...,x_m)=nH_n^{(m)}(x_1,...,x_m).\qquad(16)$$

We prove, now, an important extension of the Weyl identity, that is:

$$e^{\xi\left(x+\frac{\partial^n}{\partial x^n}\right)}=e^{x\xi+\frac{\xi^{n+1}}{n+1}}e^{\sum_{r=0}^{(n-1)}\frac{n!\xi^{r+1}}{(n-r)!(r+1)!}\left(\frac{\partial}{\partial x}\right)^{n-r}},\qquad(17)$$

where ξ being a parameter.

If we consider the exponential operator:

$$S\left(\hat{A},\hat{B};\xi\right)=e^{\xi\left(\hat{A}+\hat{B}^n\right)}\qquad(18)$$

where ξ is a parameter and $\hat{A}$ and $\hat{B}$ denote operator such that:

$$\left[\hat{A},\hat{B}\right]=\hat{A}\hat{B}-\hat{B}\hat{A}=k,$$

with *k* commuting with both of them.

The decoupling theorem for the exponential operator (18) can be proved as follows. By keeping the derivative of both sides with respect to ξ, we get:

$$\frac{\partial}{\partial\xi}S\left(\hat{A},\hat{B};\xi\right)=\left(\hat{A}+\hat{B}^n\right)S\left(\hat{A},\hat{B};\xi\right),\qquad(19)$$

and, after setting:

$$S\left(\hat{A},\hat{B};\xi\right)=e^{\xi\hat{A}}\Sigma,$$

and by using the relation:

$$e^{-\xi\hat{A}}\hat{B}^n e^{\xi\hat{A}}=\left(\hat{B}-\xi k\right)^n,$$

we finally find:

$$\frac{\partial}{\partial \xi}\Sigma = \left(\hat{B} - \xi k\right)^n \Sigma, \tag{20}$$

which can be easily integrated. Thus getting in conclusion:

$$S\left(\hat{A}, \hat{B}; \xi\right) = e^{\xi \hat{A}} e^{\sum_{r=0}^{n} \binom{n}{r} \frac{\hat{B}^{n-r} k^r \xi^{r+1}}{r+1} (-1)^r}. \tag{21}$$

It is immediately to note that identity (17) follows as a particular case with:

$$\hat{A} = x$$
$$\hat{B} = \frac{\partial}{\partial x}$$

The generalization of the Weyl identity, which we have proved above, allows us to derive the following generalized Burchnall identity:

$$\left(x + my\frac{\partial^{m-1}}{\partial x^{m-1}}\right)^n = \sum_{r=0}^{n} \binom{n}{r} H_{n-r}^{(m)}(x,y) H_r^{(m-1)}(x,y) \left(\{G\}_{s=0}^{m-2}\right), \tag{22}$$

where we have indicated with *G* the expression:

$$G = \frac{m(m-1)!\,y}{(m-1-s)!(s+1)!}\frac{\partial^{m-1-s}}{\partial x^{m-1-s}}.$$

The relation in (22), for $m = 3$, specializes as:

$$\left(x + 3y\frac{\partial^2}{\partial x^2}\right)^2 = \sum_{r=0}^{n} \binom{n}{r} H_{n-r}^{(3)}(x,y) H_r\left(3y\frac{\partial^2}{\partial x^2}, 3y\frac{\partial}{\partial x}\right), \tag{23}$$

An immediate application of these last identities is the derivation of the following Nielsen formula:

$$H_{2n}^{(m)}(x,y) = \sum_{r=0}^{n} \binom{n}{r} H_{n-r}^{(m)}(x,y) F_{n,r}^{(m-1)}(x,y), \tag{24}$$

where:

$$F_{n,r}^{(m-1)}(x,y) = \\ = H_r^{(m-1)}\left[\left\{\frac{m(m-1)!\,y}{(m-1-r)!(r+1)!}\frac{\partial^{m-1-s}}{\partial x^{m-1-s}}\right\}_{r=0}^{m-2}\right] H_n^{(m)}(x,y). \tag{25}$$

The explicit form of the $F_{n,r}^{(m-1)}(x,y)$ polynomials can be evaluated fairly straightforwardly; in the case $m = 3$, we get indeed:

$$F_{n,r}^{(2)}(x,y) = s!\sum_{r=0}^{\left[s/2\right]} \frac{(3y)^{s-r}(2s-3r)! H_{n-(2s-3r)}^{(3)}(x,y)}{(s-2r)!\,r!\left[n-(2s-3r)\right]!}. \tag{26}$$

A further application of the so far developed method is associated with the derivation of generating functions of the type:

$$G_l^{(m)}(x,y;t) = \sum_{n=0}^{+\infty} \frac{t^n}{n!} H_{n+l}^{(m)}(x,y). \tag{27}$$

Before to proceed, let us remind that [7]:

$$e^{\alpha\frac{\partial^s}{\partial x_1^s}} H_n^{(m)}(x_1,...,x_m) = \begin{cases} H_n^{(m)}(x_1,...,\alpha + x_s,...,x_m), & s \le m \\ H_n^{(m)}(x_1,...,x_m,...,\alpha), & s > m \end{cases} \tag{28}$$

and then, according with the statement in equation (22), we have:

$$G_l^{(m)}(x,y;t) = \sum_{n=0}^{+\infty} \frac{t^n}{n!}\left(x + my\frac{\partial^{m-1}}{\partial x^{m-1}}\right)^n H_l^{(m)}(x,y), \tag{29}$$

i.e.

$$G_l^{(m)}(x,y;t) = e^{\left(x + my\frac{\partial^{m-1}}{\partial x^{m-1}}\right)t} H_l^{(m)}(x,y). \tag{30}$$

Finally, by using the relation (28), we can obtain the relevant operational expression:

$$G_l^{(m)}(x,y;t) = e^{xt+yt^m} H_l^{(m)}\left(x + ymt^{m-1}, \frac{m(m-1)y}{2}t^{m-2}, ..., y\right). \tag{31}$$

These last results complete the preliminary conclusions obtained in references [5,7]. In the next and last section will be presented further comments on the families of Hermite-like polynomials and will be derived interesting operational rules.

III. Operational Rules and Multi-index Hermite Polynomials

The method described in the previous sections is devoted to the operational rules of polynomials characterized by a single index and, eventually, more than one variable. In this section we will outline the technique to extend the method to multi-index polynomials [8,9,10]. In particular, the structure and some interesting properties of the incomplete 2-dimensional Hermite polynomials, we will consider this family as example to generalize the operational method shown previously.

Let us remind that the incomplete 2-dimensional Hermite polynomials are defined by the series:

$$h_{m,n}(x,y\,|\,\tau)=m!n!\sum_{r=0}^{[m,n]}\frac{\tau^r x^{m-r}y^{n-r}}{r!(m-r)!(n-r)!}, \tag{32}$$

where $\tau\in\mathbb{R}$, $[m,n]=\min(m,n)$ and their generating function has the form:

$$\exp(xu+yv+\tau uv)=\sum_{m=0}^{+\infty}\sum_{n=0}^{+\infty}\frac{u^m}{m!}\frac{v^n}{n!}h_{m,n}(x,y\,|\,\tau)\,. \tag{33}$$

By noting that (see [1,7]), the two-variable Kampé de Fériet Hermite polynomials could be defined also by the following operational expression:

$$H_n(x,y)=e^{y\frac{\partial^2}{\partial x^2}}x^n, \tag{34}$$

it is easy to derive the analogous relation for the polynomials $h_{m,n}(x,y\,|\,\tau)$; we have, indeed:

$$e^{-\tau\frac{\partial^2}{\partial x\partial y}}(x^m y^n)=h_{m,n}(x,y\,|\,\tau)\,. \tag{35}$$

In the first section we have presented the Burchnall identity, see equation (5), and we have stated a generalization for the case of two-variable Hermite polynomials of order *m*, in section II, by equation (22). Before to proceed, it could be useful to exploit the procedure of generalization of this important identity. Let consider the operator:

$$\hat{O}_n=\left(x+my\frac{\partial^{m-1}}{\partial x^{m-1}}\right)^n, \tag{36}$$

by multiplying both sides by:

$$\frac{t^n}{n!},\ t\in\mathbb{R}\ \text{and}\ n\in\mathbb{N}$$

and then by summing up, we get:

$$\sum_{n=0}^{+\infty}\frac{t^n}{n!}\hat{O}_n=e^{t\left(x+my\frac{\partial^{m-1}}{\partial x^{m-1}}\right)}. \tag{37}$$

By using the generalized Weyl identity (eq. (21)), proved in the previous section, we can rearrange the above relation in the form:

$$\sum_{n=0}^{+\infty}\frac{t^n}{n!}\hat{O}_n=e^{xt+yt^m}e^{\sum_{r=0}^{(m-2)}\frac{m!yt^{r+1}}{(m-1-r)!(r+1)!}\frac{\partial^{m-1-r}}{\partial x^{m-1-r}}}, \tag{38}$$

and, since the generating functions of the generalized Hermite polynomials of order *m*, are [1,4]:

$$\begin{aligned}&\sum_{n=0}^{+\infty}\frac{t^n}{n!}H_n^{(m)}(x,y)=e^{xt+yt^m},\\&\sum_{n=0}^{+\infty}\frac{t^n}{n!}H_n^{(m)}(x_1,\ldots,x_m)=e^{\sum_{s=1}^{m}x_s t^s},\end{aligned} \tag{39}$$

we can rewritten the r.h.s. of the relation (38) as the product of two series involving the generalized Hermite polynomials of order *m* and we finally obtain:

$$\hat{O}_n=\sum_{s=0}^{n}\binom{n}{s}H_{n-s}^{(m)}(x,y)H_s^{(m-1)}\left(\left\{\frac{m!\,y}{(m-1-r)!(r+1)!}\frac{\partial^{m-1-r}}{\partial x^{m-1-r}}\right\}_{r=0}^{m-2}\right) \tag{40}$$

which complete prove the generalized Burchnall identity (22). It is now immediate to derive a further generalization for the incomplete 2-dimensional Hermite polynomials discussed in this section. We can indeed exploit the operational rule stated in the equation (35) to derive the following Burchnall-type identity:

$$\begin{aligned}&\left(x-\tau\frac{\partial}{\partial y}\right)^m\left(y-\tau\frac{\partial}{\partial x}\right)^n=\\&=\sum_{p=0}^{m}\sum_{q=0}^{n}\binom{m}{p}\binom{n}{q}(-\tau)^{p+q}h_{m-p,n-q}(x,y\,|\,\tau)\frac{\partial^p}{\partial y^p}\frac{\partial^q}{\partial x^q}.\end{aligned} \tag{41}$$

In section I, we have stated relevant operational identities for the two-variable Hermite polynomials as presented in the relation (9); it is immediately to note that the polynomials $h_{m,n}(x,y\,|\,\tau)$ satisfied the following identity:

$$h_{2m,2n}(x,y\,|\,\tau)=\left(x-\tau\frac{\partial}{\partial y}\right)^m\left(y-\tau\frac{\partial}{\partial x}\right)^n h_{m,n}(x,y\,|\,\tau)\,, \tag{42}$$

and then, from the formula (41), we can obtain the relevant operational identity :

$$\begin{aligned}&h_{2m,2n}(x,y\,|\,\tau)=\\&(m!n!)^2\sum_{p=0}^{m}\sum_{q=0}^{n}\frac{(-\tau)^{p+q}}{p!q!\left[(m-p)!\right]^2\left[(n-q)!\right]^2}\left[h_{m-p,n-q}(x,y\,|\,\tau)\right]^2.\end{aligned} \tag{43}$$

The aspects and the related considerations presented I this paper could be investigate in a deeper way in a forthcoming investigations. It is important to remark that many of the operational rules presented here could be generalized for a wide range of Hermite-like polynomials. Moreover, the structure of the operational techniques here described is also possible to be extended to other classes of polynomials as the

Laguerre and Legendre families. Also about this last point, we will discuss in a future paper.

REFERENCES

[1] Cesarano, C., "Monomiality Principle and related operational techniques for Orthogonal Polynomials and Special Functions", *Int. J. of Math. Models and Methods in Appl. Sci.*, to appear, 2014.

[2] Miller, W., *Lie Theory and Special functions*, Academic Press, New York, 1968.

[3] Cesarano, C., Assante, D., "A note on generalized Bessel functions", *Int. J. of Math. Models and Methods in Appl. Sci.*, 7 (6), pp 625-629, 2013.

[4] Dattoli, G., Cesarano, C., "On a new family of Hermite polynomials associated to parabolic cylinder functions", *Applied Mathematics and Computation*, 141 (1), pp. 143-149, 2003.

[5] Appell, P., Kampé de Fériet, J., "Fonctions hypergéométriques et hypersphériques. Polinomes d'Hermite", *Gauthier-Villars*, Paris, 1926.

[6] Gould, H.W., Hopper, A.T., "Operational formulas connected with two generalizations of Hermite polynomials", *Duke Math. J.*, 29 pp. 51-62 (1962).

[7] Burchnall, J.L., "A note on the polynomials of Hermite", *Quarterly ournal of Mathematics*, os-12 (1), pp. 9-11, (1941).

[8] Dattoli, G., Lorenzutta, Cesarano, C., "Bernestein polynomials and operational methods", *Journal of Computational Analysis and Applications*, 8 (4), pp. 369-377, 2006.

[9] Cesarano, C., Germano, B., Ricci, P.E., "Laguerre-type Bessel functions", Integral Transforms and Special Functions, 16 (4), pp. 315-322, 2005.

[10] Dattoli, G., Lorenzutta, S., Ricci, P.E., Cesarano, C., "On a family of hybrid polynomials", *Integral Transforms and Special Functions*, 15 (6), pp. 485-490, 2004.

Clemente Cesarano is assistant professor of Mathematical Analysis at Faculty of Engineering- International Telematic University UNINETTUNO-Rome, ITALY. He is coordinator of didactic planning of the Faculty and he also is coordinator of research activities of the University. Clemente Cesarano is Honorary Research Associates of the Australian Institute of High Energetic Materials His research activity focuses on the area of Special Functions, Numerical Analysis and Differential Equations.

He has work in many international institutions as ENEA (Italy), Ulm University (Germany), Complutense University (Spain) and University of Rome La Sapienza (Italy). He has been visiting researcher at Research Institute for Symbolic Computation (RISC), Johannes Kepler University of Linz (Austrian). He is Editorial Board member of the Research Bulletin of the Australian Institute of High Energetic Materials, the Global Journal of Pure and Applied Mathematics (GJPAM), the Global Journal of Applied Mathematics and Mathematical Sciences (GJ-AMMS), the Pacific-Asian Journal of Mathematics, the International Journal of Mathematical Sciences (IJMS), the Advances in Theoretical and Applied Mathematics (ATAM), the International Journal of Mathematics and Computing Applications (IJMCA).

Clemente Cesarano has published two books and over than fifty papers on international journals in the field of Special Functions, Orthogonal Polynomials and Differential Equations.

On Asymptotically $\mathcal{I}$-Lacunary statistical Equivalent Sequences of order α

EKREMSAVAŞ

Abstract**—**This paper presents the following definition which is a natural combination of the definition for asymptotically equivalent of order α ,where $0 < \alpha < 1$, $\mathcal{I}$ -statistically limit, and $\mathcal{I}$ -lacunary statistical convergence. Let θ be a lacunary sequence; the two nonnegative sequences $x = (x_k)$ and $y = (y_k)$ are said to be asymptotically $\mathcal{I}$ -lacunary statistical equivalent of order α to multiple L provided that for every $\varepsilon > 0$, and $\delta > 0$,

$$\{r \in \mathbb{N} : \frac{1}{h_r^{\alpha}} | \{k \in I_r : | \frac{x_k}{y_k} - L | \geq \varepsilon\} | \geq \delta\} \in \mathcal{I},$$

(denoted by $x \overset{S_\theta^L(I)^\alpha}{\sim} y$) and simply asymptotically $\mathcal{I}$ -lacunary statistical equivalent of order α if $L = 1$. In addition, we shall also present some inclusion theorems.The study leaves some interesting open problems.

Keywords**—**Asymptotical equivalent, ideal convergence, $\mathcal{I}$ -statistical convergence, $\mathcal{I}$ -lacunary statistical convergence, statistical convergence of order α .

INTRODUCTION

The concept of statistical convergence was introduce by Fast [4] in 1951.

A sequence (x_k) of real numbers is said to be statistically convergent to L if for arbitrary $\varepsilon > 0$,

$$\frac{1}{n} | \{k < n : | x_k - L | \geq \varepsilon\} | = 0,$$

where by $k < n$ we mean that $k = 0,1,2,...,n$ and the vertical bars indicate the number of elements in the enclosed set. In this case we write $st - limx = L$ or $x_k \mapsto L(st)$.

The idea of statistical convergence was further extended to $\mathcal{I}$ -convergence in [7] using the notion of ideals of $\mathbb{N}$ with many interesting consequences.

By a lacunary $\theta = (k_r)$; $r = 0,1,2,...$ where $k_0 = 0$, we shall mean an increasing sequence of non-negative integers with $k_r - k_{r-1} \to \infty$ as $r \to \infty$. The intervals determined by θ will be denoted by $I_r = (k_{r-1}, k_r]$ and $h_r = k_r - k_{r-1}$. The ratio $\frac{k_r}{k_{r-1}}$ will be denoted by q_r .

Moreover, the following concept is due to Fridy and Orhan[6].

A sequence (x_k) of real numbers is said to be lacunary statistically convergent to L (or S_θ -convergent to L) if for any $\varepsilon > 0$,

$$\lim_{r \to \infty} \frac{1}{h_r} | \{k \in I_r : | x_k - L | \geq \varepsilon\} | = 0$$

where $| A |$ denotes the cardinality of $A \subset \mathbb{N}$.

Recently in ([3] and [11]), we used ideals to introduce the concepts of $\mathcal{I}$ -statistical convergence and $\mathcal{I}$ -lacunary statistical convergence which naturally extend the notions of the above mentioned convergence.

On the other hand, in [1] a different direction was given to the study of statistical convergence where the notion of statistical convergence of order α , $0 < \alpha < 1$ was introduced by replacing n by n^α in the denominator in the definition of statistical convergence. One can also see [2] for related works.

In 1993 Marouf [9] presented definitions for asymptotically equivalent sequences and asymptotic regular matrices.Also,in 1997, Li [8] presented and studied asymptotic equivalence of sequences and summability. In 2003, Patterson [10] extended these concepts by presenting an asymptotically statistical equivalent analog of these definitions and natural regularity conditions for nonnegative summability matrices.

In present paper, we intend to unify these two approaches and we use asymptotical equivalent to introduce the concept asymptotically $\mathcal{I}$ -statistical equivalent of order α and asymptotically $\mathcal{I}$ -lacunary statistical equivalent of order α . In addition to these definitions, natural inclusion theorems shall also be presented.

Throughout by two sequences $x = (x_k)$ and $y = (y_k)$ we shall mean two sequences of real numbers.

I. MAIN RESULT

The following definitions and notions will be needed in the sequel.

Definition 1.(Marouf, [9]) Two nonnegative sequences $x = (x_k)$ and $y = (y_k)$ are said to be asymptotically equivalen**t** if

$$\lim_k \frac{x_k}{y_k} = 1$$

(denoted by $x \sim y$).

Definition 2.(Fridy, [5]) The sequence $x = (x_k)$ has statistic limit L , denoted by $st - \lim s = L$ provided that for every $\varepsilon > 0$,

$$\lim_n \frac{1}{n}\{\text{the number of } k \le n : |x_k - L| \ge \varepsilon\} = 0.$$

The next definition is natural combination of definitions 1 and 2.

Definition 3.(Patterson, [10]) Two nonnegative sequences $x = (x_k)$ and $y = (y_k)$ are said to be asymptotically statistical equivalent of multiple L provided that for every $\varepsilon > 0$,

$$\lim_n \frac{1}{n}\{\text{the number of } k < n : \frac{x_k}{y_k} - L \ge \varepsilon\} = 0$$

(denoted by $x \overset{S_L}{\sim} y$), and simply asymptotically statistical equivalent if $L = 1$.

Definition 4. A family $\mathcal{I} \subset 2^{\mathbb{N}}$ is said to be an ideal of $\mathbb{N}$ if the following conditions hold:

(a) $A, B \in \mathcal{I}$ implies $A \cup B \in \mathcal{I}$,

(b) $A \in \mathcal{I}, B \subset A$ implies $B \in \mathcal{I}$,

Definition 5. A non-empty family $F \subset 2^{\mathbb{N}}$ is said to be an filter of $\mathbb{N}$ if the following conditions hold:

(a) $\varphi \notin F$,

(b) $A, B \in F$ implies $A \cap B \in F$,

(c) $A \in F, A \subset B$ implies $B \in F$,

If $\mathcal{I}$ is a proper ideal of $\mathbb{N}$ (*i.e.*, $\mathbb{N} \notin \mathcal{I}$), then the family of sets $F(\mathcal{I}) = \{M \subset \mathbb{N} : \exists\, A \in \mathcal{I} : M = \mathbb{N} \setminus A\}$ is a filter of $\mathbb{N}$. It is called the filter associated with the ideal.

Definition 6. A proper ideal $\mathcal{I}$ is said to be admissible if $\{n\} \in \mathcal{I}$ for each $n \in \mathbb{N}$.

Throughout $\mathcal{I}$ will stand for a proper admissible ideal of $\mathbb{N}$.

Definition 7.([7]) Let $\mathcal{I} \subset 2^{\mathbb{N}}$ be a proper admissible ideal in $\mathbb{N}$. Then the sequence (x_k) of elements of $\mathbb{R}$ is said to be $\mathcal{I}$-convergent to $L \in \mathbb{R}$ if for each $\varepsilon > 0$ the set $A(\varepsilon) = \{k \in \mathbb{N} : |x_k - L| \ge \varepsilon\} \in \mathcal{I}$.

We now introduce our main definitions.

Definition 8. A sequence $x = (x_k)$ is said to be $\mathcal{I}$-statistically convergent of order α to L or $S(\mathcal{I})^\alpha$-convergent to L, where $0 < \alpha \le 1$, if for each $\varepsilon > 0$ and $\delta > 0$

$$\{n \in \mathbb{N} : \frac{1}{n^\alpha} |\{k \le n : |x_k - L| \ge \varepsilon\}| \ge \delta\} \in \mathcal{I}.$$

In this case we write $x_k \to L(S(\mathcal{I})^\alpha)$. The class of all $\mathcal{I}$-statistically convergent sequences of order α will be denoted by simply $S(\mathcal{I})^\alpha$.

Also the next definition is natural combination of definitions 1 and 8.

Definition 9. The two nonnegative sequences $x = (x_k)$ and $y = (y_k)$ are said to be asymptotically $\mathcal{I}$- statistical equivalent of order α to multiple L, where $0 < \alpha \le 1$, provided that for each $\varepsilon > 0$ and $\delta > 0$

$$\{n \in \mathbb{N} : \frac{1}{n^\alpha} |\{k \le n : |\frac{x_k}{y_k} - L| \ge \varepsilon\}| \ge \delta\} \in \mathcal{I},$$

(denoted by $x \overset{S^L(\mathcal{I})^\alpha}{\sim} y$) and simply asymptotically $\mathcal{I}$-statistical equivalent of order α if $L = 1$. Furthermore, let $S^L(\mathcal{I})^\alpha$ denote the set of x and y such that $x \overset{S^L(\mathcal{I})^\alpha}{\sim} y$.

Remark 1. If $\mathcal{I} = \mathcal{I}_{fin} = \{A \subseteq \mathbf{N} : A$ is a finite subset$\}$, asymptotically $\mathcal{I}$- statistical equivalent of order α to multiple L coincides with asymptotically statistical equivalent of order α to multiple L. For an arbitrary ideal $\mathcal{I}$ and for $\alpha = 1$ it coincides with asymptotically $\mathcal{I}$- statistical equivalent of multiple L. When $\mathcal{I} = \mathcal{I}_{fin}$ and $\alpha = 1$ it becomes only asymptotically statistical equivalent of multiple L, [10].

Definition 10. Let θ be a lacunary sequence. A sequence $x = (x_k)$ is said to be $\mathcal{I}$-lacunary statistically convergent of order α to L or $S_\theta(I)^\alpha$-convergent to L if for any $\varepsilon > 0$ and $\delta > 0$

$$\{r \in \mathbb{N} : \frac{1}{h_r^\alpha} |\{k \in I_r : |x_k - L| \ge \varepsilon\}| \ge \delta\} \in \mathcal{I}.$$

In this case we write $x_k \to L(S_\theta(\mathcal{I})^\alpha)$. The class of all $\mathcal{I}$-lacunary statistically convergent sequences of order α will be denoted by $S_\theta(\mathcal{I})^\alpha$.

We now have

Definition 11. Let θ be a lacunary sequence; the two nonnegative sequences $x = (x_k)$ and $y = (y_k)$ are said to be asymptotically $\mathcal{I}$-lacunary statistical equivalent of order α to multiple L provided that for any $\varepsilon > 0$ and $\delta > 0$

$$\{r \in \mathbb{N} : \frac{1}{h_r^\alpha} |\{k \in I_r : |\frac{x_k}{y_k} - L| \ge \varepsilon\}| \ge \delta\} \in \mathcal{I},$$

(denoted by $x \overset{S_\theta^L(I)^\alpha}{\sim} y$) and simply asymptotically $\mathcal{I}$-lacunary statistical equivalent of order α if $L = 1$. Furthermore, let $S_\theta^L(\mathcal{I})^\alpha$ denote the set of x and y such that $x \overset{S_\theta^L(\mathcal{I})^\alpha}{\sim} y$.

Remark 2. For $\alpha = 1$ the above definition coincides with asymptotically $\mathcal{I}$-lacunary statistical equivalent of multiple L. Further it must be noted in this context that asymptotically $\mathcal{I}$-lacunary statistical equivalent of order α to multiple L has not been studied till now. Obviously, if we take $\mathcal{I} = \mathcal{I}_{fin}$ asymptotically lacunary statistical equivalent of order α to multiple L is a special case of asymptotically $\mathcal{I}$-lacunary statistical equivalent of order α to multiple L.

Theorem 1. Let $0 < \alpha \le \beta \le 1$. Then $S(\mathcal{I})^\alpha \subset S(\mathcal{I})^\beta$.

Proof: Let $0 < \alpha \le \beta \le 1$. Then

$$\frac{|\{k \le n : |\frac{x_k}{y_k} - L| \ge \varepsilon\}|}{n^\beta} \le \frac{|\{k \le n : |\frac{x_k}{y_k} - L| \ge \varepsilon\}|}{n^\alpha}$$

and so for any $\delta > 0$,

$$\{n \in \mathbb{N} : \frac{|\{k \le n : |\frac{x_k}{y_k} - L| \ge \varepsilon\}|}{n^{\beta}} \ge \delta\} \subset$$

$$\{n \in \mathbb{N} : \frac{|\{k \le n : |\frac{x_k}{y_k} - L| \ge \varepsilon\}|}{n^{\alpha}} \ge \delta\}.$$

Hence if the set on the right hand side belongs to the ideal $\mathcal{I}$ then obviously the set on the left hand side also belongs to $\mathcal{I}$. This shows that $S(\mathcal{I})^{\alpha} \subset S(\mathcal{I})^{\beta}$.

Similarly we can show that

Theorem 2. Let $0 < \alpha \le \beta \le 1$. Then

(i) $S_{\theta}^{L}(\mathcal{I})^{\alpha} \subset S_{\theta}^{L}(\mathcal{I})^{\beta}$.

(ii) In particular $S_{\theta}^{L}(\mathcal{I})^{\alpha} \subset S_{\theta}^{L}(\mathcal{I})$.

Definition 12. Let θ be a lacunary sequence; two number sequences $x = (x_k)$ and $y = (y_k)$ are strong $\mathcal{I}$-asymptotically lacunary equivalent of order α to multiple L provided that for any $\varepsilon > 0$

$$\{r \in \mathbb{N} : \frac{1}{h_r^{\alpha}} \sum_{k \in I_r} |\frac{x_k}{y_k} - L| \ge \varepsilon\} \in \mathcal{I},$$

(denoted by $x \overset{N_{\theta}^{L}(I)^{\alpha}}{\sim} y$) and simply strong asymptotically $\mathcal{I}$-lacunary statistical equivalent of order α if $L = 1$. Further, let $N_{\theta}^{L}(\mathcal{I})^{\alpha}$ denote the set of x and y such that $x \overset{N_{\theta}^{L}(\mathcal{I})^{\alpha}}{\sim} y$.

We prove the following

Theorem 3. Let $\theta = \{k_r\}_{r \in \mathbb{N}}$ be a lacunary sequence, then

(a) If $x \overset{N_{\theta}^{L}(\mathcal{I})^{\alpha}}{\sim} y$ then $x \overset{S_{\theta}^{L}(\mathcal{I})^{\alpha}}{\sim} y$

(b) $N_{\theta}^{L}(\mathcal{I})^{\alpha}$ is a proper subset of $S_{\theta}^{L}(\mathcal{I})^{\alpha}$

Proof: (a) If $\varepsilon > 0$ and $x \overset{N_{\theta}^{L}(\mathcal{I})^{\alpha}}{\sim} y$, we can write

$$\sum_{k \in I_r} |\frac{x_k}{y_k} - L| \ge \sum_{k \in I_r,\ |\frac{x_k}{y_k} - L| \ge \varepsilon} |\frac{x_k}{y_k} - L| \ge \varepsilon\, |\{k \in I_r : |\frac{x_k}{y_k} - L| \ge \varepsilon\}|$$

$$\text{and so } \frac{1}{\varepsilon . h_r^{\alpha}} \sum_{k \in I_r} |\frac{x_k}{y_k} - L| \ge \frac{1}{h_r^{\alpha}} |\{k \in I_r : |\frac{x_k}{y_k} - L| \ge \varepsilon\}|.$$

Then for any $\delta > 0$

$$\{r \in \mathbb{N} : \frac{1}{h_r^{\alpha}} |\{k \in I_r : |\frac{x_k}{y_k} - L| \ge \varepsilon\}| \ge \delta\} \subseteq \{r \in \mathbb{N} : \frac{1}{h_r^{\alpha}} \sum_{k \in I_r} |\frac{x_k}{y_k} - L| \ge \varepsilon . \delta\} \in \mathcal{I}.$$

This proves the result.

(b) In order to establish that the inclusion $N_{\theta}^{L}(\mathcal{I})^{\alpha} \subseteq S_{\theta}^{L}(\mathcal{I})^{\alpha}$ is proper, let θ be given and define x_k to be $1, 2, ..., [\sqrt{h_r^{\alpha}}]$ at first $[\sqrt{h_r^{\alpha}}]$ integers in I_r and $x_k = 0$ otherwise for all $r = 1, 2, 3, \ldots$. $y_k = 1$ for all k. Then for any $\varepsilon > 0$,

$$\frac{1}{h_r^{\alpha}} |\{k \in I_r : |\frac{x_k}{y_k} - 0| \ge \varepsilon\}| \le \frac{[\sqrt{h_r^{\alpha}}]}{h_r^{\alpha}}$$

and for any $\delta > 0$ we get

$$\{r \in \mathbb{N} : \frac{1}{h_r^{\alpha}} |\{k \in I_r : |\frac{x_k}{y_k} - 0| \ge \varepsilon\}| \ge \delta\} \subseteq \{r \in \mathbb{N} : \frac{[\sqrt{h_r^{\alpha}}]}{h_r^{\alpha}} \ge \delta\}.$$

Since the set on the right hand side is a finite set and so belongs to $\mathcal{I}$ it follows that $x \overset{S_{\theta}^{L}(\mathcal{I})^{\alpha}}{\sim} y$.

On the other hand

$$\frac{1}{h_r^{\alpha}} \sum_{k \in I_r} |\frac{x_k}{y_k} - 0| = \frac{1}{h_r^{\alpha}} . \frac{[\sqrt{h_r^{\alpha}}]([\sqrt{h_r^{\alpha}}] + 1)}{2}.$$

Then

$$\{r \in \mathbb{N} : \frac{1}{h_r^{\alpha}} \sum\nolimits_{k \in I_r} |\frac{x_k}{y_k} - 0| \ge \frac{1}{4}\} = \{r \in \mathbb{N} : \frac{[\sqrt{h_r^{\alpha}}]([\sqrt{h_r^{\alpha}}] + 1)}{h_r} \ge \frac{1}{2}\}$$

$$= \{m, m+1, m+2, \ldots\}$$

for some $m \in \mathbb{N}$ which belongs to $F(\mathcal{I})$ since $\mathcal{I}$ is admissible. So the following fails $x \overset{N_{\theta}^{L}(\mathcal{I})^{\alpha}}{\sim} y$.

Remark 4. The following two conditions remain true for $0 < \alpha < 1$ is not clear and we leave them as open problems.

(2) $x \in l_{\infty}$ and $x \overset{S_{\theta}^{L}(\mathcal{I})^{\alpha}}{\sim} y \Rightarrow x \overset{N_{\theta}^{L}(\mathcal{I})^{\alpha}}{\sim} y$,

(3) $S_{\theta}^{L}(\mathcal{I})^{\alpha} \cap l_{\infty} = N_{\theta}^{L}(\mathcal{I})^{\alpha} \cap l_{\infty}$.

We now investigate the relationship between $x \overset{S^{L}(\mathcal{I})^{\alpha}}{\sim} y$ and $x \overset{S_{\theta}^{L}(\mathcal{I})^{\alpha}}{\sim} y$.

Theorem 4. Let $\mathcal{I}$ is an ideal and $\theta = \{k_r\}$ is a lacunary sequence, then

$x \overset{S^{L}(\mathcal{I})^{\alpha}}{\sim} y$ *implies* $x \overset{S_{\theta}^{L}(\mathcal{I})^{\alpha}}{\sim} y$

if $\liminf_r q_r^{\alpha} > 1$.

Proof: Suppose first that $\liminf_r q_r^{\alpha} > 1$. Then there exists $\sigma > 0$ such that $q_r^{\alpha} \ge 1 + \sigma$ for sufficiently large r which implies that

$$\frac{h_r^{\alpha}}{k_r^{\alpha}} \ge \frac{\sigma}{1 + \sigma}.$$

Since $x \overset{S^{L}(\mathcal{I})^{\alpha}}{\sim} y$, then for every $\varepsilon > 0$ and for sufficiently large r, we have

$$\frac{1}{k_r^{\alpha}} |\{k \le k_r : |\frac{x_k}{y_k} - L| \ge \varepsilon\}| \ge \frac{1}{k_r^{\alpha}} |\{k \in I_r : |\frac{x_k}{y_k} - L| \ge \varepsilon\}|$$

$$\ge \frac{\sigma}{1 + \sigma} . \frac{1}{h_r^{\alpha}} |\{k \in I_r : |\frac{x_k}{y_k} - L| \ge \varepsilon\}|.$$

Then for any $\delta > 0$, we get

$$\{r \in \mathbb{N} : \frac{1}{h_r^{\alpha}} |\{k \in I_r : |\frac{x_k}{y_k} - L| \geq \varepsilon\}| \geq \delta\}$$

$$\subseteq \{r \in \mathbb{N} : \frac{1}{k_r^{\alpha}} |\{k \leq k_r : |\frac{x_k}{y_k} - L| \geq \varepsilon\}| \geq \frac{\delta\sigma}{(1+\sigma)}\} \in \mathcal{I}.$$

This proves the result.

Remark 5. The converse of this result is not clear for $\alpha < 1$ and we leave it as an open problem.

For the next result we assume that the lacunary sequence θ satisfies the condition that for any set $C \in F(\mathcal{I})$, $\bigcup\{n : k_{r-1} < n < k_r, r \in C\} \in F(\mathcal{I})$.

Theorem 5. For a lacunary sequence θ satisfying the above condition,

$$x \overset{S_\theta^L(\mathcal{I})^\alpha}{\sim} y \text{ implies } x \overset{S^L(\mathcal{I})^\alpha}{\sim} y$$

if $\sup_r \sum_{i=0}^{r-1} \frac{h_{i+1}^{\alpha}}{(k_{r-1})^{\alpha}} = B(say) < \infty$.

Proof: Suppose that $x \overset{S_\theta^L(\mathcal{I})^\alpha}{\sim} y$ and for $\varepsilon, \delta, \delta_1 > 0$ define the sets

$$C = \{r \in \mathbb{N} : \frac{1}{h_r^{\alpha}} |\{k \in I_r : |\frac{x_k}{y_k} - L| \geq \varepsilon\}| < \delta\}$$

and

$$T = \{n \in \mathbb{N} : \frac{1}{n^{\alpha}} |\{k \leq n : |\frac{x_k}{y_k} - L| \geq \varepsilon\}| < \delta_1\}.$$

It is obvious from our assumption that $C \in F(\mathcal{I})$, the filter associated with the ideal $\mathcal{I}$. Further observe that

$$A_j = \frac{1}{h_j^{\alpha}} |\{k \in I_j : |\frac{x_k}{y_k} - L| \geq \varepsilon\}| < \delta$$

for all $j \in C$. Let $n \in \mathbb{N}$ be such that $k_{r-1} < n < k_r$ for some $r \in C$. Now

$$\frac{1}{n^{\alpha}} |\{k \leq n : |\frac{x_k}{y_k} - L| \geq \varepsilon\}| \leq \frac{1}{k_{r-1}^{\alpha}} |\{k \leq k_r : |\frac{x_k}{y_k} - L| \geq \varepsilon\}|$$

$$= \frac{1}{k_{r-1}^{\alpha}} |\{k \in I_1 : |\frac{x_k}{y_k} - L| \geq \varepsilon\}| + \ldots + \frac{1}{k_{r-1}^{\alpha}} |\{k \in I_r : |\frac{x_k}{y_k} - L| \geq \varepsilon\}|$$

$$= \frac{k_1^{\alpha}}{k_{r-1}^{\alpha}} \frac{1}{h_1^{\alpha}} |\{k \in I_1 : |\frac{x_k}{y_k} - L| \geq \varepsilon\}| + \ldots +$$

$$\frac{(k_r - k_{r-1})^{\alpha}}{k_{r-1}^{\alpha}} \frac{1}{h_r^{\alpha}} |\{k \in I_r : |\frac{x_k}{y_k} - L| \geq \varepsilon\}|$$

$$= \frac{k_1^{\alpha}}{k_{r-1}^{\alpha}} A_1 + \frac{(k_2 - k_1)^{\alpha}}{k_{r-1}^{\alpha}} A_2 + \ldots + \frac{(k_r - k_{r-1})^{\alpha}}{k_{r-1}^{\alpha}} A_r$$

$$\leq \sup_{j \in C} A_j . \sup_r \sum_{i=0}^{r-1} \frac{(k_{i+1} - k_i)^{\alpha}}{k_{r-1}^{\alpha}} < B\delta.$$

Choosing $\delta_1 = \frac{\delta}{B}$ and in view of the fact that $\bigcup\{n : k_{r-1} < n < k_r, r \in C\} \subset T$ where $C \in F(\mathcal{I})$ it follows from our assumption on θ that the set T also belongs to $F(\mathcal{I})$ and this completes the proof of the theorem.

REFERENCES

[1] R. Colak, "Statistical convergence of order α", Modern methods in Analysis and its Applications, New Delhi, India, Anamaya Pub., 121-129, 2010.

[2] R. Colak, C. A. Bektas, "λ -statistical convergence of order α", Acta Math. Scientia, 31B (3), 953-959, 2011.

[3] Pratulananda Das, E. Savas, S. K. Ghosal, "On generalizations of certain summability methods using ideals", Appl. Math. Letters, 24 , 1509 – 1514, 2011.

[4] H. Fast, "Sur la convergence statistique, Colloq. Math.", 2, 241-244, 1951.

[5] J. A. Fridy, "On statistical convergence", Analysis, 5, 301-313, 1985.

[6] J. A. Fridy and C. Orhan, "Lacunary statistical convergence", Pacific J. Math., 160, 43-51, 1993.

[7] P. Kostyrko, T. Šalát, W.Wilczynki, "I -convergence", Real Anal. Exchange, 26 (2), 669-685, 2000/2001.

[8] J. Li, "Asymptotic Equivalence of Sequences and Summability", Internat. J. Math. & Math. Sci. 20(4), 749-758, 1997.

[9] M. Marouf, "Asymptotic equivalence and summability", Internat. J. Math. Math. Sci. 16(4), 755-762, 1993.

[10] R. F. Patterson, "On Asymptotically Statistically Equivalent Sequences", Demonstratio Math. 36(1), 149-153, 2003.

[11] E. Savas, " Pratulananda Das, A generalized statistical convergence via ideals", Appl. Math. Letters, 24, 826 – 830, 2011.

[12] E.Savas, H. Gumus, "A generalization on $\mathcal{I}$ -asymptotically lacunary statistical equivalent sequences", J. Inequal. Appl., 2013:27, 2013.

[13] E. Savas, "On $\mathcal{I}$ -Asymptotically Lacunary Statistical Equivalent Sequences, Advances in Difference Equations", 2013:111, April 18, 2013.

[14] E. Savas, "Double almost statistical convergence of order α" , Adv. Difference Equ., 2013:62, 9, 2013.

Department of Mathematics, Istanbul Commerce University, Sutluce-Istanbul/ Turkey

E. Savas received the PhD degree in Mathematics for Graduate School of Natural and Applied Sciences at Firat University of Elazıg in Turkey. His research interests are in the areas of functional analysis and sequence spaces including statistical convergence, matrix transformations and fuzzy sequence spaces. He has published research articles in reputed international journals of mathematical science. He is referee and editor of mathematical journals.

L^p and BMO-solvability of the Dirichlet problem for elliptic operators

Gabriella Zecca

***Abstract*—We establish a connection between the solvability of end-point BMO and L^p Dirichlet problems for a second order divergence form elliptic operator (not necessarily symmetric) with bounded measurable coefficients. In particular, we give a lower bound for the exponent $p > 1$ in terms of the *BMO-constant* of L (see Definition 8).**

Keywords and Phrases - Dirichlet problem, Bounded mean oscillation, elliptic measure.

Math Subject Classifications. 42B37 35J25, 35R05

I. Introduction

Let $\Omega \subset \mathbb{R}^n$ denote a Lipschitz domain. For $K \geqslant 1$ we consider the class $\mathcal{E}(K)$ of measurable (not necessarily symmetric) matrix fields $A(x) \in L^\infty(\Omega)$ such that

$$\frac{|\xi|^2}{K} \leqslant \langle A(x)\xi, \xi\rangle \leqslant K\,|\xi|^2 \tag{1}$$

for a.e. $x \in \Omega$ and for any $\xi \in \mathbb{R}^n$.

We examine the classical Dirichlet boundary value problem:

$$\begin{cases} Lu = 0 \quad \text{in } \Omega \\ u_{|\partial\Omega} = f \in C(\partial\Omega) \end{cases} \tag{2}$$

where

$$L = \text{div}(A(x)\nabla\,) \tag{3}$$

is an elliptic operator whose coefficient matrix $A(x)$ belongs to $\mathcal{E}(K)$.

For $1 < p < \infty$, the problem (2) is called L^p- *solvable* and the operator (3) is said L^p-*resolutive*, if there exists a constant $C_p > 0$ for which the following holds: For any $f \in C(\partial\Omega)$ the unique solution $u \in W^{1,2}_{loc}(\Omega) \cap C(\bar{\Omega})$ to (2) satisfies the uniform estimate

$$\|Nu\|_{L^p(\partial\Omega)} \leqslant C\,\|f\|_{L^p(\partial\Omega)}\,,$$

where Nu is the nontangential maximal function,

$$Nu(x) = \sup_{y\in\mathcal{G}(x)} |u(y)|$$

(here $\mathcal{G}(x)$ is a truncated cone with vertex at x) and where C depends only on the Lipschitz character of Ω and the ellipticity of L.

In order to state a necessary and sufficient condition that problem (2) is L^p- solvable we shall now recall a key notion of the theory, namely the "elliptic measure". To this effect we assume that Ω contains the origin of $\mathbb{R}^n$ and we consider the linear functional

$$f \in C(\partial\Omega) \longrightarrow u(0)$$

G. Zecca is with the Department of Mathematics, University of Naples 'Federico II' Naples, Italy.

where $u \in W^{1,2}_{loc}(\Omega)\cap C(\overline{\Omega})$ is the unique solution of Problem (2). Then, there is a unique Borel regular probability measure ω_L on $\partial\Omega$ such that

$$u(0) = \int_{\partial\Omega} f(\sigma)d\omega_L(\sigma),$$

Such ω_L is called "elliptic measure" associated with L (see [9]).

Definition I.1. *We say that the measure ω supported on $\partial\Omega$ belongs to the Gehring class B_q, $1 < q < \infty$, if ω is absolutely continuous with respect to the surface measure σ on $\partial\Omega$, and the Radon-Nikodym derivative $w = \frac{d\omega}{d\sigma}$ verifies the "reverse Hölder inequality"*

$$\left(\frac{1}{\sigma(\Delta)}\int_\Delta w^q d\sigma\right)^{\frac{1}{q}} \leqslant \frac{B}{\sigma(\Delta)}\int_\Delta w d\sigma \tag{4}$$

with a certain constant $B \geqslant 1$ and for all surface balls $\Delta \subset \partial\Omega$.

Theorem I.1. [9] *The following conditions are equivalent ($\frac{1}{p}+\frac{1}{q}=1$): i) problem (2) is L^p- solvable; ii) the elliptic measure ω_L of the operator L belongs to the Gehring class B_q.*

We refer the reader to the papers [3], [4], [1], [6] and to [8] for more details.

In order to define the BMO-solvability for L as in [5], we need to introduce some notations.

For any $x \in \partial\Omega$ we set $B_r(x) = \{y : |y - x| \leqslant r\}$ and we denote by $\Delta_r(x)$ the surface ball $B_r(x) \cap \partial\Omega$. Moreover we denote by $T(\Delta_r) = \Omega \cap B_r(x)$ the Carleson region above $\Delta_r(x)$.

A measure μ in Ω is Carleson if there exist $r_0 > 0$ and $C > 0$ such that for all $r \leqslant r_0$,

$$\mu(T(\Delta_r)) \leqslant C\sigma(\Delta_r).$$

For such measure μ we denote by $\|\mu\|_{Car}$ the quantity

$$\|\mu\|_{Car} = \sup_{\Delta\subset\partial\Omega} (\sigma(\Delta)^{-1}\mu(T(\Delta)))^{\frac{1}{2}}$$

We say that a function $f : \partial\Omega \to \mathbb{R}$ belongs to BMO with respect to the surface measure $d\sigma$ if

$$\sup_{I\subset\partial\Omega} \sigma(I)^{-1}\int_I |f - f_I|^2 d\sigma < \infty.$$

Here $f_I = \sigma(I)^{-1}\int_I f d\sigma$. We denote by $\|f\|_{BMO(p)}$ the number

$$\|f\|_{BMO(p)} = \sup_{I\subset\partial\Omega}\left(\sigma(I)^{-1}\int_I |f - f_I|^p d\sigma\right)^{\frac{1}{p}}.$$

ISBN: 978-1-61804-225-5

It can be shown that, for any $1 \leqslant p < \infty$, $\|f\|_{BMO(2)} < \infty$ if and only if $\|f\|_{BMO(p)} < \infty$. Moreover, $\|\cdot\|_{BMO(p)}$ and $\|\cdot\|_{BMO(2)}$ are equivalent in the sense that there is a constant $C \geqslant 1$ such that the inequality

$$C^{-1}\|f\|_{BMO(p)} \leqslant \|f\|_{BMO(2)} \leqslant C\|f\|_{BMO(p)}$$

holds for any BMO function f.

Definition I.2. *The Dirichlet problem* (2) *is called BMO-solvable for L (and the operator L is said BMO-resolutive) if the solution u for continuous boundary data f satisfies*

$$\||\nabla u|^2\delta(x)dx\|_{Car} \preceq \|f\|_{BMO(2)}.$$

Here $\delta(x)$ =dist$(x, \partial\Omega)$. Equivalently, there exists a constant C such that for all continuous f,

$$\begin{aligned} &\sup_{\Delta\subset\partial\Omega} \sigma(\Delta)^{-1} \int\int_{T(\Delta)} |\nabla u|^2\delta(x)dx \\ &\leqslant C \sup_{I\subset\partial\Omega} \sigma(I)^{-1} \int_I |f - f_I|^2 d\sigma. \end{aligned} \tag{5}$$

Note that even though one defines BMO-solvability only for continuous boundary data, the solution u can be defined for any BMO function $f : \partial\Omega \to \mathbb{R}$ and moreover the estimate will hold. In addition, such a solution u will have a well-defined nontangential maximal function $Nu(x)$ for almost every point $x \in \partial\Omega$ and in the nontangential sense

$$f(x) = \lim_{y\to x, y\in\mathcal{G}(x)} u(y), \text{for a.e.} x \in \partial\Omega$$

(see [5]).

We will call BMO-constant of the operator L the quantity

$$\textit{BMO(L)} = \sup \left(\frac{\||\nabla u|^2\delta(x)dx\|_{Car}}{\|f\|_{BMO(2)}} \right)^2. \tag{6}$$

Moreover we will denote by $D_2(\sigma)$ the doubling constant of the surface measure σ on Ω, and precisely

$$D_2(\sigma) = \sup_{\Delta} \frac{\sigma(\Delta(x, 2r))}{\sigma(\Delta(x, r))}.$$

An easy computation shows that, for example, if $\Omega = \mathbb{D}$, the unit disc of $\mathbb{R}^2$, then $D_2(\sigma) = 3$ and in case $\Omega = \mathbb{B}$ the unit sphere of $\mathbb{R}^3$, then $D_2(\sigma) = 4$.

In [5] the following result is obtained (see [5], Theorem 2.2).

Theorem I.2 ([5])**.** *Assume that L is BMO-resolutive. Then there exist $p_0 > 1$ such that the L^p Dirichlet problem for L is solvable for all $p_0 < p < \infty$.*

Last result is obtained by the authors by proving that an operator L in our class $\mathcal{E}(K)$ is BMO-solvable if and only if the elliptic measure ω_L belongs to the Muckenhoupt class $A_\infty = \cup B_q$ with respect to the surface measure on the boundary of the domain of solvability Ω. And when the density of harmonic measure with respect to surface measure belongs to some B_{q_0}, using Theorem I.1, it turns out that the Dirichlet problem is L^{p_0} solvable where $1/q_0 + 1/p_0 = 1$. The range of solvability (p_0, ∞) can be then obtained by observing that $B_{q_0} \subset B_q$ for $q < q_0$.

In this note our aim is to give an upper bound for such exponent p_0 in terms of the BMO constant of L appearing in (8). In particular our main result is the following

Theorem I.3. *Let $\Omega \subset \mathbb{R}^n$ be a Lipschitz domain and let L be a divergence form elliptic operator with bounded coefficiens, satisfying the strong ellipticity condition. Assume the operator L be BMO-resolutive. Then L is L^p resolutive, for all $p \geqslant 1 + \rho_0$ where*

$$\rho_0 = C \cdot D_2(\omega_L)^2 \cdot BMO(L) + e \cdot \log D_2(\sigma). \tag{7}$$

Here $C = C(n)$, $D_2(\omega_L)$ is the doubling constant of the elliptic measure ω_L and $BMO(L)$ is the BMO constant of L defined in (8)*.*

We note explicitely that a similar result can be obtained in the context of the Orlicz boundary data (see [13], [14]).

Finally, we note that using [12] Theorem 1.3, by Theorem I.2 it is easy to prove a simultaneous BMO-solvability result for two different operators without assumption on the distance of the operator's coefficients near the boundary.

II. Proof of Theorem I.3

A key ingredient in our proof will be the following result:

Theorem II.1 ([5])**.** *Assume that L is BMO resolutive. Then the ellipic measure ω_L belongs to A_∞. In particular, for any $\varepsilon > 0$, assuming $\eta = e^{-\frac{Cd^2\bar{C}}{\varepsilon}}$, for all surface ball $\Delta \subset \partial\Omega$ and for all measurable subset $E \subset \Delta$,*

$$\frac{\sigma(E)}{\sigma(\Delta)} < \eta \Longrightarrow \frac{\omega_L(E)}{\omega_L(\Delta)} < \varepsilon \tag{8}$$

Here $C = C(n)$, $d = D_2(\omega_L)$ is the doubling constant of ω_L and $\bar{C} = BMO(L)$ is the BMO-constant of L.

Proof. The thesis can be obtained by following the proof of Theorem 2.1 in [5]. □

proof of Theorem I.3. Using Theorem II.1, the statement of Theorem I.3 follows by using a well known argument (see for example [7]). For the convenience of the reader we give here some details.

Assume that L is BMO resolutive. Then, by Theorem II.1, for any $\varepsilon > 0$, assuming $\eta = e^{-\frac{Cd^2\bar{C}}{\varepsilon}}$, for all surface ball $\Delta \subset \partial\Omega$ and for all measurable subset $E \subset \Delta$,

$$\frac{\sigma(E)}{\sigma(\Delta)} < \eta \Longrightarrow \frac{\omega_L(E)}{\omega_L(\Delta)} < \varepsilon \tag{9}$$

Moreover, since $\omega_L << \sigma$ we consider the Radon-Nikodym derivative $w = d\omega_L/d\sigma$. To obtain the thesis of Theorem I.3, we shall prove that for $\varepsilon \in (0, 1)$ one can determine $h = h(\varepsilon, d, \bar{C}, n, \Omega)$ such that $\omega_L \in B_{1+h}(d\sigma)$. To this aim we will use a classical argument due to Coiffman and Feffermann [2] and Muckenhoupt [10]. Let us fix $0 < \varepsilon < 1$ and consider the $\eta \in (0, 1)$ associated to ε according to (11). Let $\Delta \subset \partial\Omega$ be a surface ball. We take an increasing sequence $\lambda_0 < \lambda_1 < ... < \lambda_k < ...$ with $\lambda_0 = \fint_\Delta w d\sigma$ and, for any $k \in \mathbb{N}$, $\lambda_k =$

$\lambda_0 \left(\frac{S}{\eta}\right)^k$, where $S = D_2(\sigma)$ is the doubling constant of the surface measure σ on Ω.

Now we make the Calderòn-Zygmund decomposition of Δ for the function w and the value λ_0, that is we consider a family $\Delta_{0,j}$ of disjoint surface ball satisfying

$$\begin{aligned} &\lambda_0 < \fint_{\Delta_{0,j}} w d\sigma \leqslant S\lambda_0 \\ &w(x) \leqslant \lambda_0 \qquad a.e.x \notin \cup_{j\in\mathbb{N}}\Delta_{0,j} =: D_0. \end{aligned} \tag{10}$$

Then, we make the Calderòn-Zygmund decomposition of any $\Delta_{0,j}$ for the function w and the value λ_1. In this way we obtain a family $\Delta_{1,j}$ of disjoint surface ball satisfying

$$\begin{aligned} &\lambda_1 < \fint_{\Delta_{1,j}} w d\sigma \leqslant S\lambda_1 \\ &w(x) \leqslant \lambda_1 \qquad a.e.x \notin \cup_{j\in\mathbb{N}}\Delta_{1,j} =: D_1, \end{aligned} \tag{11}$$

and so on. In this way we obtain a family $\Delta_{k,j}$ of surface balls such that

$$\begin{aligned} &\forall k, \ \{\Delta_{k,j}\}_{j\in\mathbb{N}} \text{ is a disjoint family} \\ &\lambda_k < \fint_{\Delta_{k,j}} w d\sigma \leqslant S\lambda_k \\ &w(x) \leqslant \lambda_k \qquad a.e.x \notin \cup_{j\in\mathbb{N}}\Delta_{k,j} =: D_k, \end{aligned} \tag{12}$$

Moreover, since each $\Delta_{k+1,j}$ is contained in $\Delta_{k,i}$ for some i, than $D_{k+1} \subset D_k$.

We have

$$\begin{aligned} S\lambda_k &\geqslant \frac{1}{\sigma(\Delta_{k,i})} \int_{\Delta_{k,i}\cap D_{k+1}} w d\sigma \\ &= \frac{1}{\sigma(\Delta_{k,i})} \sum_{\Delta_{k+1,j}\subset\Delta_{k,i}} \int_{\Delta_{k+1,j}} w d\sigma \\ &> \lambda_{k+1} \frac{\sigma(\Delta_{k,i}\cap D_{k+1})}{\sigma(\Delta_{k,i})}. \end{aligned} \tag{13}$$

Thus,

$$\frac{\sigma(\Delta_{k,i}\cap D_{k+1})}{\sigma(\Delta_{k,i})} < \frac{S\lambda_k}{\lambda_{k+1}} = \eta$$

and hence

$$\frac{\omega_L(\Delta_{k,i}\cap D_{k+1})}{\omega_L(\Delta_{k,i})} < \varepsilon.$$

Summing over i,

$$\omega_L(D_{k+1}) < \varepsilon\omega_L(D_k),$$

which leads to

$$\omega_L(D_k) < \varepsilon^k \omega_L(D_0).$$

Of course we also have

$$\sigma(D_{k+1}) \leqslant \eta\sigma(D_k)$$

and

$$\sigma(D_k) \leqslant \eta^k \sigma(D_0)$$

which implies that

$$\sigma(\cap_{k=0}^{\infty} D_k) = \lim_{k\to\infty} \sigma(D_k) = 0.$$

Then, for any $h > 0$,

$$\begin{aligned} &\int_\Delta w^{1+h} d\sigma = \int_{\Delta\setminus D_0} w^{1+h} d\sigma + \sum_{k=0}^{\infty} \int_{D_k\setminus D_{k+1}} w^{1+h} d\sigma \\ &\leqslant \lambda_0^h \omega_L(\Delta\setminus D_0) + \sum_{k=0}^{\infty} \lambda_{k+1}^h \omega_L(D_k\setminus D_{k+1}) \\ &\leqslant \lambda_0^h \left\{ \omega_L(\Delta\setminus D_0) + \sum_{k=0}^{\infty} (S\eta^{-1})^{(k+1)h} \varepsilon^k \omega_L(D_0) \right\} \\ &\leqslant \lambda_0^h \left\{ \omega_L(\Delta\setminus D_0) + (S\eta^{-1})^h \sum_{k=0}^{\infty} ((S\eta^{-1})^h \varepsilon)^k \omega_L(D_0) \right\}. \end{aligned} \tag{14}$$

Now, if we take $h > 0$ small enough in order to have $(S\eta^{-1})^h\varepsilon < 1$, i.e.

$$h < \frac{\varepsilon \log(\varepsilon^{-1})}{Cd^2\bar{C} + \varepsilon \log S} \tag{15}$$

the series in the right hand side of (16) will have a finite sum and we shall get

$$\begin{aligned} \int_\Delta w^{1+h} d\sigma &\leqslant C\lambda_0^h \left(\omega_L(\Delta\setminus D_0) + \omega_L(D_0)\right) \\ &= C \left(\fint_\Delta w d\sigma\right)^h \omega_L(\Delta) \end{aligned}$$

that is $\omega_L \in B_{1+h}(d\sigma)$. At this point, using Theorem I.1 the thesis easily follows. □

REFERENCES

[1] L. Caffarelli, E. Fabes, S. Mortola and S. Salsa, *"Boundary behavior of non-negative solutions of elliptic operators in divergence form"*, Ind. U. Math. J., **30**, (1981) 621-640;

[2] Coifmann, R. Fefferman, *"Weighted norm inequalities for maximal functions and singular integrals"*, Studia Math., **51** (1974), 241-250.

[3] B. E. J. Dahlberg, *"On estimates of harmonic measure"*, Arch. Rat. Mech. Anal., **65**, (1977), 272-288;

[4] B. E. J. Dahlberg, *"On the Poisson integral for Lipschitz and C^1 domains"*, Studia Math., **66**, (1979), 7-24;

[5] M. Dindos, C. Kenig, J.Pipher "*BMO Solvability and the A_∞ Condition for Elliptic Operator* ". J. Geom. Anal. (2011) 21 78-95;

[6] R. Fefferman, C. Kenig and J. Pipher, *"The Theory of Weights and the Dirichlet Problem for Elliptic Equations"* Annals of Math., **134**, (1991), 65-124;

[7] J. Garcia-Cuerva, J. L. Rubio de Francia, *"Weighted norm inqualities and related topics"*, North- Holland Math. Stud., vol. **116**, North-Holland, Amsterdam, (1985);

[8] C. E. Kenig, *"Harmonic Analysis Techniques for Second Order Elliptic Boundary Value Problems"*, Conference Board of the Mathematical Sciences, Amer. Math. Soc. **83**, (1991);

[9] C. E. Kenig, H. Koch, J. Pipher and T. Toro "*A new approach to absolute continuity of the elliptic measure, with applications to non-symmetric equations"* Adv. Math. **153**, 2 (2000) 231-298;

[10] B. Muckenhoupt, *"Weighted norm inqualities for the Hardy maximal function"*, Trans. Amer. Math. Soc., **165**, (1972), 207-226;

[11] C. Sbordone, *"Sharp embeddings for classes of weights and applications"*, Rend Accad. Naz. delle Scienze detta dei XL, *Memorie di Matematica e Applicazioni* 123^0 **XXIX**, fasc. 1, (2005), 339-354;

[12] C. Sbordone, G.Zecca *" The L^p -solvability of the Dirichlet problem for planar elliptic equations, sharp results."* J. Fourier Anal. Appl. 15 (2009), no. 6, 871-903.

[13] G. Zecca, *"On the Dirichlet problem with Orlicz boundary data"*, Boll. Unione Mat. Ital. Sez. B Artic. Ric. Mat. (8) 10 (2007), no. 3, 661–679;

[14] G. Zecca, *"The unsolvability of the Dirichlet problem with $L(logL)^\alpha$ boundary data"*, Rend. Acc. Sc. Fis. Mat. Napoli, **72**, (2005) 71-80.

ISBN: 978-1-61804-225-5

Some advantages of the hybrid methods, which used the first derivative of the solution of the considered problem

G.Mehdiyeva, M.Imanova, V.Ibrahimov

Department of Computational mathematics
Baku State University

Abstract— The scientists began investigate of the solution of ODE from the XVII century. Many famous mathematicians as Newton, Leibniz, Bernoulli, D' Alembert, Euler, Cauchy and etc. have considered solving of the ordinary differential equations. For solving these equations the scientists from the different country have constructed many methods. Here, with the help of the compare known results are shown some advantages of the hybrid methods. Are constructed the hybrid methods with the order of accuracy $p = 8k$. Here, is suggested concrete hybrid method of the fractional step type with the order of accuracy $p = 8$ for $k = 1$ for which uses the first order derivative of the solution of the initial value problem.

***Keywords*—**Initial value problem for ODE, hybrid methods, degree and stability of the hybrid methods, the relation between of the degree and order of the hybrid methods.

I. Introduction

There is a wide arsenal of numerical methods for solving ordinary differential equation of the first order. Remark, that like Clairaut, many scientists have applied of the indirect-numerical method investigates practical problems (see, for example [1, p.132-133]). However, Euler found the shortcomings of existing methods and has constructed a direct method, which now is called the explicit Euler method (see [2, p. 289]). Euler has determined also the shortcomings of his method and suggested two ways to correct the indicated shortcomings. One of them is the use of Taylor's formula. The replacing the higher-order derivatives in Taylor's formula the first derivative, Runge-Kutta (in the beginning of XX century) and Adams (in the middle of XIX century) have constructed numerical methods, that generalizes the one and multistep methods accordingly. However, to solving of the following initial-value problem:

$$y' = f(x, y),\ y(x_0) = y_0. \qquad (1)$$

Here proposed use of the second derivative of the solution of problem (1) for construction of hybrid methods.

It is known that the Runge-Kutta methods, which applied to solving of problem (1), may be written as follows:

$$y_{n+1} = y_n + h\sum_{i=1}^{s} b_i K_i^{(s)}, \qquad (2)$$

$$K_i^{(s)} = f(x_n + \alpha_i h, y_n + h(\beta_{1,s}K_1^{(s)} + \beta_{2,s}K_2^{(s)} + ... + \beta_{s,s}K_s^{(s)})),$$

$$i = 1,2,..., s.$$

Usually this method is called the implicit Runge-Kutta method.

Let us consider the generalization of the Adams method, which can be written as the following:

$$\sum_{i=0}^{k} \alpha_i y_{n+i} = h\sum_{i=0}^{k} \beta_i f_{n+i}. \qquad (3)$$

In references, this method is called the k-step method with constant coefficients. Note that, there are some relationships between methods Runge-Kutta and multistep (see for example [3], [4]). But the implicit Runge-Kutta methods correspond to the forward-jumping methods, which are received from the method (3) for the values $\alpha_k = \alpha_{k-1} = ... = \alpha_{k-m+1} = 0$ and $\alpha_{k-m} \neq 0$. As follows from this for the application of forward-jumping methods may be replaced by application of implicit Runge-Kutta methods. Therefore taking into account of the some advantages of forward-jumping methods in the work [5] considered of application of these methods to solving Volterra integral equations.

In the middle of the XX century, scientists have constructed procedures which are called hybrid methods. One of papers devoted to the construction of hybrid methods

The authors with express their thanks to academician Ali Abbasov for his suggestion that the investigate the computational aspects. This work was supported by the Science Development Foundation of Azerbaijan (Grand EIF-2011-1(3)-82/27/1).

G.Yu.Mehdiyeva - doctor of science, PhD, professor, head of chair of Computational mathematics of Baku State University, Baku, Azerbaijan (corresponding author to provide phone 994125106048 e-mail: imn_bsu@mail.ru)

V.R.Ibrahimov - doctor of science, PhD, professor of the department of Computational mathematics of Baku State University, Baku, Azerbaijan (e-mail: ibvag@mail.com)

M.N.Imanova is with the Baku State University, PhD, teacher of department of Computational mathematics, Baku, Azerbaijan (e-mail: imn_bsu@mail.ru)

belongs to Gear (see [6]-[10]). In general form this method may be written as follows:

$$\sum_{i=0}^{k} a_i y_{n+i} = h\sum_{i=0}^{k} \beta_i f_{n+i} + h\beta f_{n+k-\nu} \quad (0 < \nu < 1). \quad (4)$$

Gear's method is a hybrid method of type (3). One of the first hybrid methods of type (2) was constructed in [11] and has the following form:

$$y_{n+1} = y_n + h(K_1 + K_2)/2. \quad (5)$$

where

$$K_1 = f(x_n + \frac{3-\sqrt{3}}{6}h,\ y_n + h(K_1 + \frac{3-2\sqrt{3}}{3}K_2)/4);$$

$$K_2 = f(x_n + \frac{3+\sqrt{3}}{6}h,\ y_n + h(\frac{3+2\sqrt{3}}{3}K_1 + K_2)/4).$$

Remark that the method (5) constructed on the basis of trapezoidal method and belongs to a class of implicit Runge-Kutta methods . For using the methods (5) here have proposed the following scheme, which recalls a predictor-corrector methods applying to investigation of the implicit multistep methods:

$$K_1 = f(x_n + \frac{3-\sqrt{3}}{6}h,\ y_n + h(\hat{K}_1 + \frac{3-2\sqrt{3}}{3}\hat{K}_2)/4);$$

$$K_2 = f(x_n + \frac{3+\sqrt{3}}{6}h,\ y_n + h(\frac{3+2\sqrt{3}}{3}\hat{K}_1 + \hat{K}_2)/4).$$

Obviously, if $\hat{K}_1 = K_1$ and $\hat{K}_2 = K_2$ from this we receive the method (5). But if the quantity $\hat{K}_1$ and $\hat{K}_2$ is defined as:

$$\hat{K}_1 = f(x_n + \frac{3-\sqrt{3}}{6}h,\ y_n + \frac{3-\sqrt{3}}{6}hf(x_n + \frac{3-\sqrt{3}}{12}h,\ y_n + \frac{3-\sqrt{3}}{12}f_n)),$$

$$\hat{K}_2 = f(x_n + \frac{3+\sqrt{3}}{6}h,\ y_n + \frac{3+\sqrt{3}}{6}hf(x_n + \frac{3+\sqrt{3}}{12}h,\ y_n + \frac{3+\sqrt{3}}{12}f_n)),$$

then one can be obtain the explicit method. However, for a simpler method the quantity $\hat{K}_1$ and $\hat{K}_2$ may be determined as follows:

$$\hat{K}_1 = f(x_n + (3-\sqrt{3})h/6,\ y_n + (3-\sqrt{3})hf_n/6),$$

$$\hat{K}_2 = f(x_n + (3+\sqrt{3})h/6,\ y_n + (3+\sqrt{3})hf_n/6).$$

Now consider the determination of the quantity K_1 and K_2 in the following form:

$$K_1 = f(x_{n+1/2-\alpha}, y_{n+1/2-\alpha}),$$

$$K_2 = f(x_{n+1/2+\alpha}, y_{n+1/2+\alpha}) \quad (\alpha = \sqrt{3}/6).$$

In this case the method (5) is converted to a symmetric hybrid method of the multistep type.

Note that often the hybrid methods are constructed in the symmetric form. Similar methods may be written in the following general form (see for example [7]-[10]):

$$\sum_{i=0}^{k} \alpha_i y_{n+i} = h\sum_{i=0}^{k} \beta_i f_{n+i} + h\hat{\beta}_0 f_{n+m+s} + h\hat{\beta}_k f_{n+k+m-s},$$

$$(s > 0;\ m - s > 0;\ m + s \le k).$$

It is clear that hybrid method in simple form can be written as:

$$\sum_{i=0}^{k} \alpha_i y_{n+i} = h\sum_{i=0}^{k} \beta_i f_{n+i+l_i} \quad (|l_i| < 1). \quad (6)$$

Now consider to construction of the methods on junction of the methods (6) and the methods of Adams.

II. ON ONE GENELALIZATION OT THE METHOD (6)

This method is more precise than corresponding classic methods of Runge-Kutta and Adams. If to generalize this, then in result we receive the following:

$$\sum_{i=0}^{k} \alpha_i y_{n+i} = h\sum_{i=0}^{k} \beta_i f_{n+i} + h\sum_{i=0}^{k} \gamma_i f_{n+i+l_i} \quad (|l_i| < 1). \quad (7)$$

Obviously, that the method (7) - is the hybrid method of the multistep type with the constant coefficients. Note that the integer-valued quantity p is called the degree of the method (7) if the following asymptotic equality is holds:

$$\sum_{i=0}^{k} (\alpha_i y(x+ih) - h\sum_{i=0}^{k} (\beta_i y'(x+ih) + \beta_i y'(x+(i+l_i)h))) = \quad (8)$$

$$= O(h^{p+1}),\ h \to 0.$$

Note that usually the definition of the order of accuracy of the hybrid methods of multistep type is identical of the definition of the degree of ordinary multistep methods.

The stability of method (7) may be defined according to the definition of the stability for multistep methods (see [12]). One of the basic issues in the investigation of the this method is the relationship between its degree and order. Before determining the relationship, let us consider some restrictions imposed on the coefficients of method (7).

A: The coefficients $\alpha_i, \beta_i, \gamma_i$ and $l_i, (i = 0,1,2,...,k)$ are the real numbers; moreover, $\alpha_k \neq 0$.

B: The characteristic polynomials

$$\rho(\lambda) \equiv \sum_{i=0}^{k} \alpha_i \lambda^i;\ \sigma(\lambda) \equiv \sum_{i=0}^{k} \beta_i \lambda^i;\ \gamma(\lambda) \equiv \sum_{i=0}^{k} \gamma_i \lambda^{i+l_i}$$

have no common multiple different from constant.

C: $\sigma(1) + \gamma(1) \neq 0$ and $p \ge 1$.

With the help of the methods of undetermined coefficients, we can examine the definition of the quantities $\alpha_i, \beta_i, \gamma_i, l_i$ $(i = 0,1,2,...,k)$, so we will consider the following expansion:

$$y(x+ih) =$$

$$= y(x) + ihy'(x) + \frac{(ih)^2}{2!}y''(x) + ... + \frac{(ih)^p}{p!}y^{(p)}(x) + O(h^{p+1}), \quad (9)$$

$$y'(x+ih) =$$
$$= y'(x) + ihy''(x) + \frac{(ih)^2}{2!}y'''(x) + ... + \frac{(ih)^{p-1}}{(p-1)!}y^{(p)}(x) + O(h^p), \quad (10)$$

where $x = x_0 + nh$ is a fixed point.

Note that the values of the coefficients of the multistep method in some sense are connected with the relationship between the order and degree of method (7); therefore, we require the following lemma.

Lemma. Let $y(x)$ be a sufficiently smooth function, and assume that conditions A, B, and C are holds. In order to make the method (7) had a degree p, satisfaction of its coefficients of the following conditions are necessary and sufficient:

$$\sum_{i=0}^{k}\alpha_i = 0,\ \sum_{i=0}^{k} i\alpha_i = \sum_{i=0}^{k}(\beta_i + \gamma_i),$$
$$\sum_{i=0}^{k}\frac{i^l}{l!}\alpha_i = \sum_{i=0}^{k}\frac{i^{l-1}}{(l-1)!}\beta_i + \sum_{i=0}^{k}\frac{(i+l_i)^{l-1}}{(l-1)!}\gamma_i, \quad (11)$$
$$(l = 2,3,..., p).$$

Proof. We first prove that if method (7) has the degree p, then the coefficients $\alpha_i, \beta_i, \gamma_i, l_i$ $(i = 0,1,2,...,k)$ will satisfy the system of nonlinear algebraic equations given in (11).

Taking into account that the method (7) has the degree p, then by using Taylor expression (9) and (10) in the left hand-side of asymptotic equality (8). We have:

$$\left(\sum_{i=0}^{k}\alpha_i\right)y(x) + h\sum_{i=0}^{k}\left(i\alpha_i - \beta_i - \gamma_i\right)y'(x) +$$
$$+ h^2\sum_{i=0}^{k}\left(\frac{i^2}{2}\alpha_i - i\beta_i - (i+l_i)\gamma_i\right)y''(x) + ... + \quad (12)$$
$$+ h^p\sum_{i=0}^{k}\left(\frac{i^p}{p!}\alpha_i - \frac{i^{p-1}}{(p-1)!}\beta_i - \frac{(i+l_i)^{p-1}}{(p-1)!}\gamma_i\right)y^{(p)}(x) = O(h^{p+1}),$$
$$h \to 0.$$

If take in account that the method (7) has the degree p, then we obtain the following:

$$\sum_{i=0}^{k}\alpha_i y(x) + h\sum_{i=0}^{k}(i\alpha_i - \beta_i - \gamma_i)y'(x) +$$
$$+ h^2\sum_{i=0}^{k}(\frac{i^2}{2} - i\beta_i - (i+l_i)\gamma_i)y''(x) + ... \quad (13)$$
$$+ h^p\sum_{i=0}^{k}(\frac{i^p}{p!}\alpha_i - \frac{i^{p-1}}{(p-1)!}\beta_i - \frac{(i+l_i)^{p-1}}{(p-1)!}\gamma_i)y^{(p)}(x) = 0.$$

It is known that $1, x, x^2, ..., x^p$ forms a linearly independent system; therefore, equality (13) is equivalent to the following:

$$\sum_{i=0}^{k}\alpha_i = 0,\ \sum_{i=0}^{k}(i\alpha_i - \beta_i - \gamma_i) = 0, ..., \quad (14)$$
$$\sum_{i=0}^{k}(\frac{i^p}{p!}\alpha_i - \frac{i^{p-1}}{(p-1)!}\beta_i - \frac{(i+l_i)^{p-1}}{(p-1)!}\gamma_i) = 0.$$

We now will prove that if the coefficients of the method (7) are the solution of the nonlinear system (11), then its degree is equal to p. Indeed, if we used the system of equalities of (14) into equality (12), then we obtain the asymptotic equality of (8). From this asymptotic equality it follows that method (7) must have the degree p. It is easy to determine that for the chosen values $l_i = 0$ $(i = 0,1,...,k)$, the system (11) is linear and coincides with the known systems used for defining the coefficients of the multistep method with constant coefficients. Subject to the conditions from $|l_0| + |l_1| + ... + |l_k| \neq 0$, the system (11) is nonlinear. This system contains $p+1$ equations in $4k+4$ unknowns and is homogeneous; it must possess the zero solution, and for system (11) have a non-zero solution, suppose that the condition $4k+4 > p+1$ is holds. Hence, we obtain that there are methods of type (7) with the order $p \le 4k+2$.

Consider the construction methods of type (6) and suppose that $k = 1$. Then, under the assumption that $\alpha_1 = -\alpha_0 = 1$ and $\gamma_1 = \gamma_0 = 0$, from the system of (11) we will have the following system for the determined of variables β_0, β_1, l_0 and l_1:

$$\begin{aligned} &\beta_0 + \beta_1 = 1,\\ &l\beta_0 + \gamma\beta_1 = 1/2,\\ &l^2\beta_0 + \gamma^2\beta_1 = 1/3,\\ &l^3\beta_0 + \gamma^3\beta_1 = 1/4. \end{aligned} \quad (15)$$

Here, $l = l_0$, and $\gamma = 1 + l_1$. Solving this nonlinear system of equations for l and γ in result receive the following quadratic equation:

$$l^2 - l + 1/6 = 0.$$

The value of γ is determined from the equation $\gamma + l = 1$. Note that the method with the degree $p = 4$ can be written as follows:

$$y_{n+1} = y_n + h(f_{n+l_0} + f_{n+1+l_1})/2. \quad (16)$$

Here $l_1 = -l_0;\ l_0 = (3-\sqrt{3})/6,\ 1+l_1 = (3+\sqrt{3})/6$. For this aim consider to applying hybrid method (16). Need to know the value of the $y_{n+1/2+\sqrt{3}/6}$, y_{n+l_0} and $y_{n+1/2-\sqrt{3}/6}$. Note, that these variables are independent of y_{n+1}, because that method (16) is explicit. But therefore, there still exist implicit hybrid methods. For example, consider the following method:

$$y_{n+1} = y_n + h(3f_{n+1/3} + f_{n+1})/4. \quad (17)$$

This method is an implicit hybrid method with degree $p = 3$ and is A-stable (see [13]).

Consider method (7) for $k = 1$. In this case, assuming that $\alpha_1 = -\alpha_0 = 1$, the system (15) takes the following form:

$$\beta_0+\beta_1+\gamma_0+\gamma_1=1,$$
$$\beta_1+l_0\gamma_0+l_1\gamma_1=1/2,$$
$$\beta_1+l_0^2\gamma_0+l_1^2\gamma_1=1/3,$$
$$\beta_1+l_0^3\gamma_0+l_1^3\gamma_1=1/4,$$
$$\beta_1+l_0^4\gamma_0+l_1^4\gamma_1=1/5,$$
$$\beta_1+l_0^5\gamma_0+l_1^5\gamma_1=1/6.$$

The solution of this nonlinear system yields the following:

$$\beta_0=\beta_1=1/12,\ \gamma_0=\gamma_1=5/12,$$
$$l_0=1/2-\sqrt{5}/10,\ l_1=1/2+\sqrt{5}/10.$$

The corresponding method with degree $p=6$ takes the following form:

$$y_{n+1}=y_n+h(f_{n+1}+f_n)/12+$$
$$+5h(f_{n+1/2-\sqrt{5/10}}+f_{n+1/2+\sqrt{5/10}})/12\ \ (p=6). \qquad (18)$$

To apply hybrid methods to solving of some problems, we should know the values of $y_{n+1/2-\sqrt{5/10}}$ and $y_{n+1/2+\sqrt{5/10}}$, and the accuracy of these values should have order at least $O(h^6)$. Note that hybrid method (18) is implicit and that when applying it to solving of initial value problem (1), is used a predictor-corrector scheme containing only one explicit method. Therefore, we consider the construction of an explicit method (in one variant) has the following form:

$$y_{n+1}=y_n+hf_n/9+h((16+\sqrt{6})f_{n+(6-\sqrt{6})/10}+$$
$$+(16-\sqrt{6})f_{n+(6+\sqrt{6})/10})/36. \qquad (19)$$

This method is explicit and has degree $p=5$.

To use method (19) we must define $y_{n+(6-\sqrt{6})/10}$ and $y_{n+(6+\sqrt{6})/10}$. The technique used to calculate these quantities determines the properties of the block method.

Suppose that the approximated values of the solution of problem (1) the mesh points $x_n+(1-\sqrt{5}/5)h/2$ and $x_n+(1+\sqrt{5}/5)h/2$ have been identified by some method. Then (18) may be considered as equation in the unknowns y_{n+1}, whose solution is usually obtained via iterative processes. In contrast, we suggest a predictor-corrector method, which recalls block methods. It is easy to show that first one can calculate the values of according to method (19) and then correct these values by the method (18). We therefore constructed an algorithm for applying method (19) to solving of problem (1).

Note that can be acquainted with application of hybrid methods to numerical solution of Volterra integral and integro-differential equations in [14]-[16]. And in [17] for solving problem (1) is constructed hybrid method with degree $p=7$ for $k=3$ by using collocation approach.

It follows that the investigation of hybrid methods is more difficult than the known. Consider the following hybrid method:

$$y_{n+1}=y_n+h(64y'_{n+1}+98y'_{n+1/2}+18y'_n)/360+$$
$$+h(18y'_{n+1/2+\beta/2}+98y'_{n+1/2}+64y'_{n+1/2-\beta/2})/360, \qquad (20)$$
$$(\beta=\sqrt{21}/14).$$

This stable method is one step and have the degree $p=8$. In the next we show that this method is not received from the method (7) as the special case.

Remark that, the method (20) is available for solving problem (1), which is not contained in the method (7) as the special case. But if we change h by $2h$ and use it in the formula (20), then we receive the method, which is including in class methods of type (7). Note that this method can be written as the following:

$$y_{n+2}=y_n+h(64y'_{n+2}+98y'_{n+1}+18y'_n)/180+$$
$$+h(18y'_{n+1+\beta}+98y'_{n+1}+64y'_{n+1-\beta})/180. \qquad (21)$$

Now consider the construction of some procedure for solving problem (1) by using hybrid methods with the degree $p=4,\ p=5$ and $p=6$. Note that these methods are constructed for $k=1$ (the characteristic polynomial has one root which is define as the $\lambda=1$), and all of them are stable. Methods (16) and (19) are explicit, whereas method (18) is implicit. However, the application of explicit hybrid methods requires some additional auxiliary formulas. To this end, we construct an algorithm for method (16).

Algorithm 1. Applies method (16) to the solution of problem (1).

Step 1. Calculate y_{n+l} and y_{n+1-l} by with the following block method:

$$y_{n+l}=y_n+lhf_n,$$
$$\hat{y}_{n+l}=y_n+lh(f_n+\bar{f}_{n+l})/2,\ \ (\bar{f}_m=f(x_m,\bar{y}_m),\ \ m=0,1,2,...),$$
$$y_{n+l}=y_n+lh(5f_n+8\hat{f}_{n+l})/12-$$
$$-lhf(x_n+2lh,y_n+2lh\hat{f}_{n+l})/12,$$
$$(\hat{f}_m=f(x_m,\hat{y}_m),\ \ m=0,1,2,...).$$

Repeat this scheme for $l:=(3-\sqrt{3})/6$ and $1+l=(3+\sqrt{3})/6$

Step 2. Calculate y_{n+1} according to method (16). Here, we compute the values of the quantities y_{n+l} and y_{n+1+l} to within $O(h^4)$, which suffices for this algorithm.

Now, we construct an algorithm for applying method (19).

Algorithm 2. Applies method (19) to the numerical solution of problem (1), assuming that the values y_0 and $y_{1/2}$ have been determined with the required accuracy.

Step I. Set $\hat{y}_{n+1}=y_n+hy'_{n+1/2}$,

Step II. Set $y_{n+1}=y_n+h(\hat{y}'_{n+1}+4y'_{n+1/2}+y'_n)/6$,

Step III. Set $y_{n+3/2} = y_{n+1/2} + h(7y'_{n+1} - 2y'_{n+1/2} + y'_n)/6,$

Step IV. Compute

$$y_{n+\alpha} = y_n + \alpha h y'_n + \alpha^2 h((\alpha^2 - 12\alpha + 6)y'_{n+3/2} -$$
$$-(3\alpha^2 - 48\alpha + 27)y'_{n+1} + +(3\alpha^2 - 60\alpha + 54)y'_{n+1/2} -$$
$$-(\alpha^2 - 24\alpha + 33)y'_n)/18$$

for $\alpha = \frac{6-\sqrt{6}}{10}$ and $\alpha = \frac{6+\sqrt{6}}{10}$.

Step V. Conclude that

$$y_{n+1} = y_n + hf_n/9 + h((16+\sqrt{6})f_{n+(6-\sqrt{6})/10} +$$
$$+(16-\sqrt{6})f_{n+(6+\sqrt{6})/10})/36.$$

For demonstrate algorithm 1 consider to application of its to the solving of the next problem:

$y' = \cos x,\ y(0) = 0$ (Exact solution as $y(x) = \sin x$).

Results tabulated in table 1.

Step size	**Variable** x	**Error of the algorithm 1**
$h = 0.05$	0.10	$0.14E-09$
	0.40	$0.56E-09$
	0.70	$0.93E-09$
	1.00	$0.12E-08$

Conclusion. We have constructed a multistep hybrid method with the degree $4 \le p \le 6$ for $k = 1$, and with the degree $p = 8$ for $k = 2$. It is known that for $k = 1$, the ordinary k-step method has maximal degree $p_{\max} = 2$, which yields a trapezoidal method. However, the hybrid approach, which constructed here has maximal degree $p_{\max} = 6$, although the application of the trapezoid method is simpler than applying hybrid procedure. Using the Euler explicit method in place of the predictor method, one can construct a predictor-corrector scheme for the practical application of the trapezoidal method. Remark that for the construction of the stable methods with the degree $p = 2k + 2$ can be used multistep methods with second derivatives (see, for example [15]-[25]). In this paper, we have used the block method to construction of algorithms for using hybrid methods. The method, having the degree $p = 4$, was described in algorithm 1, and algorithm 2 formulated to using of the method (19). Note that after some modifications, algorithm 2 may be realized for using method (18). In the end, let us remark that for $k = 2$, we have constructed stable methods of type (7) with degree $p = 8$ and by using that shown how can be receive the one step method (20) from the two step method (21). Method (20) is one step hybrid method and different from method (7). Consequently the methods of type (20) are more accurate, than the methods of type (7). Thus we receive that the hybrid methods have some unknown properties and therefore investigation of those methods are interesting.

REFERENCES

[1] *Subbotin M.F.* Kurs nebesnoy mekhaniki // t.2, ONTI, Moskow, 1937, 404p.

[2] *Euler L.* Integral calculus // T.1, Gos.izd of engineering and technical literature, 1956, P.415.

[3] *Skvortsov L.M.* Explicit two-step Runge-Kutta methods // Math. modeling, v. 21, 9, 2009, P. 54-65.

[4] *Mehdiyeva G.Yu., Nasirova I.I., Ibrahimov V.R.* On some connections between Runge-Kutta and Adams methods // Transactions issue mathematics and mechanics series of physical-technical and mathematical science, No5, 2005, P.55-62.

[5] *Mehdiyeva G.Yu., Imanova M.N., Ibrahimov V.R.* On one application of forward jumping methods. Applied Numerical Mathematics, Volume 72, October 2013, p. 234–245.

[6] *Mehdiyeva G.Yu., Imanova M.N., Ibrahimov V.R.* On one generalization of hybrid methods // Proceedings of the 4th international conference on approximation methods and numerical modeling in environment and natural resources Saidia, Morocco, may 23-26, 2011, P. 543-547.

[7] *Butcher J.C.* Numerical methods for ordinary differential equations. John Wiley and sons, Ltd, Second Edition, 2008.

[8] *Butcher J.C.* A modified multistep method for the numerical integration of ordinary differential equations. J. Assoc. Comput. Math., v.12, 1965, pp.124-135.

[9] *Gear C.S.* Hybrid methods for initial value problems in ordinary differential equations . SIAM, J. Numer. Anal. v. 2, 1965, p. 69-86.

[10] *G.K. Gupta.* A polynomial representation of hybrid methods for solving ordinary differential equations. Mathematics of comp., volume 33, number 148, 1979, P.1251-1256.

[11] *Hammer P.C., Hollingsworth J.W.* Trapezoildal methods of approximating solution of differential equations // MTAC-vol. 9, 1955, p.92-96.

[12] *Dahlquist G.* Convergence and stability in the numerical integration of ordinary differential equations // Math. Scand. 1956, 4, p.33-53.

[13] *Ibrahimov V.R.* On a nonlinear method for numerical calculation of the Cauchy problem for ordinary differential equation // Diff. equation and applications. Pron. of II International Conference Russe. Bulgarian, 1982, pp. 310-319.

[14] *Makroglou A.* Hybrid methods in the numerical solution of Volterra integro-differential equations. Journal of Numerical Analysis 2, 1982, pp.21-35.

[15] *Mehdiyeva G., Imanova M., Ibrahimov V.* The application of the hybrid method to solving the Volterra integro-differential equation. World Congress on Engineering 2013, London, U.K., 3-5 July, 2013, p.186-190

[16] *Mehdiyeva G., Imanova M., Ibrahimov V.* On a Research of Hybrid Methods. Numerical Analysis and Its Applications, Springer, 2013, p. 395-402.

[17] *Areo E.A., R.A. Ademiluyi, Babatola P.O.* Accurate collocation multistep method for integration of first order ordinary differential equations // J.of Modern Math.and Statistics, 2(1): 1-6, 2008, P. 1-6

[18] G. Dahlquist, Stability and Error Bounds in the Numerical Integration of Ordinary Differential Equations. Trans. Of the Royal Inst. Of Techn. Stockholm, Sweden, Nr. 130, 1959, 87pp.

[19] *Kobza J.* Second derivative methods of Adams type // Applikace Mathematicky, 1975, №20, p.389-405.

[20] *Ibrahimov V.* On the maximal degree of the k-step Obrechkoff's method. Bulletin of Iranian Mathematical Sociaty, Vol.28, №1, 2002, p. 1-28.

[21] *Enrite W.H.* Second derivative multistep methods for stiff ordinary differential equations, SIAM, J.Numer.Anal., 1974, №2, p.321-332.

[22] *Iserles A. and Norset S.P.* Two-step method and Bi-orthogonality. Math. of Comput., 180 (1987) 543-552.

[23] *Hairier E., Norsett S.P., and Wanner G.* Solving ordinary differential equations. *(Russian) M., Mir, 1990, 512 p.*

[24] *Mehdiyeva G., Imanova M., Ibrahimov V.* An application of the hybrid methods to the numerical solution of ordinary diff erential equations of second order. Kazakh National University named after Al-Farabi Journal

of treasury series mathematics, mechanics, computer science, Almaty №4 (75) 2012, p. 46-54.

[25] *Mehdiyeva G., Imanova M., Ibrahimov V.* A way to construct an algorithm that uses hybrid methods. Applied Mathematical Sciences, HIKARI Ltd, Vol. 7, 2013, no. 98, p.4875-4890.

On the convergence of two iterative methods for k-strictly pseudo-contractive mappings in CAT(0) spaces

A. Şahin and M. Başarır

***Abstract*—** In this paper, we prove the demiclosedness principle for k-strictly pseudo-contractive mappings and establish the Δ-convergence theorem of the cyclic algorithm for such mappings in CAT(0) spaces. Also, we give the strong convergence theorem of the modified Halpern iteration for k-strictly pseudo-contractive mappings in CAT(0) spaces. Our results extend and improve the corresponding recent results announced by many authors in the literature.

***Keywords*—** CAT(0) space, fixed point, k-strictly pseudo-contractive mapping, iterative method.

I. Introduction

LET C be a nonempty subset of a Hilbert space X. Recall that a mapping $T:C\to C$ is said to be k-strictly pseudo-contractive if there exists a constant $k\in[0,1)$ such that

$$\|Tx-Ty\|^2 \le \|x-y\|^2 + k\|(I-T)x-(I-T)y\|^2,\ \forall x,y\in C.$$

A point $x\in C$ is called a fixed point of T if $x=Tx$. We will denote the set of fixed points of T by $F(T)$. Note that the class of k-strictly pseudo-contractions includes the class of nonexpansive mappings T on C as a subclass. That is, T is nonexpansive if and only if T is 0-strictly pseudo-contractive. The mapping T is also said to be pseudo-contractive if $k=1$ and T is said to be strongly pseudo-contractive if there exists a constant $\lambda\in(0,1)$ such that $T-\lambda I$ is pseudo-contractive. Clearly, the class of k-strictly pseudo-contractive mappings is the one between classes of nonexpansive mappings and pseudo-contractive mappings. Also we remark that the class of strongly pseudo-contractive mappings is independent from the class of k-strictly pseudo-contractive mappings. Recently, many authors have been devoting the studies on the problems of finding fixed points for k-strictly pseudo-contractive mappings (see, e.g., [1]- [3]).

We define the concept of k-strictly pseudo-contractive mapping in a CAT(0) space as follows.

Let C be a nonempty subset of a CAT(0) space X. A mapping $T:C\to C$ is said to be k-strictly pseudo-contractive if there exists a constant $k\in[0,1)$ such that

$$d(Tx,Ty)^2 \le d(x,y)^2 + k\big(d(x,Tx)+d(y,Ty)\big)^2,\ \forall x,y\in C. \quad (1)$$

Acedo and Xu [4] introduced a cyclic algorithm in a Hilbert space. We modify this algorithm in a CAT(0) space.

Let $x_0\in C$ and $\{\alpha_n\}$ be a sequence in $[a,b]$ for some $a,b\in(0,1)$. The cyclic algorithm generates a sequence $\{x_n\}$ in the following way:

$$\begin{cases} x_1=\alpha_0x_0\oplus(1-\alpha_0)T_0x_0,\\ x_2=\alpha_1x_1\oplus(1-\alpha_1)T_1x_1,\\ \vdots\\ x_N=\alpha_{N-1}x_{N-1}\oplus(1-\alpha_{N-1})T_{N-1}x_{N-1},\\ x_{N+1}=\alpha_Nx_N\oplus(1-\alpha_N)T_0x_N,\\ \vdots \end{cases}$$

or, shortly,

$$x_{n+1}=\alpha_nx_n\oplus(1-\alpha_n)T_{[n]}x_n,\ \forall n\ge 0, \quad (2)$$

where $T_{[n]}=T_i$, with $i=n\ (mod N)$, $0\le i\le N-1$. By taking $T_{[n]}=T$ for all n in (2), we obtain the Mann iteration in [5].

In this paper, motivated by the above results, we prove the demiclosedness principle for k-strictly pseudo-contractive mappings in a CAT(0) space. Also we present the strong and Δ-convergence theorems of the cyclic algorithm and the modified

This paper was supported by Sakarya University Scientific Research Foundation (Project number: 2013-02-00-003).

A. Şahin is with Department of Mathematics, Faculty of Sciences and Arts, Sakarya University, Sakarya, 54187, TURKEY (e-mail: ayuce@sakarya.edu.tr).

M. Başarır is with Department of Mathematics, Faculty of Sciences and Arts, Sakarya University, Sakarya, 54187, TURKEY (corresponding author, phone: +902642955990; fax: +902642955950; e-mail: basarir@sakarya.edu.tr).

Halpern iteration which is introduced for Hilbert space by Hu [6] for such mappings in a CAT(0) space.

II. Preliminaries on CAT(0) space

A metric space X is a CAT(0) space if it is geodesically connected and if every geodesic triangle in X is at least as 'thin' as its comparison triangle in the Euclidean plane. It is well known that any complete, simply connected Riemannian manifold having non-positive sectional curvature is a CAT(0) space. Other examples include Pre-Hilbert spaces (see [7]), Euclidean buildings (see [8]), $\mathbb{R}$-trees (see [9]), the complex Hilbert ball with a hyperbolic metric (see [10]) and many others. For a throughout discussion of these spaces and of the fundamental role they play in geometry, we refer the reader to Bridson and Haefliger [7].

Fixed point theory in a CAT(0) space has been first studied by Kirk (see [11], [12]). He showed that every nonexpansive mapping defined on a bounded closed convex subset of a complete CAT(0) space always has a fixed point. Since then the fixed point theory in a CAT(0) space has been rapidly developed and many papers have appeared (see e.g., [13]-[16]). It is worth mentioning that fixed point theorems in a CAT(0) space (specially in $\mathbb{R}$-trees) can be applied to graph theory, biology and computer science (see, e.g., [9], [17]-[20]).

Let (X,d) be a metric space. A *geodesic path* joining $x \in X$ to $y \in X$ (or more briefly, a *geodesic* from x to y) is a map c from a closed interval $[0,l] \subset \mathbb{R}$ to X such that $c(0) = x$, $c(l) = y$ and $d(c(t), c(t')) = |t - t'|$ for all $t, t' \in [0,l]$. In particular, c is an isometry and $d(x,y) = l$. The image of c is called a *geodesic* (or *metric*) *segment* joining x and y. When it is unique, this geodesic is denoted by $[x,y]$. The space (X,d) is said to be a *geodesic space* if every two points of X are joined by a geodesic and X is said to be a *uniquely geodesic* if there is exactly one geodesic joining x to y for each $x, y \in X$.

A *geodesic triangle* $\Delta(x_1, x_2, x_3)$ in a geodesic metric space (X,d) consist of three points in X (the vertices of Δ) and a geodesic segment between each pair of vertices (the edges of Δ). A *comparison triangle* for geodesic triangle $\Delta(x_1, x_2, x_3)$ in (X,d) is a triangle $\bar{\Delta}(x_1, x_2, x_3) = \Delta(\bar{x}_1, \bar{x}_2, \bar{x}_3)$ in the Euclidean plane $\mathbb{R}^2$ such that $d_{\mathbb{R}^2}(\bar{x}_i, \bar{x}_j) = d(x_i, x_j)$ for $i, j \in \{1,2,3\}$. Such a triangle always exists (see [7]).

A geodesic metric space is said to be a CAT(0) space [7] if all geodesic triangles of appropriate size satisfy the following comparison axiom:

Let Δ be a geodesic triangle in X and $\bar{\Delta}$ be a comparison triangle for Δ. Then, Δ is said to satisfy the CAT(0) *inequality* if for all $x, y \in \Delta$ and all comparison points $\bar{x}, \bar{y} \in \bar{\Delta}$,

$$d(x,y) \le d_{\mathbb{R}^2}(\bar{x}, \bar{y}).$$

If x, y_1, y_2 are points in a CAT(0) space and if y_0 is the midpoint of the segment $[y_1, y_2]$, then the CAT(0) inequality implies that

$$d(x, y_0)^2 \le \frac{1}{2} d(x, y_1)^2 + \frac{1}{2} d(x, y_2)^2 - \frac{1}{4} d(y_1, y_2)^2.$$

This is the (CN) inequality of Bruhat and Tits [21]. In fact (see [7], p.163), a geodesic metric space is a CAT(0) space if and only if it satisfies the (CN) inequality. It is worth mentioning that the results in a CAT(0) space can be applied to any $CAT(k)$ space with $k \le 0$ since any $CAT(k)$ space is a $CAT(k')$ space for every $k' \ge k$ (see [7], p.165).

Let $x, y \in X$ and by Lemma 2.1 (iv) of [13] for each $t \in [0,1]$, there exists a unique point $z \in [x, y]$ such that

$$d(x,z) = td(x,y), \quad d(y,z) = (1-t)d(x,y). \tag{3}$$

From now on, we will use the notation $(1-t)x \oplus ty$ for the unique point z satisfying (3). We now collect some elementary facts about CAT(0) spaces which will be used in sequel the proofs of our main results.

Lemma 1 *Let X be a* CAT(0) *space. Then*
(i) (see [13], Lemma 2.4) for each $x, y, z \in X$ and $t \in [0,1]$, one has

$$d((1-t)x \oplus ty, z) \le (1-t)d(x,z) + td(y,z),$$

(ii) (see [13], Lemma 2.5) for each $x, y, z \in X$ and $t \in [0,1]$, one has

$$d((1-t)x \oplus ty, z)^2 \le (1-t)d(x,z)^2 + td(y,z)^2 - t(1-t)d(x,y)^2.$$

III. Demiclosedness principle for k-strictly pseudo-contractive mappings

In 1976 Lim [22] introduced a concept of convergence in a general metric space setting which is called Δ-convergence. Later, Kirk and Panyanak [23] used the concept of Δ-convergence introduced by Lim [22] to prove on the CAT(0) space analogs of some Banach space results which involve weak convergence. Also, Dhompongsa and Panyanak [13] obtained the Δ-convergence theorems for the Picard, Mann and Ishikawa iterations in a CAT(0) space for nonexpansive mappings under some appropriate conditions.

We now give the definition and collect some basic properties of the Δ-convergence.

Let X be a complete CAT(0) space and $\{x_n\}$ be a bounded sequence in X. For $x \in X$, we set

$$r(x,\{x_n\}) = \limsup_{n\to\infty} d(x,x_n).$$

The *asymptotic radius* $r(\{x_n\})$ of $\{x_n\}$ is given by

$$r(\{x_n\}) = \inf\{r(x,\{x_n\}) : x \in X\}.$$

The *asymptotic center* $A(\{x_n\})$ of $\{x_n\}$ is the set

$$A(\{x_n\}) = \{x \in X : r(x,\{x_n\}) = r(\{x_n\})\}.$$

It is known that in a complete CAT(0) space, $A(\{x_n\})$ consists of exactly one point (see [24], Proposition 7).

Definition 1 *([22], [23]) A sequence $\{x_n\}$ in a* CAT(0) *space X is said to be Δ-convergent to $x \in X$ if x is the unique asymptotic center of $\{u_n\}$ for every subsequence $\{u_n\}$ of $\{x_n\}$. In this case, we write $\Delta\text{-}\lim_{n\to\infty} x_n = x$ and x is called the Δ-limit of $\{x_n\}$.*

Lemma 2

i) Every bounded sequence in a complete CAT(0) *space always has a Δ-convergent subsequence. (see [23], p.3690)*

ii) Let C be a nonempty closed convex subset of a complete CAT(0) *space and let $\{x_n\}$ be a bounded sequence in C. Then the asymptotic center of $\{x_n\}$ is in C. (see [25], Proposition 2.1)*

Lemma 3 *([13], Lemma 2.8) If $\{x_n\}$ is a bounded sequence in a complete* CAT(0) *space with $A(\{x_n\}) = \{x\}$, $\{u_n\}$ is a subsequence of $\{x_n\}$ with $A(\{u_n\}) = \{u\}$ and the sequence $\{d(x_n,u)\}$ is convergent then $x = u$.*

Let C be a closed convex subset of a CAT(0) space X and $\{x_n\}$ be a bounded sequence in C. We denote the notation

$$\{x_n\} \mapsto w \Leftrightarrow \Phi(w) = \inf_{x\in C} \Phi(x) \tag{4}$$

where $\Phi(x) = \limsup_{n\to\infty} d(x_n,x)$.

Nanjaras and Panyanak [26] gave a connection between the "$\mapsto$" convergence and Δ-convergence.

Proposition 1 *([26], Proposition 3.12) Let C be a closed convex subset of a* CAT(0) *space X and $\{x_n\}$ be a bounded sequence in C. Then $\Delta\text{-}\lim_{n\to\infty} x_n = p$ implies that $\{x_n\} \mapsto p$.*

The purpose of this section is to prove *demiclosedness principle for k-strictly pseudo-contractive mappings in a* CAT(0) *space* by using the convergence defined in (4).

Theorem 1 *Let C be a nonempty closed convex subset of a complete* CAT(0) *space X and $T : C \to C$ be a k-strictly pseudo-contractive mapping such that $k \in \left[0,\frac{1}{2}\right)$ and $F(T) \neq \emptyset$. Let $\{x_n\}$ be a bounded sequence in C such that $\Delta\text{-}\lim_{n\to\infty} x_n = w$ and $\lim_{n\to\infty} d(x_n,Tx_n) = 0$. Then $Tw = w$.*

Proof By the hypothesis, $\Delta\text{-}\lim_{n\to\infty} x_n = w$. From Proposition 1, we get $\{x_n\} \mapsto w$. Then we obtain $A(\{x_n\}) = \{w\}$ by Lemma 2 (ii) (see [26]). Since $\lim_{n\to\infty} d(x_n,Tx_n) = 0$, then we get

$$\Phi(x) = \limsup_{n\to\infty} d(x_n,x) = \limsup_{n\to\infty} d(Tx_n,x) \tag{5}$$

for all $x \in C$. In (5) by taking $x = Tw$, we have

$$\begin{aligned}\Phi(Tw)^2 &= \limsup_{n\to\infty} d(Tx_n,Tw)^2 \\ &\le \limsup_{n\to\infty}\left\{d(x_n,w)^2 + k(d(x_n,Tx_n)+d(w,Tw))^2\right\} \\ &\le \limsup_{n\to\infty} d(x_n,w)^2 + k\limsup_{n\to\infty}\left(d(x_n,Tx_n)+d(w,Tw)\right)^2 \\ &= \Phi(w)^2 + kd(w,Tw)^2 \end{aligned} \tag{6}$$

The (CN) inequality implies that

$$d\left(x_n,\frac{w\oplus Tw}{2}\right)^2 \le \frac{1}{2}d(x_n,w)^2 + \frac{1}{2}d(x_n,Tw)^2 - \frac{1}{4}d(w,Tw)^2.$$

Letting $n \to \infty$ and taking superior limit on the both sides of the above inequality, we get

$$\Phi\left(\frac{w\oplus Tw}{2}\right)^2 \le \frac{1}{2}\Phi(w)^2 + \frac{1}{2}\Phi(Tw)^2 - \frac{1}{4}d(w,Tw)^2.$$

Since $A(\{x_n\}) = \{w\}$, we have

$$\Phi(w)^2 \le \Phi\left(\frac{w\oplus Tw}{2}\right)^2 \le \frac{1}{2}\Phi(w)^2 + \frac{1}{2}\Phi(Tw)^2 - \frac{1}{4}d(w,Tw)^2.$$

which implies that

$$d(w,Tw)^2 \le 2\Phi(Tw)^2 - 2\Phi(w)^2. \tag{7}$$

By (6) and (7), we get $(1-2k)d(w,Tw)^2 \le 0$. Since $k \in \left[0,\frac{1}{2}\right)$, then we have $Tw = w$ as desired.

Now, we prove the Δ-convergence of the cyclic algorithm for k-strictly pseudo-contractive mappings in a CAT(0) space.

Theorem 2 *Let C be a nonempty closed convex subset of a complete* CAT(0) *space X and $N \geq 1$ be an integer. Let, for each $0 \leq i \leq N-1$, $T_i : C \to C$ be k_i-strictly pseudo-contractive mappings for some $0 \leq k_i < \frac{1}{2}$. Let $k = \max\{k_i; 0 \leq i \leq N-1\}$, $\{\alpha_n\}$ be a sequence in $[a,b]$ for some $a,b \in (0,1)$ and $k < a$. Let $F = \cap_{i=0}^{N-1} F(T_i) \neq \varnothing$. For $x_0 \in C$, let $\{x_n\}$ be a sequence defined by (2). Then the sequence $\{x_n\}$ is Δ-convergent to a common fixed point of the family $\{T_i\}_{i=0}^{N-1}$.*

Proof Let $p \in F$. Using (1), (2) and Lemma 1, we have

$$\begin{aligned} d(x_{n+1}, p)^2 &= d(\alpha_n x_n \oplus (1-\alpha_n)T_{[n]}x_n, p)^2 \\ &\leq \alpha_n d(x_n, p)^2 + (1-\alpha_n)d(T_{[n]}x_n, p)^2 \\ &\quad - \alpha_n(1-\alpha_n)d(x_n, T_{[n]}x_n)^2 \\ &\leq \alpha_n d(x_n, p)^2 + (1-\alpha_n)\left\{d(x_n, p)^2 + kd(x_n, T_{[n]}x_n)^2\right\} \\ &\quad - \alpha_n(1-\alpha_n)d(x_n, T_{[n]}x_n)^2 \\ &= d(x_n, p)^2 - (1-\alpha_n)(\alpha_n - k)d(x_n, T_{[n]}x_n)^2 \qquad (8) \\ &\leq d(x_n, p)^2. \end{aligned}$$

This inequality guarentees that the sequence $\{x_n\}$ is bounded and $\lim_{n\to\infty} d(x_n, p)$ exists for all $p \in F$. By (8), we also have

$$\begin{aligned} d(x_n, T_{[n]}x_n)^2 &\leq \frac{1}{(1-\alpha_n)(\alpha_n - k)}\left[d(x_n, p)^2 - d(x_{n+1}, p)^2\right] \\ &\leq \frac{1}{(1-b)(a-k)}\left[d(x_n, p)^2 - d(x_{n+1}, p)^2\right] \end{aligned}$$

Since $\lim_{n\to\infty} d(x_n, p)$ exists, we obtain $\lim_{n\to\infty} d(x_n, T_{[n]}x_n) = 0$. To show that the sequence $\{x_n\}$ is Δ-convergent to a common fixed point of the family $\{T_i\}_{i=0}^{N-1}$, we prove that

$$\omega_w(x_n) = \bigcup_{\{u_n\} \subseteq \{x_n\}} A(\{u_n\}) \subseteq F$$

and $\omega_w(x_n)$ consists of exactly one point. Let $u \in \omega_w(x_n)$. Then, there exists a subsequence $\{u_n\}$ of $\{x_n\}$ such that $A(\{u_n\}) = \{u\}$. By Lemma 2, there exists a subsequence $\{v_n\}$ of $\{u_n\}$ such that $\Delta\text{-}\lim_{n\to\infty} v_n = v \in C$. By Theorem 1, we have $v \in F$ and by Lemma 3, we have $u = v \in F$. This shows that $\omega_w(x_n) \subseteq F$. Now we prove that $\omega_w(x_n)$ consists of exactly one point. Let $\{u_n\}$ be a subsequence of $\{x_n\}$ with $A(\{u_n\}) = \{u\}$ and let $A(\{x_n\}) = \{x\}$. We have already seen that $u = v$ and $v \in F$. Finally, since $\{d(x_n, v)\}$ is convergent, we have $x = v \in F$ by Lemma 3. This completes the proof.

IV. The Strong Convergence Theorem for the Modified Halpern Iteration

In [6], Hu introduced a modified Halpern iteration. We modify this iteration in CAT(0) spaces as follows.

For an arbitary initial value $x_0 \in C$ and a fixed anchor $u \in C$, the sequence $\{x_n\}$ is defined by

$$\begin{cases} x_{n+1} = \alpha_n u \oplus (1-\alpha_n)y_n, \\ y_n = \dfrac{\beta_n}{1-\alpha_n} x_n \oplus \dfrac{\gamma_n}{1-\alpha_n} Tx_n, \ \forall n \geq 0, \end{cases} \qquad (9)$$

where $\{\alpha_n\}, \{\beta_n\}, \{\gamma_n\}$ are three real sequences in $(0,1)$ satisfying $\alpha_n + \beta_n + \gamma_n = 1$. Clearly, the iterative sequence (9) is a natural generalization of the well known iterations.

(i) If we take $\beta_n = 0$ for all n in (9), then the sequence (9) reduces to the Halpern's iteration in [27].

(ii) If we take $\alpha_n = 0$ for all n in (9), then the sequence (9) reduces to the Mann iteration in [5].

In this section, we prove the strong convergence of the modified Halpern's iteration in a CAT(0) space.

Recall that a continous linear functional μ on ℓ_∞, the Banach space of bounded real sequences, is called a Banach limit if $\|\mu\| = \mu(1,1,...) = 1$ and $\mu(a_n) = \mu(a_{n+1})$ for all $\{a_n\}_{n=1}^{\infty} \subset \ell_\infty$.

Lemma 4 *(see [28], Proposition 2) Let $\{a_1, a_2, ...\} \in \ell_\infty$ be such that $\mu(a_n) \leq 0$ for all Banach limits μ and $\limsup_{n\to\infty}(a_{n+1} - a_n) \leq 0$. Then, $\limsup_{n\to\infty} a_n \leq 0$.*

Lemma 5 *Let C be a nonempty closed convex subset of a complete* CAT(0) *space X, $T : C \to C$ be a k-strictly pseudo-contractive mapping with $k \in [0,1)$ and $S : C \to C$ be a mapping defined by $Sz = kz \oplus (1-k)Tz$, for $z \in C$. Let $u \in C$ be fixed. For each $t \in [0,1]$, the mapping $S_t : C \to C$ defined by*

$$S_t z = tu \oplus (1-t)Sz = tu \oplus (1-t)(kz \oplus (1-k)Tz), \text{ for } z \in C,$$

has a unique fixed point $z_t \in C$, that is,

$$z_t = S_t(z_t) = tu \oplus (1-t)S(z_t). \qquad (10)$$

Proof As it has been proven in [29], if T is a k-strictly pseudo-contractive mapping with $k \in [0,1)$, S is a nonexpansive mapping such that $F(S) = F(T)$. Then, from

Lemma 2.1 in [14], the mapping S_t has a unique fixed point $z_t \in C$.

Lemma 6 *Let X, C, T and S be as in Lemma 5. Then, $F(T) \neq \varnothing$ if and only if $\{z_t\}$ given by (10) remains bounded as $t \to 0$. In this case, the following statements hold:*
1) $\{z_t\}$ converges to the unique fixed point z of T which is nearest to u,
2) $d^2(u,z) \le \mu\, d^2(u,x_n)$ for all Banach limits μ and all bounded sequences $\{x_n\}$ with $\lim_{n\to\infty} d(x_n, Tx_n) = 0$.

Proof If $F(T) \neq \varnothing$, then we have $F(S) = F(T) \neq \varnothing$. Also, if $\lim_{n\to\infty} d(x_n, Tx_n) = 0$, we obtain that

$$\begin{aligned} d(x_n, Sx_n) &= d(x_n, kx_n \oplus (1-k)Tx_n) \\ &\le (1-k)d(x_n, Tx_n) \to 0 \text{ as } n \to \infty. \end{aligned}$$

Thus, from Lemma 2.2 in [14], the rest of the proof of this lemma can be seen.

The following lemma can be found in [30].

Lemma 7 *(see [30], Lemma 2.1) Let $\{a_n\}$ be a sequence of non-negative real numbers satisfying the condition*

$$a_{n+1} \le (1-\gamma_n)a_n + \gamma_n\sigma_n, \ \forall n \ge 0,$$

where $\{\gamma_n\}$ and $\{\sigma_n\}$ are sequences of real numbers such that
(1) $\{\gamma_n\} \subset [0,1]$ and $\sum_{n=1}^{\infty}\gamma_n = \infty$,
(2) either $\limsup_{n\to\infty}\sigma_n \le 0$ or $\sum_{n=1}^{\infty}|\gamma_n\sigma_n| < \infty$.
Then, $\lim_{n\to\infty} a_n = 0$.

We are now ready to prove our main result.

Theorem 3 *Let C be a nonempty closed convex subset of a complete* CAT(0) *space X and $T: C \to C$ be a k-strictly pseudo-contractive mapping such that $0 \le k < \dfrac{\beta_n}{1-\alpha_n} < 1$ and $F(T) \neq \varnothing$. Let $\{x_n\}$ be a sequence defined by (9). Suppose that $\{\alpha_n\}$, $\{\beta_n\}$ and $\{\gamma_n\}$ satisfy the following conditions:*

C1) $\lim_{n\to\infty}\alpha_n = 0$,
C2) $\sum_{n=1}^{\infty}\alpha_n = \infty$,
C3) $\lim_{n\to\infty}\beta_n \neq k$ and $\lim_{n\to\infty}\gamma_n \neq 0$..

Then the sequence $\{x_n\}$ converges strongly to a fixed point of T.

Proof We divide the proof into three steps. In the first step we show that $\{x_n\}, \{y_n\}$ and $\{Tx_n\}$ are bounded sequences. In the second step we show that $\lim_{n\to\infty} d(x_n, Tx_n) = 0$. Finally, we show that $\{x_n\}$ converges to a fixed point $z \in F(T)$ which is nearest to u.
First step: Take any $p \in F(T)$, then, from Lemma 1 and (9), we have

$$\begin{aligned} & d(y_n, p)^2 \\ &\le \frac{\beta_n}{1-\alpha_n} d(x_n, p)^2 + \frac{\gamma_n}{1-\alpha_n} d(Tx_n, p)^2 - \frac{\beta_n\gamma_n}{(1-\alpha_n)^2} d(x_n, Tx_n)^2 \\ &\le \frac{\beta_n}{1-\alpha_n} d(x_n, p)^2 + \frac{\gamma_n}{1-\alpha_n}\left(d(x_n, p)^2 + kd(x_n, Tx_n)^2\right) \\ &\quad - \frac{\beta_n\gamma_n}{(1-\alpha_n)^2} d(x_n, Tx_n)^2 \\ &= d(x_n, p)^2 - \frac{\gamma_n}{1-\alpha_n}\left(\frac{\beta_n}{1-\alpha_n} - k\right) d(x_n, Tx_n)^2 \\ &\le d(x_n, p)^2. \end{aligned}$$

Also, we obtain

$$\begin{aligned} & d(x_{n+1}, p)^2 \\ &\le \alpha_n d(u, p)^2 + (1-\alpha_n)d(y_n, p)^2 - \alpha_n(1-\alpha_n)d(u, y_n)^2 \\ &\le \alpha_n d(u, p)^2 \\ &\quad + (1-\alpha_n)\left\{ d(x_n, p)^2 - \frac{\gamma_n}{1-\alpha_n}\left(\frac{\beta_n}{1-\alpha_n} - k\right) d(x_n, Tx_n)^2 \right\} \\ &\quad - \alpha_n(1-\alpha_n)d(u, y_n)^2 \\ &= \alpha_n d(u, p)^2 + (1-\alpha_n)d(x_n, p)^2 - \gamma_n\left(\frac{\beta_n}{1-\alpha_n} - k\right) d(x_n, Tx_n)^2 \\ &\quad - \alpha_n(1-\alpha_n)d(u, y_n)^2 \qquad (11) \\ &\le \alpha_n d(u, p)^2 + (1-\alpha_n)d(x_n, p)^2 \\ &\le \max\left\{ d(u, p)^2, d(x_n, p)^2 \right\}. \end{aligned}$$

By induction,

$$d(x_{n+1}, p)^2 \le \max\left\{ d(u, p)^2, d(x_0, p)^2 \right\}.$$

This proves the boundedness of the sequence $\{x_n\}$, which leads to the boundedness of $\{Tx_n\}$ and $\{y_n\}$.
Second step: In fact, we have from (11) (for some appropriate constant $M > 0$) that

$$
\begin{aligned}
&d(x_{n+1}, p)^2 \\
&\le \alpha_n d(u, p)^2 + (1-\alpha_n) d(x_n, p)^2 - \gamma_n \left(\frac{\beta_n}{1-\alpha_n} - k \right) d(x_n, Tx_n)^2 \\
&= \alpha_n (d(u, p)^2 - d(x_n, p)^2) + d(x_n, p)^2 \\
&\quad - \gamma_n \left(\frac{\beta_n}{1-\alpha_n} - k \right) d(x_n, Tx_n)^2 \\
&\le \alpha_n M + d(x_n, p)^2 - \gamma_n \left(\frac{\beta_n}{1-\alpha_n} - k \right) d(x_n, Tx_n)^2,
\end{aligned}
$$

which implies that

$$
\gamma_n \left(\frac{\beta_n}{1-\alpha_n} - k \right) d(x_n, Tx_n)^2 - \alpha_n M \le d(x_n, p)^2 - d(x_{n+1}, p)^2. \tag{12}
$$

If $\gamma_n \left(\frac{\beta_n}{1-\alpha_n} - k \right) d(x_n, Tx_n)^2 - \alpha_n M \le 0$, then

$$
d(x_n, Tx_n)^2 \le \frac{\alpha_n}{\gamma_n \left(\frac{\beta_n}{1-\alpha_n} - k \right)} M,
$$

and hence the desired result is obtained by the conditions (C1) and (C3).

If $\gamma_n \left(\frac{\beta_n}{1-\alpha_n} - k \right) d(x_n, Tx_n)^2 - \alpha_n M > 0$, then following (12), we have

$$
\begin{aligned}
&\sum_{n=0}^{m} \left[\gamma_n \left(\frac{\beta_n}{1-\alpha_n} - k \right) d(x_n, Tx_n)^2 - \alpha_n M \right] \\
&\le d(x_0, p)^2 - d(x_{m+1}, p)^2 \\
&\le d(x_0, p)^2.
\end{aligned}
$$

That is

$$
\sum_{n=0}^{\infty} \left[\gamma_n \left(\frac{\beta_n}{1-\alpha_n} - k \right) d(x_n, Tx_n)^2 - \alpha_n M \right] < \infty.
$$

Thus

$$
\lim_{n\to\infty} \left[\gamma_n \left(\frac{\beta_n}{1-\alpha_n} - k \right) d(x_n, Tx_n)^2 - \alpha_n M \right] = 0.
$$

Then we get

$$
\lim_{n\to\infty} d(x_n, Tx_n) = 0. \tag{13}
$$

Third step: Using the condition (C1) and (13), we obtain

$$
\begin{aligned}
&d(x_{n+1}, x_n) \le d(x_{n+1}, Tx_n) + d(Tx_n, x_n) \\
&\le \alpha_n d(u, Tx_n) + (1-\alpha_n) d(y_n, Tx_n) + d(Tx_n, x_n) \\
&\le \alpha_n d(u, Tx_n) + (1-\alpha_n) \left(\frac{\beta_n}{1-\alpha_n} d(x_n, Tx_n) \right) + d(Tx_n, x_n) \\
&= \alpha_n d(u, Tx_n) + (\beta_n + 1) d(x_n, Tx_n) \\
&\to 0, \text{ as } n \to \infty.
\end{aligned}
$$

Also, from (13), we have

$$
d(x_n, y_n) \le \frac{\gamma_n}{1-\alpha_n} d(x_n, Tx_n) \to 0, \text{ as } n \to \infty. \tag{14}
$$

Let $z = \lim_{t\to 0} z_t$, where z_t is given by (10) in Lemma 5. Then, z is the point of $F(T)$ which is nearest to u. By Lemma 6 (2), we have $\mu(d(u, z)^2 - d(u, x_n)^2)) \le 0$ for all Banach limits μ. Moreover, since $\lim_{n\to\infty} d(x_{n+1}, x_n) = 0$,

$$
\limsup_{n\to\infty} \left[\left(d(u, z)^2 - d(u, x_{n+1})^2 \right) - \left(d(u, z)^2 - d(u, x_n)^2 \right) \right] = 0.
$$

If we take $a_n = d(u, z)^2 - d(u, x_n)^2$ in Lemma 4, then we obtain

$$
\limsup_{n\to\infty} \left(d(u, z)^2 - d(u, x_n)^2 \right) \le 0. \tag{15}
$$

It follows from the condition (C1) and (14) that

$$
\begin{aligned}
&\limsup_{n\to\infty} \left(d(u, z)^2 - (1-\alpha_n) d(u, y_n)^2 \right) \\
&= \limsup_{n\to\infty} \left(d(u, z)^2 - d(u, x_n)^2 \right).
\end{aligned} \tag{16}
$$

By (15) and (16), we have

$$
\limsup_{n\to\infty} \left(d(u, z)^2 - (1-\alpha_n) d(u, y_n)^2 \right) \le 0. \tag{17}
$$

We observe that

$$
\begin{aligned}
&d(x_{n+1}, z)^2 \\
&\le \alpha_n d(u, z)^2 + (1-\alpha_n) d(y_n, z)^2 - \alpha_n (1-\alpha_n) d(u, y_n)^2 \\
&\le \alpha_n d(u, z)^2 + (1-\alpha_n) d(x_n, z)^2 - \alpha_n (1-\alpha_n) d(u, y_n)^2 \\
&= (1-\alpha_n) d(x_n, z)^2 + \alpha_n [d(u, z)^2 - (1-\alpha_n) d(u, y_n)^2].
\end{aligned}
$$

It follows from the condition (C2) and (17), using Lemma 7, that $\lim_{n\to\infty} d(x_n, z) = 0$. This completes the proof of Theorem 3.

We obtain the following corollary as a direct consequence of Theorem 3.

Corollary 1 *Let X, C and T be as Theorem 3. Let $\{\alpha_n\}$ be a real sequence in $(0,1)$ satisfying the conditions (C1) and (C2). For a constant $\delta \in (k,1)$, an arbitary initial value $x_0 \in C$ and a fixed anchor $u \in C$, let the sequence $\{x_n\}$ be defined by*

$$x_{n+1} = \alpha_n u \oplus (1-\alpha_n)(\delta x_n \oplus (1-\delta)Tx_n), \quad \forall n \geq 0. \qquad (18)$$

Then the sequence $\{x_n\}$ is strongly convergent to a fixed point of T.

Proof If, in proof of Theorem 3, we take $\beta_n = (1-\alpha_n)\delta$ and $\gamma_n = (1-\alpha_n)(1-\delta)$, then we get the desired conclusion.

Remark 1 *The results in this section contain the strong convergence theorems of the iterative sequences (9) and (18) for nonexpansive mappings in a* CAT(0) *space. Also, these results contain the corresponding theorems proved for these iterative sequences in a Hilbert space.*

REFERENCES

[1] I. Inchan, "Strong convergence theorems for a new iterative method of k-strictly pseudo-contractive mappings in Hilbert spaces," Computers and Mathematics with Applications, vol. 58, pp. 1397-1407, 2009.

[2] J. S. Jung, "Some results on a general iterative method for k-strictly pseudo-contractive mappings," Fixed Point Theory and Applications, 2011:24, doi:10.1186/1687-1812-2011-24, 11 pages, 2011.

[3] S. Li, L. Li, L. Zhang and X. He, "Strong convergence of modified Halpern's iteration for a k-strictly pseudocontractive mapping," Journal of Inequalities and Applications, 2013:98, doi:10.1186/1029-242X-2013-98, 2013.

[4] G. L. Acedo and H. K. Xu, "Iterative methods for strict pseudo-contractions in Hilbert spaces," Nonlinear Anal., vol. 67, no. 7, pp. 2258-2271, 2007.

[5] W. R. Mann, "Mean value methods in iteration," Proceedings of the American Mathematical Society, vol. 4, pp. 506-513, 1953.

[6] L. G. Hu, "Strong convergence of a modified Halpern's iteration for nonexpansive mappings," Fixed Point Theory and Applications, vol. 2008, Article ID 649162, 9 pages, doi: 10.1155/2008/649162, 2008.

[7] M. R. Bridson and A. Haefliger, *Metric Spaces of Non-Positive Curvature*, vol. 319, Grundlehren der Mathematischen Wissenschaften, Springer, Berlin, Germany, 1999.

[8] K.S. Brown, *Buildings*, Springer, NewYork, NY, USA, 1989.

[9] W. A. Kirk, "Fixed point theorems in CAT(0) spaces and $\mathbb{R}$-trees," Fixed Point Theory and Applications, vol. 2004, no. 4, pp. 309–316, 2004.

[10] K. Goebel and S. Reich, *Uniform Convexity, Hyperbolic Geometry and Nonexpansive Mappings*, vol. 83 of Monographs and Textbooks in Pure and Applied Mathematics, Marcel Dekker Inc., New York, NY, USA, 1984.

[11] W. A. Kirk, "Geodesic geometry and fixed point theory," in Seminar of Mathematical Analysis (Malaga/Seville, 2002/2003), vol. 64 of Coleccion Abierta, pp. 195–225, University of Seville, Secretary of Publications, Seville, Spain, 2003.

[12] W. A. Kirk," Geodesic geometry and fixed point theory II," in International Conference on Fixed Point Theory and Applications, pp. 113–142, Yokohama Publishers, Yokohama, Japan, 2004.

[13] S. Dhompongsa and B. Panyanak, "On Δ-convergence theorems in CAT(0) spaces," Computers and Mathematics with Applications, vol. 56, no. 10, pp. 2572–2579, 2008.

[14] S. Saejung, "Halpern's iteration in CAT(0) spaces," Fixed Point Theory and Applications, vol. 2010, Article ID 471781, 13 pages, 2010.

[15] A. Şahin and M. Başarır, "On the strong and Δ-convergence theorems for nonself mappings on a CAT(0) space," Proceedings of the 10th IC-FPTA, July 9-18 2012, Cluj-Napoca, Romania, pp. 227-240, 2012.

[16] A. Şahin and M. Başarır, "On the strong convergence of a modified S-iteration process for asymptotically quasi-nonexpansive mappings in a CAT(0) space," Fixed Point Theory and Applications, 2013:12, doi:10.1186/1687-1812-2013-12, 10 pages, 2013.

[17] M. Bestvina, "R-trees in topology, geometry, and group theory," in Handbook of Geometric Topology, pp. 55–91, North-Holland, Amsterdam, The Netherlands, 2002.

[18] R. Espinola and W. A. Kirk, "Fixed point theorems in R-trees with applications to graph theory," Topology and Its Applications, vol. 153, no. 7, pp. 1046–1055, 2006.

[19] W. A. Kirk, "Some recent results in metric fixed point theory," Journal of Fixed Point Theory and Applications, vol. 2, no. 2, pp. 195–207, 2007.

[20] C. Semple and M. Steel, *Phylogenetics*, vol. 24 of Oxford Lecture Series in Mathematics and Its Applications, Oxford University Press, Oxford, UK, 2003.

[21] F. Bruhat and J. Tits, "Groupes réductifs sur un corps local," Inst. Hautes Études Sci. Publ. Math., vol. 41, pp. 5–251, 1972.

[22] T. C. Lim, "Remarks on some fixed point theorems," Proceedings of the American Mathematical Society, vol. 60, pp. 179-182, 1976.

[23] W.A. Kirk and B. Panyanak, "A concept of convergence in geodesic spaces," Nonlinear Analysis: Theory, Methods and Applications, vol. 68, no. 12, pp. 3689–3696, 2008.

[24] S. Dhompongsa, W. A. Kirk and B. Sims, "Fixed point of uniformly lipschitzian mappings," Nonlinear Analysis: Theory, Methods and Applications, vol. 65, no.4, pp. 762–772, 2006.

[25] S. Dhompongsa, W. A. Kirk and B. Panyanak, "Nonexpansive set-valued mappings in metric and Banach spaces," Journal of Nonlinear and Convex Analysis, vol. 8, no. 1, pp. 35–45, 2007.

[26] B. Nanjaras and B. Panyanak, "Demiclosed principle for asymptotically nonexpansive mappings in CAT(0) spaces," Fixed Point Theory and Applications, vol. 2010, Article ID 268780, doi: 10.1155/2010/268780, 14 pages, 2010.

[27] B. Halpern, "Fixed points of nonexpanding maps," Bulletin of the American Mathematical Society, vol. 73, no. 6, pp. 957–961, 1967.

[28] N. Shioji and W. Takahashi, "Strong convergence of approximated sequences for nonexpansive mappings in Banach spaces," Proceedings of the American Mathematical Society, vol. 125, no. 12, pp. 3641–3645, 1997.

[29] H. Zhou, "Convergence theorems of fixed points for k-strict pseudo-contractions in Hilbert space," Nonlinear Anal., vol. 69, pp. 456-462, 2008.

[30] H. K. Xu, "An iterative approach to quadratic optimization," Journal of Optimization Theory and Applications, vol. 116, no. 3, pp. 659–678, 2003.

Solution of an Optimal Control Problem with Mathcad

G. Meladze[1], D. Devadze[2] and V. Beridze[3]

1. Saint Andrew the first-called Georgian University at Patriarchate of Georgia, Tbilisi, Georgia. Email: h_meladze@hotmail.com
2. Department of Computer Science, Batumi Shota Rustaveli State University, Batumi, Georgia. Email: david.devadze@gmail.com
3. Department of Computer Science, Batumi Shota Rustaveli State University, Batumi, Georgia. Email: vakhtangi@yahoo.com

Abstract — The paper deals with optimal control problems whose behavior is described by an elliptic equations with Bitsadze–Samarski nonlocal boundary conditions. The theorem about a necessary and sufficient optimality condition is given. The existence and uniqueness of a solution of the conjugate problem are proved. A numerical method of the solution of an optimal problem by means of the Mathcad package is presented.

Keywords — Elliptic equation, nonlocal boundary value problem, Bitsadze–Samarski problem, optimal control.

INTRODUCTION

Nonlocal boundary value problems are a very interesting generalization of classical problems and at the same time they are obtained in a natural manner when constructing mathematical models of real processes and phenomena in physics, engineering, sociology, ecology and so on [1]–[3]. The Bitsadze–Samarski nonlocal boundary value problem [4] arose in connection with mathematical modeling of processes occurring in plasma physics. Intensive studies of Bitsadze–Samarski nonlocal problems [5] and its various generalizations began in the 80s of the last century [4]–[6].

The present paper deals with optimal control problems whose behavior is described by Helmholtz equation with Bitsadze–Samarski nonlocal boundary conditions [7]. Necessary optimality conditions are established by using the approach worked out in [8]-[10] for controlled systems of general type. To investigate the conjugate problem we use the algorithm reducing nonlocal boundary value problems to a sequence of Dirichlet problems. Such a method makes it possible not only to solve the problem numerically, but also to prove the existence of its solution [5].

In the paper: the Bitsadze–Samarski boundary value problem for Helmholtz equations is considered. An optimal control problem is stated for a nonlocal boundary value problem with an integral quality test. A theorem about a necessary and sufficient optimality condition is formulated. The existence and uniqueness of a solution of the conjugate problem are proved. A numerical method is presented for solving an optimal problem by means of the Mathcad package.

I. STATEMENT OF THE OPTIMAL CONTROL PROBLEM

Let $\overline{G}$ be the rectangle, $\overline{G} = [0,1]\times[0,1]$, Γ be the boundary of the domain G, $0 < x_0 < 1$, $\gamma_0 = \{(x_0, y) : 0 \le y \le 1\}$, $\gamma = \{(1, y) : 0 \le y \le 1\}$,

$a(x,y), b(x,y), c(x,y), d(x,y) \in L_p(\overline{G})$, $p > 2$,

$0 \le q(x,y) \in L_\infty(\overline{G})$.

Let U be an arbitrary bounded set from R. Every function $\omega(x,y) : G \to U$ will be called a control. The set U is called the control domain. A function $\omega(x,y)$ is called an admissible control if $\omega(x,y) \in L_p(G)$, $p > 2$. The set of all admissible controls is denoted by Ω.

For each fixed $\omega(x,y) \in \Omega$ in the domain $\overline{G}$ let us consider the following Bitsadze–Samarski boundary value problem for Helmholtz equations:

$$\frac{\partial^2 u}{\partial x^2} + \frac{\partial^2 u}{\partial y^2} - q(x,y)u = a(x,y)\omega(x,y) + b(x,y), \ (x,y) \in G, \tag{1.1}$$

$$u(x,y) = 0, \ (x,y) \in \Gamma \setminus \gamma,$$

$$u(1,y) = \sigma u(x_0, y), \ 0 \le y \le 1, \ 0 < \sigma < 1.$$

The solution of the problem (1.1) exists, is unique and belongs to the space $W_2^2(G) \cap \overset{\circ}{W}{}_2^1(G)$ [10].

We consider the functional

$$I(\omega) = \iint_G [c(x,y)u(x,y) + d(x,y)\omega(x,y)]\, dxdy \tag{1.2}$$

and state the following optimal control problem: Find a function $\omega_0(x,y) \in \Omega$, for which the solution of problem (1.2) gives functional (1.2) a minimal value. A function $\omega_0(x,y) \in \Omega$ will be called an optimal control, and the corresponding solution $u_0(x,y)$ an optimal solution.

Theorem. *Let ψ_0 be the solution of the adjoint problem*

$$\frac{\partial^2\psi}{\partial x^2}+\frac{\partial^2\psi}{\partial y^2}-q(x,y)\psi=-c(x,y),\ (x,y)\in G\setminus\gamma_0,$$
$$\psi(x,y)=0,(x,y)\in\Gamma, \tag{1.3}$$
$$\frac{\partial\psi(x_0^+,y)}{\partial x}-\frac{\partial\psi(x_0^-,y)}{\partial x}=\sigma\frac{\partial\psi(1,y)}{\partial x},\ 0\le y\le 1.$$

Then for (u_0,ω_0) *to be optimal it is necessary and sufficient that the principle of minimum*

$$\inf_{\omega\in U}[d(x,y)+a(x,y)\psi_0(x,y)]\omega= \\ =[d(x,y)+a(x,y)\psi_0(x,y)]\omega_0 \tag{1.4}$$

be fulfilled almost everywhere on G [11].

II. Existence and Uniqueness of a Solution of the Conjugate Problem

We write a solution of the conjugate problem (1.3) in the form $\psi=w+w^*$, where w^* is the solution of the Dirichlet problem

$$\frac{\partial^2 w^*}{\partial x^2}+\frac{\partial^2 w^*}{\partial y^2}-q(x,y)w^*=-c(x,y),\ (x,y)\in G, \tag{2.1}$$
$$w^*(x,y)=0,\ (x,y)\in\Gamma,$$

and w is the solution of the nonclassical boundary value problem

$$\frac{\partial^2 w}{\partial x^2}+\frac{\partial^2 w}{\partial y^2}-q(x,y)w=0,\ (x,y)\in G\setminus\gamma_0,$$
$$w(x,y)=0,\ (x,y)\in\Gamma,$$
$$\frac{\partial w(x_0^+,y)}{\partial x}-\frac{\partial w(x_0^-,y)}{\partial x}= \tag{2.2}$$
$$=\sigma\frac{\partial w(1,y)}{\partial x}+\sigma\frac{\partial w^*(1,y)}{\partial x},\ 0\le y\le 1.$$

As is known [12], problem (2.1) has a unique solution that belongs to the space $W_2^2(G)\cap\overset{\circ}{W}{}_2^1(G)$. Therefore it remains for us to investigate problem (2.1). To this end, we consider the iteration process

$$\frac{\partial^2 w^{k+1}}{\partial x^2}+\frac{\partial^2 w^{k+1}}{\partial y^2}-q(x,y)w^{k+1}=0,(x,y)\in G\setminus\gamma_0,$$
$$w^{k+1}(x,y)=0,\ (x,y)\in\Gamma,$$
$$\frac{\partial w^{k+1}(x_0^+,y)}{\partial x}-\frac{\partial w^{k+1}(x_0^-,y)}{\partial x}= \tag{2.3}$$
$$=\sigma\frac{\partial w^k(1,y)}{\partial x}+\varphi(y),\ 0\le y\le 1,\ k=0,1,2,\ldots,$$

where $\varphi(y)=\sigma\frac{\partial w^*(1,y)}{\partial x}$, $w^0(x,y)$ is the initial approximation which can be assumed to be equal to zero. Let $z^{(k)}(x,y)=w^{(k+1)}(x,y)-w^{(k)}(x,y)$, then from equalities (2.3) we obtain

$$\frac{\partial^2 z^k}{\partial x^2}+\frac{\partial^2 z^k}{\partial y^2}-q(x,y)z^k=0,\ (x,y)\in G\setminus\gamma_0,$$
$$z^k(x,y)=0,\ (x,y)\in\Gamma,$$
$$\frac{\partial z^k(x_0^+,y)}{\partial x}-\frac{\partial z^k(x_0^-,y)}{\partial x}= \tag{2.4}$$
$$=\sigma\frac{\partial z^{k-1}(1,y)}{\partial x},\ 0\le y\le 1,\ k=1,2,3,\ldots.$$

In the Space $W_2^2(G\setminus\gamma_0)\cap\overset{\circ}{W}{}_2^1(G)$ problem (2.4) is equivalent to the following problem [13], [14]

$$\frac{\partial^2 z^k}{\partial x^2}+\frac{\partial^2 z^k}{\partial y^2}-q(x,y)z^k= \\ =-\sigma\delta(x_0-x)\frac{\partial z^{k-1}(1,y)}{\partial x},\ (x,y)\in G, \tag{2.5}$$
$$z^k(x,y)=0,\ (x,y)\in\Gamma,\ k=1,2,3,\ldots,$$

where $\delta(x_0-x)$ is the Dirac function. Let us introduce the notation

$$f(x,y)=-\sigma\delta(x_0-x)\frac{\partial z^{(k-1)}(1,y)}{\partial x}.$$

Since $f(x,y)\in W_2^{-1}(G)$, the solution of problem (2.5) exists, is unique and belongs to the space $\overset{\circ}{W}{}_2^1(G)$ [12]. Moreover, if $G(x,y,\xi,\eta)$ is the Green's function of problem (2.5), then the solution can be represented as follows

$$z^{(k)}(x,y)= \\ =\iint_G\sigma G(x,y,\xi,\eta)\delta(x_0-\xi)\frac{\partial z^{(k-1)}(1,\eta)}{\partial x}\,d\xi d\eta= \tag{2.6}$$
$$=\int_0^1\sigma G(x,y,x_0,\eta)\frac{\partial z^{(k-1)}(1,\eta)}{\partial x}d\eta.$$

Furthermore, taking the property of the Green's function into account [13], [14], from equality (2.6) it follows that $z^{(k)}(x,y)\in W_2^2(G\setminus\gamma_0)\cap\overset{\circ}{W}{}_2^1(G)$, hence we define the trace of the function $\frac{\partial}{\partial x}(z^{(k)}(1,y))$ which belongs to the space $W_2^{1/2}(0,1)$. Thus, using (2.6) we can write

$$\frac{\partial z^{(k)}(1,y)}{\partial x}=\int_0^1\sigma\frac{\partial G(1,y,x_0,\eta)}{\partial x}\cdot\frac{\partial z^{(k-1)}(1,\eta)}{\partial x}d\eta. \tag{2.7}$$

Next, using the Cauchy–Bunyakovsky inequality, from equality (2.7) we obtain

$$\int_0^1[\frac{\partial z^{(k)}(1,y)}{\partial x}]^2dy\le \\ \le\sigma^2\int_0^1\int_0^1[\frac{\partial G(1,y,x_0,\eta)}{\partial x}]^2dxdy\cdot\int_0^1[\frac{\partial z^{(k-1)}(1,\eta)}{\partial x}]^2d\eta. \tag{2.8}$$

Denote

$$\theta=\sigma\left\|\frac{\partial G(1,y,x_0,\eta)}{\partial x}\right\|_{L_2([0,1]\times[0,1])},$$

then from (2.8) we obtain the estimate

$$\left\|\frac{\partial z^{(k)}(1,y)}{\partial x}\right\|_{L_2[0,1]} \le \theta \left\|\frac{\partial z^{(k-1)}(1,y)}{\partial x}\right\|_{L_2[0,1]}. \quad (2.9)$$

Let $\sigma < 1/\left\|\frac{\partial}{\partial x}(G(1,y,x_0,\eta))\right\|$, then $\theta < 1$ and estimate (2.9) implies that the series $\sum_{k=1}^{\infty}\frac{\partial}{\partial x}(z^{(k)}(1,y))$ converges. This means that the sequence $\left\{\frac{\partial w^{(k)}(1,y)}{\partial x}\right\}$ converges, where

$$\frac{\partial w^{(k)}(1,y)}{\partial x} =$$

$$= \sum_{i=0}^{k-1}\left[\frac{\partial w^{(i+1)}(1,y)}{\partial x} - \frac{\partial w^{(i)}(1,y)}{\partial x}\right] + \frac{\partial w^{(0)}(1,y)}{\partial x}$$

in the norm of the space $L_2[0,1]$. Therefore equality (2.6) implies the convergence of the series $\sum_{k=1}^{\infty} z^{(k)}(x,y)$, and thereby the convergence of the iteration sequence $\{w^{(k)}(x,y)\}$:

$$\lim_{k\to\infty} w^{(k)}(x,y) = w(x,y),$$

where $w(x,y) \in W_2^2(G\setminus\gamma_0) \cap \overset{\circ}{W}{}_2^1(G)$. Further it is not difficult to prove that the function $w(x,y)$ is the solution of problem (2.2).

Let us prove the uniqueness of the solution. Assume that $w_1(x,y)$ and $w_2(x,y)$ are two generalized solutions of problem (2.2). Then their difference $z(x,y) = w_1(x,y) - w_2(x,y)$ is the solution of the problem

$$\frac{\partial^2 z}{\partial x^2} + \frac{\partial^2 z}{\partial y^2} - q(x,y)z = 0,\ (x,y) \in G\setminus\gamma_0,$$

$$z(x,y) = 0,\ (x,y) \in \Gamma, \quad (2.10)$$

$$\frac{\partial z(x_0^+,y)}{\partial x} - \frac{\partial z(x_0^-,y)}{\partial x} = \sigma\frac{\partial z(1,y)}{\partial x},\ 0 \le y \le 1.$$

By the same reasoning as above we obtain $z(x,y) = 0$. We have thereby proved the existence and uniqueness of the solution of problem (1.3).

III. Algorithm of the Solution of an Optimal Control Problem

The scheme of the solution of an optimal control problem is as follows:

1. to find a solution $\psi_0(x,y)$, we first solve the adjoint problem (1.3);

2. using the function $\psi_0(x,y)$ from (1.4), we construct the optimal control $\omega_0(x,y)$;

3. to find an optimal solution $u_0(x,y)$, we solve problem (1.1).

As we have shown, a solution of the adjoint problem can be written in the form $\psi = w + w^*$, where w^* is the solution of the Dirichlet problem (2.1), and w is the solution of the nonclassical boundary value problem (2.2). For the solution of problem (2.2) we consider the iteration process (2.3). Problem (2.3) is equivalent to the following problem

$$\frac{\partial^2 w^{k+1}}{\partial x^2} + \frac{\partial^2 w^{k+1}}{\partial y^2} - q(x,y)w^{k+1} =$$

$$= \delta(x_0 - x)(\sigma\frac{\partial w^k(1,y)}{\partial x} + \varphi(y)),\ (x,y) \in G, \quad (3.1)$$

$$w^{k+1}(x,y) = 0,\ (x,y) \in \Gamma,\ k = 0,1,2,\ldots,$$

where $\varphi(y) = \sigma\frac{\partial w^*(1,y)}{\partial x}$, $w^0(x,y)$ is the initial approximation.

For the solution of problem (1.1) we consider the iteration process

$$\frac{\partial^2 u^{k+1}}{\partial x^2} + \frac{\partial^2 u^{k+1}}{\partial y^2} - q(x,y)u^{k+1} =$$

$$= a(x,y)\omega + b(x,y),\ (x,y) \in G,$$

$$u^{k+1}(x,y) = 0,\ (x,y) \in \Gamma\setminus\gamma, \quad (3.2)$$

$$u^{k+1}(1,y) = \sigma u^k(x_0,y),\ 0 \le y \le 1,\ 0 < \sigma < 1,$$

$$k = 0,1,2,\ldots.$$

IV. Numerical Realization of the Problem by Means of the Mathcad

To obtain a numerical solution of problems (3.1) and (3.2), at each iteration step we use the built-in function **relax(a, b, c, d, e, f, u, rjac)** in the Mathcad [15], [16].

The function **relax** returns the square matrix, where the position of an element in the matrix corresponds to its position inside the square domain, while the value corresponds to an approximate solution at this point.

The arguments of the function **relax** are as follows:

a, **b**, **c**, **d**, **e** are square matrices of one and the same size, containing the coefficients of a differential equation. In particular, for a Helmholtz equation the coefficients are $a_{i,j} = b_{i,j} = c_{i,j} = d_{i,j} = 1$, $e_{i,j} = -4 - q_{i,j}$, where $q_{i,j}$ are the values of $q(x,y)$ in the respective node inside the square domain;

f is a square matrix containing the values of the right-hand part of the equation in the respective node inside the square domain;

u is a square matrix containing the boundary values of the function at the domain edges, and also the initial approximation of the solution in the interior nodes of the square domain;

rjac is the parameter controlling the relaxation process convergence. It may vary in the range from 0 to 1, but an optimal value depends on the particulars of the problem.

As an example let us consider problems (1.1) and (1.3),where $q(x,y)=x+y$, $a(x,y)=1$, $b(x,y)=0$, $c(x,y)=1$, $d(x,y)=1$, $\omega(x,y)=1$, $x_0=1/2$.

The results of the numerical solution of problems (1.1) and

(1.3) are graphically shown in Fig. 1. and Fig. 2.

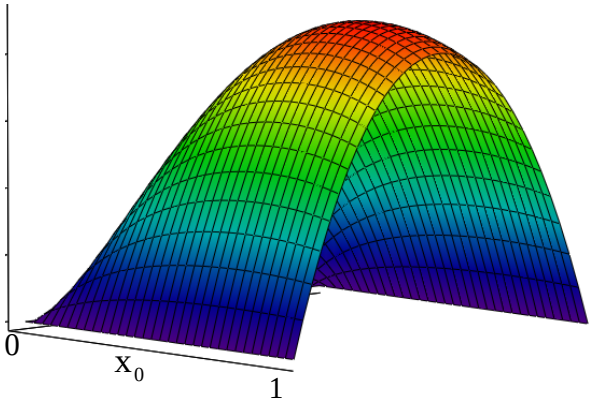

Fig. 1. Solution Bitsadze–Samarski problem

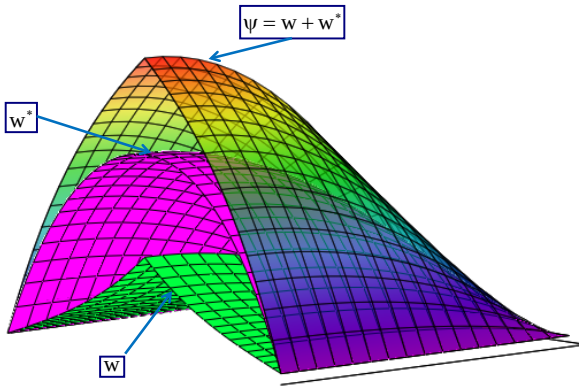

Fig. 2. Solution adjoint problem

REFERENCES

[1] V. V. Shelukhin, A non-local in time model for radionuclides propagation in Stokes fluid. Dinamika Sploshn. Sredy No. 107 (1993), 180–193, 203, 207.

[2] C. V. Pao, Reaction diffusion equations with nonlocal boundary and nonlocal initial conditions. J. Math. Anal. Appl. 195 (1995), No. 3, 702–718.

[3] E. Obolashvili, Nonlocal problems for some partial differential equations. Appl. Anal. 45 (1992), No. 1-4, 269–280.

[4] A. V. Bitsadze and A. A. Samarskii, On some simple generalizations of linear elliptic boundary problems. (Russian) Dokl. Akad. Nauk SSSR 185 (1969), 739-740; English transl.: Sov. Math., Dokl. 10 (1969), 398–400.

[5] D. G. Gordeziani, On the methods of solution of one class of nonlocal boundary value problems. Tbilisi State University Press, Tbilisi, 1986.

[6] D. V. Kapanadze, On a nonlocal Bitsadze-Samarski boundary value problem. (Russian) Differentsial'nye Uravneniya 23 (1987), No. 3, 543–545, 552.

[7] D. Devadze, V. Beridze. A Control Optimal Problem for Helmholtz Equations with Bitsadze–Samarski Boundary Conditions. Proceedings of A. Razmadze Mathematical Institute. 2013. Vol. 161. pp. 47-53.

[8] D. Sh. Devadze and V. Sh. Beridze, Optimality conditions for quasilinear differential equations with nonlocal boundary conditions. UMN 68 (2013), No. 4. pp 179-180.

[9] V. I. Plotnikov, Necessary and sufficient conditions for optimality and conditions for uniqueness of the optimizing functions for control systems of general form. (Russian) Izv. Akad. Nauk SSSR Ser. Mat. 36 (1972), 652–679.

[10] G. Berikelashvili. On the Solvability of a Nonlocal Boundary Value Problem in the Weighted Sobolev Spaces. Proceedings of A. Razmadze Mathematical Institute 119 (1999), 3-11

[11] G. V. Meladze, T. S. Tsutsunava, and D. Sh. Devadze, An optimal control problem for quasi-linear differential equations of first order on the plane with nonlocan boundary conditions. Tbilisi State University Press, Tbilisi, 1987, deposited at the Georgian Institute of Technical and Scientific Information, 25.12.87, No. 372, Г87, 61 p.

[12] O. A. Ladizhenskaya and N. N. Uraltseva, Linear and quasi-linear equations of elliptic type. (Russian) Nauka, Moscow, 1973.

[13] V. S. Vladimirov, The equations of mathematical physics. (Russian) Fourth edition. "Nauka", Moscow, 1981.

[14] S. L. Sobolev, The Equations of Mathematical Physics. (Russian) Gosudarstv. Izdat. Tehn.-Teor. Lit., Moscow–Leningrad, 1950.

[15] D. V. Kiryanov, Mathcad 14. BHV-Petersburg, St. Petersburg, 2007.

[16] M. Herhager and J. Partoll, Mathcad 2000: The Complete Guide: Trans. with Ger.-K. Publishing Group, BHV, 2000.

Review of Cases of Integrability in Dynamics of Lower- and Multidimensional Rigid Body in a Nonconservative Field of Forces

Maxim V. Shamolin

***Abstract*—Study of the dynamics of a multidimensional solid depends on the force-field structure. As reference results, we consider the equations of motion of low-dimensional solids in the field of a medium-drag force. Then it becomes possible to generalize the dynamic part of equations to the case of the motion of a solid, which is multidimensional in a similarly constructed force field, and to obtain the full list of transcendental first integrals. The obtained results are of importance in the sense that there is a nonconservative moment in the system, whereas it is the potential force field that was used previously.**

***Index Terms*—Case of integrability, dynamic part of motion equations, multidimensional rigid body.**

I. Introduction

THIS activity presents itself the review of either obtained earlier or new cases of integrability in Dynamics of two-dimensional, three-dimensional, and four-dimensional rigid body being in a nonconservative field of forces. The studied problems are described in terms of dynamic systems with so-called variable dissipation with zero mean.

The problem of research of complete choice of transcendental first integrals of the systems with dissipation is rather actual too, and majority of scientific activities was dedicated to it. New class of dynamic systems having the periodic coordinate is introduced in consideration. Due to the presence in such systems the nontrivial groups of symmetries it was shown that the considered systems possess the variable dissipation with zero mean that means the dissipation in the system is equal to zero for the period on available periodical coordinate, although both the sop of energy and its dissipation can be present in the different domains of the phase space of the system. On the base of obtained material the dynamic systems arising in Dynamics of a rigid body were analyzed. As the result the series of the cases of complete integrability of the motion equations in terms of transcendental functions and expressing through the finite combination of elementary functions were discovered. The certain generalizations on the conditions of integrability of more general classes of nonconservative dynamic systems (Dynamics of four-dimensional rigid body) were obtained.

January 18, 2014

Maxim V. Shamolin is with the Institute of Mechanics, Lomonosov Moscow State University, Moscow, 119192, Russian Federation; e-mail: shamolin@rambler.ru, shamolin@imec.msu.ru (see also http://shamolin2.imec.msu.ru).

II. Preliminary

The activity presents the review of both earlier obtained and also new cases of integrability in two-, three-, and four-dimensional rigid body dynamics in a nonconservative force field. The problems studied are described in terms of so-called zero mean variable dissipation dynamic systems.

Therefore, we study nonconservative systems for which the methods for studying, for example, Hamiltonian systems is not applicable in general. Therefore, for such systems, it is necessary, in some sense, to ”directly” integrate the main equation of dynamics. We generalize old cases and also obtain new cases of complete integrability in transcendental functions in two-, three-, and four-dimensional rigid body dynamics in a nonconservative force field.

Of course, in the general case, it is sufficiently difficult to construct some theory of integrating nonconservative systems (even of low dimension). But in a number of cases where the systems considered have additional symmetries, we succeed in finding first integrals through finite combinations of elementary functions [1].

We obtain a whole spectrum of complete integrability cases for nonconservative dynamical systems having nontrivial symmetries. Moreover, in almost all cases, each of the first integrals is expressed through a finite combination of elementary functions, being one transcendental function of its variables. In this case, the transcendence is understood in the complex analysis sense, when after continuation of given functions to the complex domain, they have essentially singular points. The latter fact is stipulated by the existence of attracting and repelling sets in the system (for example, attracting and repelling foci).

We discover new integrable cases of motion of a rigid body, including that in the classical problem of motion of a spherical pendulum in an over-run medium flow.

In [1], [2], [3], [4] we study the general aspects of integrability of so-called variable dissipation dynamic systems. For the beginning we give the visual characteristic of those systems. Therefore, in this case, we will speak of systems with the variable dissipation, where the term ”variable” refers not to the value of the dissipation coefficient, but to the possible alternation of its sign (therefore, it is more reasonable to use the term sign-alternating).

We introduce the class of autonomous dynamic systems having one periodic phase coordinate, and therefore, possessing the certain symmetries which are typical for the pendulum-like

ISBN: 978-1-61804-225-5

systems. We show that offered class of systems are embedded to the class of zero mean variable dissipation systems by natural way, i.e., on the average, for the period of the existing periodic coordinate, the sop and diffusing to energy balance to each other in certain sense. We offer the examples of pendulum-like systems on lower-dimension manifolds from dynamics of a rigid body in a nonconservative field of force [1], [5].

In [1], [6] we study the certain general conditions of integrability in elementary functions for the systems both on two-dimensional planes and the tangent bundle of one-dimensional sphere (i.e., two-dimensional cylinder), and two-dimensional sphere (the four-dimensional manifold). Therefore, we offer the interesting example of three-dimensional phase pattern of pendulum-like system which describes the motion of spherical pendulum, placed in an over-run medium flow [1], [5], [6].

Since we present the cases of complete integrability in spatial rigid body dynamics of the motion in a nonconservative field, we deal with three (at first thought) independent properties:

i) the distinguished class of systems with the symmetries above;

ii) the fact that this class of systems consists of systems with zero mean variable dissipation (in the having periodic variable), which allows us to consider them as "almost" conservative systems;

iii) in certain (although lower-dimensional) cases, these systems have the complete tuple of first integrals, which are transcendental in general (from the viewpoint of complex analysis).

In [1] the obtained results are systematized on study of the dynamic equations of the motion of symmetrical two-dimensional $(2D-)$ rigid body which residing in a certain nonconservative field of the forces. Its type is unoriginal from dynamics of the real rigid bodies interacting with a resisting medium on the laws of a jet flow, under which the nonconservative tracing force acts onto the body, and it either forces the value of the velocity of a certain typical point of the rigid body to remain as constant in all time of motion, that means the presence in system of nonintegrable servo-constraint, or forces the center of mass of the body to move rectilinearly and uniformly in all time of motion, that means the presence in system of nonconservative pair of the forces (see also [6], [7]).

Therefore, in [1] the additional transcendental first integral expressing through the finite combination of elementary functions is found to having analytical nonintegrable constraint, and in [8], [9], [10] the same was made to having analytical first integral (the square of the center of mass) only.

New obtained results are systematized and given in invariant form. Herewith, the additional dependence of the moment of the nonconservative force on the angular velocity is introduced. The given dependence can be wide-spread and on the cases of the motions in the spaces of higher dimensions.

In [1], [11] the obtained results are systematized on study of the dynamic equations of the motion of symmetrical three-dimensional $(3D-)$ rigid body which residing in a certain nonconservative field of the forces. Its type is also unoriginal from dynamics of the real rigid bodies interacting with a resisting medium on the laws of a jet flow, under which the nonconservative tracing force acts onto the body, and it either forces the value of the velocity of a certain typical point of the rigid body to remain as constant in all time of motion, that means the presence in system of nonintegrable servo-constraint, or forces the center of mass of the body to move rectilinearly and uniformly in all time of motion, that means the presence in system of nonconservative pair of the forces.

Therefore, in [10], [11], [12] three additional transcendental first integrals expressing through the finite combination of elementary functions are found to having analytical invariant relations (nonintegrable constraint and the integral on the equality to zero one of the component of angular velocity), and in [11], [12], [13] the same was made to having analytical first integrals (the square of the center of mass and the integral on the equality to zero one of the component of angular velocity) only.

In [1] we declare the general aspects of dynamics of multi-dimensional rigid body, i.e., the notion of angular velocity tensor, the joint dynamic equations of the motion on direct product $\mathbf{R}^n \times \mathrm{so}(n)$, the Euler and Rivals formulas in multi-dimensional case.

The question on tensor of inertia of four-dimensional $(4D-)$ rigid body is considered. In this activity it is proposed to study two possible cases logically on principal moments of inertia, i.e., when there exists *two* relations on the principal moments of inertia:

(i) when there exist *three* equal principal moments of inertia ($I_2 = I_3 = I_4$);

(ii) when there exist *two pairs* of equal moments of inetria ($I_1 = I_2, I_3 = I_4$).

In [12], [13], [14] the obtained results are systematized on study of the dynamic equations of the motion of symmetrical four-dimensional $(4D-)$ rigid body which residing in a certain nonconservative field of the forces for the case (i). Its type is also unoriginal from dynamics of lower-dimensional real rigid bodies interacting with a resisting medium on the laws of a jet flow, under which the nonconservative tracing force acts onto the body, and it either forces the value of the velocity of a certain typical point of the rigid body to remain as constant in all time of motion, that means the presence in system of nonintegrable servo-constraint, or forces the center of mass of the body to move rectilinearly and uniformly in all time of motion, that means the presence in system of nonconservative pair of the forces.

Therefore, in [13], [14], [15] four additional transcendental first integrals expressing through the finite combination of elementary functions are found to having four analytical invariant relations (nonintegrable constraint and three integrals on the equalities to zero some of the components of angular velocity tensor), and in [14], [15], [16] the same was made to having four analytical first integrals (the square of the center of mass and three integrals on the equalities to zero some of the components of angular velocity tensor) only.

The results are pertained to the case when all the interaction of a medium with the body is concentrated on that part of the body surface that has the form of three-dimensional disk,

ISBN: 978-1-61804-225-5

TABLE I
CLASSIFICATION OF THE CASES OF INTEGRABILITY FROM TWO-DIMENSIONAL SYMMETRIC RIGID BODY DYNAMICS IN $\mathbf{E}^2$ TO FOUR-DIMENSIONAL DYNAMICALLY SYMMETRIC RIGID BODY DYNAMICS IN $\mathbf{E}^4$

Dimension of a Rigid Body	Constraint Condition	
	$v \equiv \text{const}$ ($\beta_2 \equiv \text{const}$)	$\mathbf{V}_C \equiv \mathbf{const}$
$\mathbf{E}^2$	$h = 0$ $\oplus$	$h = 0$ $\oplus$
	$h \neq 0$ $\oplus$	$h \neq 0$ $\oplus$
$\mathbf{E}^3$	$h = 0$ $\oplus$	$h = 0$ $\oplus$
$(I_2 = I_3)$	$h \neq 0$ $\oplus$	$h \neq 0$ $\oplus$
$\mathbf{E}^4$	$h = 0$ $\oplus$	$h = 0$ $\oplus$
$(I_2 = I_3 = I_4)$	$h \neq 0$ $\oplus$	$h \neq 0$ $\oplus$
$\mathbf{E}^4$	$h = 0$ $\oplus$	$h = 0$ $\ominus$
$(I_1 = I_2,\ I_3 = I_4)$	$h \neq 0$ $\oplus$	$h \neq 0$ $\ominus$

herewith, the force interaction is concentrated in the direction which is perpendicular to this disk. These results are systematized and given in invariant form. Herewith, the additional dependence of the moment of the nonconservative force on the angular velocity is introduced. The given dependence can be wide-spread and on the cases of the motions in the spaces of higher dimensions.

In this activity the obtained results are systematized on study of the dynamic equations of the motion of symmetrical four-dimensional ($4D-$) rigid body which residing in a certain nonconservative field of the forces for the case (ii). Its type is also unoriginal from dynamics of lower-dimensional real rigid bodies interacting with a resisting medium on the laws of a jet flow, under which the nonconservative tracing force acts onto the body, and it forces both the value of the velocity of a certain typical point of the rigid body and the certain phase variable to remain as constant in all time, that means the presence in system of nonintegrable servo-constraints.

Therefore, in this activity two additional transcendental and three analytical first integrals expressing through the finite combination of elementary functions are found to having four analytical invariant relations (two nonintegrable constraints and two integrals on the equalities to zero some of the components of angular velocity tensor).

The results which are obtained now are pertained to the case when all the interaction of a medium with the body is concentrated on that part of the body surface that has the form of two-dimensional disk, herewith, the force interaction is concentrated in two-dimensional plane which is perpendicular to this disk. These results are systematized and given in invariant form. Herewith, the additional dependence of the moment of the nonconservative force on the angular velocity is introduced. The given dependence can be wide-spread and on the cases of the motions in the spaces of higher dimensions.

And so, in [16], [17], [18] the cases of integrability in lower- and multi-dimensional dynamics of a rigid body placed in a nonconservative force field. To systemize we shall place all of them to the following table.

The notifications $h = 0$ (or $h \neq 0$) mean that the dependence of the force field on the components of angular velocity tensor is present (or is absent) in the system.

The sign $\oplus$ means that the case is placed to this review.

Two signs $\ominus$ in the right below corner of the table mean that these two cases are not placed to this review (indeed, this activity is devoted to the case $I_1 = I_2,\ I_3 = I_4$ only).

Nevertheless, the corresponding results have already obtained for the case $I_2 = \ldots = I_n$ of symmetric n-dimensional rigid body, and those results are not also placed to this review.

Many results of this work were regularly reported at numerous workshops, including the workshop "Actual Problems of Geometry and Mechanics" named after professor V. V. Trofimov led by D. V. Georgievskii and M. V. Shamolin.

III. CASES OF INTEGRABILITY CORRESPONDING TO A RIGID BODY MOTION IN FOUR-DIMENSIONAL SPACE

In this section the new results are systematized on study of the equations of the motion of dynamically symmetrical four-dimensional ($4D-$) rigid body which residing in a certain nonconservative field of the forces in the case of special dynamical symmetry. Its type is unoriginal from dynamics of the real lower-dimensional rigid bodies of interacting with a resisting medium on the laws of a jet flow, under which the nonconservative tracing force acts onto the body and forces both the value of the velocity of a certain typical point of the rigid body and the certain phase variable to remain as constant in all time, that means the presence in system of nonintegrable servo-constraints.

Previously, in [1], the author showed the complete integrability of the equations of body planeparallel motion in a resisting medium under the conditions of streamline flow around when the system of dynamical equations has a first integral that is a transcendental (having essentially singular points in the sense of the theory of functions of one complex variable) function of quasi-velocities. At that time, it was assumed that the interaction of the medium with the body is concentrated on the part of the body surface that has the form of a (one-dimensional) plate.

Later on, in [2], [5], [18], the plane problem was generalized to the spatial (three-dimensional) case where the system of dynamical equations has a complete tuple of transcendental first integrals. It was assumed here that the whole interaction of the medium and the body is concentrated on a part of the body surface that has the form of a plane (two-dimensional) disk.

In this section the results which are obtained now are pertained to the case when all the interaction of a medium with the body is concentrated on that part of the body surface that has the form of two-dimensional disk, herewith, the force interaction is concentrated in two-dimensional plane which is perpendicular to this disk. These results are systematized and given in invariant form. Herewith, the additional dependence of the moment of the nonconservative force on the angular velocity is introduced. The given dependence can be wide-spread and on the cases of the motions in the spaces of higher dimensions.

ISBN: 978-1-61804-225-5

IV. More general problem of the motion with the tracing force

Let consider the motion of a homogeneous dynamically symmetric rigid body with "the front end-wall" (two-dimensional disk interacting with a medium which filling the four-dimensional space) in the field of force **S** of the resistance under the conditions of quasistationarity.

Let $(v, \alpha, \beta_2, \beta_1)$ are the coordinates of the vector velocity of a certain typical point D of a rigid body (D is the center of two-dimensional disk) such that α is the angle between the vector $\mathbf{v}_D$ and the plane Dx_1x_2, β_2 is the angle measured in the plane Dx_1x_2 up to the projection of the vector $\mathbf{v}_D$ on the plane Dx_1x_2, β_1 is the angle mesured in the plane Dx_3x_4 up to the projection of the vector $\mathbf{v}_D$ on the plane Dx_3x_4,

$$\Omega = \begin{pmatrix} 0 & -\omega_6 & \omega_5 & -\omega_3 \\ \omega_6 & 0 & -\omega_4 & \omega_2 \\ -\omega_5 & \omega_4 & 0 & -\omega_1 \\ \omega_3 & -\omega_2 & \omega_1 & 0 \end{pmatrix}$$

is the angular velocity tensor of the body, $Dx_1x_2x_3x_4$ is the coordinate system related to the body, herewith, the straight line CD lies in the plane Dx_1x_2 (C is the center of mass), and the axes Dx_3, Dx_4 lie in the disk plane, $I_1,\ I_2 = I_1,\ I_3,\ I_4 = I_3,\ m$ are the inertia–mass characteristics.

Let accept the following decompositions in the projections on the axes of the coordinate system $Dx_1x_2x_3x_4$:

$$\mathbf{DC} = \{\sigma \sin\gamma, -\sigma\cos\gamma, 0, 0\},$$
$$\mathbf{v}_D = \{v\cos\alpha\sin\beta_2, v\cos\alpha\cos\beta_2,$$
$$v\sin\alpha\cos\beta_1, v\sin\alpha\sin\beta_1\}. \quad (1)$$

Herewith, in our case the decomposition will be also correct for the function of a medium interaction on four-dimensional body:

$$\mathbf{S} = \{S_1, S_2, 0, 0\}, \quad (2)$$

herewith

$$S_1 = S\sin\gamma,\ S_2 = -S\cos\gamma,\ \gamma = \text{const}, \quad (3)$$

i.e. in this case $\mathbf{F} = \mathbf{S}$, and the angle γ is measured in the plane Dx_1x_2.

Then those part of dynamic equations of the body motion (including and in the case of Chaplygin analytical functions, see below) which describes the center of mass motion and corresponds to the space $\mathbf{R}^4$ under which the tangent forces to three-dimensional disk are absent, has the form:

$$\dot v\cos\alpha\sin\beta_2 - \dot\alpha v\sin\alpha\sin\beta_2 + \dot\beta_2 v\cos\alpha\cos\beta_2 -$$
$$-\omega_6 v\cos\alpha\cos\beta_2 + \omega_5 v\sin\alpha\cos\beta_1 - \omega_3 v\sin\alpha\sin\beta_1 -$$
$$-\sigma(\omega_6^2+\omega_5^2+\omega_3^2)\sin\gamma - \sigma(\omega_4\omega_5+\omega_2\omega_3)\cos\gamma +$$
$$+\sigma\dot\omega_6\cos\gamma = \frac{S_1}{m}, \quad (4)$$

$$\dot v\cos\alpha\cos\beta_2 - \dot\alpha v\sin\alpha\cos\beta_2 - \dot\beta_2 v\cos\alpha\sin\beta_2 +$$
$$+\omega_6 v\cos\alpha\sin\beta_2 - \omega_4 v\sin\alpha\cos\beta_1 + \omega_2 v\sin\alpha\sin\beta_1 +$$
$$+\sigma(\omega_6^2+\omega_4^2+\omega_2^2)\cos\gamma + \sigma(\omega_4\omega_5+\omega_2\omega_3)\sin\gamma +$$
$$+\sigma\dot\omega_6\sin\gamma = \frac{S_2}{m}, \quad (5)$$

$$\dot v\sin\alpha\cos\beta_1 + \dot\alpha v\cos\alpha\cos\beta_1 - \dot\beta_1 v\sin\alpha\sin\beta_1 -$$
$$-\omega_5 v\cos\alpha\sin\beta_2 + \omega_4 v\cos\alpha\cos\beta_2 - \omega_1 v\sin\alpha\sin\beta_1 +$$
$$+\sigma(\omega_4\omega_6-\omega_1\omega_3)\sin\gamma - \sigma(\omega_5\omega_6+\omega_1\omega_2)\cos\gamma -$$
$$-\sigma\dot\omega_5\sin\gamma - \sigma\dot\omega_4\cos\gamma = 0, \quad (6)$$

$$\dot v\sin\alpha\sin\beta_1 + \dot\alpha v\cos\alpha\sin\beta_1 + \dot\beta_1 v\sin\alpha\cos\beta_1 +$$
$$+\omega_3 v\cos\alpha\sin\beta_2 - \omega_2 v\cos\alpha\cos\beta_2 + \omega_1 v\sin\alpha\cos\beta_1 -$$
$$-\sigma(\omega_2\omega_6+\omega_1\omega_5)\sin\gamma + \sigma(\omega_3\omega_6-\omega_1\omega_4)\cos\gamma +$$
$$+\sigma\dot\omega_3\sin\gamma + \sigma\dot\omega_2\cos\gamma = 0, \quad (7)$$

where

$$S = s(\alpha)v^2,\ \sigma = CD,\ v > 0. \quad (8)$$

Later on, the auxiliary matrix for the calculation of the moment of the resisting force has the form

$$\begin{pmatrix} 0 & 0 & x_{3N} & x_{4N} \\ S_1 & S_2 & 0 & 0 \end{pmatrix}, \quad (9)$$

then those part of the dynamic equations of the body motion which describes the body motion around the center of mass, and corresponds to the Lie algebra so(4), has the form:

$$(\lambda_4+\lambda_3)\dot\omega_1 + (\lambda_3-\lambda_4)(\omega_3\omega_5+\omega_2\omega_4) = 0, \quad (10)$$

$$(\lambda_2+\lambda_4)\dot\omega_2 + (\lambda_2-\lambda_4)(\omega_3\omega_6-\omega_1\omega_4) =$$
$$= -x_{4N}\left(\alpha,\beta_1,\beta_2,\frac{\Omega}{v}\right)s(\alpha)v^2\cos\gamma, \quad (11)$$

$$(\lambda_4+\lambda_1)\dot\omega_3 + (\lambda_4-\lambda_1)(\omega_2\omega_6+\omega_1\omega_5) =$$
$$= -x_{4N}\left(\alpha,\beta_1,\beta_2,\frac{\Omega}{v}\right)s(\alpha)v^2\sin\gamma, \quad (12)$$

$$(\lambda_3+\lambda_2)\dot\omega_4 + (\lambda_2-\lambda_3)(\omega_5\omega_6+\omega_1\omega_2) =$$
$$= x_{3N}\left(\alpha,\beta_1,\beta_2,\frac{\Omega}{v}\right)s(\alpha)v^2\cos\gamma, \quad (13)$$

$$(\lambda_1+\lambda_3)\dot\omega_5 + (\lambda_3-\lambda_1)(\omega_4\omega_6-\omega_1\omega_3) =$$
$$= x_{3N}\left(\alpha,\beta_1,\beta_2,\frac{\Omega}{v}\right)s(\alpha)v^2\sin\gamma, \quad (14)$$

$$(\lambda_1+\lambda_2)\dot\omega_6 + (\lambda_1-\lambda_2)(\omega_4\omega_5+\omega_2\omega_3) = 0. \quad (15)$$

Thus, the following direct product of four-dimensional manifold on the Lie algebra so(4) is the phase space of the tenth order system (4)–(7), (10)–(15):

$$\mathbf{R}^1 \times \mathbf{S}^3 \times \text{so}(4). \quad (16)$$

We notice right now that the system (4)–(7), (10)–(15), by virtue of the having dynamical symmetry

$$I_1 = I_2,\ I_3 = I_4, \quad (17)$$

possesses the cyclic first integrals

$$\omega_1 \equiv \omega_1^0 = \text{const},\ \omega_6 \equiv \omega_6^0 = \text{const}. \quad (18)$$

ISBN: 978-1-61804-225-5

Herewith, hereinafter we shall consider the dynamics of the system on zero level:

$$\omega_1^0 = \omega_6^0 = 0. \tag{19}$$

And if there exists the more general problem of the body motion with the certain tracing force **T**, which acts on the plane Dx_1x_2 and providing the fulfillment of the following equalities in all time of the motion

$$v \equiv \text{const}, \ \beta_2 \equiv \text{const}, \tag{20}$$

that in the system (4)–(7), (10)–(15) the values

$$T_1 + S_1, \ T_2 + S_2 \tag{21}$$

will stand instead of F_1 and F_2 accordingly.

As a result of corresponding value choice T of the tracing force it is possible to obtain formally the fulfillment of the equalities (20) in all time of the motion. Really, if we express formally the value T by virtue of the system (4)–(7), (10)–(15) we shall obtain for $\cos\alpha \neq 0$:

$$T_1 = T_{1,v,\beta 2}(\alpha, \beta_1, \Omega) =$$
$$= -m\sigma(\omega_5^2 + \omega_3^2)\sin\gamma - m\sigma(\omega_4\omega_5 + \omega_2\omega_3)\cos\gamma +$$
$$+m\omega_5 v \sin\alpha\cos\beta_1\cos^2\beta_2 - m\omega_3 v\sin\alpha\sin\beta_1\cos^2\beta_2 +$$
$$+m\omega_4 v\sin\alpha\cos\beta_1\sin\beta_2\cos\beta_2 -$$
$$-m\omega_2 v\sin\alpha\sin\beta_1\sin\beta_2\cos\beta_2 - s(\alpha)v^2 \times$$
$$\times\left[\sin\gamma - \frac{m\sigma}{I_1+I_3}\frac{\sin\alpha}{\cos\alpha}\sin\beta_2\cdot\Lambda_{v,\beta_2}\left(\alpha,\beta_1,\frac{\Omega}{v}\right)\right], \tag{22}$$

$$T_2 = T_{2,v,\beta 2}(\alpha, \beta_1, \Omega) =$$
$$= m\sigma(\omega_4^2 + \omega_2^2)\cos\gamma + m\sigma(\omega_4\omega_5 + \omega_2\omega_3)\sin\gamma -$$
$$-m\omega_4 v\sin\alpha\cos\beta_1\sin^2\beta_2 + m\omega_2 v\sin\alpha\sin\beta_1\sin^2\beta_2 -$$
$$-m\omega_5 v\sin\alpha\cos\beta_1\sin\beta_2\cos\beta_2 +$$
$$+m\omega_3 v\sin\alpha\sin\beta_1\sin\beta_2\cos\beta_2 + s(\alpha)v^2 \times$$
$$\times\left[\cos\gamma - \frac{m\sigma}{I_1+I_3}\frac{\sin\alpha}{\cos\alpha}\cos\beta_2\cdot\Lambda_{v,\beta_2}\left(\alpha,\beta_1,\frac{\Omega}{v}\right)\right], \tag{23}$$

where

$$\Lambda_{v,\beta_2}\left(\alpha,\beta_1,\frac{\Omega}{v}\right) = x_{3N}\left(\alpha,\beta_1,\beta_2,\frac{\Omega}{v}\right)\cos\beta_1 +$$
$$+x_{4N}\left(\alpha,\beta_1,\beta_2,\frac{\Omega}{v}\right)\sin\beta_1. \tag{24}$$

The conditions (18)–(20) are used at the obtaining of the equalities (22) and (23).

It makes possible to look at this procedure from two positions. In first, the transformation of the system has occurred at presence of the tracing (control) force in the system which provides the consideration of interesting classes of the motion (20). In second, it makes possible to look at this like the procedure which allows to deflate the system. Really, the system (4)–(7), (10)–(15) as a result of that action generates an independent system of the sixth order of the following type:

$$\dot\alpha v\cos\alpha\cos\beta_1 - \dot\beta_1 v\sin\alpha\sin\beta_1 - \omega_5 v\cos\alpha\sin\beta_2 +$$
$$+\omega_4 v\cos\alpha\cos\beta_2 - \sigma\dot\omega_5\sin\gamma - \sigma\dot\omega_4\cos\gamma = 0, \tag{25}$$

$$\dot\alpha v\cos\alpha\sin\beta_1 + \dot\beta_1 v\sin\alpha\cos\beta_1 + \omega_3 v\cos\alpha\sin\beta_2 -$$
$$-\omega_2 v\cos\alpha\cos\beta_2 + \sigma\dot\omega_3\sin\gamma + \sigma\dot\omega_2\cos\gamma = 0, \tag{26}$$

$$(I_1+I_3)\dot\omega_2 = -x_{4N}\left(\alpha,\beta_1,\beta_2,\frac{\Omega}{v}\right)s(\alpha)v^2\cos\gamma, \tag{27}$$

$$(I_1+I_3)\dot\omega_3 = -x_{4N}\left(\alpha,\beta_1,\beta_2,\frac{\Omega}{v}\right)s(\alpha)v^2\sin\gamma, \tag{28}$$

$$(I_1+I_3)\dot\omega_4 = x_{3N}\left(\alpha,\beta_1,\beta_2,\frac{\Omega}{v}\right)s(\alpha)v^2\cos\gamma, \tag{29}$$

$$(I_1+I_3)\dot\omega_5 = x_{3N}\left(\alpha,\beta_1,\beta_2,\frac{\Omega}{v}\right)s(\alpha)v^2\sin\gamma, \tag{30}$$

in which the parameters v, β_2 are added to the constant parameters specified above.

A. Two systems of the discourses on integrability

Remark (on analytical first integrals). Obviously that the system (25)–(30) possesses two analytical first integrals which are expressed in terms of the finite combination of the elementary functions:

$$\omega_2\sin\gamma - \omega_3\cos\gamma = W_1' = \text{const}, \tag{31}$$

$$\omega_4\sin\gamma - \omega_5\cos\gamma = W_2' = \text{const}. \tag{32}$$

First of all this means that the system (25)–(30) can be reduced to the fourth order system on its own four-dimensional phase manifold.

Hereafter, it makes possible to develop by the following ways under the study of the system (25)–(30) (i.e. to accept the following systems of the discourses).

I. In first, it makes possible "not to notice" the existence in the system the first integrals of the forms (31), (32). Then conducting the series of the equivalent transformations it can possible try to reduce the investigated system (25)–(30) to the equivalent system in which the reduction to the systems of lower dimensionality will occur. Herewith, it is sufficient to get the quantity of the independent first integrals smaller then previous one on two units for the complete system integration, by virtue of (31), (32).

II. In second, it makes possible to use the first integrals (31), (32) expressing two interested phase variables from the list $\omega_2, \omega_3, \omega_4, \omega_5$. Herewith, we shall get just the fourth order system as the system which is the reduction of the system (25)–(30) to the certain four-dimensional phase manifold.

In the beginning we shall choose the system of the discourses **I**.

Really, the system (25)–(30) is equivalent to

$$\dot\alpha v\cos\alpha - \omega_5 v\cos\alpha\cos\beta_1\sin\beta_2 + \omega_4 v\cos\alpha\cos\beta_1\cos\beta_2 +$$
$$+\omega_3 v\cos\alpha\sin\beta_1\sin\beta_2 - \omega_2 v\cos\alpha\sin\beta_1\cos\beta_2 -$$
$$\sigma\dot\omega_5\sin\gamma\cos\beta_1 - \sigma\dot\omega_4\cos\gamma\cos\beta_1 +$$
$$+\sigma\dot\omega_3\sin\gamma\sin\beta_1 + \sigma\dot\omega_2\cos\gamma\sin\beta_1 = 0, \tag{33}$$

$$\dot\beta_1 v\sin\alpha + \omega_3 v\cos\alpha\cos\beta_1\sin\beta_2 - \omega_2 v\cos\alpha\cos\beta_1\cos\beta_2 +$$

ISBN: 978-1-61804-225-5

$$+\omega_5 v\cos\alpha\sin\beta_1\sin\beta_2-\omega_4 v\cos\alpha\sin\beta_1\cos\beta_2+$$
$$+\sigma\dot{\omega}_3\sin\gamma\cos\beta_1+\sigma\dot{\omega}_2\cos\gamma\cos\beta_1+$$
$$+\sigma\dot{\omega}_5\sin\gamma\sin\beta_1+\sigma\dot{\omega}_4\cos\gamma\sin\beta_1=0, \quad (34)$$

$$\dot{\omega}_2=-\frac{v^2}{I_1+I_3}x_{4N}\left(\alpha,\beta_1,\beta_2,\frac{\Omega}{v}\right)s(\alpha)\cos\gamma, \quad (35)$$

$$\dot{\omega}_3=-\frac{v^2}{I_1+I_3}x_{4N}\left(\alpha,\beta_1,\beta_2,\frac{\Omega}{v}\right)s(\alpha)\sin\gamma, \quad (36)$$

$$\dot{\omega}_4=\frac{v^2}{I_1+I_3}x_{3N}\left(\alpha,\beta_1,\beta_2,\frac{\Omega}{v}\right)s(\alpha)\cos\gamma, \quad (37)$$

$$\dot{\omega}_5=\frac{v^2}{I_1+I_3}x_{3N}\left(\alpha,\beta_1,\beta_2,\frac{\Omega}{v}\right)s(\alpha)\sin\gamma, \quad (38)$$

Let introduce new quasivelocities in the system. We shall transform the values $\omega_2,\omega_3,\omega_4,\omega_5$ by means of the composition of the following rotations for this:

$$\begin{pmatrix} z_1 \\ -z_2 \end{pmatrix}=T_*(-\beta_1)\begin{pmatrix} \omega_3 \\ \omega_5 \end{pmatrix},$$
$$\begin{pmatrix} z_3 \\ -z_4 \end{pmatrix}=T_*(-\beta_1)\begin{pmatrix} \omega_2 \\ \omega_4 \end{pmatrix}, \quad (39)$$

where

$$T_*(\beta_1)=\begin{pmatrix} \cos\beta_1 & -\sin\beta_1 \\ \sin\beta_1 & \cos\beta_1 \end{pmatrix}, \quad (40)$$

and also

$$\begin{pmatrix} w_1 \\ w_2 \end{pmatrix}=T_*(\beta_2)\begin{pmatrix} z_3 \\ z_1 \end{pmatrix},$$
$$\begin{pmatrix} w_3 \\ w_4 \end{pmatrix}=T_*(-\beta_2)\begin{pmatrix} -z_4 \\ z_2 \end{pmatrix}. \quad (41)$$

Thus, the following relations are correct:

$$\begin{aligned} z_1&=\omega_3\cos\beta_1+\omega_5\sin\beta_1,\\ z_2&=\omega_3\sin\beta_1-\omega_5\cos\beta_1,\\ z_3&=\omega_2\cos\beta_1+\omega_4\sin\beta_1,\\ z_4&=\omega_2\sin\beta_1-\omega_4\cos\beta_1,\\ w_1&=-z_1\sin\beta_2+z_3\cos\beta_2,\\ w_2&=z_3\sin\beta_2+z_1\cos\beta_2,\\ w_3&=z_2\sin\beta_2-z_4\cos\beta_2,\\ w_4&=z_4\sin\beta_2+z_2\cos\beta_2. \end{aligned} \quad (42)$$

As is seen from (33)–(38), on the manifold

$$O_2=\left\{(\alpha,\beta_1,\omega_2,\omega_3,\omega_4,\omega_5)\in\mathbf{R}^6:\ \alpha=\frac{\pi}{2}k,\ k\in\mathbf{Z}\right\} \quad (43)$$

it is impossible to resolve the system uniquely relatively to $\dot{\alpha},\ \dot{\beta}_1$. Thus, the violation of the uniqueness theorem is happened on the manifold (43) formally. Moreover, in first, the indefiniteness is happened for even or odd k by the reason of degeneration of the coordinates $(v,\alpha,\beta_1,\beta_2)$ which are parameterized the three-dimensional sphere (but are not the classical spherical coordinates), and, in second, it is happened the evident violation of the uniquiness theorem for odd k because of the first equation of (33) degenerates for this case.

Really, Jacobian of the transformation $x_1,x_2,x_3,x_4\longrightarrow v,\alpha,\beta_1,\beta_2$

$$\begin{aligned} x_1&=v\cos\alpha\sin\beta_2,\\ x_2&=v\cos\alpha\cos\beta_2,\\ x_3&=v\sin\alpha\cos\beta_1,\\ x_4&=v\sin\alpha\sin\beta_1 \end{aligned} \quad (44)$$

is equal to

$$v^3\cos\alpha\sin\alpha,$$

in what it differs from Jacobian of the transformation under the transition to the generalized spherical coordinates v,α,β_1,β_2, which, in turn, is equal to

$$v^3\sin\alpha\sin\beta_1.$$

It follows that the system (33)–(38) outside of and only outside of the manifold (43) is equivalent to the system

$$\dot{\alpha}=-w_3+\frac{\sigma v}{I_1+I_3}\frac{s(\alpha)}{\cos\alpha}\cdot\Lambda_{v,\beta_2}\left(\alpha,\beta_1,\frac{\Omega}{v}\right), \quad (45)$$

$$\dot{z_4}=-\frac{v^2}{I_1+I_3}s(\alpha)\cos\gamma\cdot\Lambda_{v,\beta_2}\left(\alpha,\beta_1,\frac{\Omega}{v}\right)+$$
$$+z_3\left[w_1\frac{\cos\alpha}{\sin\alpha}-\frac{\sigma v}{I_1+I_3}\frac{s(\alpha)}{\sin\alpha}\cdot\Pi_{v,\beta_2}\left(\alpha,\beta_1,\frac{\Omega}{v}\right)\right], \quad (46)$$

$$\dot{z_3}=\frac{v^2}{I_1+I_3}s(\alpha)\cos\gamma\cdot\Pi_{v,\beta_2}\left(\alpha,\beta_1,\frac{\Omega}{v}\right)-$$
$$-z_4\left[w_1\frac{\cos\alpha}{\sin\alpha}-\frac{\sigma v}{I_1+I_3}\frac{s(\alpha)}{\sin\alpha}\cdot\Pi_{v,\beta_2}\left(\alpha,\beta_1,\frac{\Omega}{v}\right)\right], \quad (47)$$

$$\dot{z_2}=-\frac{v^2}{I_1+I_3}s(\alpha)\sin\gamma\cdot\Lambda_{v,\beta_2}\left(\alpha,\beta_1,\frac{\Omega}{v}\right)+$$
$$+z_1\left[w_1\frac{\cos\alpha}{\sin\alpha}-\frac{\sigma v}{I_1+I_3}\frac{s(\alpha)}{\sin\alpha}\cdot\Pi_{v,\beta_2}\left(\alpha,\beta_1,\frac{\Omega}{v}\right)\right], \quad (48)$$

$$\dot{z_1}=\frac{v^2}{I_1+I_3}s(\alpha)\sin\gamma\cdot\Pi_{v,\beta_2}\left(\alpha,\beta_1,\frac{\Omega}{v}\right)-$$
$$-z_2\left[w_1\frac{\cos\alpha}{\sin\alpha}-\frac{\sigma v}{I_1+I_3}\frac{s(\alpha)}{\sin\alpha}\cdot\Pi_{v,\beta_2}\left(\alpha,\beta_1,\frac{\Omega}{v}\right)\right], \quad (49)$$

$$\dot{\beta}_1=w_1\frac{\cos\alpha}{\sin\alpha}-\frac{\sigma v}{I_1+I_3}\frac{s(\alpha)}{\sin\alpha}\cdot\Pi_{v,\beta_2}\left(\alpha,\beta_1,\frac{\Omega}{v}\right), \quad (50)$$

or finally

$$\dot{\alpha}=-w_3+\frac{\sigma v}{I_1+I_3}\frac{s(\alpha)}{\cos\alpha}\cdot\Lambda_{v,\beta_2}\left(\alpha,\beta_1,\frac{\Omega}{v}\right), \quad (51)$$

$$\dot{w_4}=-\frac{v^2}{I_1+I_3}s(\alpha)\sin(\beta_2+\gamma)\cdot\Lambda_{v,\beta_2}\left(\alpha,\beta_1,\frac{\Omega}{v}\right)+$$
$$+w_2\left[w_1\frac{\cos\alpha}{\sin\alpha}-\frac{\sigma v}{I_1+I_3}\frac{s(\alpha)}{\sin\alpha}\cdot\Pi_{v,\beta_2}\left(\alpha,\beta_1,\frac{\Omega}{v}\right)\right], \quad (52)$$

$$\dot{w_3}=\frac{v^2}{I_1+I_3}s(\alpha)\cos(\beta_2+\gamma)\cdot\Lambda_{v,\beta_2}\left(\alpha,\beta_1,\frac{\Omega}{v}\right)-$$
$$-w_1\left[w_1\frac{\cos\alpha}{\sin\alpha}-\frac{\sigma v}{I_1+I_3}\frac{s(\alpha)}{\sin\alpha}\cdot\Pi_{v,\beta_2}\left(\alpha,\beta_1,\frac{\Omega}{v}\right)\right], \quad (53)$$

ISBN: 978-1-61804-225-5

$$\dot{w_2} = \frac{v^2}{I_1+I_3} s(\alpha)\sin(\beta_2+\gamma)\cdot \Pi_{v,\beta_2}\left(\alpha,\beta_1,\frac{\Omega}{v}\right) -$$

$$-w_4\left[w_1\frac{\cos\alpha}{\sin\alpha} - \frac{\sigma v}{I_1+I_3}\frac{s(\alpha)}{\sin\alpha}\cdot\Pi_{v,\beta_2}\left(\alpha,\beta_1,\frac{\Omega}{v}\right)\right], \quad (54)$$

$$\dot{w_1} = \frac{v^2}{I_1+I_3} s(\alpha)\cos(\beta_2+\gamma)\cdot \Pi_{v,\beta_2}\left(\alpha,\beta_1,\frac{\Omega}{v}\right) +$$

$$+w_3\left[w_1\frac{\cos\alpha}{\sin\alpha} - \frac{\sigma v}{I_1+I_3}\frac{s(\alpha)}{\sin\alpha}\cdot\Pi_{v,\beta_2}\left(\alpha,\beta_1,\frac{\Omega}{v}\right)\right], \quad (55)$$

$$\dot{\beta_1} = w_1\frac{\cos\alpha}{\sin\alpha} - \frac{\sigma v}{I_1+I_3}\frac{s(\alpha)}{\sin\alpha}\cdot\Pi_{v,\beta_2}\left(\alpha,\beta_1,\frac{\Omega}{v}\right), \quad (56)$$

where

$$\Pi_{v,\beta_2}\left(\alpha,\beta_1,\frac{\Omega}{v}\right) = -x_{4N}\left(\alpha,\beta_1,\frac{\Omega}{v}\right)\cos\beta_1 +$$

$$+x_{3N}\left(\alpha,\beta_1,\frac{\Omega}{v}\right)\sin\beta_1, \quad (57)$$

and the function $\Lambda_{v,\beta_2}(\alpha,\beta_1,\Omega/v)$ is represented in the form (24).

Hereafter, the dependence on the groups of the variables $(\alpha,\beta_1,\beta_2,\Omega/v)$ is understood like the complicated dependence on $(\alpha,\beta_1,\beta_2,z_1/v,z_2/v,z_3/v,z_4/v)$ (or $(\alpha,\beta_1,\beta_2,w_1/v,w_2/v,w_3/v,w_4/v)$) by virtue of (42).

The violation of the uniqueness theorem is happened for the system (33)–(38) on the manifold (43) for odd k in following sense: the regular phase trajectory of the system (33)–(38) passes through nearly any point from the manifold (43) for odd k intersecting the manifold (43) under right angle, and also there exist the phase trajectory which coincides completely with the specified point in all moments of time. But those are the different trajectories physically since the different values of the tracing force correspond them. Let show this.

As it is shown above, it is necessary to choose the values T_1 and T_2 for $\cos\alpha \neq 0$ in the form of (22) and (23) to fulfill the constraints (20).

Let

$$\lim_{\alpha\to\pi/2}\frac{s(\alpha)}{\cos\alpha}\Lambda_{v,\beta_2}\left(\alpha,\beta_1,\frac{\Omega}{v}\right) = L\left(\beta_1,\beta_2,\frac{\Omega}{v}\right). \quad (58)$$

Let note that $|L| < +\infty$ iff, when

$$\lim_{\alpha\to\pi/2}\left|\frac{\partial}{\partial\alpha}\left(\Lambda_{v,\beta_2}\left(\alpha,\beta_1,\frac{\Omega}{v}\right)s(\alpha)\right)\right| < +\infty. \quad (59)$$

The necessary values of the tracing force for $\alpha = \pi/2$ should be found from the equalities

$$T_1 = T_{1,v,\beta 2}\left(\frac{\pi}{2},\beta_1,\Omega\right) =$$

$$= -m\sigma(\omega_5^2+\omega_3^2)\sin\gamma - m\sigma(\omega_4\omega_5+\omega_2\omega_3)\cos\gamma +$$

$$+m\omega_5 v\cos\beta_1\cos^2\beta_2 - m\omega_3 v\sin\beta_1\cos^2\beta_2 +$$

$$+m\omega_4 v\cos\beta_1\sin\beta_2\cos\beta_2 - m\omega_2 v\sin\beta_1\sin\beta_2\cos\beta_2 +$$

$$+v^2\frac{m\sigma}{I_1+I_3}\sin\beta_2\cdot L, \quad (60)$$

$$T_2 = T_{2,v,\beta 2}\left(\frac{\pi}{2},\beta_1,\Omega\right) =$$

$$= m\sigma(\omega_4^2+\omega_2^2)\cos\gamma + m\sigma(\omega_4\omega_5+\omega_2\omega_3)\sin\gamma -$$

$$-m\omega_4 v\cos\beta_1\sin^2\beta_2 + m\omega_2 v\sin\beta_1\sin^2\beta_2 -$$

$$-m\omega_5 v\cos\beta_1\sin\beta_2\cos\beta_2 + m\omega_3 v\sin\beta_1\sin\beta_2\cos\beta_2 -$$

$$-v^2\frac{m\sigma}{I_1+I_3}\cos\beta_2\cdot L, \quad (61)$$

where the values of $\omega_2,\omega_3,\omega_4,\omega_5$ are arbitrary.

On the other hand, if we make the rotation around a certain point W by means of the tracing force it will be necessary to choose the projections of the tracing force in the form of

$$T = T_1\left(\frac{\pi}{2},\beta_1,\beta_2,\Omega\right) = \frac{mv^2}{R_{01}}, \quad (62)$$

$$T = T_2\left(\frac{\pi}{2},\beta_1,\beta_2,\Omega\right) = \frac{mv^2}{R_{02}}, \quad (63)$$

where R_{01}, R_{02} are the projections of the cut CW onto the corresponding axes of the coordinates.

The equalities (22), (23) and (62) (63) define, generally speaking, the different values of the tracing force T for almost all the points of the manifold (43), and that is proved the suitable remark.

V. Case of the absence of the dependence of the moment of the nonconservative forces on the angular velocity

A. Reduced system

Similarly to the choice of the Chaplygin analytical functions, we shall accept the dynamic functions s, x_{3N} and x_{4N} as the following form:

$$s(\alpha) = B\cos\alpha,\ A,B>0,\ v\neq 0,$$

$$x_{3N}\left(\alpha,\beta_1,\beta_2,\frac{\Omega}{v}\right) = x_{3N0}(\alpha,\beta_1) = A\sin\alpha\cos\beta_1, \quad (64)$$

$$x_{4N}\left(\alpha,\beta_1,\beta_2,\frac{\Omega}{v}\right) = x_{4N0}(\alpha,\beta_1) = A\sin\alpha\sin\beta_1,$$

which convinces us that the dependence of the moment of the nonconservative forces on the angular velocity is absent in considered system (and there exist the dependences on the angles α,β_1,β_2 only).

Herewith, the functions $\Lambda_{v,\beta_2},\Pi_{v,\beta_2}$, appearing in the system (51)–(56), have the following forms:

$$\Lambda_{v,\beta_2}\left(\alpha,\beta_1,\frac{\Omega}{v}\right) = A\sin\alpha,\ \Pi_{v,\beta_2}\left(\alpha,\beta_1,\frac{\Omega}{v}\right)\equiv 0. \quad (65)$$

Then the dynamic part of the motion equations (the system (51)–(56)) will have the form as the following analytical system by means of the nonintegrable constraints (20) outside of and only outside of the manifold (43)

$$\dot{\alpha} = -w_3 + \frac{\sigma ABv}{I_1+I_3}\sin\alpha, \quad (66)$$

$$\dot{w_4} = -\frac{ABv^2}{I_1+I_3}\sin(\beta_2+\gamma)\sin\alpha\cos\alpha + w_1 w_2\frac{\cos\alpha}{\sin\alpha}, \quad (67)$$

$$\dot{w_3} = \frac{ABv^2}{I_1+I_3}\cos(\beta_2+\gamma)\sin\alpha\cos\alpha - w_1^2\frac{\cos\alpha}{\sin\alpha}, \quad (68)$$

ISBN: 978-1-61804-225-5

$$\dot{w_2} = -w_1 w_4 \frac{\cos\alpha}{\sin\alpha}, \tag{69}$$

$$\dot{w_1} = w_1 w_3 \frac{\cos\alpha}{\sin\alpha}, \tag{70}$$

$$\dot{\beta_1} = w_1 \frac{\cos\alpha}{\sin\alpha}, \tag{71}$$

If we introduce the dimensionless variables, parameters and differentiability as follows:

$$w_k \mapsto n_0 v w_k,\ k = 1,2,3,4,\ n_0^2 = \frac{AB}{I_1 + I_3},$$
$$b = \sigma n_0,\ \ < \cdot >= n_0 v <'>, \tag{72}$$

we shall reduce the system (66)–(71) to the form

$$\alpha' = -w_3 + b\sin\alpha, \tag{73}$$

$$w_4' = -\sin(\beta_2+\gamma)\sin\alpha\cos\alpha + w_1 w_2 \frac{\cos\alpha}{\sin\alpha}, \tag{74}$$

$$w_3' = \cos(\beta_2+\gamma)\sin\alpha\cos\alpha - w_1^2 \frac{\cos\alpha}{\sin\alpha}, \tag{75}$$

$$w_2' = -w_1 w_4 \frac{\cos\alpha}{\sin\alpha}, \tag{76}$$

$$w_1' = w_1 w_3 \frac{\cos\alpha}{\sin\alpha}, \tag{77}$$

$$\beta_1' = w_1 \frac{\cos\alpha}{\sin\alpha}, \tag{78}$$

As is seen, the independent fifth order system (73)–(77) on its own five-dimensional manifold was formed in the sixth order system (73)–(78) which can be considered on its own six-dimensional manifold

$$T\mathbf{S}^2 \times \mathbf{R}^2 \tag{79}$$

— the direct product of the tangent stratification $T\mathbf{S}^2$ of two-dimensional sphere $\mathbf{S}^2$ on two-dimensional plane.

Furthermore, the independent third order subsystem

$$\alpha' = -w_3 + b\sin\alpha, \tag{80}$$

$$w_3' = \cos(\beta_2+\gamma)\sin\alpha\cos\alpha - w_1^2 \frac{\cos\alpha}{\sin\alpha}, \tag{81}$$

$$w_1' = w_1 w_3 \frac{\cos\alpha}{\sin\alpha}, \tag{82}$$

was formed from the sixth order system (73)–(78), and also (while dependent) second order system

$$w_4' = -\sin(\beta_2+\gamma)\sin\alpha\cos\alpha + w_1 w_2 \frac{\cos\alpha}{\sin\alpha}, \tag{83}$$

$$w_2' = -w_1 w_4 \frac{\cos\alpha}{\sin\alpha}, \tag{84}$$

and the equation

$$\beta_1' = w_1 \frac{\cos\alpha}{\sin\alpha} \tag{85}$$

can be chosen.

In general, for the complete integrability of the system (73)–(78) it is sufficient to know five independent first integrals. However, after the partition of the system on three parts (the system (80)–(82), the system (83), (84) and the equation (85)) for the complete integrability it is sufficient to know two independent first integrals of the system (80)–(82), one — of the system (83), (84) (after the reduction of the latter system to the independent subsystem) and one more first integral which "joining" the equation (85).

Immediately we shall notice that the latter discourses are typical for the choice of the system of discourses **I** (see above). Really, while we "do not notice" the existence of two analytical first integrals (31), (32). Therefore, when we get two independent first integrals of the independent third order system (80)–(82), and also the first integral "joining" the equation (85), we shall have the complete tuple of the independent first integrals of the fourth order system (80)–(82), (85). The obtained assigned complete tuple (three integrals) and together with the analytical first integrals (31), (32) forms the complete tuple of five first integrals of the sixth order system (80)–(85).

Hereafter, in particular, it will is seen that the composition of the analytical first integrals (31), (32) gives the first integral of the (potentially separated) system (83), (84).

B. Complete list of invariant relations

At the beginning we compare the third order system (80)–(82) to the nonautonomous second order system

$$\begin{aligned} \frac{dw_3}{d\alpha} &= \frac{\cos(\beta_2+\gamma)\sin\alpha\cos\alpha - w_1^2\cos\alpha/\sin\alpha}{-w_3 + b\sin\alpha}, \\ \frac{dw_1}{d\alpha} &= \frac{w_1 w_3 \cos\alpha/\sin\alpha}{-w_3 + b\sin\alpha}. \end{aligned} \tag{86}$$

Let rewrite the system (86) on algebraic form using the substitution $\tau = \sin\alpha$

$$\begin{aligned} \frac{dw_3}{d\tau} &= \frac{\cos(\beta_2+\gamma)\tau - w_1^2/\tau}{-w_3 + b\tau}, \\ \frac{dw_1}{d\tau} &= \frac{w_1 w_3/\tau}{-w_3 + b\tau}. \end{aligned} \tag{87}$$

Later on, if we introduce the uniform variables by the formulas

$$w_1 = u_1\tau,\ w_3 = u_2\tau, \tag{88}$$

we shall reduce the system (87) to the following form:

$$\begin{aligned} \tau\frac{du_2}{d\tau} + u_2 &= \frac{\cos(\beta_2+\gamma) - u_1^2}{-u_2 + b}, \\ \tau\frac{du_1}{d\tau} + u_1 &= \frac{u_1 u_2}{-u_2 + b}, \end{aligned} \tag{89}$$

that is equivalent to

$$\begin{aligned} \tau\frac{du_2}{d\tau} &= \frac{\cos(\beta_2+\gamma) - u_1^2 + u_2^2 - bu_2}{-u_2 + b}, \\ \tau\frac{du_1}{d\tau} &= \frac{2u_1 u_2 - bu_1}{-u_2 + b}. \end{aligned} \tag{90}$$

Let compare the second order system (90) to the nonautonomous first order equation

$$\frac{du_2}{du_1} = \frac{\cos(\beta_2+\gamma) - u_1^2 + u_2^2 - bu_2}{2u_1 u_2 - bu_1}, \tag{91}$$

which is reduced uncomplicated to the complete differential:

$$d\left(\frac{u_2^2 + u_1^2 - bu_2 + \cos(\beta_2+\gamma)}{u_1}\right) = 0. \tag{92}$$

ISBN: 978-1-61804-225-5

And so, the equation (91) has the following first integral:

$$\frac{u_2^2+u_1^2-bu_2+\cos(\beta_2+\gamma)}{u_1}=C_1=\text{const}, \tag{93}$$

which in former variables is looked like

$$\frac{w_3^2+w_1^2-bw_3\sin\alpha+\cos(\beta_2+\gamma)\sin^2\alpha}{w_1\sin\alpha}=C_1=\text{const}. \tag{94}$$

Remark 8.1. Let consider the system (80)–(82) with zero mean variable dissipation which becomes the conservative for $b=0$:

$$\begin{aligned}&\alpha'=-w_3,\\ &w_3'=\cos(\beta_2+\gamma)\sin\alpha\cos\alpha-w_1^2\frac{\cos\alpha}{\sin\alpha},\\ &w_1'=w_1w_3\frac{\cos\alpha}{\sin\alpha}.\end{aligned} \tag{95}$$

It has two the analytical first integrals of the forms

$$w_3^2+w_1^2+\cos(\beta_2+\gamma)\sin^2\alpha=C_1^*=\text{const}, \tag{96}$$

$$w_1\sin\alpha=C_2^*=\text{const}. \tag{97}$$

It is obviously that the ratio of two the first integrals (96), (97) is also the first integral of the system (95). But for $b\neq 0$ each of functions

$$w_3^2+w_1^2-bw_3\sin\alpha+\cos(\beta_2+\gamma)\sin^2\alpha \tag{98}$$

and (97) are not the first integrals of the system (80)–(82) separately. However, the ratio of the functions (98), (97) is the first integral of the system (80)–(82) for any b.

Later on, let find the evident form of the additional first integral of the third order system (80)–(82). At the beginning for this we shall transform the invariant relation (93) for $u_1\neq 0$ as follows:

$$\left(u_2-\frac{b}{2}\right)^2+\left(u_1-\frac{C_1}{2}\right)^2=\frac{b^2+C_1^2}{4}-\cos(\beta_2+\gamma). \tag{99}$$

As is seen, the parameters of given invariant relation should satisfy the condition

$$b^2+C_1^2-4\cos(\beta_2+\gamma)\geq 0, \tag{100}$$

and the phase space of the system (80)–(82) is stratified on the family of the surfaces which is assigned by the equality (99).

Thus, by virtue of the relation (93) the first equation of the system (90) has the form

$$\tau\frac{du_2}{d\tau}=\frac{2(\cos(\beta_2+\gamma)-bu_2+u_2^2)-C_1U_1(C_1,u_2)}{-u_2+b}, \tag{101}$$

where

$$U_1(C_1,u_2)=\frac{1}{2}\{C_1\pm\sqrt{C_1^2-4(u_2^2-bu_2+\cos(\beta_2+\gamma))}\}, \tag{102}$$

herewith, the constant of the integration C_1 is chosen from the condition (100).

Therefore, the quadrature for the search of the additional first integral of the system (80)–(82) has the form ($q_1=\cos(\beta_2+\gamma)-bu_2+u_2^2$)

$$\int\frac{d\tau}{\tau}=\int\frac{(b-u_2)du_2}{2q_1-C_1\{C_1\pm\sqrt{C_1^2-4q_1}\}/2}. \tag{103}$$

The left-hand side (accurate to the additive constant), obviously, is equal to

$$\ln|\sin\alpha|. \tag{104}$$

If

$$u_2-\frac{b}{2}=p_1,\ b_1^2=b^2+C_1^2-4\cos(\beta_2+\gamma), \tag{105}$$

then the right-hand side of the equality (103) has the form

$$\begin{aligned}&-\frac{1}{4}\int\frac{d(b_1^2-4p_1^2)}{(b_1^2-4p_1^2)\pm C_1\sqrt{b_1^2-4p_1^2}}-\\ &-b\int\frac{dp_1}{(b_1^2-4p_1^2)\pm C_1\sqrt{b_1^2-4p_1^2}}=\\ &=-\frac{1}{2}\ln\left|\frac{\sqrt{b_1^2-4p_1^2}}{C_1}\pm 1\right|\pm\frac{b}{2}I_1,\end{aligned} \tag{106}$$

where

$$I_1=\int\frac{dp_3}{\sqrt{b_1^2-p_3^2}(p_3\pm C_1)},\ p_3=\sqrt{b_1^2-4p_1^2}. \tag{107}$$

Three cases are possible for the calculation of the integral (107).

I. $b>2$.

$$\begin{aligned}I_1=&-\frac{1}{2\sqrt{b^2-4}}\ln\left|\frac{\sqrt{b^2-4}+\sqrt{b_1^2-p_3^2}}{p_3\pm C_1}\pm\frac{C_1}{\sqrt{b^2-4}}\right|+\\ &+\frac{1}{2\sqrt{b^2-4}}\ln\left|\frac{\sqrt{b^2-4}-\sqrt{b_1^2-p_3^2}}{p_3\pm C_1}\mp\frac{C_1}{\sqrt{b^2-4}}\right|+\text{const}.\end{aligned} \tag{108}$$

II. $b<2$.

$$I_1=\frac{1}{\sqrt{4-b^2}}\arcsin\frac{\pm C_1p_3+b_1^2}{b_1(p_3\pm C_1)}+\text{const}. \tag{109}$$

III. $b=2$.

$$I_1=\mp\frac{\sqrt{b_1^2-p_3^2}}{C_1(p_3\pm C_1)}+\text{const}. \tag{110}$$

When we return to the variable

$$p_1=\frac{w_3}{\sin\alpha}-\frac{b}{2}, \tag{111}$$

we shall have the final form for the value I_1:

I. $b>2$.

$$\begin{aligned}I_1=&-\frac{1}{2\sqrt{b^2-4}}\ln\left|\frac{\sqrt{b^2-4}\pm 2p_1}{\sqrt{b_1^2-4p_1^2}\pm C_1}\pm\frac{C_1}{\sqrt{b^2-4}}\right|+\\ &+\frac{1}{2\sqrt{b^2-4}}\ln\left|\frac{\sqrt{b^2-4}\mp 2p_1}{\sqrt{b_1^2-4p_1^2}\pm C_1}\mp\frac{C_1}{\sqrt{b^2-4}}\right|+\text{const}.\end{aligned} \tag{112}$$

II. $b<2$.

$$I_1=\frac{1}{\sqrt{4-b^2}}\arcsin\frac{\pm C_1\sqrt{b_1^2-4p_1^2}+b_1^2}{b_1(\sqrt{b_1^2-4p_1^2}\pm C_1)}+\text{const}. \tag{113}$$

III. $b=2$.

$$I_1=\mp\frac{2p_1}{C_1(\sqrt{b_1^2-4p_1^2}\pm C_1)}+\text{const}. \tag{114}$$

ISBN: 978-1-61804-225-5

So, the additional first integral was found right before for the third order system (80)–(82) i.e. it was presented the complete tuple of the first integrals which are the transcendental functions of its own phase variables.

Remark 8.2. It is necessary to substitute formally the left-hand side of the first integral (93) instead of C_1 in the expression of the found first integral.

Then the obtained additional first integral has the following structural form (which is similar to the transcendental first integral from the planeparallel dynamics):

$$\ln|\sin\alpha| + G_2\left(\sin\alpha, \frac{w_3}{\sin\alpha}, \frac{w_1}{\sin\alpha}\right) = C_2 = \text{const}. \quad (115)$$

Thus, there are already found two the independent first integrals for the integration of the sixth order system (80)–(85). And now, under the acceptance of the discourses type system **I** (see above, when as we were "do not notice" the existence of two analytical first integrals (31), (32)), and for its complete integrability it is sufficient to find one first integral for (separated potentially) system (83), (84), and also the additional first integral which "connects" the equation (85).

After the change of the variables

$$\begin{aligned} w_* &= w_3\sin(\gamma+\beta_2) + w_4\cos(\gamma+\beta_2),\\ w_{**} &= w_1\sin(\gamma+\beta_2) - w_2\cos(\gamma+\beta_2) \end{aligned} \quad (116)$$

the system (83), (84) can be reduced to the form

$$\begin{aligned} \frac{dw_*}{d\beta_1} &= -w_{**},\\ \frac{dw_{**}}{d\beta_1} &= w_*, \end{aligned} \quad (117)$$

which expects the existence of the analytical first integral:

$$w_*^2 + w_{**}^2 = C_3 = \text{const}. \quad (118)$$

Let ask the question: how is related the obtained right now first integral (118) with the analytical first integrals of the forms (31), (32)?

Really, two discourses types (**I** and **II**, see above) correspond to two following alternatives. For the complete integration of the sixth order system (25)–(30):

1) Either we find five the independent first integrals of the sixth order system (25)–(30);

2) Or we transform the sixth order system (25)–(30) such as there are stand out the independent subsystems else more low order.

So, for instance, since after observation of such coordinates as w_*, w_{**} the stratification of the system vector field is occur such as the independent second order subsystem is formed (117), it needs to find four the independent first integrals instead of five ones (three — for the integration of the fourth order system (80)–(82), (85) and one — for the integration of the separated second order system (117)).

And now, finally, let rewrite the forms of the analytical first integrals (31), (32) in new variables as follows:

$$w_{**}\cos\beta_1 - w_*\sin\beta_1 = W_1'' = \text{const}, \quad (119)$$

$$w_{**}\sin\beta_1 + w_*\cos\beta_1 = W_2'' = \text{const}. \quad (120)$$

Obviously, that the analytical first integrals (119), (120) involve the founded analytical first integral (118) (it is sufficient for this to add the squares of the left-hand side of the equalities (119), (120)).

Later on, finally, for the integration of the fourth order system (80)–(82), (85) two independent the first integrals have already founded. And for the complete its integrability it is sufficient to find one more (additional) the first integral which "joining" the equation (85).

Since

$$\frac{du_1}{d\tau} = \frac{u_1(2u_2-b)}{(b-u_2)\tau}, \ \frac{d\beta_1}{d\tau} = \frac{u_1}{(b-u_2)\tau}, \quad (121)$$

then

$$\frac{du_1}{d\beta_1} = 2u_2 - b. \quad (122)$$

Obviously, for $u_1 \neq 0$ the equality

$$u_2 = \frac{1}{2}\left(b \pm \sqrt{b_1^2 - 4\left(u_1 - \frac{C_1}{2}\right)^2}\right),$$

$$b_1^2 = b^2 + C_1^2 - 4\cos(\beta_2+\gamma), \quad (123)$$

is fulfilled, then the integration of the following quadrature:

$$\beta_1 + \text{const} = \pm\int \frac{du_1}{\sqrt{b_1^2 - 4\left(u_1 - \frac{C_1}{2}\right)^2}} \quad (124)$$

will bring to the invariant relation

$$2(\beta_1 + C_4) = \pm\arcsin\frac{2u_1 - C_1}{\sqrt{b^2 + C_1^2 - 4\cos(\beta_2+\gamma)}}, \quad (125)$$

$$C_4 = \text{const}.$$

In other words, the equation

$$\sin[2(\beta_1 + C_4)] = \pm\frac{2u_1 - C_1}{\sqrt{b^2 + C_1^2 - 4\cos(\beta_2+\gamma)}} \quad (126)$$

is fulfilled, or, under the transition to the old variables

$$\sin[2(\beta_1+C_4)] = \pm\frac{2w_1 - C_1\sin\alpha}{\sqrt{b^2 + C_1^2 - 4\cos(\beta_2+\gamma)}\sin\alpha}. \quad (127)$$

In principle, it makes possible to stop on the latter equality to achieve the additional invariant relation "connecting" the equation (85), if we add to this equality that it is necessary to substitute formally the left-hand side of the first integral (93) instead of C_1 in the latter expression.

But we shall make the certain transformations which reduce to the obtaining of the following evident form of the additional first integral (herewith, the equality (93) is used):

$$\text{tg}^2[2(\beta_1 + C_4)] = \frac{(u_1^2 - u_2^2 + bu_2 - \cos(\beta_2+\gamma))^2}{u_1^2(4u_2^2 - 4bu_2 + b^2)}. \quad (128)$$

Returning to the old coordinates, we shall obtain the additional invariant relation as the form

$$\text{tg}^2[2(\beta_1 + C_4)] =$$

$$= \frac{(w_1^2 - w_3^2 + bw_3\sin\alpha - \cos(\beta_2+\gamma)\sin^2\alpha)^2}{w_1^2(4w_3^2 - 4bw_3\sin\alpha + b^2\sin^2\alpha)}, \quad (129)$$

ISBN: 978-1-61804-225-5

or finally

$$-\beta_1 \pm \frac{1}{2}\text{arctg}\frac{w_1^2 - w_3^2 + bw_3\sin\alpha - \cos(\beta_2+\gamma)\sin^2\alpha}{w_1(2w_3 - b\sin\alpha)} = \tag{130}$$
$$= C_4 = \text{const}.$$

And so, the system of dynamic equations (4)–(7), (10)–(15) under the condition (64) has eight invariant relations in considered case: there exist the analytical nonintegrable constraints (20), the cyclic first integrals (18), (19), the first integral (94) and also there exists the first integral expressed by the relations (108)–(115) which is the transcendental function of its phase variables (in sense of complex analysis also) and expresses in terms of finite combination of the elementary functions, and finally the transcendent first integral (130) ((129)) and analytical first integral (118).

Theorem 8.1. *The system (4)–(7), (10)–(15) under the conditions (20), (64), (19) possesses eight invariant relations (the complete tuple), three of which are the transcendental functions from the complex analysis view of point. Herewith, all the relations express in terms of the finite combination of the elementary functions.*

C. Topological analogies

Let consider the following third order system of the equations:

$$\begin{aligned}&\ddot{\xi} + b_*\dot{\xi}\cos\xi + R_3\sin\xi\cos\xi - \dot{\eta_1}^2\frac{\sin\xi}{\cos\xi} = 0,\\ &\dot{\eta_1} + b_*\eta_1\cos\xi + \dot{\xi}\eta_1\frac{1+\cos^2\xi}{\cos\xi\sin\xi} = 0,\ b_* > 0,\end{aligned} \tag{131}$$

describing the fixed spherical pendulum which is placed in a flow of the filling medium under the absence of the dependence of the moment of the forces on the angular velocity, i.e. the mechanical system in the nonconservative field of the forces. In general, the order of such system should be equal to 4, but the phase variable η_1 is the cyclic, that reduces to the stratification of the phase space and the deflation.

Its phase space is the tangent stratification

$$T\mathbf{S}^2\{\dot{\xi}, \dot{\eta_1}, \xi, \eta_1\} \tag{132}$$

to two-dimensional sphere $\mathbf{S}^2\{\xi, \eta_1\}$, herewith, the equation of the big circles

$$\dot{\eta_1} \equiv 0 \tag{133}$$

assigns the family of the integral manifolds.

It is not difficult to make sure that the system (131) is equivalent to the dynamic system with the zero mean variable dissipation on the tangent stratification (132) to two-dimensional sphere. Moreover, the following theorem is equitable.

Theorem 8.2. *The system (4)–(7), (10)–(15) under the conditions (20), (138), (19) is equivalent to the dynamic system (131).*

Really, it is sufficient to accept $\alpha = \xi,\ \beta_1 = \eta_1,\ b = -b_*,\ R_3 = \cos(\gamma + \beta_2)$.

VI. Case of the dependence of the moment of the nonconservative forces on the angular velocity

A. Introduction on the dependence on the angular velocity

This section is devoted to dynamics of four-dimensional rigid body on the four-dimensional space. But since this section is devoted to the study of the case of the motion under the presence of the dependence of the moment of forces on the angular velocity tensor, we introduce such dependence from more general positions. Additionally, the given point of view helps us to introduce this dependence and for many-dimensional ones.

Let $x = (x_{1N}, x_{2N}, x_{3N}, x_{4N})$ are the coordinates of the point N of the action of the nonconservative force (of a medium interaction) to two-dimensional disk, $Q = (Q_1, Q_2, Q_3, Q_4)$ are the components not depending on the angular velocity tensor. We shall introduce the dependence of the functions $(x_{1N}, x_{2N}, x_{3N}, x_{4N})$ on the angular velocity tensor by the linear form only since given introduction itself is not obvious a priori.

And so, let accept the following dependence:

$$x = Q + R, \tag{134}$$

where $R = (R_1, R_2, R_3, R_4)$ is the vector-function containing the components of angular velocity tensor. Herewith, the dependence of the function R on the angular velocity tensor is gyroscopic:

$$R = \begin{pmatrix} R_1 \\ R_2 \\ R_3 \\ R_4 \end{pmatrix} =$$
$$= -\frac{1}{v}\begin{pmatrix} 0 & -\omega_6 & \omega_5 & -\omega_3 \\ \omega_6 & 0 & -\omega_4 & \omega_2 \\ -\omega_5 & \omega_4 & 0 & -\omega_1 \\ \omega_3 & -\omega_2 & \omega_1 & 0 \end{pmatrix}\begin{pmatrix} h_1 \\ h_2 \\ h_3 \\ h_4 \end{pmatrix}. \tag{135}$$

Here (h_1, h_2, h_3, h_4) are the certain positive parameters.

And now, with the reference to our problem, since $x_{1N} \equiv x_{2N} \equiv 0$, then

$$x_{3N} = Q_3 - \frac{h_1}{v}(\omega_4 - \omega_5),\ x_{4N} = Q_4 - \frac{h_1}{v}(\omega_3 - \omega_2). \tag{136}$$

B. Reduced system

Similarly to the choice of the Chaplygin analytical functions

$$Q_3 = A\sin\alpha\cos\beta_1,\ Q_4 = A\sin\alpha\sin\beta_1,\ A > 0, \tag{137}$$

we shall accept the dynamic functions s, x_{3N} and x_{4N} as the following form:

$$\begin{aligned}&s(\alpha) = B\cos\alpha,\ B > 0,\ h = h_1 > 0,\ v \neq 0,\ h = h_2 > 0,\\ &x_{3N}\left(\alpha, \beta_1, \beta_2, \frac{\Omega}{v}\right) = A\sin\alpha\cos\beta_1 - \frac{h}{v}(\omega_4 - \omega_5),\\ &x_{4N}\left(\alpha, \beta_1, \beta_2, \frac{\Omega}{v}\right) = A\sin\alpha\sin\beta_1 - \frac{h}{v}(\omega_3 - \omega_2),\end{aligned} \tag{138}$$

which convinces us that the additional dependence of the damping moment of the nonconservative forces (and the dispersing one in some domains of the phase space) is also present in considered system (i.e. the dependence of the moment on the angular velocity tensor is present). Moreover, $h_1 = h_2,\ h_3 = h_4$ by virtue of the dynamical symmetry (17) of the body.

Later on, let accept the system of discourses **I** which takes into account and the system of discourses **II** (see above).

We shall arouse to introduce the following variables in this section:

$$\begin{aligned} u_1 &= \omega_2 - \omega_3, \\ u_2 &= \omega_4 - \omega_5, \\ u_3 &= \omega_2 \cos\beta_2 - \omega_3 \sin\beta_2, \\ u_4 &= \omega_4 \cos\beta_2 - \omega_5 \sin\beta_2. \end{aligned} \tag{139}$$

Really, the assigned coordinates are defined correctly for

$$\cos\beta_2 \neq \sin\beta_2, \tag{140}$$

and Jacobian of the mapping is equal to

$$-\frac{1}{(\cos\beta_2 - \sin\beta_2)^2}, \tag{141}$$

herewith, the inverse transformation is assigned as follows:

$$\begin{aligned} \omega_2 &= \frac{u_3 - u_1 \sin\beta_2}{\cos\beta_2 - \sin\beta_2}, \\ \omega_3 &= \frac{u_3 - u_1 \cos\beta_2}{\cos\beta_2 - \sin\beta_2}, \\ \omega_4 &= \frac{u_4 - u_2 \sin\beta_2}{\cos\beta_2 - \sin\beta_2}, \\ \omega_5 &= \frac{u_4 - u_2 \cos\beta_2}{\cos\beta_2 - \sin\beta_2}, \end{aligned} \tag{142}$$

and the particular case

$$\cos\beta_2 = \sin\beta_2, \tag{143}$$

which simplifies the dynamic equations can be considered separately.

Then the equations (33)–(38) under the condition (138) outside of and only outside of the manifold

$$O_3 = \left\{(\alpha, \beta_1, \omega_2, \omega_3, \omega_4, \omega_5) \in \mathbf{R}^6 :\ \alpha = \frac{\pi}{2} + \pi k,\ k \in \mathbf{Z}\right\} \tag{144}$$

transform to the following equations:

$$\dot\alpha - u_3 \sin\beta_1 + u_4 \cos\beta_1 - $$
$$-\sigma n_0^2 v \sin\alpha + \sigma H_1'[-u_1 \sin\beta_1 + u_2 \cos\beta_1] = 0, \tag{145}$$

$$\dot\beta_1 \sin\alpha - \cos\alpha[u_3 \cos\beta_1 + u_4 \sin\beta_1] -$$
$$-\sigma H_1' \cos\alpha[u_1 \cos\beta_1 + u_2 \sin\beta_1] = 0, \tag{146}$$

$$\dot u_1 = -n_0^2 v^2 r_1 \sin\alpha\cos\alpha\sin\beta_1 - \frac{Bvh}{I_1 + I_3} r_1 u_1 \cos\alpha, \tag{147}$$

$$\dot u_2 = n_0^2 v^2 r_1 \sin\alpha\cos\alpha\cos\beta_1 - \frac{Bvh}{I_1 + I_3} r_1 u_2 \cos\alpha, \tag{148}$$

$$\dot u_3 = -n_0^2 v^2 \sin\alpha\cos\alpha\sin\beta_1\cos(\gamma + \beta_2) -$$
$$-\frac{Bvh}{I_1 + I_3} u_1 \cos\alpha\cos(\gamma + \beta_2), \tag{149}$$

$$\dot u_4 = n_0^2 v^2 \sin\alpha\cos\alpha\cos\beta_1\cos(\gamma + \beta_2) -$$
$$-\frac{Bvh}{I_1 + I_3} u_2 \cos\alpha\cos(\gamma + \beta_2), \tag{150}$$

where

$$r_1 = \cos\gamma - \sin\gamma \neq 0,\ n_0^2 = \frac{AB}{I_1 + I_3},\ H_1' = \frac{Bh}{I_1 + I_3}. \tag{151}$$

We note that the particular case

$$\cos\gamma = \sin\gamma\ (r_1 = 0), \tag{152}$$

which simplifies the dynamic equations can also be considered separately (similarly the case (143)).

Let introduce the following phase variables by the formulas:

$$\begin{aligned} v_1 &= -u_1 \sin\beta_1 + u_2 \cos\beta_1, \\ v_2 &= u_1 \cos\beta_1 + u_2 \sin\beta_1, \\ v_3 &= -u_3 \sin\beta_1 + u_4 \cos\beta_1, \\ v_4 &= u_3 \cos\beta_1 + u_4 \sin\beta_1. \end{aligned} \tag{153}$$

then outside of and only outside of the manifold

$$O_4 = \left\{(\alpha, \beta_1, u_1, u_2, u_3, u_4) \in \mathbf{R}^6 :\ \beta_1 = \pi k,\ k \in \mathbf{Z}\right\} \tag{154}$$

the system (145)–(150) has the form

$$\dot\alpha = -v_3 - bH_1 v_1 + b\sin\alpha, \tag{155}$$

$$\dot\beta_1 = [v_4 + bH_1 v_2]\frac{\cos\alpha}{\sin\alpha}, \tag{156}$$

$$\dot v_1 = n_0^2 v^2 r_1 \sin\alpha\cos\alpha -$$
$$-H_1' v r_1 v_1 \cos\alpha - v_2 \cdot [v_4 + bH_1 v_2]\frac{\cos\alpha}{\sin\alpha}, \tag{157}$$

$$\dot v_2 = -H_1' v r_1 v_2 \cos\alpha + v_1 \cdot [v_4 + bH_1 v_2]\frac{\cos\alpha}{\sin\alpha}, \tag{158}$$

$$\dot v_3 = n_0^2 v^2 \sin\alpha\cos\alpha\cos(\gamma + \beta_2) -$$
$$-H_1' v v_1 \cos\alpha\cos(\gamma + \beta_2) - v_4 \cdot [v_4 + bH_1 v_2]\frac{\cos\alpha}{\sin\alpha}, \tag{159}$$

$$\dot v_4 = -H_1' v v_2 \cos\alpha\cos(\gamma + \beta_2) +$$
$$+v_3 \cdot [v_4 + bH_1 v_2]\frac{\cos\alpha}{\sin\alpha}, \tag{160}$$

where we introduce as before the dimensionless parameters as follows:

$$n_0^2 = \frac{AB}{I_1 + I_3},\ b = \sigma n_0,\ [b] = 1,$$
$$H_1 = \frac{H_1'}{n_0} = \frac{Bh}{(I_1 + I_3)n_0},\ [H_1] = 1. \tag{161}$$

Let also introduce one more auxiliary change of the part of the phase variables, as follows:

$$s_1 = v_3 + bH_1 v_1,\ s_2 = v_4 + bH_1 v_2. \tag{162}$$

Then the investigated system (155)–(160) after the introduction of dimensionless variables and differentiability

$$v_k \mapsto n_0 v v_k,\ k = 1, \ldots, 4,\ \ < \cdot >= n_0 v\ <'>, \tag{163}$$

will rewrite as the form

$$\alpha' = -s_1 + b\sin\alpha, \tag{164}$$

ISBN: 978-1-61804-225-5

$$\beta_1' = s_2\frac{\cos\alpha}{\sin\alpha}, \tag{165}$$

$$s_1' = R_1\sin\alpha\cos\alpha - s_2^2\frac{\cos\alpha}{\sin\alpha} - R_1H_1v_1\cos\alpha, \tag{166}$$

$$s_2' = s_1s_2\frac{\cos\alpha}{\sin\alpha} - R_1H_1v_2\cos\alpha, \tag{167}$$

$$v_1' = R_2\sin\alpha\cos\alpha - s_2v_2\frac{\cos\alpha}{\sin\alpha} - H_1R_2v_1\cos\alpha, \tag{168}$$

$$v_2' = s_2v_1\frac{\cos\alpha}{\sin\alpha} - H_1R_2v_2\cos\alpha, \tag{169}$$

where

$$R_1 = bH_1(\cos\gamma - \sin\gamma) + \cos(\gamma+\beta_2),$$
$$R_2 = r_1 = \cos\gamma - \sin\gamma. \tag{170}$$

Obviously, that for $H_1 = 0$ formally the independent fourth order subsystem (164)–(167) stands out in the system (164)–(169) on the tangent stratification $T\mathbf{S}^2$ to two-dimensional sphere $\mathbf{S}^2\{0 < \alpha < \pi,\ 0 \le \beta_1 < 2\pi\}$, in which, in turn, it can be stand out the independent third order subsystem (164), (166), (167) on its own three-dimensional phase manifold.

But, in principle, it is just understood, since for $H_1 = 0$ we are under the conditions of absence of moment of the forces on the angular velocity tensor (see previous section and the system (80)–(82), (85)). The latter fact allows to integrate completely similarly the considered fourth order system (164)–(167), but signifies, and the considered sixth order system (164)–(169), since there exist two independent analytical first integrals (31), (32) or (119), (120) (see above on two systems of discourses **I** and **II**).

And in the given case it is great for us that $H_1 \neq 0$. Therefore, we transform the having analytical first integrals (31), (32) or (119), (120). We have the evident type of its in the different variables:

$$\frac{u_3 - u_1\sin\beta_2}{\cos\beta - 2 - \sin\beta_2}\sin\gamma - \frac{u_3 - u_1\cos\beta_2}{\cos\beta - 2 - \sin\beta_2}\cos\gamma = \\ = W_1' = \text{const}, \tag{171}$$

$$\frac{u_4 - u_2\sin\beta_2}{\cos\beta - 2 - \sin\beta_2}\sin\gamma - \frac{u_4 - u_2\cos\beta_2}{\cos\beta - 2 - \sin\beta_2}\cos\gamma = \\ = W_2' = \text{const}. \tag{172}$$

If we consider the case (20) (i.e., in particular, when the value β_2 is the identical constant along the phase trajectories), then the following analytical functions are constant on the phase trajectories of the considered system:

$$u_3(\sin\gamma - \cos\gamma) + u_1\cos(\gamma+\beta_2) = W_1^0 = \text{const}, \tag{173}$$

$$u_4(\sin\gamma - \cos\gamma) + u_2\cos(\gamma+\beta_2) = W_2^0 = \text{const}. \tag{174}$$

In another variables the latter two invariant relations have the forms

$$(v_2\cos\beta_1 - v_1\sin\beta_1)\cos(\gamma+\beta_2) + \\ +(v_4\cos\beta_1 - v_3\sin\beta_1)(\sin\gamma - \cos\gamma) = W_1^0 = \text{const}, \tag{175}$$

$$(v_2\sin\beta_1 + v_1\cos\beta_1)\cos(\gamma+\beta_2) + \\ +(v_4\sin\beta_1 + v_3\cos\beta_1)(\sin\gamma - \cos\gamma) = W_2^0 = \text{const}, \tag{176}$$

or

$$R_1v_2\cos\beta_1 - R_1v_1\sin\beta_1 + \\ +R_2[s_1\sin\beta_1 - s_2\cos\beta_1] = W_1^0 = \text{const}, \tag{177}$$

$$R_1v_2\sin\beta_1 + R_1v_1\cos\beta_1 - \\ -R_2[s_1\cos\beta_1 + s_2\sin\beta_1] = W_2^0 = \text{const}, \tag{178}$$

where

$$R_1 = \cos(\gamma+\beta_2) + bH_1(\cos\gamma - \sin\gamma),$$
$$R_2 = \cos\gamma - \sin\gamma \tag{179}$$

as before.

Later on, let express from the relations (177), (178) the values v_1, v_2. We have:

$$v_2R_1 = R_2s_2 + \psi_1(\beta_1, W_1^0, W_2^0), \tag{180}$$

$$v_1R_1 = R_2s_1 + \psi_2(\beta_1, W_1^0, W_2^0), \tag{181}$$

where

$$\psi_1(\beta_1, W_1^0, W_2^0) = W_1^0\cos\beta_1 + W_2^0\sin\beta_1,$$
$$\psi_2(\beta_1, W_1^0, W_2^0) = W_2^0\cos\beta_1 - W_1^0\sin\beta_1. \tag{182}$$

Then the system (164)–(167) has the form of the independent fourth order system:

$$\alpha' = -s_1 + b\sin\alpha, \tag{183}$$

$$s_1' = R_1\sin\alpha\cos\alpha - s_2^2\frac{\cos\alpha}{\sin\alpha} - \\ -R_2H_1s_1\cos\alpha - H_1\psi_2(\beta_1, W_1^0, W_2^0)\cos\alpha, \tag{184}$$

$$s_2' = s_1s_2\frac{\cos\alpha}{\sin\alpha} - \\ -R_2H_1s_2\cos\alpha - H_1\psi_1(\beta_1, W_1^0, W_2^0)\cos\alpha, \tag{185}$$

$$\beta_1' = s_2\frac{\cos\alpha}{\sin\alpha}. \tag{186}$$

The system (183)–(186) can be considered as the system (164)–(167) which is reduced to the levels (W_1^0, W_2^0) of the analytical first integrals (177), (178).

Obviously, that

$$\psi_1(\beta_1, 0, 0) \equiv \psi_2(\beta_1, 0, 0) \equiv 0. \tag{187}$$

Therefore, we shall consider the system (183)–(186) on the zero levels of the analytical first integrals (177), (178):

$$W_1^0 = W_2^0 = 0, \tag{188}$$

which has the form

$$\alpha' = -s_1 + b\sin\alpha, \tag{189}$$

$$s_1' = R_1\sin\alpha\cos\alpha - s_2^2\frac{\cos\alpha}{\sin\alpha} - R_2H_1s_1\cos\alpha, \tag{190}$$

$$s_2' = s_1s_2\frac{\cos\alpha}{\sin\alpha} - R_2H_1s_2\cos\alpha, \tag{191}$$

$$\beta_1' = s_2\frac{\cos\alpha}{\sin\alpha}. \tag{192}$$

The given system can be considered on the tangent stratification $T\mathbf{S}^2$ to two-dimensional sphere $\mathbf{S}^2\{0 < \alpha < \pi,\ 0 \le \beta_1 < 2\pi\}$, in which, in turn, it can be stand out the independent third

order subsystem (189)–(191) on its own three-dimensional phase manifold.

And so, for the integration of the sixth order system at the beginning we used the system of discourses **I** (see above), when we did not yet take into account the existence of two independent analytical first integrals of the forms (31), (32). In consequence we have limited (reduced) the considered sixth order system on the levels (in consequence zero) of the assigned first integrals, i.e. the system of discourses **II** was used (see above).

C. Complete list of invariant relations

At the beginning we compare the third order system (189)–(191) to the nonautonomous second order system

$$\begin{aligned}\frac{ds_1}{d\alpha}&=\frac{R_1\sin\alpha\cos\alpha-s_2^2\cos\alpha/\sin\alpha-R_2H_1s_1\cos\alpha}{-s_1+b\sin\alpha},\\ \frac{ds_2}{d\alpha}&=\frac{s_1s_2\cos\alpha/\sin\alpha-R_2H_1s_2\cos\alpha}{-s_1+b\sin\alpha}.\end{aligned}\tag{193}$$

Let rewrite the system (193) on algebraic form using the substitution $\tau=\sin\alpha$

$$\begin{aligned}\frac{ds_1}{d\tau}&=\frac{R_1\tau-s_2^2/\tau-R_2H_1s_1}{-s_1+b\tau},\\ \frac{ds_2}{d\tau}&=\frac{s_1s_2/\tau-R_2H_1s_2}{-s_1+b\tau}.\end{aligned}\tag{194}$$

Later on, if we introduce the uniform variables by the formulas

$$s_1=t_1\tau,\ s_2=t_2\tau,\tag{195}$$

we shall reduce the system (194) to the following form:

$$\begin{aligned}\tau\frac{dt_1}{d\tau}+t_1&=\frac{R_1-t_2^2-R_2H_1t_1}{-t_1+b},\\ \tau\frac{dt_2}{d\tau}+t_2&=\frac{t_1t_2-R_2H_1t_2}{-t_1+b},\end{aligned}\tag{196}$$

that is equivalent to

$$\begin{aligned}\tau\frac{dt_1}{d\tau}&=\frac{t_1^2-t_2^2-(b+R_2H_1)t_1+R_1}{-t_1+b},\\ \tau\frac{dt_2}{d\tau}&=\frac{2t_1t_2-(b+R_2H_1)t_2}{-t_1+b}.\end{aligned}\tag{197}$$

Let compare the second order system (197) to the nonautonomous first order equation

$$\frac{dt_1}{dt_2}=\frac{t_1^2-t_2^2-(b+R_2H_1)t_1+R_1}{2t_1t_2-(b+R_2H_1)t_2},\tag{198}$$

which is reduced uncomplicated to the complete differential:

$$d\left(\frac{t_1^2+t_2^2-(b+R_2H_1)t_1+R_1}{t_2}\right)=0.\tag{199}$$

And so, the equation (198) has the following first integral:

$$\frac{t_1^2+t_2^2-(b+R_2H_1)t_1+R_1}{t_2}=C_1=\text{const},\tag{200}$$

which in former variables is looked like

$$\frac{s_1^2+s_2^2-(b+R_2H_1)s_1\sin\alpha+R_1\sin^2\alpha}{s_2\sin\alpha}=C_1=\text{const}.\tag{201}$$

Remark 8.3. Let consider the system (189)–(191) with zero mean variable dissipation which becomes the conservative for $b=R_2H_1$:

$$\begin{aligned}\alpha'&=-s_1+b\sin\alpha,\\ s_1'&=R_1\sin\alpha\cos\alpha-s_2^2\frac{\cos\alpha}{\sin\alpha}-bs_1\cos\alpha,\\ s_2'&=s_1s_2\frac{\cos\alpha}{\sin\alpha}-bs_2\cos\alpha.\end{aligned}\tag{202}$$

It has two the analytical first integrals of the forms

$$s_1^2+s_2^2-2bs_1\sin\alpha+R_1\sin^2\alpha=C_1^*=\text{const},\tag{203}$$

$$s_2\sin\alpha=C_2^*=\text{const}.\tag{204}$$

It is obviously that the ratio of two the first integrals (203), (204) is also the first integral of the system (202). But for $b\neq R_2H_1$ each of functions

$$s_1^2+s_2^2-(b+R_2H_1)s_1\sin\alpha+R_1\sin^2\alpha\tag{205}$$

and (204) are not the first integrals of the system (189)–(191) separately. However, the ratio of the functions (205), (204) is the first integral of the system (189)–(191) for any b, R_2H_1.

Later on, let find the evident form of the additional first integral of the third order system (189)–(191). At the beginning for this we shall transform the invariant relation (200) for $u_1\neq 0$ as follows:

$$\begin{aligned}&\left(t_1-\frac{b+R_2H_1}{2}\right)^2+\left(t_2-\frac{C_1}{2}\right)^2=\\ &=\frac{(b+R_2H_1)^2+C_1^2-4R_1}{4}.\end{aligned}\tag{206}$$

As is seen, the parameters of given invariant relation should satisfy the condition

$$(b+R_2H_1)^2+C_1^2-4R_1\geq 0,\tag{207}$$

and the phase space of the system (189)–(191) is stratified on the family of the surfaces which is assigned by the equality (206).

Thus, by virtue of the relation (200) the first equation of the system (197) has the form

$$\tau\frac{dt_1}{d\tau}=\frac{2t_1^2-2(b+R_2H_1)t_1+2R_1-C_1U_1(C_1,t_1)}{b-t_1},\tag{208}$$

where

$$U_1(C_1,t_1)=\frac{1}{2}\{C_1\pm U_2(C_1,t_1)\},\tag{209}$$

$$U_2(C_1,t_1)=\sqrt{C_1^2-4(R_1-(b+R_2H_1)t_1+t_1^2)},$$

herewith, the constant of the integration C_1 is chosen from the condition (207).

Therefore, the quadrature for the search of the additional first integral of the system (189)–(191) has the form

$$\begin{aligned}&\int\frac{d\tau}{\tau}=\\ &=\int\frac{(b-t_1)dt_1}{2(R_1-(b+R_2H_1)t_1+t_1^2)-C_1\{C_1\pm U_2(C_1,t_1)\}/2}.\end{aligned}\tag{210}$$

The left-hand side (accurate to the additive constant), obviously, is equal to

$$\ln|\sin\alpha|. \tag{211}$$

If

$$t_1-\frac{b+R_2H_1}{2}=w_1,\ b_1^2=(b+R_2H_1)^2+C_1^2-4R_1, \tag{212}$$

then the right-hand side of the equality (210) has the form

$$-\frac{1}{4}\int\frac{d(b_1^2-4w_1^2)}{(b_1^2-4w_1^2)\pm C_1\sqrt{b_1^2-4w_1^2}}-$$
$$-(b+R_2H_1)\int\frac{dw_1}{(b_1^2-4w_1^2)\pm C_1\sqrt{b_1^2-4w_1^2}}=$$
$$=-\frac{1}{2}\ln\left|\frac{\sqrt{b_1^2-4w_1^2}}{C_1}\pm 1\right|\pm\frac{b+R_2H_1}{2}I_1, \tag{213}$$

where

$$I_1=\int\frac{dw_3}{\sqrt{b_1^2-w_3^2}(w_3\pm C_1)},\ w_3=\sqrt{b_1^2-4w_1^2}. \tag{214}$$

Three cases are possible for the calculation of the integral (214).

I. $(b+R_2H_1)^2-4R_1>0$.

$$I_1=-\frac{1}{2W_1}\times$$
$$\times\ln\left|\frac{W_1+\sqrt{b_1^2-w_3^2}}{w_3\pm C_1}\pm\frac{C_1}{W_1}\right|+$$
$$+\frac{1}{2W_1}\ln\left|\frac{W_1-\sqrt{b_1^2-w_3^2}}{w_3\pm C_1}\mp\frac{C_1}{W_1}\right|+ \tag{215}$$
$$+\text{const},$$
$$W_1=\sqrt{(b+R_2H_1)^2-4R_1}.$$

II. $(b+R_2H_1)^2-4R_1<0$.

$$I_1=\frac{1}{\sqrt{4R_1-(b+R_2H_1)^2}}\arcsin\frac{\pm C_1w_3+b_1^2}{b_1(w_3\pm C_1)}+\text{const}. \tag{216}$$

III. $(b+R_2H_1)^2-4R_1=0$.

$$I_1=\mp\frac{\sqrt{b_1^2-w_3^2}}{C_1(w_3\pm C_1)}+\text{const}. \tag{217}$$

When we return to the variable

$$w_1=\frac{s_1}{\sin\alpha}-\frac{b+R_2H_1}{2}, \tag{218}$$

we shall have the final form for the value I_1:

I. $(b+R_2H_1)^2-4R_1>0$.

$$I_1=$$
$$=-\frac{1}{2W_1}\ln\left|\frac{W_1\pm 2w_1}{\sqrt{b_1^2-4w_1^2}\pm C_1}\pm\frac{C_1}{W_1}\right|+$$
$$+\frac{1}{2W_1}\ln\left|\frac{W_1\mp 2w_1}{\sqrt{b_1^2-4w_1^2}\pm C_1}\mp\frac{C_1}{W_1}\right|+ \tag{219}$$
$$+\text{const}.$$

II. $(b+R_2H_1)^2-4R_1<0$.

$$I_1=\frac{1}{\sqrt{4R_1-(b+R_2H_1)^2}}\times$$
$$\times\arcsin\frac{\pm C_1\sqrt{b_1^2-4w_1^2}+b_1^2}{b_1(\sqrt{b_1^2-4w_1^2}\pm C_1)}+\text{const}. \tag{220}$$

III. $(b+R_2H_1)^2-4R_1=0$.

$$I_1=\mp\frac{2w_1}{C_1(\sqrt{b_1^2-4w_1^2}\pm C_1)}+\text{const}. \tag{221}$$

So, the additional first integral was found right before for the third order system (189)–(191), i.e. it was presented the complete tuple of the first integrals which are the transcendental functions of its own phase variables.

Remark 8.4. It is necessary to substitute formally the left-hand side of the first integral (200) instead of C_1 in the expression of the found first integral.

Then the obtained additional first integral has the following structural form (which is similar to the transcendental first integral from the planeparallel dynamics):

$$\ln|\sin\alpha|+G_2\left(\sin\alpha,\frac{s_1}{\sin\alpha},\frac{s_2}{\sin\alpha}\right)=C_2=\text{const}. \tag{222}$$

Thus, there are already found two the independent first integrals for the integration of the fourth order system (189)–(192). And for the complete its integrability, as specified above, it is sufficient to find the additional first integral which "connects" the equation (192).

Since

$$\frac{dt_2}{d\tau}=\frac{2t_1t_2-(b+R_2H_1)t_2}{(b-t_1)\tau},\ \frac{d\beta_1}{d\tau}=\frac{t_2}{(b-t_1)\tau}, \tag{223}$$

then

$$\frac{dt_2}{d\beta_1}=2t_1-(b+R_2H_1). \tag{224}$$

It is obvious that for $t_2\neq 0$ the following equality is fulfilled

$$t_1=\frac{1}{2}\left((b+R_2H_1)\pm\sqrt{b_1^2-(2t_2-C_1)^2}\right), \tag{225}$$
$$b_1^2=(b+R_2H_1)^2+C_1^2-4R_1,$$

then the integration of the following quadrature:

$$\beta_1+\text{const}=\pm\int\frac{dt_2}{\sqrt{b_1^2-(2t_2-C_1)^2}} \tag{226}$$

will bring to the invariant relation

$$2(\beta_1+C_3)=$$
$$=\pm\arcsin\frac{2t_1-C_1}{\sqrt{(b+R_2H_1)^2+C_1^2-4R_1}},\ C_3=\text{const}. \tag{227}$$

In other words, the equality

$$\sin[2(\beta_1+C_3)]=\pm\frac{2t_2-C_1}{\sqrt{(b+R_2H_1)^2+C_1^2-4R_1}} \tag{228}$$

is fulfilled and under the transition to the old variables

$$\sin[2(\beta_1+C_3)]=\pm\frac{2s_2-C_1\sin\alpha}{\sqrt{(b+R_2H_1)^2+C_1^2-4R_1}\sin\alpha}. \tag{229}$$

In principle, it makes possible to stop on the latter equality to achieve the additional invariant relation "connecting" the equation (192), if we add to this equality that it is necessary to substitute formally the left-hand side of the first integral (200) instead of C_1 in the latter expression.

But we shall make the certain transformations which reduce to the obtaining of the following evident form of the additional first integral (herewith, the equality (200) is used):

$$\mathrm{tg}^2[2(\beta_1+C_3)]= \\ =\frac{(t_2^2-t_1^2+(b+R_2H_1)t_1-R_1)^2}{t_2^2(2t_1-(b+R_2H_1))^2}. \qquad (230)$$

Returning to the old coordinates, we shall obtain the additional invariant relation as the form

$$\mathrm{tg}^2[2(\beta_1+C_3)]= \\ =\frac{(s_2^2-s_1^2+(b+R_2H_1)s_1\sin\alpha-R_1\sin^2\alpha)^2}{s_2^2(2s_1-(b+R_2H_1)\sin\alpha)^2}, \qquad (231)$$

or finally

$$-\beta_1\pm\frac{1}{2}\times \\ \times\mathrm{arctg}\frac{s_2^2-s_1^2+(b+R_2H_1)s_1\sin\alpha-R_1\sin^2\alpha}{s_2(2s_1-(b+R_2H_1)\sin\alpha)}= \qquad (232) \\ =C_3=\mathrm{const}.$$

And so, the system of dynamic equations (4)–(7), (10)–(15) under the condition (138) has nine invariant relations in considered case: there exist the analytical nonintegrable constraints (20), the cyclic first integrals (18), (19), the analytical first integrals (31), (32), the first integral (201) and also there exists the first integral expressed by the relations (215)–(222) which is the transcendental function of its phase variables (in sense of complex analysis also) and expresses in terms of finite combination of the elementary functions, and finally the transcendent first integral (232).

Theorem 8.3. *The system (4)–(7), (10)–(15) under the conditions (20), (138), (19), (188) possesses nine invariant relations (the complete tuple), three of which are the transcendental functions from the complex analysis view of point. Herewith, all the relations express in terms of the finite combination of the elementary functions.*

We also note that in the similar theorem 8.1 of this section the question is on the complete tuple of the first integrals which consisting on eight the first integrals, although there are exist all nine the first integrals. But at proof of theorem 8.1 the system of discourses **I** is used (se above) which implies the introduction of such phase coordinates (in particular, $w_k,\ k=1,\ldots,4$), in which the system vector field allows the additional stratifications. Herewith, the analytical first integrals (31), (32) do not use directly, that is admit to dispense by the less quantity of the first integrals.

And at proof of the theorem 8.3 the system of discourses **II** is used (see above) which implies the reduction of investigated system on (zero) levels of the analytical first integrals (31), (32). The latter fact takes into account in principal the complete tuple of the having first integrals.

D. Topological analogies

Let consider the following third order system of the equations:

$$\ddot{\xi}+(b_*-H_1^*)\dot{\xi}\cos\xi+R_3\sin\xi\cos\xi-\dot{\eta_1}^2\frac{\sin\xi}{\cos\xi}+ \\ +H_1^{**}[W_1^0\sin\eta_1-W_2^0\cos\eta_1]=0, \\ \ddot{\eta_1}+(b_*-H_1^*)\dot{\eta_1}\cos\xi+\dot{\xi}\dot{\eta_1}\frac{1+\cos^2\xi}{\cos\xi\sin\xi}+ \\ +H_1^{**}[W_1^0\cos\eta_1+W_2^0\sin\eta_1]=0,\ b_*>0,\ H_1^{**}>0, \qquad (233)$$

describing the fixed spherical pendulum which is placed in a flow of the filling medium under the presence of the dependence of the moment of the forces on the angular velocity, i.e. the mechanical system in the nonconservative field of the forces. Unlike previous activities [1], [5], [6], the order of such system is equal to 4 (but not 3) since the phase variable η_1 is not the cyclic, that does not reduce to the stratification of the phase space and the deflation.

Its phase space is the tangent stratification

$$T\mathbf{S}^2\{\dot{\xi},\dot{\eta_1},\xi,\eta_1\} \qquad (234)$$

to two-dimensional sphere $\mathbf{S}^2\{\xi,\eta_1\}$, herewith, the equation of the big circles

$$\dot{\eta_1}\equiv 0 \qquad (235)$$

assigns the family of the integral manifolds for $W_1^0=W_2^0=0$ only.

It is not difficult to make sure that the system (233) is equivalent to the dynamic system with the (zero mean) variable dissipation on the tangent stratification (234) to two-dimensional sphere. Moreover, the following theorem is equitable.

Theorem 8.4. *The system (4)–(7), (10)–(15) under the conditions (20), (138), (19) is equivalent to the dynamic system (233).*

Really, it is sufficient to accept $\alpha=\xi,\ \beta_1=\eta_1,\ b=-b_*,\ H_1=H_1^{**},\ R_2H_1=-H_1^*,\ R_1-bR_2H_1=R_3$.

VII. Conclusion

In the previous studies of the author, the problems on the motion of the four-dimensional solid were already considered in a nonconservative force field in the presence of the following force. This study opens a new cycle of works on integration of a multidimensional solid in the nonconservative field because previously, as was already specified, we considered only such motions of a solid when the field of external forces was the potential.

Acknowledgment

This work was supported by the Russian Foundation for Basic Research, project no. 12-01-00020-a.

REFERENCES

[1] M. V. Shamolin, *Methods of analysis of dynamical systems with various disssipation in rigid body dynamics*, Moscow, Russian Federation: Ekzamen, 2007.

[2] M. V. Shamolin, *Some questions of the qualitative theory of ordinary differential equations and dynamics of a rigid body interacting with a medium*, Journal of Mathematical Sciences, Vol. 110, No. 2, 2002, p. 2526–2555.

[3] M. V. Shamolin, *Foundations of differential and topological diagnostics*, Journal of Mathematical Sciences, Vol. 114, No. 1, 2003, p. 976–1024.

[4] M. V. Shamolin, *New integrable cases and families of portraits in the plane and spatial dynamics of a rigid body interacting with a medium*, Journal of Mathematical Sciences, Vol. 114, No. 1, 2003, p. 919–975.

[5] M. V. Shamolin, *Classes of variable dissipation systems with nonzero mean in the dynamics of a rigid body*, Journal of Mathematical Sciences, Vol. 122, No. 1, 2004, p. 2841–2915.

[6] M. V. Shamolin, *Structural stable vector fields in rigid body dynamics*, Proc. of 8th Conf. on Dynamical Systems (Theory and Applications) (DSTA 2005), Lodz, Poland, Dec. 12–15, 2005; Tech. Univ. Lodz, 2005, Vol. 1, p. 429–436.

[7] M. V. Shamolin, *The cases of integrability in terms of transcendental functions in dynamics of a rigid body interacting with a medium*, Proc. of 9th Conf. on Dynamical Systems (Theory and Applications) (DSTA 2007), Lodz, Poland, Dec. 17–20, 2007; Tech. Univ. Lodz, 2007, Vol. 1, p. 415–422.

[8] M. V. Shamolin, *Methods of analysis of dynamic systems with various dissipation in dynamics of a rigid body*, ENOC-2008, CD-Proc., June 30–July 4, 2008, Saint Petersburg, Russia, 6 p.

[9] M. V. Shamolin, *Some methods of analysis of the dynami systems with various dissipation in dynamics of a rigid body*, PAMM (Proc. Appl. Math. Mech.), **8**, 10137–10138 (2008) / DOI 10.1002/pamm.200810137.

[10] M. V. Shamolin, *Dynamical systems with variable dissipation: methods and applications*, Proc. of 10th Conf. on Dynamical Systems (Theory and Applications) (DSTA 2009), Lodz, Poland, Dec. 7–10, 2009; Tech. Univ. Lodz, 2009, p. 91–104.

[11] M. V. Shamolin, *New cases of integrability in dynamics of a rigid body with the cone form of its shape interacting with a medium*, PAMM (Proc. Appl. Math. Mech.), **9**, 139–140 (2009) / DOI 10.1002/pamm. 200910044.

[12] M. V. Shamolin, *The various cases of complete integrability in dynamics of a rigid body interacting with a medium*, Multibody Dynamics, ECCOMAS Thematic Conf. Warsaw, Poland, 29 June–2 July 2009, CD-Proc.; Polish Acad. Sci., Warsaw, 2009, 20 p.

[13] M. V. Shamolin, *Dynamical systems with various dissipation: background, methods, applications* // CD-Proc. of XXXVIII Summer School-Conf. "Advances Problems in Mechanics" (APM 2010), July 1–5, 2010, St. Petersburg (Repino), Russia; St. Petersburg, IPME, 2010, p. 612–621.

[14] M. V. Shamolin, *Integrability and nonintegrability in terms of transcendental functions in dynamics of a rigid body*, PAMM (Proc. Appl. Math. Mech.), **10**, 63–64 (2010) / DOI 10.1002/pamm.201010024.

[15] M. V. Shamolin, *Cases of complete integrability in transcendental functions in dynamics and certain invariant indices*, CD-Proc. 5th Int. Sci. Conf. on Physics and Control PHYSCON 2011, Leon, Spain, September 5–8, 2011. Leon, Spain, 5 p.

[16] M. V. Shamolin, *Variety of the cases of integrability in dynamics of a 2D-, 3D-, and 4D-rigid body interacting with a medium*, Proc. of 11th Conf. on Dynamical Systems (Theory and Applications) (DSTA 2011), Lodz, Poland, Dec. 5–8, 2011; Tech. Univ. Lodz, 2011, p. 11–24.

[17] M. V. Shamolin, *Cases of integrability in dynamics of a rigid body interacting with a resistant medium*, CD-proc., 23th International Congress of Theoretitical and Applied Mechanics, August 19–24, 2012, Beijing, China; Beijing, China Science Literature Publishing House, 2012, 2 p.

[18] M. V. Shamolin, *Variety of the cases of integrability in dynamics of a 2D-, and 3D-rigid body interacting with a medium*, 8th ESMC 2012, CD-Materials (Graz, Austria, July 9–13, 2012), Graz, Graz, Austria, 2012, 2 p.

ISBN: 978-1-61804-225-5

Differentiation Functors and Category Interpretation of Optimality Conditions

Simon Y. Serovajsky and Dinash M. Diarova

***Abstract*—**Operator derivatives are determined as functors. Necessary optimality conditions with category interpretation are proved for abstract optimization control problems. Finite dimensional extremum problems and an optimization control problem for nonlinear parabolic equation with state constraints are considered as examples.

***Keywords*—**Category, control, differentiation functor, operator derivative, optimality conditions.

I. Introduction

OPTIMIZATION control problems are solved by means of necessary conditions of optimality frequently. First order optimality conditions used the differentiation of the state functional (see, for example, the stationary condition, Euler equation, the variational inequality, the maximum principle, etc.). So the optimization control theory can be interpreted as an application of the differentiation theory.

The differentiation is an operation of the local linearization [1]. The nonlinear phenomenon has become weakly apparent in a small enough set. Hence the regular enough nonlinear object can be approximated by a linear one. For example, the smooth curve can be approximated in a neighbourhood of a point by its tangent in this point. However the definition of the tangent uses the derivative of the function. We apply the differentiation whenever a nonlinear object is analyzed by means of its linear approximation.

Note that the differentiation relates with the local structure of the object only. If functions (functionals, operators) are equal in a neighbourhood of a point, then it has the same derivatives in this point. So the derivative characterizes the local properties of the class of objects, but not a concrete object. These objects are equivalent in some way. This equivalence class is the germ of functions (functionals, operators) in this point [2]. Therefore there exists a natural relation between the differentiation and germs theory.

The differentiation transforms the germ of operators to a linear operator, which is its derivative in the given point. This map can be interpreted as a functor. It transforms the category, which has germs of operators as morphisms, to the category, which has linear operators as morphisms. So we can apply the categories theory [3] for the interpretation of the differentiation.

The differentiation functor was defined in [4] without the germs theory. These results were used for the analysis of unconditional extremum problems there. The definition of the differentiation functor with using germs theory and its application to the extremum theory by means of the inverse function theorem where considered in [5]. We will define partial differentiation functors. Necessary optimality conditions with category interpretation will be proved for abstract optimization control problems with using implicit function theorem. Finite dimensional extremum problems and an optimization control problem for nonlinear elliptic equation with state constraints will be considered as examples.

II. Differentiation Functor and its Application to the Extremum Theory

We consider the set of pairs (X, x), where X is a Banach space, and x is a fixed point of X. For all pairs (X, x) and (Y, y) determine an operator $L : X \to Y$ that is Frechet differentiable at the point x such that $Lx = y$. Two operators are equivalent if they coincide at a neighbourhood of the point x. The relevant equivalence class, namely the germ of the operator L at the point x, is denoted by L_x. We determine the category Γ with Banach spaces with fixed points as the objects and the germs of differentiable operators as the morphisms.

We now define a map D from Γ to the category B of Banach spaces with linear continuous operators. For all object (X, x) and the morphism L_x of the category Γ with the beginning (X, x) and the end (Y, y) we determine

$$D(X, x) = X,\ DL_x = L'(x).$$

This map is a functor. It is called the *differentiation* [4]; and the value $D\psi$ at the germ ψ is called the *derivative of the morphism* ψ of the category Γ [5].

Determine a category Σ with Banach spaces with fixed points as the objects. Consider the germs of operators that are continuously differentiable at a neighbourhood of the fixed point and have invertible derivative at this point. Let it be the morphisms of Σ. Then Σ is the subcategory Σ of Γ; besides its morphisms are isomorphisms.

S. Y. Serovajsky is with the Differential Equations and Control Theory Department, al-Farabi Kazakh National University, Almaty, 050078 Kazakhstan (corresponding author to provide phone: +7 727-275-39-34; e-mail: serovajskys@mail.ru).

D. M. Diarova is with the High Mathematics Department, Atyrau Oil Gas Institute, Atyrau, 060002, Kazakhstan (e-mail: ddiarova@mail.ru).

There exists an application of these notions to the extremum theory. Let $A: Y \to V$ be a state operator, where V and Y are Banach spaces. The state of a system is described by the equation $Ay = v$, where v is a control, and y is the state function. Suppose for all control v of V this equation has a unique solution $y = Lv$ from the space Y. Determine the state functional $I: V \to \mathbb{R}$ by the equality $I(v) = J(v) + K(Lv)$, where $J: V \to \mathbb{R}$, $K: Y \to \mathbb{R}$ are given functional. We have the problem of the minimization of the functional I on the space V.

If v is a point of the local minimum of the functional I on the space V, J_v and K_y are the morphisms of Γ, and A_y is the morphism of Σ, where $y = Lv$, then

$$DJ_v + \left[H(DA_y) \right]^{-1} DK_y = 0,$$

where H is the general cofunctor from B to the sets category that is determined by the object $\mathbb{R}$ [4]. This result was extended to the problem of the minimization of a functional on the convex set [5]. However it was an optimization problem, where the control is an absolute term of the state equation only. Besides the state functional was the sum of the functional J and K there. We will consider the general case of the state equation and the functional. So we will determine partial differentiation functors.

III. Partial Differentiation Functors and Abstract Optimization Control Problem

Consider a continuously differentiable operator $A: V \times Y \to Z$ and a functional $I: V \times Y \to \mathbb{R}$, where V,Y,Z are Banach spaces. Suppose for all control $v \in V$ there exists a unique state $y = Lv$ from Y such that $A(v, y) = 0$. We have the problem of the minimization for the functional $v \to I(v, Lv)$ on the space V.

Let (V, v), (Y, y), $(V \times Y, w)$ be objects of Γ, where $w = (v, y)$. Then A_w is the morphism of Γ. Its derivative DA_w is the pair $\left(A_v(w), A_y(w) \right)$, where $A_v(w)$ is the derivative of the map $v \to A(v, y)$ at the point v, and $A_y(w)$ is the derivative of $y \to A(v, y)$ at y. Denote by $V \oplus Y$ the coproduct of the objects of the category B. Its morphisms $A_v(w): V \to Z$, $A_y(w): Y \to Z$ determine a cocone. Then $\iota_V DA_w = A_v(w)$, $\iota_Y DA_w = A_y(w)$, where ι_V and ι_Y are the canonic inclusions of V and Y to $V \oplus Y$.

Suppose the beginning (W, w) of the morphism A_w of the category Γ is the coproduct $(V, v) \oplus (Y, y)$. The values $\iota_V DA_w$ and $\iota_Y DA_w$ are called the *partial derivatives* $D_V A_w$ and $D_Y A_w$ of A_w. We have the equalities $DA_w = D_V A_w \oplus D_Y A_w$ and $DI_w = D_V I_w \oplus D_Y I_w$. Consider the pair $F = (I, A)$ and the matrix $F'(w)$ of its partial derivatives at the point w. It is the derivative DF_w of the morphism F_w of Γ. But it is the morphism of the category B with beginning $V \oplus Y$ and $\mathbb{R} \otimes Z$, that is the product of the objects of B.

Return to our optimization control problem. It can be transformed to the problem of the minimization for the smooth functional $S = IQ$ on the space V, where $Q = \left(E, L \right)$, and E is the unit operator on V.

Theorem 1. Suppose v is a point of local minimum of the functional S on the space V, F_w is the morphism of Γ, and C_{Lv} is the morphism of Σ, where $w = (v, Lv)$, $Cy = A(v, y)$. Then

$$D(F_w Q_v) = 0. \tag{1}$$

Proof. The derivative $A_y(w)$ is invertible. So the operator L is differentiable at the point v because of the implicit function theorem. Then L_v and Q_v are morphisms of the category Γ. Therefore the functional S is differentiable; and necessary condition of local extremum $S'(v) = 0$ is true. It can be transformed to the equality $DS_v = 0$. Then the operator $R = AQ$ is differentiable too. Using state equation, from the equality $R(v + \sigma h) - Rv = 0$ for all number σ and $h \in V$, we get $R'(v) = 0$; so $DR_v = 0$. Then we obtain

$$F_w Q_v = \left(I_w, A_w \right) Q_v = \left(I_w Q_v, A_w Q_v \right) = \left(S_v, R_v \right)$$

because of the definition of the morphism F_w. So the equality (1) is true.

We give some corollaries of Theorem 1.

Corollary 1. Under the conditions of Theorem 1 we have the equality $I_v(v, y) = \left[A_v(v, y) \right]^* p$, where y is the solution of the state equation $A(v, y) = 0$, and p is the solution of the adjoint equation $\left[A_y(v, y) \right]^* p = I_y(v, y)$.

Corollary 2. Let $x = (x_0, x_1, ..., x_n)$ be a point of the local extremum of the function $f_0 = f_0(x)$ under the equalities $f_i(x) = 0$, $i = 1, 2, ..., n$; and all functions are continuously differentiable at a neighbourhood of the point x. Then its Jacobian, that is determined by the functions $f_0, f_1, ..., f_n$ at the point x, is equal to zero.

Consider the minimization problem for the function $f_0 = f_0(x)$ under the equalities $f_i(x) = 0$, $i = 1, 2, ..., n$, where $x = (x_1, ..., x_{n+r})$. Suppose all functions are smooth enough. Fixe a vector $\alpha = (\alpha_1, ..., \alpha_n)$, where $\alpha_i \in \{1, ..., n + r\}$, $\alpha_i \neq \alpha_j$ $\forall i \neq j$. Determine the matrixes

$$F_{\beta_i}^{\alpha}(x) = \begin{pmatrix} \partial_{\alpha_1} f_0(x) & ... & \partial_{\alpha_n} f_0(x) & \partial_{\beta_i} f_0(x) \\ \partial_{\alpha_1} f_1(x) & ... & \partial_{\alpha_n} f_1(x) & \partial_{\beta_i} f_1(x) \\ ... & ... & ... & ... \\ \partial_{\alpha_1} f_n(x) & ... & \partial_{\alpha_n} f_n(x) & \partial_{\beta_i} f_n(x) \end{pmatrix}, \quad i = 1, 2, ..., r,$$

where $\beta_i \in \{1,...,n+r\}$, $\beta_i \neq \beta_j$ for all $i \neq j$ and $\beta_i \neq \alpha_j$ for all *i,j*; $\partial_k f_m(x)$ is the derivative of the function f_m with respect to x_k at the point *x*.

Corollary 3. If *x* is a point of the local extremum of the function f_0 under the given constraints, then $\left|F^{\alpha}_{\beta_i}(x)\right| = 0,\ i = 1,2,...,r.$

We determine necessary conditions of the extremum without Lagrange multipliers. However these results can be transformed to the standard form.

IV. Optimization Control Problems with Constraints

Consider again a continuously differentiable operator $A: V \times Y \to Z$ and a functional $I: V \times Y \to \mathbb{R}$, where *V,Y,Z* are Banach spaces. Let *U* be a convex closed subset of *V*. Suppose for all control $v \in U$ there exists a unique state $y = Lv$ from *Y* such that $A(v, y) = 0$. We have the problem of the minimization for the functional $v \to I(v, Lv)$ on the set *U*.

Theorem 2. Under the conditions of Theorem 1 suppose *v* is a point of a local minimum for the functional $v \to I(v, Lv)$ on the set *U*. Then *v* satisfies the variational inequalities

$$\pi_i D\left(F_w Q_v\right)(u - v) \geq 0 \ \forall u \in U_i,\ i = 1,2, \tag{2}$$

where $U_1 = U$, $U_2 = V$, π_1 and π_2 are canonic projections.

Proof. Let *v* be a point of a local minimum for the functional $v \to I(v, Lv)$ on the set *U*. Then we have the inequality

$$I(\theta, L\theta) - I(v, Lv) \geq 0 \ \forall \theta \in O,$$

where the subset *O* of *U* is a neighbourhood of the point *v*. Let $u \in U$ be fixed. Chose a positive number σ such that the inclusion $v + \sigma(u - v) \in O$ is true. Determine the control $\theta = v + \sigma(u - v)$. We get

$$I\left(v + \sigma(u - v), L\left[v + \sigma(u - v)\right]\right) - I(v, Lv) \geq 0. \tag{3}$$

Let Ξ maps the morphism $\psi = L_x$ of Γ to the value *Lx*. So the derivative of the morphism satisfies the equality

$$\Xi L_{x+h} = \Xi L_x + DL_x h + \eta(h),$$

where $\left\|\eta(h)\right\| = o\left(\left\|h\right\|\right)$. Then we have

$$\Xi I_{w+h} = \Xi I_w + D_V I_w h_V + D_Y I_w h_Y + \eta_I(h),$$

$$\Xi A_{w+h} = \Xi A_w + D_V A_w h_V + D_Y A_w h_Y + \eta_A(h),$$

where $h = (h_V, h_Y)$, $\left\|\eta_I(h)\right\| = o\left(\left\|h\right\|\right)$, $\left\|\eta_A(h)\right\| = o\left(\left\|h\right\|\right)$.

Determine

$$w = (v, Lv),\ h = \left(\sigma(u - v), h_Y\right),\ h_Y = L\left[v + \sigma(u - v)\right] - Lv.$$

Using implicit function theorem, we get

$$h_Y = \sigma L'(v)(u - v) + \eta(\sigma) = \sigma DL_v(u - v) + \eta(\sigma),$$

where $\left\|\eta(\sigma)\right\| = o(\sigma)$. Then we obtain

$$\Xi I_{w+h} = \Xi I_w + \sigma D_V I_w(u - v) + \sigma D_Y I_w DL_v(u - v) + \eta_1(\sigma),$$

where $\left\|\eta_1(\sigma)\right\| = o(\sigma)$. Devise the inequality (3) by σ and pass to the limit as $\sigma \to 0$. We have

$$D_V I_w(u - v) + D_Y I_w DL_v(u - v) \geq 0 \ \forall u \in U.$$

It can be transform to

$$DS_v(u - v) \geq 0 \ \forall u \in U.$$

We have also

$$A\left(v + \sigma g, L\left(v + \sigma g\right)\right) - A(v, Lv) = 0 \ \forall g \in V.$$

So we get

$$D_V A_w g + D_Y A_w DL_u g = 0 \ \forall g \in V.$$

It is equivalent to the inequality

$$D_V A_w(u - v) + D_Y A_w DL_u(u - v) \geq 0 \ \forall u \in V.$$

Then

$$DR_v(u - v) \geq 0 \ \forall u \in V.$$

We have the equalities $\pi_1\left(F_w Q_v\right) = S_v$, $\pi_2\left(F_w Q_v\right) = R_v$. Using last inequalities, we get (2).

If $U = V$, then the variational inequality (2) can be transformed to the equality (1).

Corollary 4. Under the conditions of Theorem 2 we have the variational inequality

$$\left\langle I_v(v, y) = \left[A_v(v, y)\right]^* p, u - v \right\rangle \geq 0 \ \forall u \in U, \tag{4}$$

where $\left\langle \lambda, \mu \right\rangle$ is the value of the linear continuous functional λ at the point μ, *y* is the solution of the state equation $A(v, y) = 0$, and *p* is the solution of the adjoint equation

$$\left[A_y(v, y)\right]^* p = I_y(v, y). \tag{5}$$

The state equation has a unique solution for our case. So there exists a bijection between the set of controls and the set of the state functions. So we have equivalence between controls and states. The single pair "control-state" was considered for solving systems described by singular systems [6,7]. We consider other case as an example. Let us have an optimization problem for a system with state constraints only. There exist difficulties for solving this problem by means of standard methods because we do not know how we can variate the control for saving state constraints. However we can rearrange the control and the state function. So we will use our results with state variation.

Consider an example. Let Ω be an open bounded *n*-dimensional set. We have the equation

$$z' - \Delta z + \left|z\right|^{\rho} z = g \tag{6}$$

in the set $Q = \Omega \times (0, T)$, where z' is the derivative of *z* with respect to *t*, ρ is a positive constant for $n = 2$, and $0 < \rho \leq 2/(n-2)$ for $n > 2$. For all *g* from $Y = L_2(Q)$ this equation has a unique solution $z = Mg$ from the space

$$\left\{z \middle| z \in L_{\infty}\left(0,T; H_0^1(\Omega) \cap L_{\rho+2}(\Omega)\right),\ z' \in L_2(Q),\ z\big|_{t=0} = 0\right\},$$

besides the operator M is $*$-weakly continuous (see [8], ch. VI, Theorem 1.1). We have $H_0^1(\Omega) \subset L_{2(\rho+1)}(\Omega)$ because of Sobolev theorem. So we have $\Delta z \in L_2(Q)$. Then the solution of our boundary problem is the point of the space $V = \left\{ z \middle| \, z \in L_\infty\left(0,T;H_0^1(\Omega)\right), z' \in L_2(Q), \Delta z \in L_2(Q), z\big|_{t=0} = 0 \right\}$.

Let U be a convex closed subset of the space V. Consider the functional

$$I(z,g) = \frac{1}{2}\left\| z - \zeta \right\|^2_{L_2\left(0,T;H_0^1(\Omega)\right)} + \frac{\chi}{2}\left\| g \right\|^2_{L_2(Q)},$$

where $\zeta \in L_2\left(0,T;H_0^1(\Omega)\right)$ is a given function, $\chi > 0$, and the functions z and g satisfy the given equation. We have the problem of the minimization for the functional I under the condition $z \in U$. Using standard technique (see, for example, [9]) we prove the solvability of this problem.

Necessary conditions of optimality for nonlinear parabolic equations with state constraints are well known. It is systems with fixed final time [10-12], optimization problems with finite quantity of integral equalities and inequalities [13], pointwise constraints [14-16], and time optimal problem [17]. There exist a few results for the general state constraints. It uses regularization method [14] or Ekeland principle [18]. We will obtain standard variational inequality as necessary conditions of optimality by means of Corollary 4.

Theorem 3. The optimal control is determined by the formula

$$g = -\chi^{-1} p, \tag{7}$$

where the function p is equal to zero on the boundary of the given set and for the final time; it satisfies the conditions

$$z' - \Delta z + |z|^\rho z = -\chi^{-1} p, \tag{8}$$

$$-p' - \Delta p + (\rho+1)|z|^\rho p = q, \tag{9}$$

$$\int_Q \left(\Delta\zeta - \Delta z - q\right)(u - z)dQ \geq 0 \ \ \forall u \in U. \tag{10}$$

Proof. We use Corollary 4. Let the state function z of our system be a "control" v, and the control g be a "state function" y of the general problem. Determine the operator A by the formula $A(v,y) = v' - \Delta v + |v|^\rho v - y$. Then the operator $Lv = v' - \Delta v + |v|^\rho v$ is differentiable. So we can apply Theorem 2.

We have

$$\left\langle I_v(v,y), h \right\rangle = \int_Q \left(\nabla v - \nabla\zeta\right)\nabla h dQ = \int_Q \left(\Delta\zeta - \Delta v\right) h dQ,$$

$$\left\langle \left[A_v(v,y)\right]^* p, h \right\rangle = \left\langle p, \left[A_v(v,y)\right] h \right\rangle =$$

$$\int_Q \left(h' - \Delta h + (\rho+1)|v|^\rho h\right) p dQ =$$

$$\int_Q \left(-p' - \Delta p + (\rho+1)|v|^\rho p\right) h dQ$$

for all $h \in V$ and for all smooth functions p that is equal to zero on the boundary of the given set and for the final time. Then the variational inequality (4) can be transformed to

$$\int_Q \left[\left(\Delta\zeta - \Delta v\right) - \left(-p' - \Delta p + (\rho+1)|v|^\rho p\right)\right](u - v)dQ \geq 0$$

for all $u \in U$. We have the equalities $I_y(v,y) = \chi y$, $\left[A_y(v,y)\right]^* p = -p$. Then we transform the adjoint equation (5) to $y = -\chi^{-1} p$. So the equality (7) is true. Besides we get (8) because of the state equation (6). Determine the function q as the right side of the equality (9). Then the last variational inequality can be transformed to (10). This completes the proof of Theorem 3.

We obtained necessary conditions of optimality in the standard form. It can be solved by means of iterative methods. However this system has peculiarities [7]. The state equation is applied for finding the state function as a rule, the adjoint function is determined from the adjoint equation, and the variational inequality is used for finding the control. But we have another algorithm. If the function q is known for the fixed iteration, then we find the state function z from the variational inequality (10). Then we determine the functions p and q from the equalities (8) and (9). Hence we do not solve the state equation and the adjoint one. It is interpreted as the formulas for finding the functions p and q. The control is determined by the formula (7). The general difficulty for the fixed iteration is solving of the variational inequality (10). However it is known numerical methods for finding the solutions of variational inequalities [19]. The analogical results can be obtained for other optimization control problems with state constraints, for example for elliptic equations [20].

REFERENCES

[1] J. Dieudonné. *Foundation of modern analysis*. New York and London: Academic Press, 1969.

[2] N. Bourbaki. *Topologie générale*. Paris: Hermann, 1940, 1942, ch. 1-4.

[3] I. Bucur and A. Deleanu. *Introduction to the theory of categories and functors*. London, New York, Sydney: John Wiley & Sons LTD, 1968.

[4] S. Serovajsky Differentiation of operators and extremum conditions category interpretation. *Izvestiya vuzov. Mathematics*. 2010, no 2, pp. 66-76.

[5] S. Serovajsky. "Differentiation Functors and its Application in the Optimization Control Theory," in *Fourier Analysis and Pseudo-Differential Operators. Springer Proceedings in Mathematics & Statistics*. 2014, submitted for publication.

[6] A. V. Fursikov. *Optimal control of distributed systems. Theory and applications*. Providence: Amer. Math. Soc. 1999.

[7] J. L. Lions. *Contrôle de systèmes distribués singuliers*. Paris: Gauthier-Villars, 1983.

[8] H. Gajewski, K. Gröger, and K. Zacharias. *Nichtlineare Operatorgleichungen und Operatordifferentiagleichungen*. Berlin: Academie Verlag, 1974.

[9] J. L. Lions. *Contrôle Optimal de Systèmes Gouvernés par des Équations aux Dérivées Partielles*. Paris: Dunod, Gauthier-Villars, 1968.

[10] R. Griesse, and S. Volkwein. A primal-dual active set strategy for optimal boundary control of a nonlinear reaction-diffusion system. *SIAM. J. Control Optim.*, vol. 44, no. 2, pp. 467-494, 2005.

[11] H. R. Henríquez, and E. Hernández Stabilization of linear distributed control systems with unbounded delay. *J. Math. Anal. Appl.*, vol. 307, no. 1, pp. 321-338, 2005.
[12] S. Serovajsky. Optimal control for a singular evolutional equation with nonsmooth operator and fixed final state. *Differential equations*, vol. 43, no. 2, pp. 251-258, 2007.
[13] A. S. Matveev, and V. A. Yakubovich. *Abstract Optimization Control Theory*. SPb.: SPb. Univ, 1994.
[14] P. Neittaanmaki, and D. Tiba. *Optimal control of nonlinear parabolic systems. Theory, Algorithms, and Applications*, New York: Marcel Dekker, 1994.
[15] N. Arada, and J. P. Raymond. Optimality conditions for state-constrained Dirichlet boundary control problems. *J. Optim. Theory Appl.*, vol. 102, no. 1, pp. 51-68, 1999.
[16] A. Rösch, and F. Tröltzsch. On regularity of solutions and Lagrange multipliers of optimal control problems for semilinear equations with mixed pointwise control-state constraints. *SIAM J. Contr. Optim.*, vol. 46, no. 2, pp. 1098-1115, 2007.
[17] J. P. Raymond, and H. Zidani Pontryagin's principle for time optimal problems. *J. Optim. Theory Appl.*, vol. 101, no. 2, pp. 375-402, 1999.
[18] E. Casas Pontryagin's principle for state-constrained boundary control problems of semilinear parabolic equations. *SIAM. J. Control Optim.*, vol. 35, no. 4, pp. 1297-1327, 1997.
[19] R. Glowinski, J. L. Lions, R. Tremolier. *Numerical Analysis of Variational inequalities*. Amsterdam: North Holland, 1981.
[20] S. Serovajsky. Optimization control problems for a nonlinear elliptic equation with state constraints and state variation. *Izvestiya vuzov. Mathematics*, no. 9, pp. 81-86, 2013.

An efficient iterative method to calibrate the Balloon model using fMRI measurements

Nafiseh Khoram, Rabia Djellouli, Taous-Meriem Laleg-Kirati and Chadia Zayane

***Abstract*—The goal of this study is to propose an efficient numerical technique for calibrating the mathematical model that describes single-event related brain response when fMRI measurements are given. To this end, we have designed a solution methodology that employs a regularized Newton method in conjunction with a Kalman filtering procedure. We have applied this method to estimate the biophysiological parameters of the Balloon model that describes the hemodynamic brain responses. Illustrative results obtained with both synthetic and real fMRI measurements are presented.**

***Index Terms*—Brain response, BOLD signal, fMRI, Balloon model, Nonlinear Hemodynamical systems, Parameter estimation, Newton method, Tikhonov regularization, Kalman filter, Cubature points**

I. Introduction

THE goal of this study is to analyze numerically an inverse problem arising in the functional brain imaging. More specifically, we consider the problem of calibrating the model that describes single-event related brain response when fMRI measurements are given. This problem can be formulated as an inverse problem that falls in the category of parameter identification of a dynamical system. We propose a regularized Newton method equipped with a Kalman filtering procedure to estimate these parameters from the knowledge of some fMRI measurements. The Newton component of the proposed algorithm addresses the nonlinear aspect of the problem. The regularization feature is used to ensure the stability of the algorithm. The Kalman filter is a de-noising procedure incorporated to address the noise in the data. We have employed this method to estimate the biophysiological parameters of the so-called Balloon model, which is a dynamical system that describes the hemodynamic brain responses [1]. We have conducted a numerical investigation using synthetic data tainted with various noise levels to assess the performance of the proposed method [2]. We present results to illustrate the potential of the proposed solution methodology to accurately and efficiently estimate the biophysiological parameters. These results clearly indicate that the proposed method outperforms the Cubature Kalman Filter (CKF), a procedure that is considered to be among the most successful parameter estimation techniques [3]. Finally, we also present results obtained from using real fMRI measurements corresponding to a finger-tapping stimulus.

N. Khoram and R. Djellouli are with the Department of Mathematics and Interdisciplinary Research Institute for the Sciences, IRIS, California State University Northridge (CSUN), Northridge, USA. e-mail: nafiseh.khoram.25@my.csun.edu, rabia.djellouli@csun.edu

T. M. Laleg-Kirati and C. Zayane are with the Department of Applied Mathematics and Computational Science, King Abdullah University of Science and Technology (KAUST), KSA. e-mail: taousmeriem.laleg@kaust.edu.sa, chadia.zayane@kaust.edu.sa

TABLE I
DESCRIPTION OF STATE VARIABLES

State variables	Description	Value at rest
$f(t)$	Cerebral blood flow	1
$s(t)$	Flow inducing signal	0
$v(t)$	Normalized cerebral blood volume	1
$q(t)$	Normalized total deoxyhemoglobin content level	1

TABLE II
DESCRIPTION OF THE BIOPHYSIOLOGICAL PARAMETERS

Descriptions	Parameters
Stiffness exponent	α
Neural efficacy	ϵ
Rate of signal decaying	$\mathcal{K}$
Rate of flow-dependent elimination	$\mathcal{X}$
Hemodynamic transit time	τ
Resting net oxygen extraction fraction	E_0
Resting blood volume	V_0

II. Problem Statement

A. The Hemodynamic System: The Direct Problem

The problem of describing the single-event related hemodynamic brain response to an exogenous input can be formulated in the framework of the dynamical system theory. The model we consider is called the hemodynamical system (HDS) [4] which is a first-order nonlinear differential system given by:

$$(HDS) \quad \begin{cases} \dot{\vec{x}}(t) = & A(\vec{\theta};\vec{x}(t)) + \nu_t \\ y(t) = & H(\vec{\theta};\vec{x}(t)) + \omega_t \quad ; \qquad t \geq 0 \\ \vec{x}(0) = & \widetilde{\vec{x}}_0 \end{cases} \tag{1}$$

where the component of the state vector $\vec{x}(t) = (f(t), s(t), v(t), q(t))^T$ are defined in Table II and the biophysiological system parameters $\vec{\theta} = (\alpha, \epsilon, \mathcal{K}, \mathcal{X}, \tau, E_0, V_0)^T$ are listed in Table II. The nonlinear vector-valued function$A$ describes the underlying physiology of the continuous hemodynamic system and is given by:

$$A(\vec{\theta};\vec{x}(t)) = \begin{cases} s(t) \\ \epsilon u(t) - \mathcal{K}s(t) - \mathcal{X}(f(t)-1) \\ \tau(f(t) - v(t)^{1/\alpha}) \\ \tau(f(t)\frac{1-(1-E_0)^{1/f(t)}}{E_0} - q(t)v(t)^{(1/\alpha-1)}) \end{cases} \tag{2}$$

The real-valued function H models the observations, that is, the Blood Oxygenation Level Dependent (BOLD) signal. H is given by:

$$H(\vec{\theta};\vec{x}(t)) = V_0\,[k_1(1-q(t)) + k_2(1-q(t)/v(t)) + k_3(1-v(t))] \tag{3}$$

ISBN: 978-1-61804-225-5

Note that ν_t (resp. ω_t) is a random vector with zero mean and 4×4 positive semidefinite covariance matrix, Q_t (resp. real-valued covariance, R_t), depending on the time t. ν_t (resp. ω_t) represents the level and distribution of the noise in the process equations (resp. in the measurements). k_1, k_2 and k_3 are positive constants given by $k_1 = 7E_0$, $k_2 = 2$ and $k_3 = 2E_0 - .2$.

B. The Discrete Inverse Problem

The determination of the parameters $\vec{\theta}$ of HDS(1) from the knowledge of some BOLD signal measurements can be formulated as the following inverse parameter problem:

$$\text{(IPP)} \quad \begin{cases} \textit{Given an initial state } \widetilde{\vec{x}}_0\textit{, a control input} \\ u(t_j) = (u(t_0), u(t_1), \ldots, u(t_M))^T, \\ \textit{and a BOLD signal } \widetilde{\vec{y}} = (\widetilde{y}_0, \widetilde{y}_1, \ldots, \widetilde{y}_M)^T, \\ \textit{find } \vec{\theta} \textit{ and } \vec{x}(t) \textit{ such that:} \\ \widetilde{H}(\vec{\theta}; \vec{x}(t_j)) = \widetilde{y}_j; \qquad j = 0, 1, \ldots, M \end{cases}$$

where the tilde notation indicates a noisy quantity, and $\widetilde{y}_j$ is the noisy measured BOLD signal at time t_j, and M is the number of measurements.

III. Parameter Estimation: The Solution Methodology

The parameter identification problem IPP is an inverse problem that is difficult to solve, especially from a numerical point of view, because it is nonlinear and ill-posed. In practice, this means that small errors in the measured BOLD signal can induce large errors in the estimate of the parameters. The proposed solution methodology is based on the Tikhonov regularized Newton method (TNM) [5], since regularized iterative methods appear to be the primary candidates for solving nonlinear and ill-posed problems (see, e.g., [6], and the references therein). The Newton algorithm addresses the nonlinear aspect of IPP, whereas the Tikhonov regularization procedure is incorporated to address its ill-posed nature [7]. In addition, a Kalman-type de-noising procedure is built within the proposed method to filter the noise contaminating the considered model. More specifically, we employ the so-called cubature Kalman filter (CKF)[3]. To the best of our knowledge, this is the first time TNM is employed in conjunction with CKF resulting in a novel procedure with a great potential for solving IPP efficiently and accurately, as illustrated by the results reported in Section IV-A and Section IV-B .

A. The Regularized Newton Algorithm

The solution of the IPP by the regularized Newton algorithm incurs at each iteration m the solution of the linearized problem of the form:

$$\sum_{j=1}^{M}\sum_{l=1}^{7} \frac{\partial \widetilde{H}^{(m)}}{\partial \theta_k}(\theta_l^{(m)}; \vec{x}^{(m)}(t_j)) \frac{\partial \widetilde{H}^{(m)}}{\partial \theta_l}(\vec{\theta}^{(m)}; \vec{x}^{(m)}(t_j)) \delta\theta_l^{(m)} + \gamma \delta\theta_l^{(m)} = \sum_{j=1}^{M} \frac{\partial \widetilde{H}^{(m)}}{\partial \theta_k}(\vec{\theta}^{(m)}; \vec{x}^{(m)}(t_j)) \left(\widetilde{y}_j - y^{(m)}(t_j)\right) ; k = 1, \ldots, 7 \tag{4}$$

and then we update $\vec{\theta}^{(m+1)} = \vec{\theta}^{(m)} + \delta\vec{\theta}^{(m)}$. Note that $y^{(m)}(t) = \widetilde{H}^{(m)}(\vec{\theta}^{(m)}; \vec{x}^{(m)}(t))$, and the positive real number γ is the Tikhonov regularization parameter. The choice of γ is a balancing act between stability and accuracy [2].

The critical step in the numerical implementation of the regularized Newton method is the computation, at each iteration m, of the Jacobian $J_H^{(m)} = \left[\frac{\partial \widetilde{H}}{\partial \theta_l}(\vec{\theta}^{(m)}; \vec{x}^{(m)}(t_j))\right]$ for $j = 1, \ldots, M$ and $l = 1, \ldots, 7$. Such computation must be executed with a high level of accuracy to ensure the stability, fast convergence and computational efficiency of the proposed Newton algorithm. The evaluation of these derivatives requires the computation of the derivatives of the state vector $\vec{x}$ with respect to the parameters $\vec{\theta}$. We have stablished a theorem (see Theorem 1 page 20 in [2]) that shows that these derivatives are the solutions of ordinary differential systems similar to HDS(1) but with different right-hand-sides.

B. Cubature Kalman filtering

The CKF procedure is a nonlinear filtering procedure that is derivative-free and more importantly the number of integration points, called the cubature points, increases linearly with the state-vector dimension. The CKF algorithm evaluates the BOLD signal in two steps: (a) a time update step in which *predicted* estimates of the state-vector and error covariance matrix are delivered at the next time step, and (b) a measurement update step in which *corrected* estimates of the *predicted* values are calculated.

The Time-Update Step in CKF. For $l = 0, 1, \ldots, M$, let $\vec{x}_l$ (resp. P_l) be an estimated value of the state vector $\vec{x}$ (resp. the error covariance matrix P) at time t_l. Suppose that $\vec{x}_l$ and P_l have been evaluated up to $l = j$ where $j < M - 1$. Then, in order to compute $\vec{x}_{j+1}$ and P_{j+1}, we first calculate in this step $\widehat{\vec{x}}_{j+1}$ (resp. $\widehat{P}_{j+1}$) a *predicted* estimate of the state vector (resp. the corresponding error covariance matrix). We evaluate $\widehat{\vec{x}}_{j+1}$, by first calculating the cubature vectors as follows:

$$\vec{c}_{i,j} = S_j \vec{\xi}_i + \vec{x}_j; \qquad i = 1, 2, \cdots, 8 \tag{5}$$

where S_j results from the Cholesky factorization of the error covariance matrix P_j, that is, $P_j = S_j S_j^T$ and $\vec{\xi}_i$ is the given i^{th} column vector of the cubature points matrix (see Eq. 7, page 2112 in [3]). Then, using the process equation in HDS(1) and the cubature vectors calculated in (5), we solve the following first order differential system

$$\begin{cases} \dot{\vec{z}}_i = A(\vec{\theta}; \vec{z}_i) \\ \vec{z}_i = \vec{c}_{i,j} \end{cases} ; \qquad i = 1, \ldots, 8 \tag{6}$$

and then evaluate the i^{th} "*propagated*" cubature vectors at time t_{j+1}, that is, $\vec{z}_{i,j+1} = \vec{z}_i(t_{j+1})$. Note that, the differential system given by (6) is typically solved using Runge-Kutta methods of order 4.

The *predicted* estimate for the state at time t_{j+1} is then calculated as follows:

$$\widehat{\vec{x}}_{j+1} = \frac{1}{8}\sum_{i=1}^{8} \vec{z}_{i,j+1} \tag{7}$$

Furthermore, the *predicted* estimate for the error covariance matrix $\widehat{P}_{j+1}$ at time t_{j+1} is evaluated as follows:

$$\widehat{P}_{j+1} = \frac{1}{8}\sum_{i=1}^{8} \vec{z}_{i,j+1}\vec{c}_{i,j+1}^T - \widehat{\vec{x}}_{j+1}\widehat{\vec{x}}_{j+1}^T + Q_{j+1} \tag{8}$$

ISBN: 978-1-61804-225-5

where $Q_{j+1} = Q_{t_{j+1}}$ is the process noise covariance matrix defined in Section II-A.

The Measurement-Update Step in CKF. This step is called the correction step. The goal here is to calculate x_{j+1} and P_{j+1} by "correcting" the predicted values $\widehat{x}_{j+1}$ and $\widehat{P}_{j+1}$, and y_{j+1}, the estimated BOLD signal at time t_{j+1} is then deduced. To this end, we first evaluate $\vec{x}_{j+1}$ as follows:

$$\vec{x}_{j+1} = \widehat{\vec{x}}_{j+1} + (\widetilde{y}_{j+1} - \widehat{y}_{j+1})\,\overrightarrow{W}_{j+1} \tag{9}$$

where $\widetilde{y}_{j+1}$ is the given measured BOLD signal at time t_{j+1}, $\widehat{y}_{j+1}$ is the *predicted* BOLD signal at time t_{j+1}. It is calculated by applying the cubature quadrature rule to the measurement equation given in HDS(1) as follows:

$$\widehat{y}_{j+1} = \frac{1}{8}\sum_{i=1}^{8} H(\vec{\theta}; \widehat{\vec{c}}_{i,j+1}) \tag{10}$$

with $\widehat{\vec{c}}_{i,j+1}$ being the i^{th} "*predicted*" cubature vector obtained as follows:

$$\widehat{\vec{c}}_{i,j+1} = \widehat{S}_{j+1}\vec{\xi}_i + \widehat{\vec{x}}_{j+1}; \qquad i = 1, 2, \cdots, 8 \tag{11}$$

where the matrix $\widehat{S}_{j+1}$ results from the Cholesky factorization of the *predicted* error covariance matrix $\widehat{P}_{j+1}$ at time t_{j+1}, that is, $\widehat{P}_{j+1} = \widehat{S}_{j+1}\widehat{S}^T_{j+1}$. $\overrightarrow{W}_{j+1}$ is the so-called *Kalman gain* at time t_{j+1}, and is given by:

$$\overrightarrow{W}_{j+1} = M^{-1}_{j+1}\overrightarrow{N}_{j+1} \tag{12}$$

The real number M_{j+1}, called the *innovation covariance* value, is given by:

$$M_{j+1} = \frac{1}{8}\sum_{i=1}^{8}\Big(H(\vec{\theta}; \widehat{\vec{c}}_{i,j+1})\Big)^2 - \widehat{y}^2_{j+1} + R_{j+1} \tag{13}$$

and $R_{j+1} = R(t_{j+1})$ is the measurement noise covariance value. The vector $\overrightarrow{N}_{j+1}$, called the *cross covariance* vector, is given by:

$$\overrightarrow{N}_{j+1} = \frac{1}{8}\sum_{i=1}^{8} H(\vec{\theta}; \widehat{\vec{c}}_{i,j+1})\vec{z}_{i,j+1} - \widehat{y}_{j+1}\widehat{\vec{x}}_{j+1} \tag{14}$$

The *corrected* error covariance matrix is then evaluated as follows:

$$P_{j+1} = \widehat{P}_{j+1} - M_{j+1}\overrightarrow{W}_{j+1}\vec{W}^T_{j+1} \tag{15}$$

where $\widehat{P}_{j+1}$, M_{j+1} and $\overrightarrow{W}_{j+1}$ are given by Eqs. (8),(13) and (12) respectively.

Last, we deduce the estimated BOLD signal at time t_{j+1} as follows:

$$y_{j+1} = H(\vec{\theta}, \vec{x}_{j+1}) \tag{16}$$

IV. Illustrative Numerical Results

A. Parameter Estimation with Synthetic Data

Because of space limitations, we present the result of one numerical experiment to illustrate the potential of the proposed solution methodology for calibrating efficiently the hemodynamical system HDS(1). In this experiment a *Gaussian* control input is employed.

The synthetic BOLD signal (see Figure 1) is generated by solving the noise free hemodynamical system HDS(1) with the initial state vector $\vec{x}_0 = (1, 0, 1, 1)^T$ and the biophysiological system parameters $\vec{\theta}^*$ whose coordinates' values were used in [3] and are listed in Table III. Moreover, we consider a set of 60 measurements ($M = 60$) taken every one second ($\Delta t = 1\,\text{s}$), that is, $\widetilde{\vec{y}} \in \mathbb{R}^{60}$ and $y_j = y(j\Delta t)$. The goal of this experiment is to illustrate the robustness of the method to the noise level in the measured BOLD signal. We also compare the obtained results to the ones delivered by the CKF algorithm when applied, as suggested in [3], to the so-called *extended* hemodynamical system (see Eq. (9), p. 2112 in [3]).

TABLE III
Biophysiological parameters: Target vs. initial values.

Parameters ($\vec{\theta}$)	α	ϵ	$\mathcal{K}$	$\mathcal{X}$	τ	E_0	V_0
Target ($\vec{\theta}^*$)	.34	.54	.65	.38	.98	.32	.04
Initial guess ($\vec{\theta}^{(0)}$)	.5	.5	.5	.5	.5	.5	.5

We artificially add white noise to the data as follows: 5% to $\vec{x}_0$, 1% to the process equation, and 10% to $\vec{y}$. We use a blind guess for the initial biophysiological parameters vector $\vec{\theta}^{(0)}$ whose components are all set to .5 (see Table III). The obtained results are depicted in Figures 2-3. These results were obtained with $\gamma = 2 \times 10^{-3}$. The following observations are noteworthy:

- As reported in Table III the initial parameters' values $\vec{\theta}^{(0)}$ is selected outside the pre-asymptotic convergence region. Indeed, Figure 1 shows that the use of this initial guess with HDS(1) leads to an initial BOLD signal profile that is very far from the target (the relative error is over 300%)
- The result depicted in Figure 2 reveals that the TNM-CKF algorithm delivers a signal with an excellent accuracy level (the relative error drops to 4%) which is remarkable given the considered relatively high noise level in the data. Note that the relative error on the parameters that was initially 52% decreases monotonically and reaches 15% at convergence.
- Figure 3 indicates that TNM-CKF algorithm requires only 8 iterations to converge (the relative residual is about 9%). This illustrates the efficiency of the method and its robustness to the noise effect.
- The comparison with the result obtained when applying the CKF algorithm only, as suggested in [3], reveals that (a) the TNM-CKF method outperforms the CKF algorithm (see Figure 2), and (b) the CKF algorithm fails dramatically to calibrate HDS(1) (the relative error on the computed BOLD signal is over 80%). This numerical experiment clearly illustrates the importance of employing the TNM procedure in conjunction with CKF to accurately reconstruct the BOLD signal when starting the calibration process from a blind guess for the biophysiological parameters's values.

B. Parameter Estimation with Real Data

In this section, we calibrate the HDS(1) using real fMRI measurements corresponding to a finger tapping stimulus. More specifically, one male subject was imaged while performing a finger tapping tasks (see Table IV for the data description). The study was approved by the Institutional Review

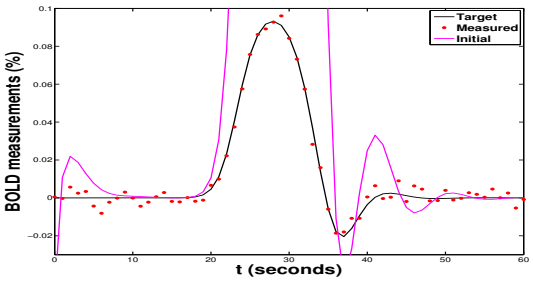

Fig. 1. Synthetic BOLD signal profiles: Target (solid-black). Measured with 10% white noise (dotted-red) and Initial (solid-magenta).

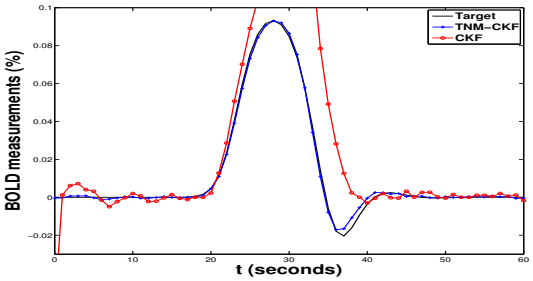

Fig. 2. Synthetic BOLD signal profiles: Target (black). Computed with TNM-CKF (blue) and computed with CKF (red).

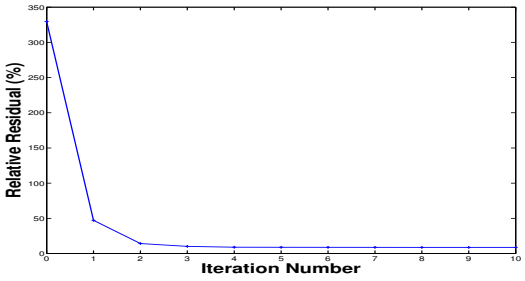

Fig. 3. Convergence history of the TNM-CKF algorithm in the case of synthetic measurements.

Board (IRB) at Nationwide Childrens Hospital, Columbus, OH. We applied the TNM-CKF using 720 BOLD measurements, $\vec{\theta}^{(0)}$ given in Table III, $\vec{x}_0 = (1, 0, 1, 1)^T$, and an *on-off* control input. Figure 4 indicates that TNM-CKF delivers a BOLD signal with an excellent accuracy (6% relative error) and Figure 5 demonstrates the convergence of the TNM-CKF algorithm after only 5 iterations.

V. Conclusion

The TNM-CKF algorithm is a solution methodology that is conceptually simple to understand and implement. The calibration results obtained with both synthetic and fMRI measurements clearly indicate that TNM-CKF algorithm is robust to the noise effect and requires few iterations to converge to an accurate solution even when starting with an initial guess value of the parameters outside the pre-assymptotic convergence region.

TABLE IV
Description of the Real Measurements.

Origin	Children's Hospital, Columbus, OH
Subject	1 male
Stimulus	Right hand finger tapping
Duration	6 minutes followed by 6 minutes rest
Voxels distribution	20 slices of 8 mm
Temporal sampling	3 seconds
Preprocessing	Filtering, smoothing and convolution
Interpolation	Matlab command 'interp1'
Number of voxels	128×128×20
Sampling time	0.01 seconds
Resolution	22 mm

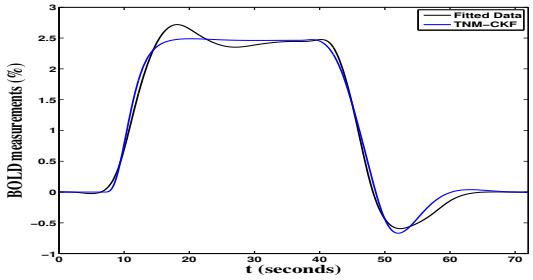

Fig. 4. BOLD signal profiles: Real (black) vs. Computed (blue).

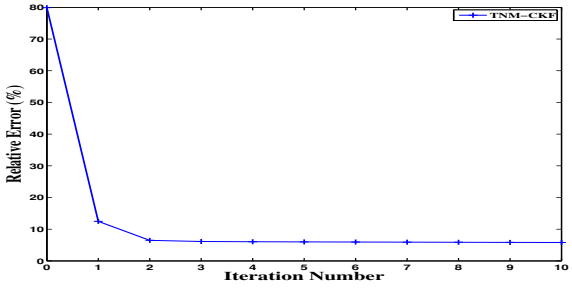

Fig. 5. Convergence history of the TNM-CKF algorithm in the case of real measurements.

Acknowledgment

The authors would like to thank Dr. Nasser Kashou, Wright State University, for providing them with the fMRI measurements and for enlightening discussions.

References

[1] K. J. Friston, E. Zarahn, O. Josephs, R. Henson, and A. Dale, "Stochastic design in event-related fMRI," *NeuroImage*, vol. 10, pp. 607–619, 1999.
[2] N. Khoram, "On the characterization of single-event related brain activity from functional magnetic resonance imaging (fmri) measurements," Master's thesis, California State University, Northridge, 2013. [Online]. Available: http://www.csun.edu/~iris/2012-2013.htm
[3] M. Havlicek, K. J. Friston, J. Jan, M. Brazdil, and V. D. Calhoun, "Dynamic modeling of neuronal responses in fmri using cubature kalman filtering," *Neuroimage.*, vol. 56, no. 4, pp. 2109–28, Jun 2011.
[4] K. J. Friston, "Variational filtering." *NeuroImage*, vol. 41, no. 3, pp. 747–66, Jul. 2008.
[5] S. F. Gilyazov and N. L. Goldman, *Regularization of ill-posed problems by iteration methods*. Kluwer Academic Publishers, 2000.
[6] R. Djellouli, *Inverse Acoustic Problems, in: Computational Methods for Acoustic Problems*. Saxe-Coburg Publications, 2008.
[7] V. Y. Tikhonov, A. N.; Arsenin, *Solutions of Ill-Posed Problems*. New York: Winston, 1977.

The Selection and Training Framework for Managers in Business Innovation and Transformation Projects

Managerial Recommendations for "The Open Group Architecture Framework" (TOGAF) Integration

Antoine Trad, prof. dr.
Webster University
Geneva, Switzerland

and

Prof. Damir KalpićKalpić, PhD
University of Zagreb
Faculty of Electrical Engineering and Computing
Zagreb, Croatia

Abstract—The riskiest factor in transforming a traditional business environment (BE) into a lean and automated BE is the role of the profile and the corresponding TOGAF managerial recommendations of the business and (e-)business transformation managers (BTM); the influence they have on the concrete implementation phase of business transformation projects (BTP).

The basic profile and "The OpenGroup Architecture Framework" (TOGAF)[66] managerial recommendations of such a business transformation manager has not been sufficiently researched in a holistic manner in order to hammer the BTM's profile and the corresponding TOGAF managerial recommendations; and that is the main goal of the authors' research [52][37][38]. In fact, currently there are no TOGAF managerial recommendations and educational curricula for such BTM profiles.

This research paper deals with the TOGAF managerial recommendations for the BTM selection and education; who has to manage the technical implementation phase of complex business transformation projects; knowing that the BTPs' implementation phase is the major cause of very high failure rates [20][21]. The implementations of such business transformation projects require a specific set of enterprise business architecture knowledge. The authors have based their research on the main fact that only around 12% of business organizations successfully terminate innovation-related business transformations projects [8].

"We know that those organizations that are consistently successful at managing innovation-related changes outperform their peers in terms of growth and financial performance" [7].

Therefore, there is an essential need for more research on the BTMs' profiles and the TOGAF related managerial recommendations. This research project presents an original set of factors and fulfills the need for an efficient tree reasoning model, in the form of a real world framework and recommendations, which affect the BTM's selection techniques. BTM selectors, professional analysts, project managers, auditors and advanced computer science students, will benefit from this research project.

Keywords *Economical competitive adavantage, TOGAF, managerial recommendations, efficient enterprise architecture, business transformation projects, business transformation manager's profile, managerial recommendations, transformation project implementation.*

I. INTRODUCTION

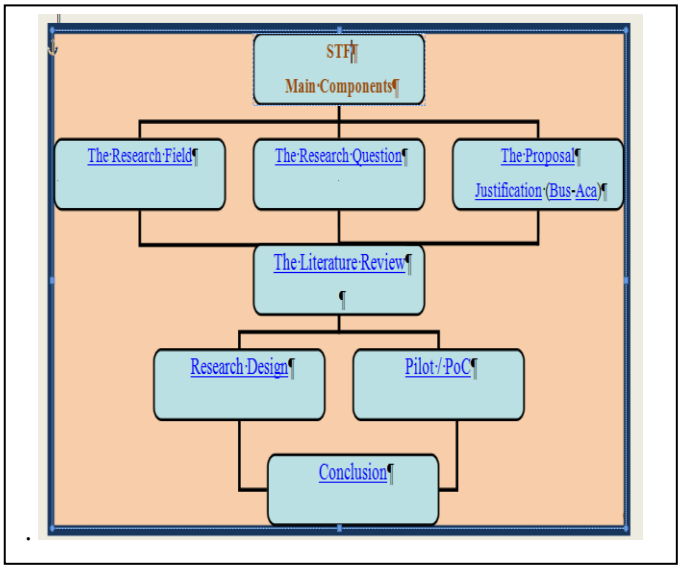

Fig. 1. The pilot Proof of Concept (PoC) development is the current research phase [52].

THE characteristics of a suitable BTM profile and the corresponding TOGAF managerial recommendations are the main goal of the authors' selection and training framework (STF) research project, which started in year 2010. In this research paper, the authors will try to present the TOGAF based managerial recommendations for such a BTM selection and education process.

This assessment and selection will be corroborated by the evaluation and monitoring of the BTM's skills [66] to integrate

innovative business processes' model (BPM) technologies into the existing BE [28].

This research's final phase uses a tunable theory based on hyper-heuristics reasoning model [25]. This reasoning model offers the optimal BTM profile and the corresponding TOGAF managerial recommendations that are adapted to complex BTPs [32][35]. These managerial recommendations are fed in the form of factors into the framework's reasoning tree, which will deliver the most important BTM characteristics or most weighted factors [35].

II. RESEARCH QUESTION AND LITERATURE REVIEW

The research project's question is: "Which business transformation managers' characteristic is optimal for the implementation phase of a(n) (e-)business transformation project? – A TOGAF Approach" [44][48][45]. The knowledge gap was acknowledged, mainly due to the fact that the existing literature and various methodologies treating business transformations offer practically no insight into the profile of the BTM as an architect of adaptive business information systems (AofABIS) and proposes the set of corresponding TOGAF managerial recommendations; who can manage the implementation phase of BTPs [1][32].

The literature review has shown that the BTM's optimal characteristic is to be a ***"TOGAF based AofABIS"***; and an important part of that phase was dedicated to the finding of factors that influence the BTMs' selection and education [44][59][63].

III. RESEARCH METHODOLOGY AND DESIGN

The authors based their research on the applicative action research (AAR) mixed method, that is mainly based on a hyper-heuristics approach [29][33]. The STF applies the positivist AAR that is designed on a model identical to the hyper-heuristics model. This heuristics model is based on a pseudo beam search tree method and has the elements described in [24][41].

The authors have implemented the STF research methodology, design and prototype [36], to support the selection of the optimal BTM profile. Such selections can be only evaluated with the help of mixed-models [3][27][64]. The STF's qualitative reasoning process model [15] uses the recommendations to give the BTP to tune the details of the BTM's profile [4][23][26].

The collection of case studies from A. Farhoomand and SAP's BTM2 perfectly correspond to the research filtering phase [6][2]. The reasoning engine will not be always perfect and adapted to all possible requirements, but it should be enhanced to make it capable of finding optimal results [33][34].

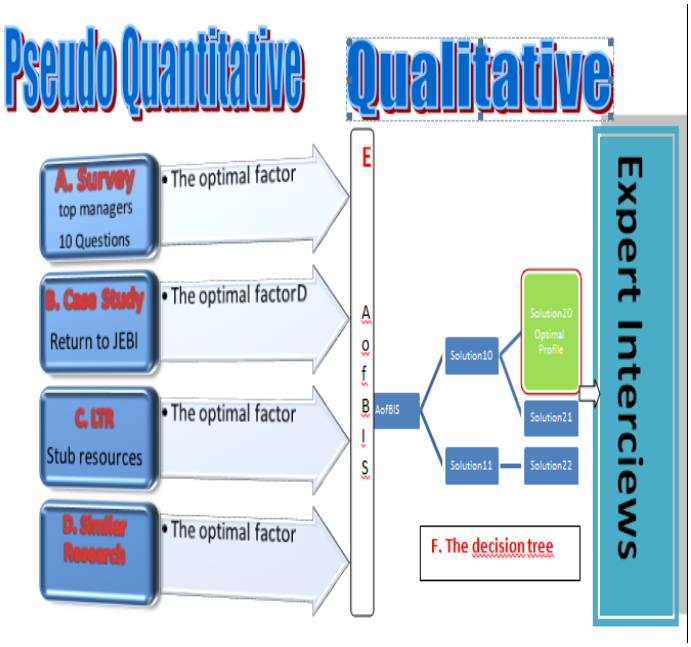

Fig. 2. The mixed method flow diagram [52] Interciews -> Interviews.

The approach to qualitative research offered the possibility to develop a real world framework and pattern [27]; that inherits TOGAF's guidelines.

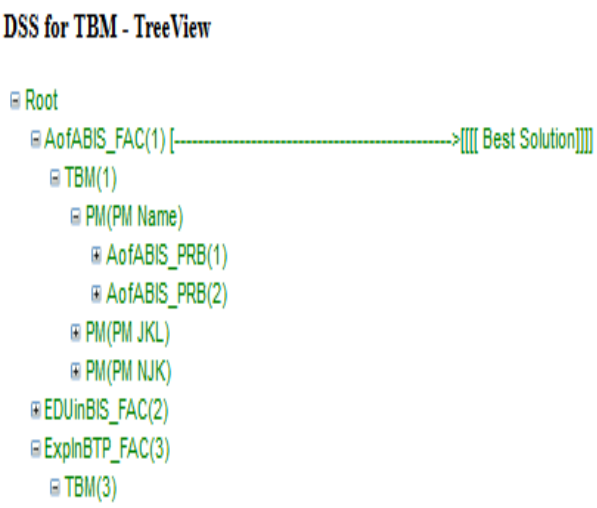

Fig. 3. *A view on the STF's tree solution node [35].*

IV. THE PILOT

The survey is the quantitative part of the mixed method that is based on the set of resulting factors, which some come from TOGAF; and hence the questions, which resulted from the literature review (Trad, Kalpić, 2013). This research process and the executed survey showed that the BTM is an AofABIS; that is a combination of roles from TOGAF [38][66]. The qualitative hyper-heuristics can be used to tune the STF factors [39]. Therefore, a concrete STF environment

was built; this STF proof of concept (PoC) and the final interviews should deliver the research's final managerial recommendations on how to select and train the right BTM profiles and to define his or her educational curriculum [2]. It will also propose how to use TOGAF as an infrastructure.

V. BTM IS A AofABIS

Understanding the BEs, enterprise architecture and the factors that affect their survival and competitiveness, is only the first step towards a successful BTP. The TBM must have in depth knowledge of: BTP architecture and its development management, business people integration, agile project management and coordination of computer engineers [22]. The BTM acts as solution designer and implementation architect [1][2].

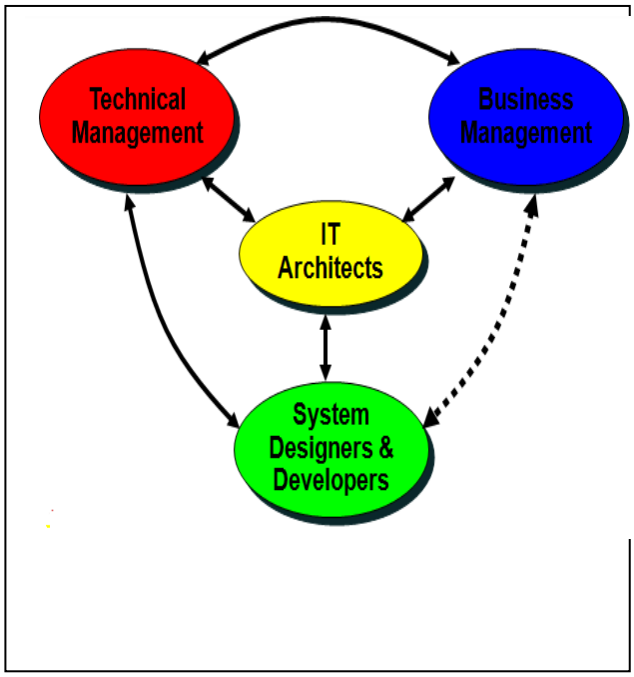

Fig. 4. *Enterprise architecture main blocks and components [65].*

Accordingly, this research project unifies resources from two distinct but related areas: business processes related information technologies and BTPs, it develops concepts for the BTM's selection and proposes a method to weight and inter-relate his or her various enterprise architecture skills with factors [50][55][66].

Estimating of BTM skills requires a profound knowledge of the enterprise business architecture, business processes (BPs), services technologies and business project management issues. That rounds up the profile of a AofABIS. The BTM is in fact a AofABS, where s/he acts as a coordinator of enterprise architecture(s) teams and coordinates their various activities. The STF will also support him or her in managing problems in real-time [38].

VI. ENTERPRISE ARCHTECTURE

Understanding the BEs and adapting the optimal enterprise architecture, assumes the BTM is capable of optimizing across the enterprise's heterogeneous dislocated processes (both manual and automated); into a holisitc integrated environment. Such an environment becomes agile to change and adapted to the enterprise's business strategy.

Executive management knows that the effective management and integration of data-information through information systems related technologies, is a key factor to BTP success, and an indispensable means to achieving ***sustainable competitive advantage***. Therefore enterprise architecture addresses this need, by providing a strategic context for the BTP.

In order finalize the BTP effectively within an enterprise, it is necessary to have a BTM who is capable to put in place an appropriate "business capability for architecture", through the: 1) organization structures, 2) roles, 3) responsibilities, 4) skills, and 5) process flows and services (The OpenGroup, TOGAF, 2011). An overview of the TOGAF "Architecture Capability" is shown in Figure 5.

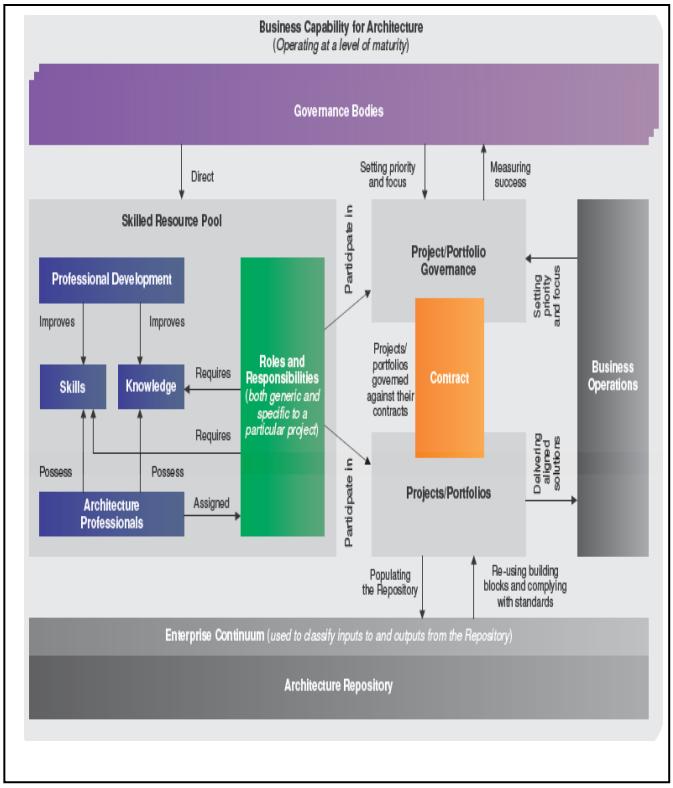

Fig. 5. *TOGAF Architecture Capability overview* [66].

ISBN: 978-1-61804-225-5

VII. TOGAF INTEGRATION

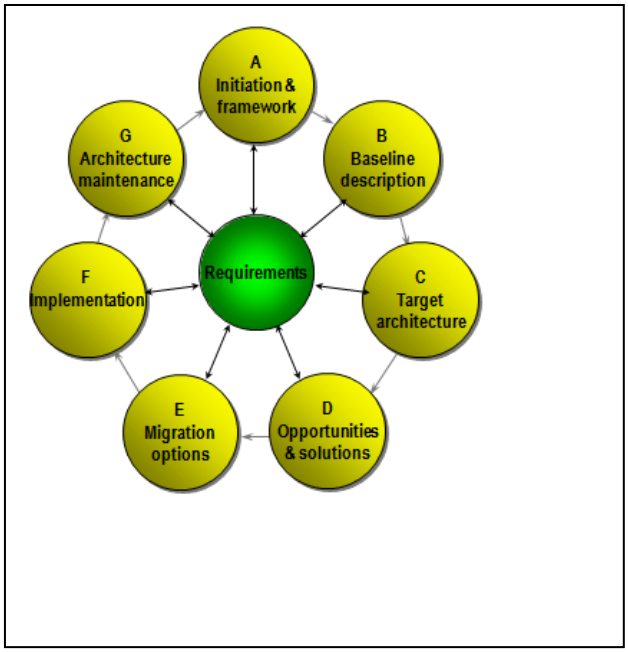

Fig. 6. *The diagram shows TOGAF's main components [35].*

The research proved the existence of a knowledge gap, as well as the necessity for the STF research project, as a complement to existing enterprise architecture standards [52][57][60][66]. What astonished the authors, during the literature review process was the superficial approach of businesses and managers towards the innovation-related business transformation processes. This research question and topic appear to be undiscovered and under-estimated. The probable reason is the approach of too much scoping of the research question and simplifying the research method to the level of "marketing like" descriptive statistics.

The STF is specialized in BTM's selection and skills definition; it recommends the integration of TOGAF's "Architecture Skills Framework" [66]; which defines the following roles: 1) Architecture Board Members, 2) Architecture Sponsor, 3) Architecture Manager and 4) Enterprise Architecture (which can be considered as a superset of Business, Data, Application and Technology Architecture). STF estimates that BTM is basically a very experienced enterprise architect or AofABIS.

The BTM as a AofABIS must have the following skills: 1) soft-skills (leadership, team-working, inter-personal skills, etc.); 2) Business Skills & Methods (typically comprising business cases, business process, strategic planning, etc.); 3) Enterprise Architecture Skills (typically comprising modelling, building block design, applications and role design, systems integration, etc.); 4) Agile program or Project Management Skills (typically comprising managing business change, project management methods and tools, etc.); 5) IT General Knowledge Skills (typically comprising brokering applications, asset management, migration planning, development of service level agreements, etc.); 6) Technical IT Skills (typically comprising software engineering, security, data interchange, data management, etc.) and 7) Legal Environment (typically comprising data protection laws, contract law, procurement law, fraud, etc.)

VIII. THE EXPERT INTERVIEW

Two BTP specialists have confirmed in interviews the need for a standardized enterprise architecture framework like TOGAF.

IX. BTP RISK READINESS ASSESSMENT

The BTM must have in-depth knowledge of the TOGAF's "Business Transformation Readiness Assessment"; which means that s/he has the "Capacity to Execute" and the ability to perform all the information technology tasks required by the BTP, including the skills, tools, processes, and management capability for the implementation phase. Lately, there has been successful execution of a similar complex endeavour, and there are appropriate processes, methods, skills, and a heuristics based model for deciding what skills and activities are needed. The BTM must also design the "Enterprise Capacity to Execute"; which is the ability of the enterprise to perform all the tasks required by the endeavour, in areas outside of information technologies (IT), including the ability to make decisions, using the built-in tree reasoning model, within the limited time constraints; that is very typical to BTPs based upon similar complexity of endeavour. There are no non-IT-specific processes, discipline, and skills to deal with this type of endeavour. The BTM has to demonstrate the ability to manage such a type of BTP environment issues and requirements. There is recognition of such a need for knowledge and skills; that reconfirms the research project's detected knowledge gap [66].

The BTM's recommended activities in the assessment process of a BTP's readiness is to address the following business transformation requirements [66]: 1) determine the readiness STF factors that will impact the BTP; 2) to present the readiness factors using STF heuristics models; 3) to assess the readiness factors, including determination of readiness factor ratings & weightings. Assess the risks for each readiness factor and identify improvement actions to mitigate the risk. Work these actions into next iterations of the agile project management plan; 4) to assess the readiness for the BTP. A "Business Transformation Readiness Assessment" can be used to evaluate and to qualify the BTP's readiness to undergo the initiative. This assessment is based upon the determination and analysis/rating of a series of selected factors; that are fed in the tuneable tree. The results of the readiness assessment should be added to the TOGAF's "Capability Assessment". These solutions are then used to select the BTM and orient him through the BTP's architecture blue-print, to identify the tasks needed for the architecture of BTP, and to identify the risks [66].

X. BTP RISK ACTIVITIES

The BTM has to identify the "Business Transformation Risks and Mitigation Activities". S/he has to identify the risks related to the "Architecture Vision" and assess the initial level of risk, that is the reasoning tree root node (e.g., catastrophic, critical, marginal, or negligible) and the number of needed iterations. S/he has also to assign a mitigation strategy for each risk that is related to a factor. TOGAF offers a risk management framework [66].

STF that incorporates TOGAF, has two levels of risk that should be managed: 1) the "Initial Level of Risk": Risk categorization prior to determining and implementing mitigating actions; 2) the "Residual Level of Risk": Risk categorization after implementation of mitigating actions (if any).

XI. TOGAF MANAGERIAL RECOMMENDATIONS

The STF research offers a set of BTM profile's selection based on the managerial recommendations for TOGAF's integration. The STF research list of TOGAF's related recommendations (sorted by Importance):

1. The BTM must be an AofABIS; who is an enterprise architect. BTMs who are basically technocrats, proactive project architecture managers and advanced knowledge specialists should be capable of supporting and designing the transformation of the (e-)business environment in a proactive manner [22][37]. In fact, BTMs must be an xcellent AofABIS [38][66].

2. The TBM must have extensive experience in business transformation projects risks and readiness assessments. The BTP's implementation phase is the main cause of high failure rates in BTPs; that is why BTMs need enterprise architecture empirical hands-on skills. That encompasses the following: 1) knowledge of business architectures (BA) and business process management (BPM), 2) automated business environments [17], 3) agile project management, 4) knowledge management & integration, 5) organizational concepts, 6) management science methodologies 7) enterprise architecture and other concrete BTP implementation artefacts [66]. Therefore the researchers recommend experienced technocrats profile [6] for such BTPs and his or her educational curriculum [64].

3. The TBM must be an avant-garde innovation project manager. The TBM must be an excellent agile project manager, who is capable of implementing a "very light version" of the disciplines TOGAF, Service Oriented Architecture and BPM. The use of BPM will enhance the management of knowledge and help in the selection of a TBM [62].

4. The TBM must be an avant-garde innovation project manager and a BTP designer. The BTMs' skills and educational curriculum must comprise the knowledge of: business and enterprise architecture, automated real-time business process environments, agile project management, organizational behaviour, management science methodologies and concrete BIS implementation phase know-how [66].

5. The TBM has a holistic profile. This research shows that the BTM is an AofABIS with holistic cross-functional skills [16]; with a business engineering education [67]. The basic profile is a flexible and intelligence-based person that has cross-functional capacities. Transformed organizations and BTMs need more than basic BIS knowledge and educational techniques to exploit the inter-related avant-garde technologies in order to successfully conduct BTPs. Managing the complexity of skills and educational concepts require a mixed method that is mainly based on action research; a hyper-heuristics model [66][9].

6. The STF is an applicable framework for decision support system (STF_DSS). TBM selection depends on the project and company context. The BTM should be supported with a configurable decision making system like the STF [31]. Such BTM's selection and education need holistic just-in-time (JIT) methodologies, similar to BTM2 [9]. The STF is a JIT systems managerial framework or "management 2.0" component for the selection of business transformation managers. The authors' aim is to convert their relevant research outcomes into a managerially useful framework and pattern [13], and its hyper-heuristics tree that is suitable for a wide class of problem instances. The authors regard this as a major business and educational benefit [4]. The STF's decision tree, results in a set of possible solutions that determine BTM's skills. This tree can be also represented as an implementation of business processes modelling (BPM). Such a solution is optimal, because then the STF knowledge is stored in the business information system [1][64].

7. The BTM must be capable of identifying the "Business Transformation Risks and Mitigation Activities" [66]; and must also be capable to identify the risks associated with the "Architecture Vision" and assess the initial level

of risk and the rate of frequency associated with it.

8. The profile and the corresponding TOGAF managerial recommendations curriculum round up the STF's business transformation managers' pattern. Therefore the BTM has to adapt the enterprise architecture method to give priority to the implementation phase; and hence develop a BTP specific architecture pattern that should include [66]:

- Architecture maturity assessment- Architecture governance processes, organization, roles, and responsibilities
- Architecture skills assessment

9. The integration of the STF in the company's business processes and knowledge environment. The use of smart tools, automated workflows, integration and advanced graphical user interfaces are making BPM cheap to use. BPM will enhance the overall business intelligence because the smart use of BPM with STF rules and analytics will help the better decisions for the selection of BTM, with more insights. S/he would be respecting existing choreography standards, enabling to deliver quick return on investment & long-term success.

XII. THE STF PROTOTYPE OF THE EMPIRICAL MODEL

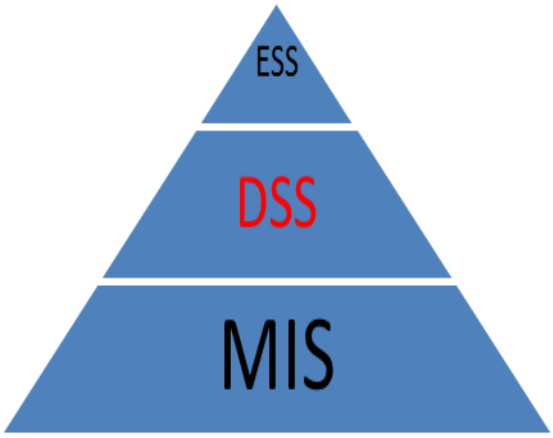

Fig. 7. *Decision systems by management level [32].*

The STF's empirical model is built to prove the research PoC, which has been developed using the Microsoft Visual Studio 2012 environment [59].

The PoC uses the Model- View- Controller (MVC) architectural pattern that collects the model data. This prototype is a real world decision support system (DSS) that can be used by middle managers [32]; where executive decision systems (ESS) is used by the executive management and management information system (MIS) by the production management, as shown in Fig. 7. The PoC is a real world system and is considered to be a concrete managerial benefit.

The PoC contains the STF's major components, and what will be primarily tested is the reasoning engine, which is based on the AAR heuristics model. This research PoC will serve to confirm the research's hypothesis and the hyper-heuristic model; that has a goal function, which calculates the best solution (DSSGoalFunction). Added to that, the authors have used interviews with experts to confirm the PoCs outcomes; which means that the STF_MHM is a mixed method based on a real world prototype. The results will be presented in the form of a set of recommendations.

XIII. THE STF'S BTM's PATTERN (STFBTMP)

The authors' aim is to convert their relevant research outcomes into a managerially useful framework [13]; and its hyper-heuristics tree processing model is used as a template that is suitable for a class of problem instances [4].

Therefore, it is planned to create a concrete STF environment that is based on a business process oriented transformation pattern [2]. This STF pattern will be in fact a STF business transformation managers' project pattern (STFBTMPP).

XIV. CONCLUSION

This is another article in a long series of research articles related to the STF research, which is based on the action research mixed method; the STF factors and TOGAF based managerial recommendations are the result of the literature review, surveys outputs, proof of concept and interviews.

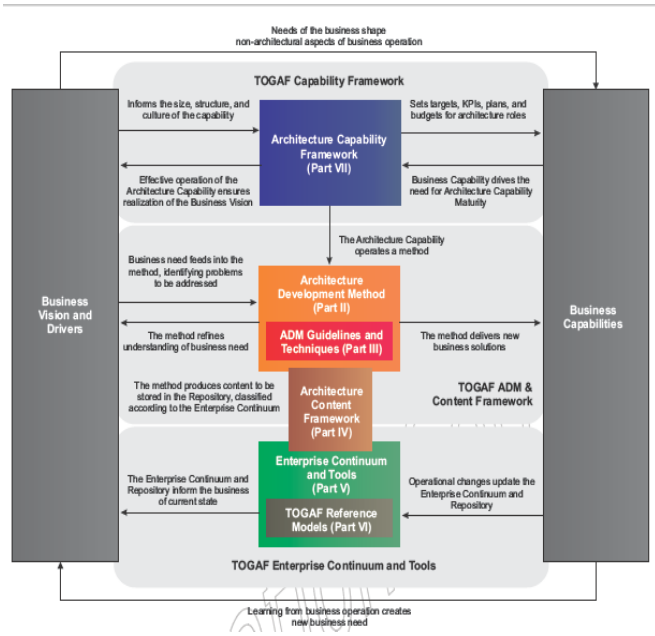

Fig. 8. *Linking Business to Business Information Technology [32].*

ISBN: 978-1-61804-225-5

The TOGAF environment permits that a BTM holistically manages the BTP; by linking the business environment and the business information technology.

These factors and TOGAF-based managerial recommendations are the base of the STF's tunable hyper-heuristics research model. In this article, the focus is on the STF's TOGAF based managerial recommendations, which are needed for finding the optimal BTMs' profiles to holistically manage the design and implementation of a BTP and the corresponding enterprise architecture.

There has been a lot developed and written on enabling success in transformation projects, but the authors propose to inspect why BTMs fail in the implementation phase of the BTP. That is mainly due to the BTMs' lack of knowledge in managing business integration and implementation and non-existence of adequate managerial recommendations. This phase's most important findings:

- Knowledge gap: The literature review proved the existence of a knowledge gap between the traditional management skills and the STF's managerial recommendations for BTP [62].
- Evolutionary Mixed Method: This research uses an evolutionary research model in order to create the initial BTM's profile based on the managerial recommendations [62].
- The STF proof of concept The PoC and interviews proved the approach and delivered the research's recommendations on how to select and educate BTMs.
- Managerial recommendations, benefits and framework: The qualitative hyper-heuristics model confirmed the survey's outcomes; and delivered the managerial recommendations and benefits. The STF research project proposes a concrete framework on how to select, train and evaluate a BTM. Hence improves the company's economical competitive advantage.
- BTM profile as an AofABIS: Actual environments produce general profiles that can hardly cope with heterogeneous complexity and fast changes. These high frequency changes are mainly due to the hyper-evolution of technology. The research proposes that the BTM is an AofABIS.
- The STFBTMP pattern: The STF's research defines the BTM profile and managerial recommendations that round up the BTM selection and educational pattern

Acknowledgment

In a work as large as this research project, technical, typographical, grammatical, or other kinds of errors are bound to be missed. In such a series of articles, it was unavoidable to allow for some overlapping. We are aware that it might be irritating to our "devoted" readers. However, this approach should enable access to general and occasional readers as well. Ultimately, all mistakes are the authors' responsibility. The authors encourage feedback from readers identifying errors in addition to comments on the work in general.

It was our great pleasure to prepare this work. Now our greater hopes are for readers to receive some small measure of that pleasure. The authors owe a special debt to Webster University who helped the first author in developing this project.

References

The references are sorted by the importance of the source to the research topic:

[1] SAP, "GBTM: Global Business Transformation Manager Master Certification (SAP Internal). July, 8th – 19th, 2013 in Potsdam, Germany, Business Transformation Academy. SAP, 2013.

[2] SAP, "BTM2: Business Process Management Business Transformation Academy". Germany. 2012.

[3] McMullen, P.R., Tarasewich, P., (2005). "A beam search heuristic method for mixed-model scheduling with setups", Int. J. Production Economics 96 (2005) 273–283. Elsevier.

[4] Vella, A., Corne, D. ; Murphy, C., (2009), "Hyper-heuristic decision tree induction". Sch. of MACS, Heriot-Watt Univ., Edinburgh, UK. Nature & Biologically Inspired Computing, 2009. NaBIC 2009. World Congress. http://ieeexplore.ieee.org/xpl/login.jsp?tp=&arnumber=5393568&url=http%3A%2F%2Fieeexplore.ieee.org%2Fxpls%2Fabs_all.jsp%3Farnumber%3D5393568, December 2nd, 2013

[5] Kalika, "eDBA, research model validation, BSI, Geneva, 2013

[6] A., Farhoomand, "Managing (e)business transformation". UK: Palgrave Macmillan, 2004.

[7] J., Tidd,. "From Knowledge Management to Strategic Competence", 2nd Edition, Imperial College, London, UK, 2006.

[8] J., Tidd, J., Bessant, "Managing Innovation, Integrating Technological, Market and Organizational Change", 4th Edition. USA: Wiley, 2009.

[9] A., Uhl, L., Gollenia, "A Handbook of Business Transformation Management Methodology", Gower. SAP. Germany. 2012.

[10] J, Whitten, L, Bentley '"Systems Analysis and Design Methods". McGraw-Hill & Irvin, 2011. USA.

[11] E., Chanaron, "DBA Workshop", GEM, 2010, Grenoble, France.

[12] Dick, B., (2002). "Action research: action and research" http://www.scu.edu.au/schools/gcm/ar/arp/aandr.html, December 2nd, 2013

[13] Markides, C. "Crossing the Chasm: How to Convert Relevant Research Into Managerially Useful Research", Journal of Applied Behavioral Science, March 2011 vol. 47 no. 1 121-134. London, UK.

[14] Quantitative, "Positivist Research Methods in Information Systems", 2010, http://dstraub.cis.gsu.edu/quant/

[15] M., Hoepft, "Choosing Qualitative Research: A Primer for Technology Education Researchers", Journal of Technology Education, Virginia Tech. 1997. USA.

[16] The Economist, "Inside the machine. A survey of E-management. Special report: E-management". The Economist. 2000, UK.

[17] F., Willaert, "XML-Based frameworks and standards for B2B e-commerce", PhD Research project, Faculteit Economische en Toegepaste Economische Wetenschappen Department. Katholieke Universiteit Leuven, 2001.

[18] IBM, Webinar, " BPM & EA for Better Business Outcomes eKit " http://www-01.ibm.com/software/info/bpm/ekit/bpmea. 2010.

[19] ECS, (2004). www.ecs.org/html/educationIssues/Research/primer/appendixA.asp

[20] Capgemini Consulting, "Business transformation: From crisis response to radical changes that will create tomorrow's business. A Capgemini Consulting survey". France, 2009.

[21] Capgemini, "Trends in Business transformation - Survey of European Executives". Capgemini Consulting and The Economist Intelligence Unit, France, 2007.

[22] Walsh, I., Kefi, H., Baskerville, R., "Managing culture creep: Toward a strategic model of user IT culture". Journal of Strategic Information Systems 19 (2010) 257–280. Journal homepage: www.elsevier.com/ locate/ jsis. Elsevier.

[23] T., Bourner, "'The research process: four steps to success", Arnold, 1996. London. United Kingdom.

[24] A., Jaszkiewicz, R., Sowiński, "The 'Light Beam Search' approach - an overview of methodology and applications", European Journal of Operational Research 113 (1999) 300-314

[25] Birudavolu, S., Nag, B., A Study of Open Innovation in Telecommunication Services: A Review of Literature & Trends. Indian Institute of Foreign Trade, India. 2011).

[26] Bruce, Deakin University, "The literature review", 2010 http://www.deakin.edu.au/library/findout/research/litrev.php#Bruce#Bruce, 2010

[27] Wes, W., "Beyond grounded theory: The use of a heuristic approach to qualitative research". Counselling and Psychotherapy Research: Linking research with practice. Taylor, Francis, 2001.

[28] S., David, D, Linthicum, "Enterprise Application Integration", Addison-Wesley Professional, 2000, USA.

[29] Quinlan,. C., 2011. "Business Research Methods". Dublin City University. Cengage Learning. Ireland. 2011.

[30] Markides, C., 2011. "Crossing the Chasm: How to Convert Relevant Research Into Managerially Useful Research", Journal of Applied Behavioral Science, March 2011 vol. 47 no. 1 121-134. London, UK.

[31] Şeref, Ravindra K. Ahuja, and Wayne L. Winston, "Developing Spreadsheet-Based Decision Support Systems", Michelle M.H. Dynamic Idea Publishing, 2007, Instructor Notes on DSS and data warehouse

[32] Laudon, K., Laudon, J., 2010. Management Information Systems, 11th Edition, Prentice Hall, USA.

[33] TechTerms , 2013, http://www.techterms.com/definition/heuristic, December 2nd, 2013

[34] Oxford Dictionaries, "heuristics", (2013). http://www.oxforddictionaries.com/definition/english/heuristic, December 2nd, 2013.

[35] Trad, A., "COSC DSS, Decision Support Systems – Labs results". Webster university 2013, Geneva, Switzerland.

[36] Trad, A., "The "Selection, and Training framework (STF) for Managers in Business Innovation Transformation Projects" - Overview of the development of the empirical model. IEEE 2013, BAME. Venice, Italy.

[37] Trad, A., Kalpić, D., "The Selection and Training Framework (STF) for Managers in Business Innovation and Transformation Projects - The Design and Implementation of the Research Model", 3rd position awarded paper. IMRA, Croatia, 2013.

[38] Trad, A., Kalpić, D., "The Selection and Training Framework (STF) for Managers in Business Innovation and Transformation Projects – The profile of an Architect of adaptive business systems", IMRA, USA. Submitted article.

[39] A., Trad, D. Kalpić, K. Fertalj, "Proactive business monitoring of the IS risk and quality". Proceedings of the 23rd International Conference on Information Technology Interfaces; 2002 June 24-27; Cavtat, Croatia. Zagreb: SRCE University Computing Center, University of Zagreb; 2002. p. 497-502.

[40] A. Trad, D. Kalpić, "Proactive Monitoring of the IS Risk and Quality", ITI 2002, Cavtat, Crotia.

[41] A. Trad, D. Kalpić, "Information Systems Risk and Quality Check (ISRQC)" – Practical Implementation. Proceedings of the International Conference on Information Technology Interfaces; 2002 Pula, Croatia. Zagreb: SRCE University Computing Center, University of Zagreb.

[42] A. Trad, "Audit, Control and Monitoring Design Patterns (ACMDP) for Autonomous Robust Systems (ARS)". International Journal of Advanced Robotic Systems, 2005, Volume y, Number x (200x), ISSN 1729-8806.

[43] A. Trad, "The Mobilere Transformation, by the use of BPEL and SOA", 2008, Geneva, Switzerland.

[44] A. Trad, "GEM DBA Workshop – Research Design" – Poster Presentation, March, 2011, Webster University, Geneva, Switzerland.

[45] A. Trad, D. Kalpić, "The Selection, Training, Follow and Evaluation STF for Managers in Business Innovation Transformation Projects "A Holistic Overview. IEEE 2011, Conference on Information Technology Interfaces; Cavtat, Croatia.

[46] A. Trad, D. Kalpić, "The "Selection, Training, Follow and Evaluation (STF), for Manager's in Business Innovation Transformation Projects - The Human Factor". Conference on Information Technology Interfaces; Cavtat; 2011.

[47] A. Trad, "STF for BTMs. DBA Proposal". Grenoble Ecole de Management, 2011, Grenoble, France.

[48] A, Trad, "The "Selection and Training STF, for Managers in Business Innovation Transformation Projects - The Proposal", GEM, 2011, France.

[49] Trad, A, "STF - The Selection and Training Framework Research Survey System". IBISM, Lausanne, Switzerland. 2013.

[50] Trad, A., Kalpić, D., "The Selection, and Training Framework (STF) for Managers in Business Innovation Transformation Projects" - The Background. , Conference on Information Technology Interfaces; Cavtat, 2013, Croatia.

[51] Trad, A., Kalpić, D., "The Selection, and Training Framework (STF) for Managers in Business Innovation Transformation Projects -The Profile" -. , Conference on Information Technology Interfaces; Cavtat, 2013, Croatia.

[52] Trad, A., Kalpić, D., "The Selection, and Training framework (STF) for Managers in Business Innovation Transformation Projects - The Literature Review". IEEE 2013, Centeris. Portugal

[53] Trad, A., "The Selection, and Training STF for Managers in Business Innovation Transformation Projects - The BPM and services implementation factors". Emerald, 2013, USA

[54] Trad, A., Kalpić, D,, "Transformation Quality and Risk Check (RQRC) – Theoretical Basis". Proceedings of the 23rd International Conference on Information Technology Interfaces; 1999 Jun 15-18; Pula, Croatia. Zagreb: SRCE University Computing Center, University of Zagreb; 1999. p. 497-502.

[55] Trad, A., "STF for BTMs. DBA Proposal." Grenoble Ecole de Management, Grenoble, France. 2011.

[56] Trad A, "The initial Proposal", GEM, France. 2010.

[57] Trad A, "The Selection and Training Framework (STF), for Managers in Business Innovation Transformation Projects - The Final Proposal", GEM, France. 2011.

[58] Trad A, "The Selection and Training Framework (STF) for Managers in Business Innovation Transformation Projects - The literature review", GEM, 2013, France.

[59] Trad, A., Kalpić, D., "The Selection, and Training Framework (STF) for Manager's in Business Innovation Transformation Projects – Educational Recommendations". 2014, EDEN; Zagreb. Croatia. Submitted research paper.

[60] Santa Cruz University, Write a literature review . http://library.ucsc.edu/help/howto/write-a-literature-review, 2011.

[61] Kelada, Why do the majority of change initiatives fail and what to do about it - The example of TQM - GEM, Grenoble. 2009.

[62] Trad, A., Kalpić, D., "The Selection, and Training framework (STF) for Managers in Business Innovation Transformation Projects - The Final Interview". IEEE 2014, Centeris. Portugal. Paper to be submitted.

[63] Trad, A., Kalpić, D., "The Selection, and Training Framework (STF) for Manager's in Business Innovation Transformation Projects – Managerial Recommendations". 2014, EDEN; Zagreb. Croatia. Submitted research paper.

[64] Trad, A., Kalpić, D., "The Selection, and Training Framework (STF) for Manager's in Business Innovation Transformation Projects – The Mathematical Model". 2014, EUROPMET; Interlaken. Switzerland. Submitted research paper.

[65] TOGAF, "TOGAF". The Open Group. www.open-group.com/togaf. USA. 2014.

[66] OpenGroup TOGAF, "Open Group Standard-TOGAF® Guide, Version 9.1". The Open Group. USA. 2011.

[67] HEC, (2014). http://www.hec.ulg.ac.be/en/node/1470. Belgium.

ADI methods for three-dimensional fractional diffusions

Moreno Concezzi, Renato Spigler
Department of Mathematics and Physics,
University "Roma Tre", Rome, Italy,
concezzi@mat.uniroma3.it, spigler@mat.uniroma3.it.

***Abstract*—ADI methods can be generalized to solve numerically multidimensional fractional diffusion equations, which describe fluid flows through porous media better than classical diffusion equations. A new, unconditionally stable, second-order and well balanced in space, third-order in time ADI scheme has been constructed and its convergence accelerated by an extrapolation technique coupled with the *PageRank* algorithm.**

***Index Terms*—anomalous (fractional) diffusion in three dimensions; Alternating Direction Implicit (ADI) methods; extrapolation; PageRank.**

I. Introduction

Diffusive flow problems occur in a number of applications, and hence have been extensively studied. Important examples are provided by seepage flows, groundwater hydraulics, and fluid dynamics in porous media; see [10], [2], e.g.. In 1856, H. Darcy [5] derived his celebrated equation, the "Darcy's law", that is $\mathbf{q} = -\mathbf{K}\nabla p$, where p is the pressure, $\mathbf{q} = (q_1, q_2, q_3)$ the fluid velocity, the indices referring to the three directions, x, y, and z, and $\mathbf{K} = (K_1, K_2, K_3)$ the percolation tensor. Below, we assume $\mathbf{K}$ diagonal. Darcy obtained such a rule through experiments on saturated flows of water through a column of soil, In heterogeneous media, when the flow is continuous and the Darcy's law holds, choosing the main directions of the percolation as the coordinate directions and neglecting gravity effects, the partial differential equation (PDE) describing a single-phase isothermal seepage flow can be written as

$$\nu^{-1} p_t = \nabla\cdot(\mathbf{K}\nabla p) + f(x_1, x_2, x_3, t),\ (x_1, x_2, x_3) \in \Omega, \quad (1)$$

[16], [7], [11], where p_t denotes time partial derivative and Ω is a given open bounded domain of $\mathbf{R}^3$ where the percolation occurs. The associated boundary conditions are given by $p(x_1, x_2, x_3, t)|_{\partial\Omega} = \Phi(x_1, x_2, x_3, t)$, and the initial condition by $p(x_1, x_2, x_3, 0) = \varphi(x_1, x_2, x_3)$, for suitable functions Φ, φ; ν^{-1} is the specific storage coefficient (taken constant), and $f(x_1, x_2, x_3, t)$ is some source or sink term.

Equation (1) was derived assuming the seepage flow to be continuous, and the Darcy's law does *not* hold in general for real seepage flows. Hence, in 1998 J. He [7] proposed a modified form of the Darcy's law, formulating it in terms of *fractional* Riemann-Liouville derivatives [14], that is as

$$\mathbf{q} = -\mathbf{K}\nabla^\alpha p, \qquad \nabla^\alpha := \left(\frac{\partial^{\alpha_1}}{\partial x_1^{\alpha_1}}, \frac{\partial^{\alpha_2}}{\partial x_2^{\alpha_2}}, \frac{\partial^{\alpha_3}}{\partial x_3^{\alpha_3}}\right),$$

where the operator ∇^α, with $\alpha := (\alpha_1, \alpha_2, \alpha_3)$, was introduced. The more general equation for seepage flow with fractional derivatives was thus obtained,

$$\nu^{-1} p_t = \partial_i^{\beta_i}\left(K_i \partial_i^{\alpha_i} p\right) + f(x_1, x_2, x_3, t), \quad (2)$$

where $\partial_i\beta_i \equiv \partial^{\beta_i}/\partial x_i$, and we used the summation convention. Here, $0 < \beta_i < 1$, $0 < \alpha_i \leq 1$, and $1 < \beta_i + \alpha_i \leq 2$, for $i = 1, 2, 3$.

Given the importance but, at the same time, the unavailability of analytic solutions to *fractional* partial differential equations (fPDEs), many authors have proposed, over the years, numerical methods to solve them, see [9], [17], [15], [21], [18], [19], [20], e.g. Yet, numerical methods for handling efficiently high-dimensional fPDEs seem to be rather few.

In this paper, we consider the 3D fPDE in (2) on the bounded domain, $\Omega := \prod_{i=1}^3 (0, L_i)$, and the time interval $(0, T]$. We assume that such a fractional equation has a unique and sufficiently smooth solution, when subject to Dirichlet boundary conditions, and some initial condition. The fractional operators involved Riemann-Liouville derivatives of order α_i, β_i, with respect to x_i. Other useful definitions of fractional derivatives exist, and among these, the Grünwald-Letnikov fractional derivative is for us most relevant, see [14], while the so-called *shifted* Grünwald-Letnikov derivative will be used in the numerical schemes. Fractional Riermann-Liouville derivatives of sufficiently regular functions coincide with those intended in the sense of Grünwald-Letnikov as well as in the sense of Caputo [14].

We construct a new, well "balanced", fractional version of the Alternating Direction Implicit (ADI) method, to solve numerically 3D diffusion fPDEs. Our algorithm is *unconditionally stable* for every fractional order of space derivatives, *second-order* accurate *in space*, and *third-order* accurate *in time*. Its convergence can be sped up adopting an extrapolation technique, along with an optimization realized through Google's *PageRank* algorithm.

Composing the two Grünwald-Letnikov fractional derivatives [14], the fPDE above becomes

$$\nu^{-1} p_t = K_i \partial_i^{\gamma_i} p + f(x, y, z, t) \quad \text{in}\,\Omega \times (0, T], \quad (3)$$

where we set $\gamma_i := \beta_i + \alpha_i$, for $i = 1, 2, 3$, and the K_i's are positive constants. Below, we construct a "fractional Alternating Direction Implicit" (fADI) scheme to solve numerically such a problem.

ISBN: 978-1-61804-225-5

II. FADI SCHEMES

We discretize space and time, as usual, setting $x_i^m := m_i h_i$ for $m_i = 0, 1, 2, \ldots, M_i$, $h_i := \frac{L_i}{M_i}$, and similarly for the time variable. The numerical approximation to $p(x_1^{m_1}, x_2^{m_2}, x_3^{m_3}, t^n)$, provided by the scheme at such points will be denoted by $p^n_{m_1,m_2,m_3}$, and similarly for the source term, f, and the boundary and initial values. The first-order derivative $\partial_t p$ in (3) is approximated by finite differences, and assume that p is sufficiently regular, so that the operators $\partial_i^{\gamma_i}$ can be discretized using the shifted fractional Grünwald-Letnikov derivative. Thus, we obtain the implicit scheme

$$\begin{aligned}&\frac{p^{n+1}_{m_1,m_2,m_3} - p^n_{m_1,m_2,m_3}}{\tau}\\ &= \frac{K_i}{h_i^{\gamma_i}} \sum_{s=0}^{m_i+1} g_{\gamma_i,s}\, p^{n+1}_{m_i+1-s,m_2,m_3}\\ &+ \frac{K_2}{h_2^{\gamma_2}} \sum_{s=0}^{m_2+1} g_{\gamma_2,s}\, p^{n+1}_{m_1,m_2+1-s,m_3}\\ &+ \frac{K_3}{h_3^{\gamma_3}} \sum_{s=0}^{m_3+1} g_{\gamma_3,s} p^{n+1}_{m_1,m_2,m_3+1-s} + f^{n+1}_{m_1,m_2,m_3},\end{aligned} \tag{4}$$

where the coefficients g's are defined in [14]. The fractional discrete operator

$$\delta_1^{\gamma_1} p^{n+1}_{m_1,m_2,m_3} := \frac{1}{h_1^{\gamma_1}} \sum_{s=0}^{m_1+1} g_{\gamma_1,s} p^{n+1}_{m_1+1,m_2,m_3}, \tag{5}$$

is known to provide an $\mathcal{O}(h_1)$ approximation of the Grünwald-Letnikov shifted fractional derivative of order γ_1, see [13], etc. The scheme in (4) can be rewritten in a more compact form as

$$\begin{aligned}&(1 - K_1\tau\delta_1^{\gamma_1} - K_2\tau\delta_2^{\gamma_2} - K_3\tau\delta_3^{\gamma_3})\, p^{n+1}_{m_1,m_2,m_3}\\ &= p^n_{m_1,m_2,m_3} + \tau f^n_{m_1,m_2,m_3}.\end{aligned} \tag{6}$$

In can be shown that the scheme in (4) has a *local truncation* error of order $\mathcal{O}(\tau) + \sum_{i=1}^3 \mathcal{O}(h_i)$, and is *unconditionally* stable.

Equation (6) (or (4)) yields a *linear* system of equations for $p^{n+1}_{m_1,m_2,m_3}$. Others than in the classical ADI method, such a system is not sparse, but a *large dense* linear system of equations. This calls for suitable efficient numerical methods, hopefully also unconditionally stable.

As in the classical ADI methods, we split the computations into three steps, corresponding to the three directions, x_1, x_2, and x_3, each step requiring a reduced computational load. An extra, higher-order, term is added to the left-hand side of equation (6), so to factor the operator into three parts, without affecting the overall convergence rate,

$$\begin{aligned}&(K_1K_2\tau^2\delta_1^{\gamma_1}\delta_2^{\gamma_2} + K_1K_3\tau^2\delta_1^{\gamma_1}\delta_3^{\gamma_3}\\ &+ K_2K_3\tau^2\delta_2^{\gamma_2}\delta_3^{\gamma_3} - K_1K_2K_3\tau^3\delta_1^{\gamma_1}\delta_2^{\gamma_2}\delta_3^{\gamma_3})\, p^{n+1}_{m_1,m_2,m_3}.\end{aligned} \tag{7}$$

Thus, we obtain the scheme

$$\begin{aligned}&(1 - K_1\tau\delta_1^{\gamma_1})(1 - K_2\tau\delta_2^{\gamma_2})(1 - K_3\tau\delta_3^{\gamma_3})\, p^{n+1}_{m_1,m_2,m_3}\\ &= p^n_{m_1,m_2,m_3} + \tau f^n_{m_1,m_2,m_3}.\end{aligned} \tag{8}$$

Splitting (8) in the three dimensions, we obtain the *unbalanced* scheme, which provides the solution at time t^{n+1},

$$(1 - K_1\tau\delta_1^{\gamma_1})\, p^{n+1/3}_{m_1,m_2,m_3} = p^n_{m_1,m_2,m_3} + \tau f^n_{m_1,m_2,m_3}, \tag{9}$$

$$(1 - K_2\tau\delta_2^{\gamma_2})\, p^{n+2/3}_{m_1,m_2,m_3} = p^{n+1/3}_{m_1,m_2,m_3}, \tag{10}$$

and

$$(1 - K_3\tau\delta^{\gamma_3})\, p^{n+1}_{m_1,m_2,m_3} = p^{n+2/3}_{m_1,m_2,m_3}, \tag{11}$$

which turns out to be of the first order in space [10].

We propose now a new *balanced* splitting of the ADI scheme in (8), which provides the solution at time t^{n+1} through three more balanced steps, obtained replacing the previous right-hand sides with $p^n_{m_1,m_2,m_3} + \frac{\tau}{3} f^n_{m_1,m_2,m_3}$, $p^{n+1/3}_{m_1,m_2,m_3} + \frac{\tau}{3} f^n_{m_1,m_2,m_3}$, and $p^{n+2/3}_{m_1,m_2,m_3} + \frac{\tau}{3} f^n_{m_1,m_2,m_3}$, respectively.

It can be shown that such second choice provides an algorithm second-order accurate in space and third-order in time [4].

Since the "load" represented by the source term enters this second scheme in a more balanced way, it is expected that such an algorithm performs better when there is little anisotropy, i.e., when the fractional orders γ_i, $i = 1, 2, 3$, do not differ appreciably.

Taking into account the boundary values $p^{n+1/3}_{0,m_2,m_3}$ and $p^{n+2/3}_{M_1,m_2,ma-3}$, we can construct the coefficients of the matrix, say A, of the linear system concerning the first step, see [4]. Then, using the boundary values $p^{n+2/3}_{m_1,0,m_3}$ and $p^{n+2/3}_{m_1,M_2,m_3}$, we obtain the matrix, say B, of the linear system concerning te second step. For each fixed (m_1, m_3), such a matrix presents some similarity with A. Finally, using the boundary values $p^{n+1}_{m_1,m_2,0}$ and $p^{n+1}_{m_1,m_2,M_3}$, we obtain the matrix C of the linear system concerning the third step, which, again, for each fixed (m_1, m_2), is analogous to A.

Examining the three matrices A, B, C, above, it can be seen that, at each time step, it is only required to solve, for each fixed pair (m_2, m_3) (at each x_1-level) a linear upper *triangular* system of size $M_1 - 1$, and similarly for the other systems. We refer to [4] for more details.

III. NUMERICAL IMPLEMENTATION

Here we apply our numerical method to solve 3D fractional diffusion problems. An example is given to illustrate its performance.

Our algorithm can be *optimized*, achieving an appreciable *acceleration*, exploiting Google's *PageRank* algorithm [8]. This method will be associated to an *extrapolation* technique, which determines the coefficients which make it optimal. A considerable amount of CPU time can be saved just resorting to the *extrapolation* technique [1]. This procedure also increases the accuracy of our algorithm up to the *third order* in time, see [3], [12]. The *extrapolated solution*, $q^n(\tau)$, is evaluated as

$$q^n(\tau) = \psi_1\, p^n(\tau) + \psi_2\, p^n\left(\frac{3}{4}\tau\right) + \psi_3\, p^n\left(\frac{\tau}{2}\right) + \psi_4\, p^n\left(\frac{\tau}{4}\right), \tag{12}$$

where the coefficients ψ's are suitably determined, see [4]. Here we have displayed the dependence of p^n on τ.

IV. A numerical example

Let the linear three dimensional fPDE

$$\begin{aligned}&\nu^{-1}\partial_t p = K_{11}\ {}_0D_1^\alpha p + K_{21}\ {}_1D_2^\alpha p + K_{12}\ {}_0D_2^\beta p\\&+K_{22}\ {}_2D_2^\beta p + K_{13}\ {}_0D_3^\gamma p + K_{23}\ {}_3D_2^\gamma p\\&+d_1\,\partial_1 p + d_2\,\partial_2 p + d_3\,\partial_3 p + f(x_1,x_2,x_3,t),\end{aligned} \tag{13}$$

where ${}_aD_b^\alpha p$ denotes the fractional Riemann-Liouville derivative of p of order α, in the interval $[a,b]$, be considered on the domain $(x_1,x_2,x_3)\in[0,2]^3$, $0<t\le T$, with

$$\begin{aligned}K_{11}&=\Gamma(3-\alpha)\,x_1^\alpha, & K_{21}&=\Gamma(3-\alpha)(2-x_1)^\alpha\\K_{12}&=\Gamma(3-\beta)\,x_2^\beta, & K_{22}&=\Gamma(3-\beta)(2-x_2)^\beta\\K_{13}&=\Gamma(3-\gamma)\,x_1^\gamma, & K_{23}&=\Gamma(3-\gamma)(2-x_3)^\gamma,\end{aligned}$$

$$d_i=\frac{1}{4}x_i,\quad i=1,2,3,$$

and the forcing term

$$\begin{aligned}&f(x_1,x_2,x_3,t)\\&:=-4\,e^{-t}x_1^2x_2^2x_3^2(x_1-2)(x_2-2)\\&(x_3-2)(3x_1x_2x_3-5x_1-5x_2-5x_3+8)\\&-[l_\alpha(x_1,x_3,t)+l_\gamma(x-3,x_1,t)+l_\alpha(x_2,x_1,t)\\&+l_\beta(x_1,x_2,t)+l_\beta(x_3,x_2,t)+l_\gamma(x_2,x_3,t)].\end{aligned} \tag{14}$$

Here $l_\delta(u,v,t) := g(u,t)\,h_\delta(v)$, being $g(u,t) := 32\,e^{-t}u^2(2-u)^2$, and

$$h_\delta(u):=u^2+(2-u)^2-\frac{3(u^3+(2-u)^3)}{3-\delta}+\frac{3(u^4+(2-u)^4)}{(3-\delta)(4-\delta)},$$

where δ can be α, β or γ.

Dirichlet homogeneous boundary conditions are imposed, as well as the initial condition

$$p(x_1,x_2,x_3,0)=4x_1^2(2-x_1)^2x_2^2(2-x_2)^2x_3^2(2-x_3)^2.$$

The analytical solution to such a problem is given by

$$p(x_1,x_2,x_3,t)=4x_1^2e^{-t}(2-x_1)^2x_2^2(2-x_2)^2x_3^2(2-x_3)^2,$$

see [6], and it is used to *validate* our 3D algorithm and test its performance.

TABLE I
L^∞ and L^2 norm discrepancies for the Example, when the *balanced* scheme is used, at time $T=1$, for several values of N, and $\tau=h=2/N$.

(α,β,γ)	N	$\|q^n_{fADI}-q^n_{ADI}\|_\infty$	$\|q^n_{fADI}-q^n_{ADI}\|_2$
(1.2, 1.2, 1.2)	256	6.1758 E-7	3.8458 E-6
	512	2.2548 E-7	7.8442 E-7
(1.4, 1.5, 1.6)	256	2.8287 E-7	1.1205 E-6
	512	3.7852 E-8	3.7854 E-7
(1.9, 1.9, 0.9)	256	1.1582 E-7	5.7852 E-7
	512	1.7855 E-8	5.0023 E-7
(2.0, 2.0, 2.0)	256	8.1158 E-8	8.7852 E-7
	512	1.7852 E-8	6.7852 E-8

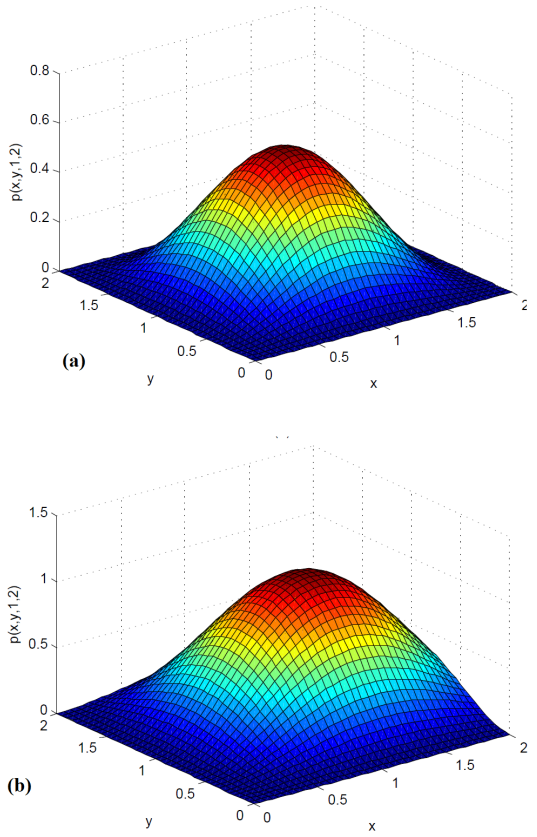

Fig. 1. (a) Classical solution (obtained by a fine grid numerical ADI method with $\tau=h/16$ and $h=1/64$), and (b) exact (analytical) fractional diffusion solution with $(\alpha,\beta,\gamma)=(1.4,1.5,1.6)$, for $x_3=1$ and $T=2$. The same forcing function was used in both cases.

Fig. 1 shows clearly the effect of replacing ordinary derivatives, (α,β,γ) = $(2,2,2)$, with fractional derivatives. Here, (α,β,γ) = $(1.4,1.5,1.6)$, which implies *anomalous* diffusion.

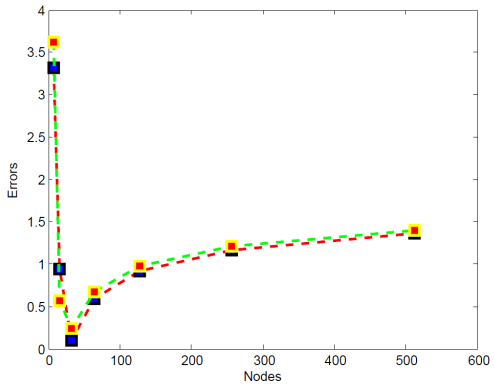

Fig. 2. Absolute numerical error between the exact and the numerical solution of the fPDE of the Example, at $T=2$, with $(\alpha,\beta,\gamma)=(1.4,1.5,1.6)$.

Fig. 2 shows the numerical errors $\|q^n-P^n\|$, in the L^2 and L^∞ norms, on a log-scale, being $P^n\equiv p(x_{m_1},x_{m_2},x_{m_3},t^n)$ the exact solution to the fPDE, and $q^n\equiv q,\tau$ is its approximation given obtained through equation (12).

ISBN: 978-1-61804-225-5

V. Conclusion

An ADI method has been constructed to solve numerically multidimensional fractional diffusion equations. The algorithm is unconditionally stable, second-order in space, third-order in time, and its convergence can be made faster by some extrapolation strategy and the *PageRank* algorithm. The scheme is better balanced with repect to previously existing schemes, assigning an equal weight to the three steps, in each space direction. More details can be found in [4].

Acknowledgment

This work was supported, in part, by the Italian GNFM-INdAM.

References

[1] Chen, S.,Liu, F., *ADI-Euler and extrapolation methods for the two dimensional fractional advection-dispersion equation*, J. Appl. Math. Comp., **26**, 295-311, 2008.

[2] Chou, H., Lee, B., and Chen, C, *The transient infiltration process for seepage flow from cracks*, Western Pacific Meeting, Advances in Subsurface Flow and Transport: Eastern and Western Approaches III, Eos Trans. AGU, 2006.

[3] Concezzi, M., Spigler, R., *Numerical solution of two-dimensional fractional diffusion equations by a high-order ADI method*, Commun. Appl. Ind. Math., 2013, printed online; **3**, No. 2 (2012), in print. [http://dx.doi.org/10.1685/journal.caim.421]

[4] Concezzi, M., Spigler, R., *An ADI method for the numerical solution of 3D fractional reaction-diffusion equations in porous media*, 2014, submitted.

[5] Darcy, H., *Les fontaines publique de la Ville de Dijon*, Western Paris, France: Dalmont, 1856.

[6] Deng, W., Chen, M., *Efficient numerical algorithms for three-dimensional fractional partial differential equations*, arXiv:1303.4628v1, 2013.

[7] He, J., *Approximate analytical solution for seepage flow with fractional derivatives in porous media*, Comput. Methods Appl. Mech. Eng. **167**, 57-68, 1998.

[8] Kamvar, S., Haveliwala, T., Manning, C., and Golub, G., *Extrapolation Methods for Accelerating PageRank Computations*, Welfth International World Wide Web Conference, 2003.

[9] Liu, F., Anh, V., Turner, I., Zhunag, P.*Numerical simulation for solute transport in fractal porous media*, ANZIAM J. **45**, 461-473., 2004.

[10] Liu, Q., Liu, F., Turner, I., and Anh, V., *Numerical simulation for the* $3D$ *seepage flow with fractional derivatives in porous media*, IMA J. Appl. Math. **74** , 178-200, 2009.

[11] Luo, Z.-J., Zhang, Y.-Y., and Wu, Y.-X., *Finite element numerical simulation of three-dimensional seepage control for deep foundation pit dewatering*, Hydrodyn. **20**, 596-602, 2008.

[12] Marchuk, G.I., and Shaidurov, V.V., *Difference Methods and Their Extrapolations*, Springer-Verlag, New York, 1983.

[13] Meerschaert, M. M. and Tadjeran, C., *Finite difference approximations for fractional advection-dispersion flow equations*, J. Comput. Appl. Math. **172**, 65-77. 2004.

[14] Podlubny, I., *Fractional Differential Equations*, New York: Academic Press, 1999.

[15] Roop, J. P., *Computational aspects of FEM approximation of fractional advection dispersion equations on bounded domains in* R^2, J. Comput. Appl. Math. **193**, 243-268, 2006.

[16] Rushton, K. R. and Redshaw, S. C, *Seepage and Groundwater Flow*, Brisbane, Australia: Wiley-Interscience Publication, 1979.

[17] Shen, S. and Liu, F., *Error analysis of an explicit finite difference approximation for the space fractional diffusion with insulated ends*, ANZIAM J. **46**, 871-887, 2005.

[18] Smith, D.D., *Numerical Solution of Partial Differential Equations: Finite Difference Methods*, Oxford Applied Mathematics and Computing Sciences Series, Oxford University Press, 1990.

[19] Yu, Q., Liu, F., Anh, V., and Turner, I., *Solving linear and nonlinear space-time fractional reaction-diffusion equations by Adomian decomposition method*, Int. J. Numer. Methods Eng. **74**, 138-158., 2008.

[20] Zhang, H., Liu, F., and Anh, V., *Numerical approximation of Lévy-Feller diffusion equation and its probability interpretation*, J. Comput. Appl. Math. **206**, 1098-1115, 2007.

[21] Zhuang, P., and Liu, F., *Implicit difference approximation for the time fractional diffusion equation*, J. Appl. Math. Comput. **22**, 87-99, 2006.

A Suggested Modification of Millionshchikov's Zero-Fourth Cumulant Hypothesis

Christos Mamaloukas, Amitabha Chanda, Himandri Pai Mazumdar

***Abstract*—**Over a few decades researchers, working in the field of turbulence, are examining the zero-fourth cumulant model, proposed by Millionshchikov. Numbers of modifications have been suggested. In some cases the problem of negative energy at the initial stage is observed and further modification is suggested. Some have tried to point out that the value of fourth cumulant may not remain zero all through the hierarchy of eddies vis-à-vis over all length scales and suggested different modification.

In the present paper we have tried to suggest a new model. Its viability has also been examined to some extent. In the final period decay of isotropic turbulence, the smallest eddies of the largest wave number only are active. Viscous dissipation of turbulent energy in the form of thermal energy takes place in this final period. The largest wave number is defined as $k_\infty = \left(\frac{\nu^3}{2}\right)^{-\frac{1}{4}}$. In the final period decay, neither inertia force nor pressure gradient takes part in the decay process. But these two terms, in fact, are the sources of third order moment.

Keeping this in mind we have tried to develop a model for fourth cumulant, expressed as $\tilde{K}_4 = \overline{\tilde{u}^4} - \overline{\left(\tilde{u}^2\right)^2}$ in wave number space. In the present case we would use the symbol $\tilde{u}$ only, since in isotropy $\overline{\tilde{u}_1^4} = \overline{\tilde{u}_2^4} = \overline{\tilde{u}_3^4}$ and $\overline{\tilde{u}_1^2} = \overline{\tilde{u}_2^2} = \overline{\tilde{u}_3^2}$. With targets given above, we present a model of $\tilde{K}_4$.

***Keywords*—**Millionschikov's hypothesis, zero-fourth cumulant hypothesis, homogeneous and isotropic turbulence, Hermite polynomial.

I. Introduction

In "zero fourth cumulant hypothesis" of Millionshchikov [1] second and fourth order moments are related as in normal distribution. The hypothesis goes also by the name of quasi-normal hypothesis. Millionshchikov has proposed that the two point distribution of simultaneous velocity amplitudes in a turbulent flow is quasi-normal. A lot of research has been done on this hypothesis. Research papers of legendary mathematicians like Heisenberg [2], Obukhov [3], Batchelor [4], Chandrasekhar [5] and Reid and Proudman [6] mentioning. Experimental results have also been analyzed by Batchelor and Uberoi [7] to verify the authenticity of this hypothesis.

Heisenberg has extended the hypothesis to the distribution of Fourier coefficients in two times. On the other hand, Reid and Proudman examined the hypothesis in the decay of homogenous turbulence using three point simultaneous velocity fluctuations. Chandrasekhar has studied the hypothesis in hydromagnetic turbulence. Along with the experimental works of Batchelor and Uberoi, the theoretical works conducted by Ghosh [8] may be mentioned.

Recently, there is a spurt of work considering the viability or otherwise of this hypothesis. Bos & Rubenstein [9], Chen, H., Herring, J.R., Kerr, R.M., & Kraichnan R.H [10], Chen, S. & Kraichnan, R.H. [11], Mazumdar, H.P. & C. Mamaloukas [12] and Mamaloukas [13] have studied the hypothesis in detail.

Suggestions have also been forwarded from time to time to modify the hypothesis. Ogura [14] has suggested some modification. Mirabel [15] has incorporated some modification to remove the discrepancies presented in the suggestion made by Ogura. The suggestion vis-à-vis objection regarding the viability of Millionshchikov hypothesis forwarded by Kraichnan [16] is note-worthy. In the present paper we shall try to suggest a modification of the "zero-fourth cumulant hypothesis" of Millionshchikov. We would confine our study to one-point one-time correlations in isotropic turbulence, and in wave number space as well.

II. Equations of Motion in Isotropic Turbulence

We have studied homogenous and isotropic turbulence. It is observed that in the final period of decay only the smallest eddies are active and viscous dissipation is the only mechanism through which turbulent energy decays in the form of thermal energy. The size or the length scale of these smallest eddies is given as $\lambda_0 = \left(\frac{\nu^3}{2}\right)^{\frac{1}{4}}$. In wave number space these smallest eddies have the largest wave number, as $k_\infty = \left(\frac{\nu^3}{2}\right)^{-\frac{1}{4}}$. In the final period of decay neither inertial force nor pressure gradient takes part in the decay process. But these

C. Mamaloukas, Department of Statistics, Athens University of Economics and Business, Athens, 10434, Greece, email: mamkris@aueb.gr
C. Amitabha, Visiting Faculty, Calcutta University, P36/1, Manasbag, Kolkata 700056, India, email: amitabha39@yahoo.co.in and amitabha39@gmail.com.
H.P. Mazumdar, Indian Statistical Institute, Calcutta -- 700035, India, email: hpmi2003@yahoo.com

two terms, in fact, are the sources of third order moment. We now try to examine this point from the Navier-Stokes equation of homogenous and isotropic turbulence. The unit density, incompressible homogenous and isotropic fully developed turbulent flow in absence of external force is governed by the following equations.

$$\frac{\partial u(x,t)}{\partial t}+\left[u(x,t)\cdot\nabla u(x,t)-\nabla p(x,t)\right]=\nu\Delta u(x,t) \qquad (1)$$
$$\nabla u(x,t)=0$$

Kraichnan & Panda [17] observe that in turbulent flow the variance of the nonlinear term in the Navier-Stokes equations i.e. $\left[u(x,t)\cdot\nabla u(x,t)-\nabla p(x,t)\right]$ is on average smaller than what would be expected from a Gaussian estimate. More precisely, if one constructs a flow field consisting of random statistically independent Fourier modes exhibiting the same energy spectrum as the turbulent flow considered, the variance of the nonlinear term will be larger than that of the original field. This depletion of nonlinearity is the result of a self-organization process of the turbulent flow, a process which is, itself, due to the nonlinear term in the Navier-Stokes equations. Kraichnan and Panda give importance on the velocity-vorticity alignment in turbulent flows. They show it to be one expression of a more general, underlying property of nonlinear systems. We consider that this depletion of nonlinearity is an important feature of turbulent flows, since the nonlinearity of the N-S equations is the heart of the turbulence problem.

The nonlinear term of the Navier-Stokes equations is a vector and its mean value is zero in isotropic turbulence. It is important to study the strength of the fluctuations of the nonlinear term and its depletion.

In order to examine the strength of the fluctuations of the nonlinear term and its depletion, we focus on the nonlinearity spectrum, which we shall define below. This spectrum measures the strength of the fluctuations of the nonlinear term as a function of scale, just like the energy spectrum does for the strength of velocity fluctuations. Whereas the characterization of the energy spectrum has received an enormous amount of attention in the field of turbulence research, only very few investigations consider the nonlinearity spectrum. To our knowledge, only the works by Chen, Herring & Kraichnan, Nelkin & Tabor [18] and Ishihara, T., Kaneda, Y., Yokokawa, M., Itakura, K. , & Uno, A [19] have considered this quantity. Chen et al. performed low resolution Direct Numerical Simulations and compared their results to the Direct Interaction Approximation (DIA). No information was obtained on the inertial range behavior of this quantity, since the Reynolds number was too low in their simulations. Higher Reynolds numbers could in principle be obtained by using the DIA, but physically incorrect behavior is observed by Kraichnan in the inertial range dynamics of the original Eulerian DIA. Nelkin & Tabor considered only the scaling of the potential part of the advection term, assuming that the full nonlinear term scales as its potential part. Only the high resolution simulations by Ishihara et al. give an idea on the inertial range scaling of several fourth order spectra.

It is shown by Bos & Rubenstein that, in the inertial and dissipation range, the nonlinearity spectrum is given by

$$w(k)=\tilde{u}^{\frac{2}{3}2^{\frac{3}{4}}}k^{\frac{1}{3}}f(k\eta).$$

For very high Reynolds numbers $\tilde{u}$ is the root-mean-square (rms) velocity fluctuation. The function $f(k\eta)$ tends to a constant value in the inertial range and its value is approximately 0.8 times the value of its Gaussian estimate.

The total depletion of nonlinearity is found to exhibit some sub-Gaussian behavior. Gryanik & Hartmann [20] have observed from CBL data that the Millionshchikov hypothesis of quasi-normal (Gaussian) distribution of the one-point fourth-order moments fails for convective boundary layer conditions. This is because the effect of the semi organized coherent structures (plumes) leads to skewed distributions; the third-order moments are non-zero. It must be connected with a certain order in the flows, but how this manifests itself in an instantaneous flow field cannot be guessed from the statistical considerations presented here. The nonlinear term consists of two parts: the advection term and the pressure gradient term. The pressure spectrum, (Gotoh & Fukayama [21]) $\pi(k)$ scales approximately as $\pi(k)\sim 2^{\frac{4}{3}}k^{-\frac{1}{3}}f(k\eta)$ and the pressure gradient spectrum scales as $\nabla\pi(k)\sim 2^{\frac{3}{4}}k^{-\frac{7}{3}}f(k\eta)$

It may be noted, however, that this scaling appears only at relatively high Reynolds number, compared to the appearance of K41 [22] scaling for the energy spectrum. It is shown by Bos & Rubenstein that at large Reynolds numbers the mean square nonlinearity is proportional to the Gaussian value, the ratio being 0.65. The variance of the nonlinearity is therefore dominantly determined by the advection term. The depletion of nonlinearity implies hereby directly a depletion of the sweeping compared to the kinematic sweeping induced by a field consisting of independent Fourier modes. Recent works of Hans C. Eggers and Martin Greinerb [23] and Servidio, S., Matthaeus, W. H., & Dmitruk, P. [24] are worth mentioning.

In this context we refer to the work by Chen, H., Herring, J.R., Kerr, R.M., & Kraichnan, R.H., which discusses the possibility of a reduction of sweeping in turbulence. They argue that third order cumulants are small but nonzero quantities. But in the pre-viscous dissipation ranges, dominated by large eddies of smaller wave number k triple order interaction are so great in number that their total contribution cannot be ignored to get to the realistic analysis of turbulence. Chen, H., Herring, J.R., Kerr, R.M., & Kraichnan, R.H. argue that a complete reduction of sweeping is improbable for stochastically forced turbulence. Their arguments are not in disagreement with the experimental results, obtained thereafter.

The dependence of the large and small scales and the sweeping is influenced, as estimated, by purely kinematic

arguments and is partially but definitely not completely suppressed. In this light, the depletion of nonlinearity can also be interpreted as a reduction of Eulerian acceleration, suggesting a larger Eulerian coherence for turbulence than for advection by random Fourier modes. The possible link of this enhanced coherence with inertial range and dissipation range intermittency is not clear at present. The super-Gaussian values of the large-scales of the nonlinearity spectrum were shown to be related to the non-Gaussianity of the Reynolds-stress-fluctuation spectrum. The physical importance of this relation for the dynamics of turbulent flow seems to deserve further research.

We mention here that a similar picture (large-scale super-Gaussian behavior and sub-Gaussian inertial range and dissipation range behavior), was observed in the depletion of advection (Bos et al.), where the inertial range scaling of the advection spectrum also displayed a constant reduction with respect to its Gaussian value.

III. The Present Model

Given above the background of study of nonlinearity vis-à-vis third order moment of turbulent flow we would now try to present a new model of one point one time moment in homogenous and isotropic turbulence of incompressible fluid with unit density. The main considerations used for constructing the model may be enumerated as below.

1. At the viscous dissipation range i.e where $k \to \infty$, turbulence energy dissipates only in the form of thermal energy. In this range interaction among eddies of different size ceases to exist. Distribution of Fourier components of velocity fluctuation is assumed Gaussian. Zero-fourth cumulant hypothesis is strictly followed in this range.
2. As wave number becomes smaller and smaller a part of turbulence energy, not the whole, dissipates as thermal energy and the residual part is involved in interacting with Fourier modes of velocity fluctuations and cascading from smaller wave number to larger wave number. As k progresses to the smallest number, it crosses universal equilibrium range and large eddy range one after the other. In this passage the ratio between dissipated thermal energy and internal energy involved in interaction and cascading becomes less and less. In these ranges third order interaction is non-zero which indicates the strict presence of third order cumulant, however small it may be.

In consideration of the above points, we now present the following model, It may be noted that we are restricting our study to wave number space only of isotropic turbulence.

$$1.\ \tilde{K}_4 = \overline{\tilde{u}^4} - \overline{\left(\tilde{u}^2\right)^2} = 0 \text{ for } k = k_\infty, \text{ and}$$

$$2.\ \tilde{K}_4 = \overline{\tilde{u}^4} - \overline{\left(\tilde{u}^2\right)^2} > 0 \text{ for } k << k_\infty$$

With targets given above we present a near-Gaussian model of distribution of *u*. The probability density of the proposed model is given as below.

$$\omega = \frac{1}{\sigma\sqrt{2\pi}} e^{-\frac{u^2}{2\sigma^2}} \left\{1 + U\left(1 - \frac{k}{k_\infty}\right)\sum_{i=3}^{\infty} \frac{c_i}{i!} H_i\left(\frac{u}{\sigma}\right)\right\} \quad (2)$$

Here $U = 0$ for $k \approx k_\infty$, and U=1 for $k < k_\infty$. In addition c_i's are given as below,

$$c_3 = \frac{\overline{x^3}}{\sigma^3},\ c_4 = \frac{\overline{x^4}}{\sigma^4} - 3,\ c_5 = \frac{\overline{x^5}}{\sigma^5} - 10\frac{\overline{x^3}}{\sigma^3} \quad (3)$$

H is the Hermite polynomial. The first three Hermite polynomials in the above expression are given as below,

$$\begin{aligned} H_3(x) &= 8x^3 - 12x \\ H_4(x) &= 16x^4 - 48x^2 + 12 \\ H_5(x) &= 32x^5 - 160x^3 + 120x \end{aligned} \quad (4)$$

ω being a probability density, it becomes equal to unity, if summed up over all Fourier modes. So, integrating over the whole range of *u* we get the following condition.

$$\int \omega du = 1 \quad (5)$$

ω becomes a Gaussian probability density ω' in viscous dissipation range and fourth cumulant becomes equal to zero satisfying zero-fourth cumulant hypothesis of Millionshchikov. But in the other ranges it is not so.

For viscuous dissipation range, when $k \to \infty$ we have the following expression for ω,

$$\omega' = \frac{1}{\sigma\sqrt{2\pi}} e^{-\frac{u^2}{2\sigma^2}} \quad (6)$$

ω' in (6) is the probability density of Gaussian distribution, that supports zero-fourth cumulant hypothesis. For other ranges $\left(k << k_\infty\right)$ we shall use the expression ω'' for ω' to show the difference of these two probability densities. ω'' is given as below,

$$\omega'' = \frac{1}{\sigma\sqrt{2\pi}} e^{-\frac{u^2}{2\sigma^2}} \left\{1 + \sum_{i=3}^{\infty} \frac{c_i}{i!} H_i\left(\frac{u}{\sigma}\right)\right\} \quad (7)$$

It may be noted that the near-Gaussian probability, expressed by ω'' is far from Gaussian ω'

Integrating (7) over the whole range of values of *u* we get as below,

$$\omega'' du = \int \left\{ \frac{1}{\sigma\sqrt{2\pi}} e^{-\frac{u^2}{2\sigma^2}} \left\{ 1 + \sum_{i=3}^{\infty} \frac{c_i}{i!} H_i\left(\frac{u}{\sigma}\right) \right\} \right\} du \quad (8)$$

From (8) we can find the third order cumulant as below,

$$\int u^3 \omega'' du = \int u^3 \left\{ \frac{1}{\sigma\sqrt{2\pi}} e^{-\frac{u^2}{2\sigma^2}} \left\{ 1 + \sum_{i=3}^{\infty} \frac{c_i}{i!} H_i\left(\frac{u}{\sigma}\right) \right\} \right\} du \quad (9)$$

The third order cumulant is zero in Gaussian distribution. But for the present near-Gaussian distribution (9) we have the following expression for third order cumulant, after using (6)

$$\int u^3 \omega'' du = \int u^3 \left\{ \frac{1}{\sigma\sqrt{2\pi}} e^{-\frac{u^2}{2\sigma^2}} \sum_{i=3}^{\infty} \frac{c_i}{i!} H_i\left(\frac{u}{\sigma}\right) \right\} du \quad (10)$$

IV. Conclusion

It has been opined by Kraichnan that even if zero fourth cumulant theory of Millionshchikov does not hold good in fully developed turbulence, third order interaction is weak. Only because of large number of these interactions their total impact cannot be ignored. As a result, there is a nonzero third cumulant indicating non-Gaussianity in distribution of velocity components. From this understanding it may be conjectured that velocity components are distributed in a near Gaussian pattern. In this paper we have considered one time one point moments in isotropic turbulence. In the background of the sets of weak third order interaction we have used Hermite polynomial to build a non-Gaussian probability density for ranges beyond viscous dissipation range.

We have ignored any change in the distribution of third order interaction in different ranges of turbulence. It may be observed that different non Gaussian probability densities may be considered by suitably truncating Hermite polynomials in their expressions. But the authenticity of such exercise would depend on experimental verification. This may be an open problem.

References

[1] M. D. Millionshchikov. 1941. Dokl. AN SSSR, v32, no.3.
[2] Heisenberg, W. 1948. Z. Physik, 124, 628.
[3] Obukhov, A.M. 1949. Doklady Akad. Nauk. S.S.S.R. 66, 17.
[4] Batchelor, G.K. 1951.Proc. Cambridge Phi. Soc., 47, 359.
[5] Chandrasekhar, S. Proc. 1951. Roy. Soc. (London), A210, 18.
[6] Reid, W.H. & I. Proudman. 1954. Trans. Roy. Soc. (London), A247, 163.
[7] Uberoi. 1953. J. Aeronautical Sc.20, 197.
[8] Ghosh K.M. 1972, Indian Journal of Pure and Appl.Math.,Vol. 3, No.1, p. 157
[9] Bos & Rubenstein. arXiv:1308.0213v1. Aug, 2013.
[10] Chen, H. , Herring, J.R. , Kerr, R.M. , & Kraichnan, R.H. 1989. Phys. Fluids A, 1, 1844.
[11] Chen, S & Kraichnan, R.H. 1989. Phys. Fluids A, 1, 2019.
[12] H. P. Mazumdar and Christos Mamaloukas. 2012. Athens ATINER Conference Paper Series, no. MAT 2012-0103.
[13] C. Mamaloukas, “A New Look at the Final-Period Decay of Homogeneous Isotropic Turbulence”, International Mathematical Forum, Vol. 8, 2013, no. 10, 495 – 499
[14] Y. Ogura. .1963. J Fluid Mech., v16, no.1.
[15] A. P. Mirabel. 1969. Izv AN SSSR, Mekhanika Zhidvos l Gaza., v4, no.5, pp 171-176.
[16] Kraichnan, R.H. 1957. Physical Review. V 107, no. 6.
[17] R.H. Kraichnan & R. Panda 1988. Phys. Fluids, 31, 2395.
[18] Nelkin, M. & Tabor, M. 1990. Phys. Fluids A, 2, 81.
[19] Ishihara, T. , Kaneda, Y. , Yokokawa, M. , Itakura, K. , & Uno, A. 2003. J. Phys. Soc. Japan, 72.
[20] Gryanik, V.M & Hartmann, 2005. J. Workshop on Interdisciplinary Aspects of Turbulence. Schlo_ Ringberg at Lake Tegernsee.
[21] Gotoh, T. & Fukayama, D. 2001. Phys. Rev. Lett., 86, 3775.
[22] Kolmogorov, A.N. 1941. Dokl. Akad. Nauk. SSSR, 30, 301.
[23] Hans C. Eggersa and Martin Greinerb, arXiv:hep-ph/0011291v1
[24] Servidio, S. , Matthaeus, W. H. , & Dmitruk, P. 2008. Phys. Rev. Lett., 100, 095005.

3-D modelling of fractal nanoclusters using the iterated affine transformations systems method

Avilov S. V., Zhukalin D.A., Bitutskaya L.A., Domashevskaya E.P.

***Abstract*—** In the current work an approach for fractal nanocluster 3-D modelling is proposed using the iterated affine transformations system method. The symmetry of regular polyhedra concept is applied. It is shown that the models can be used to interpret experimental results.

***Keywords*—** fractal, nanocluter, symmetry, polyhera, modelling, iterated affine transformations

I. Introduction

THE concept of reflection, turn and translation symmetries is widely used in crystallography to describe the formation principles of crystals [1,2]. However, nanosystems do not conform with Euclidean geometry's principles and often form a variety non-Euclidean structures, including fractal structures with adaptive and biogenic properties [3-5]. These structures may seem chaotic, however it was found that the addition of components such as CNTs into a dispersed system can modify the morphology and properties of the resulting hybrid system without affecting the chemical composition [6,7]. Nowadays there is no universal method to describe such complex systems, which could characterize their symmetrical transformations combined with chaotic quality.

II. METHOD

A new 3-D modeling method based on the iterated affine systems algorithm [8,9] is proposed to describe the morphology of fractal nanosystems. The choice of the symmetry is of primary importance for the fractal formation, thus by defining the relative spacial arrangement of the contracting affine reflections of a primary space it is possible to create a kernel cluster that will define the symmetry of the resulting dot fractal structure.

For instance, to describe the morphology of a GaSb [10,11] cluster with an icosahedral fractal symmetry [3,12] 12 reflections of a singular cube in Cartesian space are placed in the vertices of an icosahedron and one additional reflection is placed in the middle denoting a central cluster (Fig. 1). Each of the reflections have a primarily defined contraction ratio. The used system of affine transformation matrixes is the following:

$$T_1\left(\begin{bmatrix} x \\ y \\ z \end{bmatrix}\right) = \begin{bmatrix} 0.333 & 0. & 0. \\ 0. & 0.333 & 0. \\ 0. & 0. & 0.333 \end{bmatrix} \begin{bmatrix} x \\ y \\ z \end{bmatrix} + \begin{bmatrix} 0.333 \\ 0.333 \\ 0.333 \end{bmatrix}$$

$$T_2\left(\begin{bmatrix} x \\ y \\ z \end{bmatrix}\right) = \begin{bmatrix} 0.333 & 0. & 0. \\ 0. & 0.333 & 0. \\ 0. & 0. & 0.333 \end{bmatrix} \begin{bmatrix} x \\ y \\ z \end{bmatrix} + \begin{bmatrix} 0.333 \\ 0.475 \\ 0.421 \end{bmatrix}$$

$$T_3\left(\begin{bmatrix} x \\ y \\ z \end{bmatrix}\right) = \begin{bmatrix} 0.333 & 0. & 0. \\ 0. & 0.333 & 0. \\ 0. & 0. & 0.333 \end{bmatrix} \begin{bmatrix} x \\ y \\ z \end{bmatrix} + \begin{bmatrix} 0.333 \\ 0.475 \\ 0.246 \end{bmatrix}$$

$$T_4\left(\begin{bmatrix} x \\ y \\ z \end{bmatrix}\right) = \begin{bmatrix} 0.333 & 0. & 0. \\ 0. & 0.333 & 0. \\ 0. & 0. & 0.333 \end{bmatrix} \begin{bmatrix} x \\ y \\ z \end{bmatrix} + \begin{bmatrix} 0.333 \\ 0.192 \\ 0.421 \end{bmatrix}$$

$$T_5\left(\begin{bmatrix} x \\ y \\ z \end{bmatrix}\right) = \begin{bmatrix} 0.333 & 0. & 0. \\ 0. & 0.333 & 0. \\ 0. & 0. & 0.333 \end{bmatrix} \begin{bmatrix} x \\ y \\ z \end{bmatrix} + \begin{bmatrix} 0.333 \\ 0.192 \\ 0.246 \end{bmatrix}$$

$$T_6\left(\begin{bmatrix} x \\ y \\ z \end{bmatrix}\right) = \begin{bmatrix} 0.333 & 0. & 0. \\ 0. & 0.333 & 0. \\ 0. & 0. & 0.333 \end{bmatrix} \begin{bmatrix} x \\ y \\ z \end{bmatrix} + \begin{bmatrix} 0.421 \\ 0.333 \\ 0.475 \end{bmatrix}$$

$$T_7\left(\begin{bmatrix} x \\ y \\ z \end{bmatrix}\right) = \begin{bmatrix} 0.333 & 0. & 0. \\ 0. & 0.333 & 0. \\ 0. & 0. & 0.333 \end{bmatrix} \begin{bmatrix} x \\ y \\ z \end{bmatrix} + \begin{bmatrix} 0.421 \\ 0.333 \\ 0.192 \end{bmatrix}$$

$$T_8\left(\begin{bmatrix} x \\ y \\ z \end{bmatrix}\right) = \begin{bmatrix} 0.333 & 0. & 0. \\ 0. & 0.333 & 0. \\ 0. & 0. & 0.333 \end{bmatrix} \begin{bmatrix} x \\ y \\ z \end{bmatrix} + \begin{bmatrix} 0.246 \\ 0.333 \\ 0.475 \end{bmatrix}$$

$$T_9\left(\begin{bmatrix} x \\ y \\ z \end{bmatrix}\right) = \begin{bmatrix} 0.333 & 0. & 0. \\ 0. & 0.333 & 0. \\ 0. & 0. & 0.333 \end{bmatrix} \begin{bmatrix} x \\ y \\ z \end{bmatrix} + \begin{bmatrix} 0.246 \\ 0.333 \\ 0.192 \end{bmatrix}$$

This work was supported by the project FP7-IRSES-295260 "ECONANOSORB" under Marie Curie Actions of the 7th Framework Program of European Union

Avilov S.V. – PhD candidate, Department of Solid State Physics and Nanostructures of Voronezh State University
E-mail: slava_avilov@hotmail.com
Zhukalin D.A. – PhD candidate, Department of Physics of Semiconductors and Microelectronics of Voronezh State University
E-mail: d.zhukalin@mail.ru
Bityutskaya L.A. - PhD, Department of Physics of Semiconductors and Microelectronics of Voronezh State University
E-mail: me144@phys.vsu.ru
Domashevskaya E.P. – grand PhD, professor, Department of Solid State Physics and Nanostructures of Voronezh State University
E-mail: me144@phys.vsu.ru

$$T_{10}\left(\begin{bmatrix} x \\ y \\ z \end{bmatrix}\right) = \begin{bmatrix} 0.333 & 0. & 0. \\ 0. & 0.333 & 0. \\ 0. & 0. & 0.333 \end{bmatrix} \begin{bmatrix} x \\ y \\ z \end{bmatrix} + \begin{bmatrix} 0.475 \\ 0.421 \\ 0.333 \end{bmatrix}$$

$$T_{11}\left(\begin{bmatrix} x \\ y \\ z \end{bmatrix}\right) = \begin{bmatrix} 0.333 & 0. & 0. \\ 0. & 0.333 & 0. \\ 0. & 0. & 0.333 \end{bmatrix} \begin{bmatrix} x \\ y \\ z \end{bmatrix} + \begin{bmatrix} 0.475 \\ 0.246 \\ 0.333 \end{bmatrix}$$

$$T_{12}\left(\begin{bmatrix} x \\ y \\ z \end{bmatrix}\right) = \begin{bmatrix} 0.333 & 0. & 0. \\ 0. & 0.333 & 0. \\ 0. & 0. & 0.333 \end{bmatrix} \begin{bmatrix} x \\ y \\ z \end{bmatrix} + \begin{bmatrix} 0.192 \\ 0.421 \\ 0.333 \end{bmatrix}$$

$$T_{13}\left(\begin{bmatrix} x \\ y \\ z \end{bmatrix}\right) = \begin{bmatrix} 0.333 & 0. & 0. \\ 0. & 0.333 & 0. \\ 0. & 0. & 0.333 \end{bmatrix} \begin{bmatrix} x \\ y \\ z \end{bmatrix} + \begin{bmatrix} 0.192 \\ 0.246 \\ 0.333 \end{bmatrix}$$

After the kernel cluster is defined, a random point is generated inside the primary cube. The affine transformation matrix functions that were used to build the icosahedral reflections are in series randomly applied to the point's coordinates and the generated coordinates are stored in an array, which is then displayed (Fig. 2).

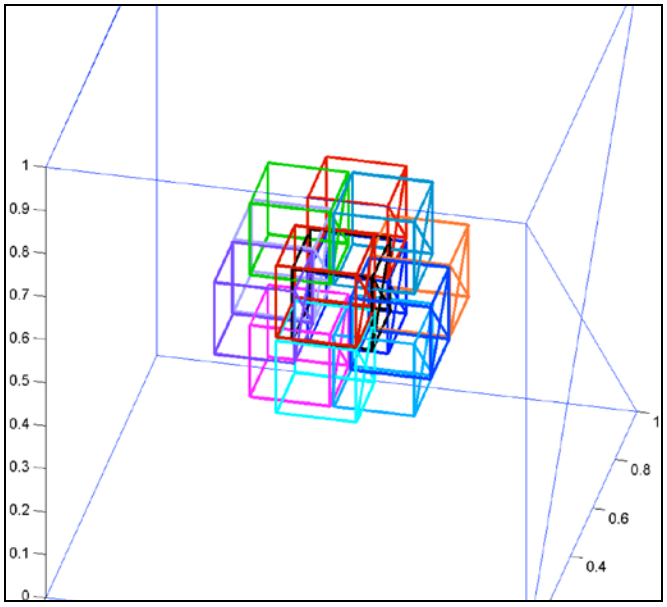

Fig. 1. The 13 affine reflections of a singular cube.

The achieved model being randomly generated has the chaotic properties of real systems. However every next generated model can not be clearly singled out due to the invariance, achieved by the large number of points.

The model conforms with the used RVE-based modelling method [13] where after generating a law for particle space occupation the space is extrapolated to larger scale levels. However, the presented model clearly describes the intrinsic symmetry of nanoclusters, conforms to their finiteness and fractal scale independency.

In [6] a CNT doped dispersed hydrated system $CaSO_4 - H_2O - CNT$ was studied where a chaotic fractal system of short CNTs turned into a symmetrical fractal system with the

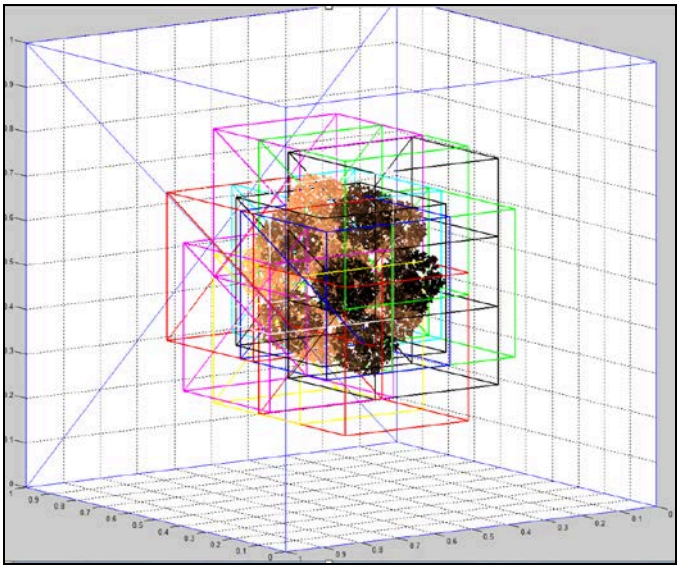

Fig. 2. The fractal dot model with an icosahedral symmetry, 30 000 dots with the corresponding affine reflections of a singular cube.

introduction of gyps. The symmetry of the resulting hybrid clusters can be described by the octahedral symmetry using the following affine transformations system

$$T_1\left(\begin{bmatrix} x \\ y \\ z \end{bmatrix}\right) = \begin{bmatrix} 0.500 & 0. & 0. \\ 0. & 0.500 & 0. \\ 0. & 0. & 0.500 \end{bmatrix} \begin{bmatrix} x \\ y \\ z \end{bmatrix} + \begin{bmatrix} 0.250 \\ 0.250 \\ 0.250 \end{bmatrix}$$

$$T_2\left(\begin{bmatrix} x \\ y \\ z \end{bmatrix}\right) = \begin{bmatrix} 0.250 & 0. & 0. \\ 0. & 0.250 & 0. \\ 0. & 0. & 0.250 \end{bmatrix} \begin{bmatrix} x \\ y \\ z \end{bmatrix} + \begin{bmatrix} 0.125 \\ 0.375 \\ 0.375 \end{bmatrix}$$

$$T_3\left(\begin{bmatrix} x \\ y \\ z \end{bmatrix}\right) = \begin{bmatrix} 0.250 & 0. & 0. \\ 0. & 0.250 & 0. \\ 0. & 0. & 0.250 \end{bmatrix} \begin{bmatrix} x \\ y \\ z \end{bmatrix} + \begin{bmatrix} 0.375 \\ 0.625 \\ 0.375 \end{bmatrix}$$

$$T_4\left(\begin{bmatrix} x \\ y \\ z \end{bmatrix}\right) = \begin{bmatrix} 0.250 & 0. & 0. \\ 0. & 0.250 & 0. \\ 0. & 0. & 0.250 \end{bmatrix} \begin{bmatrix} x \\ y \\ z \end{bmatrix} + \begin{bmatrix} 0.625 \\ 0.375 \\ 0.375 \end{bmatrix}$$

$$T_5\left(\begin{bmatrix} x \\ y \\ z \end{bmatrix}\right) = \begin{bmatrix} 0.250 & 0. & 0. \\ 0. & 0.250 & 0. \\ 0. & 0. & 0.250 \end{bmatrix} \begin{bmatrix} x \\ y \\ z \end{bmatrix} + \begin{bmatrix} 0.375 \\ 0.125 \\ 0.375 \end{bmatrix}$$

$$T_6\left(\begin{bmatrix} x \\ y \\ z \end{bmatrix}\right) = \begin{bmatrix} 0.250 & 0. & 0. \\ 0. & 0.250 & 0. \\ 0. & 0. & 0.250 \end{bmatrix} \begin{bmatrix} x \\ y \\ z \end{bmatrix} + \begin{bmatrix} 0.375 \\ 0.375 \\ 0.125 \end{bmatrix}$$

$$T_7\left(\begin{bmatrix} x \\ y \\ z \end{bmatrix}\right) = \begin{bmatrix} 0.250 & 0. & 0. \\ 0. & 0.250 & 0. \\ 0. & 0. & 0.250 \end{bmatrix} \begin{bmatrix} x \\ y \\ z \end{bmatrix} + \begin{bmatrix} 0.375 \\ 0.375 \\ 0.625 \end{bmatrix}$$

which generates the following affine reflections and resulting model (Fig. 3).

ISBN: 978-1-61804-225-5

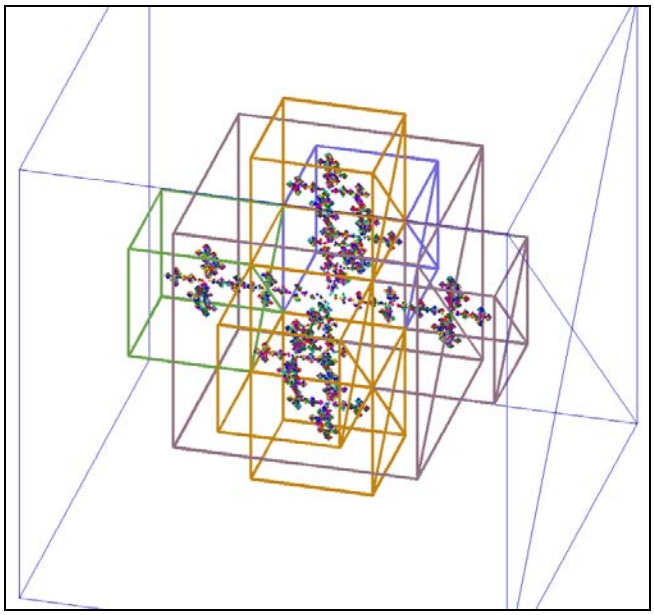

Fig. 3. The affine reflections for an octahedral symmetric system and the generated fractal dot model, 20 000 dots.

By introducing random deformations to the primary reflections the morphology of the resulting cluster is also affected (Fig. 4, 5).

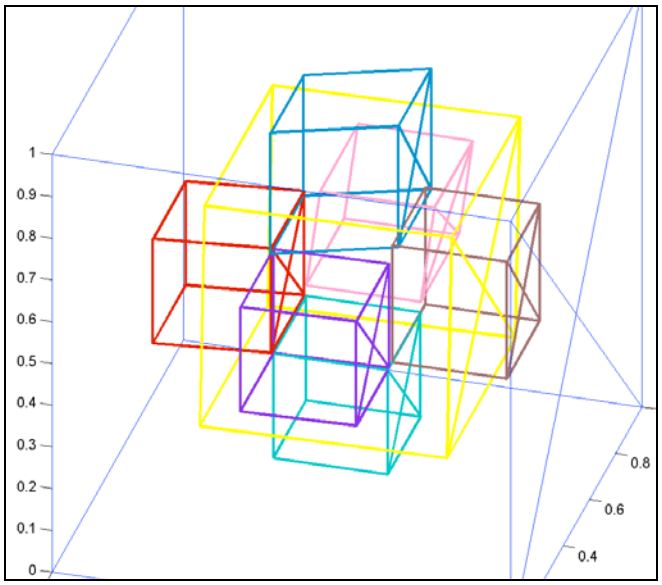

Fig. 4. An octahedral symmetrical model. The randomly modified affine reflections of a singular cube.

III. Conclusion

The obtained symmetrical objects qualitatively better represent real structures, keeping the chaotic properties of natural objects, that are not represented in purely deterministic fractal models. The further development of the method can show the importance of the regular polyhedra symmetries for the formation of nanoclusters. The method is capable of describing fractal systems of different kinds and could be used for fractal nanosystems' symmetry characterization.

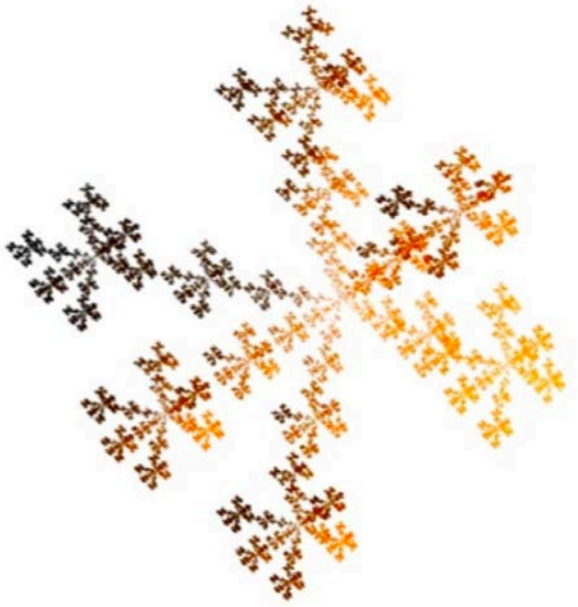

Fig. 5. The 3-D dot symmetrical octahedral model generated with minor random modifications to the affine transformations system.

References

[1] J. Robertson, "Fractals in physics edited by L. Pietronero and E. Tosatti". Acta Crystallographica Section 1986 A 42, 408.
[2] P Radaelli,. "Symmetry in Crystallography: Understanding the International Tables". OUP 2011, Oxford.
[3] E.A. Lord, A.L. Mackay, S. Ranganathan, "New Geometries for New Materials". 2006, Cambridge University Press.
[4] E. Ruiz-Hitzky, M. Darder, P. Aranda, "An Introduction to Bio-nanohybrid Materials, in: Bio-inorganic Hybrid Nanomaterials". Wiley-VCH Verlag GmbH & Co. KGaA, 2008, pp. 1–40.
[5] A.J. Patil, S. Mann,. "Bio-inorganic Nanohybrids Based on Organoclay Self-assembly, in: Bio-inorganic Hybrid Nanomaterials". Wiley-VCH Verlag GmbH & Co. KGaA, 2008, pp. 239–270.
[6] L.A. Bityutskaya, P.A. Golovinski, D.A. Zhukalin, E. V. Alekseeva, S.V. Avilov, A.N. Lukin. "Fractal coagulation of polydispersed hydrated mineral systems, doped with CNT". Condensed Matter and Interphases Journal, 2013,Volume 15, N1, p.59-64
[7] D.A. Zhukalin, D.G. Kulikov, L.A. Bityutskaya, E.V Bogatikov, M.V. Anisimov, L.A. Novikova, L.I. Belchinskaya, F. Reussner, "The catalytic properties of nanomaterials doped by carbon nanotubes". Materials of national conference with international participation "Chemistry, physics and technology of the surface." Kiev, 2013, p. 19
[8] R.M. Crownover, "Introduction to fractals and chaos", Jones and 1995, Bartlett books in mathematics. Jones and Bartlett.
[9] T. Ju, S. Schaefer, R. Goldman, "Recursive turtle programs and iterated affine transformations". Computers & Graphics 28, 2004, 991–1004.
[10] L.A. Bityutskaya, T. Kutcelyk. "Hierarchy of the Scales of Fractal GaSb Superclusters". ECASIA'2013 : 15th European Conference on Applications of Surface and Interface Analysis, 13-18th Oct. 2013 .— Cagliari, Sardinia (Italy), 2013 . p. 164
[11] T. Kutcelyk, L.A. Bityutskaya, "Obtainment and Properties of Selforganized Gallium Antimonide Superclusters". IVC-19 /ICN+T 2013 and Partner Conferences Paris, France, Sept. 9-13, 2013 : final Programme .— Paris (France), 2013 .— p. 1176-1177
[12] J. Feder,. "Fractals, Physics of Solids and Liquids". 1988, Springer.
[13] D. Weidt, Ł. Figiel, "Finite strain compressive behaviour of CNT/epoxy nanocomposites: 2D versus 3D RVE-based modeling". Computational Materials Science 82, 2014, 298–309.

ISBN: 978-1-61804-225-5

Local quartic C^2 spline quasi-interpolation on 3D bounded domains

Catterina Dagnino, Paola Lamberti and Sara Remogna

Abstract—Given a 3D bounded domain, in this paper we present new quasi-interpolating spline schemes, based on trivariate C^2 quartic box splines on type-6 tetrahedral partitions with approximation order four. They are of near-best type, i.e. with coefficient functionals obtained by minimizing an upper bound for their infinity norm. Such quasi-interpolants can be used for the reconstruction of gridded volume data and their higher smoothness is useful, for example, when functions have to be reconstructed with C^2 smoothness.

Moreover, we give norm and error bounds. Finally, some numerical tests, illustrating the approximation properties of the proposed quasi-interpolants, and comparisons with other known spline methods are presented.

Keywords—Trivariate box spline, quasi-interpolation, type-6 tetrahedral partition, approximation order, gridded volume data.

I. Introduction

In this paper we consider the problem of constructing appropriate non-discrete models from given discrete volume data. The development of such trivariate models is important because it is the theoretical basis for many applications, such as scientific visualization, computer graphics and medical imaging. Indeed, the volume data sets typically represent some kind of density acquired by devices like CT or MRI sensors. Such a type of input data is structured, so that the samples are arranged on a regular three-dimensional grid.

In several approaches the underlying mathematical models use trivariate tensor-product splines (see e.g. [2], [17]), but they use piecewise polynomials of high degree and they usually require (approximate) derivative data at certain prescribed points.

Schemes represented by blending sums of univariate and bivariate C^1 quadratic spline quasi-interpolants (see e.g. [14], [15]), quite close to tensor-product ones, provide approximation order three.

Lower total degree C^1 spline models based on trivariate splines defined on type-6 tetrahedral partitions [11], [16] yield approximation order two.

Recently, methods based on trivariate box splines with C^2 smoothness have been proposed [5], [7], [8], [13]. They achieve approximation order four, but they are defined on the whole space $\mathbb{R}^3$. If we use them on a bounded domain Ω of $\mathbb{R}^3$, we need data points outside Ω for their construction. Since the function f to be approximated may not be defined outside Ω, in the applications it is important to obtain spline models using data points inside or on the boundary of the domain.

Department of Mathematics, University of Torino, via C. Alberto 10, 10123 Torino, Italy. E-mail: catterina.dagnino@unito.it, paola.lamberti@unito.it, sara.remogna@unito.it

Here we propose and analyse new quasi-interpolants expressed as linear combination of scaled translates of the trivariate C^2 quartic box spline B [12] on a type-6 tetrahedral partition and local functionals, defined as linear combinations of values of f at specific points inside or on the boundary $\partial\Omega$ of the domain Ω. Such operators are exact on the space $\mathbb{P}_3$ of trivariate polynomials of total degree at most three and they have approximation order four. They are of near-best type, i.e. with coefficient functionals obtained by minimizing an upper bound for their infinity norm (see e.g. [1], where the concept of "near-best" is given in the bivariate case). The main problem in their construction consists in finding the coefficient functionals associated with boundary generators (i.e. scaled translate box splines with supports not completely inside Ω), involving only data points inside or on the boundary of the domain. Furthermore, we give norm and error bounds. Finally, some numerical tests, illustrating the approximation properties of the proposed quasi-interpolants, and comparisons with other known spline methods are presented.

II. Quasi-interpolation in the spline space $S_4^2(\Omega, \mathcal{T}_{\mathbf{m}})$

Let m_1, m_2 and m_3 be positive integers and let $\Omega = [0, m_1 h] \times [0, m_2 h] \times [0, m_3 h]$, $h > 0$, be a parallelepiped subdivided into $m_1 m_2 m_3$ equal cubes and endowed with the type-6 tetrahedral partition $\mathcal{T}_{\mathbf{m}}$, $\mathbf{m} = (m_1, m_2, m_3)$ (see Fig. 1).

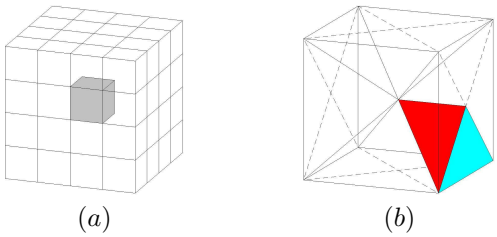

(a) (b)

Fig. 1. (a) Cube partition. (b) Uniform type-6 tetrahedral partition, obtained by subdividing each cube into 24 tetrahedra.

Let

$$\mathcal{A} = \left\{ \alpha = (i,j,k), \quad \begin{array}{l} -1 \le i \le m_1 + 2, \\ -1 \le j \le m_2 + 2, \\ -1 \le k \le m_3 + 2; \end{array} \quad \alpha \notin \mathcal{A}' \right\},$$

ISBN: 978-1-61804-225-5

with $\mathcal{A}'$ the set of indices defined by

$$\begin{aligned}\mathcal{A}' = \quad & \{(i,-1,-1),\ (i,m_2+2,-1),\\ & (i,-1,m_3+2),\ (i,m_2+2,m_3+2),\\ & \text{for } -1 \le i \le m_1+2,\\ & (-1,j,-1),\ (m_1+2,j,-1),\\ & (-1,j,m_3+2),\ (m_1+2,j,m_3+2),\\ & \text{for } 0 \le j \le m_2+1,\\ & (-1,-1,k),\ (m_1+2,-1,k),\\ & (-1,m_2+2,k),\ (m_1+2,m_2+2,k),\\ & \text{for } 0 \le k \le m_3+1\}.\end{aligned}$$

We define the space generated by the B-splines $\{B_\alpha, \alpha \in \mathcal{A}\}$

$$S_4^2(\Omega, \mathcal{T}_{\mathbf{m}}) = \left\{ s = \sum_{\alpha\in\mathcal{A}} a_\alpha B_\alpha,\ \ a_\alpha \in \mathbb{R} \right\},$$

where

$$\begin{aligned} B_\alpha(x,y,z) &= B_{i,j,k}(x,y,z)\\ &= B\left(\tfrac{x}{h} - i + 1, \tfrac{y}{h} - j + 1, \tfrac{z}{h} - k + 3\right),\end{aligned}$$

whose supports are centered at

$$C_\alpha = C_{i,j,k} = \left(\left(i-\frac{1}{2}\right)h, \left(j-\frac{1}{2}\right)h, \left(k-\frac{1}{2}\right)h\right) \quad (1)$$

and overlap with Ω, are the scaled translates of B, the box spline of degree four with C^2 smoothness [12], whose support is the truncated rhombic dodecahedron centered at $(\frac{1}{2}, \frac{1}{2}, \frac{5}{2})$ and contained in the cube $[-2,3] \times [-2,3] \times [0,5]$.

We remark that $S_4^2(\Omega, \mathcal{T}_{\mathbf{m}})$ is a subspace of the whole space of all trivariate C^2 quartic splines on $\mathcal{T}_{\mathbf{m}}$. Moreover, it is well-known that $\mathbb{P}_3 \subset S_4^2(\Omega, \mathcal{T}_{\mathbf{m}})$ and $\mathbb{P}_4 \not\subset S_4^2(\Omega, \mathcal{T}_{\mathbf{m}})$.

In the space $S_4^2(\Omega, \mathcal{T}_{\mathbf{m}})$ we define quasi-interpolants (QIs) of the form

$$Qf = \sum_{\alpha\in\mathcal{A}} \lambda_\alpha(f) B_\alpha, \quad (2)$$

where

$$\lambda_\alpha(f) = \sum_{\beta\in F_\alpha} \sigma_\alpha(\beta) f_\beta, \quad (3)$$

are linear combinations of values $f_\beta = f(M_\beta)$ of f at specific points $\{M_\beta = M_{i,j,k} = (s_i, t_j, u_k),\ \beta \in F_\alpha,\ F_\alpha \subset \mathcal{A}^M\}$ that lie in some neighbourhood of the support of $B_\alpha \cap \Omega$, with

- $\mathcal{A}^M = \{(i,j,k), 0 \le i \le m_1+1, 0 \le j \le m_2+1, 0 \le k \le m_3+1\}$;
- $s_0 = 0,\ \ s_i = (i-\frac{1}{2})h,\ \ 1 \le i \le m_1,\ \ s_{m_1+1} = m_1 h;$
  $t_0 = 0,\ \ t_j = (j-\frac{1}{2})h,\ \ 1 \le j \le m_2,\ \ t_{m_2+1} = m_2 h;$
  $u_0 = 0,\ \ u_k = (k-\frac{1}{2})h,\ \ 1 \le k \le m_3,\ \ u_{m_3+1} = m_3 h;$
- $\{\sigma_\alpha(\beta)\}$ real numbers, obtained so that $Qf \equiv f$ for all f in $\mathbb{P}_3$.

In the definition of the functionals, we consider a number of data points greater than the number of conditions we are imposing, in order to obtain a system of equations with free parameters, that we choose by minimizing an upper bound for the infinity norm of the operator Q.

From (3), it is clear that, for $\|f\|_\infty \le 1$ and $\alpha \in \mathcal{A}$, $|\lambda_\alpha(f)| \le \|\sigma_\alpha\|_1$, where σ_α is the vector with components $\sigma_\alpha(\beta)$. Therefore, since the scaled translates of B form a partition of unity [3], we deduce immediately

$$\|Q\|_\infty \le \max_{\alpha\in\mathcal{A}} |\lambda_\alpha(f)| \le \max_{\alpha\in\mathcal{A}} \|\sigma_\alpha\|_1.$$

Now, we can try to find a solution of the minimization problem

$$\min\left\{ \|\sigma_\alpha\|_1 : \sigma_\alpha \in \mathbb{R}^{\mathrm{card}(F_\alpha)}, V_\alpha \sigma_\alpha = b_\alpha \right\},$$

where $V_\alpha \sigma_\alpha = b_\alpha$ is the linear system expressing that Q is exact on $\mathbb{P}_3$.

Now, we explain the logic behind our approach, proposing a general method for the construction of coefficient functionals (3).

Fixed the scaled translate box spline $B_\alpha = B_{i,j,k}$, for any $n \ge 1$, we define $\Lambda_\alpha^n = \Lambda_{i,j,k}^n$ the octahedron centered at the point $C_{i,j,k}$, given in (1), with vertices $C_{i\pm n,j,k}$, $C_{i,j\pm n,k}$, $C_{i,j,k\pm n}$. We denote by $\bar{\Lambda}_\alpha^n = \bar{\Lambda}_{i,j,k}^n$ the set of points $\Lambda_{i,j,k}^n \cap \left[\left(\mathbb{Z} - \frac{1}{2}\right)h\right]^3$ (see Figs. 2 and 3 for $n = 2$ and 3, respectively).

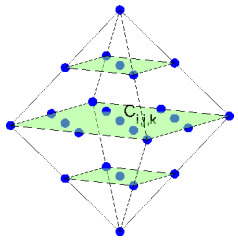

Fig. 2. The octahedron $\Lambda_{i,j,k}^n$ with the corresponding points $\bar{\Lambda}_{i,j,k}^n$, for $n = 2$.

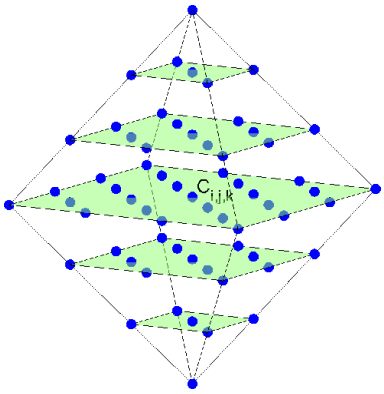

Fig. 3. The octahedron $\Lambda_{i,j,k}^n$ with the corresponding points $\bar{\Lambda}_{i,j,k}^n$, for $n = 3$.

If, for a fixed n, we used the points in $\bar{\Lambda}_\alpha^n$, as data points in the definition (3) of the coefficient functional $\lambda_\alpha(f)$, some of them could lie outside Ω. Therefore, in order to have all data points inside or on the boundary of Ω, we project them on $\partial\Omega$, obtaining a new set that we still call $\bar{\Lambda}_\alpha^n$. We remark that $\bar{\Lambda}_\alpha^n \subset \mathcal{A}^M$.

Then, for the construction of $\lambda_\alpha(f)$, we impose the exactness of Q on $\mathbb{P}_3$, getting twenty conditions (or less than twenty in case of symmetry). Thus, we choose a starting value for n, we construct a scheme for the coefficient functional based on the data point set $\bar{\Lambda}_\alpha^n$ and containing at least twenty unknown parameters (or less than twenty in case of symmetry). We solve

the resulting linear system and, in case of free parameters, we minimize the norm $\|\sigma_\alpha\|_1$.

In order to reduce such a norm, we increase the value of n and we repeat the process above explained.

Since a large number of QIs can be constructed, we have to choose a specific n for each coefficient functional in (2). For this choice we have taken into account the following remarks: since the norm reduction slows down as n increases, we have to strike a balance between n and the value $\|\sigma_\alpha\|_1$, in order to keep the data points in a neighbourhood of the support of $B_\alpha \cap \Omega$. Therefore, following this approach and taking into account the values of $\|\sigma_\alpha\|_1$ and n, we define a particular QI whose coefficient functionals are given in [6].

Now we give an upper bound for the infinity norm of the proposed quasi-interpolating operator and error estimates for it [6].

Theorem 1. *For the operator Q, the following bound holds*

$$\|Q\|_\infty \leq 9.945.$$

Standard results in approximation theory [3], [4] allow us to immediately deduce the following theorem.

Theorem 2. *Let $f \in C^4(\Omega)$ and $|\gamma| = 0, 1, 2, 3$ with $\gamma = (\gamma_1, \gamma_2, \gamma_3)$, $|\gamma| = \gamma_1 + \gamma_2 + \gamma_3$. Then there exist constants $K_\gamma > 0$ such that*

$$\|D^\gamma (f - Qf)\|_\infty \leq K_\gamma h^{4-|\gamma|} \max_{|\beta|=4} \left\|D^\beta f\right\|_\infty,$$

where $D^\beta = D^{\beta_1\beta_2\beta_3} = \frac{\partial^{|\beta|}}{\partial x^{\beta_1} \partial y^{\beta_2} \partial z^{\beta_3}}$.

III. Numerical tests

Now we present some numerical results in order to illustrate both the approximation properties and the visual quality of our C^2 trivariate splines. Box splines are evaluated by an algorithm based on the Bernstein-Bézier form of the box spline, proposed by Kim and Peters [9] and, since we deal with volumetric data, we visualize some isosurfaces of our trivariate quasi-interpolating splines, generated as a very fine triangular mesh by using the Matlab procedure `isosurface` [10].

We want to compare our method with other ones proposed in the literature [11], [14], [16], therefore we consider the same test functions there presented, i.e.

- the Marschner-Lobb function

$$f_1(x,y,z) = \frac{1}{2(1+\beta_1)}\left(1 - \sin\frac{\pi z}{2} + \beta_1\left(1 + \cos\left(2\pi\beta_2 \cos\left(\frac{\pi\sqrt{x^2+y^2}}{2}\right)\right)\right)\right)$$

  with $\beta_1 = \frac{1}{4}$ and $\beta_2 = 6$ on $\Omega = [-1,1]^3$. This function is extremely oscillating and therefore it represents a difficult test for any efficient three-dimensional reconstruction method;
- the smooth trivariate test function of Franke type

$$f_2(x,y,z) = \frac{1}{2}e^{-10((x-\frac{1}{4})^2+(y-\frac{1}{4})^2)} + \frac{3}{4}e^{-16((x-\frac{1}{2})^2+(y-\frac{1}{4})^2+(z-\frac{1}{4})^2)} + \frac{1}{2}e^{-10((x-\frac{3}{4})^2+(y-\frac{1}{8})^2+(z-\frac{1}{2})^2)} - \frac{1}{4}e^{-20((x-\frac{3}{4})^2+(y-\frac{3}{4})^2)}$$

  on $\Omega = [0,1]^3$;
- $f_3(x,y,z) = \frac{1}{9}\tanh(9(z-x-y)+1)$ on $\Omega = [-\frac{1}{2},\frac{1}{2}]^3$.

Here we assume $m_1 = m_2 = m_3 = m$ and $m = 16, 32, 64, 128$. For the evaluation of Qf, we consider a $139 \times 139 \times 139$ uniform three-dimensional grid G of points in the domain and, for each test function, we compute the maximum absolute error

$$E_S f := \max_{(u,v,w)\in G} |f(u,v,w) - Sf(u,v,w)|,$$

with $S = Q$, S_q, S_c, R_1 where

- Qf is our quasi-interpolant with approximation order four and $\lambda_\alpha(f)$ given in [6];
- $S_q f$ is the quadratic C^1 quasi-interpolant with approximation order two, studied by Nürnberger et al. [11];
- $S_c f$ is the cubic C^1 quasi-interpolant with approximation order two, studied by Sorokina and Zeilfelder [16];
- $R_1 f$ is the near-best quasi-interpolant with approximation order three, defined as blending sum of univariate and bivariate C^1 quadratic spline quasi-interpolants, on a partition of Ω into vertical prisms with triangular sections, studied by Remogna and Sablonnière [14].

We report the results in Table I with an estimate of the approximation order, rf, obtained by the logarithm to base two of the ratio between two consecutive errors.

TABLE I
Maximum absolute errors and numerical convergence orders.

m	$E_Q f_1$	rf_1	$E_{S_q} f_1$	rf_1	$E_{S_c} f_1$	rf_1	$E_{R_1} f_1$	rf_1
16	2.0(-1)						1.9(-1)	
32	1.3(-1)	0.6	1.8(-1)		1.8(-1)		1.5(-1)	0.4
64	6.5(-2)	1.0	1.2(-1)	0.5	1.2(-1)	0.5	3.2(-2)	2.2
128	2.1(-2)	1.7	4.0(-2)	1.6	4.0(-2)	1.6	4.6(-3)	2.8
m	$E_Q f_2$	rf_2	$E_{S_q} f_2$	rf_2	$E_{S_c} f_2$	rf_2	$E_{R_1} f_2$	rf_2
16	1.7(-2)		4.3(-2)		4.3(-2)		6.6(-3)	
32	8.0(-4)	4.4	1.1(-2)	2.0	1.1(-2)	2.0	8.2(-4)	3.0
64	5.2(-5)	3.9	2.8(-3)	2.0	2.8(-3)	2.0	9.8(-5)	3.1
128	3.3(-6)	4.0	6.9(-4)	2.0	6.9(-4)	2.0	8.5(-6)	3.5
m	$E_Q f_3$	rf_3	$E_{S_q} f_3$	rf_3	$E_{S_c} f_3$	rf_3	$E_{R_1} f_3$	rf_3
16	6.2(-3)		8.8(-3)				6.2(-3)	
32	8.2(-4)	2.9	2.4(-3)	1.9			1.1(-3)	2.5
64	8.9(-5)	3.2	6.3(-4)	1.9			1.7(-4)	2.7
128	7.9(-6)	3.5	1.6(-4)	2.0			1.7(-5)	3.3

Comparing the results, we can notice that using our C^2 quartic splines, the error decreases faster than using S_q, S_c and R_1, except in case of function f_1 for which the errors are comparable.

Moreover, in order to explore the volumetric data and to show the good approximation properties of the operator Q, here proposed, we visualize some isosurfaces of the trivariate C^2 splines approximating the considered test functions.

In Fig. 4(a), we show the isosurface obtained from f_1 with isovalue $\rho = 1/2$, i.e. a view on the set of all points $(x,y,z) \in [-1,1]^3$, such that $f_1(x,y,z) = \rho$. In Fig. 4(b), we show the isosurface of the approximating spline Qf_1 with isovalue $\rho = 1/2$, with $m = 64$ and the maximal error is color coded from red $\approx 6.5 \cdot 10^{-2}$ to blue $= 0$.

Moreover, a visualization of the spline Qf_2, for $m = 32$, using isovalues $\rho = -0.1$, 0, 0.1, 0.2, 0.5 and 0.8, is shown in Fig. 5, where we color coded the maximal error from red

ISBN: 978-1-61804-225-5

to blue (see the colorbar in each figure). For a qualitative visual comparison with competing methods, we can refer to the corresponding isosurfaces shown in [11] and we can notice the good performances of our method.

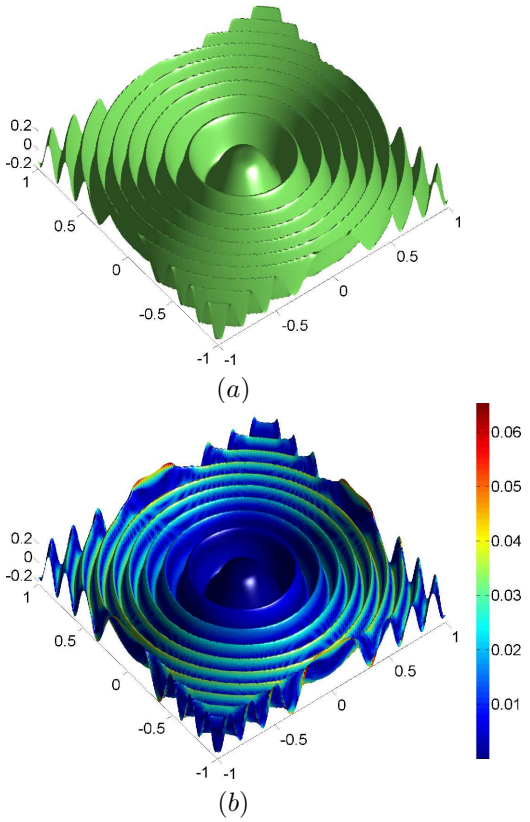

Fig. 4. For the isovalue $\rho = 1/2$ the isosurface of (a) f_1 and (b) Qf_1, with $m = 64$.

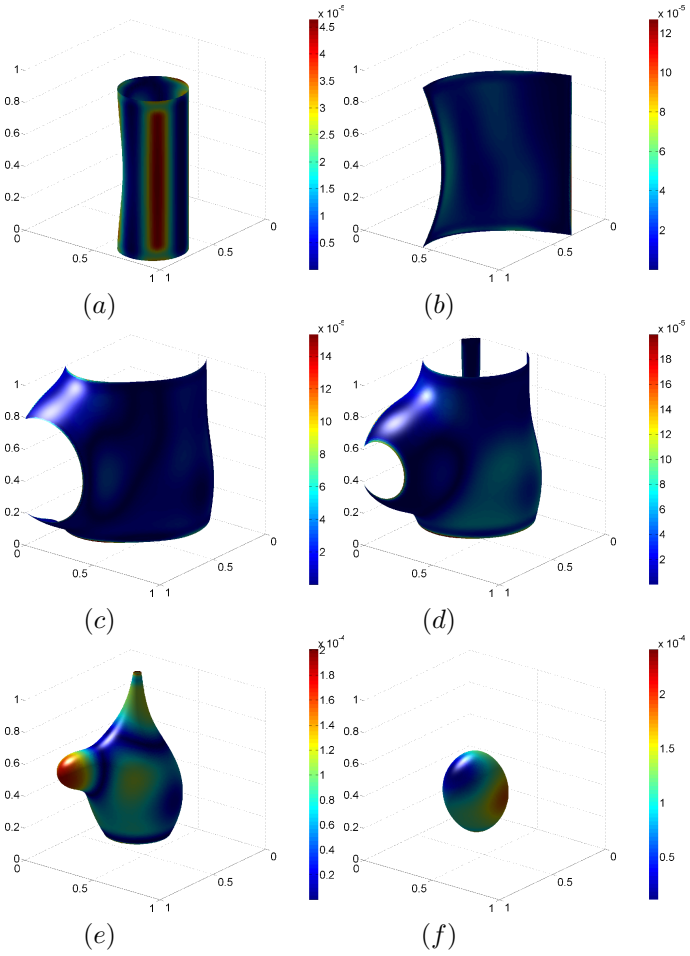

Fig. 5. Isosurfaces of Qf_2 for $m = 32$, with isovalues (a) $\rho = -0.1$, (b) $\rho = 0$, (c) $\rho = 0.1$, (d) $\rho = 0.2$, (e) $\rho = 0.5$ and (f) $\rho = 0.8$.

IV. Conclusion

In this paper, we have presented new quasi-interpolating spline schemes, more precisely of near-best type, defined on 3D bounded domains and based on trivariate C^2 quartic box splines on type-6 tetrahedral partitions with approximation order four. Due to their use for the reconstruction of gridded volume data, their construction involves only data points either inside or on the boundary of the domain. We have also given norm and error estimates and presented some numerical tests, illustrating the approximation properties of the proposed quasi-interpolants, and comparisons with other known spline methods.

Finally we refer to [6] for some examples based on real world data that can be considered as typical for many applications, where a precise evaluation and a high visual quality are the goals of visualization. In particular, starting from a discrete set of data, we have obtained a non-discrete model of the real object with C^2 smoothness.

References

[1] D. Barrera, M.J. Ibáñez, P. Sablonnière, D. Sbibih, On near-best discrete quasi-interpolation on a four-directional mesh, J. Comput. Appl. Math. 233 (2010) 1470-1477.

[2] L. Barthe, B. Mora, N. Dodgson, M.A. Sabin, Triquadratic reconstruction for interactive modelling of potential fields. In: Proc. Shape Modeling International 2002, IEEE Computer Society (2002) 145-153.

[3] B.D. Bojanov, H.A. Hakopian, A.A. Sahakian, Spline functions and multivariate interpolation. Kluwer, Dordrecht, 1993.

[4] C. de Boor, K. Höllig, S. Riemenschneider, Box splines. Springer-Verlag, New York, 1993.

[5] C. Dagnino, P. Lamberti, S. Remogna, Numerical integration based on trivariate C^2 quartic spline quasi-interpolants, BIT Numerical Mathematics 53 (2013) 873-896.

[6] C. Dagnino, P. Lamberti, S. Remogna, Trivariate local quartic C^2 quasi-interpolating splines on type-6 tetrahedral partitions of bounded domains, arXiv:1312.5552 [math.NA] (2013)

[7] A. Entezari, T. Möller, Extensions of the Zwart-Powell Box Spline for Volumetric Data Reconstruction on the Cartesian Lattice. IEEE Trans. Vis. Comput. Graph. 12 (5) (2006) 1337-1344.

[8] A. Entezari, M. Mirzargar, L. Kalantari, Quasi-interpolation on the Body Centered Cubic Lattice. IEEE Trans. Vis. Comput. Graph. 28 (3) (2009) 313-328.

[9] M. Kim, J. Peters, Fast and stable evaluation of box-splines via the BB-form. Numer. Algor. 50 (4) (2009) 381-399.

[10] MATLAB, Volume Visualization Documentation, The MathWorks, http://www.mathworks.it/help/techdoc/ref/isosurface.html.

[11] G. Nürnberger, C. Rössl, H.P.Seidel, F. Zeilfelder, Quasi-interpolation by quadratic piecewise polynomials in three variables. Comput. Aided Geom. Design 22 (2005) 221-249.

[12] J. Peters, C^2 surfaces built from zero sets of the 7-direction box spline. In: IMA Conference on the Mathematics of Surfaces (Ed. G. Mullineux), Clarendon Press (1994) 463-474.

[13] S. Remogna, Quasi-interpolation operators based on the trivariate seven-direction C^2 quartic box spline, BIT Numerical Mathematics 51 (2011) 757-776.

ISBN: 978-1-61804-225-5

[14] S. Remogna, P. Sablonnière, On trivariate blending sums of univariate and bivariate quadratic spline quasi-interpolants on bounded domains. Computer Aided Geometric Design 28 (2011) 89-101.
[15] P. Sablonnière, Quadratic spline quasi-interpolants on bounded domains of $\mathbb{R}^d,\ d = 1, 2, 3$. Rend. Sem. Mat. Univ. Pol. Torino 61 (3) (2003) 229-246.
[16] T. Sorokina, F. Zeilfelder, Local quasi-interpolation by cubic C^1 splines on type-6 tetrahedral partitions. IMA J. Numer. Anal. 27 (1) (2007) 74-101.
[17] T. Theußl, T. Möller, J. Hladuvka, M. Gröller, Reconstruction issues in volume visualization. In: Data Visualization: State of the Art, Proc. of IEEE Visualization 2002 (2002) 1-8.

ISBN: 978-1-61804-225-5

Addressing the Feasibility of the Parameters of Strongly Regular Graphs with a MacLaurin Series Approach

Vasco Moço Mano and Luís Almeida Vieira.

***Abstract*—In the environment of Euclidean Jordan algebras, we consider a Jordan frame associated to the adjacency matrix of a strongly regular graph and construct a MacLaurin series with an element of the frame. From this series we establish feasibility conditions for the existence of strongly regular graphs.**

***Keywords*-Strongly regular graph, Euclidean Jordan algebra, Matrix analysis.**

I. Introduction

On the article *Strongly regular graphs, partial geometries and partially balanced designs*, [1], R. C. Bose introduced a class of regular graphs governed by a set of four parameters. One very challenging problem concerning these graphs, lately called strongly regular, is to find good feasibility conditions over their parameter sets, in order to filter potential strongly regular graphs. A short survey on the theory of strongly regular graphs is made in Section II.

Throughout this paper we take an Euclidean Jordan algebraic approach to address this problem. By considering a special Euclidean Jordan algebra associated to the adjacency matrix of a strongly regular graph, Section IV, we constructed a MacLaurin series that allowed us to establish some feasibility conditions over the set of parameters of a strongly regular graph, Section V.

Euclidean Jordan algebras were introduced in the paper [2] and, since then, they have been applied to different branches of mathematics. For instance, there are applications to statistics, [3], to interior point methods, [4] or [5] and to combinatorics, [6], [7], [8]. The basic definitions and main results for our work are presented in Section III.

We finish our paper with some experimental results where we test our admissibility conditions as well as some conclusions, Section VI.

II. General Concepts on Strongly Regular Graphs

Along this paper, we consider only simple graphs, that is, graphs without loops and parallel edges, herein called graphs.

A graph in which all pairs of vertices are adjacent (non-adjacent) is called a *complete* (*null*) graph. The number of neighbors of a vertex v in $V(X)$ is called the *degree* of v. If all vertices of a graph X have degree k, for some natural number k, then X is *k-regular*.

We associate to a graph X an n by n matrix $A = [a_{ij}]$, where each $a_{ij} = 1$, if $v_iv_j \in E(X)$, otherwise $a_{ij} = 0$, called the *adjacency* matrix of X. The eigenvalues of A are simply called the eigenvalues of X.

A non-null and not complete graph X is *strongly regular* with parameters (n, k, a, c) if it is k-regular, each pair of adjacent vertices has a common neighbors and each pair of non-adjacent vertices have c common neighbors. It is well known that the parameter set, (n, k, a, c), of a strongly regular graph satisfy the following equality

$$k(k-a-1) = (n-k-1)c. \tag{1}$$

Also (see, for instance, [9]), the eigenvalues of a strongly regular graph X with parameters (n, k, a, c) are k, θ and τ, where θ and τ are given by

$$\theta = \frac{a-c+\sqrt{(a-c)^2+4(k-c)}}{2} \tag{2}$$

$$\tau = \frac{a-c-\sqrt{(a-c)^2+4(k-c)}}{2}. \tag{3}$$

Note that θ and τ, usually called the *restricted eigenvalues* of X, are such that the former is positive and the latter is negative. Their multiplicities can also be obtained from the parameters of X as follows (see, for instance, [9]):

$$m_\theta = \frac{1}{2}\left(n-1-\frac{(\theta+\tau)(n-1)+2k}{\theta-\tau}\right) \tag{4}$$

$$m_\tau = \frac{1}{2}\left(n-1+\frac{(\theta+\tau)(n-1)+2k}{\theta-\tau}\right), \tag{5}$$

where m_θ and m_τ are the multiplicities of θ and τ, respectively.

If X is a strongly regular graph with parameters (n, k, a, c), then its complement graph, $\overline{G}$ is also strongly regular with parameters $(n, \bar{k}, \bar{a}, \bar{c})$, where

$$\bar{k} = n-k-1, \tag{6}$$

$$\bar{a} = n-2-2k+c, \tag{7}$$

$$\bar{c} = n-2k+a. \tag{8}$$

A very important problem on the study of these graphs is to find suitable admissibility conditions over their parameter sets in order to allow us to decide whether a given parameter set can produce a strongly regular graph or not. We have already presented some trivial feasibility conditions for the parameters

Vasco Moço Mano and Luís Vieira is with Department of Civil Engineering of Faculty of Engineering of University of Porto, Portugal e-mail: vascomocomano@gmail.com and lvieira@fe.up.pt.

Manuscript received April 19, 2005; revised January 11, 2007.

of a strongly regular graph. In fact, it is clear that given any natural numbers k, a and c, equality (1) has to produce a natural n. Using a same kind of reasoning, formulas (4) and (5) must produce natural numbers for m_θ and m_τ. Finally, note that while (6) and (8) yield positive numbers, the same is not guaranteed for (7). Besides these trivial feasibility conditions, there are many nontrivial conditions widely used for checking the feasibility of a parameter set of a strongly regular graph.

The eigenvalues of a strongly regular graph satisfy the following inequalities, known as the *Krein conditions*, [11]:

$$(\theta+1)(k+\theta+2\theta\tau) \leq (k+\theta)(\tau+1)^2, \quad (9)$$
$$(\tau+1)(k+\tau+2\theta\tau) \leq (k+\tau)(\theta+1)^2. \quad (10)$$

It was also proved (see [12]) that the multiplicities of the eigenvalues satisfy the so-called *Seidel's absolute bounds*:

$$n \leq \frac{m_\theta(m_\theta+3)}{2}, \quad (11)$$
$$n \leq \frac{m_\tau(m_\tau+3)}{2}. \quad (12)$$

These inequalities where improved by Neumaier (see [13]) in some particular cases.

Finally, A. E. Brouwer obtained the following condition (see [14]), known as *the claw bound*:

$$2(\theta+1) \leq \tau(\tau+1)(c+1), \quad (13)$$

if $c \neq \tau^2$ and $c \neq \tau(\tau+1)$.

We say that a parameter set (n,k,a,c) is *feasible* if all of the above conditions are satisfied. With these conditions, many of the parameter sets are discarded as possible parameters sets of strongly regular graphs. However, to decide whether a set of parameters is the parameter set of a strongly regular graph it is one of the main problems on the study of strongly regular graphs. In fact, there are still many parameter sets for which we do not know if they correspond to a strongly regular graph. To address some of these open problems we studied the relationship between these graphs and Euclidean Jordan algebras, which will be presented in Section III.

It is worth notice that the Krein conditions (9)-(10) and the Seidel's absolute bounds (11)-(12) are special cases of general inequalities obtained for association schemes, since strongly regular graphs are symmetric association schemes with two classes. For more information on these more complex combinatorial structures it is suggested the reading of [10], for instance.

III. A short introduction to Euclidean Jordan algebras

In this section relevant concepts for our work are shortly surveyed. These can be seen, for instance, in [15].

Let $\mathcal{V}$ be a real vector space with finite dimension and a bilinear mapping $(u,v) \mapsto u \bullet v$ from $\mathcal{V} \times \mathcal{V}$ to $\mathcal{V}$, such that for each $u \in \mathcal{V}$ the algebra spanned by u is associative. Then, $\mathcal{V}$ is called a real *power associative* algebra. If $\mathcal{V}$ contains an element, e, such that for all u in $\mathcal{V}$, $e \bullet u = u \bullet e = u$, then e is called the *unit* element of $\mathcal{V}$.

Considering a bilinear mapping $(u,v) \mapsto u \bullet v$, if for all u and v in $\mathcal{V}$ we have (J_1) $u \bullet v = v \bullet u$ and (J_2) $u \bullet (u^2 \bullet v) = u^2 \bullet (u \bullet v)$, with $u^2 = u \bullet u$, then $\mathcal{V}$ is called a *Jordan algebra*. If $\mathcal{V}$ is a Jordan algebra with unit element, then $\mathcal{V}$ is power associative (see [15]). Along this paper we only consider finite dimensional real Jordan algebras.

Given a Jordan algebra $\mathcal{V}$ with unit element e, if there is an inner product $< \cdot, \cdot >$ that verifies the equality $< u \bullet v, w > = < v, u \bullet w >$, for any u, v, w in $\mathcal{V}$, then $\mathcal{V}$ is called an *Euclidean Jordan algebra*.

An element c in an Euclidean Jordan algebra $\mathcal{V}$, with unit element e, is an *idempotent* if $c^2 = c$. Two idempotents c and d are *orthogonal* if $c \bullet d = 0$. An idempotent is *primitive* if it is non-zero and cannot be written as the sum of two non-zero idempotents.

We call the set $\{c_1, c_2, \ldots, c_k\}$ a *complete system of orthogonal idempotents* if

(i) $c_i^2 = c_i, \forall i \in \{1, \ldots, k\}$;
(ii) $c_i \bullet c_j = 0, \forall i \neq j$ and
(iii) $c_1 + c_2 + \cdots + c_k = e$.

Additionally, if every c_i, $i \in \{1, \ldots, k\}$ is primitive, $\{c_1, c_2, \ldots, c_k\}$ is called a *Jordan frame*.

Let $\mathcal{V}$ be an Euclidean Jordan algebra with unit element e. Then, for every u in $\mathcal{V}$, there are unique distinct real numbers $\lambda_1, \lambda_2, \ldots, \lambda_k$, and an unique complete system of orthogonal idempotents $\{c_1, c_2, \ldots, c_k\}$ such that

$$u = \lambda_1 c_1 + \lambda_2 c_2 + \cdots + \lambda_k c_k, \quad (14)$$

with $c_j \in \mathbb{R}[u]$, $j = 1, \ldots, k$, see [15, Theorem III.1.1]. These λ_j's are the eigenvalues of u and (14) is called the *first spectral decomposition* of u. A similar result for Jordan frames is given in [15, Theorem III.1.2] and we obtain the second spectral decomposition that is analogous to (14). The difference is that in the second spectral decomposition the λ's are not all distinct and appear with their respective multiplicities.

The *rank* of an element u in $\mathcal{V}$ is the least natural number k, such that the set $\{e, u, \ldots, u^k\}$ is linearly dependent (where $u^k = u \bullet u^{k-1}$), and we write $\text{rank}(u) = k$. This concept is expanded by defining the rank of the algebra $\mathcal{V}$ as the natural number $\text{rank}(\mathcal{V}) = \max\{\text{rank}(u) : u \in \mathcal{V}\}$. The elements of $\mathcal{V}$ with rank equal to the rank of $\mathcal{V}$ are the *regular* elements of $\mathcal{V}$. This set of the regular elements is an open and dense subset in $\mathcal{V}$. If u is a regular element of $\mathcal{V}$, with $r = \text{rank}(u)$, then the set $\{e, u, u^2, \ldots, u^r\}$ is linearly dependent and the set $\{e, u, u^2, \ldots, u^{r-1}\}$ is linearly independent. Thus we may conclude that there exist unique real numbers $a_1(u), \ldots, a_r(u)$, such that $u^r - a_1(u)u^{r-1} + \cdots + (-1)^r a_r(u)e = 0$, where 0 is the null vector of $\mathcal{V}$. Making the necessary adjustments we obtain the polynomial in λ

$$p(u,\lambda) = \lambda^r - a_1(u)\lambda^{r-1} + \cdots + (-1)^r a_r(u), \quad (15)$$

that is called the *characteristic polynomial* of u, where each coefficient a_i is a homogeneous polynomial of degree i in the coordinates of u in a fixed basis of $\mathcal{V}$. Although the characteristic polynomial is defined for a regular element of $\mathcal{V}$, we can extend this definition to all the elements of $\mathcal{V}$, since each polynomial a_i is homogeneous and the set of regular

ISBN: 978-1-61804-225-5

elements of $\mathcal{V}$ is dense in $\mathcal{V}$. The roots of the characteristic polynomial of u, $\lambda_1, \lambda_2, \ldots, \lambda_r$, are called the eigenvalues of u. Furthermore, the coefficients $a_1(u)$ and $a_r(u)$ of the characteristic polynomial of u, are called the *trace* and the *determinant* of u, respectively.

IV. A Jordan Frame Associated to a Strongly Regular Graph

We consider a strongly regular graph in the environment of Euclidean Jordan algebras, in a similar way as we did in [8].

From now on we consider the Euclidean Jordan algebra of real symmetric matrices of order n, $\mathcal{V}$, such that $\forall A, B \in \mathcal{V}$, $A \bullet B = (AB + BA)/2$, where AB is the usual product of matrices. Furthermore, the inner product of $\mathcal{V}$ is defined as $< A, B >= \text{tr}(AB)$, where tr$(\cdot$ denotes the classical trace of matrices, that is the sum of its eigenvalues.

Let X be a strongly regular graph with parameter set (n, k, a, c) and let A be the adjacency matrix of X with three distinct eigenvalues, namely the degree of regularity k, and the restricted eigenvalues θ and τ, given in (2) and (3). Now we consider the Euclidean Jordan subalgebra of $\mathcal{V}$, $\mathcal{V}'$, spanned by the identity matrix of order n, I_n, and the powers of A. Since A has three distinct eigenvalues, then $\mathcal{V}'$ is a three dimensional Euclidean Jordan algebra with rank$(\mathcal{V}') = 3$.

Let $\mathcal{B} = \{E_0, E_1, E_2\}$ be the Jordan frame of $\mathcal{V}'$ associated to A, with

$$\begin{aligned} E_0 &= \frac{A^2 - (\theta+\tau)A + \theta\tau I_n}{(k-\theta)(k-\tau)} = \frac{J_n}{n}, \\ E_1 &= \frac{A^2 - (k+\tau)A + k\tau I_n}{(\theta-\tau)(\theta-k)}, \\ E_2 &= \frac{A^2 - (k+\theta)A + k\theta I_n}{(\tau-\theta)(\tau-k)}, \end{aligned}$$

where J_n is the matrix whose entries are all equal to 1. The elements of $\mathcal{B}$ can be rewritten under the basis $\{I_n, A, J_n - A - I_n\}$ of $\mathcal{V}'$ in the following manner:

$$\begin{aligned} E_0 &= \frac{\theta-\tau}{n(\theta-\tau)} I_n + \frac{\theta-\tau}{n(\theta-\tau)} A \\ &+ \frac{\theta-\tau}{n(\theta-\tau)} (J_n - A - I_n), \\ E_1 &= \frac{|\tau| n + \tau - k}{n(\theta-\tau)} I_n + \frac{n+\tau-k}{n(\theta-\tau)} A \\ &+ \frac{\tau-k}{n(\theta-\tau)} (J_n - A - I_n), \\ E_2 &= \frac{\theta n + k - \theta}{n(\theta-\tau)} I_n + \frac{-n+k-\theta}{n(\theta-\tau)} A \\ &+ \frac{k-\theta}{n(\theta-\tau)} (J_n - A - I_n). \end{aligned}$$

Let $\mathcal{M}_n(\mathbb{R})$ the space of square matrices with real entries and by $\mathcal{M}_{m,n}(\mathbb{R})$ the space of $m \times n$ matrices with real entries. We consider the *Hadamard product*, defined for two matrices A, B of order n as the componentwise product: $(A \circ B)_{ij} = A_{ij} B_{ij}$ and the *Kronecker product*, for matrices $C = [c_{ij}] \in \mathcal{M}_{m,n}(\mathbb{R})$ and $D = [d_{ij}] \in \mathcal{M}_{p,q}(\mathbb{R})$, defined by

$$C \otimes D = \begin{pmatrix} c_{11}D & \cdots & c_{1n}D \\ \vdots & \ddots & \vdots \\ c_{m1}D & \cdots & c_{mn}D \end{pmatrix}.$$

We now introduce a specific notation that will be used in the following sections. Consider the natural number p. Then, for $A \in M_n(\mathbb{R})$, we denote by $A^{\circ p}$ and $A^{\otimes p}$ the *Hadamard power* of order p of A and the *Kronecker power* of order p of A, respectively, with $A^{\circ 1} = A$ and $A^{\otimes 1} = A$.

V. A Feasibility Condition Associated to a MacLaurin Series

Consider the idempotent E_2 given in the previous section. The eigenvalues of E_2 are given by

$$\begin{aligned} q_0 &= \frac{\theta n + k - \theta}{n(\theta-\tau)} + \frac{-n+k-\theta}{n(\theta-\tau)} k \\ &+ \frac{k-\theta}{n(\theta-\tau)} (n-k-1), \\ q_1 &= \frac{\theta n + k - \theta}{n(\theta-\tau)} + \frac{-n+k-\theta}{n(\theta-\tau)} \theta \\ &+ \frac{k-\theta}{n(\theta-\tau)} (-\theta-1), \\ q_2 &= \frac{\theta n + k - \theta}{n(\theta-\tau)} + \frac{-n+k-\theta}{n(\theta-\tau)} \tau \\ &+ \frac{k-\theta}{n(\theta-\tau)} (-\tau-1). \end{aligned}$$

From E_2 we build the following partial sum:

$$\begin{aligned} S_{2l} &= \sum_{j=1}^{2l} (-1)^{j-1} \frac{(E_2^{\circ 2})^{\circ(2j-1)}}{2j-1} \\ &+ \frac{1}{3} \left(\frac{\theta n + k - \theta}{n(\theta-\tau)} \right)^3 \frac{1 - \left(\frac{\theta n + k - \theta}{n(\theta-\tau)} \right)^l}{1 - \left(\frac{\theta n + k - \theta}{n(\theta-\tau)} \right)^4} I_n. \end{aligned}$$

Since $\mathcal{V}'$ is closed under the Hadamard product and $\mathcal{B}$ is a basis of $\mathcal{V}'$, we can write S_{2l} as:

$$S_{2l} = \sum_{i=0}^{2} q_{S_{2l}}^i E_i,$$

where the $q_{S_{2l}}^i$, $i \in \{0, 1, 2\}$ are the eigenvalues of S_{2l}. We prove that $q_{S_{2l}}^i \geq 0, \forall i \in \{0, 1, 2\}$. First, we note the following identity regarding one of the eigenvalues of $E_2^{\circ 2}$:

$$\begin{aligned} &\left(\frac{\theta n + k - \theta}{n(\theta-\tau)} \right)^2 + \left(\frac{-n+k-\theta}{n(\theta-\tau)} \right)^2 k \\ &+ \left(\frac{(k-\theta)}{n(\theta-\tau)} \right)^2 (n-k-1) = \frac{\theta n + k - \theta}{n(\theta-\tau)}. \end{aligned}$$

Secondly, since all of the eigenvalues of E_2 are smaller in modulus that q_0, then the summands of S_{2l}, when $j-1$ is odd are smaller, in modulus, than

$$\left(\frac{\theta n + k - \theta}{n(\theta-\tau)} \right)^{2j-1}.$$

ISBN: 978-1-61804-225-5

For this assertion we also use the property

$$\lambda_{\max}((A_1 \circ \cdots \circ A_i)) \leq \lambda_{\max}((A_1)) \ldots \lambda_{\max}((A_i)),$$

where $\lambda_{\max}(A)$ denotes the maximum eigenvalue of the matrix A. Therefore, we conclude that all the eigenvalues of S_{2l} are nonnegative.

Now we consider the series:

$$\begin{aligned} S_\infty &= \left[\arctan\left(\frac{(\theta n+k-\theta)}{n(\theta-\tau)}\right)^2 \right. \\ &+ \left. \frac{1}{3}\left(\frac{\theta n+k-\theta}{n(\theta-\tau)}\right)^3 \frac{1}{1-\left(\frac{\theta * n+k-\theta}{n(\theta-\tau)}\right)^4}\right] I_n \\ &+ \arctan\left(\frac{-n+k-\theta}{n(\theta-\tau)}\right)^2 A \\ &+ \arctan\left(\frac{k-\theta}{n(\theta-\tau)}\right)^2 (J_n - A - I_n). \end{aligned}$$

Let q_∞^i, $i \in \{0,1,2\}$ be the eigenvalues of S_∞ such that

$$S_\infty = \sum_{i=0}^{2} q_\infty^i E_i.$$

Then, since $q_\infty^i = \lim_{l\to} q_{S_{2l}}^i$, for $i \in \{0,1,2\}$, and $q_{S_{2l}}^i \geq 0$, $\forall i \in \{0,1,2\}$, we conclude that $q_\infty^i \geq 0$, $\forall i \in \{0,1,2\}$.

Finally, we consider the new matrix, $S_{2\infty}$, obtained as

$$S_{2\infty} = E_2 \circ S_\infty.$$

The eigenvalues of $S_{2\infty}$ are also nonnegative because of the non-negativity of the eigenvalues of E_2 and S_∞ and the property $\lambda_{\min}(A \circ B) \geq \lambda_{\min}(A)\lambda_{\min}(B)$, where $\lambda_{\min}(A)$ denotes the minimum eigenvalue of the matrix A. From the non-negativity of the eigenvalues of $S_{2\infty}$ we establish the following result.

Theorem 1: Let X be a strongly regular graph with parameter set (n,k,a,c) and three distinct eigenvalues, k, θ and τ. If $k < n/3$ and $\theta < |\tau| - 2/3$, then

$$k \leq \frac{1}{3}(3\theta+1)^3. \tag{16}$$

Proof: Let $q_{2\infty}^i$, $i \in \{0,1,2\}$ be the eigenvalues of $S_{2\infty}$ such that

$$S_{2\infty} = \sum_{i=0}^{2} q_{2\infty}^i E_i.$$

We have already proved that all the eigenvalues of $S_{2\infty}$ are nonnegative. In particular, we have that $q_{2\infty}^0 \geq 0$, that is

$$\begin{aligned} 0 &\leq \frac{\theta n+k-\theta}{n(\theta-\tau)}\left[\arctan\left(\frac{(\theta n+k-\theta)}{n(\theta-\tau)}\right)^2 \right. \\ &+ \left. \frac{1}{3}\left(\frac{\theta n+k-\theta}{n(\theta-\tau)}\right)^3 \frac{1}{1-\left(\frac{\theta * n+k-\theta}{n(\theta-\tau)}\right)^4}\right] \\ &+ \frac{-n+k-\theta}{n(\theta-\tau)}\arctan\left(\frac{-n+k-\theta}{n(\theta-\tau)}\right)^2 k \\ &+ \frac{k-\theta}{n(\theta-\tau)}\arctan\left(\frac{k-\theta}{n(\theta-\tau)}\right)^2 (n-k-1). \end{aligned} \tag{17}$$

Since, for any strongly regular graph, we have $q_0 = 0$, then inequality (17) can be rewritten as

$$\begin{aligned} 0 &\leq \frac{\theta n+k-\theta}{n(\theta-\tau)}\left[\arctan\left(\frac{(\theta n+k-\theta)}{n(\theta-\tau)}\right)^2 \right. \\ &- \left. \arctan\left(\frac{k-\theta}{n(\theta-\tau)}\right)^2\right] \\ &+ \frac{1}{3}\left(\frac{\theta n+k-\theta}{n(\theta-\tau)}\right)^4 \frac{1}{1-\left(\frac{\theta * n+k-\theta}{n(\theta-\tau)}\right)^4} \\ &+ \frac{n+k-\theta}{n(\theta-\tau)}\left[\arctan\left(\frac{-n+k-\theta}{n(\theta-\tau)}\right)^2 k \right. \\ &- \left. \arctan\left(\frac{k-\theta}{n(\theta-\tau)}\right)^2\right] k. \end{aligned}$$

Applying Lagrange's Theorem to the function $\arctan$ in the intervals

$$\left[\left(\frac{k-\theta}{n(\theta-\tau)}\right)^2, \left(\frac{\theta n+k-\theta}{n(\theta-\tau)}\right)^2\right],$$

$$\left[\left(\frac{k-\theta}{n(\theta-\tau)}\right)^2, \left(\frac{n-k+\theta}{n(\theta-\tau)}\right)^2\right]$$

and making some straightforward majorations, one obtains

$$\begin{aligned} 0 &\leq \frac{\theta n+k-\theta}{n(\theta-\tau)}\frac{1}{1+\left(\frac{k-\theta}{n(\theta-\tau)}\right)^4}\frac{\theta}{(\theta-\tau)}\frac{\theta n+2k-2\theta}{n(\theta-\tau)} \\ &+ \frac{1}{3}\left(\frac{\theta n+k-\theta}{n(\theta-\tau)}\right)^4 \frac{1}{1-\left(\frac{\theta n+k-\theta}{n(\theta-\tau)}\right)^4} \\ &+ \frac{-n+k-\theta}{n(\theta-\tau)}\frac{1}{1+\left(\frac{-n+k-\theta}{n(\theta-\tau)}\right)^4}\frac{1}{\theta-\tau}\frac{n-2k+2\theta}{n(\theta-\tau)}k. \end{aligned}$$

ISBN: 978-1-61804-225-5

Since $k \leq n/3$ one obtains:

$$\begin{aligned} 0 \quad \leq \quad & \frac{1+\left(\frac{n-k+\theta}{n(\theta-\tau)}\right)^4}{1+\left(\frac{k-\theta}{n(\theta-\tau)}\right)^4}\frac{3\theta+1}{3(\theta-\tau)}\frac{\theta}{\theta-\tau}\frac{3\theta+2}{3(\theta-\tau)} \\ + \quad & \left(1+\left(\frac{n-k+\theta}{n(\theta-\tau)}\right)^4\right)\frac{1}{3}\left(\frac{3\theta+1}{3(\theta-\tau)}\right)^4 \\ \cdot \quad & \frac{1}{1-\left(\frac{3\theta+1}{3(\theta-\tau)}\right)^4}\Bigg] \\ + \quad & \frac{-n+k-\theta}{n(\theta-\tau)}\frac{1}{\theta-\tau}\frac{n-2k+2\theta}{n(\theta-\tau)}k. \end{aligned}$$

Now, since $\theta < |\tau| - 2/3$, then we conclude that

$$\frac{3\theta+1}{3(\theta-\tau)}\frac{1}{1-\left(\frac{3\theta+1}{3(\theta-\tau)}\right)^4} \leq 1$$

and

$$\frac{3\theta+1}{3(\theta-\tau)}\frac{\theta}{\theta-\tau}\frac{3\theta+2}{3(\theta-\tau)} \leq \left(\frac{3\theta+1}{3(\theta-\tau)}\right)^3,$$

then we conclude that

$$\begin{aligned} & \frac{n-k+\theta}{n(\theta-\tau)}\frac{n-2*k+\theta}{n(\theta-\tau)}\frac{1}{\theta-\tau)}k \leq \Big(\frac{1+\left(\frac{n-k+\theta}{n(\theta-\tau)}\right)^4}{1+\left(\frac{(k-\theta)}{n(\theta-\tau)}\right)^4} \\ + \quad & \frac{1+\left(\frac{n-k+\theta}{n(\theta-\tau)}\right)^4}{3}\Big)\Big(\frac{3\theta+1}{3(\theta-\tau)}\Big)^3 \end{aligned} \tag{18}$$

Using the fact that $k < n/3$ and making an algebraic manipulation of the right member of (18) we come to inequality (19):

$$\frac{2}{3(\theta-\tau)}\frac{1}{3(\theta-\tau)}\frac{1}{\theta-\tau}k \leq \frac{461}{243}\left(\frac{3\theta+1)}{3(\theta-\tau)}\right)^3 \tag{19}$$

Finally, rewriting inequality (19) and since $461/1458 < 1/3$, we obtain

$$k \leq \frac{1}{3}(3\theta+1)^3.$$

■

Applying the result presented in Theorem 1 to the complement graph, one obtains the following corollary.

Corollary 1: Let X be a strongly regular graph with parameter set (n,k,a,c) and three distinct eigenvalues, k, θ and τ. If $k > 2n/3 - 1$ and $|\tau| < \theta + 4/3$, then

$$n-k-1 \leq \frac{1}{3}(3|\tau|-2)^3. \tag{20}$$

VI. Numerical Results and Conclusions

In this section we present some experimental results for the feasibility conditions obtained in Section V. We consider the following notation:

$$q_{\theta k} = \frac{1}{3}(3\theta+1)^3 - k$$

and

$$q_{\tau k} = \frac{1}{3}(3|\tau|-2)^3 - (n-k-1).$$

We also consider the parameter sets $P_1 = (961, 312, 41, 130)$, $P_2 = (1225, 352, 24, 132)$, $P_3 = (1024, 385, 36, 210)$ and the respective complement parameter sets $\overline{P}_1 = (961, 648, 465, 378)$, $\overline{P}_2 = (1225, 872, 651, 545)$ and $\overline{P}_3 = (1024, 638, 462, 290)$.

In Table I we present some experimental results for the inequality of Theorem 1.

Param.	P_1	P_2	P_3
θ	2.0	2.0	1.0
τ	-91.0	-110.0	-175.0
$q_{\theta k}$	-197.7	-237.7	-363.7

TABLE I
NUMERICAL RESULTS FOR $P_1 = (961, 312, 41, 130)$, $P_2 = (1225, 352, 24, 132)$ AND $P_3 = (1024, 385, 36, 210)$.

In Table II we present some experimental results for the inequality of Corollary 1.

Param.	$\overline{P}_1$	$\overline{P}_2$	$\overline{P}_3$
θ	90.0	109.0	174.0
τ	-3.0	-3.0	-2.0
$q_{\theta k}$	-197.7	-237.7	-363.7

TABLE II
NUMERICAL RESULTS FOR $\overline{P}_1 = (961, 648, 465, 378)$, $\overline{P}_2 = (1225, 872, 651, 545)$ AND $\overline{P}_3 = (1024, 638, 462, 290)$.

Analyzing the results obtained for the inequalities of Theorem 1 and Corollary 1 we can conclude, from inequality (16), that when $k < n/3$ the value of k cannot be too big compared with the value of θ and, from inequality (20), when $k > 2n/3 - 1$, the value of $n - k - 1$ cannot be too big compared with the absolute value of τ.

Acknowledgment

1) Vasco Moço Mano is supported in part by FEDER funds through COMPETE Operational Programme Factors of Competitiveness ("Programa Operacional Factores de Competitividade") and by Portuguese funds through the Center for Research and Develpment in Mathematics and Applications and the Portuguese Foundation for Science and Technology ("FCT - Fundação para a Ciência e a Tecnologia") within project PEest-C/MAT/UI4106/2011 with COMPETE number FCOMP-01-0124-FEDER-022690.
2) Luís Vieira research funded by the European Regional Development Fund through the program COMPETE and by the Portuguese Government through the Center of Mathematics of University of Porto and the Portuguese Foundation for Science and Technology ("FCT - Fundação para a Ciência e a Tecnologia") under the project PEest-C/MAT/UI0144/2011.

REFERENCES

[1] R. C. Bose, *S*trongly regular graphs, partial geometries and partially balanced designs, Pacific J. Math 13, 389-419, 1963.

[2] P. Jordan, J. v. Neuman and E. Wigner, *On an algebraic generalization of the quantum mechanical formalism*, Annals of Mathematics, Vol 35, 29–64, 1934.

[3] H. Massan and E. Neher, *Estimation and testing for lattice conditional independence models on Euclidean Jordan algebras*, Ann. Statist., Vol 26, 1051–1082, 1998.

[4] L. Faybusovich, *Euclidean Jordan algebras and Interior-point algorithms*, J. Positivity, Vol 1, 331–357, 1997.

[5] L. Faybusovich, *Linear systems in Jordan algebras and primal-dual interior-point algorithms*, Journal of Computational and Applied Mathematics, Vol 86,148–175, 1997.

[6] D. M. Cardoso and L. A. Vieira, *Euclidean Jordan Algebras with Strongly Regular Graphs*, Journal of Mathematical Sciences, Vol 120, 881–894, 2004.

[7] V. M. Mano, E. A. Martins and L. A. Vieira, *Feasibility conditions on the parameters of a strongly regular graph*, Electronic Notes in Discrete Mathematics, 38, 607–613, 2011.

[8] V. M. Mano and L. A. Vieira, *Admissibility Conditions and Asymptotic Behavior of Srongly Regular Graphs*, International Journal of Mathematical Models and Methods in Applied Sciences, Issue 6, Vol 5, 1027–1034, 2011.

[9] C. Godsil and G. Royle, *Algebraic Graph Theory*, Springer, 2001.

[10] E. Bannai and T. Ito, *Algebraic Combinatorics. I. Association Schemes.*, Benjamin-Cummings, Menlo Park, CA, 1984.

[11] Jr. L. L. Scott,, *A condition on Higman's parameters*, Notices of Amer. Math. Soc., 20 A-97, 721-20-45, 1973.

[12] Ph. Delsarte, J. M. Goethals and J. J. Seidel, *Bounds for system of lines and Jacobi polynomials*, Philips Res. Rep. 30, 91-105, 1975.

[13] A. Neumaier, *New inequalities for the parameters of an association scheme*, Combinatorics and Graph Theory, Springer Lecture Notes 885, pp. 365-367.

[14] A. E. Brouwer and J. H. van Lint, *Strongly regular graphs and partial geometries, Enumeration and Design* Academic Press, 1982.

[15] J. Faraut and A. Korányi, *Analysis on Symmetric Cones* Oxford Science Publication, 1994.

ISBN: 978-1-61804-225-5

Mathematical modeling of large forest fires initiation and spread

Valeriy A. Perminov

***Abstract*—**It is presented mathematical model for description of heat and mass transfer processes at crown and large forest fires initiation and spread, taking into account their mutual influences. Mathematical model of forest fire was based on an analysis of experimental data and using concepts and methods from reactive media mechanics. The paper suggested in the context of the general mathematical model of forest fires give a new mathematical setting and method of numerical solution of a problem of a forest fire modeling. The boundary-value problem is solved numerically using the control volume methods and method of splitting according to physical processes. In this context, a study - mathematical modeling - of the conditions of forest fire initiation and spreading that would make it possible to obtain a detailed picture of the change in the velocity, temperature and component concentration fields with time, and determine as well as the conditions of forest fires initiation and spread is of interest.

***Keywords*—** Mathematical model, forest fire, turbulence, combustion, control volume, discrete analogue.

I. Introduction

One of the objectives of these studies is the improvement of knowledge on the fundamental physical mechanisms that control forest fires initiation and spread. A great deal of work has been done on the theoretical problem of how forest fire initiation. In forest there are two steps for crown forest fire initiation: spread of fire from crow to crown and crown fires are initiated by convective and radiative heat transfer from surface fires. However, convection is the main heat transfer mechanism. Firstly crown forest fire initiation have been studied and modeled by Van Wagner [1]. There are three simple crown properties: crown base height, bulk density and moisture content of forest fuel in this theory. Also crown fire initiation have been studied and modeled in detail (eg: Alexander [2], Van Wagner [3], Xanthopoulos, [4], Rothermel [5,6], Van Wagner, [7], Cruz [8], Albini [9], Scott, J. H. and Reinhardt, E. D. [10].The discussion of the problem of modeling forest fires is provided by a group of co-workers at Tomsk University (Grishin [11], Grishin and Perminov [12], Perminov [13,14]). The general mathematical model of forest fires was obtained by Grishin [11] based on an analysis of known and original experimental data [11,15], and using concepts and methods from reactive media mechanics. The physical two-phase models used in [16-17] may be considered as a continuation and extension of the formulation proposed by Grishin and Perminov [12-14]. However, the investigation of crown fires has been limited mainly to cases studied of forest fires initiation in two dimensional settings and did not take into account space properties of these phenomena. One of the objectives of these studies is the improvement of knowledge on the fundamental physical mechanisms that control forest fires initiation and spread. A great deal of work has been done on the theoretical problem of how forest fire initiation. In forest there are two steps for crown forest fire initiation: spread of fire from crow to crown and crown fires are initiated by convective and radiative heat transfer from surface fires. However, convection is the main heat transfer mechanism. Firstly crown forest fire initiation have been studied and modeled by Van Wagner [1]. There are three simple crown properties: crown base height, bulk density and moisture content of forest fuel in this theory. Also crown fire initiation have been studied and modeled in detail (eg: Alexander [2], Van Wagner [3], Xanthopoulos, [4], Rothermel [5,6], Van Wagner, [7], Cruz [8], Albini [9], Scott, J. H. and Reinhardt, E. D. [10].The discussion of the problem of modeling forest fires is provided by a group of co-workers at Tomsk University (Grishin [11], Grishin and Perminov [12], Perminov [13,14]). The general mathematical model of forest fires was obtained by Grishin [11] based on an analysis of known and original experimental data [11,15], and using concepts and methods from reactive media mechanics. The physical two-phase models used in [16-17] may be considered as a continuation and extension of the formulation proposed by Grishin and Perminov [12-14]. However, the investigation of crown fires has been limited mainly to cases studied of forest fires initiation in two dimensional settings and did not take into account space properties of these phenomena.

V.A. Perminov is with theTomsk Polytechnic University; Russia 634050, Tomsk, Lenina Avenue, 30 (Phone: +7-3822563650; fax: +7-3822563650; e-mail: valerperminov@gmail.com).

ISBN: 978-1-61804-225-5

II. Physical and Mathematical Model

It is assumed that the forest during a forest fire can be modeled as 1) a multi-phase, multistoried, spatially heterogeneous medium; 2) in the fire zone the forest is a porous-dispersed, two-temperature, single-velocity, reactive medium; 3) the forest canopy is supposed to be non-deformed medium (trunks, large branches, small twigs and needles), affects only the magnitude of the force of resistance in the equation of conservation of momentum in the gas phase, i.e., the medium is assumed to be quasi-solid (almost non-deformable during wind gusts); 4) let there be a so-called "ventilated" forest massif, in which the volume of fractions of condensed forest fuel phases, consisting of dry organic matter, water in liquid state, solid pyrolysis products, and ash, can be neglected compared to the volume fraction of gas phase (components of air and gaseous pyrolysis products); 5) the flow has a developed turbulent nature and molecular transfer is neglected; 6) gaseous phase density doesn't depend on the pressure because of the low velocities of the flow in comparison with the velocity of the sound. Let the coordinate reference point x_1, x_2 , x_3= 0 be situated at the centre of the domain of surface forest fire source at the height of the roughness level, axis $0x_1$ directed parallel to the horizontal surface to the right in the direction of the unperturbed wind speed, axis $0x_2$ directed perpendicular to $0x_1$ and axis $0x_3$ directed upward (Fig. 1).

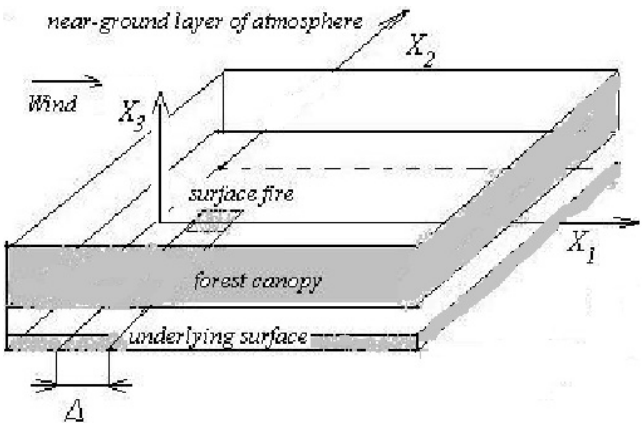

Fig. 1 Schematic of a forest fire domain.

Using the results of [11-14] and known experimental data [15] we have the following sufficiently general equations, which define the state of the medium in the forest fire zone, written using tensor notation

$$\frac{\partial \rho}{\partial t}+\frac{\partial}{\partial x_j}(\rho v_j)=\dot{m},\ j=1,2,3,\ i=1,2,3; \tag{1}$$

$$\rho\frac{dv_i}{dt}=-\frac{\partial P}{\partial x_i}+\frac{\partial}{\partial x_j}(-\rho\overline{v_i'v_j'})-\rho s c_d v_i\,|\,\vec{v}\,|- \tag{2}$$

$$-\rho g_i-\dot{m}v_i;$$

$$\rho c_p\frac{dT}{dt}=\frac{\partial}{\partial x_j}(-\rho c_p v_j'\overline{T'})+q_5R_5-\alpha_v(T-T_s)+ \tag{3}$$

$$+k_g(cU_R-4\sigma T^4)$$

$$\rho\frac{dc_\alpha}{dt}=\frac{\partial}{\partial x_j}(-\rho\overline{v_j'c_\alpha'})+R_{5\alpha}-\dot{m}c_\alpha\ ,\ \alpha=\overline{1,5}; \tag{4}$$

$$\frac{\partial}{\partial x_j}\left(\frac{c}{3k}\frac{\partial U_R}{\partial x_j}\right)-kcU_R+4k_S\sigma T_S^4+4k_g\sigma T^4=0, \tag{5}$$

$$k=k_g+k_S;$$

$$\sum_{i=1}^{4}\rho_i c_{pi}\varphi_i\frac{\partial T_S}{\partial t}=k_s(cU_R-4\sigma T_S^4)+ \tag{6}$$

$$+q_3R_3-q_2R_2+\alpha_V(T-T_S);$$

$$\rho_1\frac{\partial\varphi_1}{\partial t}=-R_1,\rho_2\frac{\partial\varphi_2}{\partial t}=-R_2, \tag{7}$$

$$\rho_3\frac{\partial\varphi_3}{\partial t}=\alpha_C R_1-\frac{M_C}{M_1}R_3,\rho_4\frac{\partial\varphi_4}{\partial t}=0;$$

$$\sum_{\alpha=1}^{5}c_\alpha=1,\ p_e=\rho RT\sum_{\alpha=1}^{5}\frac{c_\alpha}{M_\alpha},\vec{v}=(v_1,v_2,v_3),\vec{g}=(0,0,g)$$

$$\dot{m}=(1-\alpha_c)R_1+R_2+\frac{M_c}{M_1}R_3+R_{54}+R_{55},$$

$$R_{51}=-R_3-\frac{M_1}{2M_2}R_5,R_{52}=\nu_g(1-\alpha_c)R_1-R_5,$$

$$R_{53}=0,R_{54}=\alpha_4R_1,R_{55}=\frac{\alpha_5v_3}{v_3+v_{3*}}R_3.$$

$$R_1=k_1\rho_1\varphi_1\exp(-\frac{E_1}{RT_S}),R_2=k_2\rho_2\varphi_2T^{-0.5}\exp(-\frac{E_2}{RT_S}),$$

$$R_3=k_3\rho\varphi_3S_\sigma c_1\exp(-\frac{E_3}{RT_S}),$$

$$R_5=k_5M_2\left(\frac{c_1M}{M_1}\right)^{0.5}\left(\frac{c_2M}{M_2}\right)T^{-2.25}\exp(-\frac{E_5}{RT})\cdot$$

Here and above $\frac{\mathrm{d}}{\mathrm{d}t}$ is the symbol of the total (substantial) derivative. The system of equations (1)–(7) must be solved taking into account the initial and boundary conditions:

$$x_1=-x_{1e}:v_1=V_e,v_2=0,\frac{\partial v_3}{\partial x_1}=0,T=T_e,c_\alpha=c_{\alpha e}, \tag{8}$$

$$-\frac{c}{3k}\frac{\partial U_R}{\partial x_1}+cU_R/2=0;$$

$$x_1 = x_{1e}: \frac{\partial v_1}{\partial x_1} = 0,\ \frac{\partial v_2}{\partial x_1} = 0, \frac{\partial v_3}{\partial x_1} = 0,\ \frac{\partial c_\alpha}{\partial x_1} = 0, \quad \frac{\partial T}{\partial x_1} = 0, \frac{c}{3k}\frac{\partial U_R}{\partial x_1} + \frac{c}{2}U_R = 0; \tag{9}$$

$$x_2 = x_{20}: \frac{\partial v_1}{\partial x_2} = 0,\ \frac{\partial v_2}{\partial x_2} = 0,\ \frac{\partial v_3}{\partial x_2} = 0, \frac{\partial c_\alpha}{\partial x_2} = 0, \quad \frac{\partial T}{\partial x_2} = 0, -\frac{c}{3k}\frac{\partial U_R}{\partial x_2} + \frac{c}{2}U_R = 0; \tag{10}$$

$$x_2 = x_{2e}: \frac{\partial v_1}{\partial x_2} = 0,\ \frac{\partial v_2}{\partial x_2} = 0, \frac{\partial v_3}{\partial x_2} = 0, \frac{\partial c_\alpha}{\partial x_2} = 0, \quad \frac{\partial T}{\partial x_2} = 0, \frac{c}{3k}\frac{\partial U_R}{\partial x_2} + \frac{c}{2}U_R = 0. \tag{11}$$

$$x_3 = 0: v_1 = 0,\ v_2 = 0, \frac{\partial c_\alpha}{\partial x_3} = 0, -\frac{c}{3k}\frac{\partial U_R}{\partial x_3} + \frac{c}{2}U_R = 0, \quad v_3 = v_{30}, T = T_g,\ |x_1| \le \Delta, |x_2| \le \Delta \quad v_3 = 0,\ \ T = T_e,\ |x_1| > \Delta, |x_2| > \Delta; \tag{12}$$

$$x_3 = x_{3e}: \frac{\partial v_1}{\partial x_3} = 0,\ \frac{\partial v_2}{\partial x_3} = 0, \frac{\partial v_3}{\partial x_3} = 0, \frac{\partial c_\alpha}{\partial x_3} = 0, \quad \frac{\partial T}{\partial x_3} = 0, \frac{c}{3k}\frac{\partial U_R}{\partial x_3} + \frac{c}{2}U_R = 0. \tag{13}$$

Here α_v is the coefficient of phase exchange; ρ - density of gas – dispersed phase, t is time; v_i - the velocity components; T, T_S, - temperatures of gas and solid phases, U_R - density of radiation energy, k - coefficient of radiation attenuation, P - pressure; c_p – constant pressure specific heat of the gas phase, c_{pi}, ρ_i, φ_i – specific heat, density and volume of fraction of condensed phase (1 – dry organic substance, 2 – moisture, 3 – condensed pyrolysis products, 4 – mineral part of forest fuel), R_i – the mass rates of chemical reactions, q_i – thermal effects of chemical reactions; k_g , k_S - radiation absorption coefficients for gas and condensed phases; T_e - the ambient temperature; c_α - mass concentrations of α - component of gas - dispersed medium, index α=1,2,...,5, where 1 corresponds to the density of oxygen, 2 - to gas products of pyrolysis(carbon monoxide *CO*, CH_4 and etc.), 3 - to carbon dioxide and inert components of air, 4 - to particles of black, 5 - to particles of smoke; R – universal gas constant; M_α , M_C, and M molecular mass of α - components of the gas phase, carbon and air mixture; g is the gravity acceleration; c_d is an empirical coefficient of the resistance of the vegetation, s is the specific surface of the forest fuel in the given forest stratum. The initial values for volume of fractions of condensed phases are determined using the expressions:

$$\varphi_{1e} = \frac{d(1-\nu_z)}{\rho_1}, \varphi_{2e} = \frac{Wd}{\rho_2}, \varphi_{3e} = \frac{\alpha_c \varphi_{1e}\rho_1}{\rho_3}$$

where d -bulk density for surface layer, ν_z – coefficient of ashes of forest fuel, W – forest fuel moisture content. It is supposed that the optical properties of a medium are independent of radiation wavelength (the assumption that the medium is "grey"), and the so-called diffusion approximation for radiation flux density were used for a mathematical description of radiation transport during forest fires. To close the system (1)–(7), the components of the tensor of turbulent stresses, and the turbulent heat and mass fluxes are determined using the local-equilibrium model of turbulence (Grishin, [10]). The system of equations (1)–(7) contains terms associated with turbulent diffusion, thermal conduction, and convection, and needs to be closed. The components of the tensor of turbulent stresses $\rho\overline{v_i' v_j'}$, as well as the turbulent fluxes of heat and mass $\overline{\rho v_j' c_p T'}$, $\overline{\rho v_j' c_\alpha'}$ are written in terms of the gradients of the average flow properties using the formulas:

$$-\rho\overline{v_i v_j} = \mu_t\left(\frac{\partial v_i}{\partial x_j} + \frac{\partial v_j}{\partial x_i}\right) - \frac{2}{3}K\delta_{ij},$$

$$-\rho\overline{v_j c_p T'} = \lambda_t \frac{\partial T}{\partial x_j},\ -\rho\overline{v_j c_\alpha'} = \rho D_t \frac{\partial c_\alpha}{\partial x_j},$$

$$\lambda_t = \mu_t c_p / \mathrm{Pr}_t,\ \rho D_t = \mu_t / Sc_t,\ \mu_t = c_\mu \rho K^2/\varepsilon,$$

where μ_t, λ_t, D_t are the coefficients of turbulent viscosity, thermal conductivity, and diffusion, respectively; Pr_t, Sc_t are the turbulent Prandtl and Schmidt numbers, which were assumed to be equal to 1. In dimensional form, the coefficient of dynamic turbulent viscosity is determined using local equilibrium model of turbulence [11]. The length of the mixing path is determined using the formula $l = x_3 k_t / (1 + 2.5 x_3 \sqrt{c_d s / h})$ taking into account the fact that the coefficient of resistance c_d in the space between the ground cover and the forest canopy base is equal to zero, while the constants k_t = 0.4 and $h=h_2-h_1$ (h_2, h_1 – height of the tree crowns and the height of the crown base). It should be noted that this system of equations describes processes of transfer within the entire region of the forest massif, which includes the space between the underlying surface and the base of the forest canopy, the forest canopy and the space above it, while the appropriate components of the data base are used to calculate the specific properties of the various forest strata and the near-ground layer of atmosphere. This approach substantially simplifies the technology of solving problems of predicting the state of the medium in the fire zone numerically. The thermodynamic, thermophysical and structural characteristics correspond to the forest fuels in the canopy of a different (for example pine [10,12]) type of forest.

ISBN: 978-1-61804-225-5

III. Numerical Method and Results

The boundary-value problem (1)–(13) was solved numerically using the method of splitting according to physical processes [13]. In the first stage, the hydrodynamic pattern of flow and distribution of scalar functions was calculated. The system of ordinary differential equations of chemical kinetics obtained as a result of splitting [13] was then integrated. A discrete analog was obtained by means of the control volume method using the SIMPLE like algorithm [13,18]. The accuracy of the program was checked by the method of inserted analytical solutions. The time step was selected automatically.

Fields of temperature, velocity, component mass fractions, and volume fractions of phases were obtained numerically. Figures 2 illustrates the time dependence of dimensionless temperatures of gas (1) and condensed phases (2), Figure 3. – mass concentrations of gas components (1- oxygen, 2- gas products of pyrolysis), and Figure.4 - relative volume fractions of solid phases (1), moisture (2) and coke (3) at crown base of the forest (V_e=5m/s). At the moment of ignition the gas combustible products of pyrolysis burns away, and the concentration of oxygen is rapidly reduced. The temperatures of both phases reach a maximum value at the point of ignition. The ignition processes is of a gas - phase nature, i.e. initially heating of solid and gaseous phases occurs, moisture is evaporated. Then decomposition process into condensed and volatile pyrolysis products starts, the later being ignited in the forest canopy.

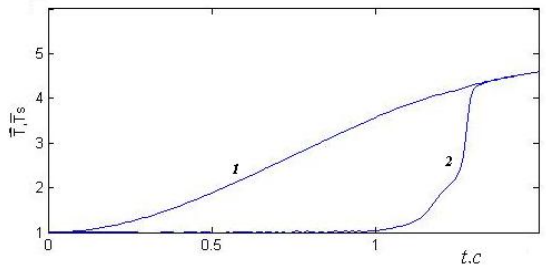

Fig. 2. Temperature of gas (1 - $\bar{T}$) and solid phase (2 - $\bar{T}_S$);
$\bar{T}$ =T/T_e , $\bar{T}_S$ =T_S/T_e, T_e=300K.

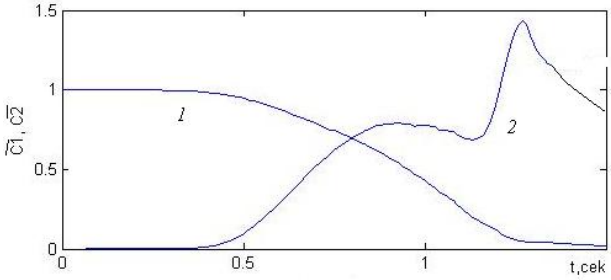

Fig. 3. Concentration of oxygen (1- $\bar{C}_1$) and gas products of pyrolysis (2- $\bar{C}_2$); $\bar{c}_\alpha = c_\alpha / c_{1e}, c_{1e} = 0.23$.

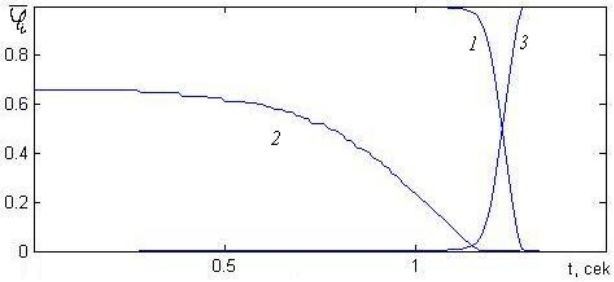

Fig. 4. Volume fractions of solid phase:
$1-\bar{\varphi}_1 = \varphi_1 / \varphi_{1e}$, $2-\bar{\varphi}_2 = \varphi_2 / \varphi_{2e}$, $3-\bar{\varphi}_3 = \varphi_3 / \varphi_{3e}$.

Note also that the transfer of energy from the fire source takes place due to radiation; the value of radiation heat flux density is small compared to that of the convective heat flux. As a result of heating of forest fuel elements, moisture evaporates, and pyrolysis occurs accompanied by the release of gaseous products, which then ignite. At $V_e \neq 0$, the wind field in the forest canopy interacts with the gas-jet obstacle that forms from the forest fire source and from the ignited forest crown and burn away in the forest canopy. Forest fire begins to spread in the forest canopy. The distribution of temperature, concentrations of gas products of pyrolysis and oxygen in the forest fire front are presented in the Figure 5.

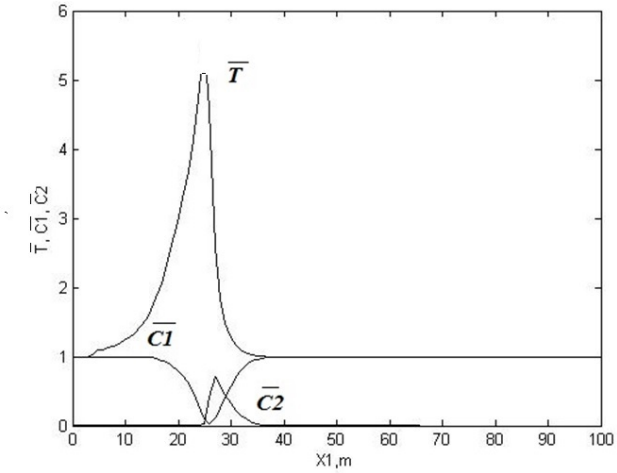

Fig. 5. The distribution of gas phase temperature ($\bar{T}$ ($\bar{T} = T / T_e, T_e = 300K$), concentrations of gas products of pyrolysis $\bar{c}_2 (\bar{c}_2 = c_2 / c_{1e}, c_{1e} = 0.23)$ and oxygen $\bar{c}_1 (\bar{c}_1 = c_1 / c_{1e})$ in forest fire front.

It is seen that the combustion wave looks like as a soliton. The oxygen concentration drops to near zero in front of a fire. It is consumed in the combustion of the pyrolysis products, the concentration of which is reached their maximum before the maximum of temperature.

Figures 6 – 7 present the distribution of temperature $\bar{T}$ ($\bar{T} = T / T_e, T_e = 300K$) (1- 1.5, 2 - 2., 3 – 2.6, 4 – 3, 5 –

3.5, 6 – 4.) for gas phase, concentrations of oxygen $\overline{c}_1$ (1 – 0.1, 2 – 0.5, 3 – 0.6, 4 – 0.7, 5 – 0.8, 6 – 0.9) and volatile combustible products of pyrolysis $\overline{c}_2$ (1 – 1., 2- 0.1, 3 – 0.05, 4 – 0.01) ($\overline{c}_\alpha = c_\alpha / c_{1e}, c_{1e} = 0.23$) at different instants of time for wind velocity V_e= 5 m/s (Fig.6) and V_e= 10 m/s (Fig.7). The distribution of isotherms of combustion temperature shows the moving of forest fire front with time. Figure 16 shows that with the increase of wind speed up to 10 m/s increases the rate of fire spread to 5 m/sec.

Ignition of forest due to spotting is one of the most difficult aspects to understand the behavior of fires. The phenomenon of spotting fires comprises three sequential mechanisms: generation, transport and ignition of recipient fuel. The present mathematical model and results of calculation are used to illustrate picture of the formation of large fires by combining small combustion sources arising from the transfer of firebrands. In order to understand these mechanisms, many calculation experiments have been performed. In the Figures 8 - 12 the process of formation large forest fire front as a result of integration of various sources of combustion is showed. The distributions of temperature for gas phase(*a*), concentrations of oxygen (*b*) and volatile combustible products of pyrolysis (c) at different times (I - t=3 sec., II - t=6 sec, III - t=12 sec.) for V_e= 5 m/s are presented. There are present the same values of isotherms and isolines of concentration for $\overline{c}_1$ and $\overline{c}_2$ as well as in the Figures 6-7. If the sources of ignition from the burning particles are arranged in a triangle, the processes of formation of the forest fire front are shown in Figures 8-9. In the second case (Figure 9), the right ignition source in the x_2 direction was 2 times less than in the first case (Figure 8). If all three combustion sources are situated on the same line, the formation of the combustion front is shown in Figure 10. Rather interesting picture of the formation of the front fire is implemented in the case of four combustion sources are located at the corners of a rectangle (Figure 11.) or trapezoid (Figure 12.).

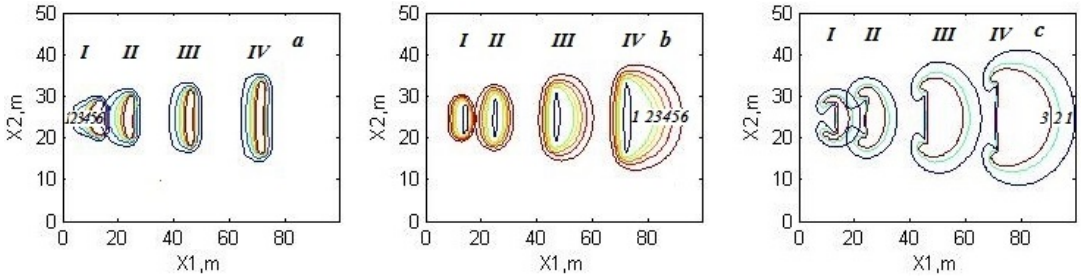

Fig. 6. The distribution of *a*) temperature for gas phase, *b)* concentration of oxygen and c) volatile combustible products of pyrolysis; V_e= 5 m/s, at different instants of time: I - t=3 sec., II - t=6 sec, III - t=12 sec., IV - t= 20 sec.

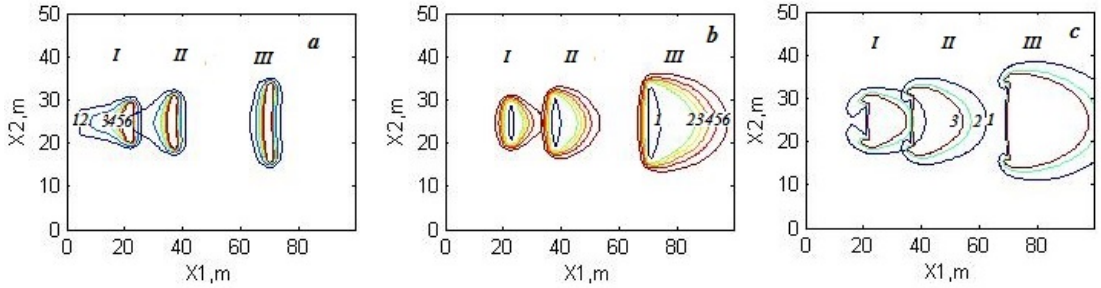

Fig. 7. The distribution of *a*) temperature for gas phase, *b)* concentrations of oxygen and c) volatile combustible products of pyrolysis; V_e= 10 m/s, at different instants of time: I - t=3 sec., II - t=6 sec, III - t=12 sec., IV - t= 20 sec.

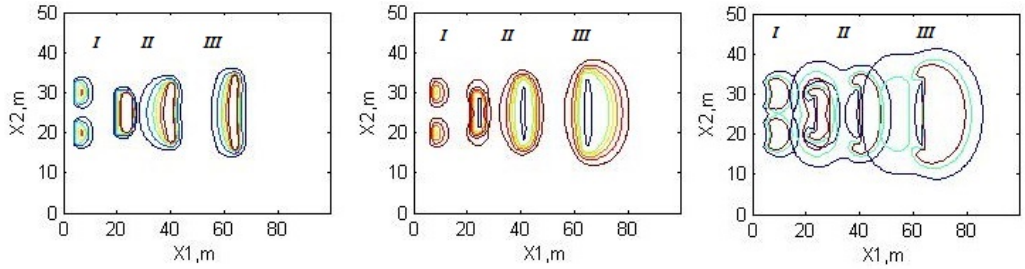

Fig. 8. The distribution of temperature for gas phase, concentrations of oxygen and volatile combustible products of pyrolysis.

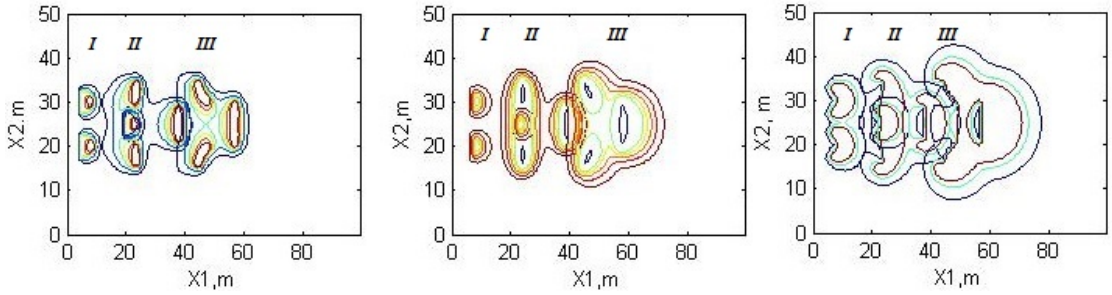

Fig. 9. The distribution of temperature for gas phase, concentrations of oxygen and volatile combustible products of pyrolysis.

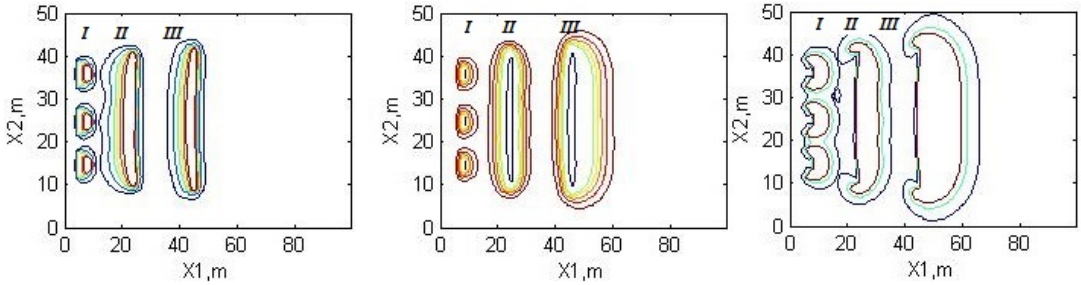

Fig. 10. The distribution of temperature for gas phase, concentrations of oxygen and volatile combustible products of pyrolysis.

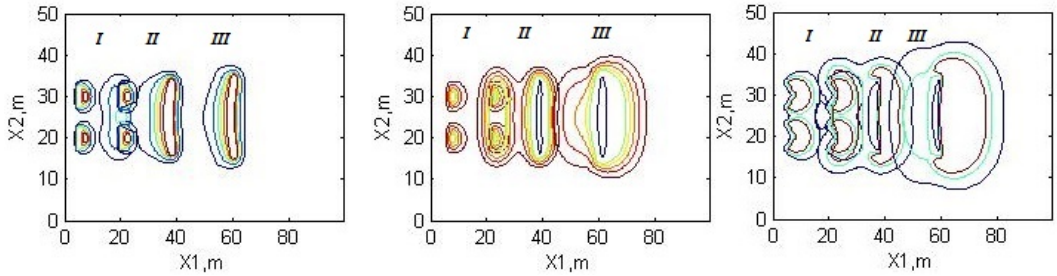

Fig. 11 The distribution of temperature for gas phase, concentrations of oxygen and volatile combustible products of pyrolysis.

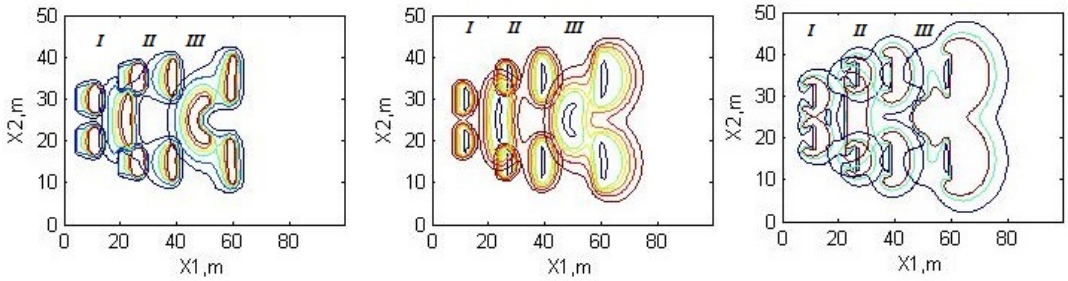

Fig. 12. The distribution of temperature for gas phase, concentrations of oxygen and volatile combustible products of pyrolysis.

IV. Conclusion

Using of this model gives an opportunity to describe the different conditions of the large forest fires initiation and spread taking account different weather conditions and state of forest combustible materials, which allows applying the given model for prediction and preventing fires. It overestimates the rate of crown forest fire spread that depends on crown properties: bulk density, moisture content of forest fuel, wind velocity and etc. The model proposed here gives a detailed picture of the change in the temperature and component concentration fields with time, and determine as well as the influence of different conditions on the crown forest fire spreading for the different cases of inhomogeneous of distribution of sources of forest fires initiation. The results of calculation of the rate of crown forest fires are agreed with the laws of physics and experimental data.

References

[1] C.E.Van Wagner, "Conditions for the start and spread of crown fire", Canadian Journal of Forest Research, vol. 7, 1977, pp. 23-34.

[2] M.E. Alexander, "Crown fire thresholds in exotic pine plantations of Australasia", PhD thesis, Department of Forestry, Australian National University, Australia, 1998.

[3] C.E. Van Wagner, "Prediction of crown fire behavior in conifer stands", Proc. '10th conference on fire and forest meteorology. Ottawa, Ontario. (Eds D. C. MacIver, H. Auld and R. Whitewood), 1989, pp. 207-212.

[4] G. Xanthopoulos, "Development of a wildland crown fire initiation model", PhD thesis, University of Montana, USA, 1990.

[5] R.C. Rothermel, "Crown fire analysis and interpretation", Proc. International conference on fire and forest meteorology. Missoula, Montana, USA, 1991.

[6] R.C. Rothermel, "Predicting behavior of the 1988 Yellowstone Fires: projections versus reality", Int. Journal of Wildland Fire, vol. 1, 1991, pp. 1-10.

[7] C.E.Van Wagner, "Prediction of crown fire behavior in two stands of jack pine", Canadian Journal of Forest Research, vol. 23, 1999, pp. 445-449.

[8] M.G. Cruz, "Predicting crown fire behavior to support forest fire management decision-making", Proc. IV International conference on forest fire research, Luso-Coimbra, Portugal. (Ed. D. X. Viegas), 11 [CD-ROM]. (Millpress), 2002.

[9] F.A. Albini, "Modeling ignition and burning rate of large woody natural fuels", Int. Journal of Wildland fire, vol. 5, 1995, pp. 81-91.

[10] J.H. Scott, "Assessing crown fire potential by linking models of surface and crown fire behavior", USDA Forest Service, Rocky Mountain Forest and Range Experiment Station. Fort Collins: RMRS-RP-29, (Colorado, USA), 2001.

[11] A.M. Grishin, Mathematical Modeling Forest Fire and New Methods Fighting Them, Publishing House of Tomsk University, Tomsk, Russia, 1997.

[12] A.M. Grishin, V.A. Perminov, "Mathematical modeling of the ignition of tree crowns", Combustion, Explosion, and Shock Waves, vol. 34, 1998, pp. 378-386.

[13] V.A. Perminov, "Mathematical Modeling of Crown and Mass Forest Fires Initiation With the Allowance for the Radiative - Convective Heat and Mass Transfer and Two Temperatures of Medium", Ph.D Thesis, Tomsk State University, Russia, 1995.

[14] V.A. Perminov, "Mathematical modeling of crown forest fire initiation", Proc. III International conference on forest fire research and 14th conference on fire and forest meteorology, Luso, Portugal. (Ed. D.X.Viegas) (1998), pp. 419-431.

[15] E.V. Konev, The physical foundation of vegetative materials combustion, Nauka, Novosibirsk, Russia, 1977.

[16] D. Morvan, J.L. Dupuy, "Modeling of fire spread through a forest fuel bed using a multiphase formulation", Combustion and Flame, vol. 127, 2001, pp. 1981-1994.

[17] D. Morvan, J.L. Dupuy, "Modeling the propagation of wildfire through a Mediterranean shrub using a multiphase formulation", Combustion and Flame, vol. 138, 2004, pp. 199-210.

[18] S.V. Patankar, Numerical Heat Transfer and Fluid Flow, Hemisphere Publishing Corporation, New York, USA, 1981.

Elliptic Curves Over The Quadratic Field

Seddik Abdelalim , Abdelhakim Chillali, and Said ELHAJJI

***Abstract*—**In this paper, we introduce some fundamental results of the elliptic curve over the quadratic field. After we create an elliptic curve over the quadratic field with an element of infinite order.[2,3,4].

***Keywords*—**Elliptic Curves, Quadratic Fields, Infinite Order...

Subject Classification: 14Gxx, 16Lxx, 16Zxx, 11Hxx, 11Txx.

I. Introduction

We introduce some importants results over the ring of integers of the quadratic fields.

Definition 1. The quadratic field is any extension of degree two over the rational field $\mathbb{Q}$.

Theorem 2. All quadratic field is of the form $\mathbb{Q}(\sqrt{d})$, where d is an integer without square factor.

Proposition 3. Let $K=\mathbb{Q}(\sqrt{d})$, is a quadratic field where d is an integer without square factor.

1. If $d\equiv 2 \mod 4$ or $d\equiv 3 \mod 4$ then the integer ring of K is the set of $a+b\sqrt{d}$ where $a,b\in\mathbb{Z}$.
2. If $d\equiv 1 \mod 4$ then the integer ring of K is the set of $\frac{1}{2}(a+b\sqrt{d})$ where $a,b\in\mathbb{Z}$ and $a\equiv b \mod 2$.

Definition 4. An elliptic curve over the quadratic field $K=\mathbb{Q}(\sqrt{d})$, is curve that is given by Weierstrass equation: $Y^2Z=X^3+AXZ^2+BZ^3$, where $A,B\in K$.[1,5].

This work was supported in part by the Laboratory of Mathematics, Computing and Application , Faculty of sciences University of Mohamed V Agdal, BP.1014 . Rabat, Morocco.

S. Abdelalim: Laboratory of Mathematics, Computing and Application, Department of Mathematical and computer, Faculty of sciences University of Mohamed V Agdal, BP.1014 . Rabat, Morocco. seddikabd@hotmail.com

A. Chillali: Department of Mathematics, USMBA, FST, FEZ, MOROCCO. chil2015@hotmail.fr

S. Elhajji: Laboratory of Mathematics, Computing and Application, Department of Mathematical and computer, Faculty of sciences University of Mohamed V Agdal, BP.1014 . Rabat, Morocco.elhajji@fsr.ac.ma

II. Elliptic Curves over the quadratic field whit an element of infinite order

PleaseIn this section we introduce some lemmas for created an elliptic Curves over quadratic field whit an element of infinite order.

Let $E_{A,B}$ an elliptic curve over the quadratic field K given by Weierstrass equation:

$$Y^2Z=X^3+AXZ^2+BZ^3, \text{ where } A,B\in K.$$

Lemma 1. Let $A,B\in\mathbb{Z}[i]$, $K=\mathbb{Q}[i]$ and $P=(x,y)$ an element of finite order in $E_{A,B}$.

If $(x,y)\in(\mathbb{Z}[i])^2$ then $y=0$ or $y^2\mid 4A^3+27B^2$.

Proof

Let $E_{A,B}$ an elliptic curve over the quadratic field $K=\mathbb{Q}[i]$ given by Weierstrass equation:

$$y^2=x^3+Ax+B, \text{ with } A,B\in\mathbb{Z}[i].$$

Let $P=(x,y)\in E_{A,B}$. Suppose that P has finite order.

If $x,y\in\mathbb{Z}[i]$, then by Lutz Nagelle Theorem [2], we have:

$$\text{if } y\neq 0 \text{ then } y^2\mid 4A^3+27B^2..$$

Lemma 2. Let $E_{A,B}$ an elliptic curve over the quadratic field $K=\mathbb{Q}[i]$ given by Weierstrass equation:

$$y^2=x^3+Ax+B, \text{ with } A,B\in\mathbb{Z}[i].$$

Then, there exists $A',B'\in\mathbb{Z}[i]$ such that $|A'|\geq|A|$ and $|B'|\geq|B|$ which the elliptic curve $E_{A',B'}$ have a point of infinite order.

Proof

Let $E_{A,B}$ an elliptic curve over the quadratic field $K=\mathbb{Q}[i]$ given by Weierstrass equation:

$$y^2=x^3+Ax+B, \text{ with } A,B\in\mathbb{Z}[i].$$

We pose:

$$A'=-(3|A|+1)^2,$$

$$B'=(3|B|+3)^2,$$

$$x_1=3|A|+1,$$

and $y_1 = 3|B|+3.$

We have:

$$\begin{aligned} x_1^3 + A' x_1 + B' &= (3|A|+1)^3 - (3|A|+1)^2 \times (3|A|+1) + (3|B|+3)^2 \\ &= (3|A|+1)^3 - (3|A|+1)^3 + (3|B|+3)^2 \\ &= (3|B|+3)^2 \\ &= y_1^2 \end{aligned}$$

It's clair that $Q = (x_1, y_1) \in E_{A',B'}$.

Suppose that Q has finite order, so by lemma2.1 we have:

$$\begin{aligned} y_1^2 \mid 4A'^3 + 27B'^2 &\Rightarrow 3 \mid 4A'^3 + 27B'^2 \\ &\Rightarrow 3 \mid 4A'^3 \\ &\Rightarrow 3 \mid A' \end{aligned}$$

Which is absurd because: $A' = -(3|A|+1)^2$

Lemma 3. Let $K = \mathbb{Q}(\sqrt{d})$ and $E_{A,B}$ an elliptic curve over K given by Weierstrass equation:

$$y^2 = x^3 + Ax + B, \text{ with } A, B \in \mathbb{Z}[\sqrt{d}].$$

Then, there exists $A', B' \in \mathbb{Z}[\sqrt{d}]$ such that $|A'| \geq |A|$ and $|B'| \geq |B|$ which the elliptic curve $E_{A',B'}$ over K have a point of an infinite order.

Proof Let $K = \mathbb{Q}(\sqrt{d})$ and $E_{A,B}$ an elliptic curve over K given by Weierstrass equation:

$$y^2 = x^3 + Ax + B, \text{ with } A, B \in \mathbb{Z}[\sqrt{d}].$$

We suppose:

$$T = sup\{|A|+1; |B|+1\},$$

$$A' = 2T,$$

$$B' = 3^2 T^2,$$

$$x_1 = \frac{1}{3},$$

and $$y_1 = \frac{1+3^4 T}{3^3}.$$

We have:

$$\begin{aligned} x_1^3 + A' x_1 + B' &= \tfrac{1}{3^6} + \tfrac{2T}{3^2} + 3^2 T^2 \\ &= \tfrac{1+2\times 3^4 \times T + 3^8 T^2}{3^6} \\ &= (\tfrac{1++3^4 T}{3^3})^2 \\ &= y_1^2. \end{aligned}$$

Such that , $Q = (x_1, y_1) \in E_{A',B'}$, so by lemma2.1 we have: Q has an infinite order.

ACKNOWLEDGMENT

I would thank Laboratory of Mathematics, Computing and Application for his helpful comments and suggestions.

REFERENCES

[1] A. Chillali, Elliptic Curves of the Ring, International Mathematical Forum, Vol. 6, no. 31 (2011), 1501-1505.

[2] S. Abdelalim, A. Chillali, S. Elhajji, Elliptic Curve Over The Rational Filed Whit Element Of Infinite Order, International Journal of Algebra, vol. 7, no. 19, (2013), 929-933.http://dx.doi.org/10.12988/ija.2013.311119

[3] N. Koblitz, Elliptic curve cryptosystems, Mathematics of Computation, vol. 48 (1987), 203-209.

[4] E. Lutz, Sur l'quation y2 = x3 dans les corps p-adic Math, J. Reine Angew, 1937.

[5] B. Mazur, Rational isogenies of prime degree, an appendix by D. Gold-feld,Invent. Math 1978.

[6] P. Samuel , Théorie Algébrique Des Nombres ISBN 2 7056 5589 1 deuxième Edition collection Hermann 1997.

S. Abdelalim: Laboratory of Mathematics, Computing and Application, Department of Mathematical and computer, Faculty of sciences, University of Mohamed V Agdal, BP.1014 . Rabat, Morocco.

A. Chillali: Department of Mathematics, USMBA, FST, FEZ, MOROCCO.

S. Elhajji: Laboratory of Mathematics, Computing and Application, Department of Mathematical and computer, Faculty of sciences, University of Mohamed V Agdal, BP.1014 . Rabat, Morocco.

On the geometry of luxury

Andrea Mantovi

***Abstract*—**A class of transcendental preferences is employed as an explicit representation of the luxury-necessity dichotomy which admits a smooth Cobb-Douglas limit. The analytical tractability of the model enables us to represent explicitly Marshallian demand and income elasticity of demand. The noncommutativity of scale and substitution effects, and measured by Lie brackets of the corresponding vector fields, is employed in order to define a measure of deviation from scale symmetry which is profoundly connected with Shephard's distance.

***Keywords*—** Cobb-Douglas functions, homotheticity, luxury, scale effect, income effect, substitution effect, Lie bracket.

I. Introduction

IN 1928 Cobb and Douglas [1] set forth a pathbreaking theory of aggregate manufacturing production, based on a highly tractable functional form of production function. Through the decades, such a function has proved extremely relevant for both production and consumption analysis, so as to become "perhaps the most ubiquitous function in all of economics." [2].

Being homothetic, Cobb-Douglas (CD) functions embody the scale symmetry of production and consumption problems, which has been long recognized as a benchmark property with noticeable implications (in first instance, the factorization of expenditure functions). In a recent paper, Mantovi [3] deepens the benchmark nature of homothetic models in terms of the commutativity of expansion and substitution effects. True, by their scale invariance, homothetic functions cannot represent general traits of preferences.

Definitely, to some extent, the luxury-necessity dichotomy can accommodate general traits of preferences. Departing from the scale symmetry of homothetic expansion paths (rays), the luxury-necessity dichotomy posits that, roughly speaking, expansion paths bend monotonically towards luxury. It is the aim of the present contribution to discuss a class of transcendental preferences for luxury which enable us to solve explicitly the consumption problem, maintain the pleasant analytical tractability of CD models, and then introduce a differential measure of luxury which complements and improves upon income elasticity of demand (IED).

The plan of the rest of the paper is as follows. In section 2 we introduce our preferences, solve the consumption problem, and represent explicitly income elasticity of demand. In section 3 we introduce our measure of luxury, and discuss its connection with Shephard's distance. A final section sketches potential lines of progress.

II. A model of luxury-necessity dichotomy

A. Transcendental preferences for luxury

Consider the 2-parameter class of preferences represented by the ordinal utility functions

$$U_{a,\varepsilon}(x,y) = x^{a}(ye^{\varepsilon y})^{1-a} \tag{1}$$

Such functions belong to the class of *transcendental* functions [6], and then to the class of *generalized power* production functions [7]. The class (1) is parametrized by the parameter $a \in (0,1)$, and by the "luxury" parameter $\varepsilon \in [0,\infty)$, which 'injects' increasing luxury into good y; generalizes the corresponding CD parameter in that (1) approach the CD form for $\varepsilon \to 0$.

Indifference curves for the class (1) read

$$x(y;u) = u^{\frac{1}{a}}(ye^{\varepsilon y})^{\frac{a-1}{a}} \tag{2}$$

Sample curves (2) are represented in Figure 1.

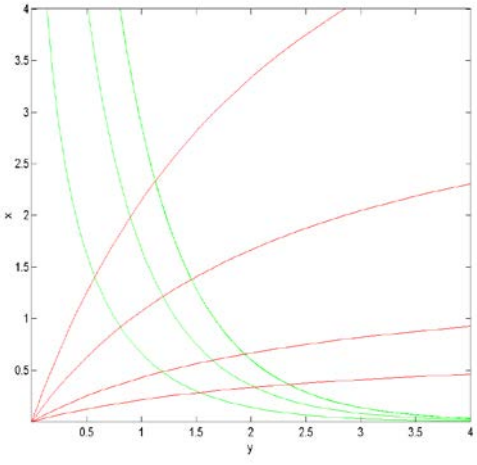

Figure 1. Sample indifference curves (utility levels 2, 4, 6) for the agent $(a,\varepsilon) = (0.75, 0.4)$ against expansion paths $p_x/p_y = 1, 2, 5, 10$.

As expected, utility curves approach the corresponding CD curves in the "no-luxury" limit $y \to 0$.

ISBN: 978-1-61804-225-5

B. Marshallian demand

By the analytical tractability of preferences (1), we are in a position to solve the consumption problem with only minor deviations from the analytics of CD models. The FOC

$$MRS = \frac{\frac{\partial U}{\partial y}}{\frac{\partial U}{\partial x}} = \frac{p_y}{p_x} = \frac{1-a}{a}\frac{x}{y}(1+\varepsilon y)$$
$$\Rightarrow \quad xp_x = \frac{a}{1-a}\frac{yp_y}{1+\varepsilon y} \tag{3}$$

is a smooth generalization of the corresponding CD condition, (a condition, evidently, independent of the utility representation), and provides a Cartesian equation for expansion paths.

Marshallian demand functions satisfy the budget balance condition; therefore, assume all income is spent, plug (3) into the budget constraint and obtain the simple quadratic equation

$$\varepsilon\, y^2 + \left(\frac{1}{1-a} - \varepsilon\frac{I}{p_y}\right)y - \frac{I}{p_y} = 0 \tag{4}$$

whose positive solution

$$y_{1,2} = \frac{1}{2\varepsilon}\left(-\frac{1}{1-a} + \varepsilon\frac{I}{p_y} \pm \sqrt{\left(\frac{1}{1-a} - \varepsilon\frac{I}{p_y}\right)^2 + 4\varepsilon\frac{I}{p_y}}\right) \tag{5}$$

establishes the Marshallian demand of the luxury good for the agent (a,ε). Notice, and enter such an expression via their ratio, so as to guarantee homogeneity of degree 0.

The simplicity of the function (5), a combination of elementary functions, enables us to plot Engle curves for both the goods with great analytical control. Evidently, given (5), the Marshallian demand for the necessary good is uniquely determined by the budget constraint. Consistently with the cartesian representation of expansion paths (eq. 3), the necessary good is subject to satiation: for any pair p_x, p_y, the upper bound $\overline{x} = \frac{a}{1-a}\frac{p_y}{p_x}\frac{1}{\varepsilon}$ for the consumption of the necessary good is the satiation level, which, as expected, varies with relative price, and shrinks for increasing ε.

On the other hand, the consumption of the luxury good, as income increases, "takes it all": for large enough income, the necessity share becomes negligible, and Engel curves for luxury are linear. Figure 2 provides a transparent representation of such a simple pattern, which witnesses the effectiveness of our consumption model in representing fundamental traits of behavior.

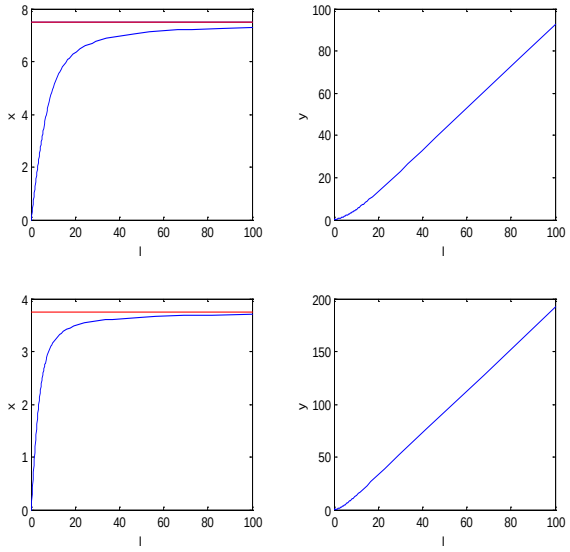

Figure 2. Engel curves for the agent (a,ε) = (0.75, 0.4) for unit prices (above) and $p_x=2p_y$ (below) for both luxury (right) and necessary (left) good.

C. Income elasticity of demand

IED exceeding 1 is the standard indicator of a good being a luxury good (see for instance [7] for a landmark theoretical/empirical analysis). By the analytical tractability of our model we are in a position to write simple explicit solutions for such an indicator. For the sake of definiteness, consider unit prices, and then optimal consumption as a function of the expenditure $I = x + y$. Then, equation (4) reduces to $0 = y^2 + (10 - I)y - 2.5I$, whose positive solution reads

$$y(I) = \frac{1}{2}\left(I - 10 + \sqrt{(I-10)^2 + 10I}\right) \tag{6}$$

The graph of (6) is the Engel curve for the luxury commodity at identical prices for the agent . Differentiate (6) and divide by itself and obtain the expression

$$\frac{I}{y^*}\frac{dy^*}{dI} = I\,\frac{1 + \frac{I - 10 + 5}{\sqrt{(I-10)^2 + 10I}}}{I - 10 + \sqrt{(I-10)^2 + 10I}} \tag{7}$$

for IED as a function of expenditure (income) I. The plot of (7) function is given in Figure 3.

ISBN: 978-1-61804-225-5

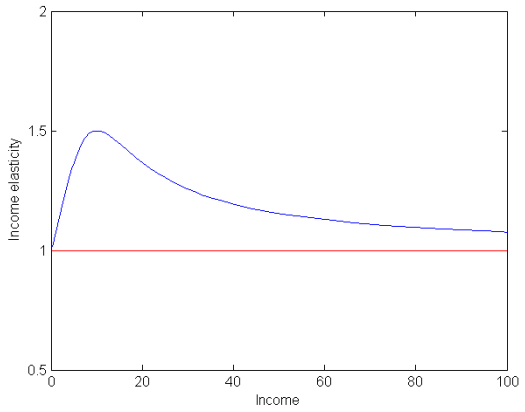

Figure 3. Income elasticity of demand as a function of income for the agent $(a,\varepsilon) = (0.75, 0.4)$.

As expected, such a plot approaches 1 for vanishing expenditure (in which preferences approach the CD limit), display an initial phase of growth (driven by the bending of the expansion path) which culminates in a peak, after which the function approaches asymptotically 1 from above (as the expansion path approach the asymptotic satiation of necessity.

The transparency of such a picture witnesses the effectiveness of our model of preferences. True, the curve represented in Figure 2 spans a vertical range [1,1.5], and the question raises naturally as to which of such values should be considered a 'preferred' indicator of the luxury effect driving the agents under inspection. Evidently, if, ceteris paribus, we increase ε, we obtain a curve with the same qualitative behavior and with a magnification in the vertical direction.

In fact, IED is a function of dual variables (prices and income). Building on the philosophy represented in [3, 4] we can define a primal indicator representing a 'departure' from the scale symmetry (homotheticity) of CD models which bears a close connection with Shephard' distance.

III. Measuring Luxury via Lie Brackets

Along the line of though discussed by [3] one can employ vector fields on consumption space the model globally relevant economic effects, and then employ Lie brackets as measures of noncommutativity of such effects. We already know ([3]) that in the CD limit $\varepsilon \to 0$ our agents display commutation of expansion and substitution effects. In addition, we expect noncomutativity to onset for positive ε, and to increase with such a parameter.

The vector field on our consumption set generating scale effects (SCE) reads [3,4]:

$$\mathbf{Z} = x\frac{\partial}{\partial x} + y\frac{\partial}{\partial y} \tag{8}$$

It is a radial vector field whose components do coincide with the coordinates of the base, and such that, for any function f homogeneous of degree d, Euler's theorem can be written $\mathbf{Z}(f) = d\ f$. Recall, scale transformation define the rationale for Shephard's distance [9], which provides a primal representation of preferences equivalent to the one given by a utility function.

As of the vector field generating substitution effects (SUE), let us follow [3], and notice that the vector field

$$\begin{aligned}\tilde{\mathcal{S}} &= \frac{\partial U}{\partial y}\frac{\partial}{\partial x} - \frac{\partial U}{\partial x}\frac{\partial}{\partial y} \\ &= e^{\varepsilon(1-a)y}\left((1-a)x^{a}y^{-a}(1+\varepsilon y)\frac{\partial}{\partial x} - ax^{a-1}y^{1-a}\frac{\partial}{\partial y}\right)\end{aligned} \tag{9}$$

is tangent to indifference curves, so that

Let the ratio y/x be the coordinate on indifference curves by means of which we want to parametrize SUE; such a choice is pivotal for the consistency of our framework, in that such a parametrization of SUE is *adapted* to SCE. Compute the normalization function, i.e. the action of the vector field (23) on the function y/x,

$$\mathcal{N}_{\frac{y}{x}} = \tilde{\mathcal{S}}\left(\frac{y}{x}\right) = \left(\frac{\partial U}{\partial y}\frac{\partial}{\partial x} - \frac{\partial U}{\partial x}\frac{\partial}{\partial y}\right)\left(\frac{y}{x}\right)$$

$$= -e^{\varepsilon(1-a)y}x^{a-2}y^{1-a}(1+(1-a)\varepsilon y) = -\frac{1}{x^2}\chi_{a,\varepsilon}(y)U_{a,\varepsilon}(x,y) \tag{10}$$

As expected, we face the emergence of the deviation factor χ. Thus, the proper SUE vector field results in

$$\mathcal{S} \equiv \frac{\tilde{\mathcal{S}}}{\mathcal{N}_{\frac{y}{x}}} == -(1-a)\,x^{2}y^{-1}\frac{1+\varepsilon y}{\chi_{a,\varepsilon}(y)}\,\frac{\partial}{\partial x} + \frac{ax}{\chi_{a,\varepsilon}(y)}\frac{\partial}{\partial y} \tag{11}$$

so that $\mathcal{S}\left(\frac{y}{x}\right) = 1$, with the correct CD limit for $\varepsilon \to 0$ (Mantovi, 2013a). The vector field (25) is clearly independent of the utility representation,

Thus, we are in a position to compute the Lie bracket between the substitution vector field (11) and scaling vector field (8) by means of the standard algebra [10, p. 153] and obtain

$$[\mathcal{S},\mathbf{Z}]_x = \mathcal{S}_x \frac{\partial Z_x}{\partial x} + \mathcal{S}_y \frac{\partial Z_x}{\partial y} - Z_x \frac{\partial \mathcal{S}_x}{\partial x} - Z_y \frac{\mathcal{S}_x}{\partial y}$$

$$= -(1-a)x^2 y^{-1} \frac{1+\varepsilon y}{\chi(y)} \cdot 1 + ax \frac{1}{\chi(y)} \cdot 0$$
$$- x(a-1)2xy^{-1} \frac{1+\varepsilon y}{\chi(y)} - y(1-a)x^2 y^{-2} \frac{1+\varepsilon y}{\chi(y)}$$
$$+ y(1-a)x^2 y^{-1} \frac{d}{dy}\left(\frac{1+\varepsilon y}{\chi(y)}\right)$$

$$= (1-a)x^2 \frac{d}{dy}\left(\frac{1+\varepsilon y}{\chi(y)}\right) \qquad (12)$$

$$[\mathcal{S},\mathbf{Z}]_y = \mathcal{S}_x \frac{\partial Z_y}{\partial x} + \mathcal{S}_y \frac{\partial Z_y}{\partial y} - Z_x \frac{\partial \mathcal{S}_y}{\partial x} - Z_y \frac{\partial \mathcal{S}_y}{\partial y}$$

$$= -(1-a)x^2 y^{-1} \frac{1+\varepsilon y}{\chi(y)} \cdot 0 + ax \frac{1}{\chi(y)} \cdot 1$$
$$- xa \frac{1}{\chi(y)} - y \cdot 0 \frac{1}{\chi(y)} - yax \frac{d}{dy}\frac{1}{\chi(y)}$$

$$= -yax \frac{d}{dy}\frac{1}{\chi(y)} \qquad (13)$$

We thereby verify that the vector field with components (12) and (13) is radial, on account of the simple derivatives

$$\frac{d}{dy}\left(\frac{1+\varepsilon y}{\chi(y)}\right) = \frac{a\varepsilon}{(1+(1-a)\varepsilon y)^2}$$
$$\frac{d}{dy}\frac{1}{\chi(y)} = \frac{(a-1)\varepsilon}{(1+(1-a)\varepsilon y)^2} \qquad (14)$$

To sum up, the vector field with components (12) and (13) is a consistent measure of deviation from scale symmetry (homotheticity), in which scale effects and substitution effects do commute [3].

$$[\mathcal{S},\mathbf{Z}] = \varepsilon \frac{a(1-a)}{(1+(1-a)\varepsilon y)^2}\left(x^2 \frac{\partial}{\partial x} + xy \frac{\partial}{\partial y}\right)$$
$$= \varepsilon\, a(1-a) \frac{x}{\chi_{a,\varepsilon}{}^2(y)} \mathrm{Z} \equiv L(x,y;a,\varepsilon)\, \mathrm{Z} \qquad (15)$$

Such a vector field, as expected, is radial, in that the failure of the infinitesimal path employed in standard discussions [10 Spivak] to close up takes place in the radial direction, and is uniform in *x*/*y*. Figure 4 provides an intuitive setting with respect to which to pin down the insight connecting (15) with Shephard's distance.

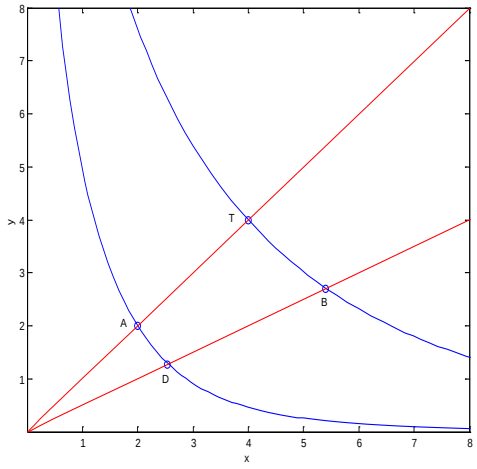

Figure 4. The noncommutativity of finite scale effects and substitution effects: the loop ATBD is closed since AT and DB represent different scale effects.

As represented in Figure 4, closed loops must entail different scale effects: the scale effect connecting D and B is larger than the scale effect connecting A with T since such scale effects connect point on a higher indifference curve with points on different indifference curves, we are given a monotone pattern of Shephard's distances between the points on the upper curve and the lower utility level. Such measures are the finite correspondent of the infinitesimal measure (15), which defines an "index" of luxury as a function of primal variables and of the parameters of the model. We thereby obtain a natural representation of the connection between Shephard's distance and the commutativity of SCE and SUE

IV. Perspectives

The "index" of luxury we been arguing about, evidently, is shaped by the properties of the specific functional form (1). Still, the degree of generality embodied by our model, in which the bending of expansion path increases with ε, enables us to believe in the 'universality' of the insights thereby conveyed.

On the one hand, by their analytical tractability, the preferences (1) seem to represent a promising building block for theoretical general equilibrium analysis. On the other hand, the well behavior of the consumption pattern discussed leads one to conjecture potential applications to the positive theory of general equilibrium. On the other hand, the relevance of potential empirical applications may rest on the smooth Cobb-Douglas limit of our model.

Overall productive efficiency as tailored by [5] seems to be a natural playground for our approach, on account of the close link established in [3] between, on the one hand, standard and

reversed Farrel decompositions, and, on the other hand, the commutativity of expansion and substitution effects.

ACKNOWLEDGMENT

The author acknowledges profound comments by Paolo Fabbri (Department of Economics, Parma) and G. Corneo (Department of Economics, Freie Universität, Berlin).

REFERENCES

[1] W. Cobb and P. H. Douglas, "A Theory of Production," *American Economic Review*, vol. 18, no. 1, pp. 139–165, March 1928.
[2] R. G. Chambers, *Applied production analysis*. Cambridge University Press, 1988.
[3] A. Mantovi, "On the commutativity of expansion and substitution effects," *Journal of Economics*, vol. 110, no. 1, pp. 83-105, September 2013.
[4] A. Mantovi, "Differential duality," *Working paper 2013-EP05, Dipartimento di Economia, Università degli Studi di Parma*.
[5] P. Bogetoft, R. Färe, and B. Obel, "Allocative efficiency of technically inefficient units," *European Journal of Operational Research*, vol. 168, no. 2, pp. 450–462, January 2006.
[6] A. Halter, H. Carter, J. Hocking, "A Note on the Transcendental Production Function," *Journal of Farm Economics*, vol. 39, pp. 966-974, 1957.
[7] A. de Janvry, "The Class of Generalized Power Production Functions," *American Journal of Agricultural economics*, vol. 54, pp. 234-237, 1972.
[8] A. Deaton, J. Muellbauer, "An Almost Ideal Demand System," *American Economic Review*, vol. 70, no. 3, pp. 312–326, June 1980.
[9] R. Shephard, *Cost and Production Functions*. Princeton University Press, 1953.
[10] M. Spivak, *A Comprehensive Introduction to Differential Geometry, Volume one, Third edition*. Publish or Perish, 1999.

A. **Mantovi**, PhD in Physics (Parma), lecturer in microeconomics at the Department of Economics in Parma, has published monographs (Carocci Editore) on corporate governance and dividend policies as contributions to the theory of the firm. His published papers (see for instance RePEc) deal with the connection between the investment and the agency problem, and the foundations of the microeconomics of consumption.

End Fuel prices and their drivers in the Czech Republic

Ladislav Tyll, Filip Fingl

Abstract - This paper deals with understanding drivers influencing the end price of fuels in the Czech Republic and ramifications for relevant companies. Its aim is to provide a comprehensive understanding of all relevant elements that have been influencing end prices of gasoline and diesel during last 8 years, understand their leverage and uncover which of those were the most important for this development. These are then researched using mainly graphical analysis and statistical tools. The delivery is that both prices of gasoline and diesel are highly correlated with the price development of crude oil and the prices of their respective commoditized barges expressed in the nominal value of CZK. It was also discovered that there are visible tendencies for asymmetrical pricing reaction and reaction lags, which could serve as a basis for a follow-up work. We also tried to examine the level in which Czech crown as a national currency provides cushion against up and down swings in commodity markets. Based on these findings several conclusive recommendations for relevant companies were built and delivered.

Keywords - Barge, crude oil price effect, Czech end fuel market, diesel price, exchange rate, gasoline price

I. Introduction

The role of end fuel prices is very important in every country, and the Czech Republic is no different, because apart from providing private customers with means of transportation, they influence a large part of the economy, since they make a significant part of the cost structure of transport and logistics companies, which make up a backbone of many important industries. Therefore understanding what drives these prices could help better grasp on their dynamics and provide valuable insights into how could certain companies be able to optimize their purchasing decisions. Third one that there is a tendency to drive price up, however their decrease tends to be much more subtle, i.e. so called asymmetric pricing. Last but not least we tried to examine the role of the Czech currency in mitigating up and down swings in commodity markets. All these hypotheses come from general notions of this market in the Czech Republic and will be scrutinized throughout the paper. The final outcome should be a set of applicable recommendations or insights for relevant companies, which could help them to understand what is happening to the prices, what kind of patterns there are and which business implications therefore arise from it.

II. Theoretical background and former studies overview

To understand pricing mechanism in respective markets we used a study done by Asche, Gjølberg and Volker [1] providing a fairly compelling analysis on a possible exogenous character of crude oil price development and an interesting work by Johansen [2] providing a framework for understanding long-run price relationships between crude oil and refined products and mutually between these products, however unfortunately not covering gasoline and diesel. For the purposes of this paper the most important finding is that crude oil prices are only weakly exogenous, which means that in the long-run, which is the major focus of this paper, there is no reverse feed of the end product prices back to crude oil price, hence crude oil price could be considered as an independent variable. It is important to mention though that the study provides an evidence of a slight reversed feed in the short-run, which will be also of the interest, however since this paper is focused only on the Czech market, which is in the whole magnitude quite negligible.

Rao [3] seeks to understand if there is a causality between the development of crude oil prices and the refined products, where he eventually concludes that there is, in fact, a causal relationship. Whereas the market itself is very distant from the researched one, the heterogeneity of the character of fuels can provide a base for the thinking in the work, especially since these findings are backed but numerous other studies.

A deeper analysis of trends between crude oil and gasoline prices is provided by Mirantes et al. [4], where they demonstrate the non-stationarity of crude oil and refined products and on the other hand stationarity of refining margins and their co-integration with a long-term dynamics, which further supports the hypothesis that there is a tight correlation between crude oil prices and refined products and also that refining margins tend to remain stable and quite easily observable over the course of time.

Another hypothesis is provided by Radchenko [5], who argues that in the end gasoline market there are lags in changes of the gasoline price in response to the changes on the crude oil market. This hypothesis was tested on empirical data gathered in the US between 1991 and 2002 however again the character of these reaction does not discriminate its existence

ISBN: 978-1-61804-225-5

also on the Czech market and can therefore provide one reasoning for imperfect reactions of the end market.

In its other paper, Radchenko [6] further develops the idea of the oil price volatility and the response from the gasoline market however here he presents a hypothesis, that reactions towards the crude oil price development on the gasoline market are asymmetric, meaning that the reaction on an upward movement of oil prices is sharper than the other way around. A similar conclusion is drawn by Bettendorf et al. [7] based on a study conducted on the Dutch market between 1996 and 2004, which concluded that these changes are indeed asymmetrical with a stronger reaction to an upward change in a spot price, therefore this behavior is not typical only for US market. According to our research we may see the same behavior of price also in the Czech market.

Further theoretical background on this problematic is provided by Chevillon and Rifflard [8], where it is enlighten how OPEC is able to shift the balance of power using its oligopolistic power. A deeper elaboration on how oil markets work and why it is possible to use spot prices for understanding the dynamics of the industry, even though the industry itself deals predominantly on the contract basis is offered by Fattouh [9] from the Oxford Institute for Energy Studies. Based on his argumentation, since the oil market is to a substantial extent, a physical market, futures prices should converge to the spot market because of the arbitrage opportunities.

Regarding the relation between the oil prices and the value of USD Novotný [10] in his work very convincingly illustrates how Brent price is linked to the USD exchange rate. The development itself has been observed since 1990s however Novotný goes further and seeks to examine the relationship between the price of oil and USD, since that is the currency in which it is traded. After analyzing the strength and direction of the relationship, he offers a point of view, which concludes that there is indeed a negative correlation. This finding should therefore strongly reflect into the price of oil expressed in Czech currency or to be more precise, to dampen it, since the growth of oil price means a drop in the nominal value of USD, which should theoretically mean a drop of its value against CZK, if everything else remains unchanged.

A paper on a similar topic was presented by Breitenfellner and Cuaresma [11], where they devote their time to exploring the linkage between crude oil prices and USD/EUR exchange rate and conclude that the negative correlation has several main reasons, among others efficiency of the monetary market and investments in crude oil related asset markets. Therefore they present a very similar conclusion as Novotný did.

A relationship between global economic development and crude oil prices was researched by He et al.[12], concluding a strong influence of the economic development on the crude oil prices (supporting the development of crude oil prices during the crisis). We used these studies as our inputs and we tried to go further to prove them on the Czech market with time series ending in year 2013.

III. Methodology

For understating the relationship between the crude oil (independent variable) and prices of barges and end prices of fuels (dependent variables) correlation analysis was used [13]. The same was applied for the mutual relationship between value of CZK in relation to USD and the oil prices. For our purposes we used the Pearson product-moment correlation coefficient, which is the most widely used. To understand the possible volatility of individual time series, mean and standard deviation was used.

Time series reflecting the development of end prices were cleared of VAT and excise tax to properly reflect changes in the underlying commodity.

To understand leverages correctly, it is necessary to untwist elements involved in this process and the magnitude of their impact.

Market-driven factors consist of elements which impact on the final price of fuels is determined by rationales arising through the interaction of different players on the market. In this group there are several significant factors to be considered, namely the crude oil price, then costs connected with each element of the supply chain involved in the process of extracting and delivering the final product (in this case, costs of refinement, distribution, marketing and margins of all involved parties, i.e. refineries, transportation companies, wholesalers and retailers) and finally relevant exchange rates. The most important exchange rate for the sake of this work is the CZK/USD ER, since all relevant quotes are denominated in USD.

Within the **administrative factors** we examined taxes, namely the Value Added Tax (VAT) and the excise tax. In recent years we had to include into our consideration also EU directives concerning minimal contents of bio-originated matters. However these factors contribute quite significantly on the end price of fuels (more than 50 %) they will not be included into our consideration since they are more or less stable over longer period of time and because their changes are more predictable.

Lastly, a group of **external factors** which do not directly fit into either of aforementioned groups. Here we may include for instance seasonality or the phase of the economic cycle.

Despite the fact, that there are certain distinctions between the price creation of gasoline and diesel, a significant part of their price creation is similar therefore they can be researched jointly to a certain extent.

IV. Construction of the Fuel End Price in the Czech Republic

The crude oil and its markets constitute only the first component of the pricing. The second component covers the process of the purchase and physical delivery of the raw resource to the Czech Republic.

Tariffs connected with transporting crude oil are quite distinctive. There are generally two types of tariffs; cost-based and negotiated, whereas the latter type prevails for the transit tariffs. In general, the way how these tariffs are established and calculated shows significant difference from country to country and even with comparable methodology the spread of margins seems to be quite wide. Another issue is that since in

the majority of relevant countries these tariffs are negotiated on the state level and then implemented through the bilateral intergovernmental agreements, they are often subject to confidentiality rules and therefore it is difficult to understand the whole extent and therefore underpin the average costs relevant to the transferred amount [14].

Another element worth understanding is refinery margins, which could then help us to break down the overall margin to its three elements, i.e. refinery, wholesale and retail margins.

According to Czech National Bank (CNB) these margins have oscillated between 0,5 % and 3,5 % in case of gasoline, whereas the oscillation in case of diesel was somewhere between 3 – 6,5 % during the last two years. Based on the data from CNB, it seems reasonable to use a rough margin of about 1,5 for gasoline and 4,5 % for diesel [15].

However in most of the calculations we used prices cleared of VAT and excise tax, it is worth to mention also these taxes for better understanding of final price construction. Since the beginning of year 2012 the VAT is 21 % and the absolute amount of the Excise Tax added to gasoline is 12,84 CZK and for diesel 10,95 CZK.

Since all important supply-chain-wise components have already been introduced it is possible to estimate the remaining margin on the final price. The gross margin reflects not only margins of retailers, however also costs connected with transportation and distribution on the Czech territory. The end price construction illustrates Table I.

Table I - Construction of the end price of gasoline and diesel

	Gasoline		Diesel	
Elements	Price (CZK)	Share (%)	Price (CZK)	Share (%)
Crude oil price	14,7	40 %	14,7	40,3 %
Transportation	0,7	1,9 %	0,7	1,9 %
Refinery margin	0,56	1,5 %	1,63	4,5 %
Gross margin	1,85	5 %	3,03	8,3 %
Excise Tax	12,84	34,9 %	10,95	30 %
VAT	6,36	21 %	6,31	21 %
End price	36,7	100 %	36,4	100 %

Source: CNB, CCS and various
Note: Annual averages were used for prices and exchange rate conversions

The exchange rate component is mentioned at the end of this part, since it stands a little bit aside of previous ones, however it has an importance for all of them. A more thorough analysis will be carried out later on, to uncover what kind of leverage the exchange rate really has and when it works in favor or against the development offered prices. For the sake of this model, a model rate of 20,18 CZK/USD was used to remain consistent with conversions, which have already been introduced.

V. Impact of Oil Price and Exchange Rate Development on the Nominal Oil Price Calculated in CZK

As we may see in bellow mentioned Fig. 1 there is a negative correlation between exchange rate CZK/USD and crude oil prices. The national stand alone currency provides a cushion for Czech customers since it softens all the up and down swings in crude oil prices and thus it provides additional stability for country economy.

Fig. 1 - Impact of oil price and ER development on the nominal oil price calculated in CZK

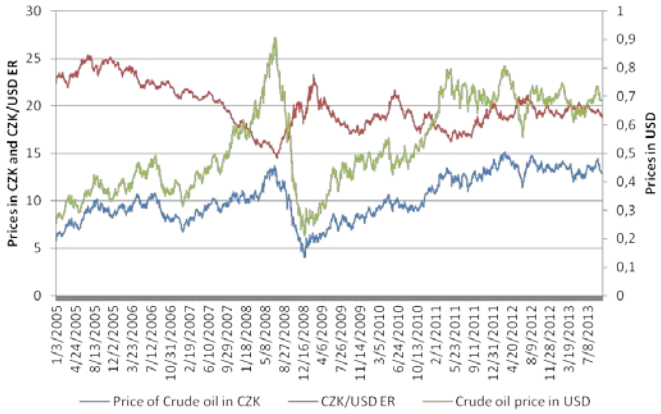

Source: Thomson Reuters, CSS, own calculations

VI. Crude Oil Price and Barges

To uncover impacts on the end prices we examined also FOB barges of gasoline and diesel delivered to ARA exchange. According to literature barges delivered to Rotterdam would have been better indicators in relation to the Czech Republic, however they are not accessible, and barges delivered to ARA should equally reflect the market conditions in case of wholesale prices of respective fuels. It is necessary to bear in mind that these prices are quotes for purchases done in the Netherlands, therefore the real wholesale prices of fuels in the Czech Republic will be slightly higher because of the inland premium, which represents an incorporation of virtual additional costs connected with a theoretical (or actual) delivery of these products to the Czech territory [16].

To be more precise, we used 10 ppm Barge FOB Antwerp-Rotterdam-Amsterdam (ULSD-10-B-ARA) for Diesel and 10 ppm premium unleaded gasoline FOB ARA (PU-10PP-ARA) for gasoline. The quotes used reflect the daily middle price of spot contracts.

The price development of respective barges tightly copy the price development of crude oil with a strong correlation with Brent spot prices (in particular 0,85 in case of gasoline and 0,9 for diesel). And as we learned there is marginally stronger correlation between crude oil prices and the end prices in the Czech Republic (0,94 for gasoline and 0,949 for diesel) rather than between barges and the end prices (0,938 for gasoline and 0,944 for diesel). Thus we used for further analysis Brent spot prices, since it constitutes the deciding rationale in the price creation of refined commodities in case of gasoline and diesel for end customers. However to examine lags between inputs changes and end price changes it was worth to use barges, where it is better apparent.

VII. Analysis of the End Fuel Prices in the Czech Republic

For our analysis we used the database of CCS company [17] which provides daily averages for Natural 95 (the most

common gasoline with an octane rating of 95) and Nafta (diesel) again between January 4, 2005 and September 23, 2013. Before diving into the analysis it is important to mention few remarks concerning the analyzed set of data. This set is based on data taken from payments by bank cards, therefore a significant amount of data from cash payments might be missing, which might cause a certain extent of distortion in the analyzed time series, especially at the beginning of the data set, where the penetration of card payments was limited and therefore it is possible that this data is omitting several data sets, which might have influenced the average price.

Second limitation is that these prices are reflecting daily averages for the whole country, therefore they might be negatively (in terms of objectivity) influenced by two factors: possible price wars taking place in certain regions, where stronger players might try to take out weaker participants, and by sales of fuels imported illegally without a proper duty payment. Both of these factors might have a mitigating effect on the "real" average price, however given the number of gas stations and observations present in the sample, it seems sound to assume that this data set provides a solid picture of fuel prices and their development over the years.

The prices of both gasoline and diesel were cleared of VAT and the Excise Tax to better understand the development of market-driven factors. In this part the oil price were recounted using the daily exchange rate available on the pages of CNB.

We also tried to test the hypothesis of a generally quite spread notion of a so called "seasonality" of prices on the Czech market, which should allegedly reflect the situation when prices of fuels go up during the summer, where they should be presumably driven by growing demand, because of vacations, etc.

The logic of this notion is understandable, however severely limited and as it is possible to see from the graph, it fails to materialize on the Czech market. Even a possible increase in the demand during the summer is not therefore sufficient to overthrow the influence of crude oil prices, which are more sensitive to the overall economic development and market activities than to a possible growth in demand of fuels because of travelling during the summer in the western hemisphere.

If anything, it would probably make more sense for crude oil prices to go up during the winter propelled by a growing demand for other refined products during this time of a year. The literature and analyzed data however do not provide a tangible proof, that seasonality is a reoccurring pattern, which has a clear impact of prices. The thing is rather that the naturally growing demand during winter months is clashing with news about supply capacities and the general mood on the markets [18].

Fig. 2 - Comparison of crude oil prices, diesel barge prices and end diesel price in CZK

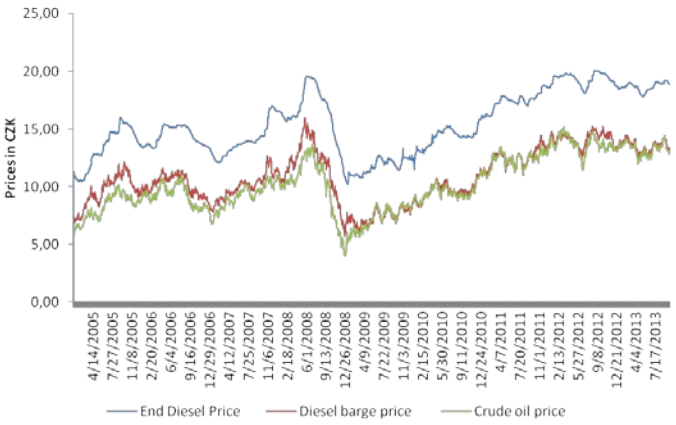

Source: *Source: EIA, CNB, CCS, Thomson Reuters, own calculations*
Note: End diesel prices cleared of VAT and excise tax as explained in the text

VIII. Is end pricing of fuels on the Czech market truly asymmetric?

Graphs developed in previous chapter visually support the hypothesis that results presented by Ratschenko [6] or Bettendorf et al. [7] concerning asymmetric pricing could be relevant also for the Czech market. In order to develop this hypothesis further and understand whether it is truly supported by data we will compare the daily relative differential in changes of prices of Natural 95, nafta and the respective barges. The underlying logic is to understand the difference between differentials in cases of increasing and decreasing prices.

As mentioned in the Methodology chapter, the analysis will be carried out by subtracting the relative daily changes in end pricing and pricing of commodities. This should provide two types of insights. First of all, the comparisons of slopes of upward and downward trends should provide an idea whether end market pricing is truly asymmetric (to be more precise, if the trajectory of upward movement is concave and the trajectory of the downward movement as well relative to the underlying development then the asymmetry is present) and if there are any lags concerning the reaction on a change (which would manifest in negative differential in case of upward trend or vice versa).

On following graphs you can see the relative differential day by day for gasoline and diesel. The comparison is done against prices of barges, since they visually seem to better reflect short-term price shocks relevant for the retail market.

Fig. 3 - Moving average of reactions towards price change in underlying commodity

ISBN: 978-1-61804-225-5

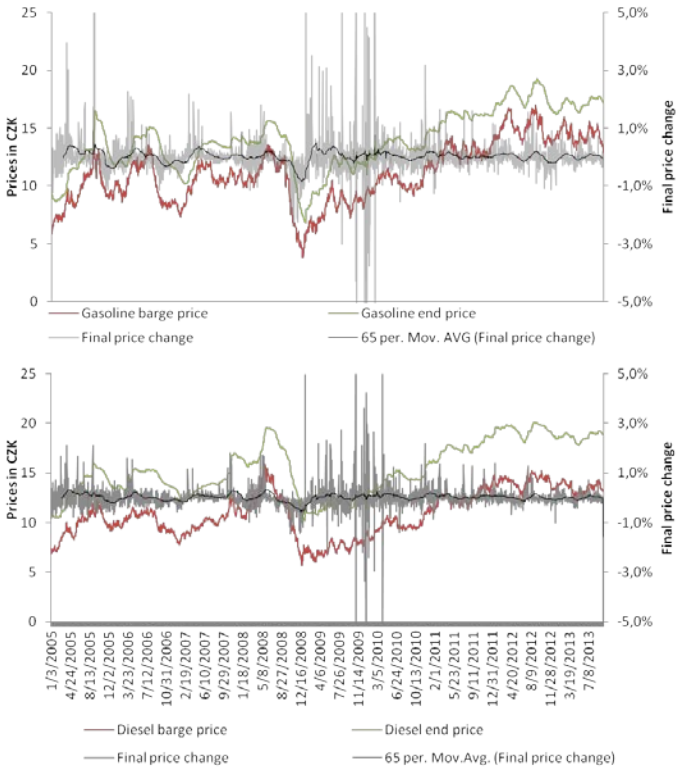

Source: Thomson Reuters, CSS, own calculations

These figures further confirm that the reaction toward an increase in price is generally more significant that the reaction towards the decrease with a stronger inclination towards higher upward volatility in cases of growth of the underlying commodity. The moving average of 65 periods reflecting the average daily reaction towards changes in end prices also indicates an asymmetric pricing in respective to the development of the barge price, which is visible in both cases despite diesel being less sensitive. However it is also visible that the reaction is becoming somehow less sensitive with increase absolute value of the end price. This can have several reasons, where some of those were developed by Lewis and presented by Bettendorf et al.[7]. According to this, customers have myopic expectations, meaning that their expectations are based on past observations, i.e. if they observe lower prices only minimum of them decides to search for better prices, since they are satisfied by this result and they have only a very limited idea, what the "fair" price should be, which puts a lot of sense into a quite gradual decrease of the end price. On the other hand, when the cost element increases, companies tend to react very sharply on this incentive to remain profitable. This can also to a certain extent explain a less sensitive reaction towards the increase in commodity prices when the price of the end fuel is high. This development is actually rendering the remaining parts of the cost structure less demanding in the relative sense, providing retailers with a more leeway in terms of realizing the profit and therefore also presumably tightening the competitive environment, where participants are reluctant to increase prices, since the competitive response might not follow this tactics, which could cause a loss of customers to cheaper competitors.

The statistical estimation of how big the lag really is and where exactly is located, is a bit beyond the scope of this study and a good incentive to deepen the analysis in some follow-up econometrical work, however it is possible to understand it is relative frequency. To do this, two data will be observed. Firstly, what is the average differential (difference between change in barges and change in end prices) and in how many cases the reaction on the end market was reversed. This should provide us with a sense how sizeable the dissonancy really is.

The average differential, showing the relative difference between intraday changes, is 1,3 % over the set with a standard deviation of almost 1,7 % for gasoline, signalling that there are indeed significant differences between the daily change of the barge and the end price adjustment. For diesel this average is a bit lower, of 1,1 %, though the standard deviation is again higher of 1,3 %, suggesting that both fuels follow very similar patterns of behaviour. Another interesting insight is, that the relative frequency of reversed reactions (an end price adjustment which is opposite in terms of change to the change of the barge) for gasoline is over 30 %, namely 975 out of 3195 observations, which shows that the lags in adjustment are relatively frequent, and this number does not change very much for diesel (30,2 %).

There are several factors which might help to explain this at first sight surprising behaviour. One was offered by Radschenko [5] by stating that 97 % of price shocks are perceived only as swings which will be very quickly corrected by the market itself. The explanation could be however based on the fact, that gas stations have only limited ways how to adjust their prices to immediate changes. Based on the correlation with crude oil and barges pricing, it seems fair to assume that a gas station will set its prices in line with these price developments. However it has only limited time frame to do that and therefore it is not able to perfectly adapt to intraday changes. For instance if the gas station is setting its prices for the following day in the evening, it cannot observe what will happen the next day, which would then explain this slightly peculiar result. The other thing might be that this thesis is working with averages of spot prices, however the high and low values can also influence a behaviour of gas stations by biasing their expectations to higher/lower prices and thus diverging their pricing from the underlying asset.

On the following figure prices of gasoline barge and end gasoline price are translated to an index more accurately showing the delayed reaction as well as a certain ignorance concerning sudden developments in the barge price. It is likely that these two observed patterns are mutually dependent because of their nature (since the reaction on the initial price change could be lagged, a participant is able to observe a following price adjustment, which is mitigating the impact of short-run price shocks).

The limited volatility of the end price is also very well documented on Fig. 4, where the index showing gasoline prices is much less volatile with an average of 1,5 and standard deviation of 0,28 than the barge index with an average of 1,9 and a standard deviation of 0,44 giving a narrower interval of distribution of +- one standard deviation by almost 10 %.

This figure is also providing yet another graphical proof that the pricing is asymmetric with a generally concave character,

which is reflecting the aforementioned tendency to reflect the upward trend more quickly than the opposing one. In the last period there are visible tendencies of a trend alternation to the convex curve, possibly reflecting the behaviour implied by the Lewis theory mentioned in the previous paragraphs.

It is visible that diesel prices expressed in indexes more tightly follow barge prices changes, which might be possibly caused by the seemingly lower volatility of the data set from day to day, which could suggest that if the change is not that strong on daily basis, gas stations have higher trust in the market and therefore they are more ready to make the change earlier. The tendency to asymmetrical pricing seems to be slightly weaker than in case of gasoline with quite quick adjustments towards both increases and decreases in the price. One reason of this could be that unlike gasoline diesel prices are targeting also corporate customers which are presumably more price sensitive and have a better overview of conditions on the market. Therefore the reaction is forced by the competitive pressures. Nevertheless it is still present.

Fig. 4 - Indexed expression of changes in barges and end prices of gasoline and diesel

Source: Thomson Reuters, CSS, own calculations

According to the presented data and their analysis it is therefore possible to conclude that the retail market of fuels in the Czech Republic shows signs of both asymmetric pricing and lags in reaction to changes, which both could be utilized by relevant companies.

IX. Conclusion and Practical Implication

This paper sought to provide a comprehensive analysis of all important factors involved in the end gasoline and diesel price creation in the Czech Republic with a major focus on delivering an understandable and applicable insights for companies, which could benefit from understanding them.

Whilst a significant number of factors is involved, it has been concluded that there are only few ones (namely prices of crude oil, prices of gasoline and diesel barges and exchange rate), which directly influence the pricing on daily basis and they are in the same time relatively easy to be observed.

The analysis of USD prices of crude oil and CZK/USD exchange rate also showed that there tend to be a strong inverse relationship between the prices of crude oil and the nominal rate of CZK/USD resulting into the fact that this exchange rate poses as a cushion for the volatile development of oil prices mitigating its impact in the prices expressed in CZK.

Following that, a strong positive relationship between crude oil, gasoline and diesel end prices and their respective barges has been established, leaving only narrow margin of differences, caused mainly by asymmetrical reactions and reaction lags.

Asymmetrical reactions of the end price to price changes in underlying commodities were present on the whole set of data, manifested by a generally concave shape of the reaction curve, pointing to a quicker adjustment to increasing price than vice versa. This trend tends to be stronger, when the end prices of fuels are relatively lower, likely relating to the hypothesis of Lewis, that companies tend to firstly secure at least some profitability, however after fulfilling this goal they start to incorporate the circumstances defined by their competitive landscape into their decision making. There are also numerous reaction lags presented, resulting in an imperfect adjustment of the end prices, which are however still very closely reflecting the development in underlying commodities.

All these insights provide several implications for concerned companies. There are generally two kinds of companies which can benefit from the outcomes of this work. Those might be either gas stations which can better understand the dynamics of the industry and therefore adjust their adaptation patterns. The second group consists of companies, which cost structure contains fuel. They tend to refrain from doing long-run hedging bets, because of cost savings or because of the variety of their business and they are not in the same time able to flexibly translate additional costs arising from fuel price fluctuations to their end customer pricing. This could be typically for instance a smaller size transportation company, which tends to buy larger quantities of fuel at given points of time and would like to understand what kind of patterns are reoccurring to better plan its purchasing decision and what kind of risks it will face doing so.

This paper provides a substantial amount of insights based on empirical data and analysis of long-run time series to be correspondingly instrumental, yet it also brings up several interesting questions which could be researched and possibly bring deeper dive into this dilemma.

There are two main rationales upon which these companies can react. It is the operational, or more of a ”day-to-day” reaction and strategy, which helps to understand what will happen in the future.

From the operational point of view, both types of companies are expected to be able to a certain extent to plan ahead therefore they have some flexibility in their adjustments to the current development. Both groups are good off with observing spot prices of Brent or possibly barge prices development (however since these data are not publicly available as complete time series, the Brent time series should be good enough, since there is a very strong correlation), exchange rate

of CZK and USD and make adjustments based on these two or three time series.

For gas stations it is important to understand, what is the expected development in the end price to be able to find the balance between realizing as much profit per litre as possible whereas staying competitive price-wise. With that in mind a gas stations want to know what will happen to the end price when the underlying commodity changes.

First of all, it is important to follow the price of crude oil/appropriate barge calculated into CZK currency, which is the most telling factor. In this case it is possible to generally expect an existence of an exchange rate pillow, which will mitigate the swings in the price of the underlying commodity, therefore the impact in the end price will not be that volatile as a rule. With this observation there are then basically three modus operandi. If the underlying price goes up, gas stations can expect that if the current end price is relatively low, the adjustment will be quite quick and closely resemble the growth of the commodity price. This gives them a chance to make a quick adjustment and therefore extract additional profits. If the end price is however already high, it is a good idea to see how the market will adjust, since there is a good chance for the adjustment not to be that rapid, because other participants in the market are starting to be more aware of their competitors' behaviour and they are less willing to rapidly increase the price.

On the other hand, if the underlying asset price goes down, it is safe to assume that other players will adjust their retail prices only very gradually and therefore the same thing could be done by an individual gas station, which in the same time does not have to react immediately, since there are frequent time lags present, suggesting that the translation of the shocks occurring in commodities to the end price is delayed, which gives a leeway to that particular gas station, because the reaction does not have to be prompt.

Apart from these factors, which should be observed on a day-to-day basis, there are also long-term factors, which change very predictably and the magnitude of change is rather limited, nevertheless there are several things to this, about which is necessary to have an idea. In this context this is mainly the development of administrative factors, i.e. the tax burden and possibly content of bio-originated matters. All these factors influence the price however their effect is very well predictable.

To conclude, it is fair to mention that an individual gas station should seek to understand the particular development in its whereabouts. This dilemma is already outside of the scope of this work, yet it is important to stress that there might be differences in pricing and price adjustments based on physical location. A good strategy perhaps might be to run a mystery shopping around its whereabouts, prepare a time series and compare it with outcomes of this work.

In case of the second group of companies, the underlying logic is very much the same as for gas stations only in their case they need to understand how it is possible to mitigate the impact on their costs. They should therefore tend to purchase as soon as possible during the bullish development of the market thus taking advantage of reaction lags and surpassing the adjustment of gas stations. On the other hand, when facing more of a diving trend, it seems to be a good idea to wait for some time to make the purchase since the adjustment of the end price tends to be more gradual.

The strategic perspective is then shared for both these players, because it mainly deals with understanding what will be the future development. This is again beyond the scope of this work and generally a quite problematic field, since forecasting of the price development of commodities is always a knotty job.

Despite this there are several points to be made. As it was already mentioned, there are two main groups of variables coming into play there, which could be subject to forecasting efforts. The first is the price of crude oil/barges and second is the exchange rate. In case of the first one, it is a good idea is to observe trends accompanying its underlying factors (such as demand versus supply conditions, overall trends in consumption, etc.) as well as how it is perceived by investors, or to put it differently, how they treat it in connection to other commodities (as we already saw, there is currently a growing correlation between oil prices and prices of other commodities, suggesting that this is a place where we can extract some information). It could be also useful to monitor the nominal rate of USD as well as its effective rate, which can also hint about the prices of crude oil. For future development of crude oil prices it might be also relevant to observe prices of relevant futures, which were in the past able to implicitly forecast the development more precisely than analytics, however it is questionable how they are doing post-crisis [19]. It is though still important to keep in mind that this foretelling is based on empirical data from the past and therefore has only limited implications for the future development.

REFERENCES

[1] Asche F., Gjølberg O., Volker T., Price relationships in the petroleum market: an analysis of crude oil and refined product prices, Energy Economics, 25 (2003), 289–301

[2] Johansen, S., Juselius, K.,Maximum likelihood estimation and inference on cointegration—with applications to the demand for money. Oxf. Bull. Econ. 2009, Stat. 52, 169–210.

[3] Rao G., The Relationship between Crude and Refined Product Market: The Case of Singapore Gasoline Market using MOPS Data, University of South Pacific, 2008, [Online], Available at: [http://mpra.ub.uni-muenchen.de/7579/1/MPRA_paper_7579.pdf], Accessed: 1.12.2013

[4] Mirantes G. et al., Crude Oil And Refined Products: A Common Long-Term Trend, 2008 [Online]. Available at: [https://editorialexpress.com/cgi-bin/conference/download.cgi?db_name=forofinanzas2008&paper_id=86], Accessed: 5.10.2013

[5] Radchenko S., Lags in the response of gasoline prices to changes in crude oil prices: The role of short-term and long-term shocks, Energy Economics, Volume 27, Issue 4, July 2005, Pages 573–602

[6] Radchenko S., Oil price volatility and the asymmetric response of gasoline prices to oil price increases and decreases, Energy Economics, Volume 27, Issue 5, September 2005, Pages 708–730

[7] Bettendorf et al., Do daily retail gasoline prices adjust asymmetrically?, Journal of Applied Statistics, Vol. 36, No. 4, April 2009, 385–397

[8] Chevillon G., Rifflart Ch., Physical market determinants of the price of crude oil and the market premium, Energy Economics, 2009, Volume 31, Issue 4, Pages 537-549

[9] Fattouh B., An Anatomy of the Crude Oil Pricing Systém, The Oxford Institute for Energy Studies, University of Oxford 2011

[10] Novotný F., The Link between the Brent Crude Oil Price and the US Dollar Exchange Rate, Prague Economic Papers, 2 (2012), 220-232
[11] Breitenfellner A. et al., 2009, Determinants of Crude Oil Prices: Supply, Demand, Cartel or Speculation?, Monetary Policy and Economy, Q4/2009, 111-136
[12] He, Y., Wang S., Lai, K. K., Global Economic Activiy and Crude Oil Prices: A Cointegration Analysis, Energy Economics, 32 (2010), 868–876
[13] Hindls et al.,Statistika pro ekonomy, Professional Publishing 2006, issue 7, Prague
[14] Energy Charter Secretariat, 2012, Bringing Oil to the Market: Transport Tariffs and Underlying Technologies for Cross-Border Crude Oil and Products Pipelines
[15] CNB, 2012, Faktory vývoje maloobchodních cen pohonných hmot, [Online], Available at: [http://www.cnb.cz/cs/menova_politika/zpravy_o_inflaci/2012/2012_II/boxy_a_prilohy/zoi_2012_II_box_2.html], Accessed: 15.11.2013
[16] Unipetrol, 2013, Výroční zpráva Unipetrolu za rok 2012, [Online], Available at: [http://www.unipetrol.cz/cs/vztahy-s-investory/regulatorni-oznameni/detail/Vyrocni-zprava-Unipetrolu-za-rok-2012/]
[17] CCS, 2013, Radar vývoje cen PHM, [Online], Available at: [http://www.ccs.cz/pages/phm2.php], Accessed: 20.10.2013
[18] Procházka J., 2010, Jsou marže čerpařů opravdu přemrštěné?, Cyrrus
[19] ČNB, 2006, Ceny ropy a benzínu v prognóze ČNB, [Online], Available at: [http://www.cnb.cz/cs/menova_politika/zpravy_o_inflaci/2006/2006_cervenec/boxy_a_prilohy/zoi_2006_cervenec_box2.html], Accessed: 10.12.2013

Ladislav Tyll, MBA., Ph.D. is assistant professor at the University of Economics Prague and in the same time runs his own consulting company. His major points of interests and job are corporate strategy and international business.

Approximation of a wanted flow via topological sensitivity analysis

Mohamed Abdelwahed

Abstract—We propose an optimization algorithm for the geometric control of fluid flow. the used approach is based on the topological sensitivity analysis method. It consists in studying the variation of a cost function with respect to the insertion of a small obstacle in the domain. Some theoretical and numerical results are presented in 2D and 3D.

Keywords—Sensitivity analysis, topological gradient, shape optimization, Stokes equations.

I. Introduction

THE optimal control of fluid flows has long been receiving considerable attention by engineers and mathematicians due to its importance in many applications involving fluid related technology [11], [16]. There is a wealth of literature on optimal control of flows through suction and injection of fluid along domain boundaries, see e.g. [7], [12]. In the context of design, one of the first studies is found in [18]. It is devoted to determine a minimum drag profile submerged in a homogeneous, steady, viscous fluid by using optimal control theories for distributed parameter systems. Next, many shape optimization methods are introduced to determine the design of minimum drag bodies [8], [15], [19], diffusers [5], and airfoils [6], [17]. The majority of works dealing with optimal design of flow domains fall into the category of shape optimization and are limited to determine the optimal shape of an existing boundary.

It is only recently that topological optimization has been developed and used in fluid design problems. It can be used to design features within the domain allowing new boundaries to be introduced into the design. In this context, one of the first approaches is proposed by Borvall and Petersson in [3]. They implemented the relaxed material distribution approach to minimize the power dissipated in Stokes flow. To approximate the no-slip condition along the solid-fluid interface they used a generalized Stokes problem to model fluid flow throughout the domain. Later, this approach has been generalized by Guest and Prévast in [9]. They treated the material phase as a porous medium where fluid flow is governed by Darcy's law. For impermeable solid material, the no-slip condition is simulated by using a small value for the material permeability to obtain negligible fluid velocities at the nodes of solid elements. The flow regularization is expressed as a system of equations; Stokes flow governs in void elements and Darcy flow governs in solid elements.

M. Abdelwahed is with the Department of Mathematics, College of Science, King Saud University, Riyadh 11451, Kingdom of Saudi Arabia e-mail: mabdelwahed@ksu.edu.sa.

In this paper, we propose a new, fast and accurate optimization algorithm based on topological sensitivity analysis [1], [2], [10], [13], [14], [20]. It consists in studying the variation of a cost function with respect to a small topological perturbation of the fluid flow domain.

To present the basic idea, let us consider a domain $\Omega \subset \mathbb{R}^d$, $d = 2, 3$ and a cost function $j(\Omega) = J(\Omega, u_\Omega)$, where u_Ω is the velocity field solution to Stokes problem defined in Ω. For $\varepsilon > 0$, let $\Omega_\varepsilon = \Omega \backslash \overline{(x_0 + \varepsilon\omega)}$ be the fluid domain obtained by inserting a small obstacle $x_0 + \varepsilon\omega$ in Ω, where $x_0 \in \Omega$ and $\omega \subset \mathbb{R}^d$ is a fixed bounded domain containing the origin, whose boundary $\partial\omega$ is connected and piecewise of class $\mathcal{C}^1$. The topological sensitivity analysis method leads to an asymptotic expansion of the function j in the following form:

$$j(\Omega_\varepsilon) = j(\Omega) + f(\varepsilon)g(x_0) + o(f(\varepsilon)),$$

where $f(\varepsilon)$ is a scalar positive function going to zero with ε. This expression is called the topological asymptotic expansion and g is called the topological gradient. The function g is very easy to compute. In order to minimize the cost function, the best location to insert a small obstacle in Ω is where g is negative. In fact if $g(x_0) < 0$, we have $j(\Omega_\varepsilon) < j(\Omega)$ for small ε. Starting with this observation, a topological optimization algorithm can then be constructed. The optimal design is obtained using an iterative process building a sequence of geometries $(\Omega_k)_k$ with $\Omega_0 = \Omega$. At the k^{th} iteration the topological gradient g_k is computed in Ω_k and the new geometry Ω_{k+1} is obtained by inserting an obstable ω_k in the domain

ISBN: 978-1-61804-225-5

Ω_k; $\Omega_{k+1} = \Omega_k \backslash \overline{\omega_k}$. The obstacle ω_k is defined by a level set curve of g_k

$$\omega_k = \{x \in \Omega_k, \text{ such that } g_k(x) \leq c_k < 0\},$$

where c_k is chosen in such a way that the cost function j decreases as most as possible. This algorithm can be seen as a descent method where the descent direction is determined by the topological sensitivity g_k and the step length is given by the volume variation $meas(\Omega_k \backslash \Omega_{k+1})$.

The paper is organized as follows. In section 2, we give a statement of the optimization problem. Section 3 is devoted to a topological sensitivity analysis for the Stokes equations. The obtained results are valid for a large class of cost functions. Similar analysis is developed by Guillaume and SidIdris in [10]. Their approach is based on an adaptation of the adjoint method and a domain truncation technique that provides an equivalent formulation of the PDE in a fixed functional space. In this work, we derive a simplified topological sensitivity analysis for the Stokes equations without using the truncation technique. In section 4, we present some numerical experiments showing the efficiency of our approach.

II. Topological optimization problem

Consider a viscous incompressible fluid flow in a bounded domain $\Omega \subset \mathbb{R}^d$, $d = 2, 3$. We assume that the fluid flow is governed by the Stokes equations.
We denote by $\Omega \backslash \overline{\omega_\varepsilon}$ the perturbed domain, obtained by inserting a small obstacle $\omega_\varepsilon = x_0 + \varepsilon\omega$ in the initial domain flow Ω. In $\Omega \backslash \overline{\omega_\varepsilon}$, the velocity u_ε and the pressure p_ε are solution to

$$\left\{ \begin{array}{rcl} -\nu\Delta u_\varepsilon + \nabla p_\varepsilon &= F & \text{in } \Omega \backslash \overline{\omega_\varepsilon} \\ \text{div } u_\varepsilon &= 0 & \text{in } \Omega \backslash \overline{\omega_\varepsilon} \\ u_\varepsilon &= 0 & \text{on } \Gamma \\ u_\varepsilon &= 0 & \text{on } \partial\omega_\varepsilon. \end{array} \right. \quad (1)$$

where ν is the (constant) fluid kinematic viscosity, and F is a given body force per unit of mass. Note that for $\varepsilon = 0$, $(u_0\,,\, p_0)$ is solution to

$$\left\{ \begin{array}{rcl} -\nu\Delta u_0 + \nabla p_0 &= F & \text{in } \Omega \\ \text{div } u_0 &= 0 & \text{in } \Omega \\ u_0 &= 0 & \text{on } \Gamma. \end{array} \right. \quad (2)$$

Consider now a design function j of the form

$$j(\Omega \backslash \overline{\omega_\varepsilon}) = J_\varepsilon(u_\varepsilon), \quad (3)$$

where J_ε is defined on $H^1(\Omega \backslash \overline{\omega_\varepsilon})^d$ for $\varepsilon \geq 0$
Our aim is to determine the optimal location of the obstacle ω_ε in the domain Ω in order to minimize the cost function $J_\varepsilon(u_\varepsilon)$. Then, the optimization problem we consider is given as follows:

$$\begin{array}{l} \min\limits_{\omega_\varepsilon \subset \Omega} J_\varepsilon(u_\varepsilon) \text{ such that, for some } p_\varepsilon, \\ (u_\varepsilon, p_\varepsilon) \text{ is a solution of (1) in } \Omega \backslash \overline{\omega_\varepsilon}. \end{array} \quad (4)$$

To this end, we will derive a topological asymptotic expansion of the function j with respect to ε.

III. Topological sensitivity analysis

In our topological sensitivity analysis, we have to distinguish the cases $d = 2$ and $d = 3$. This is due to the fact that the fundamental solutions $(E,\ \Pi)$ to the Stokes equations in $\mathbb{R}^2$ and $\mathbb{R}^3$ have essentially different asymptotic behaviour at infinity. We have if $d = 3$

$$E(y) = \frac{1}{8\pi\nu r}\Big(I + e_r e_r^T\Big),$$
$$\Pi(y) = \frac{y}{4\pi r^3}$$

and if $d = 2$

$$E(y) = \frac{1}{4\pi\nu}\Big(-\log(r)I + e_r e_r^T\Big),$$
$$\Pi(y) = \frac{y}{2\pi r^2},$$

with $r = ||y||$, $e_r = y/r$ and e_r^T is the transposed vector of e_r.

Next we assume that J_ε satisfies the following assumption.

Hypothesis 3.1: i) J_0 is differentiable with respect to u, its derivative being denoted by $DJ_0(u)$. ii) There exists a real number δJ such that $\forall\, \varepsilon \geq 0$

$$\begin{array}{rl} J_\varepsilon(u_\varepsilon) - J_0(u_0) = & DJ_0(u_0)(\widehat{u}_\varepsilon - u_0) \\ & + f(\varepsilon)\delta J + o(\varepsilon), \end{array} \quad (5)$$

where f is a scalar function and $\widehat{u}_\varepsilon$ is an extension of u_ε in Ω respectively defined by:

$$f(\varepsilon) = \left\{ \begin{array}{ll} \varepsilon & \text{if } \ d = 3, \\ -1/\log(\varepsilon) & \text{if } \ d = 2, \end{array} \right.$$

$$\widehat{u}_\varepsilon = \left\{ \begin{array}{ll} u_\varepsilon & \text{in } \Omega \backslash \overline{\omega_\varepsilon}, \\ 0 & \text{in } \omega_\varepsilon. \end{array} \right.$$

A- The three dimensional case: Let $(U,\ P)$ denotes a solution to

$$\left\{ \begin{array}{rcl} -\nu\Delta U + \nabla P &= 0 & \text{in } \mathbb{R}^3 \backslash \overline{\omega} \\ \text{div } U &= 0 & \text{in } \mathbb{R}^3 \backslash \overline{\omega} \\ U &\longrightarrow 0 & \text{at } \infty \\ U &= -u_0(x_0) & \text{on } \partial\omega. \end{array} \right. \quad (6)$$

We start the derivation of the topological asymptotic expansion with the following estimate of the

ISBN: 978-1-61804-225-5

$H^1(\Omega\backslash\overline{\omega_\varepsilon})$ norm of $u_\varepsilon(x) - u_0(x) - U(x/\varepsilon)$. This estimate plays a crucial role in the derivation of our topological asymptotic expansion. It describes the velocity perturbation caused by the presence of the small obstacle ω_ε.

Proposition 3.1: There exists $c > 0$, independent of ε, such that for all $\varepsilon > 0$ we have

$$\|u_\varepsilon(x) - u_0(x) - U(x/\varepsilon)\|_{1,\Omega\backslash\overline{\omega_\varepsilon}} \leq c\,\varepsilon.$$

The following corollary follows from Proposition 3.1. It gives the behaviour of the velocity u_ε when inserting an obstacle. The principal term of this perturbation is given by the function U, solution to (6).

Corollary 3.1: We have

$$u_\varepsilon(x) = u_0(x) + U(x/\varepsilon) + O(\varepsilon), \quad x \in \Omega\backslash\overline{\omega_\varepsilon}.$$

We are now ready to derive the topological asymptotic expansion of the cost function j. It consists in computing the variation $j(\Omega\backslash\overline{\omega_\varepsilon}) - j(\Omega)$ when inserting a small obstacle inside the domain. The leading term of this variation involves the solution to a boundary integral equation (see Theorem 3.1).

Theorem 3.1: [13] If the assumption 3.1 holds, the function j has the following asymptotic expansion

$$j(\Omega\backslash\overline{\omega_\varepsilon}) = \quad j(\Omega) + \varepsilon\left[\Big(-\int_{\partial\omega}\eta(y)\ \text{ds(y)}\Big).v_0(x_0) + \delta J\right] + o(\varepsilon),$$

where v_0 is the solution to the adjoint problem

$$\begin{cases} -\nu\Delta v_0 + \nabla q_0 &= -DJ(u_0) \quad \text{in } \Omega \\ \text{div } v_0 &= 0 \quad \text{in } \Omega \\ v_0 &= 0 \quad \text{on } \Gamma. \end{cases}$$

The function $\eta \in H^{-1/2}(\partial\omega)^3$ is the solution to the following boundary integral equation

$$\int_{\partial\omega} E(y-x)\,\eta(x)\ \text{ds}(x) = -u_0(x_0), \quad \forall y \in \partial\omega.$$

In the particular case where $\omega = B(0,1)$, the density η is given explicitly $\eta(y) = -\dfrac{3\nu}{2}u_0(x_0), \quad \forall y \in \partial\omega$.

Corollary 3.2: If $\omega = B(0,1)$, under the assumption 3.1 we have

$$j(\Omega\backslash\overline{\omega_\varepsilon}) = \quad j(\Omega) + \varepsilon\Big[6\pi\nu\,u_0(x_0).v_0(x_0) + \delta J\Big] + o(\varepsilon).$$

B- The two dimensional case: In the two dimensional case we have the following asymptotic expansion.

Theorem 3.2: If the assumption 3.1 holds, j admits the following asymptotic expansion

$$j(\Omega\backslash\overline{\omega_\varepsilon}) = j(\Omega) + \quad \tfrac{-1}{\log(\varepsilon)}\Big[4\pi\nu\,u_0(x_0).v_0(x_0) + \delta J\Big] + o\Big(\tfrac{-1}{\log(\varepsilon)}\Big).$$

IV. Numerical examples

We consider a tank Ω filled with a viscous and incompressible fluid. The aim is to determine the optimal shape of the fluid flow domain minimizing a given objective function.

Our implementation is based on the following optimization algorithm. We apply an iterative process to build a sequence of geometries $(\Omega_k)_{k\geq 0}$ with $\Omega_0 = \Omega$. At the k^{th} iteration the topological gradient g_k is computed in Ω_k and the new geometry Ω_{k+1} is obtained by inserting an obstacle ω_k in the domain Ω_k; $\Omega_{k+1} = \Omega_k\backslash\overline{\omega_k}$. The obstacle ω_k is defined by a level set curve of g_k

$$\omega_k = \{x \in \Omega_k, \text{ such that } g_k(x) \leq c_k < 0\},$$

where c_k is chosen in such a way that the cost function j decreases as much as possible.

The algorithm :

- Initialization: choose $\Omega_0 = \Omega$, and set $k = 0$.
- Repeat until $g_k \geq 0$ in Ω_k:
  - solve the Stokes equations in Ω_k,
  - solve the associated adjoint problem in Ω_k,
  - compute the topological sensitivity $g_k(x)$ $\forall x \in \Omega_k$,
  - determine the obstacle ω_k,
  - set $\Omega_{k+1} = \Omega_k\backslash\overline{\omega_k}$,
- $k \longleftarrow k+1$.

This algorithm can be seen as a descent method where the descent direction is determined by the topological sensitivity g_k and the step length is given by the volume variation $meas(\Omega_k\backslash\Omega_{k+1})$. The natural optimality condition $g_k(x) \geq 0, \forall x \in \mathcal{O}_k$ is used as stopping criteria [4].

Approximation of a wanted flow. The aim is to determine the optimal shape $\mathcal{O}^* \subset \Omega$ of the fluid flow domain such that the velocity $u_{\mathcal{O}^*}$, solution to the Stokes equations in $\mathcal{O}^*$, approximate a wanted flow w_d defined in a fixed domain $\Omega_m \subset \Omega$. The optimal shape $\mathcal{O}^*$ can be characterized as the solution to the following topological optimization problem

$$\min_{\mathcal{O}\subset\Omega}\int_{\Omega_m}|u_{\mathcal{O}} - w_d|^2\text{dx},$$

where $u_{\mathcal{O}}$ is the solution to the Stokes equations in $\mathcal{O} \subset \Omega$. This test is treated in two and three dimensional cases. In 2D, the tank $\Omega = [0, 1.5] \times$

ISBN: 978-1-61804-225-5

$[0,1]$, the domain $\Omega_m = [0,1.5] \times [0.8,1]$ and the velocity field w_d is defined by: $w_d = (1,0)$ in Ω_m and $w_d = (0,0)$ elsewhere. The numerical results are described in Figure 1. A 3D extension of this case is presented in Figure 2.

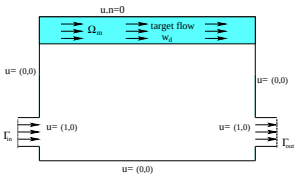

(a) The initial geometry Ω

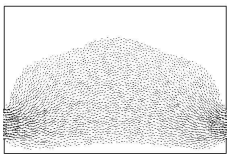

(b) The velocity field in the initial domain

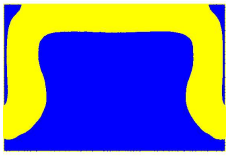

(c) The optimal domain is obtained in only 3 iterations

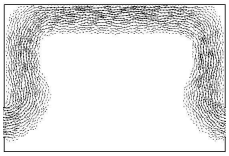

(d) The velocity field in the obtained domain

Fig. 1. Approximation of a wanted flow: 2D case

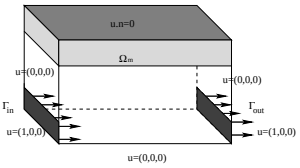

(a) The initial geometry

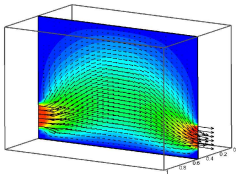

(b) The velocity field in the initial domain

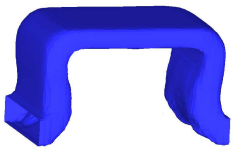

(c) The optimal domain is obtained in only 4 iterations

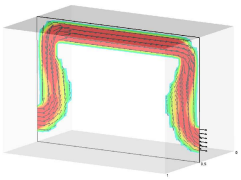

(d) The velocity field in the obtained domain

Fig. 2. Approximation of a wanted flow: 3D case

REFERENCES

[1] G. Allaire, F. Jouve, A-M. Toader , Structural optimization using sensitivity analysis and a level-set method, J. Comput. Phys., 194 (1), 2004, 363-393.

[2] M. Bendsoe , Optimal topology design of continuum structure: an introduction, Technical report, Departement of mathematics, Technical University of Denmark, DK2800 Lyngby, Denmark, 1996.

[3] T. Borrvall, J. Petersson , Topological optimization of fluids in Stokes flow, Inter. J. Numer. Methods Fluids, 41 (1), 2003, 77-107.

[4] G. Buttazzo, G. Dal Maso , Shape optimization for Dirichlet problems: Relaxed formulation and optimality conditions, Appl. Math. Optim., 23, 1991, 17-49.

[5] H. Cabuk, V. Modi , Optimum plane diffusers in laminar flow, J. of Fluid Mechanics, 237, 1992, 373-393.

[6] E.M. Cliff, M. Heinkenschloss, A. Shenoy , Airfoil design by an all-at-once method, Inter. J. Compu. Fluid Mechanics, 11, 1998, 3-25.

[7] O. Ghattas, J-H. Bark , Optimal control of two and three dimensional incompressible Navier-Stokes flows, Journal of Computational Physics, 136, 1997, 231-244.

[8] R. Glowinski, O. Pironneau , On the numerical computation of the minimum drag profile in laminar flow, J. of Fluid Mechanics, 72, 1975, 385-389.

[9] J. K. Guest, J. H. Prévost , Topology optimization of creeping fluid flows using a Darcy-Stokes finite element, Inter. J. Numer. Methods in Engineering, 66, 2006, 461-484.

[10] Ph. Guillaume, K.Sid Idris , Topological sensitivity and shape optimization for the Stokes equations, SIAM J. Control Optim., 43(1), 2004, 1-31.

[11] M.D. Gunzburger , Perspectives in flow control and optimization, Advances in Design and Control, SIAM, Philadelphia, PA, 2003.

[12] M. Gunzburger, H. Kim, S. Manservisi , On a shape control problem for the stationary Navier-Stokes equations, M2AN Math. Model. Numer. Anal. , 34 (6), 2000, 1233-1258.

[13] M. Hassine, S. Jan, M. Masmoudi , From differential calculus to $0-1$ topological optimization, SIAM J. Cont. Optim., 45 (6), 2007, 1965-1987.

[14] M. Hassine, M. Masmoudi , The topological sensitivity analysis for the Quasi-Stokes problem, ESAIM, COCV J., 10, 2004, 478-504.

[15] D.W. Kim, M.U. Kim , Minimum drag shape in two two-dimensional viscous flow, Inter. J. Numer. Methods in Fluids, 21, 1995, 93-111.

[16] B. Mohammadi, O. Pironneau , Applied shape optimization for fluids, Numerical Mathematics and Scientific Computation, Oxford University Press, New York, 2001.

[17] O. Pironneau , On optimum profiles in Stokes flow, J. of Fluid Mechanics, 59, 1973, 117-128.

[18] O. Pironneau , On optimal design in fluid mechanics, J. Fluid Mech., 64, 1974, 97-110.

[19] O. Pironneau , Optimal Shape Design for Elliptic Systems, Springer, Berlin, 1984.

[20] J. Sokolowski, A. Zochowski , On the topological derivative in shape optimization, SIAM J. Control Optim., 37 (4), 1999, 1251-1272.

Runoff as a Stochastic Process

Giuliano Vitali

University of Bologna - Italy
giuliano.vitali@unibo.it

***Abstract*—Runoff stationary critical flow is investigated as a stochastic process by means of two routing simulation models, a stream confluence, which has beens interpreted as a Marcus-Lushnikov coalescence process, and a channel splitting model, which has ben interpreted as a Markov chain over a regular tree. Despite of the expected similarity due to expection that they should be seen as one the backward of the other, the initiation and the stopping methods using in algorithms influence strongly stream size distribution.**

***Index Terms*—runoff, stochastic processes**

I. Introduction

Runoff is a fundamental process in surface hydrology, related to phenomena as erosion, landslides and flooding, all issues of growing importance for civil risks and food security in a climate-change scenario.

Runoff takes place at any rainfall event and its intensity and duration are related to scale and period of runoff: in practice it occurs when rainfall rate is greater than infiltration rate, and when the process reach a certain scale it is the main driver of hydrological network, both feeding and forming it. At basin scale routing models are widely used to forecast how streams collect water from its catchment area: in such approaches the watershed is represented in terms of homogeneous surfaces where runoff is interpreted by simple dynamics as the mean-field Kinematic Wave one ([4],[1]).

Though the complexity of routing models justify such lumped approach, physically-based models have been continuously chased as an El-Dorado ([6]) because of the need to describe the very nature of runoff process mat a field scale.

One of major problem in developing a physical model of runoff stay in surface complexity, which is usually represented in terms of roughness, a concept related to a number of measurable variables (e.g. pocket density, average depth, ..) with a strong spatial variability.

The present approach is aimed to identify which stochastic processes are suitable to model runoff at such a scale, an issue which is faced interfacing the phenomenological description to stochastic language by means of simulation models.

Phenomenology

Runoff is a process occurring over a surface which normally owns depressions (pockets) with a size ranging from the scale of mm to that of dm.

During a rainfall randomly falling droplets are collected by those depressions, and when rainfall intensity exceeds pocket leakage (infiltration) a cascade begins 1.

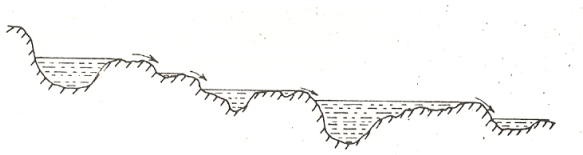

Fig. 1. Sketch of pocket cascade (from [1])

As those depression have different height, capacity and location, spilling occurs in a random direction feeding the closest pocket. Streams merges and increase in size and sone generate rills and channels 2..

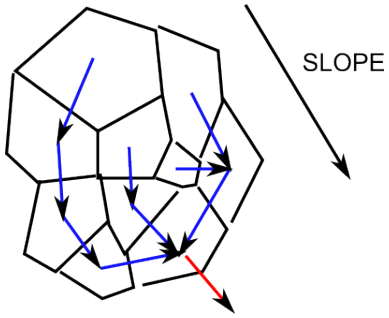

Fig. 2. Divide of a surface forming a pocket cascade

In 2D view runoff field may be seen as made of pockets whose centers are located randomly as nodes of a lattice.

Toy model #1

To simulate runoff a depression lattice can be easily generated by means of a random (uniform) distribution, while Thiessen - Voronoi geometrical approach can be used to generate a polygonal divide of the surface (see figure 3). From the catchment area boundary poligons are conveniently removed.

The generated coverage is related to a pocket size distribution reported in figure 4 (right side).

Such a coverage is used to produce a discharge network, assigning each node (pocket) a downstream child on the base of slope (giving the main flow direction), distance and angle.

Stream network generation procedure is based on two steps:

- for each node (pocket) identification of downward child node is made whose multiplicity is increased.
- starting from nodes with multiplicity 0 (source pockets), streams are drawn to child nodes whose resolved multiplicity is reduced while increasing the size of the stream that will emerge from it;
- the last step is repeated for the nodes reaching a residual multiplicity equal to 0, till zeroing the nodes.

ISBN: 978-1-61804-225-5

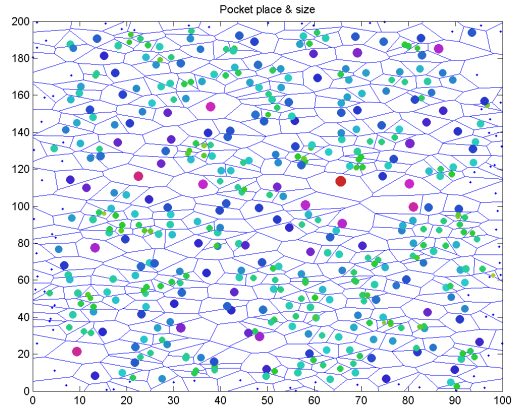

Fig. 3. 2D distribution of 500 pockets generated in Matlab with ***random('uniform')*** function and their Thiessen-Voronoi spatialization

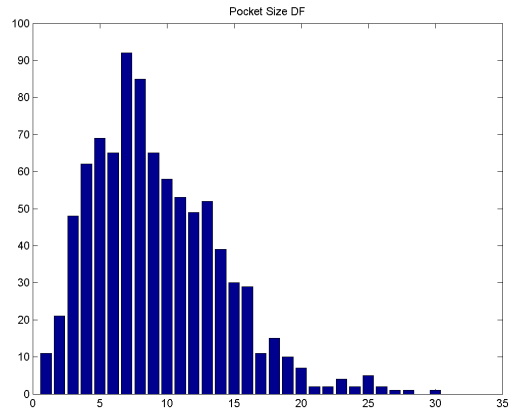

Fig. 4. Distribution of pocket size

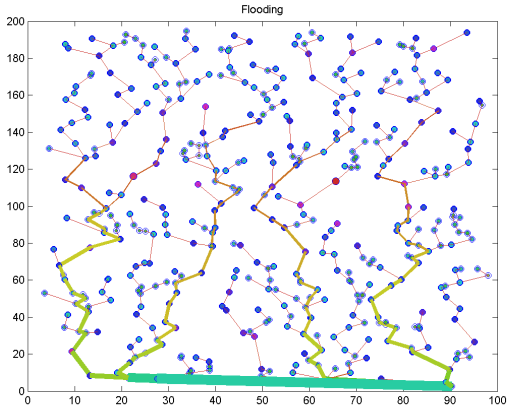

Fig. 5. Criptical flow routing obtained from the divide in figure 3

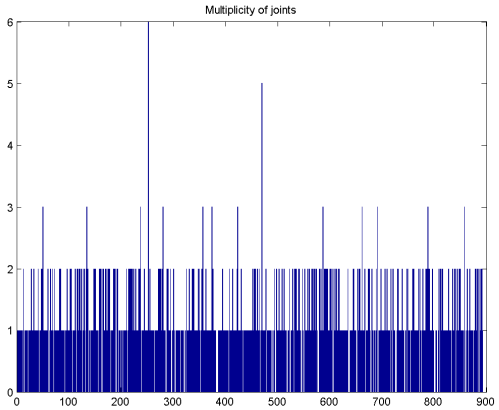

Fig. 6. Confluence multiplicity of nodes in figure 3

Such an algorithm does not simulate true dynamics, as confluence nodes stay in a dormant state till every uphill nodes are waken up (residual multiplicity goes to 0).

So doing a routing network is generated corresponding to **stationary critical flow** that is a full stream saturation under a constant rainfall regime without considering surface floods (stream merging) and erosion **(hard surface** assumption). Under these hypothesys it is possible to identify two kind of pockets, 'sources' (tree leaves) which feed the network, and 'confluence nodes' representing those pockets where streams merge to one another 5.

Node multiplicity is shown in figure 6 where, apart a large number of 'sources'a certain amount of nodes with more than 2 confluences are also present.

Figure 7 reports the distributions of stream size (flow).

Toy Model #2

Another way of generating a runoff routing can be easily obtained as a binary branching scheme going back from the outlet channel. Figure 8 has been obtained by successive random bifurcations (split has been obtained using a uniform distribution), stopping the process when the branch size reaches 1/1000 of that of main stream; branches total to around 4000.

Model #2 as much as Model #1 can be useful to develop rainfall-runoff models at field scale to study the response to roughness.

Both models support a delay which can be easily related to stream size, though it doesn't perform any leaf node spatializatiom: to assign each graph leaf a pocket without leaving empty spaces, additional rules should be added further (e.g. as in basin-scale models, [5]).

II. Coalescence and Branching processes

The models used above make runoff similar to other phenomena widely studied in the literature in terms of stochastic processes, as coalescence of particles in dispersed media (aerosols and hydrosols), formation of agglomeration of emulsion droplets (oil separation) or coagulation (before gelation), solid state avalanche breakdown in electronics.

Marcus-Lushnikov model

Model#1 can be seen as a Marcus-Lushnikov (ML) coalescence process, where a couple of particles (streams) with a

ISBN: 978-1-61804-225-5

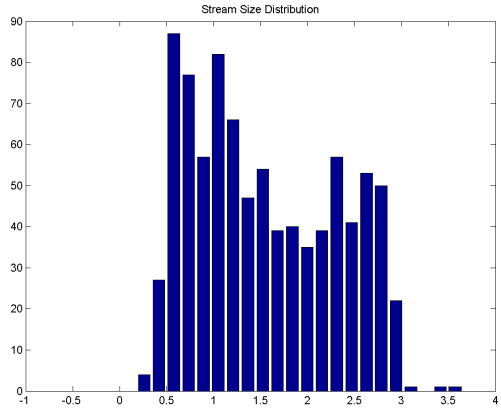

Fig. 7. Distribution of log of stream size

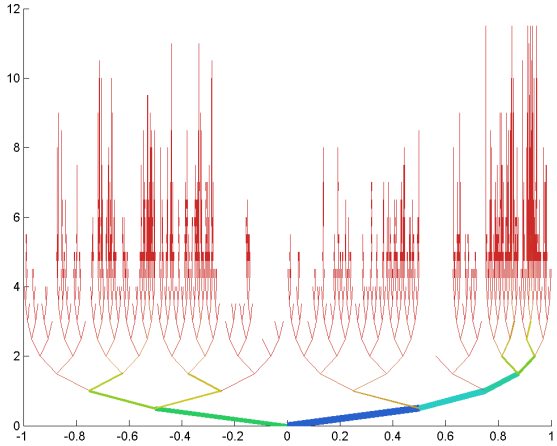

Fig. 8. Bottom-up reconstruction of a runoff process; x-axis is an arbitrary cohordinate systems used just for display purposes whereas on y-axis is the number of splits

given mass (flow) coalesce (merge) to a new entity conserving their mass:

$$(x) + (y) \rightarrow (x + y)$$

It is a particular Markov chain process considering $n(> 1)$ finite mass particles of mass $(x_1, .., x_n) \in (0, \infty)^n$, with total mass $M(= \sum_{i=1,n} x_i)$.

Such a process has been formerly described from Lushnikov ([2]) introducing the state of the system:

$$Q = n_1, .., n_g, ..$$

which is a mass distribution function where n_g is the number of particles of size g : each time a coalescence event takes place, two bins decrease of one unit and one of them increases of one unit

$$Q^+ = n_1, .., n_l - 1, ..n_m - 1, ..n_{l+m} + 1, ..$$

therefore the mass distribution integral $|Q| = \sum n_i$ is not time-conservative, while the total mass $M = \sum y_i \cdot n_i$does.

In the case of runoff, assuming that particles (source pockets/streams) of the same size, namely $n(x, 0) = N \cdot \delta(x_0)$, the process is made a discrete one, and all the downhill stream sizes are multiple (g is multiplicity) of the source one (which can be easily related to roughness).

Therefore the distribution transformation process: $Q \rightarrow Q^+$ can be represented by the **rate** $A(Q^+, Q)$:

$$A(Q^+, Q) = K_{l,m} \cdot n_l(Q) \cdot [n_m(Q) - \delta(l, m)]$$

where $n_g(Q)$ is the number of particles with size g in the state Q, and $K_{l,m}$ is the probability of coalescence of two streams of size l and m respectively.

As model #1 is describing a **steady state regime,** Marcus-Lushnikov process should be considered as a space process; however as it is not possible to observe every particles (streams) of the system simultaneously, we have to look at the process in terms of strips of length δz where an injection of 'new' source streams occur and the total number of streams is conserved:

$$Q \quad \rightarrow \quad Q^+ + \{N - |Q^+|, 0, .., 0\}$$

where$|Q|$ is the number of streams in the considered state.

Splitting model

Even if split process (also know as binary branching/Galton-Watson p.) seems the better candidate to represent model #2, it is also obvious that branching is not an option as split probability refers to the partitioning of a particle of mass l:

$$(l) \rightarrow (x) + (l - x) \quad ; \quad 0 < x < l$$

Therefore partitioning occurs on a graph which in first instance can be assumed to be a regular tree, and the process is a Markov chain on a tree (see e.g. [3]) where, at each branching, a new Markov chain is initiated. Therefore in a backward runoff process it applies repetitively, starting from the main channel, which after n steps reduces its size by:

$$r_n = x_1 \cdot \ldots \cdot x_i \cdot y_1 \cdot \ldots \cdot y_{n-i} \quad : \quad y = 1 - x$$

In fact runoff Model #2 has some discrepancies with such a split process:

- stream length is not taken into account so probability of branching after a fixed roughness dependent time/space interval is considered to be 1;
- at branching the partitioning probability density is random (uniform);
- branch production is stopped as a roughness-dependent size is reached, that is when $L \cdot r_n < L_0$.

As a dead event takes place, the particle is no more split, therefore the process stops. Distribution of stream size is shown in the figure 9 where after applying a log transformation to size, a gaussian-like behavior appear, which suggests an interpretation in terms of diffusive models.

ISBN: 978-1-61804-225-5

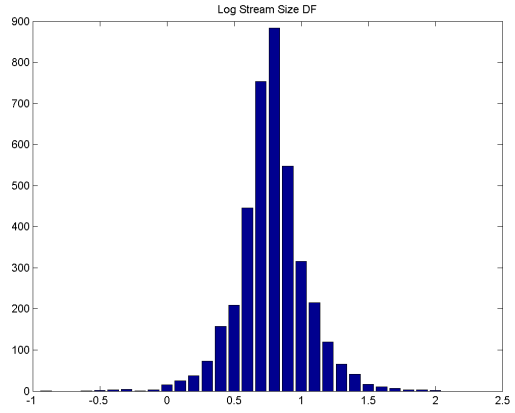

Fig. 9.

III. Conclusions

The study analyzes the possibility to represent runoff in terms of a couple of stochastic processes, the coalescence (Marcus-Lushnikov) and the splitting one, revealing that the former one could be used once introducing an injection of particles to conserve their number. The process which can be used to represent the inverse runoff model could be a simple Markov chain over a regular tree, with a death term to consider the reaching of a stream of its birth point. Even if both routing models seem to be sound with the physical interpretation, initiation and stopping methods used in routing algorithms don't allow them to produce the same distributions of stream sizeo.

References

[1] Daniel Hillel. *Applications of Soil Physics*. 1980.
[2] A A Lushnikov. Field-theory methods in coagulation theory. *Physics of Atomic Nuclei*, 74(8):1096–1106, 2011.
[3] Russell Lyons and Yuval Peres. *Probability on Trees and Networks*. -, 2010.
[4] Jeffrey E Miller. Basic concepts of kinetic-wave models. Technical report, U. S. GEOLOGICAL SURVEY, 1984.
[5] B M Troutman and M R Karlinger. *Spatial Channel Network Models in Hydrology*, chapter 4, pages 85–127. World Scientific, 1996.
[6] David A Woolisher. Search for Phsically Based Runoff Model - A Hydrologic El-Dorado ? *J.of Hydraulic Eng.*, march:122–129, 1996.

Giuliano Vitali was born in Italy, 1962. With a degree in Physics and PhD in Environmental Physics, he is Full Researcher at University of Bologna at Dept.of Agricultural Sciences, where he carry on researches and hold lectures in Soil Physics, Land Surface Hydrology, Atmosphere Physics, Theoretical Ecology and Crop Production System.

ISBN: 978-1-61804-225-5

Weakly Extension

Mostafa Zeriouh, M'hamed Ziane, Seddik Abdelalim and Hassane Essanouni

***Abstract*—**In this paper, let p a prime number and A an abelian $p-$group . We defined weak extension property and we establish the result follows: for all $x\in A,$ if $<x>$ is a direct summand of A while there exists $m_x\in\mathbb{Z}$ such that $\alpha(x)-m_x x\in A^1,$ where $\alpha\in Aut(A)$ satisfies the weak extension property and A^1 is the first Ulm subgroup of A.

***Keywords*—**Abelian goups, $p-$group, order, direct sums of cyclic groups, basic subgroups, monomorphism group, automorphism group.

I. Introduction

IN 1987, P. Schupp showed, in [3], that the extension property in the category of groups, characterizes the inner automorphisms. M. R. Pettet gives, in [4], a simpler proof of Schupp's result and shows that the inner automorphisms of a group are also characterized by the lifting property in the category of groups. The automorphisms of abelian $p-$groups having the extension property in the category of abelian $p-$groups are characterized in [1].

Definition 1. Let Γ a class of abelian $p-$groups and let $A\in\Gamma$. We say that automorphism α of A has the weak extension property if for all $B\in\Gamma$ and any monomorphism of groups $\lambda: A\to B$ and if there exists an element m in $\mathbb{N}^*$ such that the restriction of λ to mA is an isomorphism between mA and mB then there exists $\tilde{\alpha}\in Aut(B)$ such that the following diagram is commutative:

$$\begin{array}{ccc} A & \xrightarrow{\lambda} & B \\ \alpha\downarrow & & \downarrow\tilde{\alpha} \\ A & \xrightarrow{\lambda} & B \end{array}$$

This work was supported in part by the Department of Mathematical and Computer Sciences , Faculty of sciences , University of Mohamed first, BP.717 60000, Oujda, Morocco.

M. Zeriouh: Department of Mathematical and Computer Sciences , Faculty of sciences , University of Mohamed first, BP.717 60000, Oujda, Morocco. zeriouhmostafa@gmail.com

M. Ziane: Department of Mathematical and Computer Sciences , Faculty of sciences , University of Mohamed first, BP.717 60000, Oujda, Morocco.

S. Abdelalim: Laboratory of Mathematics, Computing and Application, Department of Mathematical and computer, Faculty of sciences University of Mohamed V Agdal, BP.1014 . Rabat, Morocco. seddikabd@hotmail.com

H. Essanouni: Laboratory of Mathematics, Computing and Application, Department of Mathematical and computer, Faculty of sciences University of Mohamed V Agdal, BP.1014 . Rabat, Morocco.

II. Main result

Theorem 1. Let A an abelian $p-$groups and α an automprphism of A which satisfies the weakly extension property.

If for all $x\in A$ such that:

$$\begin{cases} o(x)=p^r \ \ where \ \ r\in\mathbb{N}^* \\ A =<x>\oplus A' \ \ where \ A' \ is \ a \ subgroup \ of \ A \end{cases}$$

then there exists $m_x\in\mathbb{Z}$ such that $\alpha(x)-m_x x\in A^1$.

Proof

Let $x\in A$ such that $o(x)=p^r$ where $r\in\mathbb{N}^*$ and $A=<x>\oplus A'$ where A' is a subgroup of A.

Since $\alpha(x)\in A$ then there exists $m_x\in\mathbb{Z}$ such that

$$\alpha(x)=m_x x+a' \text{ where } a'\in A' \qquad (1)$$

Prove that $a'\in(A')^1$, assume the contrary: $a'\notin(A')^1$.

Let B a basic subgroup of group A' therefore by theorem 32.4 [3] we have:

$$B=\bigoplus_{n\geq 1} B_n \text{ with } \begin{cases} B_n=\bigoplus\limits_{i\in I_n}<x_{n,i}> \\ o(x_{n,i})=p^n, \ \forall i\in I_n \end{cases}$$

and with $B_n^*=\bigoplus\limits_{j>n} B_j$, $\forall n\geq 1$, we have: $\forall n\geq 1$,

$$A'=B_1\oplus\cdots\oplus B_n\oplus A_n \text{ where } A_n=B_n^*+p^nA'$$

so there exists $m\geq 1$ such that:

$$a'=b_1+\cdots+b_m+a_m \qquad (2)$$

where all the $b_i\in B_i$, $a_m\in A_m$ and $b_m\neq 0$.

Consider the group G such that $G=<y>\oplus A'$

With $y\in A$ and $o(y)=p^{r+m}$.

We define a group homomorphism λ from $A=<x>\oplus A'$ to $G=<y>\oplus A'$ by:

$$\begin{cases}\lambda(x)=p^m y\\ \lambda(b_i)=b_i \quad , \quad \forall b_i\in B_i\\ \lambda(a_m)=a_m \quad , \quad \forall a_m\in A_m\end{cases} \qquad (3)$$

λ is clearly a monomorphism of groups. Indeed,

if $a\in ker(\lambda)$ then $\lambda(a)=0$

i.e. $\exists(m_x,a')\in\mathbb{Z}\times A'$ such that $a=m_x x+a'$

and $\lambda(m_x x+a')=0$

by (2) we have: $0=\lambda(m_x x+a')$

i.e. $0=\lambda(m_x x+b_1+\cdots+b_m+a_m)$

and (3) show that: $0=m_x p^m y+b_1+\cdots+b_m+a_m$

i.e. $0=m_x p^m y+a'$

then $0=m_x p^m y=a'$

which implies that $p^{r+m}\mid m_x p^m$

i.e. $p^r\mid m_x$

thus $\exists t\in\mathbb{Z}$ such that $m_x=tp^r$

hence $m_x x=tp^r x=t\times 0=0$

i.e. $m_x x+a'=0$

then $ker(\lambda)=0$ which implies that λ is a monomorphism. The other hand we have:

$$p^{r+m}A=p^{r+m}A' \quad \text{and} \quad p^{r+m}G=p^{r+m}A'$$

thus the restriction of λ to $p^{r+m}A$ is an isomorphism from $p^{r+m}A$ to $p^{r+m}G$ (more precisely: $\lambda|_{p^{r+m}}=id_{p^{r+m}}$).

Using the fact That α checks the weak extension property then there exists $\tilde{\alpha}\in Aut(G)$ such that the following diagram is commutative:

$$\begin{array}{ccc} A & \xrightarrow{\lambda} & G\\ \alpha\downarrow & & \downarrow\tilde{\alpha}\\ A & \xrightarrow{\lambda} & G\end{array}$$

i.e. $\forall x\in A,\quad \lambda\alpha(x)=\tilde{\alpha}\lambda(x) \qquad (4)$

by (1) and (2) we have :

$$\begin{aligned}\lambda\alpha(x)&=\lambda(m_x x+a')\\ &=\lambda(m_x x+b_1+\cdots+b_m+a_m)\end{aligned}$$

then $\alpha\lambda(x)=m_x p^m y+b_1+\cdots+b_m+a_m \quad (5)$

and by (3) we have:

$$\begin{aligned}\tilde{\alpha}\lambda(x)&=\tilde{\alpha}(p^m y)\\ &=p^m\tilde{\alpha}(y)\end{aligned}$$

and since $\tilde{\alpha}(y)$ is an element of $G=<y>\oplus A'$

while $\tilde{\alpha}(y)=ky+b_1'+\cdots+b_m'+a_m' \quad (6)$

where all the $b_i'\in B_i$ and $a_m'\in A_m$

then by (3) and (6) we have :

$$\begin{aligned}\tilde{\alpha}\lambda(x)&=\tilde{\alpha}(p^m y)\\ &=p^m\,\tilde{\alpha}(y)\\ &=p^m(ky+b_1'+\cdots+b_m'+a_m')\\ &=kp^m y+p^m a_m' \qquad (7)\end{aligned}$$

(4), (5) and (7) show that :

$$m_x p^m y+b_1+\cdots+b_m+a_m=kp^m y+p^m a_m' \qquad (8)$$

Consider now the projection pr_m of G on B_m

(8) implies that :

$$pr_m(m_x p^m y+b_1+\cdots+b_m+a_m)=pr_m(kp^m y+p^m a_m')$$

i.e. $b_m=0$

which is absurd , hence $a'\in(A')^1$.

But since $(A')^1\subseteq A^1$

while $a'\in A^1$

i.e. $\alpha(x)-m_x x\in A^1$.

We proved that for all $x\in A$, if $<x>$ is a direct summand of A while there exists $m_x\in\mathbb{Z}$ such that $\alpha(x)-m_x x\in A^1$, where $\alpha\in Aut(A)$ satisfies the weak extension property and A^1 is the first Ulm subgroup of A.

ACKNOWLEDGMENT

I would thank professor Abdelhakim Chillali for his helpful comments and suggestions.

REFERENCES

[1] S. Abdelalim and H. Essannouni, Characterization of the automorphisms of an Abelian group having the extension property, vol. 59, Portugaliae Mathematica. Nova Srie 59.3, 325-333, 2002.
[2] L. Fuchs, Infinite Abelian Groups, vol. 1 Academic press New York, 1970.
[3] P. E Schupp, A Characterizing of Inner Automorphisms, Proc of A.M.S V 101, N 2. 226-228, 1987.
[4] M.R. Pettet, On Inner Automorphisms of Finite Groups, Proceeding of A.M.S. V 106, N 1, 1989.

M. Zeriouh: Department of Mathematical and Computer Sciences , Faculty of sciences , University of Mohamed first, BP.717 60000, Oujda, Morocco. zeriouhmostafa@gmail.com

M. Ziane: Department of Mathematical and Computer Sciences , Faculty of sciences , University of Mohamed first, BP.717 60000, Oujda, Morocco.

S. Abdelalim: Laboratory of Mathematics, Computing and Application, Department of Mathematical and computer, Faculty of sciences University of Mohamed V Agdal, BP.1014 . Rabat, Morocco. seddikabd@hotmail.com

H. Essanouni: Laboratory of Mathematics, Computing and Application, Department of Mathematical and computer, Faculty of sciences University of Mohamed V Agdal, BP.1014 . Rabat, Morocco.

Product life cycle cost

Doros Alexandra ,Dumitru Grazziella Corina, Irimescu Mihaela Alina,

Abstract**—**The life cycle cost of a product consists in the analysis technique that takes into account the total cost of ownership, throughout the entire lifespan of the product, from its conception and projection, to its decommissioning or disposal. The analysis of the life cycle cost allows for the selection of the products that register the lowest life cycle cost, from a range of multiple possible alternatives. Even if from a technological perspective, some of the suggested products might seem eligible, they can prove to be unprofitable, when analyzed through the lens of economic justification. The combination between engineering and economy ensures business success.

Keywords**—**life cycle cost, producer costs, target costing, user costs, value analysis.

I. INTRODUCTION

THE acquisition cost is used at a large scale as the main or even the only criterion in the decision making process regarding the design of a new product or service. The acquisition cost, however, tackles only certain superficial aspects, which cannot be considered sufficient for financing a product or service. The purchasing cost constitutes only the tip of the iceberg, while the rest of the costs related to the product's life cycle define and complete the iceberg.

The life cycle cost throughout the entire life of the product reveals "unexpected" costs and constitutes a particularly useful instrument for management. The use of the life cycle cost technique is justified when it comes to products with a long life cycle and with considerable costs, in order to develop the best decisions for their purchase.

In Berliner's and Brimson's vision, the concept of product life cycle cost consists in the *"accumulation of costs for activities that occur over the entire life cycle of a product, from inception to abandonment by the manufacturer and consumer"* (Berliner and Brimson 1988).

The product or service life cycle cost represents *"the sum of the costs the owner must incur in order to procure a product/service, to exploit it according to its operating specifications and to dispose of it, meaning all the direct and indirect costs associated with the design, projection, development, production, exploitation, maintenance and disposal throughout its entire anticipated lifespan"* (AC/323 (SAS-028)TP/37, RTO Tehnical Report Tr-058).

Therefore, the assessment of product life cycle cost constitutes *the process of economic analysis of total ownership cost evaluation, which, apart from the acquisition cost also comprises other costs such as: installation cost, operation and support cost, maintenance cost, conversion cost and / or disposal cost.*

The objective of product life cycle cost analysis, abbreviated from here on LCC, is to choose the most efficient approach of the cost, from a series of alternatives, in order to attain the lowest long term ownership cost. LCC is an economic model on product life cycle. The balance between cost elements is achieved when LCC is diminished. The LCC analysis offers very important information for the decision making process regarding the design, development and exploitation of the product.

At the basis of LCC establishment stands John Ruston's motto: "It's unwise to pay too much, but it's foolish to spend too little." The product life cycle cost analysis gives the best results when the art of technology and science fuse together with economy, so as to construct a rational development process of a business.

It is natural to raise the question regarding the moment when the technique of the product life cycle cost appeared.

The global approach of costs is not a modern method; it has been developed in the 60's by the Department of Defense of the US, which controlled the entire life cycle of weapon systems: research, development, design, manufacturing, installation, exploitation, maintenance and activation.

The employment of product life cycle cost analysis in the case of military systems consists in the fact that the operation and support costs are clearly superior to the procurement cost, and the decisions made in the designing and planning phase highly influence the assessment of the entire life cycle cost. In the military field (Cernat and Baban 2006), the cost of exploitation, maintenance and disposal of equipment exceeds the initial procurement cost several times. This is why product life cycle cost analysis is necessary in the justification of the selection of a particular product.

Product life cycle cost formula is:

$$LCC = \sum_{t=0}^{n} \frac{C_t}{(1+d)^t}$$

Where:

LCC- product life cycle cost

C_t – the sum of relevant costs, comprising initial costs and future costs, from which we deduce the cash flows that can be obtained in the year *t* (negative residual value)

n – the number of years in the study period.

d – real discount rate used to adjust cash flows and bringing them to a current value.

II. WHY DO WE NEED PRODUCT LIFE CYCLE COST ANALYSIS?

LCC can be used as an instrument in the decision-making process at a managerial level, meant to solve dividing conflicts, focusing on facts, money and time.

ISBN: 978-1-61804-225-5

The typical conflict of interests in most of the entities emerges from the pursuit of distinct aspects, characteristic to each and every department in the organization (Barringer, David and Baringer&Associates 2003):

- Project engineering seeks to minimize capital costs as a sole criterion;
- Maintenance engineering wants to minimize the repair times as sole purpose;
- Production has as only objective the maximization of operational hours;
- Viability engineering is concentrated solely on eliminating malfunctions;
- Accounting wants to maximize the present net value of the project;
- Shareholders' only objective is the increase of their wealth.

Thus, above all, management has the role to mediate conflicts and make timely decisions to meet the needs of all the above mentioned categories, efforts being directed towards obtaining the lowest product life cycle cost. Engineers need to think like managers and act like economists to maximize the profit of the organization, mainly because cost becomes the main factor in the company's profitability equation.

III. Producer Costs

The analysis of life cycle costs structure, from the perspective of the producer must establish a thorough understanding of its role, which is identifying the activities that generate suppressible or reducible expenses. This also constitutes a challenge for management accounting to calculate costs that have not been materialized yet.

A very important role in the creation of the product is played by the marketing department, which establishes the selling price that must be higher than the total cost. The cost that is intended to be achieved, starting from the selling price, is called target costing and has been widely debated in the literature. The concept has been developed and employed in the Japanese enterprises, even in the early 70's, especially in the automobile industry.

The target costing represents the maximum cost that can be incurred under certain quality requirements and considering the objective of profitability.

Target costing has to be established from the early stages of product design, so that the engineers should run cost management from the upstream of product manufacturing. Philip Kotler underlined the importance the design phase has in placing the future product on the market, because this stage establishes the quality, functionality, cost and targeted profit margins, all of which influence the competitiveness of the product on the market (Kotler 1997).

In order to attain target costing, certain techniques are employed, one of which is still paid an important amount of attention to: value analysis. This method was created by engineer Miles, at General Electric, in the US, in 1947.

Value analysis is a procedure of product analysis, with the purpose of improving it, leading to cost reduction and utility increase. This method establishes that the product is valuable only if costs are minimized, a condition for being profitable, too and client satisfaction is maximized, so as to prove its utility.

In other words, the objective of this method consists in establishing an effective compromise between the cost and the function of a product, ensuring a necessary and sufficient quality level.

Value analysis method resides in the identification of a product's functions, in the ranking of these functions and in establishing the utility each of them has in the total cost of the product, in order to decide "the material costs that can be tampered with". It was found that the design stage is responsible for 75% of the cost of a product and that cost reduction possibilities can be carried out only on the remaining 25%.

IV. User Costs

Apart from "*the analysis in one's own kitchen*", suppliers have to put themselves in the buyers' position and calculate the total costs supported by them along the entire life cycle of the product. They should then judge from the clients' perspective whether the purchasing of the product or service in question is profitable or not. This way, the additional costs, apart from the acquisition price paid to the seller, are revealed.

For a better illustration of the theoretical elements debated above, take the following example: a buyer wants to purchase a car. Before the acquisition, they build several scenarios in which they calculate the total product life cycle cost, in order to take the best decision. The analysis of the various alternatives starts from the following assumptions: expenditures are considered to be made at the end of each year; the expected duration of exploitation of the car is 4 years, at an estimated 30,000 km a year; all models use gas as fuel, (purchase price of 1,3 euro / liter); the car's insurance costs are 4% of its acquisition price; estimated inflation rate is 6%; discount rate is set at 10%; at the end of four years, the owner intends to sell the car, the residual value is considered to be obtained at the time of sale. The alternatives would be the following:

- car A: Purchase price of the car is 14,000 euros, fuel usage 9%, recommended maintenance is every 15,000 km or every 6 months, average maintenance cost is estimated to be 200 euros, salvage value is 5,500 euro;
- car B: Purchase price of the car is 16,000 euro, fuel usage 8%, recommended maintenance is every 10,000 km or 6 months, average maintenance cost is estimated to be 250 euro, salvage value is 6,000 euro;
- car C: Purchase price of the car is 20,000 euro, fuel usage 7%, the dealer offers a special service package, which consists in free maintenance and service for 3 years or for the first 90,000 km; the average estimated cost of a maintenance visit is 300 euros, the interval between tune ups being of 15.000 km; salvage value is 9,500 euros.

For a clearer illustration, consider the table below:

Table I The initial information

Vehicle	Purchase price (euro)	Fuel usage (liters/100km)	Annual insurance (euro)	Maintenance cost (euro)	Salvage value (euro)
Car A	14,000	9	560	200	5,500
Car B	16,000	8	640	250	6,000
Car C	20,000	7	800	300	9,500

Source: *own calculus*

Establishing fuel expenses during the first year:

- for car A: $30{,}000 \quad km * 9\% * 1{,}3 \quad euros / litre = 3{,}510 \quad euros$
- for car B: $30{,}000 \quad km * 8\% * 1{,}3 \quad euros / litre = 3.120 \quad euros$
- for car C: $30{,}000 \quad km * 7\% * 1{,}3 \quad euros / litre = 2.730 \quad euros$

Establishing maintenance and service expenses for the first year:

- for car A:

$$\frac{30.000 \quad km}{15.000 \quad km} = 2 \quad \text{Maintenance visits / year;}$$

The annual cost of maintenance visits = 2*200 euros = 400 euros

- for car B:

$$\frac{30.000 \quad km}{10.000 \quad km} = 3 \quad \text{Maintenance visits / year;}$$

The annual cost of maintenance visits = 3*250 euros = 750 euros

- for car C:

For the first 3 years (or 90,000 km) maintenance visits are free of charge; therefore we will incur expenses only in the 4th year:

$$\frac{30{,}000 \quad km}{15{,}000 \quad km} = 2 \quad visits \text{ during the } 4^{th} \text{ year}$$

Maintenance visits costs during the 4th year = 2*300 euros = 600 euros

ISBN: 978-1-61804-225-5

Table II The calculation of the actual value of expenses incurred during the 4 years

		Fuel cost	Maintenance and service costs	Insurance costs	Inflation	Discount rate	Present value of the fuel cost (1x4x5)	Present value of the maintenance and service cost (2x4x5)	Present value of the insurance cost (3x4x5)	Total present value of the cost (6+7+8)
Car A		1	2	3	4	5	6	7	8	9
	Year 1	3,510	400	560	$(1+6\%)^1$	$\frac{1}{(1+10\%)^1}$	3,382.36	385.45	539.64	*4,307.45*
	Year 2	3,510	400	560	$(1+6\%)^2$	$\frac{1}{(1+10\%)^2}$	3,259.37	371.44	520.01	*4,150.82*
	Year 3	3,510	400	560	$(1+6\%)^3$	$\frac{1}{(1+10\%)^3}$	3,140.85	357.93	501.10	*3,999.88*
	Year 4	3,510	400	560	$(1+6\%)^4$	$\frac{1}{(1+10\%)^4}$	3,026.63	344,92	482.88	*3,854.43*
	TOTAL						*12,809.21*	*1,459.74*	*2,043.63*	*16,312.59*
Car B	Year 1	3,120	750	640	$(1+6\%)^1$	$\frac{1}{(1+10\%)^1}$	3,006.55	722.73	616.73	*4,346*
	Year 2	3,120	750	640	$(1+6\%)^2$	$\frac{1}{(1+10\%)^2}$	2,897.22	696.45	594.30	*4,187.96*
	Year 3	3,120	750	640	$(1+6\%)^3$	$\frac{1}{(1+10\%)^3}$	2,791.86	671.12	572.69	*4,035.67*
	Year 4	3,120	750	640	$(1+6\%)^4$	$\frac{1}{(1+10\%)^4}$	2,690.34	646.72	551.86	*3,888.92*
	TOTAL						*11,385.97*	*2,737.01*	*2,335.58*	*16,458.56*
Car C	Year 1	2,730	-	800	$(1+6\%)^1$	$\frac{1}{(1+10\%)^1}$	2,630.73	-	770.91	*3,401.64*
	Year 2	2,730	-	800	$(1+6\%)^2$	$\frac{1}{(1+10\%)^2}$	2,535.06	-	742.88	*3,277.94*
	Year 3	2,730	-	800	$(1+6\%)^3$	$\frac{1}{(1+10\%)^3}$	2,442.88	-	715.86	*3,158.74*
	Year 4	2,730	600	800	$(1+6\%)^4$	$\frac{1}{(1+10\%)^4}$	2,354.05	517.37	689.83	*3,561.25*
	TOTAL						*9,962.72*	*517.37*	*2,919.48*	*13,399.57*

Source: own calculus

Note: the amounts are in euro.

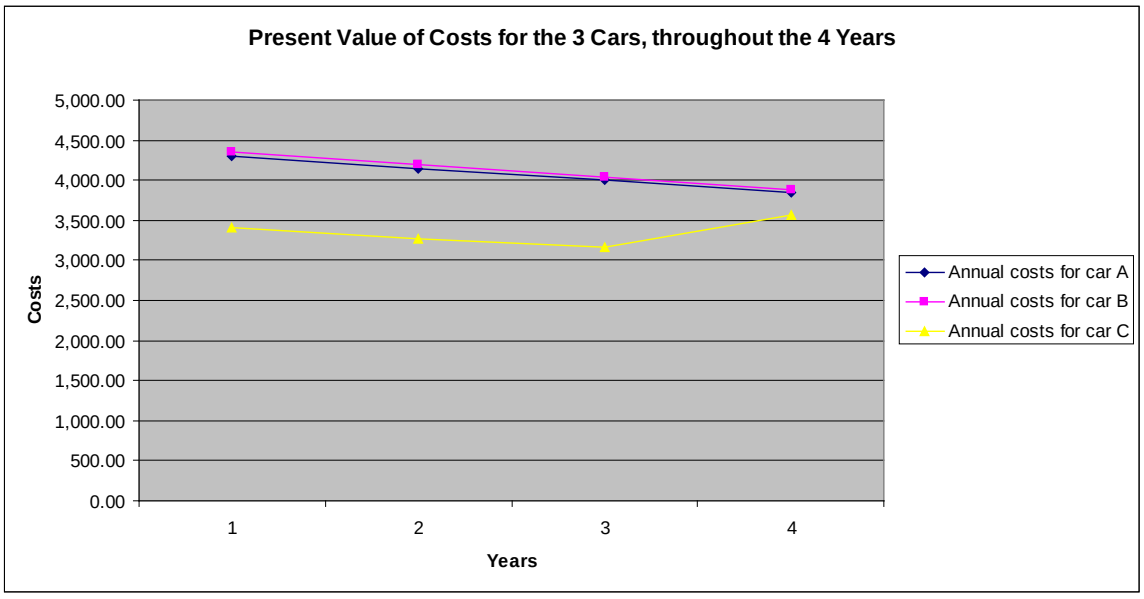

Fig.1 Present value of costs for the 3 cars, throughout the 4 years

Table III Life Cycle Cost Calculation

	Purchase price (euros)	Current salvage value (euros)	Current value of costs suffered during 4 years	Total life cycle cost
0	1	2	3	4=1-2+3
car A	14,000	3,756.57	16,312.59	26,556.02
car B	16,000	4,098.08	16,458.56	28,360.48
car C	20,000	6,488.63	13,399.57	26,910.94

Source: own calculus

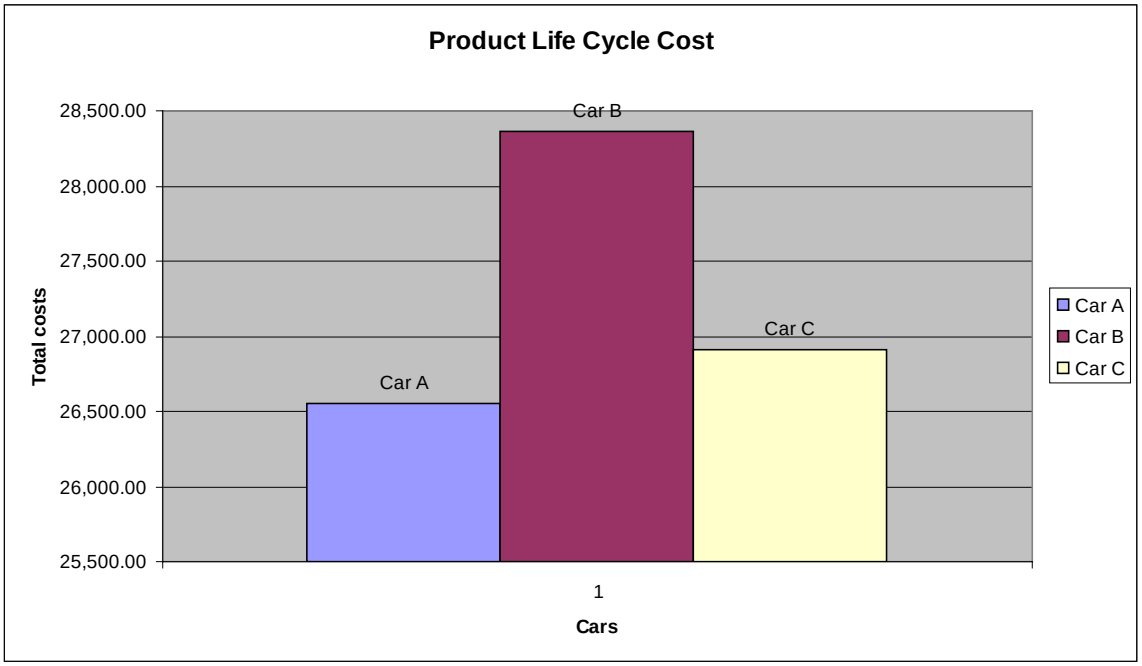

Fig.2 Product life cycle cost
Source: own analysis

ISBN: 978-1-61804-225-5

As illustrated in the figures above, car A registers the lowest life cycle cost, but is quite close to the cost registered by car C. The final decision should take into consideration quality factors.

The adoption of product life cycle cost analysis stems from the companies' need to collaborate better, to adapt faster, to create an innovative content and to have greater flexibility and real time response capacity.

V. The Advantages And Disadvantages Of Assessing Product Life Cycle Cost

LCC offers critical information regarding the global decision making process, but does not provide the final answer.

The *advantages* of this method can be synthesized as follows:

- It ensures a complete picture from a financial perspective, taking into account the initial cost, but also all the costs and benefits throughout the entire life cycle of the product.
- It allows for comparisons between different combinations of measures and the selection of the best alternative, which will maximize the economies and financial profitability of the entity; the analysis of the influence of different manufacturing methods provides the best option for the completion of the product.
- LCC grants the possibility of analyzing repairs cost, which is very useful when assessing the necessity of maintenance, and maintenance costs.
- It offers information for establishing warranty and repairs costs, useful both to suppliers and users.
- It supports the selling strategy of the dealers, taking into account the level of the product, the general exploitation experience and the rate of decommissioning for the user.
- It presents the financial benefits of the product in terms familiar to the economic departments, for instance: net present value, internal rate of return, cash flows.

Far from representing a perfect analysis instrument, despite the significant series of advantages of life cycle cost analysis, we have to be rational and look at the glass half empty, too – its disadvantages.

The *disadvantages* of LCC analysis emerge from the uncertainties we come across when estimating the total life cycle cost of the product. Apart from the purchasing cost, the only known set value, the rest of the costs are only estimated values, governed by uncertainties. Therefore, the LCC analysis:

- Does not offer precise values; this does not mean, however, that it provides wrongful information; it is only a matter of satisfactory or unsatisfactory information.
- It works with limited data bases, the estimations lacking precision: the precision errors are difficult to establish because the variations obtained through statistical methods are at times significant.
- It sometimes requires considerable amounts of information, which is usually unavailable and much of it lacks credibility; gathering the input data can be a real challenge.
- It is difficult to learn and implement.
- It presents information that is useful only if it is the result of team work, engaging different departments of the entity.

LCC does not consist in determining the total cost for an alternative product, but, quite on the contrary, in the capacity to compare the cost of the other possibilities and in establishing which alternative offers the best value for each spent unit.

VI. Conclusions

The life cycle cost of a product has proven to be a useful instrument in the decision making process related to investments. It includes in the analysis countless costs, transformed in economic models by the *present net value*. The comparison between life cycle costs helps us make the correct investment decision. A small selling price usually provides necessary information for the purchasing decision, and a large selling price has to be compared with the entire lifespan of the product. The present net value requires decisions related to the time of maintenance and to the type of maintenance / cost of replacement which will be incurred; these aspects are given by the time and methods employed to detect flaws, using reliable technology.

In our opinion, LCC analysis provides a better evaluation of long term cost efficiency, compared to the alternative methods, which rely only on the initial cost (initial investment) or on a short term operational cost.

LCC is an analysis process that has valuable results when art and science are intertwined in an accurate judgment.

In order to underline the utility of product life cycle cost analysis we often employ the proverb: "in the country of the blind the one-eyed man is king", meaning that this technique helps us optimize the idea of product cost to an extent large enough so as to be competitive on the market.

ISBN: 978-1-61804-225-5

REFERENCES

C. Berliner, and J. A. Brimson, "Cost Management for Today's Advanced Manufacturing: The CAM-I Conceptual Design", Harvard Business School Press, Boston, (1988).

H. P. Barringer, P. E. David, and P. Weber, "Life cycle Cost Tutorial", Fifth International Conference on Process Plant Reliability, Houston, Texas, October 2-4 (1996).

H. Bouquin, „Contabilitate de gestiune", Ed. TipoMoldova, Iaşi (2004).

C. Dumitru, and C. Ioanăş, "Contabilitatea de gestiune şi evaluarea performanţelor", Editura Universitară, Bucureşti (2005).

K. S. Fuller and S. R. Petersen, "Life Cycle Costing Manual for the Federal Energy Management Program", National Institute of Standards and Tehnology Handbook 135, Washington (1996).

P. Kotler, "Managementul marketingului", Ed. Teora, Bucureşti (1997).

T. Mearig, N. Coffee, and M. Morgan, "Life Cycle Cost Analysis" Handbook, State of Alaska, Department of Education&Early Development, first edition (1999).

M. Ristea, L. Possler, and K. Ebbeken, "Calculaţia şi managementul costurilor", Editura Teora, Bucureşti (2000).

AC/323 (SAS-028)TP/37, RTO Tehnical Report Tr-058, Cost Structure and Life Cycle Costs for Military Systems.

H. P Barringer, P.E. David, and Baringer&Associates, Inc, „A Life Cycle Cost Summary", paper presented on International Conference of Maintenance Societies (ICOMS). Avaible: http://www.barringer1.com/pdf/LifeCycleCostSummary.pdf

Cernat, M. and Băban, C. „Costul pe ciclul de viaţă al echipamentelor militare" (2006). Avaible: www.dpa.ro/rp/publicatii/rtm/.../studii/RTM2006_1_3.pdf.

Fuller, S. "Life Cycle Cost Analysis (LCCA)", National Institute of Standards and Technology (NIST), 2008. Avaible: www.wbdg.org/resources/lcca.php.

Hall effect on MHD flow and heat transfer over an unsteady stretching permeable surface in the presence of thermal radiation and a heat source/sink

Stanford Shateyi, University of Venda , South Africa and Gerald , Marewo, University of Swaziland, Swaziland

Abstract—This paper employs the computational iterative approach known as Spectral Local Linearization Method (SLLM) to analyze Hall effect on MHD flow and heat transfer over an unsteady stretching permeable surface in the presence of thermal radiation and heat source/sink. To demonstrate the reliability of our proposed method, we made comparison with Matlab $bvp4c$ routine technique and excellent agreement was observed. The governing partial equations are transformed into a system of ordinary differential equations by using suitable similarity transformations. The results are obtained for velocity, temperature, skin friction and Nusselt number.

Keywords—Hall effect;stretching sheet ; thermal radiation, heat source/sink.

I. Introduction

Theoretical studies of magnetohydrodynamic flow and heat transfer over stretching surfaces have received great attention by virtue of their numerous applications in the fields of metallurgy, chemical engineering and biological systems. Such applications include geothermal reservoirs, wire and fiber coating, food stuff processing, reactor fluidization, enhanced oil recovery, packed bed catalytic reactors, and cooling of nuclear reactors. The primary aim in extrusion is to maintain the quality of the surface of the extricate.

Examples of such studies include Sakiadis[1], [2] did pioneering work on boundary layer flow on a continuously moving surface. Shateyi and Motsa [3] carried out a numerical analysis of the problem of magnetohydrodynamic boundary layer flow, heat and mass transfer rates on steady two-dimensional flow of an electrically conducting fluid over a stretching sheet embedded in a non-Darcy porous medium in the presence of thermal radiation and viscous dissipation. Shateyi [4] investigated thermal radiation and buoyancy effects on heat and mass transfer over a semi-infinite stretching surface with suction and blowing. Singh et al. [5] investigated two dimensional unsteady flow of a viscous incompressible fluid about a stagnation point on a permeable stretching sheet. Shateyi and Motsa [6] numerically investigated the unsteady heat, mass and fluid transfer over a horizontal stretching sheet. More recently, Shateyi and Marewo [7] studied the magnetohydrodynamic boundary layer flow with heat and mass transfer of an UCM fluid over a stretching sheet in the presence of viscous dissipation and thermal radiation.

Governing equations modeling MHD flow and heat transfer over stretching surfaces are highly nonlinear thereby exact solutions are impossible to obtain. Therefore, numerical solutions have always been developed and modified, as a bid of getting more accurate and stable solutions. The current study seeks to investigate the Hall effect on MHD flow and heat transfer over an unsteady stretching permeable surface in the presence of thermal radiation and a heat source/sink. We propose to numerically solve the present problem using a recently developed iterative method known as Spectral Local Linearization Method (SLLM), Motsa [8]. The SLLM approach is based on transforming nonlinear ordinary differential equation into an iterative scheme. The iterative scheme is then blended with Chebyshev spectral method ([9]).

II. Model Formulation

We consider an unsteady two-dimensional laminar MHD boundary layer flow and heat transfer of an incompressible, viscous and electrically conducting fluid over a continuously moving stretching permeable surface.

S. Shateyi is with the Department of Mathematics and Applied Mathematics, University of Venda, , X5050, 0950 South Africa e-mail: stanford.shateyi@univen.ac.za.

G.T. Marewo is with the University of Swaziland, Department of Mathematics, Private Bag 4, Kwaluseni, Swaziland Email:

Manuscript received January, 2014

The flow is subjected to a transverse magnetic field of strength B_0 and the Hall current is taken into account in this study.

The relevant governing equations of fluid flow and heat transfer are,

$$\frac{\partial u}{\partial x}+\frac{\partial v}{\partial y}=0, \tag{1}$$

$$\frac{\partial u}{\partial t}+u\frac{\partial u}{\partial x}+v\frac{\partial u}{\partial y}=\nu\frac{\partial^2 u}{\partial y^2}-\frac{\sigma B^2}{\rho(1+m^2)}(u+mw), \tag{2}$$

$$\frac{\partial w}{\partial t}+u\frac{\partial w}{\partial x}+v\frac{\partial w}{\partial y}=\nu\frac{\partial^2 w}{\partial y^2}-\frac{\sigma B^2}{\rho(1+m^2)}(mu-w), \tag{3}$$

$$\frac{\partial T}{\partial t}+u\frac{\partial T}{\partial x}+v\frac{\partial T}{\partial y}=\alpha\frac{\partial^2 T}{\partial y^2}-\frac{1}{\rho c_p}\frac{\partial q_r}{\partial y}+\frac{Q}{\rho c_p}(T-T_\infty). \tag{4}$$

The associated boundary conditions to the current problem are:

$$\begin{aligned} &u=U_w(x,t),\ v=V_w,\ T=T_w(x,t), \quad \text{at}\ \ y=0,\\ &u\to 0,\ w\to 0,\ T\to T_\infty \quad \text{as}\ \ y\to\infty, \end{aligned} \tag{5}$$

where u, v and w are the velocity components along x, y and z directions, respectively and t is the time. T is the temperature within the fluid, c_p is the specific heat at constant pressure, α is the thermal diffusivity, ν is the kinematic viscosity of the fluid density, $T_w(x,t)$ is the temperature on the stretching surface, T_∞ is the ambient temperature with $T_w > T_\infty$. We have $V_w=-(\nu U_w/x)^{1/2}f(0)$ representing the mass transfer at the surface with $V_w>0$ for injection and $V_w<0$ for suction. We also have $U_w(x,t)=ax/(1-ct)$, where a (stretching rate) and c are positive constants, with $ct<1$. It is noted that the stretching rate $a/(1-ct)$ increases with time since $a>0$. The surface temperature of the sheet varies with the distance x from the origin and time t and takes the form:

$$T_w(x,t)=T_\infty+\frac{b^2x}{2\nu(1-ct)^{3/2}}, \tag{6}$$

where b is a constant with $b\geq 0$.

A. Similarity Transformation

Following Ishak et al. [10], we introduce the following dimensionless functions f and θ, and the similarity variable η.

$$\eta=\left(\frac{b}{\nu(1-ct)}\right)^{\frac{1}{2}}y,\ \psi(x,y,t)=\left(\frac{\nu b}{1-ct}\right)^{\frac{1}{2}}xf(\eta),$$
$$T(x,y,t)=T_\infty+\frac{b^2x}{2\nu(1-ct)^{\frac{3}{2}}}\theta(\eta),\quad B^2=\frac{B_0^2}{(1-ct)}. \tag{7}$$

By using the Rosseland approximation, the radiative heat flux is given by

$$q_r=-\frac{4\sigma^*}{3K^*}\frac{\partial T^4}{\partial y}, \tag{8}$$

where $\sigma*$ and K^* are respectively, the Stephan-Boltzman constant and the mean absorption coefficient. Assuming that the temperature differences within the flow are such that T^4 can be expressed as a linear function. Expanding T^4 in a Taylor series about T_∞ and neglecting higher order terms we get

$$T^4\cong 4T_\infty T-3T_\infty^4. \tag{9}$$

By using the above transformations, the governing partial differential equations are transformed into a system of non-dimensional nonlinear and coupled ordinary differential equations as follows:

$$f'''+ff''-f'^2-A(f'+\frac{1}{2}\eta f'')-\frac{M}{1+m^2}(f'+mg)=0, \tag{10}$$

$$g''+fg'-f'g-A(g+\frac{1}{2}\eta g')+\frac{M}{1+m^2}(mf'-g)=0, \tag{11}$$

$$\left(1+\frac{4}{3}R\right)\theta''+Pr(f\theta'-2f'\theta)-Pr\frac{A}{2}(3\theta+\eta\theta')+\delta\theta=0, \tag{12}$$

Here $M^2=\sigma B_0^2/\rho a$, $A=c/a$ is a parameter that measures the unsteadiness, $Pr=\nu/\alpha$ is the Prandtl number, $R=4\sigma^*T_\infty^3/kK_s$ is the thermal radiation parameter. The boundary conditions are

$$f(0)=f_w,\quad f'(0)=1,\ \ \theta(0)=1\ \ g(0)=0, \tag{13}$$
$$f'\to 0,\quad \theta\to 0,\quad g\to 0,\quad \text{as}\ \ \eta\to\infty, \tag{14}$$

where $f(0)=f_w$ with $f_w<0$ or $f_w>0$ corresponding to injection or suction, respectively. The physical engineering quantities of interest in this problem are the skin friction coefficients in the $x-$ and $z-$ directions and the local Nusselt number number, Nu_x which are defined

as:

$$C_{fx} = -\frac{2\mu(\partial u/\partial y)_{y=0}}{\rho U_w^2} = -2Re_x^{-1/2} f''(0),$$
$$C_{fz} = \frac{2\mu(\partial w/\partial y)_{y=0}}{\rho U_w^2} = 2Re_x^{-1/2} g'(0),$$
$$Nu_x = \frac{x q_w}{\kappa(Tw - T_\infty)}, \tag{15}$$

where $\tau_w = \mu\left(\frac{\partial u}{\partial y}\right)_{y=0}$ is the wall shear stress, and $q_w = -\kappa\left(\frac{\partial T}{\partial y}\right)_{y=0}$ is the surface heat flux, where μ and κ are the dynamic viscosity and thermal conductivity, respectively.

III. Method of solution

If we let $f' = p$ then equations (10-12) become

$$p'' + fp' - p^2 - A\left(p + \frac{\eta}{2}p'\right) - \frac{M}{1+m^2}(p + mg) = 0 \tag{16}$$

$$g'' + fg' - pg - A\left(g + \frac{\eta}{2}g'\right) + \frac{M}{1+m^2}(mp - g) = 0 \tag{17}$$

$$\left(1 + \frac{4}{3}R\right)\theta'' + Pr(f\theta' - 2p\theta) - Pr\frac{A}{2}(3\theta + \eta\theta') + \delta\theta = 0 \tag{18}$$

Equations (16-18) together with the change of variable $f' = p$ may be written as

$$L_1 + N_1 = H_1 \tag{18}$$
$$L_2 + N_2 = H_2 \tag{19}$$
$$L_3 + N_3 = H_3 \tag{20}$$
$$L_4 + N_4 = H_4 \tag{21}$$

IV. Results and Discussion

The numerically results iteratively generated by the SLLM for the main parameters that have significant effects on the flow properties are presented in this section. All the SLLM results presented in this work were obtained using $N = 50$ collocation points, and were are glad to high light that convergence was achieved as few as six iterations. We take the infinity value η_∞ to be 40. The magnetic field is taken quite strong by assigning large values of M to ensure generation of Hall currents. Unless otherwise stated, the default values for the parameters are taken as $M = 1,\ Pr = 0.71,\ \sigma = 0.5,\ R = 1,\ m = 0.5,\ f_w = 1$. In order to validate our numerical method, it was compared to MATLAB routine $bvp4c$ which is an adaptive Lobatto quadrature iterative scheme.

In Table I we present a comparison between the SLLM approximate results and the $bvp4c$ results for selected default values of the stretching parameter A. It can be clearly seen from this table that there is an excellent agreement between the results from the two methods. Also Table I shows that an increase in the unsteadiness parameter leads to increases in the skin-friction coefficients in both directions. Also the heat transfer gradient increases as the values of the unsteadiness parameter increase. The negative values of $f''(0)$ mean that the solid surface exerts a drag force on the fluid. This is due to the development of the velocity boundary layer which in the current study is caused solely by the stretching sheet. In Table II we display the effect of the magnetic parameter on the skin friction coefficients and the Nusselt number. The magnetic parameter M represents the significance of the magnetic field on the flow properties. As the magnetic strength increases, the dragging effect is clearly seen by the significant increments in the skin friction. We also observe that increasing the values of the Hartman number leads to the lowering of the values of the Nusselt number. Application of a strong magnetic field reduces the velocity which in turn increases heat diffusion within the fluid flow. This physically explains why heat transfer at the wall is reduced as M is increased.

TABLE I
Comparison of the SLLM results of $-f''(0),\ g'(0),\ -\theta'(0)$ with those obtained by $bvp4c$ for different values of the unsteadiness parameter.

	$-f''(0)$		$g'(0)$		$-\theta'(0)$	
A	$bvp4c$	SLLM	$bvp4c$	SLLM	$bvp4c$	SLLM
1	2.06334	2.06334	0.17552	0.17552	0.95974	0.95974
2	2.27278	2.27278	0.15185	0.15185	1.30759	1.30759
3	2.46650	2.46650	0.134598	0.134598	1.54422	1.54422

TABLE II
Comparison of the SLLM results of $-f''(0),\ g'(0),\ -\theta'(0)$ with those obtained by $bvp4c$ for different values of the magnetic parameter.

	$-f''(0)$		$g'(0)$		$-\theta'(0)$	
M	$bvp4c$	SLLM	$bvp4c$	SLLM	$bvp4c$	SLLM
1	2.06334	2.06334	0.17552	0.17552	0.51730	0.51730
3	2.40060	2.40060	0.41758	0.41758	0.46088	0.46088
5	2.69188	2.69188	0.59380	0.59380	0.43117	0.43117

Table III displays the influence of the Hall current on the skin friction coefficients as well as the Nusselt number. The skin friction coefficient is reduced as the values of the Hall current parameter increase. This explains why the skin friction coefficient in the axial direction. However, in the transverse direction the skin

friction increases as the Hall current increases. There is slight effect of the Hall current on Heat transfer rate on the stretching surface. The influence of suction/injection

TABLE III
COMPARISON OF THE SLLM RESULTS OF $-f''(0),\ g'(0),\ -\theta'(0)$ WITH THOSE OBTAINED BY $bvp4c$ FOR DIFFERENT VALUES OF THE HALL PARAMETER.

	$-f''(0)$		$g'(0)$		$-\theta'(0)$	
m	$bvp4c$	SLLM	$bvp4c$	SLLM	$bvp4c$	SLLM
0.1	2.2059	2.2059	0.0312	0.0312	0.4978	0.497
0.5	2.1537	2.1537	0.1311	0.1311	0.5041	0.504
1.0	2.0633	2.0633	0.1755	0.1755	0.5173	0.517

parameter f_w on the axial velocity is depicted in Figure 1. The axial velocity is significantly influenced by this parameter. The velocity boundary layer is greatly enhanced when fluid is injected $(f_w < 0)$ into the flow system thereby increasing the velocity profiles. However, removing fluid from the flow system through suction, as expected drastically reduces the velocity profiles as can be clearly seen in Figure 1.

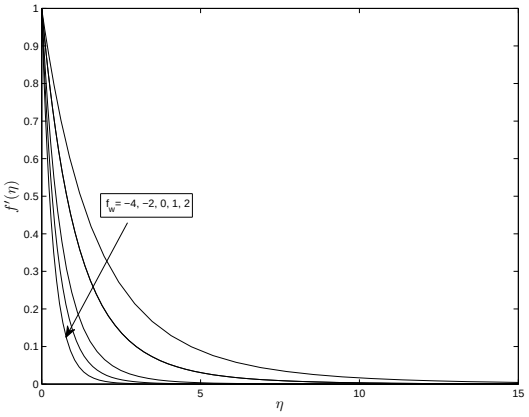

Fig. 1. Graph of the SLLM solutions for the horizontal velocity for different values of f_w.

The effect of the Hall current parameter m on the axial velocity is shown in Figure 2. The velocity is enhanced as the values of m increase. However, the axial velocity profiles approach their classical values when the Hall current parameter m becomes large $(m > 1.5)$ in our current study. Any further increase of the Hall current would make the magnetic effect insignificant.

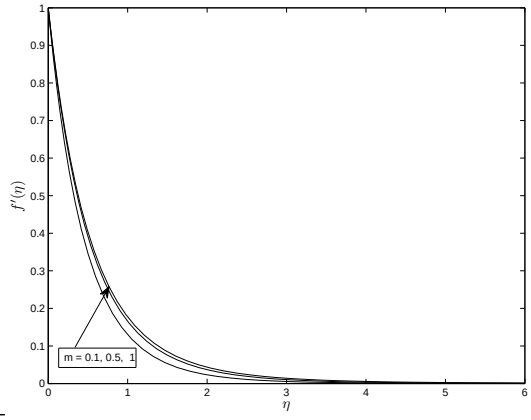

Fig. 2. Graph of the SLLM solutions for the horizontal velocity for different values of Hall parameter

The effect of the Hall current parameter on the transverse velocity is displayed in Figure 3. Increasing the values of m causes the transverse velocity to rapidly increase.

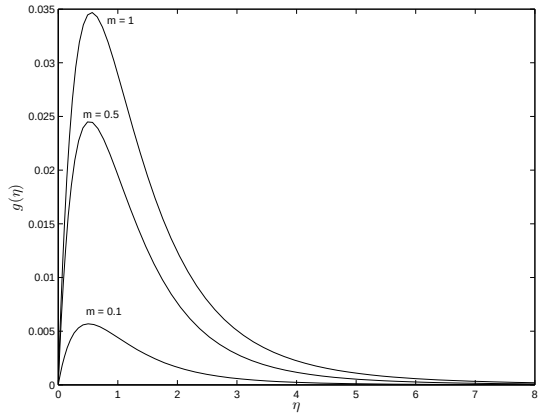

Fig. 3. Graph of the SLLM solutions for the transverse velocity for different values of the Hall parameter

In Figure 4 we have the effect of the heat source/sink parameter δ on the temperature profiles. As expected, it is observed in this figure that the temperature in the boundary layer increases with increasing values of δ. The heat absorption due to a uniform sink $(\delta < 0)$ leads to the reduction of the thermal boundary layer thickness, whereas this layer increases significantly with increases in $\delta > 0$.

ISBN: 978-1-61804-225-5

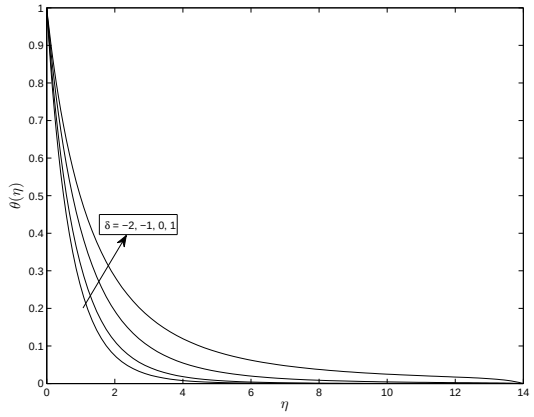

Fig. 4. Graph of the SLLM solutions of the temperature profiles for different values of heat source/sink parameter

Figure 5 is plotted to depict the influence of the thermal radiation parameter R on the temperature profiles. We clearly observe that the temperature in the boundary layer increases with increasing values of the thermal radiation parameter. This is due to the fact that the divergence of the radiative heat flux increases as the Rosseland radiative absorption K^* decreases which in turn increases the rate of radiative heat transfer to the fluid. Thus the presence of thermal radiation enhances thermal state of the fluid causing its temperature to significantly increase.

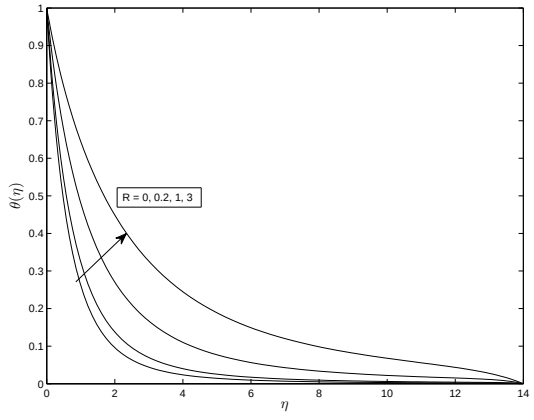

Fig. 5. Graph of the SLLM solutions of the temperature profiles for different values of thermal radiation parameter

V. Conclusion

The present work analyzed MHD unsteady flow and heat transfer of an electrically conducting fluid over a stretching sheet in the presence of thermal radiation and Hall effect. The governing partial differential equations are transformed into a system of non-linear ordinary differential equations by using suitable similarity variables. The resultant system of non-linear ordinary differential equations is solved numerically by the recently developed technique known as the Spectral Local Linearization Method. The accuracy of the SLLM is validated against the MATLAB in-built $bvp4c$ routine for solving boundary value problems. The following conclusions were drawn in our investigation.

- An excellent agreement was observed between our results and those obtained using $bvp4c$ routine technique giving confidence to our present results.
- The unsteadiness parameter A has significant effects on the velocity components and temperature profiles. The maximum axial velocity, transverse velocity and temperature profiles are attained when the flow is steady $(A = 0)$.
- Increasing the values of the magnetic field strength decreases the momentum boundary layer thickness while increasing the thermal boundary layer thickness.
- The velocity components are enhanced as the Hall parameter increases.
- The fluid temperature increases with increasing values of thermal radiation as well as a heat source.
- The heat transfer rate and the skin friction coefficient in the $x-$ direction are increased while the skin friction in the $z-$ direction decreases as the unsteadiness parameter increases.
- The skin friction coefficients are enhanced while the heat transfer rate is depressed by increasing values of the magnetic strengths.

Acknowledgment

The authors would like to thank NRF and the University of Venda for financial support.

References

[1] B. C. Sakiadis, "Boundary-layer behaviour on continuous solid surfaces: I. Boundary-layer equations for two-dimensional and axisymmetric flow," *AICHE J,* 7, 26-28, (1961).

[2] B. C. Sakiadis, "Boundary-layer behaviour on continuous solid surfaces: II. Boundary-layer equations for two-dimensional and axisymmetric flow," *AICHE J,* 7, 221-225, (1961).

[3] S. Shateyi and S. S. Motsa, "Hydromagnetic Non-Darcy Flow, Heat And Mass Transfer Over A Stretching Sheet In The Presence Of Thermal Radiation And Ohmic Dissipation," *The canadian Journal of Chemical Engineering,* 89, 13881400, (2011).

[4] S. Shateyi, "Thermal radiation and buoyancy effects on heat and mass transfer over a semi-infinite stretching surface with suction and blowing," *Journal of Applied Mathematics,* Volume 2008, doi.10.1155/2008/ 414830, 1-12, (2008).

[5] P. Singh, A. Jangid, N.S. Tomer and D. Sinha, "Effects of Thermal Radiation and Magnetic Field on Unsteady Stretching Permeable Sheet in Presence of Free Stream Velocity," *International Journal of Information and Mathematical Sciences,* 6:3, 160-166, (2010).

[6] S. Shateyi and S. S. Motsa, "Thermal radiation effects on heat and mass transfer over an unsteady stretching surface," *Mathematical Problems in Engineering,* Vol 2009, doi:10.1155/2009/965603, 1-13, (2009).

[7] S. Shateyi, and G. T. Marewo, "A new numerical approach of MHD flow, heat and mass transfer for the UCM fluid over a stretching surface in the presence of thermal radiation," *Mathematical Problems in Engineering,* Volume 2013, 1-8, doi.org/10.1155/2013/670205, (2013).

[8] S. S. Motsa, "A New Spectral Local Linearizatio Method for Nonlinear Boundary Layer Flow Problems", *Journal of Applied Mathematics,* Volume 2013, Article ID 423628, 1-15 http://dx.doi.org/10.1155/2013/423628, (2013).

[9] L. N. Trefethen, "Spectral Methods in MATLAB", SIAM, Philadelphia, (2000).

[10] A. Ishak, R. Nazar and I. Pop, "Heat transfer over an unsteady stretching permeable surface with prescribed wall temperature," Nonlinear Analysis: Real World Applications, vol. 10, pp 2909-2913, 2009.

Application of the Monte Carlo Method for the Determination of Physical Parameters of an Electrical Discharge

L. Zeghichi, L. Mokhnache, and M. Djebabra

***Abstract*—** The aim of this paper is to use of the Monte Carlo Method to try to reproduce an electrical discharge in the oxygen gas; by following the random histories of free electrons and using the sampling laws, we can determine some electrical discharge parameters. Additionally we use the simulation results to verify the electrical breakdown criteria under an homogenous field and for small distances; and the obtained results are compared with those of the literature.

***Keywords*—** Attachment, Collision probability, electrical discharge, ionization, mean free flight time, Monte Carlo method, Monte Carlo method

I. Introduction

IN their normal state of temperature and pressure, the gases are perfect insulations. The reason for this, that they contain only neutral species (molecules and atoms) [1]-[5]. The conduction in air at low field is in the region 10^{-16} — 10^{-17} A/cm^2. This current, results from cosmic radiations and radioactive substances present in earth and the atmosphere. However, when applying a sufficiently strong electric field between two electrodes immersed in a gaseous medium, it becomes more or less conductive and an electrical breakdown occurs [2]. So, the complex phenomena that occur are called electrical discharge in gases [4].

As a rule, an electrical discharge is produced mainly via ionization by collision, photo-ionization, and the secondary ionization processes. In insulating gases (also called electron-attaching gases) the process of attachment also plays an important role [6]. It follows the generation of new electrons and ions in the Townsend avalanches that grow up until a maintenance state is established. The discharge becomes then independent of the external sources which produce free electric charges in the gas.

Several studies have been made in the framework of the discharge modeling to improve the understanding of the fundamental processes of electrical discharges in gases, with the aim is to obtain good results [6]-[11].

L. Zeghichi, is now with the Department of Physics, Ouargla University, P.O Box.511, OUARGLA 30 000, Algeria(e-mail: zeghichi.leyla@univ-ouargla.dz).

L. Mokhnache is with the Electrical Engineering Department, Batna University, Batna, Algeria(e-mail: lmokhnache@yahoo.fr).

M. Djebabra is with the Institute Health and Safety, Batna University, Batna, Algeria(e-mail: ebarek_djebabra@ yahoo.fr).

A model must reproduce as finely as possible the physical phenomena involved in the studied system. The task of the modeler is first to identify the main characteristics of the physical problem, and formulate them mathematically. Because of the complexity of the studied systems, the mathematical representation is related to the choice of approximations and hypotheses that make the problem resolvable.

The Monte Carlo Method (MCM), based on stochastic laws, is used in our computation seen that it considers several stochastic events during the process of the electrical discharge; it consists in simulation of a large number of events (charged particles) by another set easily achievable (random variables). The simulation of electron motion has been performed in order to accurately calculate the ionization and the attachment rates as well the mean kinetic energy.

In this paper we will study, in the oxygen gas, the temporal evolution of an electrical discharge at an atmospheric pressure; moreover the influence of pressure and applied voltage on the breakdown inception is to be considered.

II. The Monte Carlo Method

Physical concepts of MCM applied to the study of an electrical discharge are [9]: the mean free flight time, the mean free path or null-collision Monte Carlo Method.

The application of the constant step MCM version for the study of electrons' motion, under the effect of an applied electric field, requires the evaluation process of the different physical parameters after experiencing energy loss and gain (taking into account the different processes of atomic collisions elastic or inelastic).

A. The Model

At time $t = 0$, the initial electrons are emitted from the cathode according to a cosine distribution. The energy gain of the electrons in a small time interval '*dt*' is governed by the equation of motion.

Before collision; the velocity and position components', for each electron, are given by [7]:

$$v_{x0}(i) = v_0 \sin(\theta(i))\cos(\varphi(i))$$
$$v_{y0}(i) = v_0 \cos(\theta(i))\sin(\varphi(i)) \quad (1)$$
$$v_{z0}(i) = v_0 \cos(\theta(i))$$

Where v_0 is given by:

$$v_0 = \sqrt{2\varepsilon_0 \frac{e}{m}} \quad (2)$$

And the θ and φ angles are defined as functions of a random number r such as:

$$\cos(\theta) = 2\pi r \quad (3)$$

$$\varphi = 2\pi r \quad (4)$$

The collision probability P_1, that follows the Poisson's distribution, is given by:

$$P_1 = 1 - \exp\left(\frac{dt}{Tm}\right) \quad (5)$$

Tm is the electron mean free flight time between two successive collisions; it is determined by the electron collision total cross section Q (ε) as:

$$Tm = \frac{1}{N.Q(\varepsilon).v(\varepsilon)} \quad (6)$$

where: v (ε) is the velocity of electrons and N the gas number density.

Before collision; the velocity and position components',

$$v_x(i) = v_{x0}(i)$$
$$v_y(i) = v_{y0}(i) \quad (7)$$
$$v_z(i) = v_{z0}(i) + ad$$
$$x(i) = x_0(i) + v_x(i)dt$$
$$y(i) = y_0(i) + v_y(i)dt \quad (8)$$
$$z(i) = z_0(i) + v_z dt + \frac{1}{2}a(dt)^2$$

B. Simulation Implementation

The flight time is divided into a number of smaller elements according to:

$$dt = \frac{Tm0}{K} \quad (9)$$

where: K is a sufficiently large integer and T_{m0} is the mean free flight time

The occurrence of collision between an electron and a gas molecule and its kind are determined by comparison of the collision probability P_1 with computer generated random numbers R.

The interval [0, P_1] is divided into segments of lengths that correspond to the probabilities of different types of collision after increasing scheduling of these probabilities. The remaining portion of the interval [0, 1] is for the case where no collision is possible.

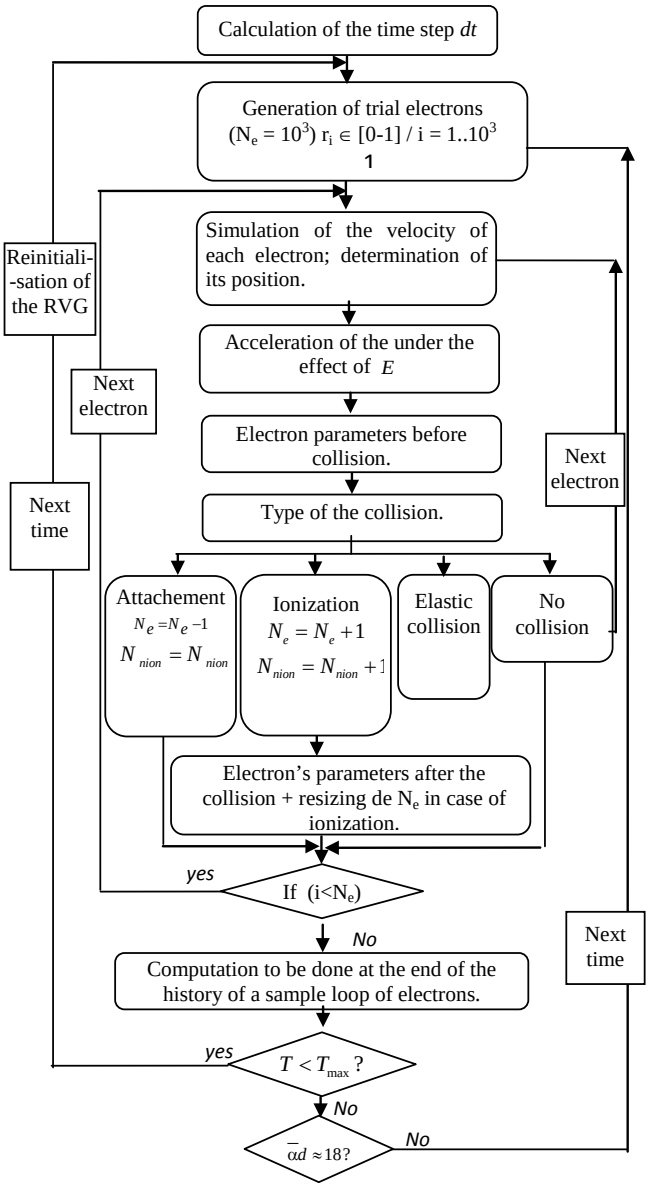

Fig. 1: Simulation's flowchart

The electron energy is described for the different processes of collision:

For the elastic collision the energy is given by:

$$\varepsilon_1 = \left(1 - 2\frac{M}{m}\cos(\delta)\right)\varepsilon_0 \quad (10)$$

where: δ is the scattering angle of the electron after the collision, m and M are, respectively, the mass of electron and an O_2 molecule and ε_0 is the electron's energy before collision.

Next to the processes of attachment, excitation and ionization, the onset energy "los" is subtracted from the electron energy as follow:

For an attachment of the electron, all its energy is to be lost, and therefore this electron is lost in the swarm.

$$\varepsilon_1 = 0 \quad (11)$$

For an exciting process of a molecule to a higher state (different rotations, vibrations and electronic excited states),

the energy of the electron is reduced with the energy needed to excite the molecule and the resulting energy is given by:

$$\varepsilon_1(m) = \varepsilon_0(m) - los \tag{12}$$

Finally, for an ionizing process, the remaining energy is shared between the primary and the ejected electrons with the ratios r and $(r-1)$ as:

$$\begin{aligned} \varepsilon_{primary} &= r(\varepsilon_0 - los) \\ \varepsilon_{ejected} &= (r-1)\times(\varepsilon_0 - los) \end{aligned} \tag{13}$$

C. Exploitation Of The Simulation Results

By means of tracking the history of each individual in a population upon appearance until its disappearance [8]; several values (the electron's energy, its position, the number of positive and negative ions, etc.) can be stored. Through averaging on the histories, different properties can be determined.

$$\bar{z} = \frac{1}{N}\sum_{i=1}^{N} z(i) \tag{14}$$

$$\bar{\varepsilon} = \frac{1}{N}\sum_{i=1}^{N} \varepsilon(i) \tag{15}$$

III. SIMULATION AND RESULTS

In this paper we describe the development of an electric discharge in the oxygen O_2 gas within plane-plane geometry. At t = 0, a number of electrons are released from the cathode with small energy (0.1 eV).The calculations of the physical parameters are performed at atmospheric pressure for an applied voltage of 57 kv. The electrical breakdown criteria are checked under different gas pressures for several voltages values. The cross section set of the O_2 molecule used is that referred in [12].

A. The Physical Parameters

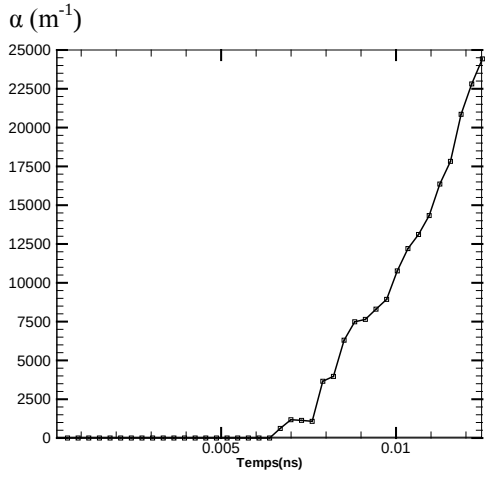

Fig. 2. Temporal variation of the ionization coefficient (P=1atm, V=57 kv)

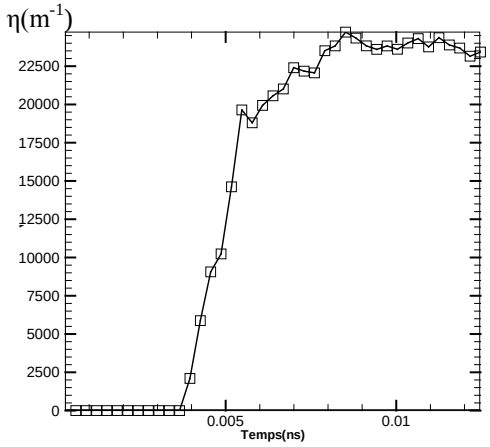

Fig. 3. Temporal variation of the attachment coefficient (P=1atm, V=57 kv)

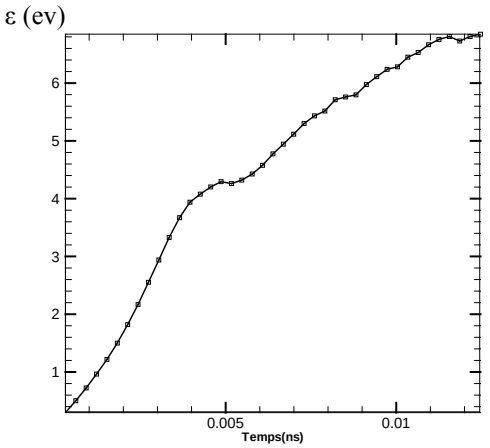

Fig. 4. Temporal variation of the mean kinetic energy (P=1atm, V=57 kv)

The figures (2, 3, and 4) represent, respectively, the temporal variation of the ionization (α), attachment (η) rates and of the mean kinetic energy. As much as the space charge accumulates in the time, the induced field increases.

In Figures (2 and 3), we note that: the ionization coefficient, in the case of the atmospheric pressure under 57kv and a temperature of 293 ° K (20 ° C), increases and reaches high values in a short delay; and that the electrons in the beginning of the discharge are attached because they have, initially, low energies and the attachment rate increases and then stabilizes at a certain value.

Figure (4) shows that the electrons have a short free path (in 2cm interval) and as the energy gain depends on the distance travelled, the mean kinetic energy of the electrons does not vary significantly.

B. Check of the Breakdown Criteria

For different pressures and different voltages with an inter-electrode distance of 2cm, the values of the ionization and attachment coefficients, and values of the mean kinetic energy are collected in the table below.

TABLE I
THE EFFECT OF THE VOLTAGE AND PRESSURE

P	V(V)	$\alpha\left(\mathrm{m}^{-1}\right)$	$\eta\left(\mathrm{m}^{-1}\right)$	$(\alpha-\eta)\times d$
	10	0.00	4.68E-01	-9.37E-03
1 torr	200	116.46	4.845873	2.23
	600	412.38	9.65E-01	8.22
	40000	737.36	2825.32	-41.76
1atm	50000	3108.40	2679.79	8.57
	55000	26693.99	25623.02	21.41
	2000	0. 00	0. 00	0. 00
5atm	20000	0. 00	5.11E-02	-1.02E-03
	60000	0. 00	91.477350	-1.80

For the voltages 10 (V), 40000 (V), 20000 (V) and 60000 (V), which correspond, respectively, to the pressures 1(torr), 1(atm) and 5(atm), the values of $(\alpha - \eta) \times d$ are negative that means that $\alpha < \eta$ and there is not effective ionization

For the voltages 200 (V), and 50000 (V) which correspond, respectively, to the pressures 1(torr) and 1(atm), the values of $(\alpha - \eta) \times d$ are positive but little because there are ionizing collisions between the electrons and molecules which are not enough to ensure that the discharge is maintained.

Electrical discharges in gases are of two types (1) non-self sustaining, (2) self sustaining. The breakdown in a gas is the transition from (1) to (2). The construction of the currents in the breakdown is due to the ionization processes in which ion-electron pairs are created by collisions with neutral atoms and their drift towards the anode and the cathode. For 1 (torr) and under 600 (V), we have a self-sustaining discharge of the Townsend type and for 1 (atm) under 55000 (V) the streamer breakdown criterion is checked.

IV. Conclusion

The idea of this paper was to use the Monte Carlo method to study the fundamental processes of an electrical discharge, which have a random quality, through computing its physical parameters.

As a result of this study, we conclude that when the voltage is sufficiently high the ionization increases and the gas becomes conductor and the current passing through is increased where the onset of the electric breakdown. In this context, we tested the electrical breakdown criteria (Townsend for low pressures and streamer for high pressures).

References

[1] J. M. Meek, J. D. Craggs, "Electrical breakdown of gases". Oxford: Clarendon Press, 1953.

[2] E. Kuffel, W. S. Zaengl and J. Kuffel, "High voltage engineering fundamentals", 2nd ed. Butterworth-Heinemann, 2000, 534p.

[3] G. G. Raju, "Dielectrics in electric field". Marcel Dekker, New York: CRC Press, 2003.

[4] Y. R. Raizer, "Gas discharge physics", Berlin: Springer-Verlag, 1991.

[5] M. S. Naidu, "High voltage engineering", 2nd ed. New York: Quebecor/Book Press, 1995.

[6] A. Settaouti and L. Settaouti , "Monte Carlo simulation of electron swarm parameters in O_2," *Eur. Phys. J. Appl. Phys*(37), 2007, pp. 335–341.

[7] G. R. Govinda Raju and J. Liu. "Simulation of Electrical Discharges in Gases– Uniform Electric Fields". *IEEE Transactions on Dielectrics and Electrical Insulation*, vol 2 (5), pp. 1004-1015, 1995.

[8] B. Djillali et B. Bachir,"Etude d'une décharge luminescente continue dans l'argon Par la méthode de Monte Carlo". CNHT'2003 – 5éme Conférence sur la Haute Tension – USTMB, 2003 (pp. 61-66). oran.

[9] G. G. Raju. "Dielectrics in Electric Fields" (Power Engineering, 19) 1st edition ed.. New York: CRC Press. 2003

[10] L. Zeghichi, L. Mokhnache and M. Djebabra, "The The Monte Carlo Method for the Study of an Electrical Discharge" 2013 IEEE International Conference on Solid Dielectrics (ICSD)

[11] L. Zeghichi, L. Mokhnache and M. Djebabra" Monte Carlo Simulation for an Electrical Discharge in O2" Advanced Materials Research Vol. 227 (2011) pp 211-214

[12] A. V. Phelps, Atomic & Molecular Physics. JILA NIST-CU website. [Online] 2005. Available: ftp://jila.colorado.edu/collision_data/electronneutral/ELECTRON.TXT

The issues of the improvement of the methodology for the assessment of reforms

Samson Davoyan, Ashot Davoyan

Abstract**—**The purpose of this article is to suggest a new methodology that will give us an opportunity to create an Integral Index of Reforms (IIR) that will include seven indexes: KOF Index of Globalization, The Democracy Index, The Corruption Perception, The Human Development, Doing Business, The Global Competitiveness Index and The Index of Economic Freedom. From both scientific and empiric perspective it is supposed that the quantitive assessment of various reforms implemented in different countries based on presented indicators of seven indexes despite the new methodology that we suggest give us the opportunity to include much more indexes.

Keywords**—** Competitiveness, democracy, efficiency, reforms, development, economic growth, corruption.

I. Introduction

In different countries of the world various reforms are implemented objectively, which pursue the aim to improve the quality of the life, increase the rating of the country and also provide the sustainable development of the country in the future [1]. On the purpose of our research we consider more important the following indexes, as their integrity will represent the features of the social-economic development of each country. From this point of view, during the last decades there have been various indexes developed by different international organizations and non-government corporations (KOF Index of Globalization by the Economist Intelligence Unit, Human Development Index by UNO, The Corruption Perception Index by Transparency International anti-corruption organization and so on), which are used to assess the institutions of different fields. Based on the new methodology, suggested by us, we have tried to create more integral index based on the following indexes, which trend will give an opportunity to assess the comparative efficiency of various reforms for different countries (24 countries in transition, 15 developed and 10 least developed countries). We have splint the countries into 3 main groups. We have highlighted the reforms implemented in 15 developed countries: Austria, Belgium, Denmark, Finland, France, Germany, Japan, Netherlands, Norway, Portugal, Singapore, Sweden, Switzerland, United Kingdom and United States.
We have also assess the comparative efficiency in 24 countries in transition countries during post-crisis period. These countries are Albania, Armenia, Azerbaijan, Bulgaria, Cambodia, Croatia, Czech Republic, Estonia, Georgia, Hungary, Kazakhstan, Kyrgyz Republic, Latvia, Lithuania, Macedonia, Moldova, Poland, Romania, Russia, Slovak Republic, Slovenia, Ukraine, Vietnam. We have also chosen 10 least developed countries: Bangladesh, Benin, Côte d'Ivoire, Gambia, Lesotho, Mali, Nepal, Senegal, Uganda and Zambia.

The integral index consists of seven indexes for the last 4 years: KOF Index of Globalization for 2010-2013, Democracy Index for 2008, 2010, 2011 and 2012, The Global Competitiveness Index for 2010-2011 and 2013-2014 periods by World Economic Forum, Doing Business for 2011-2014, Corruption Perception for 2010-2013, The Index of Economic Freedom for 2010-2013, The Human Development for 2009-2012.

Our new methodology is based on two regulator-parameters: the changes of the ranks and average of scores of the above mentioned indexes for two periods of time. As a result we have the Integral Index of Reforms.

II. Statistical Review

The integral index describes the social-economic development level and through it we assess variety of reforms for 2009-2013. On this purpose we have suggested a new methodology for the assessment of the Integral Index of Reforms based on seven different indexes.

A. The Global Competitiveness Index (GCI)

The Global Competitiveness Index (GCI) released by the World Economic Forum, which is a comprehensive tool, that measures the competitiveness of 148 countries, contains 3 sub-indexes: basic requirements, efficiency enhancers, innovation and sophistication factors, that are based on 12 pillars (institutions, infrastructure, macroeconomic environment, health and primary education, higher education and training, etc.) including 119 indicators[2].

B. Doing Business

Doing Business released by the World Bank and International Financial Corporation assesses business activity for 189 countries on the basis of 10 areas of regulation (starting a business, dealing with construction permits, getting credits, paying taxes, etc.) with 36 sub-indexes considering the survey results of organizations in different sectors of economies [3].

C. The Corruption Perception Index

The Corruption Perception Index published by Transparency International anti-corruption organization measures the perceived levels of public-sector corruption for 177 countries based on different assessments and business opinion surveys [4]. The countries, included in the rank of The Corruption Perception Index, are classified on a scale of 0 to 100. The countries, that get 0 are the highly corrupt in judicial system, media, legislative, police, business, public, educational, military areas [5].

D. The Index of Economic Freedom

The Index of Economic Freedom assesses the economic freedom of countries through 10 indicators (Business Freedom, Trade Freedom, Fiscal Freedom, Government spending, Monetary Freedom, Investment Freedom, Financial Freedom, Property Rights, Freedom from Corruption, Labor Freedom) in 185 countries [6]. All ten indicators of the Index are scaled equally. Each of them gets 0 to 100 economic freedom grading scale; countries that get 100 are the freest economies of the world. The Index has been published by The Heritage Foundation and The Wall Street Journal since 1994 [7].

E. The Human Development Index

The Human Development Index is a summary indicator that measures a standard of living, the literacy rate, the life expectancy in order to compare and assess the human potential of different countries [8].

F. The Democracy Index

The Democracy Index, compiled by the Economist Intelligence Unit, is the classification of 167 countries by the level of the democracy. The Index includes 60 indicators grouped in five categories: electoral process and pluralism, civil liberties, functioning of government, political participation, and political culture [9].

G. KOF Index of Globalization

KOF Index of Globalization compiled by the Economist Intelligence Unit. The KOF Index of Globalization measures the three main dimensions of globalization: economic, social and political. In addition to three indices measuring these dimensions, we calculate an overall index of globalization and sub-indices referring to actual economic flows:

- economic restrictions
- data on information flows
- data on personal contact
- and data on cultural proximity.

Data are available on a yearly basis for 207 countries over the period 1970 – 2010 [10].

For all represented above indexes we can say, that they are considered to be particular assessment of social-economic development. Besides they often include such indicators, that are not assessed by statistic services and therefore they can only be estimated by experimental method, which is obviously limit wide usage opportunity of these indexes. One of the most important problems is to assess the weight of each component.

III. New Methodological Approach

Using above-mentioned indexes, we represent an integral index, that assess social-economic development level for 2009-2013 based on statistic data for seven indexes (KOF Index of Globalization, The Corruption Perception, The Global Competitiveness Index, Doing Business, The Index of Economic Freedom, The Human Development, The Democracy Index). As a result we have the integral assessment of social-economic development for chosen countries.

To create the Integral Index of Reforms we calculated the ratio of observed seven indexes. Those ratios were acquired experimentally by 56 both Armenian and foreign experts who are state and non-governmental management workers, as well as economists. In the result of the assessment of the seven indices normalized coefficients were provided and the total sum of their ratios is 1.

Those coefficients are:

α_i^j - the scale of each index,

i and *j* are indexes

i=1, 2,...7 - the seven indexes,

j_1=1, 2,....15 –developed countries, j_2=1, 2,....24 countries in transition, j_3=1, 2,....10 least developed countries we evaluated. For example,

α_4^j=0,12 - the scale of The Economic Freedom Index in the Integral Index of Reforms for j_2=1, 2,....24 countries in transition,

α_4^j=0,13 - the scale of The Economic Freedom Index for j_1=1, 2,....15 countries, and

α_4^j=0,16 - the scale of The Economic Freedom Index in the Integral Index of Reforms for j_3=1, 2,....10 countries:

$$\sum_{i=1}^{7} \alpha_i^j = 1,$$

$$j = \{j_1, j_2, j_3\}$$

With the help of our methodology we first summarized the above-mentioned 7 indexes and attained 1 general index.

$$H_{\text{int}.index}^j = \sum_{i=1}^{7} \alpha_i^j N_i^j,$$

$H_{\text{int}.index}^j$ - the Integral Index of Reforms ,

i and *j* are indexes

i = 1,2,….7 – the seven indexes. For example, *i* = 4 The Economic Freedom Index,

j_2=1, 2,....24 countries in transition we evaluated

j=1 - Albania, *j*=2 – Armenia, … *j*=21 - Vietnam

α_i^j - the scale of each index,

N_i^j - the rank of the *j* country by *i* index

For example, Armenia is ranked 4 among 24 countries for 2010-2013 by the Global competitiveness index (considering the change of rank and score), therefore $N_1^2 = 4$

The first stage of creating the index was the rearrangement of the indexes included in analyze. The principle of rearrangement was based on the changes of the ranks and average of scores of the above mentioned indexes for two periods of time. Then we adjusted the change with scale coefficients substantiated methodologically. Depending on the level of the social-economic development of the country and the comparative efficiency of various reforms we used scale coefficients. For example, for those countries which had more than 7 points of improvements in rank we gave 0,1 for the change of the rank and 0,9 for the average score, for those who had more than 7 points of decrease in rank we gave 0,9 for the change of the rank and 0,1 for the average score [11].

Fig. 1, 2, 3 represent the Integral Index of Reforms in reports for 2009-2013 compare with the base year (2009) in both 24 countries in transition, 15 developed and 10 least developed countries. Fig. 4, 5, 6 represent the Integral Index of Reforms by the new methodology for 2009-2013 compare with the base year (2009). Fig. 7, 8, 9 represent the Integral Index of Reforms in reports and by the new methodology in 24 countries in transition, 15 developed and 10 least developed countries for 2009-2013.

ISBN: 978-1-61804-225-5

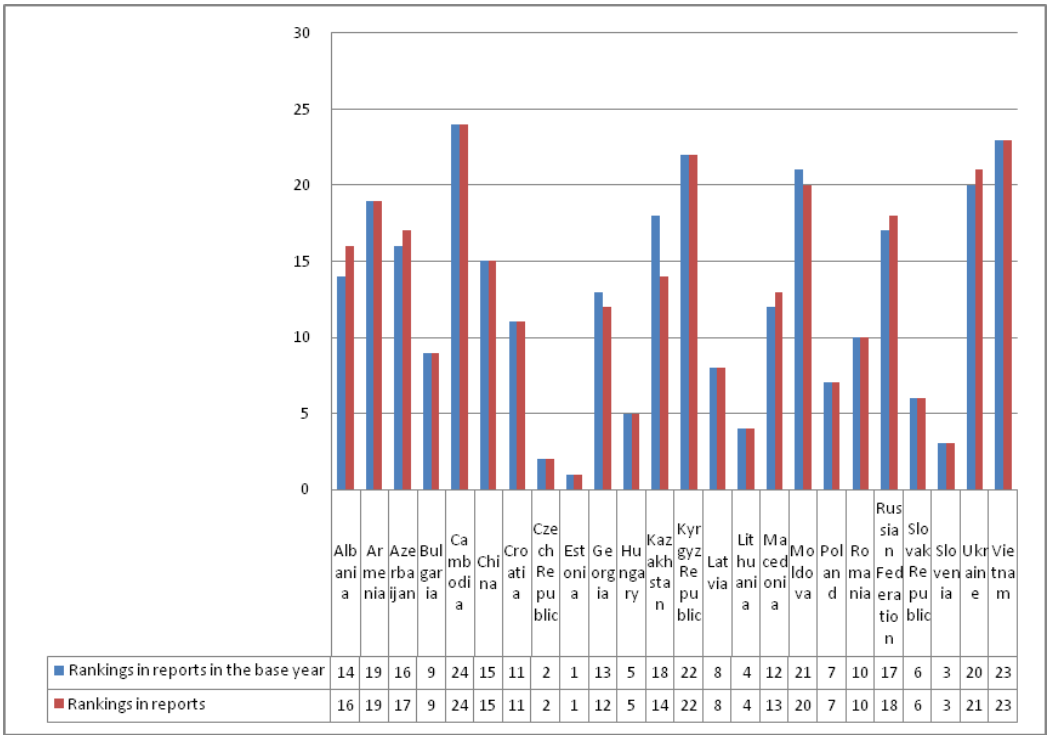

	Albania	Armenia	Azerbajian	Bulgaria	Cambodia	China	Croatia	Czech Republic	Estonia	Georgia	Hungary	Kazakhstan	Kyrgyz Republic	Latvia	Lithuania	Macedonia	Moldova	Poland	Romania	Russian Federation	Slovak Republic	Slovenia	Ukraine	Vietnam
Rankings in reports in the base year	14	19	16	9	24	15	11	2	1	13	5	18	22	8	4	12	21	7	10	17	6	3	20	23
Rankings in reports	16	19	17	9	24	15	11	2	1	12	5	14	22	8	4	13	20	7	10	18	6	3	21	23

Fig. 1. The Integral Index of Reforms in reports for 2009-2013compared with the base year (2009) in in 24 countries in transition

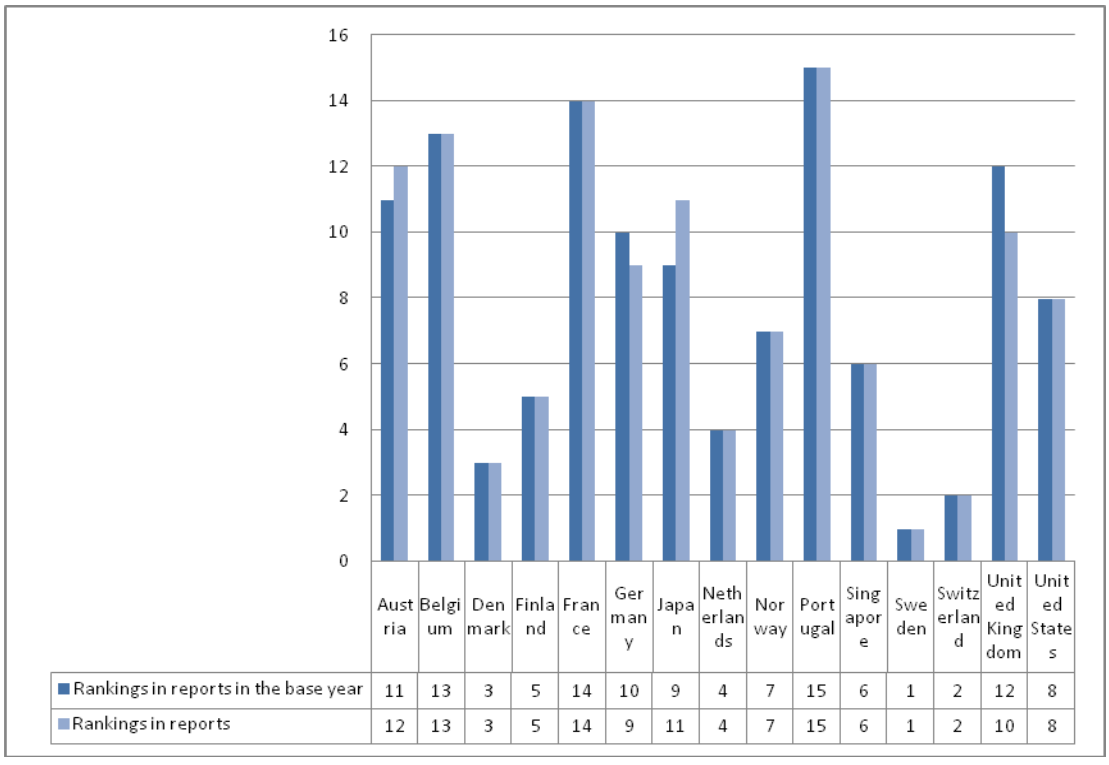

	Austria	Belgium	Denmark	Finland	France	Germany	Japan	Netherlands	Norway	Portugal	Singapore	Sweden	Switzerland	United Kingdom	United States
Rankings in reports in the base year	11	13	3	5	14	10	9	4	7	15	6	1	2	12	8
Rankings in reports	12	13	3	5	14	9	11	4	7	15	6	1	2	10	8

Fig. 2. The Integral Index of Reforms in reports for 2009-2013 compared with the base year (2009) in 15 developed countries

ISBN: 978-1-61804-225-5

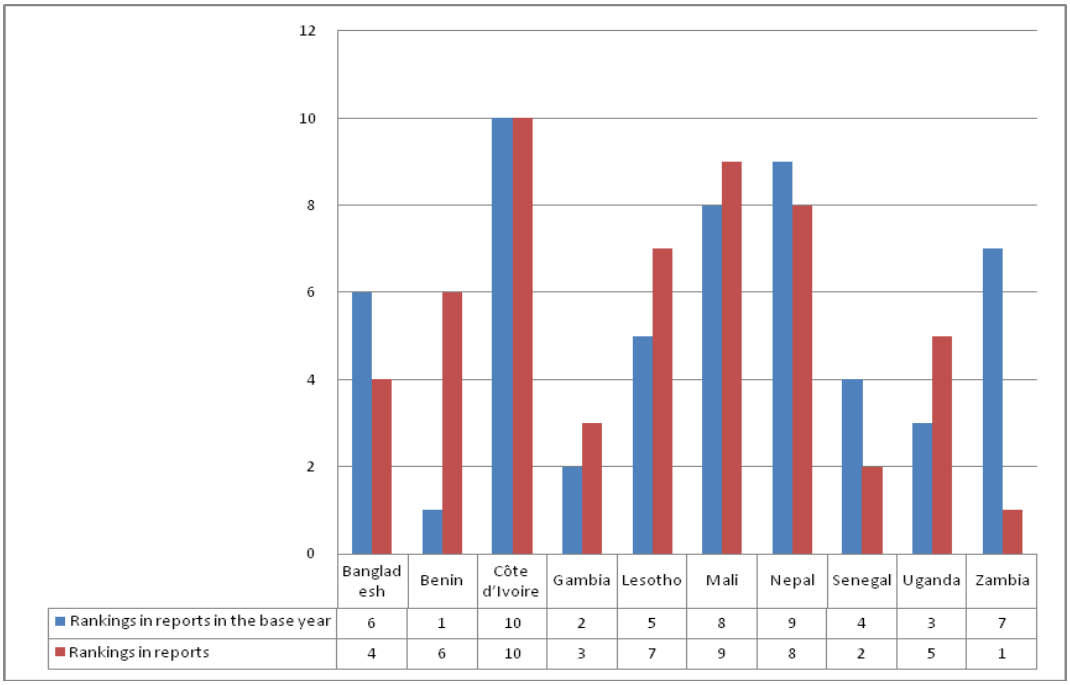

	Bangladesh	Benin	Côte d'Ivoire	Gambia	Lesotho	Mali	Nepal	Senegal	Uganda	Zambia
Rankings in reports in the base year	6	1	10	2	5	8	9	4	3	7
Rankings in reports	4	6	10	3	7	9	8	2	5	1

Fig. 3. The Integral Index of Reforms in reports for 2009-2013 compared with the base year (2009) in 10 least developed countries

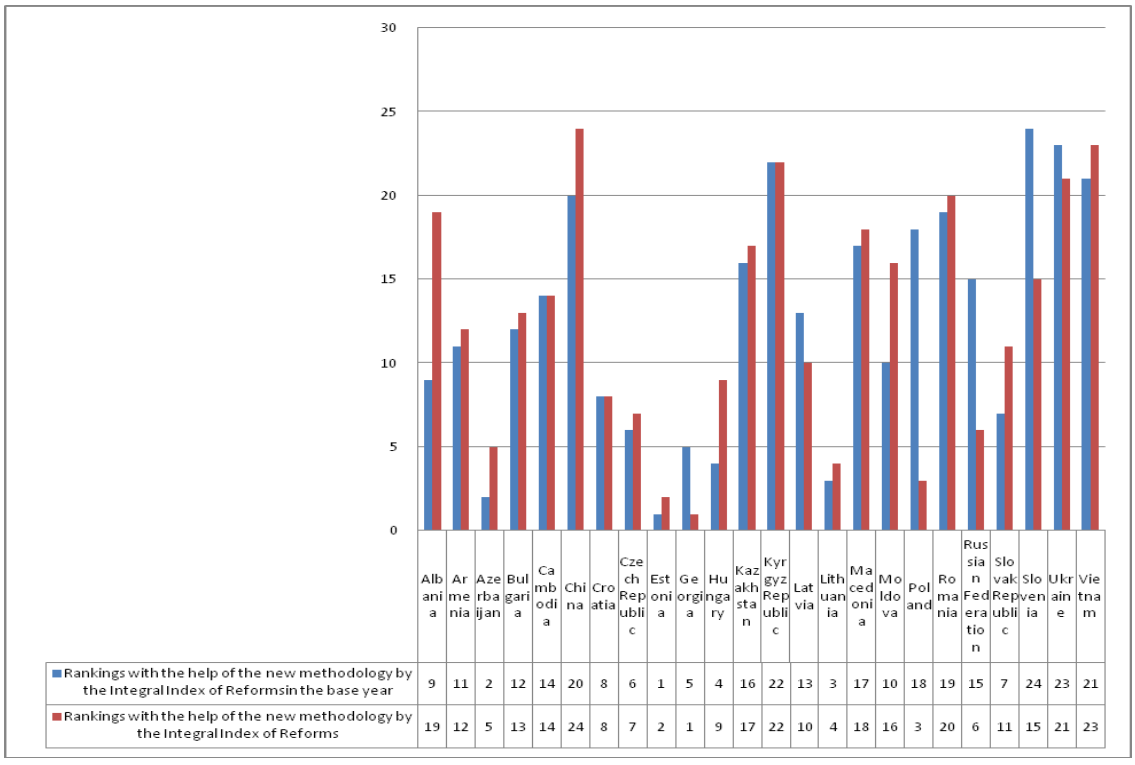

	Albania	Armenia	Azerbaijan	Bulgaria	Cambodia	China	Croatia	Czech Republic	Estonia	Georgia	Hungary	Kazakhstan	Kyrgyz Republic	Latvia	Lithuania	Macedonia	Moldova	Poland	Romania	Russian Federation	Slovak Republic	Slovenia	Ukraine	Vietnam
Rankings with the help of the new methodology by the Integral Index of Reforms in the base year	9	11	2	12	14	20	8	6	1	5	4	16	22	13	3	17	10	18	19	15	7	24	23	21
Rankings with the help of the new methodology by the Integral Index of Reforms	19	12	5	13	14	24	8	7	2	1	9	17	22	10	4	18	16	3	20	6	11	15	21	23

Fig. 4. The Integral Index of Reforms by the new methodology for 2009-2013 compared with the base year 2009 in 24 countries in transition

ISBN: 978-1-61804-225-5

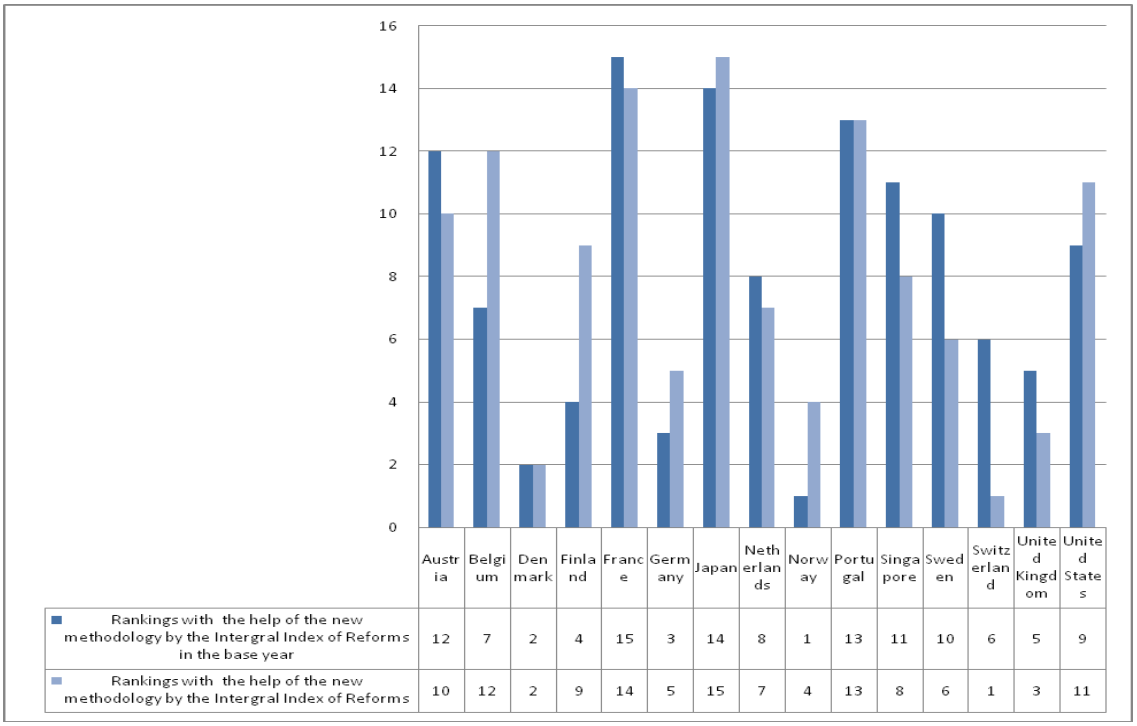

	Austria	Belgium	Denmark	Finland	France	Germany	Japan	Netherlands	Norway	Portugal	Singapore	Sweden	Switzerland	United Kingdom	United States
Rankings with the help of the new methodology by the Intergral Index of Reforms in the base year	12	7	2	4	15	3	14	8	1	13	11	10	6	5	9
Rankings with the help of the new methodology by the Intergral Index of Reforms	10	12	2	9	14	5	15	7	4	13	8	6	1	3	11

Fig. 5. The Integral Index of Reforms by the new methodology for 2009-2013 compared with the base year 2009 in 15 developed countries

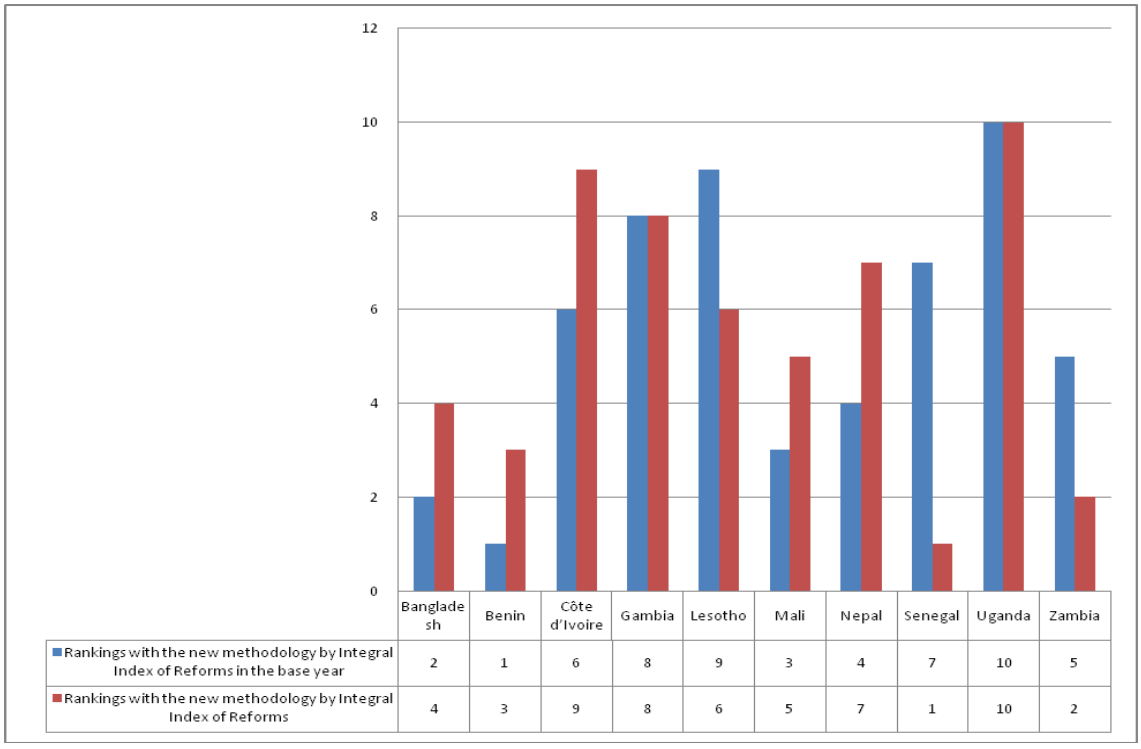

	Bangladesh	Benin	Côte d'Ivoire	Gambia	Lesotho	Mali	Nepal	Senegal	Uganda	Zambia
Rankings with the new methodology by Integral Index of Reforms in the base year	2	1	6	8	9	3	4	7	10	5
Rankings with the new methodology by Integral Index of Reforms	4	3	9	8	6	5	7	1	10	2

Fig. 6. The Integral Index of Reforms by the new methodology for 2009-2013 compared with the base year 2009 in 10 least developed countries

At the second stage countries were rearranged by the methodology mentioned above. This approach was repeated for each year combining with the previous year. As a result of the first and second stages we had a new range of countries for each index for 2009-2013.

At the third stage we gave scale coefficients to all seven indexes considering the importance and the variety of included indicators, eliminating the usage of the same indicator and

ISBN: 978-1-61804-225-5

finally we had Integral Index of Reforms of each country for 2009-2013.

Putting the indicators of α_i^j and N_i^j in the equation we will have H_i^j.

$H_{\text{int.}index}^j = \sum_{i=1}^{7} \alpha_i^j N_i^j$, For j_1=1, 2,....15 –developed countries, j_2=1, 2,....24 countries in transition and j_3=1, 2,....10 –least developed countries we assess the average of the summary for 4 years.

$(H_{i_1}^j + H_{i_2}^j + H_{i_3}^j + H_{i_4}^j)/4$

For instance, The Economic Freedom Index for Arnenia will be:

$(H_{4_1}^2 + H_{4_2}^2 + H_{4_3}^2 + H_{4_4}^2)/4$

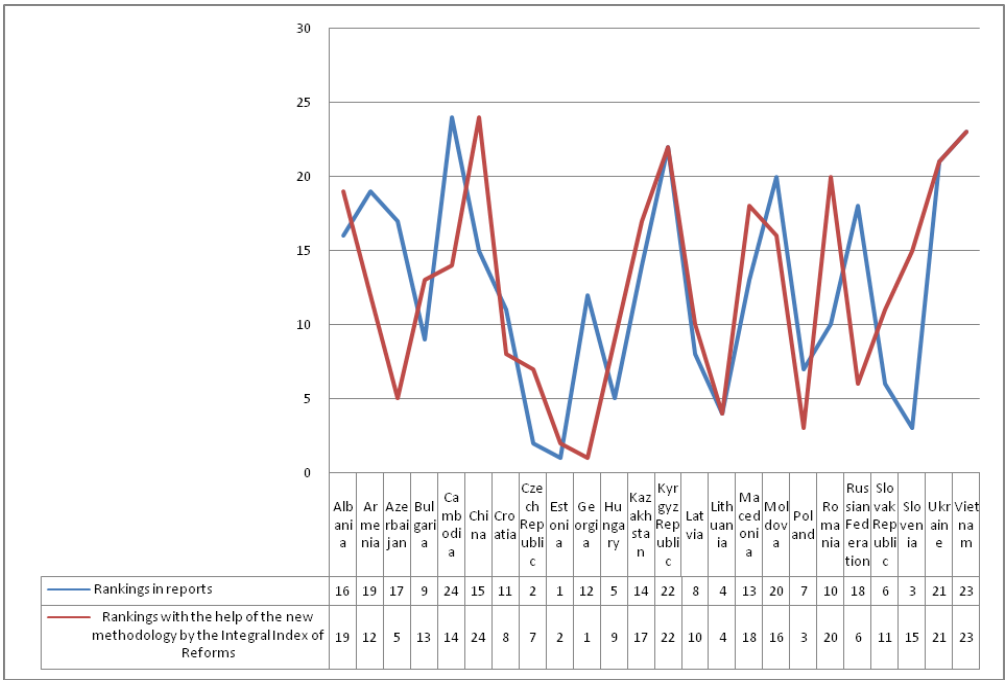

	Albania	Armenia	Azerbaijan	Bulgaria	Cambodia	China	Croatia	Czech Republic	Estonia	Georgia	Hungary	Kazakhstan	Kyrgyz Republic	Latvia	Lithuania	Macedonia	Moldova	Poland	Romania	Russian Federation	Slovak Republic	Slovenia	Ukraine	Vietnam
Rankings in reports	16	19	17	9	24	15	11	2	1	12	5	14	22	8	4	13	20	7	10	18	6	3	21	23
Rankings with the help of the new methodology by the Integral Index of Reforms	19	12	5	13	14	24	8	7	2	1	9	17	22	10	4	18	16	3	20	6	11	15	21	23

Fig. 7 The Integral Index of Reforms in reports and by the new methodology for 2009-2013 in 24 countries in transition

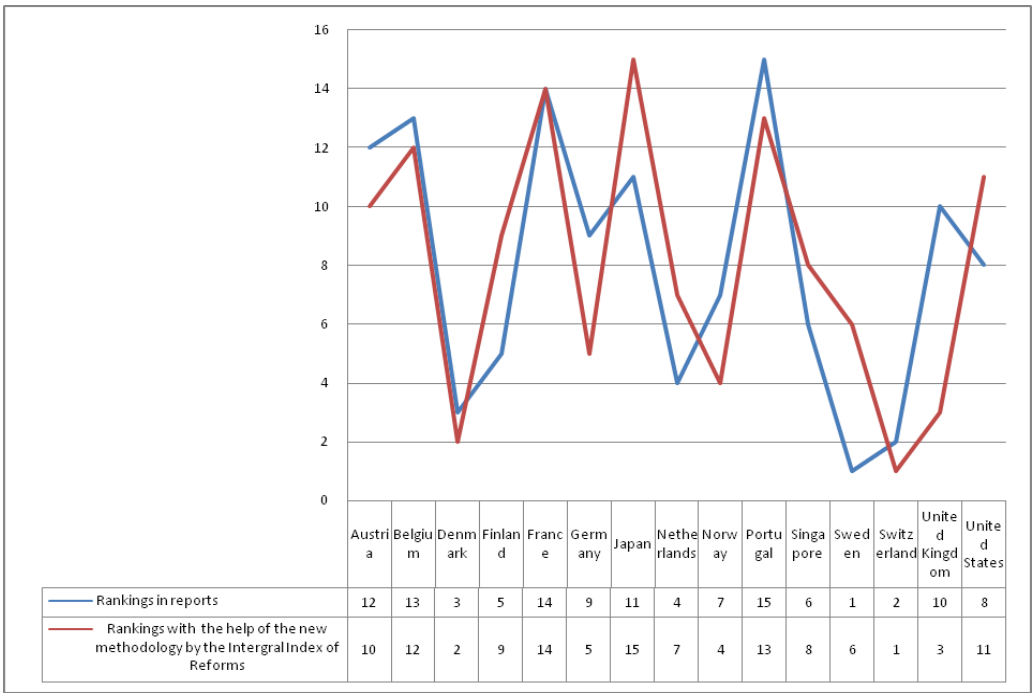

	Austria	Belgium	Denmark	Finland	France	Germany	Japan	Netherlands	Norway	Portugal	Singapore	Sweden	Switzerland	United Kingdom	United States
Rankings in reports	12	13	3	5	14	9	11	4	7	15	6	1	2	10	8
Rankings with the help of the new methodology by the Intergral Index of Reforms	10	12	2	9	14	5	15	7	4	13	8	6	1	3	11

Fig. 8. The Integral Index of Reforms in reports and by the new methodology in 15 developed countries for 2009-2013

ISBN: 978-1-61804-225-5

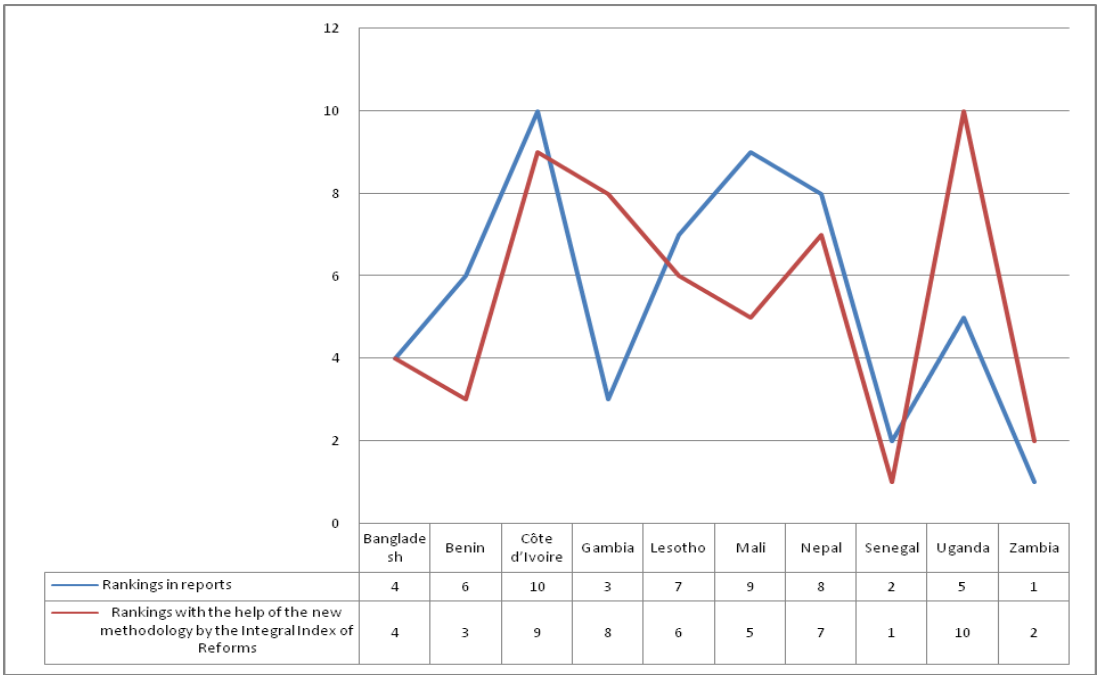

	Bangladesh	Benin	Côte d'Ivoire	Gambia	Lesotho	Mali	Nepal	Senegal	Uganda	Zambia
Rankings in reports	4	6	10	3	7	9	8	2	5	1
Rankings with the help of the new methodology by the Integral Index of Reforms	4	3	9	8	6	5	7	1	10	2

Fig. 9. The Integral Index of Reforms in reports and by the new methodology in 10 least developed countries for 2009-2013

According to the suggested methodology, we measure Integral Index of Reforms for 15 developed, 24 countries in transition and 10 least developed countries, considering the change of rank and score adjusted with scale coefficients for 2009-2013. The results witness, that the reforms for 2009-2013 have more effectively implemented in Georgia, Russia Poland, Azerbaijan, Moldova, Croatia and Armenia, but less effectively in Romania and Vietnam.

In our opinion the Integral Index of Reforms can express comparative efficiency of various reforms in each country more integrally than each of the indexes not only the ones we have included in the article, but also some indexes which are not represented in the article such as Transformation Index BTI and The index of Sustainable Economic Welfare.

REFERENCES

[1] Popov V. Shock Therapy versus Gradualism Reconsidered: Lessons from Transition Economies after 15 Years of Reforms. TIGER Working paper No. 82 p. 95, 2006

[2] The Global Competitiveness Report, The World Economic Forum, weforum.org.

[3] Doing Business Report, The World Bank, doingbusiness.org.

[4] Corruption Perceptions Index 2012: Full Source Description/Transparency International, p. 45, 2012, www.transparency.org.

[5] Kaufmann, Daniel, "Corruption, Governance and Security: Challenges for the Rich Countries and the World, " MPRA Paper 8207, University Library of Munich, Germany, p. 77, 2004.

[6] Ambassador Terry Miller, Kim R. Holmes, Edwin J. Feulner, "2012 Index of Economic Freedom", The Heritage Foundation and The Wall Street Journal, New York, p. 62, 2012, www.heritage.org.

[7] Samson Davoyan, Tatevik Sahakyan, The assessment of reforms in different countries by social-economic development integral index, World Academy of Science , Engineering and Technology, Issue 79 Stockholm, July 2013, p. 1324.

[8] United Nations Organization, UNDP.org

[9] Economist Intelligence Unit, www.eiu.com.

[10] http://globalization.kof.ethz.ch/

[11] Samson Davoyan, The assessment of the reforms in different countries using social-economic development index, Conference on The trends of changes of the world economy and the challenges in Armenia, Gyumri p.6, 2012.

Samson Davoyan, Armenia, Doctor of Economic Sciences, professor member of Association of Economists of Armenia, lecturer professor in Russian-Armenian (Slavonic) University, director of Gyumri branch of the Armenian State Economic University. Samson Davoyan was a student in 1965-1967 in Yerevan State University, faculty of economics, section of economic cybernetics, in 1967-1970 in Novosibirsk State University, personal programme study, in 1970-1973 post-graduate school of Central Economic-Mathematical Institute , in 1976- Candidate of Economic Science, in 1980- docent (associate professor), in 1994-1995 "Market economics and financial analysis" specialization retraining course in Vienna joint Institute of World Bank and U.N.O. and in Prague university by Charles, from 2003-professor, from 2003- Doctor of Economic Science (phone: 00374 91434283; e-mail: gbesei@mail.ru).

Ashot Davoyan, Armenia, PhD, senior researcher in "Ambert" research centre at Armenian State University of Economics, MBA, bachelor and master degree at Yerevan State University, master school at George Town University in the USA for 2006-2007, Finance academy in Switzerland in 2008, "Business Management" Start-up project of Skolkovo in Moscow for 2013 (phone: 00374 55401070; e-mail: ashot_davoyan@yahoo.com).

Fuzzy Delay Tumor Growth With Quiescence Cells: Stability of Steady States

Normah Maan, Khabat Barzinji, and Nor'aini Aris

***Abstract*—**This paper presents a system of delay tumor growth that describes an interaction between the proliferating and quiescent cells tumor. This system is fuzzified by parametric form of α-cut representation of symmetric triangular fuzzy number. The steady state and linear stability of fuzzy tumor growth system with quiescence and without quiescence cells are determined and analyzed. Here, we show that the trivial steady state of the system with quiescence is stable for τ=0 by Routh Hurwitz conditions. For increasing delay the steady state is unstable by using Strum theorem.

***Keywords*—**Delay tumor growth with quiescence, Steady States, Stability, Fuzzy delay tumor growth.

I. Introduction

PREDATOR-PREY interaction is the fundamental model in population dynamics. Understanding the dynamics of predator-prey models will be useful for investigating multiple species interaction. However, one of application of predator-prey interaction is tumor growth cells. Many researchers examined delay predator-prey type interaction in tumor studies where the immune or the quiescence cells play the role of predator and prey respectively [1].

Tumor cells can be divided into proliferating or cycling cells and nonproliferating or quiescent cells [2]. A cell is assumed cancerous when it has lost its ability to regulate cell growth and division (mitosis). Thus, cancer is a disease of rapid uncontrolled growth of malignant cells. In this paper the mathematical system proposed describes the delay tumor growth interaction between the proliferating and quiescent cells of two differential equations with one delay.

Yafia [3] develops a delay differential equation model for interaction of proliferating and quiescent tumor cells. However, this paper does not include immune cell nor the impact of the drugs. In fact, it may be important for cancer treatment to target the proliferating cells. Including quiescent cells in the model should be more realistic and could provide additional insight into complex system. In [4], the authors discuss the existence, uniqueness and non-negativity of solutions and they obtain that under an appropriate hypotheses and using Poincare-Bendixon theorem, the nontrivial steady state is globally asymptotically stable for the system with τ=0.

In real life, we have learned to accept that we are actually dealt with uncertainty. Modeling the real life problems in such cases, usually involves uncertainty or vagueness in some of the parameters including the tumor growth system. In this system, the condition of the patients and the tumor type can be considered as uncertain parameters. Meanwhile, the concept of fuzzy set and system was initially introduced by Zadeh [5] and has been used to model a dynamical system under possibility uncertainty [6]. Therefore, in this paper we used fuzzy concept to propose a system known as fuzzy delay tumor growth system. Specifically, the discussion on the theory and analysis of delay tumor growth system with uncertainty parameters is considered.

The organization of this paper is as follows. In Section II, tumor growth system without and with quiescent cells are given. Including dynamical analysis in a delayed system for tumor growth. In addition some definitions regarding the fuzzy number are briefly presented. In Section III, fuzzy tumor system without quiescent cells is introduced. In Section IV, two examples are given to demonstrate the results for the fuzzy delay tumor growth with quiescence cells. Finally the conclusion of the finding is given in Section V.

II. TUMOR GROWTH SYSTEM

In the absence of quiescent cells and the delay, the proliferating cells follow the logistic equation $\dot{P}(t) = bP(t)$ and the tumor becomes a malignant tumor for $b > 0$ and becomes benign for $b < 0$. In absence of proliferating cells the quiescent cells are normally absent.

A. Dynamics Analysis in a Delayed system for Tumor Growth with Quiescence

Consider the following system:

$$\begin{aligned} \frac{dP(t)}{dt} &= bP(t-\tau) - r_P(N(t))P(t) + r_Q(N(t))Q(t) \\ \frac{dQ(t)}{dt} &= r_P(N(t))P(t) - (\mu_Q + r_P(N(t)))Q(t) \end{aligned} \tag{1}$$

This work is supported in part by the Fundamental Research Scheme under grant FRGS 4F127.

N. Maan is with the Department of Mathematical Sciences, Faculty Of Science, University Teknologi Malaysia, Johor Bahru, Johor Malaysia 81310 (phone: +60197007014; fax: +607-5566162; e-mail: normahmaan@utm.my).

K. Barznji is with the Department of Mathematical Sciences, University Teknologi Malaysia . (e-mail: khabat.rasoul@yahoo.com).

N.Aris is with the Department of Mathematical Sciences, Universtiy Teknologi Malaysia (e-mail: noraini@utm.my).

In biological terms, where $P(t)$ and $Q(t)$ represent the numbers of proliferating tumor cells and quiescent tumor cells respectively. $N(t)=P(t)+Q(t)$ is the total number of tumor cells at time t, $b=\beta-\mu_P>0$ the rate of the proliferating cells where ($\beta>0$) and the division rate of the proliferating cells, $\mu_P\geq 0$ the death rate of cells of the proliferating cells, $\mu_Q\geq 0$ is the mortality rate of the quiescent cells, $r_P(N)$ is the nonlinear transition rate from the proliferating class to the quiescent class and $r_Q(N)$ is the nonlinear transition rate from the quiescent class to the proliferating class . For this tumor population, we assume that $r_P(N)$ is non-decreasing and $r_Q(N)$ is non -increasing, both rates are Lipschitz continuous on bounded sets of N in R (see Gyllenberg and Webb [4]) and the constant τ is the time delay which the proliferating cells takes to divide.

Yafia [3] analyzed system (1) and concluded that it has a trivial and unique positive steady state. Dynamical study of the system is also presented in [3] in terms of local stability of the two steady states. Yafia consider the function $f:\mathbb{R}^+\to\mathbb{R}$ and $g:\mathbb{R}^+\to\mathbb{R}$ as

$$f(x)=\mu_Q r_P(x)-b(\mu_Q+r_Q(x))$$

and

$$g(x)=b-\mu_Q-r_P(x)-r_Q(x),$$

respectively.

Assuming the hypotheses:

(A_1) $f(0)<0$,

(NA_1) $f(0)>0$,

(A_2) $f(+\infty)>0$,

(A_3) $g(x)<0$ for all $x\geq 0$,

(NA_3) $g(x)>0$ for all $x\geq 0$.

Yafia's paper proved the next three theorems where the first theorem gives the stability result for the trivial steady state while the nontrivial is not exist.

Theorem 1

Assume the hypotheses (NA_1) and (A_3). Then the trivial steady state of the system (1) is asymptotically stable for all $\tau\geq 0$.

The next theorem gives a result of instability of the trivial steady state when the nontrivial steady state exists.

Theorem 2

Assume the hypotheses (A_1) and (NA_3). Then the trivial steady state of the system (1) is unstable for all $\tau>0$.

The last theorem gives the result of change of stability of non trivial steady state.

Theorem 3

Assume the hypotheses (A_1)-(A_3) and the functions r_P (increasing function) and r_Q (decreasing function) are of class C^1. Then there exists a critical value τ_0 of the time delay, such that the nontrivial steady state is asymptotically stable, for $\tau\in[0,\ \tau_0]$ and unstable, for $\tau>\tau_0$.

B. Fuzzy Theory

Definition 1 [5]

A fuzzy number is a function such as $u:\mathbb{R}\to[0,1]$ satisfies the following properties:

1) u is normal, i.e $\exists x_0\in\mathbb{R}$ with $u(x_0)=1$.

2) u is a convex fuzzy set i.e $u(\lambda x+(1-\lambda)y)\geq\min\{u(x),u(y)\}\forall x,y\in\mathbb{R},\lambda\in[0,1]$.

3) u is upper semi-continuous on $\mathbb{R}$.

4) $\overline{\{x\in\mathbb{R}:u(x)>0\}}$ is compact where $\overline{A}$ denotes the closure of A.

Definition 2 [6]

An α-cut, u_α is a crisp set which contains all the elements of universal set X that have a membership function greater or equal to α and can be expressed as $u_\alpha=\{x\in X:\mu_u(x)\geq\alpha\}$.

Definition 3 [7]

A fuzzy number u is completely determined by any pair $u=(\underline{u},\bar{u})$ of functions $\underline{u}(\alpha),\bar{u}(\alpha):[0,1]\to\mathbb{R}$ satisfies the three conditions:

1) $\underline{u}(\alpha),\bar{u}(\alpha)$ is a bounded, monotonic , (nondecreasing, nonincreasing) left-continuous function for all $\alpha\in(0,1]$ and right-continuous for $\alpha=0$.

2) For all $\alpha\in(0,1]$ we have : $\underline{u}(\alpha)\leq\bar{u}(\alpha)$.

3) For every $u=(\underline{u},\bar{u}),v=(\underline{v},\bar{v})$ and $k>0$,

$(\underline{u+v})(\alpha)=\underline{u}(\alpha)+\underline{v}(\alpha)$

$(\overline{u+v})(\alpha)=\bar{u}(\alpha)+\bar{v}(\alpha)$

$(\underline{ku})(\alpha)=k\underline{u}(\alpha),(\overline{ku})(\alpha)=k\bar{u}(\alpha)$

Fuzzy set is a mapping from a universal set into [0,1]. Conversely, every function $\mu:X\to[0,1]$ can be represented as a fuzzy set ([5]). We can define a set $F_1=\{x\in\mathbb{R}:xisabouta_2\}$ with triangular membership function as below:

Definition 4 [5]

$$\mu_{F_1}=\begin{cases}\dfrac{x-a_1}{a_2-a_1}\,x\in[a_1,a_2)\\ 1x=a_2\\ \dfrac{-x+a_3}{a_3-a_2}\,x\in(a_2,a_3]\end{cases}$$

So the fuzzy set F can be written as any ordinary function $F=\{(x,\mu_F(x)):x\in X\}$.

III. Fuzzy tumor growth

Consider the following differential tumor equation without quiescent cells:

$$\dot{P}(t)=bP(t)\,. \qquad (2)$$

We fuzzy the equation by parametric representation of α-cut as follows: let

$$b=[b-(1-\alpha)\sigma_1,b+(1-\alpha)\sigma_1],\alpha\in[0,1]$$

and

$$b_1=(1-\mu)(b-(1-\alpha)\sigma_1)+\mu(b+(1-\alpha)\sigma_1)\,,\ \mu\in[0,1]\,.$$

Then the fuzzy system of (2) is

$$\begin{aligned}\dot{\underline{P}}&=b_1\underline{P}(t),\\ \dot{\overline{P}}&=b_1\overline{P}(t).\end{aligned} \qquad (3)$$

The fuzzy tumor system (3) has trivial steady states with the characteristic equation $(b_1-\lambda)^2=0$ and, hence the root of characteristic equation is b_1. Then if b_1 is positive the steady state is unstable and the tumor will be malignant. Otherwise the steady state is stable and the tumor will be benign.

A. Fuzzy Delay Tumor Growth System with Quiescent Cells

Now consider System (1) with assuming that there are uncertainty parameters. Here again, we fuzzify the system and let $P(t),Q(t),\mathrm{r}_P(t),r_Q(t)$ be non-negative fuzzy functions and

$$\tilde{b}=[b-(1-\alpha)\sigma_1,b+(1-\alpha)\sigma_1],$$

$$\mu_Q=[\mu_Q-(1-\alpha)\sigma_2,\mu_Q+(1-\alpha)\sigma_2],$$

where

$$b_1=(1-\mu)(b-(1-\alpha)\sigma_1)+\mu(b+(1-\alpha)\sigma_1),$$

$$b_2=(1-\mu)(\mu_Q-(1-\alpha)\sigma_2)+\mu(\mu_Q+(1-\alpha)\sigma_2).$$

By using parametric representation of α-cut (see [8]) we write the system in matrix form as follows:

$$\begin{bmatrix}\dot{\underline{P}}_\alpha(t)\\ \dot{\overline{P}}_\alpha(t)\\ \dot{\underline{Q}}_\alpha(t)\\ \dot{\overline{Q}}_\alpha(t)\end{bmatrix}=\begin{bmatrix}0&0&0&0\\0&0&0&0\\0&0&0&-b_2\\0&0&-b_2&0\end{bmatrix}\begin{bmatrix}\underline{p}_\alpha\\ \overline{P}_\alpha\\ \underline{Q}_\alpha\\ \overline{Q}_\alpha\end{bmatrix}+$$

$$\begin{bmatrix}b_1&0&0&0\\0&b_1&0&0\\0&0&0&0\\0&0&0&0\end{bmatrix}\begin{bmatrix}\underline{P}_{\alpha t}\\ \overline{P}_{\alpha t}\\ \underline{Q}_{\alpha t}\\ \overline{Q}_{\alpha t}\end{bmatrix}+\begin{bmatrix}-\bar{r}_P\overline{P}+\underline{r}_Q\underline{Q}\\ -\underline{r}_P\underline{P}+\bar{r}_Q\overline{Q}\\ \underline{r}_P\underline{P}-\bar{r}_Q\overline{Q}\\ \bar{r}_P\overline{p}-\underline{r}_Q\underline{Q}\end{bmatrix}\,. \qquad (4)$$

Where $\underline{P}_{\alpha t}=\underline{P}_\alpha(t-\tau),\overline{P}_{\alpha t}=\overline{P}_\alpha(t-\tau)$ similarly for Q. So, the system (4) is known as fuzzy delay tumor growth system.

The system (4) has trivial steady state. And the characteristic equation is :

$$\lambda^4+C\lambda^2+E+e^{-\lambda\tau}(A\lambda^3+D\lambda)+e^{-2\lambda\tau}(B\lambda^2+F)=0\,. \qquad (5)$$

Where

$$\begin{aligned}&A=-2b_1,\\ &B=b_1^2,\\ &C=-b_2^2-\underline{r}_P(0)\bar{\mathrm{r}}_P(0)-\mathrm{b}_2\bar{r}_Q(0)-\mathrm{b}_2\underline{r}_Q(0)-\underline{r}_Q(0)\bar{r}_Q(0)\\ &-\bar{r}_P(0)\bar{r}_Q(0)-\underline{r}_P(0)\underline{r}_Q(0),\\ &D=2b_2^2b_1+2b_2b_1\bar{r}_Q(0)+2b_2b_1\underline{r}_Q(0)+2b_1\underline{r}_Q(0)\bar{r}_Q(0)\\ &+\mathrm{b}_1\bar{r}_P(0)\bar{r}_Q(0)+\mathrm{b}_1\underline{r}_P(0)\underline{r}_Q(0),\\ &\mathrm{E}=\mathrm{b}_2^2\underline{r}_P(0)\bar{r}_P(0),\\ &\mathrm{F}=-b_2^2b_1^2-b_2b_1^2\bar{r}_Q(0)-\mathrm{b}_2b_1^2\underline{r}_Q(0)-\mathrm{b}_1^2\underline{r}_Q(0)\bar{\mathrm{r}}_Q(0).\end{aligned} \qquad (6)$$

In absence of delay the steady state is stable if the roots of $\lambda^4+(B+C)\lambda^2+D\lambda+(E+F)=0$ have negative real part. By Routh-Hurwitz conditions this occurs if $A>0,D>0,(E+F)>0,\mathrm{A(B+C)D}>\mathrm{D}^2+A^2(E+F)$. Now for increasing τ, $\tau\neq0$, we assume that the root of the characteristic equation (5) is $\lambda=i\mu$ and $\mu>0$. Substitute $\lambda=i\mu$ in (5) we obtain,

$$\mu^4-C\mu^2+E(\cos(\mu\tau)-i\sin(\mu\tau))(-iA\mu^3+iD\mu)+$$

$$(\cos(2\mu\tau)-i\sin(2\mu\tau))(-B\mu^2+F)=0.$$

Separating the real and imaginary parts, we get

$$\begin{aligned}&\mu^4-C\mu^2+E=-(-A\mu^3+D\mu)\sin(\mu\tau)-\\ &(-B\mu^2+F)\cos(2\mu\tau),\\ &(-A\mu^3+D\mu)\cos(\mu\tau)-(-B\mu^2+F)\cos(2\mu\tau)=0\end{aligned} \qquad (7)$$

Squaring and adding both sides of (7) gives the polynomial of degree eight as follows:

$$(\mu^4 - C\mu^2 + E)^2 - (-A\mu^3 + D\mu)^2 - (-B\mu^2 + F)^2 + 2(-A\mu^3 + D\mu)(-B\mu^2 + F)\sin(-\mu\tau) = 0. \quad (8)$$

If $\tau = \frac{n\pi}{\mu}$ then $\sin(2\mu\tau)$ =0 and let $\gamma = \mu^2$ the equation (8) can be written in terms of γ as follows:

$$\gamma^4 + (-2C - A^2)\gamma^3 + (2E + C^2 + 2AD - B^2)\gamma^2 + (-2CE - D^2 + 2BF)\gamma + (E^2 - F^2) = 0. \quad (9)$$

We look for the case when the lead coefficient of (9) is positive so, there are two cases for a positive real root can obtain. The first and simplest is ($E^2 - F^2$) < 0. Now assume ($E^2 - F^2$) >0. Since the polynomial is even, there are four roots we are focusing for these roots to be real (four of them positive or two positive and two negative or four of them negative). If four of the roots are negative we suppose to take the strum chain of polynomial (9) denoted P_0, P_1, P_2, P_3, P_4.

Let

$$P_0 = \gamma^4 - (A^2 + 2C)\gamma^3 + (2E + C^2 + 2AD - B^2)\gamma^2 + (-2CE - D^2 + 2BF)\gamma + (E^2 - F^2) = 0$$

and

$$P_1 = 4\gamma^3 - 3(A^2 + 2C)\gamma^2 + 2(2E + C^2 + 2AD - B^2)\gamma + (-2CE - D^2 + 2BF) = 0$$

The bifurcation occurs in the case ($E^2 - F^2$) >0 if and only if the lead coefficient P_2, P_3 and P_4 are positive.

Hence by division algorithm the lead coefficient of P_2, P_3, P_4 is positive which are

,,

$$\left(\frac{1}{2}(2E + C^2 + 2AD - B^2) - \frac{3}{16}(-2C - A^2)^2 > 0,\right.$$

$$-(A_2 - A_3) > 0,$$

$$-\left((E^2 - F^2) - \frac{1}{16}(-2C - A^2)(-2CE - D^2 + 2BF) - \frac{A_5}{A_2 - A_3}\left((-2CE - D^2 + 2BF) - \frac{A_1\left((E^2 - F^2) - \frac{1}{16}(-2C - A^2)(-2CE - D^2 + 2BD)\right)}{\frac{1}{2}(CE + C^2 + 2AD - B^2) - \frac{3}{16}(2C - A^2)^2}\right) > 0, \quad (10)$$

Where

$$A_1 = 3(-2C - A^2) - \frac{3(-2CE - D^2 + 2BF)}{\frac{1}{2}(2E + C^2 + 2AD - B^2) - \frac{3}{16}(2C - A^2)^2} - \frac{\frac{1}{2}(-2C - A^2)(2E + C^2 + 2AD - B^2)}{\frac{1}{2}(2E + C^2 + 2AD - B^2) - \frac{3}{16}(2C - A^2)^2},$$

$$A_2 = 2(2E + C^2 + 2AD - B^2) - \frac{4(E^2 - F^2)}{\frac{1}{2}(2E + C^2 + 2AD - B^2) - \frac{3}{16}(2C - A^2)^2} \frac{\frac{1}{16}(-2C - A^2)(-2EC - D^2 + 2BF)}{\frac{1}{2}(2E + C^2 + 2AD - B^2) - \frac{3}{16}(2C - A^2)^2},$$

$$A_3 = \frac{A_1\left(\frac{3}{4}(-2CE - D^2 + 2BF)\right)}{\frac{1}{2}(2E + C^2 + 2AD - B^2) - \frac{3}{16}(2C - A^2)^2} - \frac{\frac{1}{8}(-2C - A^2)(2E + C^2 + 2AD - B^2))}{\frac{1}{2}(2E + C^2 + 2AD - B^2) - \frac{3}{16}(2C - A^2)^2},$$

$$A_4 = \left(\frac{\frac{1}{2}(2E + C^2 + 2AD - B^2) - \frac{3}{16}(2C - A^2)^2}{A_2 - A_3}\right)$$

$$\left((-2CE - D^2 + 2BF) - \frac{A_1\left((E^2 - F^2) - \frac{1}{16}(-2C - A^2)\right.}{\frac{1}{2}(2E + C^2 + 2AD - B^2) - \frac{3}{16}(2C - A^2)^2}\right) \quad (11)$$

$$\left(\frac{A_1(-2CE - D^2 + 2BD))}{\frac{1}{2}(2E + C^2 + 2AD - B^2) - \frac{3}{16}(2C - A^2)^2}\right),$$

$$A_5 = \frac{3}{5}(-2CE - D^2 + 2BF) - \frac{1}{8}(-2C - A^2)(2E + C^2 + 2AD - B^2) - A_4$$

Proposition 1

A steady state with characteristic equation (5) is stable in the absence of delay, and become unstable with increasing delay if and only if

1) $A>0, D>0, (E+F)>0$ and
$A(B+C)>D^2+A^2(E+F)$

2) $-(\frac{1}{2}(2E+C^2+2AD-B^2)-\frac{3}{16}(-2C-A^2)^2)>0,$

$-(A_2-A_3)>0,$

$-((E^2-F^2)-\frac{1}{16}(-2C-A^2)(-2CE-D^2+2BF)-$

$\frac{A_5}{A_2-A_3}((-2CE-D^2+2BF)-$

$\frac{A_2((E^2-F^2)-\frac{3}{16}(-2C-A^2)(-2CE-D^2+2BD))}{\frac{1}{2}(CE+C^2+2AD-B^2)-\frac{3}{16}(2C-A^2)^2}>0$

Where $A, B, C, D, E, F, A_1, A_2, A_3, A_4, A_5$ are given in (6), (11).

IV. Examples

Example 1

Consider the fuzzy delay tumor system (4) with the following conditions $\mu=1, b=1, \mu_Q=1, r_P=2, r_Q=1, \sigma_1=1.2$
$\sigma_2=0.1, \sigma_4=0.2, \sigma_5=0.5$

And the initial conditions is

$(\underline{P}(0), \overline{P}(0))=(4-(1-\alpha)\sigma_4, 4+(1-\alpha)\sigma_4),$

$(\underline{Q}(0), \overline{Q}(0))=(3-(1-\alpha)\sigma_5, 3+(1-\alpha)\sigma_5).$

As can be seen in Fig. 1, the behavior of the trivial steady state is unstable since the solution does not converge to the trivial steady state. It means the conditions of Proposition 1 are satisfied.

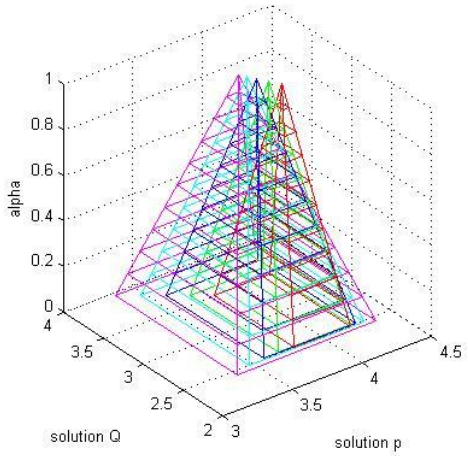

Figure 1: $\tau=20$

Example 2

We fixed all parameters as in Example 1 except for b, b is now equal to two. The solution does not converge to the trivial steady state (as in Figure 2). If b =4, the trivial steady state is also unstable (as in Figure 3).

Also, another increase of b =5 we see the trivial steady state is unstable (as in Figure 4).

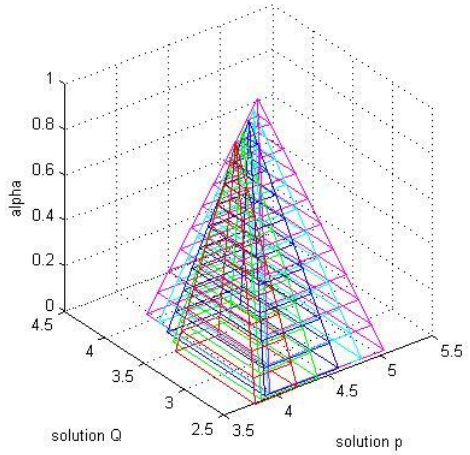

Figure 2: $\tau=20$

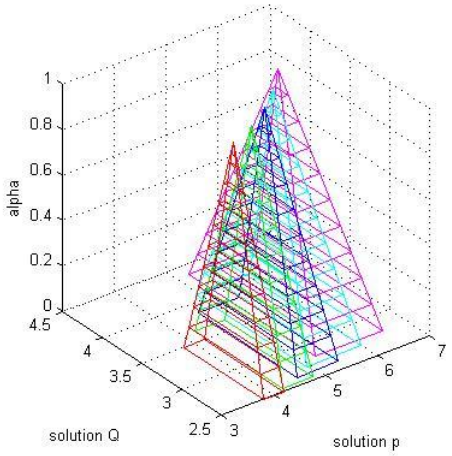

Figure 3: $\tau=20$

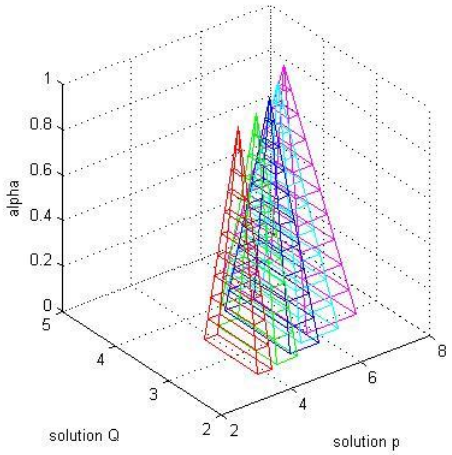

Figure 4: $\tau=20$

From above examples, physiologically it means that the fuzzy delay tumor system has stable trivial steady state when $\tau = 0$ and hence the growth of tumor is stopped by medical cure.
After extension of influence of medical cure (increasing the parameter τ) the stability of steady state is lost and the tumor starts to oscillate. The oscillations means either the tumor disappears or the patient is overcome.
If the delay τ is greater than zero, the tumor may experience a temporary appear and the trivial steady state is unstable. The tumor proliferates and it turns into necrotic mass. An increase in cell proliferation leads to an increase the concentration of many growth factors. However, it takes time for cell to up-regulate rate of growth. It means for large value of delay the fuzzy system showed irregular pattern for each cell population. And with increasing time delay in proliferation we observed periodic behavior of the number of cancerous cells. This behavior may explain periodic tumors growth and it's uncorrelated with the chemotherapy.

V. Conclusions

In this paper, we proposed a system of fuzzy delay tumor growth system by using symmetric triangular fuzzy number. The crisp tumor growth system of (2×2) system is extended to a fuzzy tumor growth of (4×4) system by using parametric form of α-cut. The fuzzy tumor growth with and without quiescence cells has trivial steady states. The fuzzy system proposed leads to the difficulty of locating the roots of the characteristic equation since the system becomes larger compare with the crisp system. Generally, the situation is more complex to arrive at general conditions on the coefficient of characteristic equation in order to describe a stability of trivial steady state. The trivial steady state for the system with quiescent cells is stable in absence of delay and increasing delay it is unstable. The applicability of the results is demonstrated by examples.

References

[1] N. Maan, K.Barzinji and N.Aris, Stability of Fuzzy Delay Differential System, Submit to Scientific World Jiournal. .
[2] B.Birkhead, E. Rankin, S. Gallivan, I. Dones and R. Rubens, A mathematical model of the development of drug resistance to cancer chemotherapy. Eur.J. Cancer Clinical Oncology 1987, pp 1421-1427.
[3] R. Yafia Dynamics Analysis and Limit Cycle in a Delayed Model for Tumor Growth with Quiescence Nonlinear Analysis: Modelling and Control, 2006 pp. 95-110. .
[4] B. Smith, M. Gyllenberg and G. F. Weeb, Quiescence in Strutured Population Dynamic:Application to tumor growth in Mathematical Population dynamic, Math. Bioscience 1991,pp. 45-62.
[5] L.A.Zadeh Fuzzy Sets, Information and Control, 1965,pp, 44-53.
[6] M. Farhi and S. Barati Fuzzy time-delay dynamical systems, Mathematics and computer sicience, 2011 pp, 44-53.
[7] I. Stefaninia,I.Sorinia and M.I.Guerraa Parametric representation of fuzzy numbers and application to fuzzy calculus, Fuzzy Sets and Systems,2007 pp, 2423-2455.
[8] N.Maan,K.Barzinji and N.Aris, Fuzzy Delay Differential Equation in Predator-prey Interaction:Analysis on Stability of Steady State of the System, ICAEM conference London 2013.

Benefit analysis weighing bulk traffic in ports multipurpose terminal

H.Elmandili, B.Nsiri, and B.Aghezzaf

***Abstract*—** This paper presents an approach which utilizes the analysis of the processes of waiting trucks at numerous stages of service in polyvalent terminals in the ports of the Kingdom, with an emphasis on the infrastructures of weighing and loading of trucks. Mathematical modeling, a study of the stability of double weighing and loading system as well as its measures of performance have been made, and developments in computing programs also facilitates these calculations, which have enabled us to specify whether the system needs additional new infrastructure, or it is sufficient to just reorganize the workings of the existing infrastructure. Thanks to the performance measures of the stochastic system identified by numerical experiments, we were able to prove the stability of the double-weighing and delivery system during the day, and explain the situation of congestion during certain periods of the day through the random arrival of trucks, and not by the instability of the system or lack of infrastructure.

***Keywords*—** Queues trucks, weighing, performance measures, stability.

I. Introduction

Climate change manifests itself in various forms around the world, but whatever form it heavily influenced the stocks of livestock and cereals of countries, which requires the import of large quantities from abroad so as to meet the demands of citizens as well as livestock rearing. Such process creates additional pressure on ports, which do not correspond with the preparations and expectations of the ports management. This contributes to the development of an enormous traffic congestion, which makes drivers and transport staff alike suffer in ports, disrupting the unloading and weighing of trucks, and causing conflicts and long delays. It is within the framework of ensuring operational management in real time in order to guarantee maximum productivity and minimize the delays that the approach I intend to adopt in this article is based. We are interested in analyzing the delivery weighing of the bulk traffic (direct exit) to the multipurpose port terminal, that is to say the goods which the vessel load directly into the trucks without delay when staying at the terminal. Afterwards, the trucks leave the port after passing through the weighbridge. Then we have a network of queues.

At the weighbridge, the route of the trucks is characterized by a probabilistic manner; the next station is the dock, if this is his second weighing, he moves outside. This is therefore a deterministic cyclic routing. Figure 1 demonstrates the physical circuit of the truck inside the multipurpose terminal. Making a field visit, we notice the existence of a traffic jam, goods of different types on the ground, trucks blocking traffic and more cars from service personnel. With regard to the weighbridges, we notice a traffic congestion due to a large number of trucks which arrive to load from the ship, and a large queue of trucks even before entering the main gate. This problem of congestion also has other impacts; longer service period, conflicts among truck drivers, and also traffic jam at the terminal especially with the goods which are put on the ground and staff cars, which can result in reducing the number of clients in the port.

These trucks, which we are discussing, are part of the port customers, because it is the importer who sent them to retrieve the goods. It is for this reason that the port cannot handle the arrival times of the trucks which is random and unbalanced during the day. But planning in advance the time slots for unloading each type of â€œvracâ€ in the case of large vessels can play an important role in avoiding such waiting for those trucks interested in a different type of â€œvracâ€ which the crane is in the process of unloading. It is therefore important to regulate the discipline of the queued trucks. In recent years, several authors have analyzed various models of queues in discrete time, and a number of new results have been reported in the literature, see [1]. The most popular model is the expectation M / G / 1 queue with a Poisson arrival process. [2].

The distribution of the duration of treatment of a service depends on numerous factors, such as the experience of staff and client characteristics [12]. The arrival rate of trucks vary from on period to another during the same day, and the distribution of arrival rate over time (also referred to as profile for early arrival of passengers, [13] depends on several criteria. For instance Barros and Falling as they addressed the aeronautical field, have taken, as criteria for passengers, the category of flights, and time of day. Thus the average arrival time in the morning is much shorter than in the afternoon [14] For the delivery that we study in this paper, the rate of entry of trucks to the multipurpose terminal is much higher in the early morning hours, and this is due to the fact that truck drivers are paid by the number of loads carried by day, hence they prefer to come early in the morning so as to return in the afternoon to take a second load. Furthermore, when the trucks arrive, they do not have the choice of weighbridges; they are obliged to go through the weighbridge they have been assigned even if there aremany other empty ones, while self-assignment of trucks at the level of weighbridges can reduce the length of waiting and delays. This principle has been effective for waiting passengers at the registration service in the airport [15] Indeed numerous air campaigns offer a free check-in service to reduce the duration of time at a registration agency. In our case we shall consider that we have a single server since the truck was not allowed to go through the other weighbridges, and we will find the

complete Kendall notation of delivery weighing, based on numerical results for a long period of time in order to go through all the possible cases of delivery weighing during the day.

The arrival time of each truck does not depend on the time of arrival of the truck that it precedes, the same goes with the length of service. Hence, we can consider an M/G/1 server. The performance of this type of server has been studied in many articles using several approaches [16] well as the discrete time Markov arrival process may include special cases such as the arrival process Bernulli [17], [18] Service to customers is measured by the average length of the queue, the average waiting time, and service levels, that is to say, the waiting time for customers must be below a certain threshold. This has been well discussed by Graham [19], who analyzed in detail the waiting process of check-in at airports, proposing an approach for performance analysis that is applicable also to queues in the ports. the field of operations research has also given many pushed together and results to optimize routing clients and assignments to servers in the system, [3], and many heuristics have been proposed for the analysis and flus scheduling [4], but in our case ,this technique will not be useful because the allocation of trucks to weighbridges is submitted to another constraint which is the position of weighbridges from the docks.

Various approaches in the literature [9, 5, 6, 7] have been proposed to improve the queues of M/G/1 type and integrate changes service time to reduce it [2, 8, 10], but most of these approaches are based on automation servers. This is often not applicable, especially when it is a system that is already in activity, and suggestions are too expensive, or that space presents a major constraint. Our approach proposes no expensive modifications that can be applied without interrupting the activity or require time or staff. Then we can increase the service capacity without increasing the cost of service.

We will begin this article by describing the physical circuit of trucks between the dock and weighbridges, analysis of the problems encountered, and accuracy of the mathematical model selected. The second chapter will primarily focus on the performance of the system through a conceptual study, then finally ending up with suggestions and conclusions of the last chapters .

II. Mathematical Modeling of the Physical Circuit of Trucks

There exist many weighbridges in multipurpose terminals as well as several docks, but in this study we shall consider that we have solely one weighbridge and only one dock, since our goal is to analyze the circuit of a truck inside the terminal, and each truck must pass through the weighbridge that it was assigned even if there other empty ones, and then through a specific dock. We may then diagram the circuit of the truck as follows :

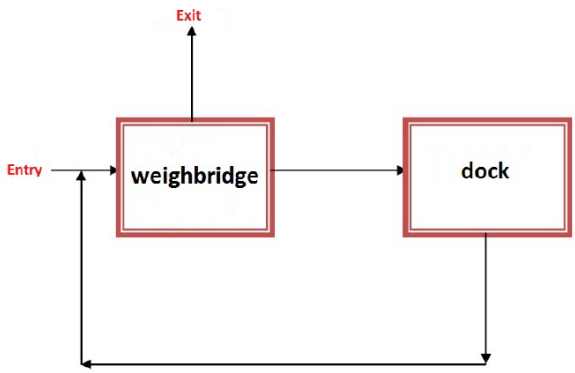

Figure 1: Physical circuit of the truck inside the multipurpose terminal

We are in the case of an open network of queues, because the trucks coming from outside circulate in a network across different stations (weighbridge, dock, back to weighbridge), then leave the network. The number of clients that may be found at any given time in an open network is not limited.

In our case, trucks represent clients, while the weighbridge and the dock represent the stations. The purpose of what follows in this chapter is to study the structure and calculate the characteristic values allowing to describe the performance of this system.

There are several mathematical models that can be chosen in this modelization, but we chose the single server model with exponential time service (time exponential service will be demonstrated in what follows). We could think of the multiple servers model with exponential time service, but we can not choose it in our case, because the average rate of service is not the same for all servers [11, 20]. The queue of trucks is at an unlimited capacity, and we are before the FCFS discipline (first come first served); the first client to arrive shall be the first to start his service, nothing then prevents a client who starts his service after it, ends before; (in the case of the arrival of two trucks that will not load the same type of goods, the crane assigned to the ship discharge one type, and once it clears its quantity, it, then, turns to the second type and so on; for instance truck 1 is interested in type X, and truck 2 is interested in type Y, if the crane is already working on the Y type, although truck 1 had arrived before truck 2, it will be served after it, because even if it has weighed before it, it will still be obliged to wait at the dock, and hence it is indeed the FCFS discipline).

By detailing our service (tare weight + load from the ship + gross weighing), we can determine the Round-Robin discipline (cyclic). Indeed, all the trucks queue move to the weighbridge alternately, conducting the tare weight, then repositioning it in a new dock for loading and so forth until the service is all completed. We deduce then that the notation of Kendall of our queue is as follows:

$$M/M/1/+\infty/+\infty/FCFS \quad (1)$$

The first element M , which denotes the inter-arrival distribution, is a Markov process since the arrival time of each truck does not depend on the time of the arrival of the truck preceding it (we will see later that this is a Markov jump

process). The second M denotes the distribution of service. It is also Markovian since the length of service of each truck does not depend on the length of service of the trucks which precede them. The third element â€œ1â€ denotes the number of servers. As we have already mentioned, each truck must go through a weighbridge even if the others are empty.

Furthermore, we shall later discuss the service as weighing + loading, then we will consider the existence of a single server (weighbridge + dock). The two infinites denote the capacity of queue which is infinite, and the users population is also infinite since the number of trucks entering the system is not limited, and therefore the FCFS denotes the discipline which we have already talked about. We aim to specify our system by characterizing the process of arrival of trucks and the process of service. For that, we shall, in what follows, consider the double weighing and loading as a single service, which can be schematized as follows:

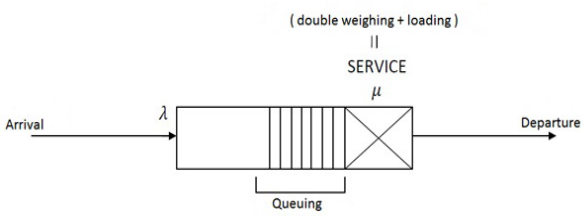

Figure 2: The trucks service in multipurpose terminal

The arrival of trucks to the system will described using a stochastic counting process $(N_t)_{t\geq 0}$.

We denote by A_n the random variable measuring the arrival time of the nth truck in the system and thus will have : $A_0 = 0$ (by agreement) and $A_n = inf\{t; N_t = n\}$,which means that the first time that the number of trucks is found in the system is equal to n.

We denote by D_n the random variable measuring the time between the arrival of $(n-1)^{th}$ truck and the n^{th} truck (inter-arrival). We have then: $D_n = A_n - A_{n-1}$.

Let us find the inter-arrivals rate λ' : We are interested in times of congestion, that is to say the moments when the inter-arrivals are very short $(D_n \leq 3)$, and this is the case of early morning hours. An observation of a dozen trucks allows us to establish the following calculations :

We have seven trucks with $D_n = 1$, two trucks with $D_n = 2$, and one truck with $D_n = 3$.

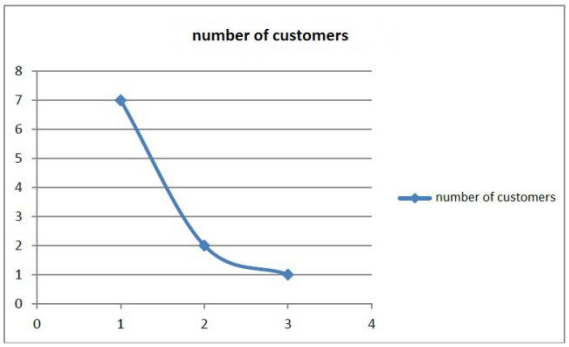

Figure 3: Number of customers for each inter-arrival.

We note that the shape of this graph is similar to that of the exponential law, and also the empirical average of inter-arrivals is:

$$E(D_n) = 1.4 \quad (2)$$

This is the average interval between two consecutive arrivals. The empirical variance of interarrivals is:

$$Var(D_n) = 0.48 \quad (3)$$

We have:

$$Var(D_n) \approx \frac{1}{E(D_n)^2} = 0.51 \quad (4)$$

However there exists a law of probability, the exponential law, such as:

$$Var(X) \approx \frac{1}{E(X)^2} \quad (5)$$

Therefore, it is logical to assume, given the digital results, and the shape of the graph, that the empirical distribution of interarrivals can be adjusted by an exponential law, with parameter:

$$\lambda' = \frac{1}{E(D_n)} = 0.71 \quad (6)$$

This is the inter-arrivals rate. In addition we have:

$A_0 = 0 \quad and \quad A_1 < A2 < A_3$

and we have : $P(D_n > t) = P(N_{t_0+t} - N_{t_0} = 0)$ since $N(t)$ is an independent process, then :

$P(D_n > t) = P(N_t = 0) = p_0(t) = e^{-\lambda t}$

but we have $N(t)$ follows the Poissonian law (λt)

so $P(D_n > t) = e^{-\lambda t} 1 - P(D_n \leq t)$

so $P(D_n \leq t) = 1 - e^{-\lambda t} \Leftrightarrow D_n$ follows the exponential law (λ) by integrating we find a density of exponential law ($\lambda exp(-\lambda t)$). so D_n follows the exponential law .

The random variables $(D_n)_{1\leq n\leq +\infty}$ are independent and identically distributed, because they shame the same probability law and are mutually independent. Therefore, the counting process $(N_t)_{t\geq 0}$ is a renewal process. We have found that the interarrivals are exponential and are characterized by a single parameter: the rate of interarrival λ' So, the process of arrival of trucks in the system is a Poissonian process.

- Time of service: We note:

S_n: the random variable measuring the start time of the n^{th} client system

Y_n: the random variable measuring the service time of the n^{th} client (the time separating the beginning and end of the service).

$$Y_n = S_n - A_n \quad (7)$$

The variables (Y_n) are independent and identically distributed. Indeed, the service time of each truck does not depend upon that of the truck that precedes it, and the distribution of service time the exponential distribution which is characterized by the property Without memory.

The following table demonstrates the consecutive service times of trucks; observation is made on the same dozen trucks we have seen previously.

truck	1	2	3	4	5	6	7	8	9	10
Y_n	82	85	61	65	60	52	53	64	68	75

Table I: Service times of trucks in minutes

The average duration (or average service time) is the mathematical expectation of the random variable (Y_n) , it is the empirical average:

$$E(Y_n) = 66.5 \quad (8)$$

The average service is:

$$\mu = \frac{1}{E(Y_n)} = 0.01 \quad (9)$$

We will now study the stability of the system.For this, let us find the average rate of arrivals λ.

The expected arrival of trucks that is the empirical average number of truck arrivals is equal to 68.16Therefore the arrival rate is:

$$\lambda = 0.014 \quad (10)$$

We have found in the foregoing the following results: The average rate service

$$\mu = 0.015 \quad (11)$$

The average rate of arrivals

$$\lambda = 0.014 \quad (12)$$

We note that

$$\lambda \prec \mu \quad (13)$$

That is to say: traffic intensity:

$$\rho = \frac{\lambda}{\mu} \prec 1 \quad (14)$$

So the queue is stable .It is true that reality shows an explosion in the same during certain period of the day. That is because in these periods, all trucks come in the same time (the same importer who sent them), and both inter-arrivals are null. It is therefore logical that with these constraints, any system will appear unstable, when it is not.

III. Performance of Service Provided to Trucks

Consider the system behavior in a given period of time, for instance between $t = 0$ et $t = \theta$. X_t is the total number of clients in the system at the instant t.

Taking interest in the system behavior of the time interval $[0, \theta]$ is tantamount to considering the â€œtransitional regimeâ€ system. We take $[0, \theta] = [0{,}960]$ in minutes . The choice of $\theta = 960$ is tantamount to considering both shifts of the day $(16h = 960min)$ to go through every possible state of the system during the day (congestion, vacancy of system, balance, explosion ,…) .

• Average rate of entry: the average rate of entry is the average number of clients who arrived to the system per unit of time. over the observation period 0.960, it is therefore:

$$d_e(\theta) = \frac{\alpha(\theta)}{\theta} \quad (15)$$

With $\alpha(\theta)$ Number of clients arriving to the system during the period so: That is to say one truck every 8 min.

• Remark :The average exit rate is the average number of clients who have left the system per unit of time. over the observation period $[0, \theta]$ it is therefore:

$$d_s(\theta) = \frac{\delta(\theta)}{\theta} \quad (16)$$

With $\delta(\theta)$ is the number of clients who have left the system during the period $[0, \theta]$.

In our case $d_s(\theta) = d_e(\theta)$ Since we have taken as time interval all shifts, and at the end of the day no truck remains in the system, so the number of trucks that arrived to the system is itself the same number leaving it.

•Total time during which the system contains n trucks: $T(n, \theta)$ Total number of trucks in the system during the observation period θ. The purpose of this paragraph is to observe the change in the number of trucks in the system over time. We have as data the " $tare$" table which contains instants of tare weighing, and "$pese$" table which contains instants of gross weighing. We define the "$fusion$" table which contains all the instants during which the system has witnessed an arrival or departure of a truck ascending. This is obtained by making an increasing fusion of two preceding tables., and the "nbr " table which, for each instant or each case of "$fusion$" table, specifies the number of trucks present in the system.

These two tables cannot be made by hand due to the large size of our database. This requires a computer program. Therefore, we have established the following algorithm .

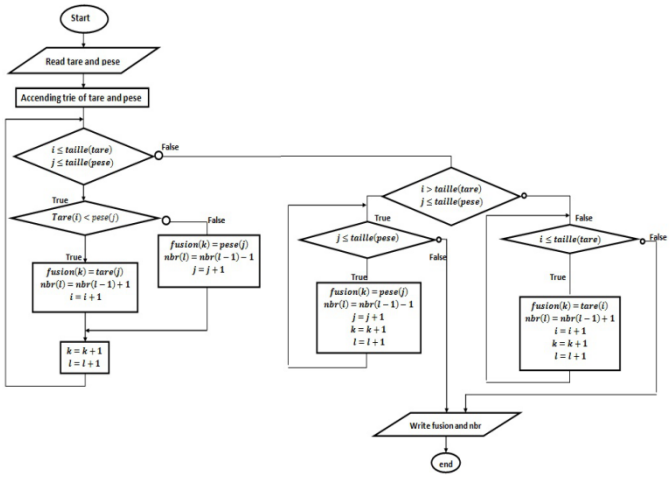

Figure 4: Examination of the change in the total number of trucks in the system

Notes:

- i and j traverse successively the two tables tare and pese.
- k and l traverse successively the two tables fusion and nbr.

This algorithm proceeds as follows: As input, we introduce the " $tare$" and "$pese$" tables, the two tables "$fusion$" and "nbr "are obtained as output.

For the "nbr " table, if the corresponding checkbox in the fusion table is an entry, we increase the number of trucks by one and if the corresponding checkbox in the fusion is a departure, we decrease the number by one.

We get the following graph after execution:

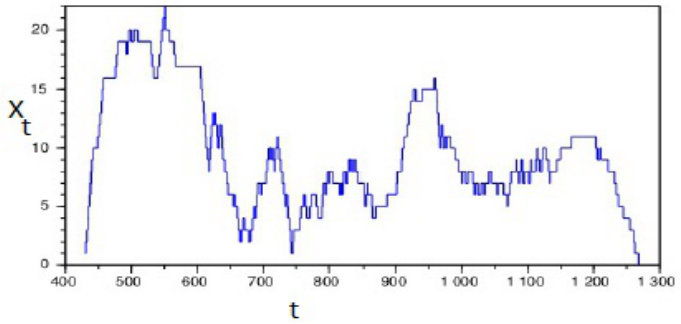

Figure 5: Total number of trucks in the system during the two shifts

It is clear that the maximum number of truck that were in the system during the period of observation 960 min is n=22.

• Remark: The number of trucks in the system decreases during the following intervals :

$[11:02:00,11:26:00]$, $[12:15:00,12:27:00]$, $[20:20:00,22:30:00]$ it will be very effective to distribute the breaks the workers take during these intervals to ensure their presence during intervals of the explosion of system .

• <u>calcul of $T(n,\theta)$ for a given number n:</u> We note the total time during which the system contains n clients $T(n,\theta)$ which we calculated as the sum of the durations during which there were n trucks in the system during the observation period θ .

It is clear that $\sum_{n=0}^{+\infty} T(n,\theta) = \theta$.

In our case, the calculation of $T(n,\theta)$ amounts to calculating $T(n,960)$ for every n with $0 \leq n \leq 22$.

The calculation of $T(n,960)$ cannot be made by hand due to the large size of our database. This requires a computer program. Therefore, we have established the following algorithm:

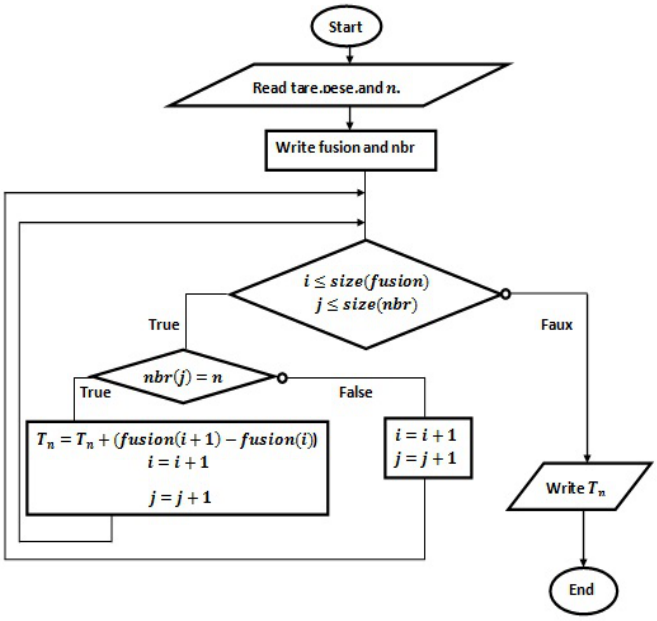

Figure 6: Calculation of the total time during which the system contains n trucks

Notes:

- i and j traverse successively the two tables fusion and nbr.
- to display fusion and nbr tables, it uses the Previous program.

The principle of this algorithm is to introduce as arguments the tables "tare" and "pese" , and n. Specifying the value of n, this algorithm gives us as output, the total time during which the system contains n clients. We obtain the following graph:

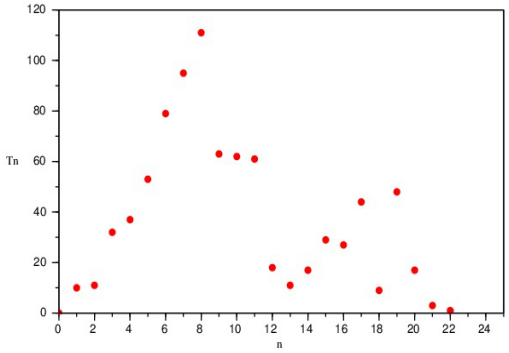

Figure 7: Total time during which the system contains n trucks

• <u>Average number of trucks:</u> the average number of trucks present in the system is the time average X_t , orX_t Over the observation period $[0,\theta]$. this is therefore the area under the curve for X_t.

$$L(\theta) = \frac{1}{\theta}\sum_{n=0}^{22} nT(n,\theta) \qquad (17)$$

We thus obtain $L(960) = 8.476$.

• <u>The average stay time:</u> the average stay time of a client in the system is, by definition, the arithmetic average of stay time of the clients who arrived into the system during the time interval $[0,\theta]$:

$$W(\theta) = \frac{1}{\alpha(\theta)}\sum_{k=1}^{\alpha(\theta)} W_k$$

With W_k is the stay time of k^{th} client in the system .

$$W(\theta) = \frac{1}{120}\sum_{k=1}^{120} W_k = 67min. \qquad (18)$$

• <u>Utilization rate U:</u> we are in the case of a single queue waiting with one server (weighbridge + dock), then we may define the utilization rate of the server which is the proportion of time during which the server is occupied in the interval $[0,\theta]$ as follow:

$$U(\theta) = \sum_{n=1}^{22} \frac{T(n,\theta)}{\theta} \qquad (19)$$

so: $U(960) = 0.872$.

That is to say during the day, the system was occupied with 87.2%.It was therefore unoccupied with 12.8%.

• <u>First remark :</u> The utilization rate of a server is also calculated is follows :

$$U(\theta) = 1 - P(0,\theta) \qquad (20)$$

With $P(0,\theta)$ is the proportion of time during which the server does not contain any client in the interval $[0,\theta]$.

• <u>Second remark:</u> The utilization rate of server $U(960)$which we have calculated represents the entire server utilization rates (weighbridge, dock, weighbridge). We may easily deduce then that the utilization of the weighbridge is the double of the preceding rate since we use the weighbridge twice .

we note U_{ble} the utilization rate of weighbridge

$$U_{ble}(\theta) = 2 \times 0.872 = 1.744 \qquad (21)$$

• <u>Third remark :</u> The inoccupation rate of the system is a very important result which allows us to specify the total length of coffee breaks the workers take. In fact, the total length of breaks should not exceed the inoccupation period of the system so as not to negatively impact the production by leaving the trucks waiting.

ISBN: 978-1-61804-225-5

IV. Proposed Method and Result

Details regarding the weighing process inside the weighbridge:

In this section, we are interested in the weighbridge, that is to say, one of three stations in our network, and more specifically the second weighing of trucks.

At the level of this station, the truck is placed on the weighbridge and the deriver descends to show the weighing ticket he had during his first weighing, and get the stamp of the customs officer along with the delivery note.

We have then an informational flow of trucks inside the weighbridge office, for it is the documents of trucks that move and not the trucks. This is yet another network of queues with three stations which are:

• Weighing: Office containing a computer system which ensures the loads of trucks and display their weight under the supervision of a weighing agent, who prints the weighing ticket containing all the necessary information of the trucks and the goods it carries.

• Customs: Office containing a customs officer who verifies whether the weight of the goods carried exceeds the declared weight, recopies on his register all the extra information on the weighing ticket, fill the exit note and on its back filled in and puts the stamp on the customs liquidation.

• Surveillance: Office containing a delivery agent who controls the quantity of the goods, ensures the delivery of the destination and records all information in order to give a delivery note.

To modeling the informational flow of trucks , we can diagram the informational flow of trucks inside the weighbridge as follows:

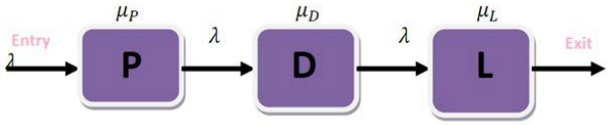

Figure 8: Informational flow of trucks at the weighbridge

• Type of queue: We have then a system which consists of three servers that work in tandem. When a client arrives, he is first directed to the ”P” server, and as soon his service is completed he is directed to the ”D”server where he performs a new service and then directed to the ”L”server. The system is described by the triplet $X_t = (X_t^1, X_t^2, X_t^3)$ where, for i=1,2,3 , X_t^i ,is the size of the system (number of clients in the queue of server i , including the client still in service by the server i). We suppose that the arrival process is a poissonian process with the parameter λ , and the times of services are independent variables, and independent of the arrival process.

We suppose that the times of services of server i follow exponential laws of parameter μ_i This is a special case of Jackson’s networks.

• Kendall’s notation : Kendall’s notation of our queue is as follows:

$$M/M/3/+\infty/+\infty/FIFO \quad (22)$$

Indeed, the arrival processes and services in the various stations are Markovian. The capacity of the queue and the servers are infinite, the number of servers is three, and the discipline of service is FIFO.

• Accuracy of the model parameters: Notice that this is indeed a network of queues. To study its parameters, we can either study the parameters of the entire system, or study the parameters of each of its various stations. We shall opt for the second option, which provides us with the maximum details for a better analysis. Concerning the arrival rate for each station, it is the same as the one found in the second chapter which is 0.014. For the service rate, it changes from one station to the other; using a stopwatch a each station, we find the following: The service time at the ”P” station is fixed in one minute, (it is fixed because it is the system that weighs). The service rate therefore is:

$$\mu_P = 1 \quad (23)$$

The service time at the ”D”station is an average of four minutes. The service rate therefore is:

$$\mu_D = \frac{1}{4} = 0.25 \quad (24)$$

The service time at the "L" station is an average of two minutes. The service rate therefore is:

$$\mu_L = \frac{1}{2} = 0.5 \quad (25)$$

Hence the service time at the weighbridge (second weighing) equals the sum of the service time at each station, it is therefore seven minutes.

We deduce then that the service rate at the weighbridge is:

$$\mu_{ble2} = \frac{1}{7} = 0.14 \quad (26)$$

To optimize the stability of a service, the most effective procedure consists in the reduction of the service time. In this context, we propose to eliminate the manual statement identified by the customs officer.

This operation takes an average of three minutes, while the weigher has a system of information which may be used by the customs.

The customs officer will therefore only verify the weight of the goods and seal the back of the exit note, and at the end of his shift he prints all the data needed from the system. The new mission of the customs shall take only 40 seconds, and then we will have a gain of 3 minutes. It is therefore a change in the ”D” station. The new service time will be one minute, and the new service rate at the level of this station will be:

$$\mu'_D = 1$$

• Remark : This change in the delay of service is interesting at the level of the weighbridge (second weighing), but at the level of the entire service (double weighing + load), three minutes remain insignificant compared with 66 minutes as the average duration of service. But throughout the day, this gain is multiplied by the number of trucks passed through the port, which gives a gain of 37% at the service time, and this will help to serve more trucks per day.

V. Suggestions

It is necessary to make other changes at the level of the remaining stations; at the level of queues, and at the level of the dock. Briefly, changes ought to be made at the level of the organization within the terminal, so for this reason we propose the following suggestions.

• At the level of the dock: When we verify the databases of the past weighing, we notice the different durations of service. We remark that the trucks have greatly exceeded the average length of service (which is 66 min). By comparing monitoring of these delays, we find that the primary reason which causes the biggest delays is attributed to the breakdown of cranes. It is true that this phenomenon is rare, but it has caused the biggest delays, which impacts on the service of trucks, as well as the length of stay and ship performance. According to the principle of the ABC method , it is necessary to focus on the problems, which despite the weakness of their appearances, cause the biggest impacts.

The crane is a lifting machine which is used as a handling tool (loading and unloading of ships). The analysis of the causes of breakdowns of cranes made it incumbent upon us to pay a visit to the technical component of the lifting gear division (LGD), and there we have noted that the cranes undergo two types of technical maintenance: CM (corrective maintenance): which can be done at any time a breakdown occurs. SPM (systematic periodic maintenance): which is necessarily done after a certain number of hours worked, and this varies according to the capacity of the crane. It is evident that once the crane is not available for the SPM, we then put a 20% margin to carry out the maintenance, for example for a crane of 100T capacity (G38001), it must undergo an SPM following every 100h worked.

By exploiting the 20% margin, we monitor the crane starting from 80h of work to 120h. As soon as the crane is available or has just completed the unloading of the ship, it is put in maintenance. This is a well-organized method. In fact, SPM check-lists are prepared and given to the company which have made an agreement to carry out the maintenances. The check-lists contain all the information about the equipment to maintain, as well as the work required. Starting from 80h of work, Technical component department prepared a card programming the lifting gear maintenance which contains the available cranes and gantries taking into account availability, the finishing date and the date of return to service, that provides the operating component ,so that it meets the program during the assignment of cranes to ships.

• Remark : It is necessary to double check if the 20% margin is well chosen. In fact, if we take the same crane of 100T capacity, with the 20% margin, it cannot undergo SPM until 120h of work instead of 100h. if we suppose that, by chance, right from the purchase of a crane, it has undergone its SPM every time after 120h, in the long run, we shall have an accumulation of SPM delays which may cause unforeseen breakdowns, which will then require CM, which means that now we will fall into the problem of delays of trucks should there be no trucks available for replacement.

• Suggestion 1 : We all know that every machine has a lifespan. By comparing the counters of cranes (number of hours worked), we have noticed that there exists a yawninggap in the number of hours worked among cranes of the same capacity. This means that the lifespan of the one with the advanced counter shall be quickly exhausted. We then propose to balance the counters via making a way to give priority to the crane with the least advanced counter when assigning cranes to ships (of course, were talking about cranes of the same capacity).

• At the organizational level: Along with the problem of the breakdowns of cranes, there is also another problem which often prevents the reduction of delay of truck service. This can be explained through the following example:

If we have a ship containing several types of goods, including wheat and corn, and the crane assigned to this ship begins unloading wheat, it will unload the corn only after it has finished the amount of wheat. So if at a certain time, a truck wishing to load corn goes to the terminal, while the crane is in the process of unloading the wheat, it shall have to wait until all the quantity of wheat carried in the ship is unloaded (every truck wishing to load wheat will be served before him and leave).

It is then impossible to decrease the delay of service trucks wishing to load the goods while while the crane unloading started by another type of goods.

• Suggestion 2 : To avoid the above problem, we propose to make the truck drivers aware of te first type of goods to be unloaded, and announce a likely margin time for the unloading of each type of goods. That way, we will have a good organization of the arrivals of trucks, and see some stability in the queues.

• Suggestion 3 : In the organizational context, we propose to put ticket machines at the main gate of the terminal, so as to be able to print tickets which contain the arrival number, thereby the truck drivers will be required to respect the order of the queue (FIFO or FCFS), which will hence make them avoid conflicts among themselves.

• Suggestion 4 : Organize well the dispatching of staff positions, and make sure that there is a supervisor during the day when the utilization rate is very high, based upon the graph representing the total number of trucks in the system during two shifts, so as to guarantee the fluidity of the flow of merchandise.

VI. Conclusion

In this article we have explained the delay trucks and congestion problems within the ports, by the hazard of truck arrivals, and not by the instability of the system. But applying the suggestions previously, we can reduce the time of the tour trucks without interrupting the activity or require budget.

This approach allowed us to win 37% of the service time. To further enhance the performance of handling within the port, and since the supply chain of the company is linked to other processes, it is beneficial to extend this study by analyzing the possibility of create deposits of bulk goods out of the ports.

References

[1] M.L. Chaudhry, in: W.K. Grassmann (Ed.), On numerical computations of some discrete-time queues, Computational Probability, Kluwer.2000.

[2] T. Koderaa, M. Miyazawab, An M=G=1 queue with Markov-dependent exceptional service times , Academic Publishers, Boston, 2001, pp. 365-407.

[3] L.Chen, N. Bostel, P. Dejax, J. Cai,L. Xi, A tabu search algorithm for the integrated scheduling problem of container handling systems in a maritime terminal. European Journal of Operational Research 181 (1), (2007)4058.

[4] J.M. Proth, N. Sauer, 1998,Scheduling of piecewise constant product flows: A Petri net approach. European Journal of Operational Research 106 (1),(1998) 45-56.
[5] A.Demiriz, U.Kula, N. Akbilek, A framework for balanced service and crossselling by using queuing science, Journal of Intelligent Manufacturing 20 (2),(2009) 249-257.
[6] A. El-Sherbiny,H. Zamani, N. Ismail, G. Mokaddis, M. Ghazal, A. El-Desokey, M.S. ELSherbeny, M.S., E.Al-Esayeh, O. Olotu, Transient solution to an infinite server queue with varying arrival and departure rate,Journal of Mathematics and Statistics 6 (1),(2010) 1-3.
[7] S.M.T.F.Ghomi, A.A.Jaafari, Simulation - A queuing theory based approach,Journal of American Science 7 (1) (2011).
[8] H. Minton, Waiting and queuing in the check-in hall: An ethnographic study of queuing and waiting for check-in services at Manchester Airport,Journal of Airport Management 2 (3),(2008) 249-264.
[9] T. Koderaa, M. Miyazawab,An M=G=1 queue with Markov-dependent exceptional service times, , Operations Research Letters 30 (2002) 231 - 244.
[10] J.F.Shortle, P.H.Brill, M.J.Fischer, D.Gross, D.M.B.Masi, An algorithm to compute the waiting time distribution for the M/G/1 queue,Journal on Computing 16 (2),(2004) 152-161.
[11] M.Snipas, E. Valakevicius, Markov model of multi-class, multi-server queuing system with priorities, Journal of Communication and Computer 7 (1), (2010)62.
[12] L.Brunetta, L. Righi,G. Andreatta ,An operations research model for the evaluation of an airport terminal: SLAM (simple landside aggregate model),Journal of Air Transport Management, 5, (1999)161-175.
[13] d. A. G. Barros,D. D. Tomber, Quantitative analysis of passenger and baggage security screening ar airports.,Journal of Advanced Transportation, 41(2),(2007) 171-193.
[14] C.Robertson, S.Shrader,D. Pendergraft, L.Johnson, K.Silbert, In E. Ycesan, C. -H. Chen, J. Snowdown, J. Charnes (Eds.), The role of modeling demand in process re-engineering, Proceedings of the Winter Simulation Conference,2002, pp. 1454-1458.
[15] R. Stolletz,Analysis of passenger queues at airport terminals, Research in Transportation Business Management 1 (1), (2011)144-149.
[16] R.Stolletz , Approximation of the non-stationary M(t)/M(t)/c(t)-queue using stationary queuing models: The stationary backlog-carryover approach, European Journal of Operational Research, 190(2) (2008) 478-493.
[17] C. Blondia, T. Theimer, A discrete-time model for ATM traffic, RACE document PRLB 123 0018 CC CD/ UST 123 0022 CC CD, October 1989.
[18] A.S. Alfa, M.F. Neuts, Modelling vehicular traffic using the discrete time Markovian arrival process, Transportation Science 29 (1995) 109-117.
[19] A.Graham, (2003). Managing airports An international perspective (2. ed). Elsevier.
[20] D.Worthington, Reflections on queue modelling from the last 50 years,Journal of the Operational Research Society 60, (2009)S83-S92.

About New Class of Volterra Type Integral Equation with Two Boundary Singularity in Kernels

N. Rajabov , S. Saidov

Abstract: -.In this work, investigation one class general Volterra type Integral Equation with two boundary logarithmic and singular points. In depend from roots corresponding characteristic equation, solution this integral equation can contain two arbitrary constants, one constant and may be having unique solution.

Key words:- singular kernel, Volterra type integral equation, boundary singularity, logarithmic singularity.

Let $\Gamma = \{x: a < x < b\}$ the set of point on real axis and consider an integral equation

$$\varphi(x) + \int_a^x \left\{K_1(x,t) + K_2(x,t) ln\left[\left(\frac{x-a}{b-x}\right)\left(\frac{b-t}{t-a}\right)\right]\right\} \frac{\varphi(t)dt}{(t-a)(b-t)} = f(x), \quad (1)$$

where $K_1(x,t)$, $K_2(x,t)$ are given functions on the rectangle $\overline{R}$ with R defined as the set $\{a < x < b\ , a < t < b\}$, $f(x)$ are given function in $\overline{\Gamma}$ and $\varphi(x)$ to be found

The theory of the integral equation type (1) with one left , one right singular point or one interior singular point at $K_2(x,t) = 0$ has been constructed in [1]. The theory of the integral equation (1) at $K_2(x,t) = 0, K_1(x,t) = A(t)$ and $K_2(x,t) = 0, K_1(x,t) \neq A(t)$ constructed in [1]-[4]. The theory of the integral equation type (1) with one left singular point has been constructed in [5].

The solution of the this equation is south in the class of function $\varphi(x) \in C[a,b)$ vanishing at the singular point $x = a$, i.e

$\varphi(x) = o[(x-a)^{\varepsilon}]$, $\varepsilon > 0$ and $x \to a$.

In point $x = b$ the solution of the equation (1) may be unbounded or vanish.

In this work, we investigate other cases integral equation(1) and corresponding him characteristic equation.

Integral equation (1) we represented in following form

$$\varphi(x) + \int_a^x \left\{K_1(a,a) + K_2(a,a) ln\left[\left(\frac{x-a}{b-x}\right)\left(\frac{b-t}{t-a}\right)\right]\right\} \frac{\varphi(t)dt}{(t-a)(b-t)} = f_1(x), \quad (2)$$

where

$$f_1(x) = f(x) - \int_a^x \left\{(K_1(x,t) - K_1(a,a)) + (K_2(x,t) - K_2(a,a)) ln\left[\left(\frac{x-a}{b-x}\right)\left(\frac{b-t}{t-a}\right)\right]\right\} . \frac{\varphi(t)dt}{(t-a)(b-t)} . \quad (3)$$

Integral equation (2) we called characteristic integral equation, corresponding to general equation(1). Consequently, problem red use to investigate the following integral equation

$$\varphi(x) + \int_a^x \left\{p + q ln\left[\left(\frac{x-a}{b-x}\right)\left(\frac{b-t}{t-a}\right)\right]\right\} \frac{\varphi(t)dt}{(t-a)(b-t)} = f(x), \quad (4)$$

where p , q are given constants.

Support that, the solution of the characteristic equation (4) exist and belongs to $C''(\Gamma)$. Also, assume $f(x) \in C''(\Gamma)$. Then differentiating both side of (4) twice arrives at an ordinary differential equation of the second order with left and right points. Writing out solution obtained ordinary differential equation according to [6] and returning to conversely, we find solution integral equation (4) . After immediately testing, be convinced that obtained solution be satisfied the equation (4) at less week conditions.

For (4) the following confirmations is obtained:

Theorem 1. *Let in integral equation (4) functi*on $f(x)$ *represents in form uniformly converges generalized power*

series

$$f(x)=\sum_{k=0}^{\infty} f_k\left(\frac{x-a}{b-x}\right)^{k+\gamma},\ \ x\in[a,b),\qquad \gamma=constant>0 \tag{5}$$

and $(k+\gamma)^2(b-a)+p(k+\gamma)+q\neq 0$ *for* $k=0,1,2,\ldots\ldots\ldots$ *The roots of the algebraic equation*

$$\lambda^2(b-a)+p\lambda+q=0 \tag{6}$$

real , different and positive , that is $p<0$, $q>0$, $D=p^2-4(b-a)q>0$ *. Then, homogeneous integral equation* (4) *in class of function* $\varphi(x)\in C[a,b)$*, vanishing in point* $x=a$*, unbounded in point* $x=b$ *has two linear independence solution of the following form*

$$\varphi_1(x)=\left(\frac{x-a}{b-x}\right)^{\lambda_1},\ \ \varphi_2(x)=\left(\frac{x-a}{b-x}\right)^{\lambda_2}, \tag{7}$$

where $\lambda_1=\frac{|p|+\sqrt{D}}{2(b-a)}$, $\lambda_2=\frac{|p|-\sqrt{D}}{2(b-a)}$.

Non homogeneous integral equation (4) *in class of function* $\varphi(x)\in C[a,b)$*, vanishing in point* $x=a$ *, unbounded in point* $x=b$ *is always solvability and its solution is given by formula*

$$\varphi(x)=\varphi_1(x)C_1+\varphi_2(x)C_2+K_\gamma^1(f), \tag{8}$$

where C_1, C_2*-arbitrary constants,*

$$K_\gamma^1(f)=\sum_{k=0}^{\infty}\frac{(k+\gamma)^2(b-a)f_k}{(k+\gamma)^2(b-a)+p(k+\gamma)+q}\left(\frac{x-a}{b-x}\right)^{k+\gamma}. \tag{9}$$

Theorem 2. *Let in integral equation (4)* $p<0$, $q>0$, $D>0$, $f(x)\in C(\overline{\Gamma})$, $f(a)=0$ *with the following asymptotic behavior*

$$f(x)=o\left[(x-a)^{\delta_1}\right],\qquad \delta_1>\lambda_1 \qquad \text{at} \qquad x\to a\,.$$

Then integral equation (4) *in class of function* $\varphi(x)\in C[a,b)$*, vanishing in point* $x=a$ *, unbounded in point* $x=b$ *is always solvability and its solution is given by formula*

$$\varphi(x)=\varphi_1(x)C_1+\varphi_2(x)C_2+K_3(f), \tag{10}$$

where C_1, C_2 *-arbitrary constants ,*

$$K_3(f)=f(x)-\frac{(b-a)^2}{\sqrt{D}}\int_a^x\{\lambda_2^2\left[\left(\frac{x-a}{b-x}\right)\left(\frac{b-t}{t-a}\right)\right]^{\lambda_2}-\lambda_1^2\left[\left(\frac{x-a}{b-x}\right)\left(\frac{b-t}{t-a}\right)\right]^{\lambda_1}\}\frac{f(t)dt}{(t-a)(b-t)}. \tag{11}$$

Characteristic*s 1.* Let in integral equation (4) parameters p,q , function $f(x)$ satisfy any condition of theorem 2. Then from (10), (11) it follows , the solution integral equation (4) $\varphi(x)\in C[a,b)$, $\varphi(a)=0$ with following asymptotic behavior

$$\varphi(x)=o\left[(x-a)^{\lambda_2}\right], \qquad \text{at} \qquad x\to a\,;$$

$\varphi(b)=\infty$ with following asymptotic behavior

$$\varphi(x)=O\left[(b-x)^{-\lambda_2}\right], \quad \text{at} \qquad x\to b\,.$$

Theorem 3. *Let in integral equation (4)* $p>0$, $q>0$, $D>0$*. Assume that a function* $f(x)\in C(\overline{\Gamma})$, $\varphi(a)=0$ *with the following asymptotic behavior*

$f(x)=o[(x-a)^{\varepsilon}]$, $\varepsilon>0$ *and* $x\to a$;

$f(b)=0$ *with the following asymptotic behavior*

$$f(x)=o\left[(b-x)^{\delta_2}\right],\qquad \delta_2>|\lambda_1| \qquad \text{at} \qquad x\to b\,.$$

Then the integral equation (4)*in class of function* $\varphi(x)\in C(\overline{\Gamma})$*, vanishing in point* $x=a$ *and* $x=b$ *has a unique solution which is given by formula*

$$\varphi(x)=f(x)-\frac{(b-a)^2}{\sqrt{D}}\int_a^x\{\lambda_2^2\left[\left(\frac{b-x}{x-a}\right)\left(\frac{t-a}{b-t}\right)\right]^{|\lambda_2|}-\lambda_1^2\left[\left(\frac{b-x}{x-a}\right)\left(\frac{t-a}{b-t}\right)\right]^{|\lambda_1|}\}\frac{f(t)dt}{(t-a)(b-t)}. \tag{12}$$

Characteristic*s 2.* Let in integral equation (4) parameters p,q , function $f(x)$ satisfy any condition of theorem 3. Then from (13) it follows the solution integral equation (4) $\varphi(x)\in C(\overline{\Gamma})$, $\varphi(a)=0$ with following asymptotic behavior

$$\varphi(x)=o[(x-a)^{\varepsilon}], \quad \varepsilon>0 \qquad \text{at} \qquad x\to a\,;$$

$\varphi(b)=0$ with following asymptotic behavior

$$\varphi(x)=o\left[(b-x)^{|\lambda_1|}\right], \quad \text{at} \qquad x\to b\,.$$

For investigation the general case integral equation (1) we represented in form (2) . Assuming for a moment that $f(x)$ is known, we can find a general solution to (2). The integral equation (2) corresponding to following characteristic equation

$$\mu^2(b-a)+K_1(a,a)\mu+K_2(a,a)=0\,.$$

Let $K_1(a,a)<0$, $K_2(a,a)>0$ and $D_1=\left(K_1(a,a)\right)^2$

$-4K_2(a,a)(b-a)>0$, and let functions $f(x)$, $K_1(x,t)$, $K_2(x,t)$ and $\varphi(x)$ be such that $f_1(x)\in C(\overline{\Gamma})$, $f_1(a)=0$ with following asymptotic behavior:

$$f_1(x)=o\big[(x-a)^{\delta_3}\big],\qquad \delta_3>\mu_1 \qquad \text{at} \qquad x\to a\ ,$$

where $\mu_1=\frac{|K_1(a,a)|+\sqrt{D_1}}{2(b-a)}$.

Then according to Theorem 2 general solution of no homogeneous integral equation (2) is

$$\varphi(x)=\Psi_1(x)C_3+\ \Psi_2(x)C_4+K_4(f_1)\equiv K_4^1[C_3,C_4\ ,f_1(x)\ ],$$

where

$$K_4(f)=f_1(x)-\frac{(b-a)^2}{\sqrt{D_1}}\int_a^x\{\mu_2^2\left[\left(\frac{x-a}{b-x}\right)\left(\frac{b-t}{t-a}\right)\right]^{\mu_2}-\mu_1^2\left[\left(\frac{x-a}{b-x}\right)\left(\frac{b-t}{t-a}\right)\right]^{\mu_1}\}\frac{f_1(t)dt}{(t-a)(b-t)},\qquad (13)$$

$$\Psi_1(x)=\left(\frac{x-a}{b-x}\right)^{\mu_1},\quad \Psi_2(x)=\left(\frac{x-a}{b-x}\right)^{\mu_2},\quad \mu_2=\frac{|K_1(a,a)|-\sqrt{D_1}}{2(b-a)}$$

and C_3 , C_4 are arbitrary constants.

Substituting for $f_1(x)$ from (13) we arrive at the solution of the following integral equation

$$\varphi(x)+\int_a^x\frac{M(x,t)}{(t-a)(b-t)}\varphi(t)dt=K_4^1[C_3,C_4\ ,f_1(x)\ ]\qquad (14)$$

where

$$M(x,t)=K_1(x,t)-K_1(a,a)\big(K_2(x,t)-K_2(a,a)\big)ln\left[\left(\frac{x-a}{t-a}\right)\left(\frac{b-t}{b-x}\right)\right]-$$

$$-\frac{(b-a)^2}{\sqrt{D_1}}\int_t^x\{\mu_2^2\left[\left(\frac{x-a}{b-x}\right)\left(\frac{b-\tau}{\tau-a}\right)\right]^{\mu_2}-\mu_1^2\left[\left(\frac{x-a}{b-x}\right)\left(\frac{b-\tau}{\tau-a}\right)\right]^{\mu_1}\}\Big[K_1(\tau,t)-K_1(a,a)+\big(K_2(\tau,t)-K_2(a,a)\big)ln\left[\left(\frac{\tau-a}{t-a}\right)\left(\frac{b-t}{b-\tau}\right)\right]\ \Big].$$

$$\frac{dt}{(t-a)(b-t)}.\qquad (15)$$

If , the kernels $K_1(x,t)$, $K_2(x,t)$ in (1) are such that for any $(x,t)\in\overline{R}$ and $(x,t)\to(a,a)$ satisfies the conditions

$$K_1(x,t)-K_1(a,a)=o\big[(x-a)^{\delta_4}(t-a)^{\delta_5}\big],\ \delta_4>\mu_1\ ,\ \delta_5>\mu_1 \text{ at } (x,t)\to(a,a),\qquad (16)$$

$$K_2(x,t)-K_2(a,a)=o\big[(x-a)^{\delta_6}(t-a)^{\delta_7}\big],\ \delta_6>\mu_1\ ,\ \delta_7>\mu_1 \text{ at } (x,t)\to(a,a)\ ,\qquad (17)$$

and $\delta_4+\delta_5>\mu_2$, $\delta_6+\delta_7>\mu_2$, then $M(a,a)=0$. In this case function

$M_1(x,t)=(t-a)^{-1}M(x,t)$ has week singularity at $t=a$.

Let function $\mathrm{f}(x)\in C(\overline{\Gamma})$, $f(a)=0$ with asymptotic behavior

$$f(x)=o\big[(x-a)^{\delta_8}\big],\ \delta_8>\mu_1 \ \text{ at } \ x\to a\ ,\qquad (18)$$

Then integral equation (14) , as second kind Volterra type integral equation with week singularity , has a unique solution , which is given by formula

$$\varphi(x)=K_4^1[C_3,C_4\ ,f_1(x)\ ]-\int_a^x\Gamma(x,t)\,K_4^1[C_3,C_4\ ,f_1(t)\ ]dt\ ,\qquad (19)$$

where $\Gamma(x,t)$ is a resolvent of the integral equation (14) and C_3,C_4 are arbitrary constants.

Thus , from the preceding discussion the theorem follows.

Theorem 4. *Let in* (1) , $K_1(x,t)\in C(\overline{R})$, $K_2(x,t)\in C(\overline{R})$, *functions* $K_1(x,t)$ $K_2(x,t)$ *in neighborhood point* $(x,t)=(a,a)$ *satisfy condition* (16), (17) *and let* $K_1(a,a)<0$, $K_2(a,a)>0$, $D_1>0$, $\mathrm{f}(x)\in C(\overline{\Gamma})$, $f(a)=0$ *with asymptotic behavior* (18) , $\delta_4+\delta_5>\mu_2$, $\delta_6+\delta_7>\mu_2$. *Then the integral equation* (1) *in class of function* $\varphi(x)\in C[a,b)$, *vanishing in point* $x=a$, *is always solvability and its solution is given by formula* (19) , *where* C_3,C_4 *are arbitrary constants.*

Characteristics *3.* Let in integral equation (1) , functions $K_1(x,t)$,$K_2(x,t)$, , $\mathrm{f}(x)$ satisfy any condition of theorem 4. Then from (19) it follows , the solution integral equation (1) $\varphi(x)\in C[a,b)$, $\varphi(a)=0$ with following asymptotic behavior

$$\varphi(x)=o[(x-a)^{\mu_2}],\qquad \text{at} \qquad x\to a\ ;$$

$\varphi(b)=\infty$ with following asymptotic behavior

$$\varphi(x)=O[(b-x)^{-\mu_2}],\qquad \text{at} \qquad x\to b\ .$$

Reference

[1] N Rajabov , Volterra type integral equation with

boundary and interior fixed singularity and super-singularity kernels and their, application, LAP LAMBERT Academic Publishing, Germany , 2011, 282 p.

[2] N. Rajabov ,S. Saidov , One-dimensional Volterra type integral equation with two boundary singular points. Herald Tajik National University, Natural science series, 2012, № 1/3(85), pp. 36-42.

[3] N. Rajabov ,S. Saidov , To theory general Volterra type integral equation with two boundary singularity. Tajik Acad. Sci. Doklady, 2012, v. 55, №7, pp. 519-525.

[4] N. Rajabov , S. Saidov , To theory one class model one-dimensional Volterra type integral equation with two boundary singular points. Proceedings XI school of young scientists : Non –local boundary value problems and problems of modern analysis and informatics. Terskol, 4-6 December 2013, pp. 55-60.

[5] N. Rajabov , About new class of Volterra type integral equation with boundary singularity in kernels. Advances in Applied Mathematics and Approximation Theory. Springer Proceedings in Mathematics and Statistics, 41, 2013, pp. 339-358.

[6] N. Rajabov , Introduction to ordinary differential equations with singular and super-singular coefficients, Dushanbe, 1998, 150p.

Vector Error Correction Model for Causality Link among the Construction, Manufacturing and Mining & Quarrying Sector in Malaysia (1991-2010)

Raza Ali Khan, M. Shahir Liew, Z.B. Ghazali, and Noor Amila

***Abstract*—** Vector error correction model (VECM) is a multivariate error correction model, which handles sets of the equation at the same time. Error correction model (ECM) converts into VECM when more than one or set of equations is involved in causality model. The model will help to understand and examine empirical long run and short run association between the concerned variables in optimal lag order. The objective of this study is to investigate causality linkage among the three important sectors namely construction, manufacturing and mining & quarrying of the Malaysian economy and estimate VECM equations for the studied sectors. The quarterly time series data from 1991Q1 – 2010 Q4 is used to understand pair wise causality and the direction of the causality link among the concerned variables. The result of the Granger causality shows that a unidirectional causality exists among the construction, manufacturing and mining and quarrying sector of the Malaysia. The construction sector has strong backward linked with manufacturing as well as mining and quarrying sector, while mining and quarrying has forward linkage with construction and manufacturing sectors. The estimated VECM equations suggest that the studied sectors have long run as well as short run associations with each other. Furthermore, it shows that the speed of adjustment toward long run equilibrium for construction, manufacturing, and mining and quarrying is 8 %., 14% and 11% respectively. The outcome of the study is valuable for the Government of Malaysia, policy makers and concerned parties of the sectors.

***Keywords*—** VECM, Causality, Linkages.

I. Introduction

The Malaysian economy is the most successful growing economy in the world. The World Economic Forum ranked Malaysia 24th most competitive nation out of 148 countries, higher than China and South Korea due to her impressive and extraordinary economic performance [1].

According to Malaysia Vision 2020, it has to achieve the title of developed nation status by the year 2020. The Government of Malaysia has to make lots of efforts and formulate its economic development policies in such a way that all major sectors of the economy contribute positive growth that accelerate the momentum of social economic development and growth of the country.

Overall economic growth depends on the sectoral growth rates, which are influenced by the linkages between the sectors. Inter sectoral linkages thus play a crucial role in the industrialization and socioeconomic development of a country. They provide opportunities for future economic activities and development of new sectors of the economy.

Therefore, it is necessary to understand the strength and direction of interdependent linkages among the sectors. An in-depth knowledge of inter-sectoral linkage is very useful for Government and policy makers as well, so that the more effective and efficient long term policies could be formulated in order to attain comprehensive development and sustainable growth in the economy.

The objective of this study is to examine the linkage among the three key sector construction, manufacturing and mining and quarrying of the Malaysian economy and development of a VECM for the construction sector. The VECM will determine the long run and short adjustment coefficient of the Malaysian construction sector (MCS).

II. Literature Review

Malaysia's rapid economic growth is the result of prompt structural changes in the economy. Its economy has undergone rapid transformation since independence. The major shift is from natural resource based economy to large scale industrialized economy.

The manufacturing, mining and quarrying and construction sector are considered as a major sector of the Malaysian economy. The economic activities of these three sectors not only play a significant role in the aggregate economy, but also affect the economic performance of each other on the basis of inter-sectorial linkages.

A. Significance of Inter-sectorial Linkages

The linkage among various sectors of the economy is one of the significant sources of economic development in a modest world. The evaluation of the strength and direction of the relationship that exists among the various sectors of the economy determines the importance of a particular sector to an economy [2]. During the last 60 years after independence of a number of colonies in Asia and Africa, the question of development received special attention and the theory of inter-sectoral linkage has created much interest and has become the primary subject of development economics.

ISBN: 978-1-61804-225-5

The sectorial configurations and the linkage among various sectors of the economy and their mutual impact on economic development and GNP, has developed multiple theories of economic growth [3]. The theory of unbalanced growth presented by Hirschman recommends that the economic development policy should emphasize on accelerating the growth of leading sectors. This would result in growth effect being shifted from the leading sectors to the other supporting sectors [4]. The enhancement in leading sector activities will significantly affect the production, employment level and per capita income of other sectors due to strong backward and forward linkage, thus have a multiplier effect on aggregate economy.

The study of inter linkages is all the more important for developing countries like Malaysia. So that's positive growth stimuli among sectors can be identified and nurtured to sustain the economic growth momentum [5]. Linkages thus play a crucial part in the industrialization of a country and generate further production activities in an economy.

The sectorial linkages are developed as a result of each sector's role as a supplier and receiver of inputs from other sectors of the economy. The manners in which two sectors link with each other is known as backward and forward linkages between the sectors.

B. Measuring Tools for Linkages

There are three analytical tools, which are widely used for measuring the strength of the linkage, sectoral economic performance and production interdependence:

1. Leontief's (1936) Input–output analysis
2. Statistical technique
3. The new econometric modeling developed by Engle and Granger

Leontief (1936) pioneered the use of the input-output analysis to gauge the backward and forward linkages between the sectors of the economy. This concept is very useful for assessing the impact associated with the growth of a particular sector [6]. The number of studies available in which input-output analysis tool used to measure linkage between the sectors.

Bon (1988) is one of the few researchers who applied the concept of Leontief input-output matrix to the construction industry and found that the input–output tool can be used for studies of the construction sector in three broad aspects: employment creation potential, role in the economy, and identification of major suppliers to the construction industry [7]. A study conducted by Rameezdeen et al, (2006), used an input-output table to analyze the significance of construction in a developing economy and its relationships with other sectors of the national economy [8]

However, more sophisticated statistical and econometric methodology is now available for measuring the strength of linkages among economic sectors. This econometric technique introduced by Engle and Granger in 1988. Many modeling studies related to economic and financial issues have applied this new technique to analyze economic relationships.

Green (1997) applied the Granger causality test to determine the relationship between GDP and residential and non-residential investment. The results suggested that residential investment causes, but is not caused by GDP, while non-residential investment does not cause, but is caused by GDP. He concluded that housing leads and other types of investment lag the business cycle [9]

A study conducted by Chan (2001) used econometric models to assess construction linkages with sectors of Singaporean economy. The result shows that some causal relationships are bi-directional, including those between the construction sector and other sectors; and the construction sector and the GDP [10].

Another study conducted under the title "An assessment of the linkages between the construction sector and other sectors of the Nigerian economy", indicates that construction significantly leads many sectors and virtually all economic sectors feedback into the construction sector. Hence mutual interdependence of construction with sectors of the economy is created [11] .

All above discussed studies have made a valuable contribution to understanding the association between construction and economic growth. However, this study examines the causality link among the construction, manufacturing and mining and quarrying sector of the Malaysian economy. The Engel Granger econometric approach is used here because of its popularity and providing better results. The long run and short run associations among the three sectors, construction, manufacturing and mining and quarrying are measured through VECM.

III. Research Methodology

The paradigm of research for this study is purely quantitative. An econometric time series analysis used to measure the causal link between the variables. VECM is established to estimate the long run and short run causality coefficient for the studied variables. This is a four steps process. At first the data variable series are tested for unit root and stationary problem. If the data series are found stationary, then move to the second step, Johansen's co-integration test is conducted to examine the number of co-integration equations in the data set. If the data set qualified the first two conditions, then the third step is to estimate VECM equations. Finally Granger causality link and their directions are identified.

A. Data and Sample Size

The study is based upon quarterly time series data on the three major sectors of the Malaysian economy, namely construction, manufacturing and mining and quarrying from 1991Q1 to 2010 Q4. The data of the concerned sector's output in money term (Ringgit million) are obtained from the department of Statistics Government of Malaysia. Each data series is converted into natural logarithm form to control the variance and maintain the uniformity in the data.

ISBN: 978-1-61804-225-5

B. Model Function

The following VECM model functions are developed on the bases of the endogenous output growth model.

lcons = f (lcons, lmanf, lminq)
lmanf = f (lcons, lmanf, lminq)
lminq = f (lcons, lmanf, lminq)
Where;
lcons = log of construction output series
lmanf = log of manufacturing sector output series
lminq = log of mining and quarrying output series

C. Unit Root Test

The major problem in time series is unit root and stationarity. Most of the time series has this fundamental problem that leads to spurious regression. To avoid this situation and make the variable stationary, the traditional way is to take the first difference of the series.

The augmented Dickey Fuller (ADF) and Philip Peron (PP) tests are used here to examine unit root and stationarity problem with the series. The ADF test for each variable series (construction, manufacturing and mining and quarrying) is conducted on the basis of Equations 1- 3 with the null hypothesis that the series has a unit root problem ($\propto_2 = 0$). The estimated t-statistic compared with the value suggested by MacKinnon for rejecting the null hypothesis. The estimated value must be equal or greater than the MacKinnon values at the 5% level of significance for rejecting the null hypothesis (H_0).

$$\Delta lcons_t = \propto_0 + \propto_1 T + \propto_2 lcons_{t-1} + \sum_{i=1}^{n} \gamma_i \Delta lcons_{t-1} + \mu_t \quad (1)$$

$$\Delta lmanf_t = \propto_0 + \propto_1 T + \propto_2 lmanf_{t-1} + \sum_{i=1}^{n} \gamma_i \Delta lmanf_{t-1} + \mu_t \quad (2)$$

$$\Delta lminq_t = \propto_0 + \propto_1 T + \propto_2 lminq_{t-1} + \sum_{i=1}^{n} \gamma_i \Delta lminq_{t-1} + \mu_t \quad (3)$$

D. Co-integration Test

The co-integration test is normally conducted after knowing the order of integration in the data series. The order of integration of data variable series is determined by the number of time series have to be differences for converting it into stationary series. If a series differenced one time to become stationary, it is known to be integrated order one I(1).

The stationary linear combination between the variables may be defined as a long run equilibrium association between the variables and called the co-integrating equation [12]. If the two or more variables are non-stationary but a linear arrangement between them is stationary, then the variable series are to be known as co-integrated.

The Johansen co-integration rank tests, Trace test and maximum Eigenvalue test are used here in order to determine the number of co-integrating equations between the concerned variables. Equation (4) is used to Trace test with the null hypothesis that there is at most " r " co-integrating vectors. Equation (5) is used for maximum eigenvalue test with the null hypothesis that the number of co-integrating vector is " r " against the alternative hypothesis the number of vectors is "r+1" [13] .

$$\delta_{trace}(r) = -T \sum_{i=r+1}^{n} \ln(1 - \bar{\delta}_i) \quad (4)$$

$$\delta_{max}(r, r+1) = -T \sum_{i=r+1}^{n} \ln(1 - \bar{\delta}_{r+1}) \quad (5)$$

Where
$\bar{\delta}_i$: Estimated characteristics root and
T: number of observation used.

E. Generalized ECM

In order to estimate the long run and short association between the concerned variables the VECM is developed. The generalized mathematical formulation of the model is described in Equation (6)

$$\Delta Y_t = \pi Y_{t-1} + \sum_{i=1}^{p-1} \alpha_i \Delta Y_{t-1} + \mu D_i + \varepsilon_t \quad (6)$$

Where
Y_t : A column vector having current values of all endogenous variables in the model.
D_t : Matrix of deterministic variables
ε_t : Vector of error terms
π, α_i , μ : Parameters

IV. Research Hypothesis

The six nulls and alternate hypotheses are established in order to examine the causal relationship between the studied sectors of the Malaysian economy.

Table 1
Research Hypotheses

Null Hypotheses	Alternate Hypotheses
lcons does not cause *lmanf*	*lcons* cause to *lmanf*
lmanf does not cause *lcons*	*lmanf* cause to *lcons*
lcons does not cause *lminq*	*lcons* cause to *lminq*
lminq does not cause *lcons*	*lminq* cause to *lcons*
lmanf does not cause *lminq*	*lmanf* cause to *lminq*
Lminq does not cause *lmanf*	*lminq* cause to *lmanf*

V. Results and Discussion Analysis

A. Unit Root Test Result

The two popular tests ADF and PP are conducted to examine the unit root and stationary problem with the variable data series. These tests are made for each variable data series by regressing Equations 1-3 with the assumption of intercept

without a trend. The null hypothesis of this test is a data variable series has a unit root problem. Both ADF and PP test results are presented in Table 2, Shows that all variables data series *lcons, lmanf* and *lminq* have a unit root problem at level because the null hypothesis was not rejected at the 5% significance level. However, at first difference all data series converted into stationary series and the null hypothesis was statistically rejected at the 5% level of significance. This implies that the unit root problem is removed from series after first differencing of the series and it becomes stationary series. The result also suggests that all the variable series are integrated order one I(1). This indicates that there is a chance of long run equilibrium association between the variables, which can be tested through co-integration examination.

Table 2.
Unit Root Test Result

Variables	Lag order	DF Test (intercept without trend)	ADF Test (intercept without trend)	PP Test (intercept without trend)
		Level	1st Diff.	1st Diff.
lcons	4	-2.7720	-2.9444*	-9.8985*
lmanf	4	-2.1610	-4.7084*	-8.3446*
lminq	4	-2.3621	-3.5707*	-9.1594*

Mackinnon critical value for rejection null hypothesis at 5%, level of significance intercept without trend is 2.9012. (* denotes rejection of null hypothesis at 5% significance level)

B. Co-integration Test Result

The Johansen co-integration rank (Trace value and maximum eigenvalue) tests are conducted to know the number of co-integrating equation in the data set. The test results are displayed in Table 3. Both Trace statistics and maximum eigenvalue statistics suggest one co-integration equation exists in the data set at the 5% significance level.

Table 3
Trace and Max. Eigenvalue test

Hyp. No of CE(s)	Trace statistics	5% critical value	Max. Eigen statistics	5% critical value
None*	39.1620*	29.7970	25.3848*	21.1316
At most 1	13.7772	15.4947	9.6348	14.2646
At most 2*	4.1425*	3.8415	4.1425*	3.8414

*denotes rejection of null hypothesis at 5% significance level

The existence of co-integration in a data set confirms the unit root test result, which has already suggested that the data series are non-stationary at level and integrated order one I(1).

Table 4 depicts the normalized co-integrating coefficient and standard error in parentheses by which normalized co-integrating equation can easily develop.

Table 4
Normalized Co-integrating Coefficient

c	lcons	lmanf	lminq
12.4698	1.0000	-0.5927 (0.1808)	-2.9113 (0.5313)

$$lcons + 0.5927lmanf - 2.9114lminq + 12.4698 \quad (7)$$

Since the unit root test has already confirmed the variables are non-stationary at a level and achieved stationarity after one differencing and now the rank tests confirmed the existence of co-integration therefore resulting model will be VECM. The three variables (lcons, lmanf and lminq) are under consideration; therefore three VECM equations are developed (Equations 8-10) at optimal lag length 4.

C. VECM for Construction Sector

A system VECM equation for the construction sector is developed with a view that construction is a function of manufacturing and mining and quarrying. The Equation (8) expresses the long run as well as short run associations between construction and other two concerned sectors manufacturing and mining and quarrying. It consists of two parts co-integration and short run association. Co-integration part represents to long run association between the variables. The first term C(1) represents to speed of adjustment. It should be negative and significant for correctness of the model.

D(*lcons*) = C(1)* (*lcons*(-1) + 0.5927**lmanf*(-1) – 2.9114**lminq*(-1) + 12.4698) + C(2)*D(*lcons*(-1)) + C(3)*D(*lcons*(-2)) + C(4)*D(*lcons*(-3)) + C(5)*D(*lcons*(-4)) + C(6)*D(*lmanf*(-1)) + C(7)*D(*lmanf*(-2)) + C(8)*D(*lamnf*(-3)) + C(9)*D(*lmanf*(-4)) + C(10)*D(*lminq*(-1)) + C(11)*D(*lminq*(-2)) + C(12)*D(*lminq*(-3)) + C(13)*D(*lminq*(-4)) + C(14) (8)

Where C(1) is long run adjustment coefficient. C(2) to C(13) are short run causality coefficients of respective variables and C(14) is a constant term. The values of all coefficients and their probabilities are presented in Table 5.

Table 5
Coefficient and Probability values

	coefficient	Std.Error	t - Stat.	Probability
C(1)*	-0.081284	0.037892	-2.145139	0.0359
C(2)*	0.305602	0.152465	2.004407	0.0495
C(3)*	0.408846	0.128464	3.182583	0.0023
C(4)*	-0.223157	0.131742	-1.693889	0.0954
C(5)*	0.462558	0.135727	3.407992	0.0012
C(6)	-0.100048	0.126905	-0.788374	0.4335
C(7)	-0.149574	0.131046	-1.141392	0.2582
C(8)	0.120316	0.127928	0.940493	0.3507
C(9)	0.017547	0.131327	0.133616	0.8941
C(10)*	-0.376710	0.158022	-2.383910	0.0203
C(11)	0.196542	0.160649	1.223426	0.2259
C(12)	0.163569	0.146864	1.113747	0.2698
C(13)*	-0.467422	0.149750	-3.121349	0.0028
C(14)	0.004409	0.005621	0.784495	0.4358

*denotes significant coefficient at 5% level of significance

ISBN: 978-1-61804-225-5

D. VECM for Manufacturing Sector

The Equation (9) is a vector error correction system equation for manufacturing sector in which manufacturing sector considered as a dependent variable while construction and mining and quarrying are independent variables. First term C(15) shows the speed of adjustment of the manufacturing sector in the long run and C(16) to C(27) are short run causality coefficient of respective independent variables construction and mining and quarrying while C(28) is a constant term. The estimated coefficient values and their probability are available in Table 6.

D(*lmanf*) = C(15)*(*lcons*(-1) + 0.5927**lmanf*(-1) – 2.9114**lminq*(-1) + 12.4698 + C(16)*D(*lcons*(-1)) + C(17)*D(*lcons*(-2)) + C(18)*D(*lcons*(-3)) + C(19)*D(*lcons*(-4)) + C(20)*D(*lmanf*(-1)) + C(21)*D(*lmanf*(-2)) + C(22)*D(*lmanf*(-3)) + C(23)*D(*lmanf*(-4)) + C(24)*D(*lminq*(-1)) + C(25)*D(*lminq*(-2)) + C(26)*D(*lminq*(-3)) + C(27)*D(*lminq*(-4))+C(28) (9)

Table 6
Coefficient and Probability Values

	coefficient	Std.Error	t - Stat.	Probab.
C(15)*	-0.136638	0.038495	-3.549489	0.0007
C(16)*	0.585337	0.154891	3.779035	0.0004
C(17)	0.110971	0.130507	0.850309	0.3985
C(18)	-0.136018	0.133838	-1.016284	0.3135
C(19)	0.236040	0.137887	1.711842	0.0920
C(20)	0.018216	0.128923	0.141297	0.8881
C(21)	-0.013417	0.133130	-0.100777	0.9201
C(22)	-0.051675	0.129964	-0.397609	0.6923
C(23)	0.082780	0.133417	0.620464	0.5373
C(24)	-0.233713	0.160536	-1.455831	0.1506
C(25)	0.264770	0.163205	1.622320	0.1099
C(26)	-0.047716	0.149200	-0.319810	0.7502
C(27)*	-0.602748	0.152132	-3.962000	0.0002
C(28)	0.010408	0.005710	1.822814	0.0732

*denotes significant coefficient at 5% level of significance

E. VECM for Mining and Quarrying Sector

The third system equation (Equation - 10) is for mining and quarrying sector, which is the function of construction and manufacturing sector. It also consists of co-integration part and short run causality. The term C(29) is long run adjustment term and C(30) to C(41) are short run causality coefficients. C(42) is a constant term. The estimated values of all coefficients C(29) to C(42) and their respective probabilities are displayed in Table 7.

D(*lminq*) = C(29)*(*lcons*(-1) + 0.5927**lmanf*(-1) – 2.9114**lminq* (-1) + C(30)*D(*lcons*(-1)) + C(31)*D(*lcons*(-2)) + C(32)*D(*lcons*(-3)) + C(33)*D(*lcons*(-4)) + C(34)*D(*lmanf*(-1)) + C(35)*D(*lmanf* (-2)) + C(36)*D(*lmanf*(-3)) + C(37)*D(*lmanf*(-4)) + C(38)*D(*lminq*(-1)) + C(39)*D(*lminq*(-2)) + C(40)*D(*lminq*(-3)) + C(41)*D(*lminq*(-4)) + C(42) (10)

Table 7
Coefficients and Probability Values

	coefficient	Std.Error	t - Stat.	Probab.
C(29)*	-0.106103	0.030689	3.457381	0.0010
C(30)*	-0.081988	0.123480	-0.663972	0.5092
C(31)	0.135579	0.104042	1.303123	0.1974
C(32)	-0.063259	0.106697	-0.592880	0.5555
C(33)*	-0.247831	0.109925	-2.254551	0.0278
C(34)	0.089794	0.102779	0.873656	0.3857
C(35)	-0.071372	0.106133	-0.672481	0.5038
C(36)	0.067957	0.103608	0.655903	0.5144
C(37)	-0.002898	0.106361	-0.027248	0.9784
C(38)	0.076341	0.127981	0.596502	0.5530
C(39)	0.117103	0.130109	0.900043	0.3716
C(40)*	0.298414	0.118944	2.508860	0.0148
C(41)*	0.391353	0.121281	3.226816	0.0020
C(42)	0.000862	0.004552	0.189393	0.8504

*denotes significant coefficient at 5% level of significance

F. Pair Wise Combine Causality analysis

The combined short run causality analysis is conducted by testing the Wald Statistics for the respective restrictions. Table 8 depicts the causality linkage results for construction, manufacturing and mining and quarrying sector under Vector Auto Regression (VAR). The three null hypotheses are rejected on the bases of Chi square and p-value of Wald test. The criterion for rejection of the null hypothesis is a P-value should be less than the level of significance i.e. 5%.

Table 8
Result of Causality Test in VECM Construction

Null hypothesis	Restrictions	P-Value
lmanf does not cause *lcons*	C(6)=C(7)= C(8)=C(9)=0	0.5703
lminq does not cause *lcons**	C(10)=C(11)= C(12)=C(13)=0	0.0001*
lcons does not cause *lmanf**	C(16)=C(17)= C(18)+C(19)=0	0.0056*
lminq does not cause *lmanf**	C(24)=C(25)= C(26)=C(27)=0	0.0001*
lcons does not cause *lminq*	C(30)=C(31)= C(32)=C(33)=0	0.2049
lmanf does not cause *lminq*	C(34)=C(35)= C(36)=C(37)=0	0.8347

*denotes the rejection of hypothesis at 5% significance level

The causality analysis identifies the direction of linkage among the concerned sectors. Figure 1 shows that there is a uni-directional causality between construction and manufacturing and the direction of link from construction to manufacturing. Similarly the linkage between construction and mining and quarrying is also uni-directional towards construction. The link between manufacturing and mining and quarrying is also uni-directional and the direction is mining and quarrying to manufacturing. However, none of the sector has causality direction towards to mining and quarrying, neither from construction nor from the manufacturing sector. This implies that the mining and quarrying sector of Malaysia

has forward linkage with construction and manufacturing sectors. Since the output of mining and quarrying consumed by the construction and manufacturing sectors as an intermediate goods (inputs) for their production such as ferrous and nonferrous metals, limestone, and granite. In contrast of this no directional causality from manufacturing either for construction or to mining and quarrying sector. This implies that the manufacturing sector output has not significant influence over construction and mining and quarrying as well.

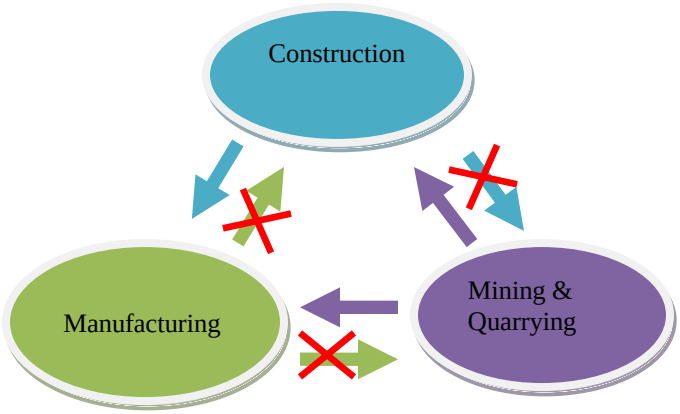

Figure 1 Causality Link

G. *Strength of the Estimated Model Equations*

The three parameters, R-Square, Durbin Watson value (D.W) and F-Statistics normally examine to test the strength, efficiency and correctness of the model. The explanatory power of the independent variable is shown by the value of R^2. The high value of R^2 may be concluded that the model is good and fit for an estimate. But the large value of R^2 does not directly imply that the model is accurate and efficient for estimation. The R^2 must be less than D.W for accurate model. The value of Durbin Watson should be in an appropriate range. The thumb rule is around 2 neither too little nor too high from 2. Both situations indicate there is an auto-correlation in the model. Third important factor is an F-statistic which should be significant. It indicates that all explanatory variables jointly influence the dependent variable. The estimated values of above discussed parameter for developed model equations are displayed in Table 9.

Table 9
Estimated model Equations Results

Parameters	Equation (8)	Equation (9)	Equation (10)
R-Square	0.6655	0.5546	0.5192
D.W	1.9384	1.9704	2.0338
F- Statistics	9.3350	5.8450	5.0687
Probability	0.0000	0.0000	0.0000

The estimated values of R^2 suggest that the VECM Equation 8 has good explanatory power while the Equation 9 and Equation 10 have moderate strength to explained respective dependent variables. The all estimated model equations are technically correct, since the R^2 is less than D.W and value of D.W is closed to 2. The F- statistics are also significant for all model equations. Therefore the estimated model equations 8, 9 and 10 have not any technical problem.

The two more conditions for good unbiased, non-spurious model are:

1) Residual of the model should be serially uncorrelated
2) Hetroskedasticity should not be exist in the residual

H. *Residual Serial Correlation Tests*

Breusch-Godfrey Serial Correlation LM Test is used to examine the residual serial correlation with the null hypothesis that there is no serial correlation in the residual series. Results of the test are presented in Table 10. There is no significant statistical evidence to reject the null hypothesis on the bases of Chi- Square probability. The probability of Chi-Square is greater than the 5% significance level in each model (Equation 8-10).

Table 10
Serial Correlation LM Test Result

Null Hypotheses	Probability Chi-Square		
	Eqn. (8)	Eqn. (9)	Eqn. (10)
No serial correlation in the residual	0.0743	0.6460	0.8286

*denotes the rejection of hypothesis at 5% significance level

I. *Hetroskedasticity Test*

The result of hetroskedasticity through ARCH is presented in Table 11. The null hypothesis, there is no hetroskedasticity in the residual series tested and found that the null hypothesis cannot be rejected in any estimated equation (Equation 8-10). This implies that the residual for each estimated equation is homoscedastic.

Table11
Hetroskedasticity Test Results

Null Hypotheses	Probability Chi-Square		
	Eqn. (8)	Eqn. (9)	Eqn. (10)
No hetroskedasticity in the residual	0.8205	0.6518	0.7539

*denotes the rejection of hypothesis at 5% significance level

VI. Conclusion

The primary objective of this study was to explore the linkages among the construction, manufacturing and mining and quarrying sectors of Malaysia and to estimate VECM equations to determine the long run and short run association among the sectors. There can be no reservation about the socio-economic significance of the three sectors for their role and contribution towards achievement of the national development goals such as poverty reduction, reducing unemployment and reducing the inequality in the Malaysian society.

ISBN: 978-1-61804-225-5

The linkages among the construction, manufacturing and mining and quarrying sectors investigated through Granger causality under restricted VAR, which suggests that the construction has uni directional backward linkages with mining and quarrying and manufacturing sector as well. In contrast the mining and quarrying has only forward linkages with construction and manufacturing sectors. However the no causal direction from manufacturing sector either for construction or to mining and quarrying..

The VECM results suggest that studied sectors have long run association .The speed of long run equilibrium adjustment for construction , manufacturing and mining and quarrying is 8% , 14% and 11% respectively.

The residuals of estimated model equations are white noise, free from serial correlation and hetroskedasticity. The results of the study are important, informative and useful for Malaysian Government, policy makers and the interested parties of the concerned sectors to develop future strategy for the growth of the concerned sectors and socio-economic development in Malaysia as well.

ACKNOWLEDGMENT

This study was conducted with the valuable support of Department of Civil Engineering, Universiti Technologi PETRONAS (UTP). The author would like to specially thank UTP for providing research facilities and environment for conducting the study.

REFERENCES

[1] P. Vijian, "The Malaysian economy: Here's to the next 50 golden years," in *Free Malaysias Today* ed. Malaysia, 2013.

[2] R. Bynoe, "Construction Sector Linkages In Barbodas," in *Presented at the Annual Review Seminar Research Department Central Bank of Barbados*, Barbados, 2009.

[3] M. Wild and O. Schwank, "Testing for Linkages in Sectoral Development: AnSVAR-Approach to South Africa," presented at the Annual Forum 2008 South Africa's, 2008.

[4] A. O. Hirschman, *The Strategy of Economic Development* vol. 10: Yale University Press, 1958 1958.

[5] G. Kaur, Bordoloi, S., Rajesh, R. , "An Empirical Investigation of the Inter-Sectoral Linkages in India," *Reserve Bank of India Occasional Papers.*, vol. 30, pp. 29-72, 2009.

[6] P. Dasgupta and D. Chakraborty, "The Structure of the Indian Economy," presented at the 15th International Input-Output Conference, Beijing, China, P.R, 2005.

[7] Bon.R, "Direct and Indirect resource utilizationby the construction sector: The case of the USA since World War II," *Habitat International*, vol. 12, pp. 49-74, 1988.

[8] R. Rameezdeena and T. Ramachandra, "Study of Linkages between Construction Sector and Other Sectors of the Srilankan Economy," *Construction Management and Economics* vol. Volume 26, Issue 5, 2008, pp. pages 499-506, 2008.

[9] R. K. Green, "Follow the leader: how changes in residential and non-residential investment predict changes in GDP," *Real Estate Economics, 25(2), 253–70*, 1997.

[10] S. C. Lean, "Empirical tests to discern linkages between construction and other economic sectors in Singapore," *Construction Management and Economics*, vol. 13, pp. 253-262, 2001.

[11] N. Saka and J. Lowe, "An Assesment of Linkages between Construction Sector and Other Sectors of Nigerian Economy," in *COBRA 2010*, Dauphine Universite Paris, 2010.

[12] R. A. Khan, Noor Amila Bt Wan Abdullah Zawawi, and M. F. Khamidi, "An Empirical Assessment of Linkage between the Construction Sector and Economic Growth (GDP) of Malaysia (2000-2010)," presented at the ICCOEE-2012 (ESTCON) Kaula Lumpur, 2012.

[13] V. Subramaniam, "Agricultural Intersectoral Linkages and their Contribution to Economic Development," PhD, College of Agriculture University of Kentucky, Lexington, Kentucky, 2010.

New Iterative Method of Cauchy problem solving for the First Order Differential Equations

Kamal younis[1], Nykolay Tsapenko[2]
[1]Department of Electrical Engineering, Salahaddin University, Erbil, Iraq
[2]Department of Mathematics, Moscow State Mining University
Email address:
younis@ieee.org (k. Younis), nt225@yandex.ru (n. Tsapenko)

Abstract
The method of Cauchy problem $y' = f(x,y)\ y(x_0) = 0$ *solving by successive approximations* $y_{n+1} = \int_{x0}^{x}\left[f(t,y_n) - f_y'(t,y_n)\right]e^{\int_t^x f_y'(t,y_n)dt}\,dt$ *is proposed. The theorem of given iterative process convergence is proved and estimations of its rapidity* $|y_{n+1} - y_n| < \frac{a}{b^{2^n-1}}$ *are received. Application of the method in solving Riccati's general equation is considered.*

Keywords: Iterative process, Cauchy problem, Riccati's equation

Inquiring rational methods of construction of Cauchy problem solving for ordinary first order differential equation is an important and enduring problem in the theory of differential equations. The most general method of integration i.e. Picar's successive approximation method demonstrate the existence and uniqueness of a solution and enables basically for seeking such a solution. However, its practical significance is considerably below the theoretical one. This fact is explained by relatively low rapidity of the convergence method for many equations. Meanwhile there is approximate integration method devised (conceived) by academician S.A Chaplygin in 1919 which converged with unusual rapidity, but unfortunately it hadn't the same degree of universality as Picar's successive approximation method. The reason of aforementioned condition is in the limitations emerging from the necessity to construct a solution on the basis of differential inequality characteristics and to make an assumption about the monotony of those operators under consideration.
The method presented below permits to be unrestricted from above mentioned undesirable characteristics of Picar's and Chaplygin's approaches to integration of Cauchy problem
Keeping at the same time their main advantages. [1]

1. The theorem on convergence of the method.

Let in the closed range G:$\{|x - x_0| \le a, |y| \le r\}$ function $f(x,y)$ is continuous and has continuous derivative$f_y'(x,y)$, then there will be such positive number h not exceeding α , that in interval $|x - x_0| \le h$ to Cauchy problem solving
$y' = f(x,y), y(x_0) = 0$ (1)
Iterative process converges:
$y_{n+1} = \int_{x0}^{x}\left[f(t,y_n) - f_y'(t,y_n)y_n\right]e^{\int_t^x f_y'(t,y_n)dt}\,dt$ (2)
And this process may be initiated by any continuous and differentiable function$y_0(x)$, so it would satisfy conditions as follows: $y_0(x_0) = 0, max|y_0(x)| \le r.$
$|x - x_0| \le h$
Proof:
If iterative process (2) converges uniformly, in this case it apparently converges to solution of integral equation
$y = \int_{x0}^{x}\left[f(t,y) - f_y'(t,y)\right]e^{\int_t^x f_y'(t,y)dt}dt$
This is simply proved to be equivalent to Cauchy problem (1). So to prove the theorem it is enough to confirm the interval existent of uniform convergence of the process (2).
First it is required to observe that from the condition of the theorem we have certain positive constants A and B for which in a whole range G the following inequalities are valid:
$$\left|f(x,y) - f_y'(x,y)y\right| \le A, \left|Re f_y'(x,y)\right| \le B\ .$$
As a result of these conditions the first term of relationship (2) produces an inequality
$|y_1| \le A\frac{e^{B|x-x_0|}-1}{B}$
Let's choose a number h from condition
$A\frac{e^{Bh}-1}{B} = r$
We'll receive
$h = \frac{1}{B}\ln\left(1 + \frac{B}{A}r\right)$ (3)
(Obviously if the right part of this relationship is in excess of a, in this case the condition must be: $h = a$).
Now as it may be stated that, all successive approximations $y_n(x), n = 0,1,2,\ldots$ In interval $[x_0 - h, x_0 + h]$ are continuous, differentiable and limited on absolute value by one and the same number r . Now we will demonstrate that, in this interval they converge uniformly.
Postulating generally that, $u_n = y_{n+1} - y_n$ we will bring the question of convergence of successive approximations to the question of convergence of series
$y_{n+1} = y_n + \sum_{k=0}^{n} u_k,\ \ n \to \infty$ (4)
To estimate the magnitude of its terms let us express U_{n+1} in terms of U_n and y_n.the iterative process (2) in differential form is as follows:
$y_{n+1}' = f(x,y_n) + f_y'(x,y_n)(y_{n+1} - y_n), y_{n+1}(x_0) = 0$
From those conditions we'll receive relationships for the functions U_n as follows:
$u_0' - f_y'(x,y_0)u_0 = f(x,y_0) - y_0'$
$u_{n+1}' - f_y'(x,y_{n+1})u_{n+1} = f(x,y_{n+1}) - y_{n+1}' =$
$= \left[\frac{f(x,y_n+u_n)-f(x,y_n)}{u_n} - f_y'(x,y_n)\right]u_n.$
Let us denote
$\alpha(x,y_n,u_n) = \frac{f(x,y_n,U_n)-f(x,y_n)}{U_n} - f_y'(x,y_n).$ (5)
Hence,
$u_0 = \int_{x_0}^{x}\left[f(t,y_0 - y_0'\right]e^{\int_t^x f_y'(t,y_o)dt}\,dt$ (6)
$u_{n+1} = \int_{x_0}^{x}\alpha(t,y_n,u_n)u_n e^{\int_t^x f_y'(t,y_{n+1})dt}\,dt$ (7)
In accordance with the conditions of the theorem, all the integrand functions in these equations in interval $[x - h, x + h]$ are uniformly

limited on absolute value. Moreover $\alpha(x, y_n, u_n) \to 0$ when $u_n \to 0$. Then establishing an order of infinitesimal value of $|\alpha(x, y_n, u_n)|$ is necessary to make some additional assumption regarding the function $f(x, y)$.the essence of the assumption will be described below and now we consider that, for all the numbers $n = 0,1,2, \ldots$ and $x \in [x_0 - h, x_0 + h]$ there is positively determined continuous function $\varepsilon(x)$ implementing the condition

$$|\alpha(x, y_n, u_n)| \le \varepsilon(x).$$

On the basic of (6), (7) we write down the recurrent inequalities

$$|u_0| \le \delta(x) = \left|\int_{x_0}^{x} \left|f(t, y_0) - y_0'\right| e^{B|x-t|} dt\right|, \quad (8)$$

$$|u_{n+1}| \le \left|\int_{x_0}^{x} \varepsilon(t)|u_n|\, e^{B|x-t|} dt\right|. \quad (9)$$

This results in estimations:

$$|u_n| \le \delta(x) \frac{\left|\int_{x_0}^{x} \varepsilon(t)dt\right|^n}{n!} \quad (10)$$

Thanks to these estimations the question of series (4) uniform convergence in the interval $|x - x_0| \le h$ Is solved positively and the statement of the theorem is proved.

An estimation of n −aapproximation deviation value $y_n(x)$ from exact solution $y(x)$:

$$|y - y_n| = \left|\sum_{k=n}^{\infty} u_k\right| \le \sum_{k=n}^{\infty} |u_k| \le \delta(x) \sum_{k=n}^{\infty} \frac{1}{k!} \left|\int_{x_0}^{x} \varepsilon(t)dt\right|^k \quad (11)$$

However, the formulation of the theorem and the proof expressed above do not give clear arguments in support of Cauchy problem solving by successive approximations (2) in comparison with the traditional process of Picar. The main advantage is in rapidity of process (2) convergence, the rate of which is not described fully by the estimation (10). Now we'll estimate absolute values of differences $\boldsymbol{u_n = y_{n+1} - y_n}$ in detail.

In addition to the condition of the theorem we'll make one of the following assumptions:

(a) If $f(x, y)$ is real-valued function of real variables, in this case in range $\overline{G}: \{|x - x_0| \le h, |y| \le r\}$ has limited second –order derivative $f_{y^2}''(x, y)$.

(b) if function $f(x, y)$ is complex valued function in this case let it be analytical in range $\bar{G}$ on argument y .then considering that for $(x, y) \in \bar{G}$ it is correct that, $\left|f_{y^2}''(x, y)\right| \le C$,

In both cases functions $\alpha(x, y_n, u_n)$ determined by equalities (5) in interval $|x - x_0| \le h$ are estimated as follows:

$$|\alpha(x, y_n, u_n)| \le \frac{C}{2}|u_n|$$

Replacing $\varepsilon(x)$ by $\frac{C}{2}|u_n|$ in the inequality (9) results the inequality

$$|u_{n+1}| \le \frac{C}{2}\left|\int_{x_0}^{x} |u_n|^2 e^{B|x-t|} dt\right|$$

Proceeding successively from one index to another we confirm that the following estimations are correct:

$$|u_n| \le \delta(x) \left[\frac{c}{2a_n}|x - x_0|\delta(x)\right]^{2^n - 1} \quad (12)$$

Where a_n is received recurrently from relationships

$$a_0 = 1, a_{n+1} = (2^{n+1} - 1)^{\frac{1}{2^{n+1}-1}} a_n^{\frac{2^{n+1}-2}{2^{n+1}-1}},$$

It is not difficult to reveal that the sequence $\{a_n\}$ is increasing monotonic and inclined towards finite limit. Hence, rewriting the inequality once again in reinforced form we obtain:

$$|u_n| \le \delta(x) \left[\frac{C}{2}|x - x_0|\delta(x)\right]^{2^n - 1}$$

Consequently, the deviation value (11) would be displayed as follows:

$$|y - y_n| \le \delta(x) \sum_{k=n}^{\infty} \left[\frac{C}{2}|x - x_0|\delta(x)\right]^{2^k - 1} \quad (13)$$

There obviously accepted that $\frac{C}{2}|x - x_0|\delta(x) < 1$

Let us note that with an aid of most rough approximation $y_0 = 0$, the function $\delta(x)$ could be estimated as follows:

$$\delta(x) < \delta_0 = \frac{r}{A} \max_{|x - x_0| \le h} |f(x,0)| \quad \text{So (13) results in an estimation}$$

$$|y - y_n| \le \delta(x) \sum_{k=n}^{\infty} \left[\frac{Ch}{2}\delta_0\right]^{2^k - 1} \quad (14)$$

This may be helpful for many practical calculations.

It remains for us to mention that the series in (13) and (14) have in comparatively more rapid convergence than the series in (11), which has Picar's process convergence rapidity.

Now we would consider the results of above described method in relation to the Riccati's general equation. [3]

1. Application of the method in relation to the Riccati's equation.

Let in the Reccati's equation

$$q' = i(k^2(x) - q^2) \quad (15)$$

Function $k(x)$ is determined and continuous in the interval $|x - x_0| \le a$. We'll construct successive approximations which converges to particular solution with initial condition $q(x_0) = k(x_o) = k_0 > 0$. Substituting $y = \frac{q(x)}{k_0} - 1$, $n = \frac{k(x)}{k_0}$ which for function y sets Cauchy problem $y' = ik_0(n^2(x) - 1 - 2y - y^2)$, $y(x_0) = 0$

For the right hand side of the equation

$f(x, y) = ik_0(n^2(x) - 1 - 2y - y^2)$,

And calculating

$f_y'(x, y) = -2ik_0(1 + y)$, $f_{y^2}''(x, y) = -2ik_0$,

$f(x, y) - f_y'(x, y)y = ik_0(n^2(x) - 1 + y^2)$

Considering that,

$|y| \le r$, $\max_{|x - x_0| \le a} |n^2(x) - 1| = m^2$

We may write down

$\left|f(x, y) - f_y'(x, y)y\right| \le k_0(m^2 + r^2) = A$,

$\left|Ref_y'(x, y)\right| \le 2k_0 r = B$,

$\left|f_{y^2}''(x, y)\right| \le 2k_0 = C$.

In accordance with formula (3) we obtain the value of the interval of iteration process (2) convergence:

$$h = \frac{1}{2k_0 r} ln\left(1 + \frac{2r^2}{m^2 + r^2}\right)$$

Making an assumption that $r = m$ we obtain $h = {}^{0,6931}/_{2k_0 m}$

Next we determine the relationship between numbers r and m when the interval of convergence has the greatest length. Assuming that $r = \theta m$, then

$$h = \frac{1}{2k_0 m} \frac{1}{\theta} ln\frac{1 + 3\theta^2}{1 + \theta^2},$$

$$\frac{dh}{d\theta} = \frac{1}{2k_0 m}\left[\frac{4}{(1 + \theta^2)(1 + 3\theta^2)} - \frac{1}{\theta^2} ln\frac{1 + 3\theta^2}{1 + \theta^2}\right].$$

The condition $\frac{dh}{d\theta} = 0$ leads to transcendental equation

$$1 - \left(1 + \frac{1}{4\theta^2} + \frac{3\theta^2}{4}\right) ln\frac{1 + 3\theta^2}{1 + \theta^2} = 0,$$

Root of which is the number $\theta^2 = 0{,}5485 \ldots$

($\theta = o, 7406 \ldots$).

Accordingly we calculate the optimal value

$$h = \frac{0{,}7231}{2k_0 m} \quad (16)$$

That we would take into the consideration when executing further calculations.

The estimation of the function $\delta(x)$ in accordance with the constant approximation $y_0 = 0$, $(q_0 = k_0)$ gives:

$$\delta(x) < \delta_0 = \frac{r}{m^2 + r^2} \max_{|x - x_0| \le h} |n^2(x) - 1| < 0{,}5m \quad (17)$$

Substituting (16), (17) into the inequality (14) we obtain:

$$|y - y_n| = \frac{|q - q_n|}{k_0} \le \sigma_n \delta(x) \quad (18)$$

Where

$\sigma_{n = \sum_{k=n}^{\infty} (0.5mk_0 h)^{2^k - 1} = \sum_{k=n}^{\infty} (0{,}181)^{2^k - 1}}$

The number σ diminishes very rapidly. Their values for the first five indexes are demonstrated in the table below:

n	0	1	2	3	4
σ_n	1,186716	0,186716	5,916x10^{-3}	6x10^{-6}	7x10^{-12}

Function $\delta(x)$ for Riccati's equation has the following shape:

$$\delta(x) = \left|\int_{x_0}^{x} |ik_0(n^2(t) - 1 - 2y_0 - y_0^2) - -y_0'|e^{B|x-t|}dt\right| =$$

$$= \frac{1}{k_0}\left|\int_{x_0}^{x} |i(k^2 - q_0^2) - q_0'|e^{B|x-t|}dt\right| \qquad (19)$$

The inequality (18) in a particular case can be refers to separately because it makes possible to estimate in the interval $|x - x_0| \le h$ a deviation from accurate solution, of any approximate solution of Riccati's equation an obligatory term of an iterative consequence (2).

$$|q - q_0| \le 1{,}1867k_0\delta(x) < \frac{0{,}2169}{h} \qquad (20)$$

Thus, the equation of estimating accuracy of some approximate Riccati's equation solving $q_0(x)$ as a matter of fact produces an estimation or calculation of corresponding integral (19).

For approximate solution presented in [3], it is possible to estimate the integral (19) obviously if the factor $k(x)$ is considered as a real, positive, monotonic and the initial point $x = x_0$ is established in such a manner that $k(x) \le k_0$.

Under these conditions, let's make proper manipulations.

The estimation of approximation of the firs type.

Let q_0 to be determined equality

$$q_0 = kexp\left\{-e^{-2i\int kdx}\int_{x_0}^{x}\frac{k'}{k}e^{2i\int kdx}dx\right\}$$

Whence

$$\delta(x) \le \frac{e^{Bh}}{K_0}\left|\int_{x_0}^{x}\left|i(k^2 - q^2) - 2ikq_0 ln\frac{k}{q_0}\right|dx\right| \le$$

$$\le \frac{1{,}71}{k_0}\left|\int_{x_0}^{x}|kq_0|2\left(sh\left|ln\frac{k}{q_0}\right| - \left|ln\frac{k}{q_0}\right|\right)dx\right|$$

In this case the value $\left|ln\frac{k}{q_0}\right|$ permits dual estimation:

$$\left|ln\frac{k}{q_0}\right| \le \begin{cases} ln\frac{k_0}{k} = |\ln n| \\ max\left|\frac{k'}{k^2}\right| = M \\ [x_0, x] \end{cases}$$

Accordingly, we obtain the dual estimation for$\delta(x)$:

$$\delta(x) \le \begin{cases} 1{,}71k_0\left|\int_{x_0}^{x}\left(n - \frac{1}{n} - 2\ln n\right)ndx\right| \\ 2.1{,}71k_0(shM - M)\left|\int_{x_0}^{x} ndx\right| \end{cases}$$

The estimation of the approximations of second type.

Let q to be determined by equality

$$q = k - e^{-2i\int kdx}\int_{x_0}^{x} k'e^{2i\int kdx}dx$$

Whence

$$\delta(x) \le \frac{e^{Bh}}{k_0}\left|\int_{x_0}^{x}|i(k^2 - q_0^2) - 2ik(k - q_0)|\,dx\right| \le$$

$$\le \frac{1{,}71}{k_0}\left|\int_{x_0}^{x}|k - q_0|^2\,dx\right|$$

For value $|k - q_0|$ we have dual estimation

$$|k - q_0| \le \begin{cases} k_0 - k \\ kM, \end{cases}$$

This results in a dual estimation for function $\delta(x)$:

$$\delta(x) \le \begin{cases} 1{,}71\frac{1}{k_0}\left|\int_{x_0}^{x}(k_0 - k)^2\,dx\right| \\ 1{,}71\frac{M^2}{k_0}\left|\int_{x_0}^{x} k^2\,dx\right| \end{cases}$$

With regard to (16) and considering that $(k_0 - k)^2 \le k_0^2 - k^2$, we have:

$$\delta(x) < \begin{cases} 1{,}71m^2k_0h \\ 1{,}71M^2k_0h \end{cases} = \begin{cases} 0{,}6182m \\ 0{,}6182\frac{M^2}{m} \end{cases}$$

Estimation of approximation of the third type.

Let q_0 to be determined by equality

$$q = k\left(1 + ke^{-2i\int kdx}\int_{x_0}^{x}\frac{k'}{k^2}e^{2i\int kdx}dx\right)^{-1}$$

Whence

$$\delta(x) \le \frac{e^{Bh}}{K_0}\left|\int_{x_0}^{x}|i(k^2 - q_0^2) - 2iq_0(k - q_0)|\,dx\right| \le$$

$$\le \frac{1{,}71}{K_0}\left|\int_{x_0}^{x}|k - q_0|^2\,dx\right|$$

The value $|k - q_0|$ is estimated as follows:

$$|k - q_0| \le \begin{cases} k_0 - k \\ \frac{M}{1-M}k \end{cases}$$

Accordingly we obtain the estimation of the function $\delta(x)$:

$$\delta(x) \le \begin{cases} 1{,}71\frac{1}{k_0}\left|\int_{x_0}^{x}(k_0 - k)^2dx\right| \\ 1{,}71\frac{M^2}{k_0(1-M)^2}\left|\int_{x_0}^{x} k^2\,dx\right| \end{cases}$$

Conclusion

In this paper we suggest a new iterative process (2), which converges to solution of Cauchy problem (1). The theorem about convergence of this process in interval$|x - x_0| \le h$, where h is given by formula (3), is proved. The value of the new method consists of its exceptional strong convergence, which is determined by inequality (14). The effectiveness of the method is illustrated in solving the general Riccati's equation.

REFERENCES

[1].Chaplygin S.A. **New method for an approximate integration of differential equations**. – Moscow, State Technical-Theoretical Publisher, 1932.

[2].Petrovsky I.G. **Lectures on the Theory of Ordinary Differential Equations**. – Moscow, Nauka, 1970.

[3].Tsapenko N.E."**New formulas for an approximate solution of the one-dimensional wave equation."** Differential Equations. – V.25, No.11, 1989.

Mathematical modelling for studying the influence of the initial stress and relaxation time on reflection waves in thermo-piezoelectric half-space

Fatimah A. Alshaikh[1] and Abo-el-nourN. Abd-alla[2]

Abstract—The aim of this study is to illustrate of the influence of the thermal relaxation time according the Lord-Shulman model and the initial stress on the reflection of plane waves in an elastic transversely isotropic thermo-piezoelectric half-space. The governing equation and suitable boundary conditions of a transversely isotropic thermo-piezoelectric medium are solved to obtain reflection coefficients when incident waves are falling at the interface between vacuum and half-space. The effects of thermal relaxation time and the initial stress are calculated numerically and shown graphically on these coefficients

Keywords—Reflection coefficients; Thermo-piezoelectricity; Thermal relaxation time; Lord-Shulman model; Cadmium Selenide; Hexagonal crystals.

Nomenclature

$E_i = -\varphi_{,i}$is the electric field,
$u_i, \varphi,$and$T$ are the mechanical displacement, electric potential and absolute temperature,
$D_i$is the electric displacement,
$\sigma_{ij}, \sigma_{kj}^o$are the stress and initial stress tensors,
$\varepsilon_{ij}$is the strain,
$\gamma_{ij}$is the thermal elastic coupling tensors
$\rho$is the density of the medium,
$C_{ijkl}$is the elastic parameters tensor,
$e_{ijk}$is the piezoelectric constants,
$P_{ij}$is the dielectric moduli,
$d_i$is the pyroelectric moduli,
$t_o$are thermal relaxation times,
$K_{ij}$is the heat conduction tensor,
$T_o$is the reference temperature,
$C_E$are the specific heat at constant strain,
$\delta_{ik}$is the Kronecker delta

[1] F. A. Alshaikh, Department of Mathematics, Faculty of Science, Jazan University, Jazan, Saudi Arabia (e-mail: dr.math999@hotmail.com).

[2] A. N.Abd-alla,Department of Mathematics, Faculty of Science, Jazan University, Jazan, Saudi Arabia (e-mail: aboelnourabdalla@yahoo.com).

I. Introduction

Piezo-thermoelasticity theories, which admit a finite speed for thermal signals, have been receiving a lot of attention for the past four decades. The theory of thermo-piezoelectricity was first proposed by Mindlin[1]. The physical laws for the thermo-piezoelectric materials have been explored by Nowacki [2]-[4].Chandrasekharaiah[5],[6] has generalized Mindlin's theory of thermo-piezoelectricity to account for the finite speed of propagation of thermal disturbances. Various authors have worked on wave propagation in isotropic thermo-piezoelectricity. For example, Sharma and Kumar [7],Sharma and Walia[8],[9], Alshaikh[10].

The problem of reflection of plane waves at a plane interface of piezoelectric and thermoelasticity media has been discussed by many authors, Abd-alla and Al-dawy[11] discussed the reflection phenomena of *SV* waves in a generalized thermoelastic medium, Sharma et. al. [12] reflection of generalized thermoelastic waves from the boundary of a half-space.The reflection waves in pyroelectric and Piezoelectric Materials investigated by Kuang and Yuan [13], Alshaikh[14] studied the reflection transverse waves in the Green- Lindsay theory for kind of smart materials under initial stress and relaxation times effect. The effect of the initial stresses on the reflection and transmission of plane wave propagation are illustrated in many recent contributions such as [15]-[19].

In the present contribution, reflection of plane waves under initial stress of a hexagonal thermo-piezoelectric solid half-space is studied. Reflection coefficients of various reflected waves are obtained and illustrated numerically for a particular model to analyze effects of initial stressand thermal relaxation.

II. Governing equations

Following Lord and Shulman [20] and Sharma and Walia[8], the constitutive relations and hexagonal thermopiezoelectric equations under initial stress and relaxation time effect for two dimensions motion are given by:

Equation of motion and Gauss's equation

$$\left.\begin{aligned} \sigma_{ij,j} + \left(u_{ik}\sigma_{kj}^o\right)_{,j} &= \rho\ddot{u}_i, \\ D_{i,i} &= 0 \end{aligned}\right\} \quad (1)$$

Heat conduction equation

$$K_{ij}T_{,ij} = T_o\left[\gamma_{ij}\left(\dot{u}_{i,j} + t_o\delta_{ik}\ddot{u}_{i,j}\right) - d_{ij}\left(\dot{\varphi}_{,i} + t_o\delta_{ik}\ddot{\varphi}_{,j}\right)\right]$$

$+\rho C_E\left(\dot{T}+\delta_{ik}\ddot{T}\right)$(2)

The strain-displacement relation and the electric field according to the quasi-static approximation have the forms as:

$$\left.\begin{aligned}\varepsilon_{ij}&=\frac{1}{2}\left(u_{i,j}+u_{j,i}\right),\\ E_i&=-\varphi_{,i}\end{aligned}\right\} i,j=1,2,3.(3)$$

Stress-strain-temperature and electric field relations

$\sigma_{ij}=C_{ijkl}\varepsilon_{kl}-e_{kij}E_k-\gamma_{ij}T$ (4)

The relation between the electric displacement, strain, electric field, and temperature

$D_i=e_{ikl}\varepsilon_{kl}+P_{ik}E_k+d_iT$ (5)

III. SOLUTION OF THE PROBLEM FOR INCIDENT *QP*-WAVE

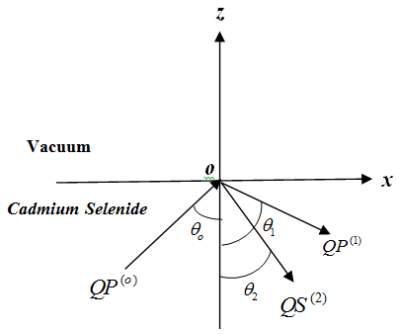

Figure 1

We consider a thermopiezoelectric plane wave *QP*propagating under initial stress through the medium, which we identify as the region $z \le 0$ and falling at the plane z = 0, with its direction of propagation making an angle θ_o with the normal to the surface. Corresponding to incident wave, we get the waves in mediumas reflected *QP*-, *QS*-, φ- and *T*- waves. The complete geometry of the problem is shown in Figure 1. Let the wave motion in this medium be characterized by the displacement $\vec{u}(u,0,w)$, the temperature T vector, and the electric potential functionφ, all these quantities being dependent only on the variablesx,z,t. We assume solution of the form (Achenbach [21]):

$(u^{(o)},w^{(o)},\varphi^{(o)},T^{(o)})=(A_o\sin\theta_o\,,A_o\cos\theta_o\,,B_o,C_o)\,exp[\vartheta_o]$

$(u^{(1)},w^{(1)},\varphi^{(1)},T^{(1)})=$

$(A_1\sin\theta_1\,,-A_1\cos\theta_1\,,B_1,C_1)\,exp[\vartheta_1]$

$(u^{(2)},w^{(2)},\varphi^{(2)},T^{(2)})=(A_2\cos\theta_2\,,A_2\sin\theta_2\,,B_2,C_2)\,exp[\vartheta_2]$ (6)

where

$\vartheta_0=ik_o(x\sin\theta_o+z\cos\theta_o-C_{Lo}t),$

$\vartheta_1=ik_1(x\sin\theta_1-z\cos\theta_1-C_{L1}t),$

$\vartheta_2=ik_2(x\sin\theta_2-z\cos\theta_2-C_{T2}t),$

Also, here $C_{L0}=\omega/k_0\,,C_{L1}=\omega/k_1\,,C_{T2}=\omega/k_2$are the velocity of incident *QP*, reflected *QP*, reflected *QS* wave.

IV. THE BOUNDARY CONDITIONS

The free mechanical boundary conditions

$\sigma_{zx}^{(O)}+\sigma_{zx}^{(1)}+\sigma_{zx}^{(2)}=0$ (7)

$\sigma_{zz}^{(O)}+\sigma_{zz}^{(1)}+\sigma_{zz}^{(2)}=0$ (8)

The electrical condition

$\varphi^{(O)}+\varphi^{(1)}+\varphi^{(2)}=0$ (9)

The thermal condition

$T^{(O)}+T^{(1)}+T^{(2)}=0$ (10)

Using equations (3-4), and (6) of hexagonal (6 mm) crystals into equations (7)-(10), we obtain the following set of equations:

$ik_o[C_{44}\sin 2\theta_o\,A_o+e_{15}\sin\theta_o\,B_o]\exp[\vartheta_0]$
$-ik_1[C_{44}\sin 2\theta_1\,A_1-e_{15}\sin\theta_1\,B_1]\exp[\vartheta_1]$
$-ik_2[C_{44}\cos 2\theta_2\,A_2-e_{15}\sin\theta_2\,B_2]\exp[\vartheta_2]=0$(11)

$ik_o[(C_{13}\sin^2\theta_o+C_{33}\cos^2\theta_o)A_o+e_{33}\cos\theta_oB_o-$
$(\gamma_3/ik_o)C_o]\exp[\vartheta_0]-ik_1[(C_{13}\sin^2\theta_1+C_{33}\cos^2\theta_1)A_1-$
$e_{33}\cos\theta_1B_1-(\gamma_3/ik_1)C_1]\exp[\vartheta_1]+ik_2[(C_{13}-$
$C_{33})sin\theta_2\cos\theta_2A_2-e_{33}\cos\theta_2B_2-$
$(\gamma_3/ik_2)C_2]\exp[\vartheta_2]=0$ (12)

$B_o exp[\vartheta_o]+B_1\,exp[\vartheta_1]+B_2\,exp[\vartheta_2]=0$(13)

$C_o exp[\vartheta_o]+C_1\,exp[\vartheta_1]+C_2\,exp[\vartheta_2]=0$(14)

Equations (11-14) must be valid for all values of *t*and x, hence

$$\left.\begin{aligned}\vartheta_o=\vartheta_1=\vartheta_2,\\ k_o\sin\theta_o=k_1\sin\theta_1=k_2\sin\theta_2,\\ k_oC_{Lo}=k_1C_{L1}=k_2C_{T2}=\omega\end{aligned}\right\} \quad (15)$$

From the above relations, we get

$$\left.\begin{aligned}k_o=k_1,\theta_o=\theta_1,C_{Lo}=C_{L1},\\ k_2/k_o=C_{Lo}/C_{T2}=\tau,\\ \sin\theta_2=\sin\theta_o/\tau\end{aligned}\right\}(16)$$

Furthermore, we should now use the equations (6) when z=0 of the media, i.e., using equations (1-2) which will give us additional relations between amplitudes

$$\left.\begin{aligned}\chi_oA_o+R_oB_o+\mu_oC_o=0,\\ \chi_1A_1+R_1B_1+\mu_1C_1=0,\\ \chi_2A_2+R_2B_2+\mu_2C_2=0\end{aligned}\right\}(17)$$

$$\left.\begin{aligned}L_oA_o+G_oB_o+S_oC_o=0,\\ L_1A_1+G_1B_1+S_1C_1=0,\\ L_2A_2+G_2B_2+S_2C_2=0\end{aligned}\right\}(18)$$

$$\left.\begin{aligned}E_oA_o+D_oB_o+F_oC_o=0,\\ E_1A_1+D_1B_1+F_1C_1=0,\\ E_2A_2+D_2B_2+F_2C_2=0\end{aligned}\right\}(19)$$

where

$\chi_o=-\sin\theta_o[\rho C_{Lo}^2-(C_{11}+\sigma_{xx}^o)\sin^2\theta_o-(C_{13}+2C_{44}+\sigma_{zz}^o)\cos^2\theta_o]$

$R_o=(e_{13}+e_{15})\sin\theta_o\cos\theta_o,\ \mu_o=-i\gamma_1\sin\theta_o/k_o$

$\chi_1=-\chi_o,\quad R_1=R_o,\quad \mu_1=-\mu_o,$

$\chi_2=\cos\theta_2[\rho C_{T2}^2-(C_{11}+\sigma_{xx}^o)\sin^2\theta_2-(C_{44}+\sigma_{zz}^o)\cos^2\theta_2+(C_{13}+C_{44})\sin^2\theta_2]$

$R_2=(e_{13}+e_{15})\sin\theta_2\cos\theta_2,\ \mu_2=-i\gamma_1\sin\theta_2/k_2,$

$L_o=-[(e_{13}+2e_{15})\sin^2\theta_o\cos\theta_o+e_{33}\cos^3\theta_o],$

$G_o=P_{11}\sin^2\theta_o+P_{33}\cos^2\theta_o,\ S_o=id_3\cos\theta_o/k_o,$

$L_1=-L_o,\quad G_1=G_o,\ S_1=-S_o,$

$L_2=[(e_{13}+e_{15}-e_{33})\sin\theta_2\cos^2\theta_2-e_{15}\sin^3\theta_2]$

$G_2=P_{11}\sin^2\theta_2+P_{33}\cos^2\theta_2,\ S_2=-id_3\cos\theta_2/k_2$

$E_o=T_o(1-ik_ot_o\delta C_{Lo})(\gamma_1\sin^2\theta_o+\gamma_3\cos^2\theta_o),$

$D_o=-T_od_3(1-ik_ot_o\delta C_{Lo})\cos\theta_o,$

$F_o=[(K_1\sin^2\theta_o+K_3\cos^2\theta_o)/C_{Lo}]-[\rho iC_E(1-ik_ot_oC_{Lo})/k_o]$

$E_1=-E_o,\quad D_1=D_o,\ F_1=-F_o,$

$E_2=-T_o(1-ik_2t_o\delta C_{T2})(\gamma_1-\gamma_3)\sin\theta_2\cos\theta_2,$

$D_2=-T_od_3(1-ik_2t_o\delta C_{T2})\cos\theta_2,$

$F_2=[\rho iC_E(1-ik_2t_oC_{T2})/k_2]-[(K_1\sin^2\theta_2+K_3\cos^2\theta_2)/C_{T2}]$

Solving equations (17-19), we can determine the reflection coefficients as:

$A_1/A_o=(\eta_1+\eta_2)/(\eta_1-\eta_2)$, (20)

$A_2/A_o = 2/(\eta_2 - \eta_1)$(21)
$B_1/B_o = -A_1/A_o$ (22)
$B_2/B_o = (A_2/A_o - 1)$ (23)
$C_1/C_o = A_1/A_o$ (24)
$C_2/C_o = -(1 + A_1/A_o)$(25)
Where
$\eta_1 = Y_oY_1/Y_2, \eta_2 = Y_3Y_4/Y_5$
$Y_o = \tau(F_oR_o - D_oR_o)/(F_2R_2 - D_2R_2)$
$Y_1 = (C_{13} - C_{33})(D_2\mu_2 - F_2R_2)\sin\theta_2\cos\theta_2 + e_{33}(E_2\mu_2 - F_2\chi_2)\cos\theta_2 + \gamma_3(D_2\chi_2 - E_2R_2)/ik_2$
$Y_2 = (C_{13}\sin^2\theta_2 + C_{33}\cos^2\theta_o)(D_o\mu_o - F_oR_o) - e_{33}(E_o\mu_o - F_o\chi_o)\cos\theta_o + \gamma_3(D_o\chi_o - E_oR_o)/ik_o$
$Y_3 = \tau(D_o\mu_o - F_oR_o)/(D_2\mu_2 - F_2R_2)$
$Y_4 = [C_{44}(D_2\mu_2 - F_2R_2)\cos2\theta_2 + e_{15}(E_2\mu_2 - F_2\chi_2)\sin\theta_2]$
$Y_5 = [C_{44}(D_o\mu_o - F_oR_o)\sin2\theta_o - e_{15}(E_o\mu_o - F_o\chi_o)\sin\theta_o]$
We obtain the amplitude ratios from the equations (20-25).

V. APPLICATION TO PARTICULAR MODEL

The reflection coefficients of reflected *QP*, *QS*, *T* and φ waves depend upon angle of incidence, angle of reflection, various elastic and thermopiezoelectric parameters, initial stress and relaxation times. The effect of these parameters on the reflection coefficients may be analyzed for particular model of the medium. For the purpose of numerical computations, the following physical constants of Cadmium Selenide (CdSe) for lower medium are considered [9]

$C_{11} = 7.41 \times 10^{10}\ \mathrm{Nm^{-2}}, C_{12} = 4.52 \times 10^{10}\ \mathrm{Nm^{-2}},$
$C_{13} = 3.93 \times 10^{10}\ \mathrm{Nm^{-2}}, C_{33} = 8.36 \times 10^{10}\ \mathrm{Nm^{-2}},$
$C_{44} = 1.32 \times 10^{10}\ \mathrm{Nm^{-2}}, \rho = 5504\ \mathrm{Kgm^{-3}},$
$e_{13} = -0.160\ \mathrm{Cm^{-2}}, e_{33} = 0.347\ \mathrm{Cm^{-2}},$
$e_{15} = -0.138\ \mathrm{Cm^{-2}}, T_o = 298\ \mathrm{K},$
$\gamma_1 = 0.621 \times 10^6\mathrm{NK^{-1}m^{-2}}, \gamma_3 = 0.551 \times 10^6\mathrm{NK^{-1}m^{-2}},$
$d_3 = -2.94 \times 10^{-6}\mathrm{CK^{-1}m^{-2}}, K_1 = K_3 = 9\ \mathrm{Wm^{-1}K^{-1}}$
$\epsilon_{11} = 8.26 \times 10^{-11}\mathrm{C^2N^{-1}m^{-2}},$
$\epsilon_{33} = 9.03 \times 10^{-11}\mathrm{C^2N^{-1}m^{-2}}$
$C_E = 260\ \mathrm{J\,Kg^{-1}K^{-1}}, \omega = 2.14 \times 10^{13}\mathrm{s^{-1}},$
$t_o = 10^{-12} = 1\ \text{pico} - \text{sec}.$

The variations of phase velocities computed from
$c_{Lo} = c_{L1} = \sqrt{C_{44} + C_{11}\sin^2\alpha + C_{33}\cos^2\alpha + v_1}/\sqrt{2\rho},$
$c_{T2} = \sqrt{C_{44} + C_{11}\sin^2\alpha + C_{33}\cos^2\alpha - v_1}/\sqrt{2\rho},$
where $v_1 = \sqrt{v_{11} + v_{12}},$
$v_{11} = [(C_{11} - C_{44})\sin^2\alpha + (C_{44} - C_{33})\cos^2\alpha]^2,$
$v_{12} = (C_{13} + C_{44})^2\sin^2 2\alpha$
Numerical computations are restricted to incident *QP* wave only. For the incidence of *QP* wave, the reflection coefficients of *QP*, *QS* and *T* waves are computed for Lord and Shulman (L-S) theory with the angle of incidence after using the above physical constants. For L-S theory, the reflection coefficients are computed for the range $0 \le \theta_o \le 90^o$ of angle of incidence, and plotted in figures 2-9 which have the following observations:

Figures 2,3,4and 5 represent the relation between the imaginary part of reflection coefficient A_1/A_o, A_2/A_o, B_2/B_o and C_2/C_o as function of incident angle θ_o for various value of relaxation time for (L-S) model. While **Figures** 6,7,8 and 9show the effect of initial stress on the imaginary part of reflection coefficient A_1/A_o, A_2/A_o, B_2/B_o and C_2/C_o as function of incident angle θ_o for (L-S) model.

The real parts of those reflection coefficients have not any influence by the change of the thermal relaxation time in the model of (Lord-Shulman). While the real parts of those reflection coefficients have some affected by the change of the initial stress (we did not give the figures and the details for these influence due to a shortcut the contribution and the details will be given in the coming search).

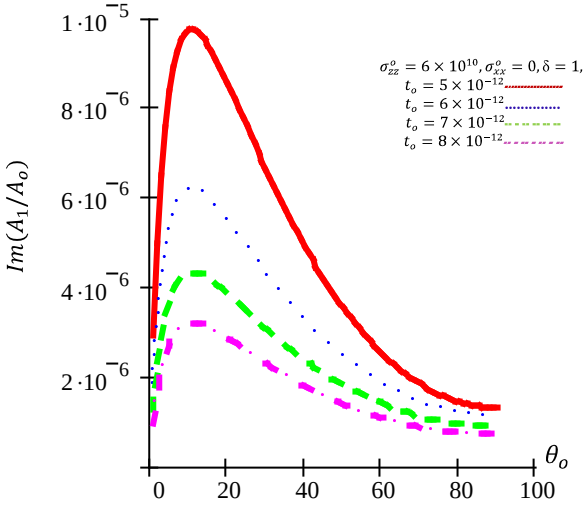

Fig. 2 Imaginary part of reflection coefficient A_1/A_o,as a function ofincidence angle $\theta_o$for various values of the relaxation times

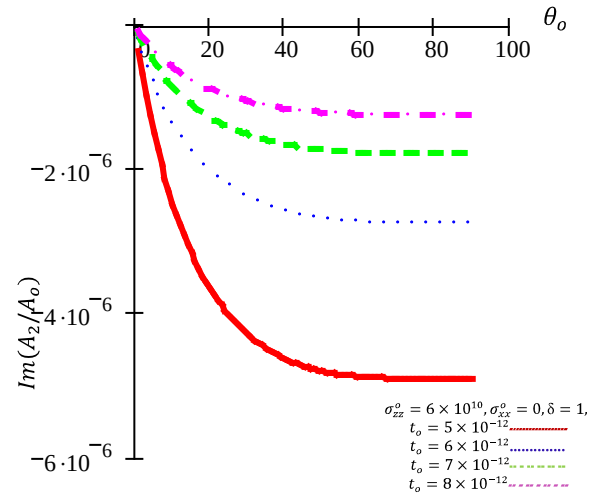

Fig. 3 Imaginary part of reflection coefficient A_2/A_oas a function of incidence angle θ_o for various values of the relaxation times.

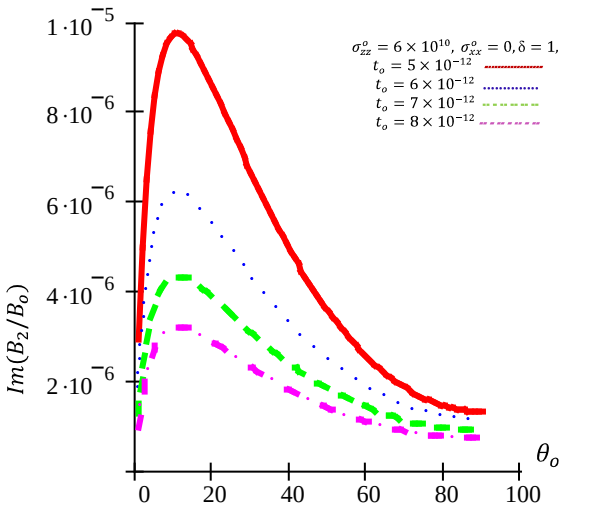

Fig. 4 Imaginary part of reflection coefficient(B_2/B_o)as a function of incidence angle$\theta_o$for various values of the relaxation times.

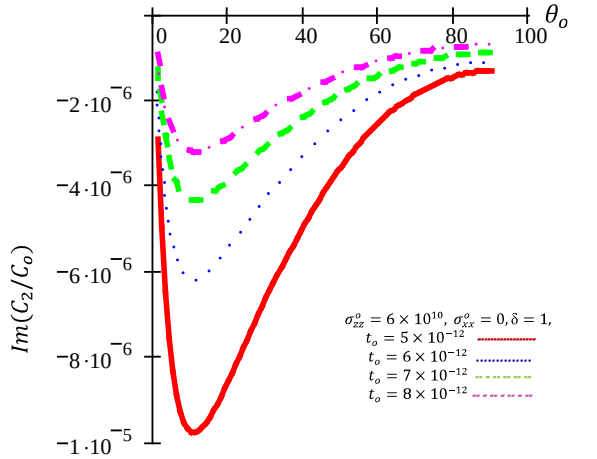

Fig. 5 Imaginary part of reflection coefficient(C_2/C_o)as a function of incidence angle $\theta_o$for various values of the relaxation times.

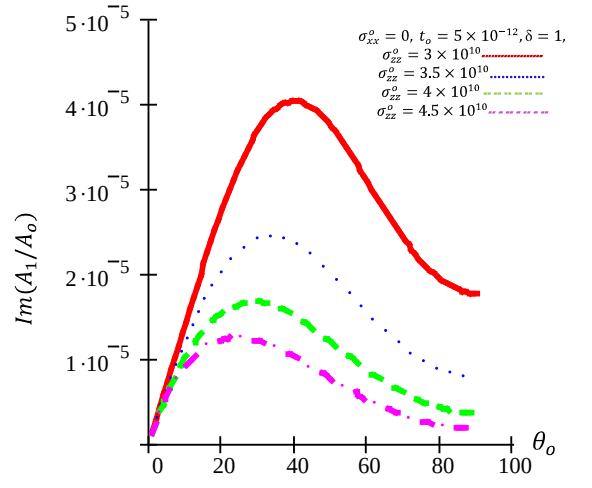

Fig. 6 Imaginary part of reflection coefficient (A_1/A_o) as a function of incidence angle $\theta_o$under effect of different values of the initial stress

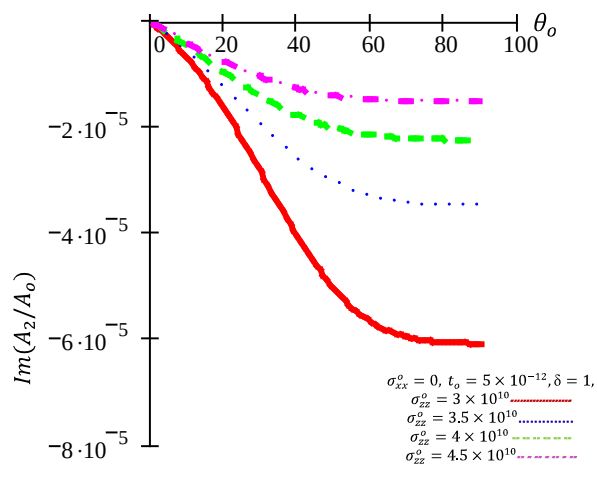

Fig. 7 Imaginary part of reflection coefficient A_2/A_o as a function of incidence angle $\theta_o$under effect of different values of the initial stress.

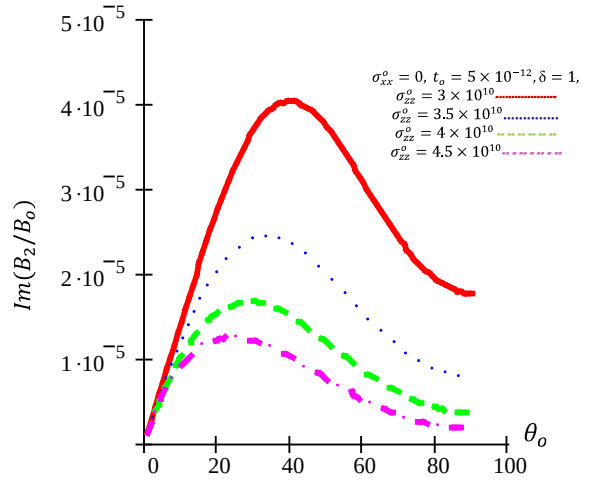

Fig. 8. Imaginary part of reflection coefficient (B_2/B_o) as a function of incidence angle $\theta_o$under effect of different values of the initial stress

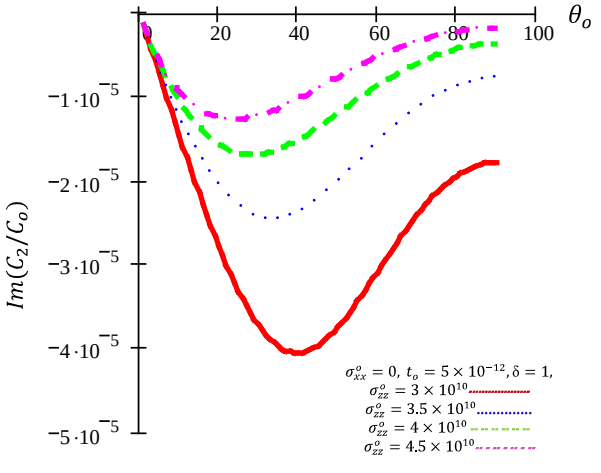

Fig. 9. Imaginary part of reflection coefficient (C_2/C_o) as a function of incidence angle θ_o under effect of different values of the initial stress.

ISBN: 978-1-61804-225-5

VI. Conclusion

Reflection of the plane waves is studied under initial stress of hexagonal thermopiezoelectric solid half-space. The reflection coefficients which dependon the angle of incidence, angle of reflection, various elastic and thermopiezoelectric parameters are computed for a particular model. From numerical computations, it is noticed that the reflection coefficients of various quasi-plane waves are affected significantly due to the presence of relaxation time and anisotropy in the medium. In particular, the *T* wave is most affected due to the presence of relaxation time and anisotropy. However, the reflection coefficients of *T* wave are much less than that of *QP* at each angle of incidence.

Acknowledgment

The authors are thankful for King Abdulaziz City for Science and Technology(KACST)for providing financial assistance to carry out thiswork via Project grant No. A-S-11-0588.

II.References

[1] R. D. Mindlin, “On the equations of motion of piezoelectric crystals,” in: N. I. Muskilishivili, Problems of continuum Mechanics, 70th Birthday Volume, SIAM, Philadelphia, pp. 282-290, 1961.

[2] W. Nowacki, “Some general theorems of thermo-piezoelectricity,” *Journal of Thermal Stresses,*vol. 1, no. 2, pp. 171–182, **1**978.

[3] W. Nowacki, “Foundation of Linear Piezoelectricity,” H. Parkus, Editor, “Interactions in Elastic Solids, ” Springer, Wein, 1979.

[4] W. Nowacki, “Mathematical models of phenomenological piezo-electricity, New Problems in Mechanics of Continua, pp. 29-49, University of Waterloo Press, Waterloo, Ontario, 1983.

[5] D. S. Chandrasekharaiah, “A Temperature-rate-dependent theory of thermopiezoelectricity”, *J. Thermal Stresses*, vol. 7, pp. 293-306, 1984.

[6] D. S. Chandrasekharaiah, “A Generalized linear thermoelasticity theory for piezoelectric media,” *ActaMechanica*, vol. 71, pp. 39-49, 1988.

[7] J. N. Sharma, M. Kumar, “Plane harmonic waves in piezo-thermoelasticmaterials,”*Indian Journal of Engineering and Material Science*, vol. 7, pp. 434-442, 2000.

[8] J.N. Sharma, V. Walia, “Further investigations on Rayleigh waves in piezothermoelasticmaterials,”*Journal of Sound and Vibration,*vol. 301, no. 1-2, pp. 189–206, 2007.

[9] J.N. Sharma, V. Walia and S.K. Gupta, “Reflection of piezo-thermoellastic waves from the charge and stress free boundary of a transversely isotropic half space,” *International Journal of Engineering Science*, vol. 46, no. 2, pp. 131–146, 2008.\

[10] F. Alshaikh, The mathematical modelling for studying the influence of the initial stresses and relaxation times on reflection and refraction waves in piezothermoelastic half-space, ”, *J. Applied Mathematics*, vol. 3, no. 8, pp. 819-832, 2012.

[11] A. N. Abd-alla and A. A. S. Al-dawy, “The reflection phenomena of SV waves in a generalized thermoelastic medium,” *International Journal of Mathematics and Mathematical Sciences*, vol. 23, no. 8**,** pp. 529–546, 2000.

[12] J.N. Sharma, V. Kumar and D. Chand, “Reflection of generalized thermoelastic waves from the boundary of a half-space,” *Journal of Thermal Stresses*, vol. 26, no. 10**,** pp.925–942,2003.

[13] Z.-B. Kuang, and X.-G. Yuan, “Reflection and transmission of waves in pyroelectric and piezoelectric materials,” Journal of Sound and Vibration, vol. 330, no. 6, 1111–1120, 2011.

[14] F. Alshaikh, Reflection of Quasi Vertical Transverse Waves in the Thermo-Piezoelectric Material under Initial Stress (Green- Lindsay Model), ”, J. *Int. J. Pure Appl. Sci. Technol.*,vol. 13, no. 1, pp.27–39,2012.

[15] A. N. Abd-alla and F. Alshaikh, "The Effect of the Initial Stresses on the Reflection and Transmission of Plane Quasi-Vertical Transverse Waves in Piezoelectric Materials", *International Journal of Mathematical and Statistical Sciences* 1:1 (2009).

[16] A. N. Abd-alla and F. Alshaikh, "Reflection and refraction of plane quasi-longitudinal waves at an interface of two piezoelectric media under initial stresses", Arch ApplMech (2009) 79: 843–857.

[17] A. N. Abd-alla and F. Alshaikh ,"The Effect of the Initial Stresses on the Reflection and Transmission of Plane Quasi-Vertical Transverse Waves in Piezoelectric Materials", World Academy Of Science, Engineering And Technology,50, pp.660-668 (2009).

[18] A. N. Abd-alla, H. A. Eshaq and H. El-haes The phenomena of reflection and transmission waves in smart nano materials, Journal of Computational and Theoretical Nanoscience, V8, pp. 1-9 (2011).

[19] A. N. Abd-alla, F. A. Al-sheikh and A. Y. Al-Hossain, "The reflection phenomena of quasi-vertical transverse waves in piezoelectric medium under initial stresses", Meccanica, 47, pp. 731-744 (2012)

[20] H. Lord and Y. Shulman, “A generalized dynamical theory of thermoelasticity,”*Journal of The Mechanics and Physics of Solid*, vol. 15, pp. 299-309, 1967.

[21] J.D. Achenbach, “Wave Propagation in Elastic Solids,” North-Holland Publishing Company- Amsterdam, 1973.

Integration of migration flows. A diffusive theory

M. Fabrizio - Department of Mathematics, University of Bologna

***Abstract*—The subject of this research is the presentation of a model for studying the integration of migration flows with the resident population. The basic element for social cohesion is the cultural level of the people involved. In this study, we hypothesize a similarity between diffusion laws of the heat and culture, represented respectively by equations on the knowledge and temperature. The integration of migration flows is described by the use of the Cahn-Hilliard equation.**

Key words: Social and economic integration, Thermodynamics, Phase transitions, Cahn-Hilliard equation.

I. Introduction

Fig.1 - Symbolic integration pictures

Fig.2 - An impressive picture that well describes migration issues

The growing role of the problems linked to migration and integration for the political and economic development of social systems is becoming very important. Stimulating interest in the mathematical modeling of migration and integration.

In this framework, the equations which describe the evolution of the culture is represented by diffusion equations on the knowledge, likewise to the equation that describes the heat diffusion.

Moreover, we suppose that the social cohesion in the integration processes is controlled by the cultural level of the populations [6],[5],[4],[7],[1],[2],[3],[9],[10].

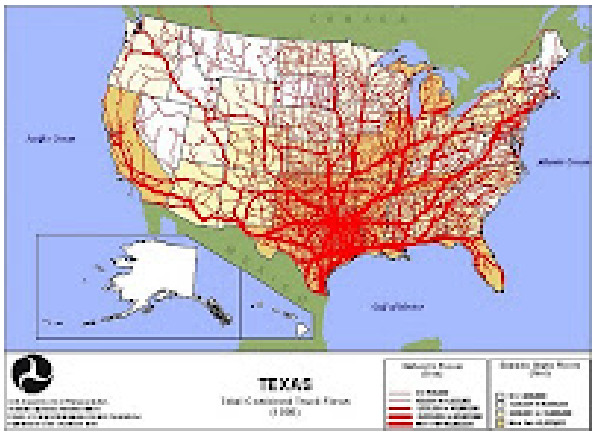

Fig.3 - The flow migration form Texas to US

ISBN: 978-1-61804-225-5

In this work we present a summary of the paper [8], in which it was studied the migration and integration of different populations by a differential system containing the Cahn-Hilliard equation. This issue describes the integration or separation law of two ethnic fluxes, according to a control factor given by the cultural levels of two populations, whose evolutions are described by a system of diffusion equations. Moreover, we assume that the homogenization process occurs when the mean of two cultural levels exceeds a critical value.

Fig.4 Diffusion process

Fig.5 - The homogenization of the mixture

Fig.6 - Integration process

II. INTEGRATION MODEL

In this section, we study the interaction of two ethnic groups A_1 and A_2 with different cultures (traditions, religions, ecc.). So in a fixed bounded domain $\Omega \subset \boldsymbol{R}^2$ and time interval $[0,T]$, the total mass M_1 and M_2 of two populations will be constants. In the following, we denote with ρ_1 and ρ_2 the local densities of the two groups, while the specific densities of the populations A_1 and A_2 are the same, denoted by ρ. Finally, the local concentration $c \in [-1,1]$ of the component A_1 is given by $c = \frac{2\rho_1 - \rho}{\rho}$. In this framework, we consider the mean velocity $\mathbf{v}$ of the mixture, defined by

$$\mathbf{v} = \frac{\rho_1 \mathbf{v}_1 + \rho_2 \mathbf{v}_2}{\rho} \tag{II.1}$$

where $\mathbf{v}_1$ and $\mathbf{v}_2$ are the velocity related with the components A_1 and A_2. Thus, the evolution of the mixture will be represented by the equation of a viscous incompressible fluid

$$\rho \dot{\mathbf{v}} = -\nabla p + \rho \nabla \cdot (\nabla c \otimes \nabla c) + \nabla \cdot \upsilon(c) \nabla \mathbf{v} + \rho \mathbf{b} \tag{II.2}$$

where p is the pressure, $\upsilon(c)$ is the viscosity coefficient depending on c, the vector $\mathbf{b}$ denotes the external body forces. Moreover, because the density of the mixture is constant., we have $\nabla \cdot \mathbf{v} = 0$

The behavior of the concentration c will be described by the Cahn-Hilliard equation

$$\rho \dot{c} = \nabla \cdot M(c) \nabla \mu \tag{II.3}$$

where $M(c)$ is the mobility such that $M(c) \geq 0$, $M(-1) = M(1) = 0$. While μ is the supplemented potential defined by

$$\mu(c, \varphi_1, \varphi_2) = \gamma \nabla^2 c - \varphi_0 H'(c) - \frac{\varphi_1 + \varphi_2}{2} L'(c) \tag{II.4}$$

where the potentials H and L are defined by

$$H(c) = \frac{1}{4}(c^2 - 1)^2 \quad , \quad L(c) = \frac{c^2}{2} \tag{II.5}$$

while $\varphi_1 > 0$ and $\varphi_2 > 0$ represent the knowledge levels of the two components, while φ_0 is a critical value, which denotes the integration-separation phase transition, controlled by the mean value $\frac{\varphi_1 + \varphi_2}{2}$. Hence, we obtain by (II.3) and (II.4) the equation on the concentration c

$$\rho \dot{c} = \nabla \cdot M(c) \nabla (\gamma \nabla^2 c - \varphi_0 H'(c) - \frac{\varphi_1 + \varphi_2}{2} L'(c)) \tag{II.6}$$

Finally, for this problem we consider the boundary conditions

$$M(c) \nabla \mu \cdot \mathbf{n} = 0 \quad , \quad at \quad \partial\Omega \tag{II.7}$$

where $\mathbf{n}$ is the unit outward normal. Then, we study the evolution of the educational level by a diffusion equation. Thus, we introduce two equations related with the knowledge, which describe the cultural balance laws of two ethnic groups

$$\rho \dot{\varphi}_1 - \frac{1}{2} \dot{L}(c) + \frac{\nu}{2} \nabla^2 \mathbf{v} = \nabla \cdot \delta_1 \nabla \varphi_1 - \alpha(\varphi_1 - \varphi_2) + \rho s_1 \tag{II.8}$$

$$\rho \dot{\varphi}_2 - \frac{1}{2} \dot{L}(c) + \frac{\nu}{2} \nabla^2 \mathbf{v} = \nabla \cdot \delta_2 \nabla \varphi_2 - \alpha(\varphi_2 - \varphi_1) + \rho s_2 \tag{II.9}$$

ISBN: 978-1-61804-225-5

where $\alpha \geq 0$, s_1 and s_2 represent the cultural supplies, while δ_1 and δ_2 are the cultural conductivity (diffusibility) of the component A_1 and A_2. Therefore, the differential system is given by the equations (II.2), (II.6), (II.8) and (II.9) with the boundaries conditions (II.7) and

$$\begin{aligned} \mathbf{v}(x,t)|_{\partial\Omega} &= 0\ ,\ \ \nabla c(x,t)\cdot\mathbf{n}(x)|_{\partial\Omega} = 0\ , \\ \nabla\varphi_1(x,t)\cdot\mathbf{n}(x)|_{\partial\Omega} &= 0\ ,\ \ \nabla\varphi_2(x,t)\cdot\mathbf{n}(x)|_{\partial\Omega} = 0 \end{aligned} \tag{II.10}$$

and the initial conditions

$$\begin{aligned} \mathbf{v}(x,0) &= \mathbf{v}_0(x)\ ,\ c(x,0) = c_0(x)\ \ ,\ \ x\in\Omega \\ \varphi_1(x,0) &= \varphi_{10}(x)\ ,\ \varphi_2(x,0) = \varphi_{20}(x)\ \ ,\ \ x\in\Omega \end{aligned} \tag{II.11}$$

The evolution of the system is well described by the following pictures.

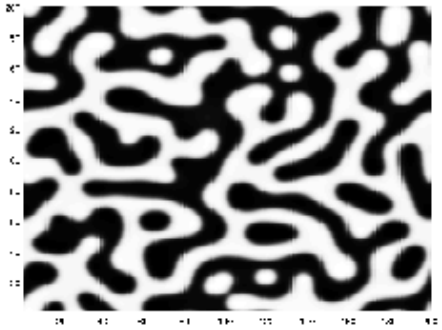

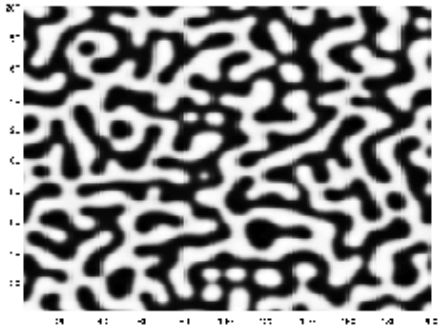

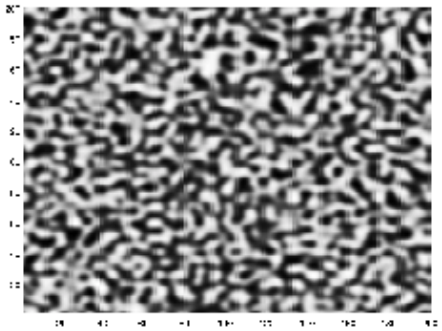

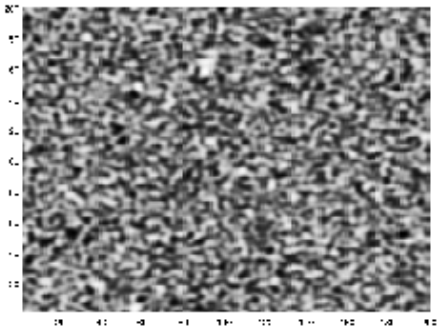

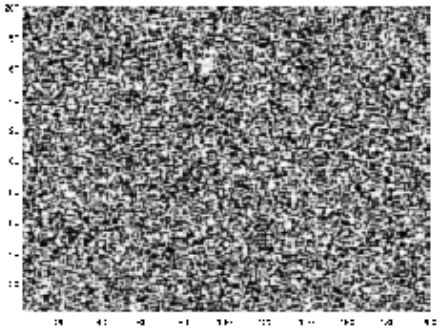

Fig.7 - The integration process by Cahn-Hilliard equation

REFERENCES

[1] C. Argyris and D. Schon, Organizational Learning: a Theory of Action Perspective, Reading, Menlo.Park:Addison-Wesley,1978.

[2] A. Berti, I. Bochicchio, *A mathematical model for phase separation: A generalized Cahn-Hilliard equation*, Math.Meth.Appl.Sci. (2011).

[3] L. Bevilacqua, A. C. Galeão, F. Pietrobon-Costa, S. L. Monteiro. Knowledge diffusion paths in a research chain. Mecanica Computacional. Vol. 24, 2061-2069. 2010.

[4] J.W. Cahn, C. M. Elliott and A. Novik–Cohen, *The Cahn–Hilliard equation with a concentration dependent mobility: motion of minus Laplacian of the mean curvature,* European J. Appl. Math. 7, No.3, 287-301.

[5] L.L. Cavalli-Sforza and M. Feldman, *Cultural Transmission and Evolution,* Princeton: Princeton University Press. 1981

[6] E. Collett, Immigrant Integration in Europe in a Time of Austerity. Migration Policy Institute. Washington 2011

[7] M. Fabrizio, C. Giorgi and A. Morro, *Phase separation in quasi-incompressible Cahn–Hilliard fluids*, European Journal of Mechanics B/Fluids **30** (2011), 281—287

[8] M. Fabrizio, J. Munoz Rivera, *An integration model for two different ethnic groups*, In press on Evolution Equations and Control Theory.

[9] M.E. Gurtin, *Generalized Ginzburg-Landau and Cahn-Hilliard equations based on a microforce balance*, Physica D **92** (1996), 178-192.

[10] G. Hedlund, *A model of knowledge management and the N-Form corporation*, Strategic Management Journal, **15**, 73-90,1994

Optimal Control Motion Planning

O. Hachour

***Abstract*—**Motion planning is one of the important tasks in intelligent control of an autonomous mobile robot. An optimal free path without collision is solicited in any design of movement of an autonomous mobile robot. The robots are compelling not for reasons of mobility but because of their *autonomy*, and so their ability to maintain a sense of position and to navigate without human intervention is paramount. To deal with optimal control concept and to present a real intelligent task, we propose an optimal control motion for autonomous mobile robot. The objective of optimization theory is to determine the control process that will cause a process to satisfy the physical constraints and at the same time minimize (or maximize) the performance measure (cost). The best response is gotten at the end where all boundary elements constraints are satisfied. Our discussion here will be restricted to systems which are described by ordinary differential equations (in state variable model). The theory developed is aimed to solve the problem of optimal control. That means that, find an admissible control which causes the systems to follow an admissible trajectory that minimize the performance. As case study of optimization theory, we have practiced the motion planning of an autonomous mobile robot where we have studied clearly the main steps of optimal control. This is a clarified model of optimal control of moving a robot where the elapsed time is the principal performance to be evaluated.

***Keywords*—** Intelligent system, optimal control, artificial intelligence, decision.

I. Introduction

The history of autonomous mobile robotics research has largely been a story of closely supervised, isolated experiments on platforms which do not last long beyond the end of the experiment. There is no universally accepted definition of the term robot. Typical definitions encompass notion of mobility, programmability, and the use sensory feedback in determining subsequent behavior [4,5].

Autonomous robots which navigate without human interventions are required in robotic fields. In order to achieve tasks, autonomous robots have to be intelligent and should decide their own action. When the autonomous robot decides its action, it is necessary to plan optimally depending on their tasks. More, it is necessary to plan a collision free path minimizing a cost such as time, energy and distance. When an autonomous robot moves from a point to a target point in its given environment, it is necessary to plan an optimal or feasible path avoiding obstacles in its way and answer to some criterion of autonomy requirements such as : thermal, energy, time, and safety for example [3,4].

A robotic system is an intelligent mobile machine capable of autonomous operations in structured and unstructured environment. It must be capable of sensing, thinking and acting. The mobile robot is an appropriate tool for investigating optional artificial intelligence problems relating to world understanding and taking a suitable action, such as , planning missions, avoiding obstacles, and fusing data from many sources.

According to the Robotics Industries Association (RIA): "A robot is a reprogrammable multifunctional manipulator designed to move material, parts, tools, or specialized devices through variable programmed motions for the performance of a variety of tasks".

This artificial *automaton* produce the remarkable repetitive actions that may be tedious and hazardous health human risks as exposure to unsafe materials like radioactive and high pressure in underwater applications.

The *automaton* mobile robots are able to react and act in structured or unstructured environments as human being. These machines are able of taking a suitable decision with appropriate best intelligence. Finally, the notion of simulating biological organism has a certain instinctive reproductive appeal and offers the possibility of satisfying our curiosity as to how come to be as we are. Being able to interact and communicate with robots in the same way we interact with people as long been a goal of Artificial Intelligence AI and robotic researches. However, much of the robotics research in the past has emphasized the goal of achieving autonomous agents.

Classical artificial intelligence systems presuppose that all knowledge is stored in a central database of logical assertions or other symbolic representation and that reasoning consist largely of searching and sequentially updating that database. While this model has been successful for disembodied reasoning system, it is problematic for robots.

The objective of intelligent mobile robots is to improve machine autonomy. This improvement concerns three (03) essential aspects. First, robots must perform efficiently some tasks like recognition, decision-making, and action which constitute the principal obstacle avoidance problems. They must also reduce the operator load by using natural language and common sense knowledge in order to allow easier decision making. Finally, they must operate at a human level with adaptation and learning capacities [5,6,7,8].

The navigation of mobile robots in an environment where stationary obstacles, and other moving objects, requires the

ISBN: 978-1-61804-225-5

existence of algorithms that are able to solve the path and motion planning problem of these robots so that collisions are avoided and the feasible path is found. On the other hand, a suitable control law has to be designed, in order for the mobile robot to execute the desired motion. The problem becomes more difficult when the parameters that describe the model and/or the workspace of the robot are not exactly known.

However, the mobile robot is an appropriate tool for investigating optional artificial intelligence problems relating to world understanding and taking a suitable action, such as, planning missions, avoiding obstacle, and finding data from many sources. Many traditional working machines already used are going through changes to become remotely operated or even autonomous. Technology has made this feasible by using advanced computer control systems.

To detect all possible obstacles, the robot is supposed to have vision system (camera). To operate in certain dynamic environments, the use of two or more sensors can guarantee to deliver acceptably accurate information all of the time. Thus the redundancy can be useful for autonomous systems as in the human sensory system

When an autonomous robot moves from a source point to a target point in its given environment it is necessary to plan an optimal or feasible path avoiding obstruction in its way and answering to autonomy requirements such as: thermal, energy, Communication Management, Mechanical design, etc.

The theory and practice of Intelligent Autonomous Robots IAR are currently among the most intensively studied and promising areas in computer science and engineering which will certainly play a primary goal role in future. These theories and applications provide a source linking all fields in which intelligent control plays a dominant role.

Technology has made this feasible by using advanced computer control systems. Also, the automotive industry has put much effort in developing perception and control systems to make the vehicle safer and easier to operate.

To perform all tasks in different environments, the vehicle must be characterized by more sever limits regarding mass volume, power consumption, autonomous reactions capabilities and design complexity.

Particularly, for planetary operations sever constraints arise from available energy and data transmission capacities, e.g., the vehicles are usually designed as autonomous units with: data transfer via radio modems to rely stations (satellite in orbit or fixed surface stations) and power from solar arrays, batteries or radio-isotope thermo electric generators (for larger vehicles).

Classical control design is generally a trial- and -error process in which various methods of analysis are used iteratively to determine the design parameters of an "acceptable" system. Acceptable system performance is generally defined in terms of time and frequency domain such as time arise, gain and phase margin, peak overshoot and bandwidth.

Radically difference performance criteria must be satisfied, however by complex, multiple-input, multiple outputs systems required to meet the demand s of modern technology. For example the design of a spacecraft attitude control system that minimizes fuel expenditure is not amenable to solution by classical methods. A new and direct approach to the synthesis of these complex systems , called optimal control theory, has been made feasible by the development of the digital computer.

This paper deals with the intelligent navigation optimal control of autonomous mobile robot in an unknown environment. The objective is to determine the control models that will cause a process a robot to move reaching the best path.

II. The Optimal Control Problem

Optimal control needs three steps to be developed which are

A. Mathematical Model

It is the model that describes the process to be controlled. The mathematical model is considered as a nontrivial part of any control problem. it is just the unified framework which it has a strong motivation before starting any control design. The objective is to obtain the simplest mathematical description that adequately predicts the response of the physical system to all anticipated inputs.

B. Physical constraints

After we have selected a mathematical model, the next step is to define the statement of physical constraints on the state and control values. The selection focus about admissibility concept. Admissibility is an important concept, because it reduces the range of values that can be assumed by the states and controls. Rather than consider all control histories and their trajectories to see which are the best (according to some criterion) we investigate those trajectories and controls that are admissible.

C. Performance measure (the cost)

In order to evaluate the performance of a system quantitatively; the designer selects a performance measure. An "optimal control" is defined as one that minimizes (or maximizes) the performance measure. In certain cases the problem statement may clearly indicate that to select for a performance measure. Whereas in other problems the selection is a subjective matter. Generally for any optimal control design the performance of a system is evaluated by a measure of the form.

$$J = h(x(tf), tf) + \int_{t0}^{tf} g(x(t), u(t), t)dt \quad (1)$$

Where t_0 and t_f are the initial and final time; *h* and *g* are scalar functions. t_f may be specified or "free" , depending on the problem statement . starting from the initial state $x(t_0)=x_0$ and applying a control signal u(t); for $t \in [t_0, t_f]$, causes a system to follow some state trajectory of the system.

The optimal control problem is to find an *admissible control U** which causes the system to follow an *admissible trajectory X**that minimizes or maximizes the performance measure [2]. In this context, an optimal control may be non unique.

A non-unique optimal control may complicate computational procedures, but they do allow the possibility of choosing among several controller configurations. This is certainly helpful to the designer, because he can then consider other factors, such as cost, size, reliability, etc; which may not have been included in the performance measure.

III. THE PROPOSED OPTIMAL CONTROL MOTION

Consider a robot shown in figure 1 is to be controlled to navigate from initial point position S to the target position T.

To simplify the model, let us approximate that the shape of the robot by a unit point mass, or by a material point in the beginning. At the end of conception we will take the size of this robot (just to be added to the material point or gravity center) . This physical format facilitates a lot of tasks. The distance of this robot from initial position at time t is denoted by d(t). The unit point mass can be accelerated, deviated, decelerated, or keeping a constant velocity.

The differential equation is given by:

$$d^{\cdot\cdot}(t) = \rho\, a(t) + \delta\, b(t) \tag{2}$$

Where :
a(t) the control vector of acceleration .
b(t) the control vector of deceleration .
ρ, σ are a weighting factors included to permit adjustment of the relative importance of the three terms in d(t).

The states variables are:

$$X_1(t) = d(t)$$
$$X_2(t) = d^{\cdot\cdot}(t) \tag{3}$$

The control variables are:

$$C_1(t) = a(t)$$
$$C_2(t) = b(t) \tag{4}$$

We define the physical constraints for the state variables as:

$$X_1(t_0) = S$$
$$X_1(t_f) = T \tag{5}$$
$$X_2(t_0) = 0$$
$$X_2(t_f) = 0 \tag{6}$$

Since the robot starts from rest (initial velocity is zero 0) and stops when reaching the target T.We can call these constraints by *admissible states* . A *history* of state values in the interval $[t_0, t_f]$ is called a state trajectory as it is shown in the figure 2 where we present an example of a single valued function of time which is denoted by x.

We assume the following constraints for the control inputs:

$$0 \le a(t) \le \max 1$$
$$-\max 2 \le b(t) \le 0 \tag{7}$$

Where max_1 is the maximum of acceleration
max_2 is the maximum of deceleration

These constraints are called admissible controls. The constraints are also called *boundary conditions* limit the system parameters.

This is certainly very useful we investigate only with those are admissible to reduce the range values and to satisfy some autonomy requirements such as: time, energy, thermal, etc. A history of control input values during the interval $[t_0, t_f]$ is called a control history.

The autonomy implies that the robot is capable of reacting to static obstacles and unpredictable dynamic events that may impede the successful execution of a task. To achieve this level of robustness, methods need to be developed to provide solutions to localization, map building, planning and control.

The robots are compelling not for reasons of mobility but because of their *autonomy*, and so their ability to maintain a sense of position and to navigate without human intervention is paramount.

For example, AGV (Autonomous Guided Vehicle) robots autonomously deliver parts between various assembly stations by following special electrical guide wires using a custom sensor. Several autonomy requirements must be satisfied to well perform the tasks of autonomous mobile robots.

After selecting the admissible trajectories (stets) and the admissible controls the next step is to evaluate the performance of a system quantitatively measure. Selecting of performance measure is the subjective matter, this is due if a nonunique existence of performance. In such cases the designer may be required to try several performance measures before selecting one which yields what he considers to be optimal performance.

For each investigated optimal control, we estimate the best performance measure. This is when a nonunique optimal control exits. Here we are seeking the absolute or global minimum of the performance measure of J, not merely local minima.

It may be helpful to visualize the optimization as shown in the figure3 . $U^{(1)}$,$U^{(2)}$,$U^{(3)}$ are points at which **J** has local or

relative minima $u^{(1)}$ is the point where J has its goal or absolute minimum.

For our case study: optimal motion planning of an autonomous mobile robots we investigate with the following performance measure:

$$J = t_f - t_0 \quad (8)$$

This is because the short elapsed time is the main necessity to reach the target without collision .we want that our autonomous mobile robot reach the target T as quickly as possible without damage taking into consideration all embedded factors of navigation while answering to the main criteria of autonomy requirements.

Navigation is one of the most challenging competences required of a mobile robot. Success in navigation requires success at the four building blocks of navigation: *perception*, the robot must interpret its sensors to extract meaningful data; *localization*, the robot must determine its position in the environment; *cognition*, the robot must decide how to act to achieve its goals; and *motion control*(see the figure 4), The robot must modulate its motor outputs to achieve the desired trajectory. Of these four components, localization plays the role to found the exact local points of the robot.

The robot has to find a collision-free trajectory between the starting configuration and the goal configuration in a static environment containing some obstacles. To this end, the robot needs the capability to build a map of the environment, which is essentially a repetitive process of moving to a new position, sensing the environment, updating the map, and planning subsequent motion. This is necessary to build the trajectory of sub positions " the feasible optimal trace line towards the target without collisions ».

When an autonomous robot moves from a source position to a target position, it must find a feasible connection between the source and the target. In other word: It is necessary to plan an optimal or feasible path avoiding obstacles in its way and answer to some criterion of autonomy requirements such as: thermal, energy, time, and safety for example.

To operate independently in unknown or partially known environments is the basic feature of an autonomous mobile robot. The autonomy implies that the robot is capable of reacting to static obstacles and unpredictable dynamic events that may impede the successful execution of a task. To achieve this level of robustness, methods need to be developed to provide solutions to localization, map building, planning and control. The development of such techniques for autonomous robot navigation is one of the major trends incurrent robotics research.

Configuration space obstacles have high artificial potentials that decline gradually with distance from the obstacle. At any instance, the robot calculates the derivative of the potential function and descends the maximal downward gradient in an effort to reach the minimum at the goal position. This calculation quickly determines the motion to take next.

For every configuration space, there is an optimal number of samples that must be selected to construct a sufficient approximation of configuration space connectivity.

Motion planning will frequently refer to motions of a robot in a 2D or 3D world that contains obstacles. The robot could model an actual robot, or any other collection of moving bodies, such as humans or flexible molecules.

A motion plan involves determining what motions are appropriate for the robot so that it reaches a goal state without colliding into obstacles. When the autonomous robot decides its action, it is necessary to plan optimally depending on their tasks and on the environments complexity.

To illustrate a complete problem formulation and to deal with principle of optimal control, let us now present the optimal control and trajectory for the autonomous mobile robot shown in the figure 6. We assume that the robot has enough fuel available to reach the target T.

The robot is simulated in different environments. To reflect the robot behavior acquired by learning in the explored environment and in new unvisited environments. The robot reacts in efficient and a satisfactory manner in these environments. The configuration of the environments changes by adding other shapes of static obstacles, in each situation the robot can navigate successfully. The flexible proposed approach is able to achieve the main task without collisions for every developed or proposed environment. The algorithm is implemented in several static environments; whereby the environment is studied in a two dimensional coordinate system. The algorithm permits the robot to move from the initial position to the desired position following an optimal estimated trajectory. Taking a suitable action and reacting at the appropriate way, the robot finds its safe way without collisions in efficient manner. The figure 5 shows one example of this training algorithm.

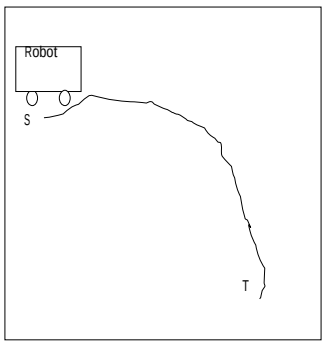

Fig. 1 A robot control problem

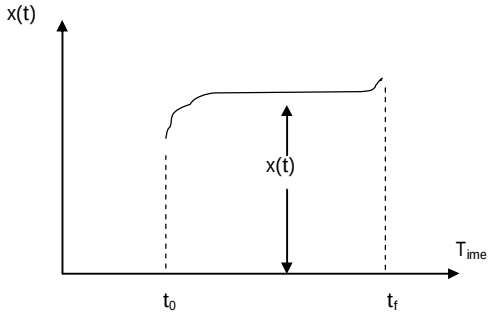

Fig.2 the state x(t) and its value

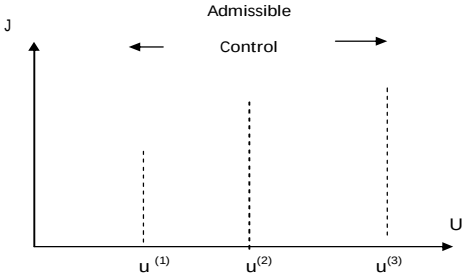

Fig.3 a representation of the optimization problem

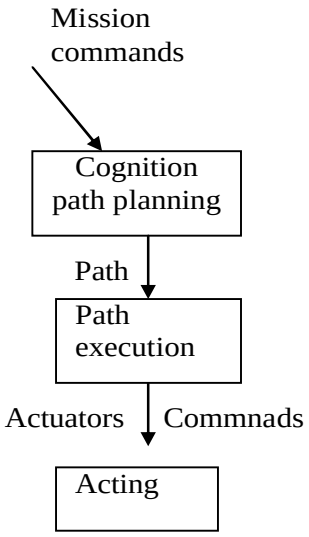

Fig. 4 Motion control

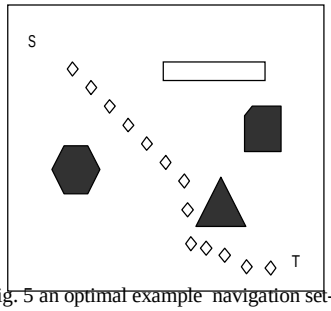

Fig. 5 an optimal example navigation set-up

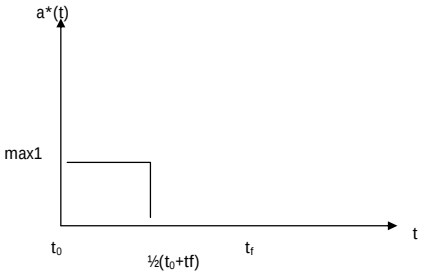

(a)

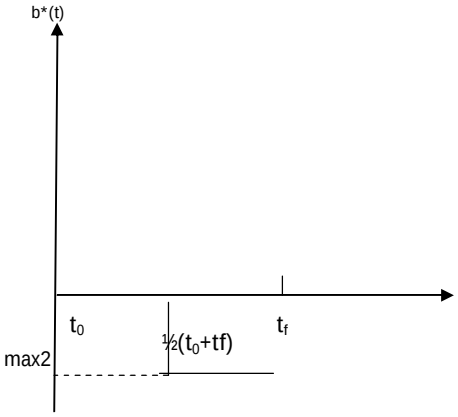

(b)

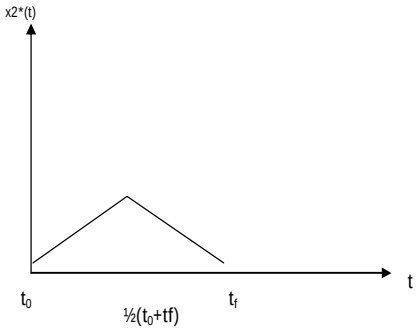

(c)

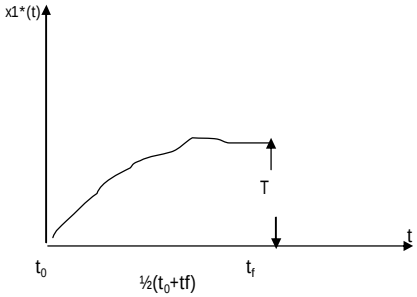

(d)

Fig.6 the optimal control and trajectory for the

IV. Conclusion

The theory and practice of Intelligent Autonomous Systems are currently among the most intensively studied and promising areas in computer science and engineering which will certainly play a primary goal role in future.

In this paper, we have presented a model of an optimal control optimal control motion for autonomous mobile robot. The objective of optimization theory is to determine the control process that will cause a process to satisfy the physical constraints and at the same time minimize (or maximize) the performance measure (cost). The best response is gotten at the end where all boundary elements constraints are satisfied..

The objective of optimal control theory is to determine the control signals that will cause a process to satisfy the physical constraints and at the same time minimize or maximize some performance measure criterion.

The theory developed is aimed to solve the problem of optimal control. That means that, find an admissible control which causes the systems to follow an admissible trajectory that minimize the performance. As case study of optimization theory, we have practiced the motion planning of an autonomous mobile robot where we have studied clearly the main steps of optimal control.

This is a clarified model of optimal control of moving a robot where the elapsed time is the principal performance to be evaluated. . This is a clarified model of optimal control of moving a robot where the elapsed time is the principal performance to be evaluated. This proposed approach has made the robot able to achieve these tasks: avoiding obstacles, deciding, perception, and recognition and to attend the target which are the main factors to be realized of autonomy requirements. Hence; the results are promising for next future work of this domain. Besides, the proposed approach can deal a wide number of environments.

References

[1] D. KIRK , Optimal control, Prentice Hall edition 1988

[2] R.F.Stengel, stochastic optimal control: theory and application, Jhon wiley & Sons edition,1986.

[3] L.R Medsker, hybrid intelligent systems, Kluwer Academic Publishers, 1995.

[4] H K. Schilling and C.Jungius : Mobile robots for planetary explorations, in Proceeding 2nd International Conference IFAC Intelligent Autonomous Vehicles, Finland, 1995, pp.110-120.

[5] O.Hachour, Pth planning of autonomous mobile robot, International Journal Of System Applications, Engineering & Developments, issue4, volume2,2008,pp.178-190.

[6] O.Hachour, The proposed Fuzzy Logic Navigation approach of Autonomous Mobile robots in unknown environments, International journal of mathematical models and methods in applied sciences, Issue 3, Volume 3, 2009 , pp 204-218.

[7] O.Hachour, the proposed hybrid intelligent system for path planning of Intelligent Autonomous Systems; International journal of mathematics and computers in simulation,Issue 3, Volume 3, 2009, Pages 133-145.

[8] O. Hachour, ,"path planning of Autonomous Mobile Robot", *International Journal of Systems Applications, Engineering & Development*, Issue4, vol.2, 2008, pp178-190.

On General Product of Two Finite Cyclic Groups one being of order 7

(Induced by π = (1) (2) (3) (4) (5) (6) (7))

S.F. El-Hadidi

Abstract—In this paper we find the general product induced by the semi special permutation π =(1)(2)(3)(4)(5)(6)(7). That is the general products of two finite cyclic groups in which one of order 7 and the other is of order m these general products can be described in terms of numerical parameters.

***Keywords*— semi special permutations, general product**

I. Introduction

If A, B are two subgroups of a group G then we say that G is the general product of A, B if and only if:
(1) G = AB
(2) A, B has no elements in common other than the identity i.e. $A \bigcap B = \{e\}$.

Now if A = {a} is a cyclic group of order m, B = {b} is a cyclic group of order n then there exist corresponding to G two semi special permutations π , ρ where π on [n], ρ on [m] such that

$$a^y b^x = b^{\pi^y x} a^{\rho^x y}, x \in [n],\ y \in [m] \quad \text{..... (1)}$$

$$\pi^m x \equiv x(mod\ n), x \in [n] \quad \text{..... (2)}$$

$$\rho^n y \equiv y(\mathrm{mod}\, m), y \in [m] \quad \text{..... (3)}$$

Where *[c]* demote to the set of dements *{1, 2, 3, …, c}*

Definition: (Semi special permutation) *A* permutation π on *[c]* is said to be semi special on *[c] iff* π *(c) = c,*

$\pi_z(x) = \pi(x+z) - \pi z$ (mod *c*), y∈[*c*] is a power depending on *z* of π

Theorem A:

(i) $a^m b^x = b^x a^m, x \in [n]$ …….. (4)

(ii) $a^y b^n = b^n a^y, y \in [m]$ …….. (5)

S.F. El-Hadidi math department, faculty of science, HelwanUniversity , Cairo, EgyptEmail: sameh2002@yahoo.com

Theorem B:

(i) The order of π divides *m* i.e. if e is the orders of π then m is a multiple of ℓ .

(ii) There exist a number $\lambda, (\lambda, \frac{m}{\ell}) = 1$ thus that

$$a^\ell b = b a^{\ell\lambda}, \ell\lambda^\mu \equiv \ell \bmod m \quad \text{..... (6)}$$

Where μ is the **g.c.d** of all $\nu - \upsilon$; ν, υ are any numbers of the principal cycle of π .

(iii) $a^\ell b^\mu = b^\mu a^\ell$.

We know that π = (1)(2)(3)(4)(5)(6)(7) is a semi special permutation on [7]

§1- The general product induced by π

Theorem 1.1: the defining relation of the general product of *G* corresponding to

$\pi = (1)(2)(3)(4)(5)(6)(7)$ is

$$G = \{a, b; a^m = b^7 = e, ab = ba^r\} \quad \text{…….. (7.1)}$$

$$r^7 \equiv 1(\mathrm{mod}\, m) \quad \text{…….. (7.2)}$$

The converse is also true i.e. for any *r* satisfying (7.2) then any group *G* generated by *a* and *b* satisfying (7.1) is the general product of {*a*}, {*b*}.

Proof:

Assume that the general product of G exist, from the equation $a^y b^y = b^{\pi^y x} a^{\rho^x y}, x \in [7], y \in [m]$, with *y*=1 we get

$ab^x = b^{\pi^1 x} a^{\rho^x 1}, x = 1,2,3,4,5,6,7$ put *x*=1 then we have

$ab = b^{\pi 1} a^{\rho 1}$

let us write $\rho 1 = r$ then $ab = ba^r$,

$ab^2 = abb = ba^r b = b\underbrace{aaa\ldots}_{r\text{-times}}\mathrm{ab}$

$ab^2 = b^2 a^{r^2}$ and so by induction we get

$$ab^7 = b^7 a^{r^7} \quad \text{..... (8)}$$

From theorem A with *n* = 7, *y* = 1

we have $ab^7 = b^7 a$ …..(9)

From 8, (9) we get $r^7 \equiv 1(\mathrm{mod}\, m)$ and so (7.2) follows.

Also we notice that {*a*} is of order m and {*b*} is of order 5 then 7.1 is the required defining relation of *G*.

ISBN: 978-1-61804-225-5

The converse is also true to do this let G be a group generated by a, b with the defining relation (7.1) and satisfying the condition (7.2) and let *x* = {0, 1, 2, 3, 4, 5,6}, *y* = {0, 1, 2, …, *m*-1} and let *H* be the set of all ordered pairs (x, y) with $x \in X, y \in Y$ with binary operation $*$ defined on *H* as follows:

$(x, y) * (x', y') = (x'', y'')$ such that

$x'' = x + x'$ (mod 7)

$y'' = r^{x'} y + y'$ (mod m)

Then it is clear that <*H*,$*$ > is a group with *e* = (0,0) as its identity element. Also if $\alpha = (0,1), \beta = (1,0)$

$\beta^x \alpha^y = (x, y)$ which implies that each element of *H* can be determined uniquely in the form $\beta^x \alpha^y$ which means that *H* is the general product of $\{\alpha\}, \{\beta\}$. since $\{\alpha\}$ is of order m and $\{\beta\}$ is of order 5 so $\left|H\right| = 7m$, it is evident to see that $\alpha^m = \beta^m = e$, $\alpha\beta = \beta\alpha^r$ which are corresponding to the defining relation of *G* and so the permutation $\pi = (1)(2)(3)(4)(5)(6)(7)$ is induced by α .

Also *H* can be considered as a homomorphic image of *G*, since $\left|G\right| \leq 7m$ and hence the two groups are isomorphic hence the theorem is proved.

Remark: It must be noted that two groups *G, L* with defining relation:

$$G = \{a, b; a^m = b^7 = e, ab = ba^r, r^7 \equiv 1(\mathrm{mod}\, m)\}$$

$$L = \{a, b; a^m = b^7 = e, ab = ba^s, s^7 \equiv 1(\mathrm{mod}\, m)\}$$

Such that $r \not\equiv s$ mod m, then $G \cong L$ if and only if $r \equiv s^6 (\mathrm{mod}\, m)$

Conclusion:

The general product of two finite cyclic groups one being of order 7, which is corresponding to $\pi = (1)(2)(3)(4)(5)(6)(7)$ is obtained by theorem 1.1 with defining relation (7.1), (7.2).

ACKNOWLEDGMENT

I want to express my thankfulness to professor dr N. G Elsharkawy for her encouragement

REFERENCES

(1)K.R.Yacoub, on general products of two finite cyclic groups one being of order 4 prove math & phys. Soc. ARE, No 21, 1957 PP 119-126.

(2)N.G. El-Sharkawy, S.F. El-Hadidi Parametric Representation of finite groups with-two independent Generators with, one Being of given order, International Jornal of mathematics and computation (IJMC). Vol.6; No. M10, March 2010, PP 27-42.

Multiscale Convergence Optimization in Constrained Molecular Dynamics Simulations

N. M. Nafati, S. Antonczak, J. Topin. J. Golebiowski.

APSM Team. ICN. UMR7272.
Scientific University of Nice. France.
Courriel : Nicolas.Nafati@unice.fr

Abstract-The energy analysis is essential for studying chemical or biochemical reactions but also for characterizing interactions between two protagonists. Molecular Dynamics Simulations are well suited to sampling interaction structures but under minimum energy. To sample unstable or high energy structures, it is necessary to apply a bias-constraint in the simulation, in order to maintain the system in a stable energy state. In MD constrained simulations of "Umbrella Sampling" type, the phenomenon of ligand-receptor dissociation is divided into a series of windows (space sampling) in which the simulation time is fixed in advance. A step of de-biasing and statistical processing then allows accessing to the Potential Force Medium (PMF) of the studied process.

In this context, we have developed an algorithm that optimizes the DM computation time regarding each reaction coordinate (distance between the ligand and the receptor); and thus can dynamically adjust the sampling time in each US-Window. The data processing consists in studying the convergence of the distributions of the coordinate constraint and its performance is tested on different ligand-receptor systems. Its originality lies in the used processing technique which combines wavelet thresholding with statistical-tests decision in relation to distribution convergence.

In this paper, we briefly describe a Molecular Dynamic Simulation, then by assumption we consider that distribution data are series of random-variables vectors obeying to a normal probality law. These vectors are first analyzed by a wavelet technique, thresholded and in a second step, their law probability is computed for comparison in terms of convergence.

In this context, we give the result of PMF and computation time according to statistic-tests convergence criteria, such as Kolmogorov Smirnov, Student tTest, and ANOVA Tests. We also compare these results with those obtained after a preprocessing with Gaussian low-pass filtering in order to follow the influence of thresholding. Finally, the results are discussed and analyzed regarding the contribution of the muli-scale processing and the more suited criteria for time optimization.

***Index* Keywords: Molecular Dynamic Simulations. Umbrella Sampling. Potential Force Medium (PMF). Convergence. Ligand – Receptor. Wavelet Thresholding. Statistical-Tests Decision. Normal Probality Law. Kolmogorov Smirnov. Student tTest. ANOVA. Gaussian low-pass filtering.**

I. INTRODUCTION

Molecular Dynamics (MD) is a sampling space based on iterative numerical integration of the equations of Newton motion. Since the time scales accessible to MD simulations are several orders of magnitude less than the time of chemical reactions, we may introduce a bias to increase the likelihood of sampling rare or unlikely events. In fact, when the energy barrier between two states to be sampled is less than KT (K: Boltzmann constant. T: system temperature in °K), the probability can be obtained in simulations at equilibrium. In the case of larger barriers, the state of higher energy will not be reached and a harmonic potential sampled must be inserted in order to obtain the Hamiltonian suitable sampling. The addition of this harmonic potential is called Umbrella-Sampling (U.S.), where the force constant of this potential is another parameter at equilibrium (or reaction coordinate at equilibrium) . This way provides a sampling that does not follow the Boltzmann statistics, but improves sampling in the vicinity of a chosen value of reaction coordinate [9][10][14].

The sampling technique is therefore constrained so as to cut the energy path connecting an initial state to a final state of the reaction in several windows, as shown in the fig1. .

According to Boltzmann statistics [10][13][17][20][23], Potential Strength Medium (PMF) noted F is given by the following formula:

$$\mathbf{F}(\boldsymbol{\xi}) = -\mathbf{K_B T} \ln(\mathbf{P}(\boldsymbol{\xi})) \quad (1)$$

Where P(ξ) is the probability distribution that represents the number of times that the system samples the reaction coordinate. The expression of P(ξ) and hence of the PMF are modified in the case of sampling constraint. The WHAM (Weigthed Average Histogram Analysis) [9][14] software

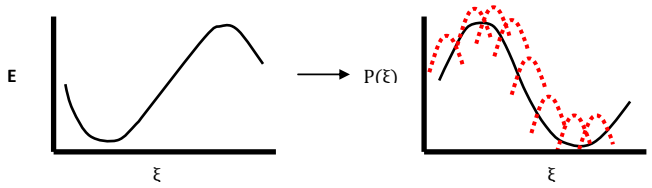

Fig1.: Schematic overall sampling by Umbrella Sampling technique under a harmonic constraint. The left curve shows the energy according to the reaction coordinate. The right one shows the probability as a function of the same parameter. The red curves having the umbrella-shaped sample windows are Umbrella-Sampling.

aims to determine the PMF through the calculation of some constants induced by the harmonic constraint.

As indicated in Fig1., two successive harmonic potential sampling windows, with a recovery given rate, lead to PMF identification up to a constant. The expression of this constant is:

$$\ln\left(\langle e^{\beta V_1(\xi)}\rangle\right) - \ln\left(\langle e^{\beta V_2(\xi)}\rangle\right) \quad (2)$$

The WHAM program corrects the value of PMF in each window by calculating the constants from (2) through the recovery of successive US windows, and thus provides the values of PMF (kcal/mol) depending on the reaction coordinate.

II. Problem Context:

A molecular dynamics simulation [10] consists in several steps of calculation:

-Energy minimization processing.

-Thermalization processing in which the protein complex is heated up to 300 °K. During this phase the thermal noise increa-ses.

-Equilibration phase processing: the energy of the system becomes minimum.

-Production Data phase: data are collected in order to compute the PMF.

The Amber software is used to achieve all these steps, and to reach among other things, different distributions of coordinate reaction (Distance between molecules), expressed in Angstroms. Each distribution is a distance-vector including a deterministic and random component. These distribution-vectors are measured at a given time in a sampling window-time whose size is set in advance. The present random component in each distribution is due to thermal agitation. The random thermal noise explains that noise components due to thermal agitation may have all sorts of values from low frequencies to very high frequencies. It greatly influences the number of iterations of the temporal sampling under a constraint reaction coordinate.

During the production phase, data distributions are collected by moving the US window along the spatial axis sampling. Therefore this sampling is directed or forced because the system is maintained in an energy potential well. Then the distribution distance estimator depends only on the distance, so the directed sampling allows to overcome the other freedom degrees.

To obtain efficient estimators of the distance-distribution, the US windows must be relatively long (approximately about several tens nanoseconds) and this for a large protein complex of approximately 5000 atoms. Consequently, our work has focused on developing algorithms that use short time windows centered around each spatial sampling. Our algorithm combines the wavelet and gaussian filtering processing with statistical convergence criteria. Our simulations have shown that this combination can reduce the cost of computing time.

III. Data formulation:

(2)

In our study, we consider that during a Dynamic Molecular Simulation, each distribution $\boldsymbol{X_i}_{\,0\le i\le N-1}$ is obtained as a stochastic measure which represents a temporal sample at a given distance. In other words, the constrained spatial sampling proceeds as follows: for each distance $\boldsymbol{D_J}_{\,0\le j\le M-1}$ from $\boldsymbol{D_0}$ to $\boldsymbol{D_{M-1}}$, we collect each distribution $\boldsymbol{X_i}_{\,0\le i\le N-1}$ at time $\boldsymbol{t_{i-1}+\Delta t}$ until the convergence of their probability distribution, then we increment the distance and repeat the process until $\boldsymbol{D_{M-1}}$.

The objective of our molecular modeling is to obtain measurements of the vibrational micro-state of the protein complex at a given distance. To do this, we have to accumulate a large number of statistical data which represent the probability distribution of the micro-states system. This statistic depends on the thermodynamics complex.

So, we denote that each distribution is a random measure such that :

$$\boldsymbol{X = X_d + \varepsilon}$$

Where $\boldsymbol{X_d}$ is the determinist component, and $\boldsymbol{\varepsilon}$ is the noise component.

So, at every spatial sampling step, we collected a series of distributions: $\{X_0, X_1, X_2, X_3, X_4, \ldots, X_{N-1}\}$ whose limit mainly depends on the speed of the probability convergence. This series is considered as a set of independent random variables, supposed to follow a normal distribution.

IV. Removing Noise with Wavelet Transformation

A. A brief overview of wavelets

The Continuous Wavelet Transform (CWT) [3][19][23] gives a time-frequency representation of signals. A wavelet

transform is a convolution of a signal X(t) with a set of functions which are generated by translations and expansions of a main function. The main function is known as the mother wavelet and the translated or expanded functions are called wavelets. Mathematically, the CWT is given by:

the translated or expanded functions are called wavelets. Mathematically, the CWT is given by:

$$\boldsymbol{W(a,b) = \frac{1}{\sqrt{a}} \int X(t)\psi(\frac{t-b}{a})\, dt} \quad (3)$$

Here $\boldsymbol{b}$ is the time translation parameter and $\boldsymbol{a}$ is the expansion parameter of the wavelet. Ψ is the mother wavelet which is non-zero only on a certain interval.

The Discrete Wavelet Transform (DWT) is similar to the Fourier transform in that a signal is decomposed in terms of a basis set of functions. In Fourier transforms the basis set involves sines and cosines and the expansion has a single parameter. In wavelet transform the expansion has two parameters and the functions (wavelets) are generated from a single "mother" wavelet [8].

Any signal can be decomposed as:

$$\boldsymbol{X(t) = \sum_a \sum_b c_{ab}\, \psi_{ab}(t)} \quad (4)$$

Where the two-parameter coefficients are given by

$$\boldsymbol{c_{ab}(a,b) = \int X(t)\, \psi_{ab}(t)\, dt} \quad (5)$$

And the wavelets $\boldsymbol{\psi_{ab}}$ obey the condition

$$\boldsymbol{\psi_{ab}(t) = 2^{\frac{a}{2}}\, \psi(2^a t - b)} \quad (6)$$

B. Removing Noise with the DWT

"De-noising" a signal with the DWT involves three steps [1][5][8][15]:

1. Transform the input signal **X** with the DWT (X is a vector whose dimension is equal to N).

2. Force to zero all transform coefficients whose magnitude falls below some percentage of the maximum magnitude. This is a thresholding operation in which the threshold is adaptively computed or not. In our simulation, we used an adaptative soft thresholding with a universal threshold [1][5][15]. given by:

$$\boldsymbol{T = \sigma \sqrt{\frac{2\log(N)}{N}}} \quad (7)$$

Where σ is the standard deviation of X.

3. Inverse DWT.

V. Principle of Statistical Tests

A hypothesis test (or statistical test) is an approach that aims to provide a decision rule which, on the basis of sample results, leads to make a choice between two statistical hypothesis. These two hypothesis are disjoint, in other word mutually exclusive.

Significance level of the test :

There is a risk, agreed in advance, of wrongly rejecting the null hypothesis H_0 when it is true, it is called the significance level of the test and the corresponding probability is noted α:

$$\boldsymbol{\alpha = P\,(\,\textbf{To Reject } H_0 \mid \textbf{when } H_0 \textbf{ is true}\,)} \quad (8)$$

At this level of significance, we affect to the statistic sampling distribution a rejection region of the null hypothesis (also called the critical region or **C**ritical **P**robability ($\mathbf{P_c}$)). The area of this region is the probability α. For example, choosing α = 0.05 means that sampling variable can take in 5% of cases, a value belonging to the rejection area of $\mathbf{H_0}$. The sampling distribution matches to a complementary region, called region of acceptance of $\mathbf{H_0}$ (or region of non-rejection) whose probability is equal to 1 - α.

From this point, we use different stochastic tests as convergence criteria. These criteria are focused on α as a threshold of acceptation or rejection of any convergence hypothesis. We set α error to 0.05 in our simulations.

As we said before, our data are samples (distance distributions) coming from the same population, which follows a probability law supposed to be normal $\mathcal{N}(\mu,\sigma)$. In our simulations we use non-parametric [2][4][6,7][12][16][21] and parametric statistic-tests [11][18][22] in order to find the best statistic-tests convergence criteria.

The statistical tests are:

- The parametric test of student (tTest), to test the sample average convergence, assuming that the variance is known.

- The non-parametric Kolmogorov Smirnov test, another non-parametric alternative to the tTest for independent samples.

- The Anova non-parametric test, to check if the difference between the sample averages can be attributed to random sampling or to the fact that the samples are really significantly different [18].

A. Student Convergence criteria

Convergence of sequences of random variables is an important concept in probability theory and statistics, in particular the study of stochastic processes. For example, several random variables from the same population converge to the same probability.

In this article, we assume that (X_i) is a sequence of real

ISBN: 978-1-61804-225-5

random variables, and that all these variables are defined on the same probability space.

Let $(\boldsymbol{F_0, F_1, F_2, \ldots\ldots, F_{N-1}})$ be the repartition functions, associated with random variables $(\boldsymbol{X_0,\ X_1,\ X_2\ \ldots\ldots, X_{N-1}})$. **F** is the repartition function of the random variable $\boldsymbol{X}$. In other words, $\boldsymbol{F_i(x)}$ is defined by $\boldsymbol{F_i(x) = P(X_i \leq x)}$ and $\boldsymbol{F}$ by $\boldsymbol{F(x) = P(\ X \leq x)}$. It is said that $\boldsymbol{X_{N-1}}$ converges to $\boldsymbol{X}$ in probability if :

$$\boldsymbol{\lim_{N\to\infty} P(|X_N - X| \geq \epsilon) = 0} \tag{9}$$

The distributions $(\boldsymbol{X_0,\ X_1,\ X_2\ \ldots\ldots, X_{N-1}})$ are considered as a set of independent random variables and are measured at each constraint spatial sampling step. In principle they should converge at a given time. [Our goal is to reduce the iteration numbers and then the cost in time of molecular dynamic simulation.

Student's **tTest** [21] can be used to statistically test the hypothesis of equality of random variables average following a normal distribution and with unknown variance.

So the bilateral symmetrical confidence interval for the mean $\boldsymbol{\mu}$ can be written as:

$$\boldsymbol{IC(n) = \left[\bar{x} - t_{1-\alpha/2}^{n-1}\cdot\sqrt{\frac{S}{n}}\ , \bar{x} + t_{1-\alpha/2}^{n-1}\cdot\sqrt{\frac{S}{n}}\right]} \tag{10}$$

where

tTest is the fractile of order $\boldsymbol{1-\frac{\alpha}{2}}$ of St(n-1) Student Law. Most **tTest** statistics have the form: $\textbf{tTest} = \frac{\mathbf{Z}}{\mathbf{s}}$, where **Z** and **s** are functions of the data. Typically, $\boldsymbol{Z}$ is designed to be sensitive to the alternative hypothesis (its magnitude tends to be larger when the alternative hypothesis is true), whereas *s* is a scaling parameter that allows the distribution of **tTest** to be determined.

And

$\bar{x} = \frac{1}{n}\ \sum_{i=1}^{n} x_n$ is the average estimator

$\boldsymbol{s = \frac{1}{n-1}\ \sum_{i=1}^{n}(x_i - \bar{x})^2}$ is the unbiased estimator of the variance.

B. Kolmogorov-Smirnov (ksTest) criteria

The **two-sample ksTest** is one of the most useful and general nonparametric methods for comparing two samples, as it is sensitive to differences in both location and shape of the empirical cumulative distribution functions [12][16].

The Kolmogorov–Smirnov test may also be used to test if two underlying one-dimensional probability distributions differ. In this case, the Kolmogorov–Smirnov statistic is:

$$\mathbf{D_n = \ sup_x|F_n(x) - F(x)|} \tag{11}$$

where $\mathbf{sup_x}$ is the supremum of the distances set. If the sample comes from a distribution F(x), then $\mathbf{D_n}$ converges to 0 almost surely. Kolmogorov strengthened this result, by effectively providing the rate of this convergence.

$$\mathbf{F_n(x) = \frac{1}{n}\sum_{i=1}^{K} I_{X_{i\leq x}}} \tag{12}$$

Where $\mathbf{I_{X_{i\leq x}}}$ is the indicator function, equal to 1 if $\mathbf{X_i \leq x}$ and equal to 0 otherwise.

Under null hypothesis, the sample comes from the distribution **F(x)** and $\sqrt{\mathbf{n}}\mathbf{D_n}$ converges to the Kolmogorov distribution, which does not depend on **F**. This result may also be known as the **Kolmogorov theorem** [12].

C. One-way ANOVA test criteria

In statistics, one-way ANalysis Of VAriance (abbreviated one-way ANOVA) is a technique used to compare mean-values of two or more samples.

ANOVA is a collection of statistical models used to analyze the differences between group mean-values and their associated procedures (such as "variation" among and between groups). In ANOVA setting, the observed variance in a particular variable is partitioned into components attributable to different sources of variation. In its simplest form, ANOVA provides a statistical test of whether or not the mean-values of several groups are equal, and therefore generalizes tTest to more than two groups.

The normal-model based ANOVA analysis assumes the independence, normality and homogeneity of the variances of the residuals. **Significance testing** ANOVA is a good example for explaining why very many statistical tests represent ratios of explained to unexplained variability. Here, we base this test on a comparison of the variance due to the between-groups variability (called *Mean Square Effect*, or MS_{effect}) with the within-group variability (called *Mean Square Error*, or Ms_{error}). Under the null hypothesis (that there are no mean differences between groups in the population), we would still expect some minor random fluctuation in the mean-values for the two groups when taking small samples. Therefore, under the null hypothesis, the variance estimated based on within-group variability should be about the same as the variance due to between-groups variability. We can compare those two estimates of variance via the *F* test (see also Fisher Distribution), which tests whether the ratio of the two variance estimates is significantly greater than 1. When a statistical test provides a highly significant ratio, we can conclude that the mean-values for the two groups are significantly different from each other.

VI. ALGORITHM ARCHITECTURE:

The Proposed algorithm is :

Step_1: Production by the Program XLeap from Amber of the Coordinate Topology Files of the complex system under study.

Step_2: Initializing input parameters (initial and final distance coordinates of the complex system.

Step_3: Calculation calibration process step.

Step_4: Production step in which molecular dynamic simulation provides data-distribution. Each iteration have to take into account the output file "restart " of the previous step as a coordinate file (Input CRD File).

Step_5: Data outputs Collection, namely the distribution of distance from the file dump.

Step_6: Subband decomposition of collected data and thresholding high frequency components. Or preprocessing by a gaussian filter of the collected data distribution.

Step_7: Data Reconstruction after the suppression of the micro-states noise. Or collecting the smooth data distribution.

Step_8: Evaluation of the convergence statistic-criteria. If the probability distribution doesn't converge then begin the process since step_4. If not the program goes on.

Step_9: Recording of production results and incrementing of the US step.

Step_10: If the final distance is not reached, then loop from step_3, if not, stop the process.

VII. Simulations and Results:

Our simulations have been made on two systems:

-**System_1**: a mixture of one molecule of NaCl (saline) and water in a box of 12 Angstroms long.

-**System_2**: Deca-Alanine, a peptide consisting of ten residues of alanine with an alpha helix form, in vacuum.

Distance distributions are considered by assuming independent random variables following a normal law probability. Their number at a given constrained distance depends strongly on the used convergence criteria.

Distance distributions are considered by assuming independent random variables following a normal law probability. Their number at a given constrained distance depends strongly on the used convergence criteria.

A. Simulation number one:

Below we give the results of the PMF in the case of System_1 and for windows of 16000 steps in time. The spatial sampling is 0.2 Angstrom. The sampling time step is 0.002 ps. The initial distance is equal to 0.5 Angstroms and the final distance is equal to 10 Angstroms. For System_2 we have the same parameters except for the distance varying from 12 to 35 Angstroms.

In this first simulation, we used a simple and effective criteria which is a parametric statistical test of normality, leading to the Confidence Interval of normality with a given confidence level [4,5]. This confidence interval contains 99% of the population when the distribution is following a normal (or Gaussian) law of probability. The character of normality is given by the probability:

$$\mathbf{P}(\mathbf{IC_{Max}} \leq \mathbf{X} \leq \mathbf{IC_{Min}}) \quad (13)$$

$$\mathbf{and}\ \mathbf{IC_{Max}} = \mu + \mathbf{3\sigma}\ \ \mathbf{when}\ \ \mathbf{IC_{Min}} = \mu - \mathbf{3\sigma}$$

From this, we deduced the following parametric criteria:

$$\mathbf{Criteria\_1} = |\,\mathbf{IC_{1_{Min}}} - \mathbf{IC_{2_{Min}}}\,| \quad (14)$$

$$\mathbf{Criteria\_2} = |\,\mathbf{IC_{1_{Max}}} - \mathbf{IC_{2_{Max}}}\,| \quad (15)$$

Below we give the PMF simulation in the case of System_1 whose window size is 16000 temporal steps. The convergence normality criteria are: Criteria_1 and Criteria_2. Their values are each fixed to 0.2, 0.1, and 0.05.

Below we give the PMF simulation in the case of System_1 whose window size is 16000 temporal steps. The convergence normality criteria are: Criteria_1 and Criteria_2. Their values are each fixed to 0.2, 0.1, and 0.05.

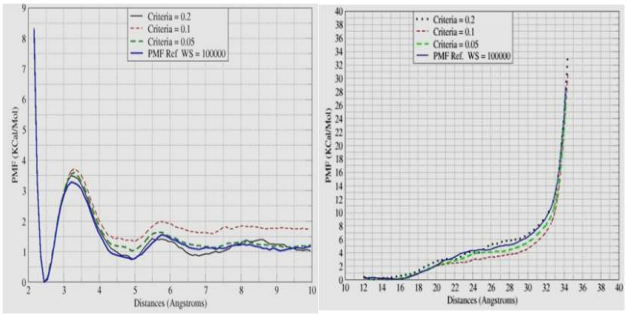

Fig2.: On the left we give the PMFs of system_1, on the right those of system_2; these for different thresholds of the normality criteria. The Umbrella Sampling Window Size (USWS) is fixed to 16000. The blue curve represents the Reference PMF (Ref. PMF) whose USWS is fixed respectively to 40000 for system_1 and 100000 for system_2. All these curves except the Ref. PMF are obtained after the convergence of their probability.

The following figure shows the time cost of these results in function of the threshold criteria values and the Umbrella Sampling Window size.

	System_1		System_2	
Criteria Threshod Values	USWS = 16000	Ref. USWS = 40000	USWS = 16000	Ref. USWS = 100000
0.2	3.232 ns	7.680 ns	40.704 ns	46.400 ns
0.1	4.576 ns		40.736 ns	
0.05	7.296 ns		42.240 ns	

Fig3.: Time costs of simulations for different test-threshold values and sizes of the Umbrella Sampling Window Size.

Observation and Discussion:

we can note that the computation time is low for the criteria threshold value of 0.2 and with PMF close to the PMF reference for both system_1 and sytsem_2 complexes. The used normality convergence criteria indicate that improvement in terms of computation time is possible for adequate test criteria threshold values. Thermal agitation induces duplication of information related to the remaining degrees of freedom. A non-optimal threshold does not filter some parasite micro-states which make information redundant, so the knowing of all the micro-states is not required to measure the PMF. In this context we assume that pre-processing the distributions could improve the convergence speed.

B. Simulation number two:

The purpose of this simulation is to see the impact of the pre-processing by a low-pass Gaussian filter and statistical convergence criteria such as Anova, tTest and skTest. The simulation conditions are identical to that of the previous case.

Note that the pre-processed distributions by a gaussian low pass filter brings a significant gain in terms of time of the probability convergence. The simulation time is reduced by a

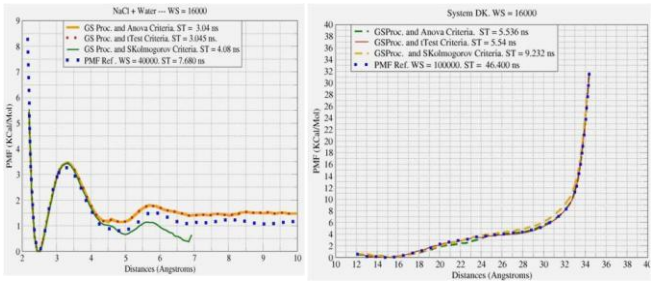

Fig4.: On the Left and right, we give respectively the PMF of system_1 and system_2 for different statistical conver-gence criteria. The distributions of micro-vibration states are pre-processed by Gaussian low-pass filter. One can see the duration of each simulation (Simulation Time=ST) according to statistical criteria. The window size (USWS) is set to 16000 steps for each simulation. Also one gives the reference curve PMF (Ref. PMF) whose size is set to 40000 for system_1, and 100000 for system_2.

factor of two for system_1 and 10 for system_2 when the convergence criteria such as ANOVA and tTest are used. Results of skTest are less satisfactory.

C. Simulation number three:

Here distributions obtained during a sampling time at a given distance are pre-processed by a denoising technique. It involves a wavelet methodology where high frequencies are thresholded (see Fig5.). The used wavelet belongs to the family of bio-orthogonal wavelet (Cubic Spline) and the chosen thresholding method is a universal soft thresholding technique. In order to see the influence of this denoising process, distributions are decomposed and thresholded until level 8. Then the signal is reconstructed and its probability is compared to the previous one by using different convergence criteria such as : skTest, tTest and finally Anova Test.

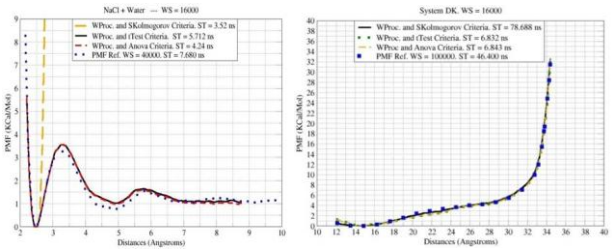

Fig5.: On the left and right we give respectively the PMFs of system_1 and system_2. The PMF curves are represented as a function of distance. The Umbrella Sampling Window Size (USWS) is fixed to 16000. The blue curve (…) represents the Reference PMF (Ref. PMF) whose USWS is fixed to 40000 and 100000 respectively for system_1 and system_2.

Observation and Discussion:

The PMF values in case of multi-scale distributions analysis are shown above (Fig5.). We can see that the cost in computation time is generally less than those of PMFs references. In system_1, a gain of 2ns to 3ns was observed in the case of tTest and ANOVA test criteria. However in the

case of skTest, divergence was observed at the beginning of the simulation.

For the Alanine complex, the computation time of each simulation is measured about 7 times lower than the reference simulation one (46.400 ns). This is in the case of tTest and ANOVA test. Regarding skTest, the computation time increased significantly (about twice the reference time).

It is also noted for the system_2 that convergence is almost perfect with respect to the PMF reference for all statistical tests.

VIII. Conclusion

The performance of the algorithm thus developed, is based on the efficiency of the stochastic convergence criteria, combined with an adaptative pre-processing. This allows to use a succession of short size windows iterated until a convergence. One reminds that a long Umbrella Sampling Window for a big protein complex leads to several days of calculation.

Here distributions of reaction coordinates are pre-processed by a methodology involving a low pass-filter, or a wavelet soft thresholding. It significantly improves and reduces the computation time of the simulations.

The results show that fact of pre-processing all micro-vibrations of high frequencies reduces the computation time. The Umbrella Sampling Method with short windows is used to perform a constrained temporal sampling.

We can assume that the use of narrow bandwidth filters eliminates some useful information (some vibrational frequencies) from the entropy, and then causes the PMF to take inifinite values.

The given algorithm unquestionably allows a reduction of the iteration number and so the time of simulation.

VIII. References

[1] A., Azzalini, M. Farge, and K. Schneider. "Nonlinear wavel et thresholding: a recursive method to determine the optimal denoising threshold," Appl. Comput. Harmon. Anal. 18(2), pp.177–185, Oct. 2004.

[2] V. Bagdonavicius, J. Kruopis, M.S. Nikulin, "Non-parametric tests for complete data," ISTE&WILEY: London&Hoboken, 2011.

[3] H. O. Bartelt, K. H. Brenner, and A.W. Ohman, "The wigner distribution function and its optical production," *Optics Communications*, 32, pp. 32-38,1980.

[4] G. W. Corder & D. I. Foreman, "*Nonparametric Statistics for Non-Statisticians: A Step-by-Step Approach*," Wiley, 2009.

[5] M. Farge, "Wavelet transforms and their applications to turbulence," Ann. Rev. Fluid Mech. , 24:395–457, 1992.

[6] Gibbons, Jean Dickinson and Chakraborti, Subhabrata "*Nonparametric Statistical Inference*," 4th Ed. CRC, 2003.

[7] T. P. Hettmansperger, J. W. McKean, "*Robust nonparametric statistical methods,"* Kendall's Library of Statistics. 5 (First ed.). London: Edward Arnold.

[8] I. Johnstone and B. Silverman, "Wavelet treshold estimators for data with correlated noise," J. R. Stat. Soc., Ser. B. Stat. Methodol. 59,pp.319–351,1997.

[9] S. Kumar, J. M. Rosenberg, D. Bouzida, R. H. Swendsen, P.A. Kollman P. A., "Multidimensional Free-Energy Calculations Using the Weighted Histogram Analysis Method," Journal of Computational Chemistry, 16, 11, pp.1339-1350. 1995.

[10] L. Charlier, "Etude des Interactions moléculaires entre molécules odorantes et protéines impliquées dans les premières étapes de la perception olfactive," Thèse de Doctorat. Université de Nice-Sophia Antipolis, Octobre, 2009.

[11] Lehmann E.L., Scheffé H. "Completeness, similar regions, and unbiased estimation," Sankhya: the Indian Journal of Statistics 10 (4), pp. 305–340,1950.

[12] Marsaglia G., Tsang WW., Wang J., "Evaluating Kolmogorov's Distribution," Journal of Statistical Software, 8(18), pp1-4,2003.

[13] Masunov A., and Lazaridis T., "Potentials of mean force between ionisable amino acid side chains in water," J. Am. Chem. Soc. 125, pp1722-1730,2003.

[14] Mills Maria and Andricioaei Loan, "An experimentally guided umbrella sampling protocol for biomolecules," J. Chem. Phys. 129(11): 114101. 2008.

[15] Mostacci E., Truntzer C., Cardot H., Duoroy P., "Méthodes multivariées combinant ondelettes et analyse en composantes principales pour le débruitage de données issues de spectrométrie de masse," *42èmes Journées de Statistique*, Marseille, France. 2010.

[16] Pratt J.W., and Gibbons, J.D., "Concepts of Nonparametric Theory," New York: Springer Verlag, 1981.

[17] Roux B., "The calculation of the potential of mean force using computer simulations," Comp. Phys. Comm., 91, pp.275–282. 1995.

[18] Shorack Galen R., and Wellner Jon A., "*Empirical Processes With Applications to Statistics*," Philadelphie, Society for Industrial & Applied Mathematics, pp.998,2009.

[19] Torrence, C., and Compo G.P., "A Practical Guide to Wavelet Analysis", Bulletin of the American Meteorological Society, 79, pp61-78,1998.

[20] Torrie G. M., and Valleau J. P., "Monte Carlo free energy estimates using non-Boltzmann sampling: application to the sub-critical Lennard-Jones fluid," Chem. Phys. Let., october 1974.

[21] Wasserman, Larry, "*All of nonparametric statistics*," Springer, 2007.

[22] Sawilowsky, Shlomo S., "Fermat, Schubert, Einstein, and Behrens–Fisher: The Probable Difference Between Two Means When $\sigma_1 \neq \sigma_2$,". Journal of Modern Applied Statistical Methods 1 (2), pp.461–472.2002.

[23] Silverman B. W.. "Wavelets in statistics: beyond the standard assumptions, Phil. Trans. R. Soc. Lond. A, 1999.

Analysing the Impact of the Monetary Policy Dynamics on Financial Imbalances- A Model Approach

Wael Bakhit
Lebanese University, Faculty of Economics and Management
Lebanese French University, Faculty of Management

Abstract — This paper employs a quarterly time series to determine the timing of structural breaks for interest rates in USA over the last 60 years. The Chow test is used for investigating the non-stationary, where the date of the potential break is assumed to be known. Moreover, an empirically examination of the financial sector to check if it is positively related to deviations from an assumed interest rate as given in a standard Taylor rule. The empirical analysis is strengthened by analysing the rule from a historical perspective and look at the effect of setting the interest rate by the central bank on financial imbalances. The empirical evidence indicates that deviation in monetary policy has a potential causal factor in the build up of financial imbalances and the subsequent crisis where macro prudential intervention could have beneficial effect. Thus, my findings tend to support the view which states that the probable existence of central banks has been one source of global financial crisis since the past decade.

Key words: Taylor rule, Financial Imbalances, Central Banks.

I INTRODUCTION

The practice of central banking has developed during the last 60 years in a way that affected their ability to target both economic growth and inflation through their effect on short interest rates and/ or growth of monetary and credit aggregates (McCallum, 1999), thus leading to the formulation of a number of simple reaction functions spanning the evolution of the monetary-policy framework. This last was consistent with the Taylor-type rules (Taylor, 1993) which showed that US monetary policy after 1986 was well characterised by a rule for the Federal Reserve's interest rate, whereby the interest rate responds with fixed, positive weights to inflation and the output gap. (Judd & Rudebusch, 1998) found as well that the Taylor rule reproduces the evolution of Federal Reserve funds rate on the basis of quarterly US Data over the 1987-1992 periods.

As a standard reference, modern central banks have relied increasingly on Taylor's conception on the formulation of monetary. First, the use of such models as documented in (Asso, Kahn, & Leeson, 2007) evolved from a long intellectual history that debated the merits of rules versus discretion [(Mccallum, 1988), (McCallum, 2000), (Goodhart, 1988, 1994), and (Taylor, 1999)]. Second, the practice comes from its simplicity, intuitiveness and focus on short-term interest rates as the instrument of monetary policy, which simply relates the policy rates directly to the goals of monetary minimizing fluctuations in inflation relative to its objective and output relative to potential output. Instead of forecasting employment, the Fed used to state its policy objectives in terms of economic growth and price stability, because of their effect on employment through what is called the Okun's law 1962 (Thornton, 2012).

The rule has been subsequently developed in a theoretical and empirical perspective in order to perform the original models and to optimize the monetary policy guidance. Thus, leading to the formulation of different versions which span the evolution of monetary policy; including econometric estimates of the coefficients for the United States by [(Judd & Rudebusch, 1998), (Clarida, Gali, & Gertler, 2000)] extended versions for the standard equation by imputing financial condition indexes, use ex-ante data to estimate the policy rule instead of ex-post (revised) data, or range from a simple monetary policy to a backward-versus forward looking. The debate is about how the objectives of monetary policy should be expended to include financial variables in order to reduce (or prevent) financial crisis.

A. Problem of the Research

The common second area of central bank responsibility is financial stability. But easy monetary policies did indeed lead to excessive credit growth that eventually bred this issue, claiming that central banks policies contribute to the build-up major imbalances.

Feedback instrument rules involve line causality between mechanical deviations in the level of the policy rate from systematic or rule-like behaviour to deviations of inflation from its target, and of output from its potential. Such deviations are identified as a potential cause for the occurrence of global imbalances, which are perceived as an important factor in the financial crisis. The literature has not reached yet consensus in this issue. In this study, there is evidence of a multiple structural breaks in the behaviour of interest rates based on political factors allowing the instability, which is in turn correlated with the monetary regime switches.

B. Research Question

The present work departs from the literature and the hypothesis and builds its analysis on two areas. Basically, an estimate of the backward-looking Taylor rule for United States with constructed variables with statistical techniques was taken into consideration. This procedure will answer the following questions: is the Fed reacting differently to levels of inflation and output above or below the target? Does the Fed attempt to hit the macroeconomic target or keep some margin of fluctuations? What about the timing of structural breaks in regressions? The linear specification of the Taylor rule has been extended with the financial indexes to check if the Fed is still reacting to the macroeconomic aggregate as to the information contained in the index.

Similarly, an application of a linear model took place where the presence of deviation in the policy rate is taken into the structure of the model. The principal objective in this area is to test the presence of ruptures in the monetary policy, whether or not such shifts occur at politically important times (e.g. near elections, with changes of party of administrations, FOMC decisions… etc.). The secondary objective is to question if the monetary policy contributes to financial imbalances.

Obviously, this paper is organised as follows:

The first section covers a construction of the variables to be used. Besides that, the second section includes econometric specifications and empirical estimates of the policy rule for different periods in the U.S presidency (the terms of Arthur Burns and William McChesney-Martin (1955-1978), the terms of Paul Volcker (1970-1987) and the terms of Greenspan and Bernanke from 1987 to date): For each period, rupture on the coefficients on output and inflation was estimated. Additionally, the third section discusses possible explanations of the findings, and finally the fourth section concludes.

II LITTERATURE REVIEW

There is of course a vast literature on monetary policy which includes financial variables to forward guidance, and finds evidence of strong linkages (transmission mechanisms) between monetary policy and financial conditions. Indeed, one of the most important issues facing central banks is their capability of correctly identifying bubbles in real time in order to justify leaning against the bubble, or prevent crisis. In (Bernake & Gertler, 2000), the issue is how to respond to **variability** in asset prices. This model incorporates non fundamental movements in asset prices into a dynamic macroeconomic framework. Authors found that it is neither necessary nor desirable for monetary policy to respond to changes in asset prices, except to the extent that they help to forecast inflationary or deflationary pressures. In (Bernanke, Gertler, & Ghilchrist, 1999) authors helped to clarify the role of credit market frictions in business fluctuations using a DSGE model. They argued that changes in credit market conditions might affect the intrinsic costs of borrowing and lending, which is associated with asymmetric information and might run financial crisis within a financial accelerator mechanism. Moreover, (Filardo, 2001) examined the macroeconomic performance of an economy where the central bank usually responds to changes in forward-looking inflation information contained in asset price inflation. The monetary policy rule is substituted by the IS-PC-AP system of equations, which is simulated with random numbers representing shocks to output, consumer price inflation, and asset price inflation. The coefficients of the model are then chosen to minimize the central banks loss function L. The view of using these asset prices to improve economic outcomes is not promising. The price inflation of housing shows some power to predict the future inflation, but stock market price inflation exhibits no power in the prediction of the future consumer price inflation. Finally, the monetary authorities should not respond to asset prices if there is any considerable uncertainty about the macroeconomic role of asset prices (if they cannot distinguish between fundamental and bubble asset price behaviour). Also, (Castro, 2008) analyzes the possibility of the rule to be augmented with financial conditions index containing information from some asset prices and financial variables. Therefore, the results indicate that the monetary behaviour of the Federal Reserve of the United States can be well described by a linear Taylor rule. It also suggests that the Fed is not reacting to the financial conditions.

Policy actions following financial crisis in which central banks just clean up after the bubble are not without risks. What has been missing in this debate so far is the possible evidence which can reveal if the central bank is the one which contributes itself to financial crisis.

A. Hypothesis:

Uncertainty in the monetary policy as claimed by Bernanke had increased in recent decades, giving rise to the volatility of interest rates as well as exchange rates. According to (FOMC, 2009), “members noted the possibility that some negative side effects might result from the maintenance of very low short-term interest rates for an extended period, including the possibility that such a policy stance could lead to excessive risk-taking in financial markets or an un-anchoring of inflation expectations.” According to the subprime crisis, the drastic change in the monetary policy stance had let to a sudden raise in the US subprime mortgage market.

H_1: Structural changes in the monetary policy stance have a significant impact on the money conditions (bank lending), related forecasts, and consequences on the volatility of the financial markets linked to it.

III METHODOLOGY

This study is concerned with the impact of deviations in interest rate on asset price inflation and output. The standard Taylor rule along with the modified version which contains looking variables is proposed, and later estimated on (Batini & Haldane, 1999). The following forms of panel regressions are estimated, where *i* represents the interest rate.

A model of possible deviation from a simple linear model was stated previously in this study. As originally described, the rule requires knowledge of only the current inflation rate and the output gap. Using Quarterly report data, a series of robustness checks and tests of the effectiveness of simple financial ratios were performed, being considered as predictors in respect to future financial crisis and analyse the impact of the deviations on financial turbulences. It is expected to find a relationship between dynamics in monetary policy decisions and financial imbalances, the mean that the Fed strategy is likely to contribute to financial crisis. In this article, imbalance is defined as a persistent deviation in asset prices from historical trend on a variety of financial indicators (credit supply, liquidity growth, financial asset prices).

The following forms of panel regressions are estimated, where *i* is the nominal interest rate, (π_t) inflation rate over the previous year, $(y_t - y^*)$ the per cent deviation of the logarithm of the real GDP (y_t) from estimate of the logarithm of its

unobserved potential level (y^*) and ε_t is a white noise error term.

The rule sets the level of the nominal federal funds rate (i_t) being equal to a natural rate that is seen as consistent with full employment (originally defined as ($i^* = 2$)), plus the inflation rate over the previous year (π_t), plus an equally weighted average of two gaps: (a) The four quarter moving average of actual inflation less a target rate (π^*), and (b) the output gap.

Generally, a brief description of the theoretical model is provided, which in turn refers to the original specification introduced by (Taylor, 1993). Although there is no consensus about the size of the coefficient of policy rule; (Taylor, 1993) assumed that the weights the Fed gave to deviations in inflation and real GDP from trend same coefficient equal to 0.5, and the equilibrium real interest rate and the inflation target equal 2%. The generalized form of the rule has been considered in order to suggest an interest rate feedback rule that describes the US monetary policy over 1955 to 2012 (the frequency is quarterly). The model takes the following form:

$$i_t = i^* + \pi_t + \alpha_\pi(\pi_t - \pi^*) + \beta_y\,(y_t - y^*) + \varepsilon_t$$

A measure of output gap, potential output, inflation and equilibrium real rate plays an important role on policymaking and is useful before proceeding to any monetary analysis. (See the Appendix 1 for details on data construction). Note that the slope coefficient on inflation in the equation is: $(1 + \alpha_\pi)$; hence the two response coefficients are: $1 + \alpha_\pi$ and β_y. Also, note that the intercept term is: $i^* - \alpha_\pi \pi^*$.

[(Clarida, Jordi , & Mark, 1998), (Orphanides, 2001), (Rudebusch, 2002) and (Castelnuovo, 2003)] are followed by including an interest rate smoothing parameter in order to avoid excessive movements in the aggregate variables subsequent to sudden and frequent change in interest rate. The Interest rate equation is entered with a lag of one quarter. Moreover, the equation is assumed to relate interest rate to lag in output gap (Orphanides, 2001) as shown in equation 2:

$$fi_t = r^* + \pi_t + \alpha_\pi(\pi_t - \pi^*) + a_y Y_t + \delta(L) Y_{t-1} + \gamma(L) fi_{t-1} + \varepsilon_t$$

In another term:

$$fi_t = r_t^* + \pi_t^* + \alpha_\pi(\pi_t - \pi^*) + a_{y1} Y_t + a_{y2} Y_{t-1} + fi_{t-1} + \varepsilon_t$$

Then, (Kahn, 2009) was followed by including financial ratios into the interest rate reaction function. Kahn found a statistically significant influence of the interest rate on financial ratio. While, (Svensson, 2003) argued that adding variables could increase the explanatory power of the rule, leading to an optimal rule in this context. This issue has been the centre of a large discussion in the literature: as some authors consider important that central banks target asset prices ((Cecchetti, Genberg, Lipsky, & Wadhwani, 2000) (Borio & Lowe, 2002), (Borio, 2005), (Goodhart & Hofmann, 2002 (Chadha, Sarno, & Valente, 2004), others disagree (Bernake & Gertler, 2000) and (Bullard & Schaling, 2002). A model of possible deviation from a simple linear model is presented.

$$fi_t = r_t + \pi_t + \alpha(\pi t - \pi) + a_{y1} Y_t + a_{y2} Y_{t-1} + fi_{t-1} + Bankindex_1 + Bankindex_2 + Bankindex_3 + Bankindex_4 + Liquidityindex + Liquidityindex(-1) + \varepsilon_t$$

The following forms of panel regressions are estimated, where (i, t) indicates respectively the loan type and time index, thus the results indicate that the Fed deviates from the interest rate target and does not pursuit the pre-announced or defined targets. This is considered an interesting result that might help in understanding part of the story behind financial crisis.

It is worth stating that the reaction function-based assessments of US monetary policy are so sensitive to the chosen potential output and inflation target which can be unreliable. Therefore, one should be careful when interpreting such variables. Orphanides argues that the Taylor rule is sensitive to the choice of the variables and the period, which may result in reaching to a different policy. The implementation is then considered to be far from being simple (Orphanides, 1997, 2001) To start with estimating variables, they are classified as follows:

A. Determining r^* and π^*

For the construction of the USA inflation objectiveπ^*, the U.S. Federal Reserve System has no official inflation target. Upon this, the HP filter technique is used to determine inflation trend. The appropriate measure of natural real interest rate because it is consistent with stable inflation and output equal to potential. (NRR) r^* for the united-states over history also presents some difficulties: r^* is likely shifting all the time (contain time subscripts because they may be time-varying). However, the policymaker took a stand where the average r^* will be over some time period. For simplicity, we set its level at 2% as it was assumed in the Taylor rule.

B. Determining i_{taylor}

The interest rate setting in the USA using annual data is analysed from 1955 to 2012. Since there was no single policy interest rate, we used short-term money market rates, i_t as a measure of the stance of monetary policy.

C. Determining y^* and $(y - y^*)$

Calculating y^* is problematic indeed. The most common in the literature is the use of Linear trend (Taylor, 1993), a quadratic trend (Clarida, Jordi , & Mark , 1998), or a Hodrick Prescott filter (Taylor, 1999).

In this paper, a structural definition of potential GDP is used which is in turn developed at the (CBO, 1995). The output gap is measured as the percentage difference between real GDP and the estimate of its potential level. In macroeconomic terms, potential output is defined as a sustainable output, that is, the level of real GDP is consistent with a stable rate of inflation (CBO, 2003, 2004). It is denoted as y^*, and the associated gap is shown in figure 1 in the appendix 2.

Clearly, the construction of the output gap seems difficult since potential output is not observed. (Orphanides, Porter, Reifschneider, Tetlow, & Finan, 2000), (Orphanides, 2001) shows that the central bank can make large and persistent mistakes in the estimation of potential output in response to productivity and cost shocks. The output estimates has an ineligible consequence on policy behaviour and inflation dynamics. Theoretically, it should provide information regarding future inflation. (Orphanides & Van Norden, 2003).

Several techniques have been traditionally used to estimate the potential output, which is usually identified as the output trend as reported at (CBO, 2004). (Taylor, 1993) simply fitted a line through log-levels of real GDP over a short sample period (1984 Q1 to 1992 Q3) as a proxy for potential output. One can also fit trends to lag factor-input and multifactor productivity data and plug these trends into an estimated production function (see CBO, 2004).

Given the applied focus of the paper, the first section profile statistical de-trending methods considered in this paper for estimating potential output:

1) The linear method
2) Moving average
3) The Hodrick-Prescott filter (The HP filter, a purely statistical method, was also used to estimate potential output and the natural rate of interest).

It is worth stating that the MA filtering, the HP filter, and the Beveridge and Nelson decomposition are often used to extract the trend from GDP directly. Indeed, the main evidence is that the HP filter methodology outperforms all models.

1. The output gap using a linear regression method.

The simplest method considered; which was used until the early 70's, involves a linear regression of (the log of) real GDP on a constant and a time trend. So, the trend in (the logarithm of) output is well approximated as a deterministic function of time, given by: $y_t = \alpha + \beta.t + \varepsilon_t$ (1)

The residuals ε_t from the regression equation provide a measure of the output gap, and y_t is the chosen measure of output (in logarithms). This method builds on the basis of an assumption that the GDP can be decomposed into the sum of a slowly evolving secular; which is classified as cycle c_t, and a transitory deviation from it; τ_t which is a linear function of time.

The results from the estimated equation are given in appendix 2. In figure 1 in appendix 2, the graph of actual and potential output is shown. In the beginning of the 1915s and throughout most of the 1920s, output was above its potential level. From 1960 until 1980, the output exceeded potential output, to later approach the fitted value after 1980.

2. MA filter

The second method, which is today's statistical filtering, assumes that the logarithm of output can be decomposed into a cyclical component c_t and a trend component τ_t, $y_t = c_t + \tau_t$ Where τ_t, is the moving average of the output.

Transform output series by a centred moving average of order 2p+1 is given by:

$$\tau_t = \sum_{i=-m_1}^{m_2} \theta_i y_{t+i} = \theta_{-m_1} y_{t-m_1} + \theta_{-m_1+1} y_{t-m_1+1} + \cdots + \theta_{m_2} y_{t+m_2} \quad (2)$$

Where, $\sum_{i=-m_1}^{m_2} \theta_i = 1$; $m_1 \geq 0, m_2 \geq 0$

3. The Hodrick-Prescott filter

Another method to calculate the trend in real share prices uses the Hodrick-Prescott filter (Hodrick & Prescott, 1997) (henceforth, HP). Time series are decomposed into a trend, a cycle, and a noise that is, $y_t = c_t + \tau_t + \varepsilon_t$

Based on this, the filter is given by the equation (3) where the trend m_t is the result of the following optimization problem:

$$\min_{\{g_t\}_{t=-1}^{T}} \left[\sum_{t=1}^{T} c_t^2 + \lambda \sum_{t=1}^{T} [(g_t - g_{t-1}) - (g_{t-1} - g_{t-2})^2]\right] \quad (3)$$

In the case of a HP filter, one also has to choose a value for the "penalty" parameter λ, which determines how smooth a trend can be. The larger the value of λ, , the smoother the growth component, and the greater the variability of output gap. A smaller value indicates a smaller importance of cyclical shock and yields a more volatile series of output gap. The larger the value, the more growth component approaches a linear time trend.

In this article, λ is set at 1600, as suggested in literature for quarterly time series (Hodrick & Prescott, 1997) also (Ravn & Uhlig, 2002), (Baxter & King, 1995), and (Backus & Kehoe, 1992) gave similar justifications..The result extracted from this method shows a large positive swing in output gap during 1950s, in the 1980s and recently (2006-2008). However, the HP filter has remained popular because of its flexibility in tracking the characteristics of the fluctuations in trend output and its simplicity in the economic literature.

IV DATA

Dataset were quarterly at the source and included the short-term interest rate (fedf) commonly used as the monetary policy instrument, the real GDP (RGDP), and the consumer price index (CPI). To generate the output gap we used the HP filter with a smoothing parameters settled on the standard value of 1600 as suggested previously in the literature. That is, □ = 100 × (ln RGDP - GDP POT). The CPI, is used to measure inflation that is, □□□ = 400 × ln (CPI) - ln (CPI).

Real-time data for the CPI and real GDP growth were respectively obtained from Bureau of Economic analysis and Bureau of Labor Statistics.

In a further step, all variables except the interest rates; measured in percent, were transformed into their fourth order log-difference form to ensure stationary given the existence of unit root in their level forms, that is, (log Xt – log Xt-4).

Similarly, the following individual asset prices have been considered: the real stock market price (RSP), the real housing price (RHP) and exchange rates (ER), a measure of financial conditions *proxied* by the financial conditions index (Goodhart & Hofmann, 2000) as an extension of the monetary conditions index, representing a linear combination of interest rates and exchange rates, to include housing and stock prices, and a broad credit aggregate. The latter represents alternatively the three categories of the balance sheets of all commercial banks in the United States: Real Estate Loan (Real_LN), consumer loans (Cons_LN), Commercial and industrial loans (Bus_Loans) and Bank credit (Inv_LN). [The model includes the variables comprised in the table 5. Other variables would be subject to a macro prudential supervision.Some credit booms could be identified as a key factor behind financial crises.

Total credits are used as an early warning indicator for systemic banking crises. The indicator used here is the credit-to- GDP and it's backward looking long-term trend (calculated by using a HP filter). To start with the calculation of the

deviation which was done from a trend (Figure 1 to 8) and a proxy of the threshold beyond the gap of credit to its long-term trend (the credit boom) gave a certain episode of financial crisis in the sample. Specifically, by comparing the financial destabilizing effects of excess liquidity versus credit growth, such global excess liquidity (household and business) are argued to be more significantly correlated to an economic bubble (house price bubble, financial bubble…). Accordingly it is more appropriate to study the impact of the leverage expansion rather than excess liquidity.

Based upon that, a broad measure of excess liquidity of banks is applied which measures the gap between the growth of the money supply and the demand for the narrow money (M0) defined as the ratio (M0/GDP) in a long-term horizon. Liquidity ratio enters the equation with a lag of one quarter to capture possible past effect of the variable on the interest rate. Panel constructed equations are estimated using the OLS estimator.

V RESULTS AND ANALYSIS

Based on the results in Tables 1, 3 and 4, the primary results of the analysis are as follows. First, consider the LS model, column 2 in table 1 presents the results of Taylor rule original version. The results show a positive significant relation between deviation in interest rates and deviation in inflation rates and output gaps variable from stance. In accordance with the main hypothesis, these results suggest that central banks tend to accord more importance to inflation rather than the output gap. Having this result confirms the empirical evidence from the literature.

Second, the Chow test (1960) for structural change in the same regression model was used with a known couple of break dates: 1970, 1979, 1987 and 2006; associated with the move of the U.S. presidential election (See Table 2). As indicated, the most major structural break in this series (indicating a significant change in both the intercept and the slope) over the period 1955-2011 occurred during the late 1970s (Table 3). This particular break may be attributed to the gradual effects of several policy changes during this time, including: (i) Deregulation in the financial industry under Volcker government (Monetary Control Act of 1980). (ii) Expansionary monetary policy stance employed by the Fed (iii) and the innovation that took hold on increasing the credit market which is associated with the functioning of the economy. All of these elements tends to decrease risk aversion over the long term and influenced on the nearly development of **systemic** crisis.

Concerning the augmented version model, it was found that credit indicators would enhance central bank performance (Table 4). To be more precise, I found that there is a positive significant relation between interest rates and all credit ratios. However, the interest rate response to credit ratios is lower than the two conventional objectives. This highlights the Federal Reserve assistance to the credit bubble: The private sector demand responds to easier monetary conditions and may shift their credit origination toward riskier borrowers.

A. Regression results

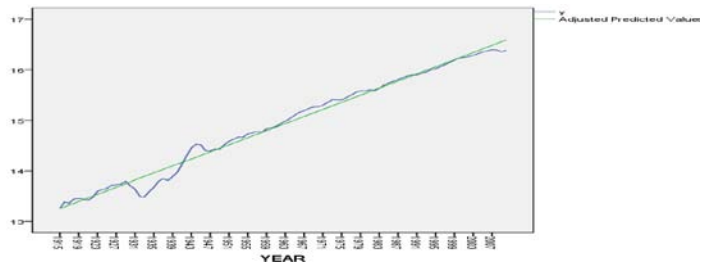

Figure 1: Potential GDP vs. actual based on linear regression estimates

R	R Square	Adjusted R Square	Std. Error of the Estimate
,993[a]	,987	,986	,11489

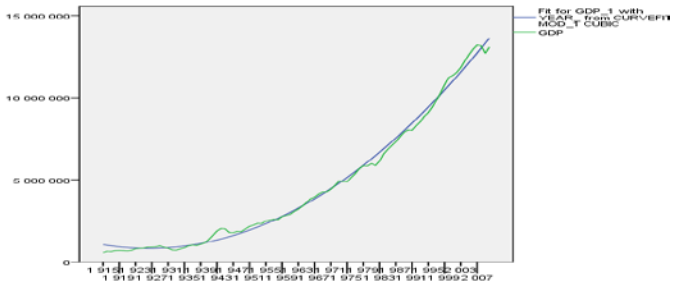

Figure 2: Potential GDP vs. actual based on MA

Model Summary and Parameter Estimates

Dependent Variable:MA(GDP,5,5)

Model Summary

	R^2	F	df_1	df_2	Sig.	Cst	b1	b2	b3
Eq. Cubic	**,997**	12,71 1,724	2	89	,00	4.44E +12	- 3,459,871 ,785	,00	,311

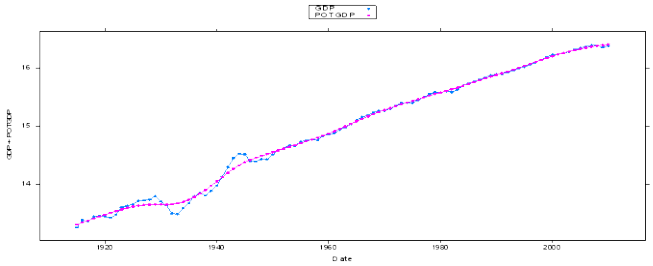

Figure 3: Potential GDP in log terms vs. actual based on HP filter estimate

1) lm (i ~ p + y)
2) **Model estimates:** where significance codes: 0 '***' 0.001 '**' 0.01 '*' 0.05 '.' 0.1 ' ' 1 and residual standard error: 2.933 on 93 degrees of freedom.(1 observation deleted due to missing)

Residuals:

Min	**1Q**	**Median**	**3Q**	**Max**
-6.0113	-1.9225	-0.4232	1.3605	11.1068

	Estimate	Std Error	t	Pr(>| t|)
(Intercept)	**0.07322**	1.1256	0.065	0.948275
p	**1.31745**	0.3372	3.907	0.000177 ***
y	**0.51222**	0.73975	0.692	0.490391

VI CONCLUDING RESULTS

The findings which declare that the monetary policy regime might have changed in significant ways over time, tend to have implications on financial stability. As drawn by the relationship between persistently low policy rates—measured by Taylor rule deviations—and financial variables- it is derived from examining the correlation and lead-lag relationships between Taylor rule deviations and financial crisis from 1955 to 2012. By responding to the inflation, this should help the central bank's ability to respond to financial disruptions that do arise. Since systemic crisis often occur at low level of inflation, when investment booms and rapid credit expands, the money created could provide the fuel of financial bubbles. Moreover, stated evidences show that the Federal Reserve Bank is not targeting the financial conditions in certain periods, so the lack of consideration to financial markets might be one of the causes of crisis such as the recent credit crunch that started in the United States. I conclude that the recurrence of financial crisis has its roots in the fact that lenders offer increasingly money and lead to a higher-risk borrowers comportment. In my view, the most important challenges to monetary policy related to structural change in this recurrent crisis episode arise from possible changes in political atmosphere. Being a causal factor for a number of recessions and degradation in economic and social conditions affecting human beings, fluctuations in interest rate policy are a significant problem in the study as we suppose. Nowadays, the recurrence of financial crisis is at a very high rate in the United States and across the world as reported by the (BIS, 2009). Unless radical changes in the US monetary policy are applied, the United states will face another one in the near future that are assumed to be more systemic because of financial innovations (securitizations, derivatives, etc.); see for example (Allen & Carletti, 2006), (Rajan, 2005), and (Sveiby, 2012) among many others who assess the systemic effects of financial innovation.

Table 1: What can Taylor rule say about monetary policy in United-States over the period (1955:1-2012:4)?

	-1	*p value*	Std. Error	-2	*p value*
Inflation-∏	0.18*** (3.57)	0.0004	0.050644	0.59*** (8.07)	0
Output gap	0.27*** (8.50)	0	0.032242	0.34*** (6.60)	0
ff(-1)	0.71*** (19.39)	0	0.036473	0.042*** (3.42)	0.0007
∏	0.30*** (7.77)	0	0.038269	1	
r	0.29*** (6.30	0	0.046511	1	
Adj. R2	0.95			0.88	
Log Likelihood	-254.83			-364.32	
HQC	2.28			3.2	
Mean dep. var	5.300173			5.300173	
S.D dep var	3.473406			3.473406	

Source: *Author calculation* (Eviews) /Table for LS regression

Table 2: Presidents of the United States of America over the period (1955-2012)

9th	**1951–1970**	William McChesney Martin	Q2, 1951 to Q1, 1970
10th	**1970–1978**	Arthur F. Burns	Q2, 1970 to Q1, 1978
11th	**1978–1979**	G. William Miller Pr	Q2, 1978 to Q3, 1979
12th	**1979-1987**	**Paul Volcker**	**Q4, 1979 to Q3, 1987**
13th	**1987-2006**	Alan Greenspan	Q4, 1987 to Q1, 2006
14th	**2006 -**	Ben Bernanke	Q2, 2006-

Table 3: Structural changes by Chow test

H_0	H_1	Statistics F	p-value	Results
1955-2012	[1955:1-1970:1:]$_{(1)\text{ and}}$ [1970:2-2012:4]$_{(2)}$	3.195	0.0244**	Structural break in 1970
1970-2012	[1970:2-1979:3] and [1979:4-2012:4]	4.072	**0.0077*** **	**Break in 1979**
1979-2012	[1979:4-1987:3] and [1987:4-2012:4]	3.798	0.0110**	Break in 1987
1987-2012	[1987:4-2006:1] and [2006:2-2012:4]	2.767	0.0426**	Break in 2006

Source: *Author*/Eviews

Common values of significance level (p-value) below which the null hypothesis will be rejected are 5% and 1%.

Table 4: Taylor rule augmented with financial variables, liquidity and credit (1955 :1-2012 :4)

	-3	*p value*	Std. Error
Inflation-∏	0.58*** (8.21)	0	0.07
Output gap	0.32*** (5.73)	0	0.055
ff(-1)	0.04*** (3.07)	0.0024	0.014
$Bankindex_1$	-0.007*** (-2.93)	0.0038	-2.93
$Bankindex_2$	0.008*** (2.03)	0.0431	0.004
$Bankindex_3$	0.0098*** (2.91)	0.004	0.003
$Bankindex_4$	0.012*** (3.88)	0.0001	0.003
Gap_DJ	0.0003*** (1.92)	0.0559	0.0002
M_0/PIE	-29.47 (24.16)	0.2238	24.15628
M_0/PIB(-1)	-28.01 (24.88)	0.2614	24.87837
Adj. R^2	0.89		
Log Likelihood	-350.25		
HQC	3.18		
Mean dep. Var	5.3		
S.D dep. Var	3.47		

Table 5: Independent variables summary

Variables	Definition	Sign (expected)	Source
Bankindex₁	1947Q1 2012Q4 // bankratio1=loaninv-loaninvtrend	+, High	*Federal Reserve Bank Author calculations Data are quarterly, in billions $.*
Bankindex₂	1947Q1 2012Q4 // bankratio2=consloan-consloantrend	+, Average	Ibid.
Bankindex₃	1947Q1 2012Q4 // bankratio3=busloan-busloantrend	+, Average	Ibid.
Bankindex₄	1947Q1 2012Q4 // bankratio4=mortgloan-morgtloantrend	+, Average	Ibid.
M_0/PE	Monetary base as percentage of gdp.	High	Federal Reserve Bank of St Louis.
Gap_DJ	Asset price gap represented by the Dow Jones *(the HP filter is used to calculate the trend).*	High	S&P Dow Jones Indices LLC › Dow Jones Averages.

ISBN: 978-1-61804-225-5

APPENDIX: Figures and tables from this article

Appendix 1

Table 1: Data

Definitions	Source
Output Gap is the proportional deviation of real GDP from its long-run trend (Hodrick & Prescott, 1997) smoothing parameter = 100.	Real Gross Domestic Product obtained from (Johnston & Williamson, 2013) for 1789 to present.
The inflation gap is obtained by taking the difference between actual and target inflation. The Fed does not have an official target rate; therefore we determine the trend inflation using the HP filter, and we redefined the inflation gap as the difference between actual inflation (percentage change in the log of the GDP deflator expressed at an annualized rate) and trend inflation.	GDP deflator obtained from (Johnston & Williamson, 2013) for 1789 to present.
i_t is measured by the commercial paper rate for the years 1879-1914 and by the federal funds rate for the years 1954-2010.	Federal Reserve Bank of Saint Louis (Louis)

Table 2: Summary of Crisis

Crisis Type	Threshold	Period	Maximum
Inflation	An annual inflation rate 20% or higher. We also examine separately the incidence of more extreme cases where inflation exceeds 40% per annum	1500-1790 1800-1913 1914-2006	173.1 159.6 9.63E+26
Currency Crashes	An annual depreciation versus the US dollar (or the relevant anchor currency) of 15% or more.	1800-1913 1914-2006	275.7 3.37E+09
Currency debasement Type I	A reduction in the metallic content of coins in circulation of 5% or more.	1258-1799 1800-1913	-56.8 -55.0
Currency debasement Type II	A currency reform where a new currency replaces a much depreciated earlier currency in circulation	The most extreme episode in our sample is the 1948 Chinese conversion at a rate of 3 million to 1	

Appendix 2

As a first step of the study it is useful to briefly review the data. In the following figure the inflation and interest rates move closely together in the period under consideration. This suggests the presence of one nominal trend. The inflation rose at the end of the 1980s, declined continuously from 1990 to 1998 and increased from 1999 to 2000 before falling again. Both the short and long term interest rate move in similar ways, with the exception of a peak in 1995 that followed a tightening of monetary policy in the US. The Dow Jones Industrial Average provides a view of the US stock market and economy. Originally, the index was made up of 11 stocks; it now contains 30 component companies in various industries. Figure 6 shows an annual time series of the U.S. Real market over the period 1915 the 2010. There is a clear trend. But in addition the earlier part of the figure marked cyclical behaviour as the economy moves from boom to recession; that's why it is important to add a cyclical component in a model for USA GDP.This evidence leads us to the 1920s, a period which marked the birth of modern central banking in the United States. Moreover, at this time the Fed was fairly independent from the government (see). The properties of the series change after the end of the Second World War and illustrate another aspect of economic and social time series that don't remain over time. The first 14 points and the last 72 points after 1945 are the layer at the bottom of the figure and suggest an orderly market. The remainder clearly reflect the subsequent turmoil in this market. The model we will examine is with an addition of a log trend as used in Taylor (1993)

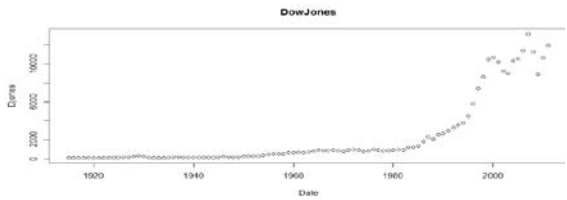

Figure 4: Dow Jones
Source: FRED economic data. Federal Reserve Bank of St Louis.

The Dow Jones Industrial Average provides a view of the US stock market and economy. Originally, the index was made up of 11 stocks; it now contains 30 component companies in various industries

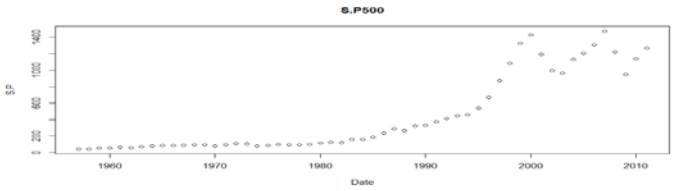

Figure 5: S&P 500

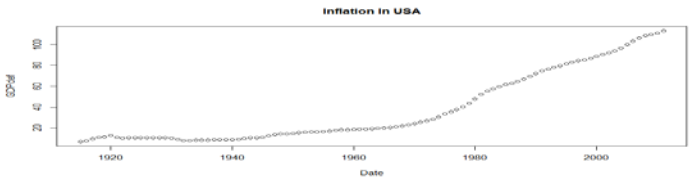

Figure 6: Inflation in USA (GDP deflator)

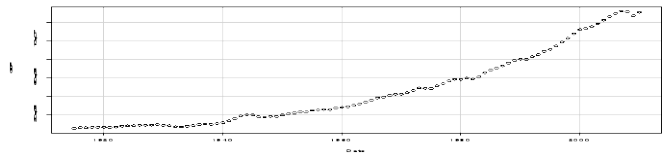

Figure 7: U.S. Real market

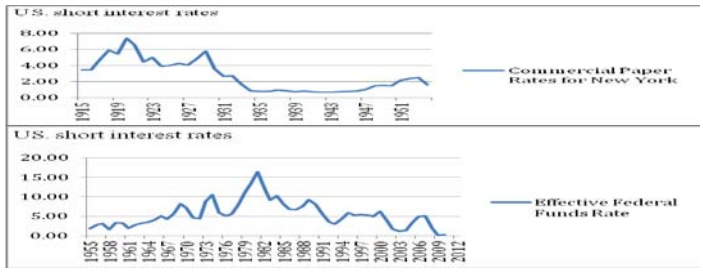

Figure 8: US. Short interest rates
Source: Federal Reserve Bank of St Louis

REFERENCES

[1] Allen, F., & Carletti, E. (2006). *Mark-to-Market Accounting and Liquidity Pricing*. Available at: http://finance.wharton.upenn.edu/~allenf/download/Vita/Allen-Carletti-MMA-200706-final.pdf

[2] Asso, P., Kahn, G., & Leeson, R. (2007). The Taylor rule and the transformation of monetary policy. *Monetary Policy Rules: From Adam*

Smith to John Taylor (p. 41). Kansas: Federal Reserve Bank of Kansas City, Economic Research Department.

[3] Backus , D., & Kehoe, P. (1992). International Evidence on the Historical Properties of Business Cycles,. *American Economic Review , 82* (4), 864-888.

[4] Batini, N., & Haldane, A. G. (1999). Forward Looking Rules for Monetary Policy. In J. Taylor, *Monetary Policy Rules* (pp. 157-202). University of Chicago Press. Available at:http://www.nber.org/chapters/c7416.pdf

[5] Baxter , M., & King, R. (1995). Measuring Business Cycles Approximate Band-Pass Filters for Economic Time Series. *NBERWorking Paper N 5022* .

[6] Bernake, B., & Gertler, M. (2000). Monetary Policy and Asset Price Volatility. *Economic Review* , 17-51.

[7] Bernanke, B., Gertler, M., & Ghilchrist, S. (1999). The Financial Accelerator in a Quantitative Business Cycle Framework. In N. Y. Princeton University, J. B. Laylor, & M. Woodford (Eds.), *Handbook of Macroeconomics* (Vol. 1, pp. 1341-1391). 1999 Elsevier Science B.V. Available at: http://faculty.wcas.northwestern.edu/~lchrist/course/Czech/BGG%201999%20Handbook%20chapter.pdf

[8] BIS. (2009). Retrieved from www.bis.org

[9] Borio, C. (2005). The Search for the Elusive Twin Goals of Monetary and Financial Stability. *DG ECFIN Annual Research Conference. 2*, pp. 1-27. Brussels: Bank for International Settlements. Available at: ec.europa.eu/economy_finance/events/2005/bxlforum1005/borio_en.pdf

[10] Borio, C., & Lowe, P. (2002). Asset prices, financial and monetary stability: exploring the nexus. *Changes in Risk Through Time: Measurement and Policy Options. 114.* Switzerland: Bank for International Settlements Working Papers. Available at: http://www.latrobefinancialmanagement.com/Research/Macroeconomics/Asset%20Prices%20Financial%20and%20Monetary%20Stability.pdf

[11] Bullard, J. B., & Schaling, E. (2002). *Why the Fed Should Ignore the Stock Market.* The Federal Reserve Bank of St. Louis. Available at: http://research.stlouisfed.org/publications/review/02/03/35-42BullardSchaling.pdf

[12] Castelnuovo, E. (2003). Taylor rules, omitted variables, and interest rate smoothing in the US. *Economics Letters , 81* (1), 55-59.

[13] Castro, V. (2008). Are central banks following a linear or non linear (augmented) Taylor rule? (N. U. Minho, Ed.) *NIPE Working Papers* .

[14] CBO. (2003, 2004). *CBO's method for estimating potential output.* The Congress of the United States, Congressional Budget Office.

[15] CBO. (1995). *Method For Estimating Potential Output.* Washington. Available:cbo.gov/sites/default/files/cbofiles/ftpdocs/3xx/doc312/potout.pdf

[16] Cecchetti, S. G., Genberg, H., Lipsky, J., & Wadhwani, S. (2000). Asset Prices and Central Bank Policy. *Central Banks and Asset Prices. 2*, pp. 1-142. Geneva: ICMB and the CEPR .Available at: http://down.cenet.org.cn/upfile/8/2010318204458149.pdf

[17] Chadha, J. S., Sarno, L., & Valente, G. (2004). Monetary Policy Rules, Asset Prices, and Exchange Rates. *IMF Staff Papers , 51* (3), 529-552. Available:www.imf.org/external/pubs/ft/staffp/2004/03/pdf/chadha.pdf

[18] Clarida, R., Jordi , G., & Mark , G. (1998). Monetary policy rules in practice: some international evidence. *european economic review* (6), 1033-1067.

[19] Clarida, R., Gali, J., & Gertler, M. (2000). Monetary Policy Rules and Macroeconomic Stability: Evidence and some Theory. *The Quarterly Journal of Economics* , 148-180.

[20] Federal Reserve Bank, Louis, available at www.research.stlouisfed.org/fred2/

[21] Filardo, A. J. (2001). *Should Monetary Policy Respond to Asset Price Bubbles? Some Experimental Results.* Available at: http://www.kc.frb.org/publicat/reswkpap/pdf/rwp01-04.pdf

[22] FOMC. (2009, November 3-4). Minutes of the Federal Open Market Committee. Wahington, NY. Available at: www.federalreserve.gov/monetarypolicy/fomcminutes20091104.htm

[23] Friedman, M., & Schwartz, A. (1960). *A monetary history of the United States, 1867-1960.* Princeton University Press.

[24] Goodhart, C. (1988). *The evolution of central banks* (Vol. 1). MIT Press Books.

[25] Goodhart, C. (1994). What should central banks do? What should be their macroeconomic objectives and operations? . *The Economic Journal* , 1424-1436.

[26] Goodhart, C., & Hofmann, B. (2002). *Asset Prices and the Conduct of Monetary Policy.* Available at: http://citeseerx.ist.psu.edu/viewdoc/download?doi=10.1.1.199.1957&rep=rep1&type=pdf

[27] Goodhart, C., & Hofmann, B. (2000). *Financial Variables and the Conduct of Monetary Policy.* Available at: http://citeseerx.ist.psu.edu/viewdoc/download?doi=10.1.1.200.8989&rep=rep1&type=pdf

[28] Hodrick, R., & Prescott, E. (1997). Postwar U.S business cycles: An empirical investigation. *Journal of Money, Credit and Banking , 29*, 1-16.

[29] Hoffmann, B. (2012). *Taylor rules and monetary policy: a global " Great Deviation "?* BIS Quarterly Review.

[30] Johnston, L., & Williamson, S. (2013). *What was the U.S. GDP then ?* . Retrieved 2013, from measuring worth. Available at: www.measuringworth.com/usgdp/

[31] Judd, J. P., & Rudebusch , G. D. (1998). Taylor's Rule and the Fed: 1970-1997. *Economic Review-Federal Reserve Bank of San Francisco* , 3-16.

[32] Kahn, G. (2009). Taylor rule deviations and financial imbalances. *Economic Review* (Q II), 63-69.

[33] Mccallum, B. (1988). Robustness properties of a rule for monetary policy. *Carnegie-Rochester conference series on public policy, 29*, pp. 173-203. North-Holland.

[34] McCallum, B. T. (2000). Alternative monetary policy rules: a comparison with historical settings for the United States, the United Kingdom, and Japan. *National Bureau of Economic Research* (w7725).

[35] McCallum, B. T. (1999). Chapter 23 Issues in the design of monetary policy rules. In B. T. McCallum, *Handbook of macroeconomics* (Vol. 1C, pp. 1483-1530). Carnegie Mellon University and National Bureau of Economic Research.

[36] Orphanides, A. (2003). Historical monetary analysis and the taylor rule. *Journal of Monetary Economics , 50* (5), 983-1022.

[37] Orphanides, A. (2001). Monetary policy rules based on real time data. *American Economic Review , 91* (4), 964-985.

[38] Orphanides, A. (1997). *Monetary Policy Rules Based on Real-Time Data.* Board of Governors of the Federal Reserve System. Available at: http://www.federalreserve.gov/pubs/feds/1998/199803/199803pap.pdf

[39] Orphanides, A., & Van Norden, S. (2003, January). The unreliability of inflation forcasts based on output gap estimates in real time. *CIRANO Scientific Series s-1* .

[40] Orphanides, A., Porter, R., Reifschneider, D., Tetlow, R., & Finan, F. (2000). Errors in the measurement of the output gap and the design of monetary policy. *Journal of Economic and Business , 52* (1/2), 117-141.

[41] Rajan, R. (2005). Has financial development made the world riskier? (pp. 313-369). Federal Reserve Bank of Kansas City.

[42] Ravn, M., & Uhlig, H. (2002). On adjusting the Hodrick-Prescott filter for the frequency of observations. *The Review of Economics and Statistics , 84* (2), 371-375.

[43] Reinhart, C., & Rogoff, K. (2011). From financial crash to debt crisis. *American Economic Review , 101* (5), 1676-1706.

[44] Rudebusch, G. D. (2002). Term structure evidence on interest rate smoothing and monetary policy inertia. *Journal of monetary economics , 49* (6), 1161-1187.

[45] Rudebusch, G., & Lars EO , S. (1999). Policy rules for inflation targeting. In B. J. Taylor, *Monetary Policy Rules* (pp. 203-262). Chicago: University of Chicago Press.

[46] Sveiby, K.-E. (2012). Innovation and the global financial crisis - systemic consequences of incompetence . *International Journal of Entrepreneurship and Innovation Management , 21* (1-2), 30-50.

[47] Svensson, L. E. (2003). What Is Wrong with Taylor Rules? Using Judgment in Monetary Policy through Targeting Rules. *Journal of Economic Literature* , 1-76. Available at: http://www.norges-bank.no/Upload/import/konferanser/2003-05-05/data/svensson.pdf

[48] Taylor, J. (1993). Discretion versus policy rules in practice. *Carnegie-Rochester Conference Series on Public Policy , 39*, 195-214.

[49] Taylor, J. (1999). The robustness and efficiency of monetary policy rules as guidelines for interest rate setting by the European Central Bank. *Journal of Monetary Economics , 43* (3), 655-679.

[50] Thorbecke, W. (2000). *A dual mandate for the federal reserve: The pursuit of price stability and full employment.* Public policy brief // Jerome Levy Economics Institute of Bard College N°60. Economics Institute of Bard.

[51] Thornton, D. (2012). The dual mandate: hast the Fed changed its objective ? *St. Louis Review , 94* (2), 177-33.*United States Congress.* (1957). Retrieved from www.congress.gov

Euro-Asia comparative study of logistics cost

Korrakot Y. Tippayawong, and Kevin Veyrat-Parisien

***Abstract*—**This study aims to describe and compare infrastructure systems of Asian and European countries. The first part is a survey to show similarities and differences between the two systems. Comparison between transportation costs is made. Road and air transports are studied, starting from Paris for Europe and from Bangkok for Asia to other cities within their respective continents. It was shown that it is not possible to rank in one part Asian countries and in second part European countries. It is better to rank Asian and European countries together because they represent the same level of development in one hand and the emerging countries in the other. Freight transport has been shown to be cheaper in Asia than in Europe, even if the price depends on destination. However, border crossing is more expensive in Asia than in European Union.

***Keywords*—**Logistics cost, supply chain management, transportation, Europe, Asia.

I. Introduction

LOGISTICS is the management of business operations, such as the acquisition, storage, transportation and delivery of goods along the supply chain. Efficiency of this operation depends on many factors. According to Wood et al. [1], infrastructure is a main criterion important to logistics excellence. Infrastructure provides information about logistics performance of a country. Developed and well maintained infrastructures make exchanges easier and it is an important attribute in order to trade with other countries.

Nowadays, Europe and Asia are two major actors of international trade. In fact, Asia's and Europe's gross domestic products surpassed that of the US. More and more exchanges are achieved between these two regions. That's why this study aims to compare Asian and European countries logistics infrastructures. Moreover, one of the major objectives is to reduce the logistics costs. This study compares different transportation costs (road and air freights) in the two places.

II. Review of Background Information

Some researchers have tried to compare logistics infrastructure between Europe and Asia. Bang [2] led a study of the logistics system in Northeast Asia where he compared their transportation systems with other major countries in the World, including the US, Germany, and the UK, shown in Table 1. In terms of road density represented by length of roadway per 1000 km^2 of land, Northeast Asian countries excluding Japan show relatively low road density, compared to Germany and the UK. It is the same remark concerning the rail transportation. For the airports (comparing area of each country and the number of airports), Germany and the UK are leading. However, this study does not take into consideration some major Asian countries, particularly Singapore and Hong Kong.

Bookbinder et al. [3] compared many European and Asian logistics systems, focusing on development and maintenance of the logistics system infrastructure. They classified the logistics systems into four general attributes in three tiers. Infrastructure was one of them as illustrated in Fig. 1.

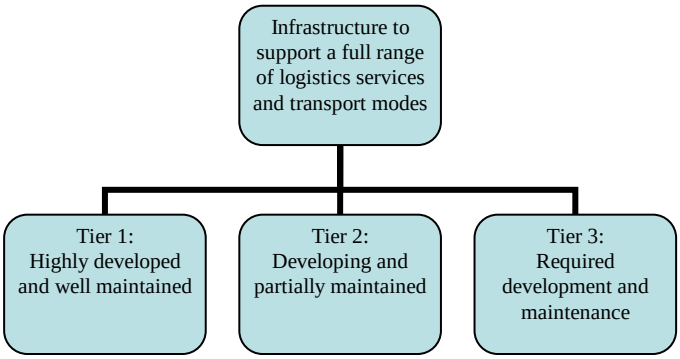

Fig. 1 Definition of logistics infrastructure tiers.

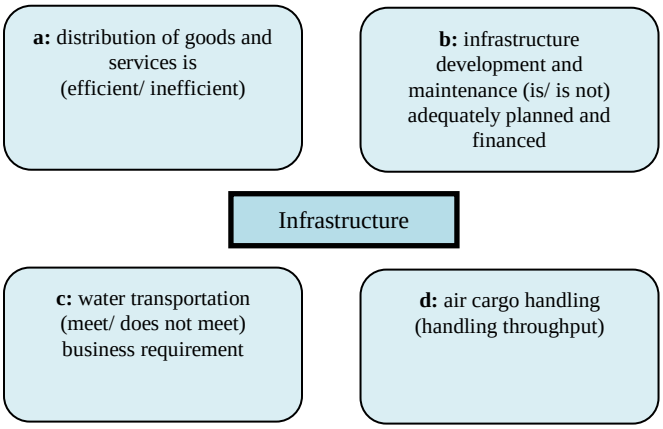

Fig. 2 Specific attributes that determines logistics infrastructure tiers.

This work was supported in part by Chiang Mai University under Center of Excellence in Logistics and Supply Chain Management grant.

K. Y. Tippayawong is with Department of Industrial Engineering, Faculty of Engineering, Chiang Mai University, Chiang Mai, 50200 Thailand. (corresponding author , phone: +66-5394-4125; fax: +66-5394-4185; e-mail: korrakot@eng.cmu.ac.th)

K. Veyrat-Parisien was with Department of Industrial Engineering, Faculty of Engineering, Chiang Mai University, Chiang Mai, 50200 Thailand. He is currently with Roger Dubuis in France, as a chief supply chain project manager. (kevin.veyrat@gmail.com)

Table 1 Overview of transport infrastructure in East Asia and other major countries (adapted from Bang [2])

		South Korea	North Korea	China	Mongolia	Japan	US	Germany	UK
	Population (million)	48.3	22.5	1287	2.7	127.2	290	82.3	60
	Area (1000 km^2)	98.5	120.5	9597	1565	377.8	9629	357.0	244.8
	Land	98.2	120.4	9326	1554	374.7	9159	349.2	241.6
	Water	0.3	0.1	271	10	3.1	470	7.8	3.2
Road	Road length (1000 km)	87.5	31.2	1400	34.0	1152	6335	230.7	371.9
	Road density (km/1000 km^2)	888	259	146	2	3050	658	231	372
Railway	Railway length (1000 km)	3125	5214	71600	1815	23170	46	231	372
	Railway density (km/1000 km^2)	31.7	43.3	7.5	1.2	61.3	45.8	230.7	371.9
Airport	Number of airport	102	72	500	50	175	14801	551	470
	Airport with paved runways	69	34	351	10	141	5131	328	334

According to the World competitiveness yearbook [4], this attribute was divided into four specific attributes (a, b, c and d), shown in Fig. 2. Based on a statistical cluster analysis, Bookbinder et al. [3] can provide a non-standardized data matrix. The standardized results do not give detail on each attribute. Table 2 provides raw ranking scores for cluster analysis. After calculation of average, the ranking of each country can be evaluated, shown in Table 3. It was shown that infrastructure development is homogeneous between Asia and Europe. It is not possible to separate between Asian and European countries. However, Table 3 also shows the noted difference between developed and emerging countries. With the occasional exception, emerging countries of Europe (Eastern European countries) and Asia (Indonesia, India, the Philippines) are at the end of the ranking. The leading countries are Singapore, Germany, Hong Kong, and France. These countries have the same level of development and maintenance. Wilson [5] regrouped countries in Europe and Central Asia (ECA) and conducted a comparative study with South Asian countries, focusing on the constraints for development of trade facilitation. For South Asia, Wilson [5] pointed out the lack of infrastructure such as poor road, rail, air and shipping link. For instance, in 2004, the percentage of paved road is approximately 37% for South Asia, while it is

Table 2 Raw ranking scores for infrastructure attribute

	Infrastructure			
	a	b	c	d
Austria	10	9	13	105
Belgium	24	23	16	27
Canada	11	12	9	51
China	25	24	30	28
Czechoslovakia	31	35	35	223
Denmark	2	3	2	46
Finland	5	4	4	124
France	6	8	15	14
Germany	4	2	3	9
Greece	38	31	28	571
Hong Kong	7	5	5	2
Hungary	27	30	33	232
India	46	47	47	64
Indonesia	41	39	43	63
Ireland	33	27	29	112
Italy	39	41	37	69
Korea	37	34	40	7
Luxembourg	9	7	17	38
Malaysia	16	13	24	40
Mexico	35	38	36	571
Netherlands	17	18	7	15
Philippines	44	40	42	50
Poland	43	42	44	176
Portugal	23	21	25	116
Russia	40	46	41	135
Singapore	1	1	1	10
Slovenia	32	36	26	359
Spain	21	15	22	55
Sweden	8	11	6	93
Taiwan	22	22	20	17
Thailand	26	26	31	24
UK	28	28	27	13
USA	13	16	14	1

Table 3 Country ranking for infrastructure attribute

	Average of specific attribute	Ranking
Singapore	9	13
Germany	23	16
Hong Kong	12	9
France	24	30
USA	35	35
Denmark	3	2
Netherlands	4	4
Luxembourg	8	15
Taiwan	2	3
Canada	31	28
Belgium	5	5
Malaysia	30	33
UK	47	47
China	39	43
Thailand	27	29
Spain	41	37
Korea	34	40
Sweden	7	17
Austria	13	24
Finland	38	36
Philippines	18	7
Portugal	40	42
Indonesia	42	44
Italy	21	25
Ireland	46	41
India	1	1
Russia	36	26
Poland	15	22
Hungary	11	6
Czechoslovakia	22	20
Slovenia	26	31
Greece	28	27
Mexico	16	14

ISBN: 978-1-61804-225-5

Table 4 Estimated air freight cost for door-to-door service to cities in Europe

	distance		Minimum charge			Per kg		
	(km)	kg	THB	USD	Euro	THB	USD	Euro
Berlin	880	70	18000	555	450	260	8	6.5
Rome	1110	70	18000	555	450	260	8	6.5
Porto	1208	70	17580	543	440	252	7.8	6.3

Table 5 Estimated air freight cost to cities in Southeast Asia

	distance	Minimum charge		Per kg	
	(km)	THB	USD	THB	USD
Vientiane	520	700	20.59	16	0.47
Hanoi	993	700	20.59	30	0.88
Hochiminh city	669	700	20.59	20	0.59
Phnom Penh	530	700	20.59	16	0.47
Yangon	584	700	20.59	18	0.53

Table 6 International priority express cost rate to Southeast Asia

	10 kg box		Additional rate per kg > 10 kg, up to 20 kg		21 kg box		Additional rate per kg > 21 kg, up to 44 kg	
	THB	USD	THB	USD	THB	USD	THB	USD
Laos	3753	110.38	137	4.03	5411	159.15	291	8.56
Cambodia	3753	110.38	137	4.03	5411	159.15	291	8.56
Vietnam	4308	126.70	191	5.62	6536	192.23	319	9.38
Myanmar	4308	126.70	191	5.62	6536	192.23	319	9.38

Table 7 Estimated air freight cost for door-to-door service to cities in Southeast Asia

	distance	Charge for 70-100 kg		
	(km)	THB	USD	Euro
Vientiane	520	280	8.7	7
Hanoi	993	125	3.9	3.1
Phnom Penh	530	125	3.9	3.1

about 86% for ECA countries. It was shown that it is not possible to separate between European and Asia countries' infrastructure. Logistics infrastructure is similar between developed countries in Europe and Asia. But, difference exists if developed and emerging countries of Europe and Asia are to be compared.

III. Logistics Cost Analysis

After the comparison of infrastructure between European and Asian countries, this part of the study presents comparison of road and air freight costs between European and Asian cities.

A. Air Freight

Estimation has been made for air freight cost from Paris to other capital cities in Europe using a freight operator. The estimated cost is displayed in Table 4. For Southeast Asia, Table 5 shows air freight cost between Bangkok and other cities in the region using Thai Airways Cargo. Table 6 shows express delivery cost to main cities in Southeast Asia. In all cases, the freight transport using a freight operator such as UPS, which delivers door-to-door service, is more expensive. In order to compare freight cost in Southeast Asia and Europe, Table 7 presents estimated air freight cost from Bangkok to three cities in Southeast Asia. With an exception of Laos, prices were found to be cheaper in Asia than in Europe.

B. Road Freight

By using an international freight operator, the transported weight using road is limited to 70 kg. This type of operator offers different services with different delivery times, prices, and insurance policies. Table 8 shows estimated road freight cost in Europe. Contrary to Asia, the border crossing fee is non-existent in European Union. Table 9 shows border crossing fee in Southeast Asia. They vary greatly, depending on which country to enter. The border crossing fee was found to account between 20 – 50% of the total transport cost.

In Europe, according to "comite national routier" which is an official French technical agency, the relative part of diesel price in the transport cost is 24%. In France, a liter of diesel bought costs 0.94 Euro or 37.7 Thai baht (THB). This value is close to the average value in Europe. So main transport cost (fuel cost) is similar between the two regions.

ISBN: 978-1-61804-225-5

Table 8 Estimated road freight cost to cities in Europe

	distance	20 kg			50 kg			70 kg		
	(km)	THB	USD	Euro	THB	USD	Euro	THB	USD	Euro
Berlin	880	12000	370	300	18000	550	450	22700	700	570
Rome	1110	12000	370	300	18000	550	450	22700	700	570
Porto	1208	12000	370	300	18000	550	450	22500	693	565

Table 9 Cost of border crossing for transport in Southeast Asia

	Total cost (THB)	Border crossing cost (THB)	Percentage of total cost (%)
Bangkok-Vientiane	547	131	24
Bangkok-Hanoi	2907	757	26
Bangkok-Phnom Penh-Hochiminh city	751	381	51
Bangkok-Yangon	760	150	20

IV. Conclusion

This study shows that globally Western European countries and developed Asian countries are equally well developed with respect to logistics infrastructures. These countries present a high level of development and maintenance. Some countries of ECA are now new EU members. This new membership could allow them to develop their logistics systems. Regarding the costs, Asian transportation is cheaper than European, as expected. It is noted here that free border crossing is a real advantage for EU members. If the border crossing tariff in Asia can be negotiated, it will encourage more trade.

Acknowledgment

We would like to thank secretarial staff at the Department of Industrial Engineering, Faculty of Engineering, Chiang Mai University for assistance.

References

[1] D. F. Wood, A. Barone, P. Murphy, and D. L. Wardlow, "Logistics and transportation in different parts of the World," in *International Logistics*, London: Chapman & Hall, 1995, ch. 3.
[2] H. K. Bang, "Toward an integrated logistics system in Northeast Asia," *East Asian Review*, vol. 16, pp. 111-121, 2004.
[3] J. H. Bookbinder, and C. S. Tan, "Comparison of Asian and European logistics systems," *International Journal of Physical Distribution and Logistics Management*, vol. 33, pp. 36-58, 2003.
[4] S. Garelli, World Competitiveness Report, EMF Foundation, Geneva, Switzerland, 1999.
[5] J. S. Wilson, "Integration and trade facilitation in South Asia and ECA: contrast and commonalities," PRAL seminar, 2004.

Korrakot Y. Tippayawong graduated with B.Eng. in industrial engineering from Chiang Mai University, Thailand, M.Eng. in industrial engineering and management from Swinburne University of Technology, Australia, and D.Eng. in decision science from Tokyo Institute of Technology, Japan. She is currently an assistant professor at the Department of Industrial Engineering, Chiang Mai University. Her fields of specialization are SCM, Logistics, and Performance Measurement.

Kevin Veyrat-Parisien was a research engineer at the Department of Industrial Engineering, Chiang Mai University. He is now working with Roger Dubuis Co., Ltd., in France, as a chief supply chain project manager.

Is the cost function still linear? An empirical study

Bassam Baroma

***Abstract*—**the main objective of this study is to estimate the cost function behavior amid the new manufacturing environment. Because accountants have always assumed linearity of the cost function and economists the converse (non-linearity), this study's goal is to discover its actual behavior (linear or non-linear). This study depends upon descriptive and inductive extrapolations of the cost function: by collecting actual cost data from two companies. The first one represents traditional manufacturing environment (T) whilst the second new manufacturing environment (M) for 24 months from {1/1/2010- 1/1/2012}. Results indicate that the best model to represent the cost function for (T) company is non-linear (logarithmic model) (R^2 =92.1%); conversely, the best model for (M) company is in fact the multiple linear one (R^2 =71.2%), following its non-linear counterpart (logarithmic model) (R^2 =67.2%).

***Key words*—**linear cost function, non-linear cost function, cost classification, Activity Based Costing, Egypt

I. Introduction

Accounting literature has hitherto assumed the linearity of the cost function; hypotheses call for variable costs to change alongside variations in production volumes and for fixed costs to remain unvaried. The assumption about linear cost function by accountants was due to the following reasons[1], and [12]:

a) The production process and Industrial environment were simply and there were availability of production materials, labors and other services

b) Regular or traditional level of technology used by industries.

c) The desire of Accountants to ease the calculations of cost of product unit and ease to prepare cost function.

All previous factors led to use of an approximate cost function en lieu of a real one; and with the appearance of new manufacturing variables. Because the volume of production was not the only variable influencing cost function behavior, the importance of estimating it decreased. Thence costdefinition shifted from the concept of cost based on volume to the concept of activity-based costing and cost classification shifted from variable cost and fixed cost to flexible cost and committed cost .

II. Disadvantages of volume based costing system

The volume based costing system uses drivers related to the volume to aggregate costs, such as direct labor, machine hour and direct material; it also measures the consumption of overhead resources[9],[11], and[12].

Risks related to the application of the volume based costing system are the following:

a) Clear cause- and-effect relationship between cost accumulation and activity unit.

b) Simple production process rely upon judgmental allocation bases.

c) Distorts the cost of activity unit.

III. Features of new manufacturing environment

There are many features within new manufacturing environment, namely the following[17]:

a) The elements of variable costs in the short run are direct materials and power and the remaining elements represent fixed costs. Moreover, they are increasing in non-financial measures and decreasing in financial measures

b) The time of product life cycle decreased, so the importance of traditional cost report decreased in the operational control.

ISBN: 978-1-61804-225-5

c) There exists increasing importance for activity based costing which helps implementation control upon cost drivers

d) A fall in the percentage ratio of direct labor to total costs.

e) Decreasing in the cost of product within achieving economies of scale[2].

(f) The greater in the production of finished goods, the shorter in the products' life cycle

IV. Activity based costing (ABC): background, definition and elements

The introduction of activity based costing (ABC) began in the late 1980s by Prof. Kaplan and Prof. Cooper in the Harvard Business School. They published many papers together related to ABC such as "Relevance lost: the rise and fall of management accounting" and "Relevance regained". The activity based costing system involves the utilization of a diversity of cost drivers containing volume-based cost drivers and non-volume- based cost drivers. The definition of volume-based cost drivers relates to the fact that cost drivers, consuming by products, are proportional to product volume. Other cost drivers which are not related to volume-based cost drivers are considered as non-volume-based cost drivers[5], [6], and [14].

Activity based costing (ABC) uses non-volume-based cost drivers (activities) as cost drivers instead of volume of production such as number of setup, purchase order, inspections, parts, and the time spent on activities[7], and [9].

In general, the activity based costing system is defined as a costing system which uses a range of cost drivers associated to product volume[4], and[13].

The difference between volume-based system and non-volume based system (ABC system) is that volume based system uses only one large cost pool in a large cost center (may be a department or a manufacturing unit), whereas in ABC system a traditional cost center may accommodate several cost pools to reflect diversity in non-volume based cost drivers[9], [16], and [18].

The use of activities as cost drivers leads to a distinctive between value added and non-value added activities and enhances firm operations performance.

V. Research methodologies

A. Data collection and variables definition

This paper uses the descriptive inductive approach to analyze the results of empirical study and describes the types and forms of cost functions. It collects actual cost data related to two types of manufacturing firms, traditional manufacturing environment (T) and new manufacturing environment (M), for 24 months from (1/1/2010 to 1/1/2012), to arrive a proposal model to cost function.

B. Model development

This study depends on statistical regression models to estimate the forms and types of cost functions. The models use divided to: (a) linear regression models contain simple linear regression and multiple linear regressions. (b) Non-linear regression models contain Logarithmic model (LOG), Growth model and power model.

VI. Statistical analysis and results

The objective of this study is estimating the form and type of cost function within the traditional environment represented by (T) company, and new environment represented by (M) company. The study has applied linear and non-linear models to estimate the cost function (linear or non-linear function) using actual data from two companies (T and M). Table (I) summarizes the results for applying linear and non-linear models using R^2 (which represents the percentage change in dependent variable due to change in independent variables).

Table I

Models applied	R^2
SIG (F)	
Firstly: Linear models	
1-simple linear regression	
1-1-linear function	
(T) Company	68.1%
0.001	
(M) Company	14%
0.126	
1-2-quadratic function	
(T) Company	68.6%
0.005	
(M) Company	19.6%
0.195	

1-3-cubic function

(T) Company 68.6%
0.005

(M) Company 19.6%
0.195

2-multiple linear regression:

(T) Company 89.8%
0.385

(M) Company 71.4%
0.138

Secondly: non-linear regression

Logarithmic model (Enter method)

(T) Company 92.1%
0.308

(M) Company 67.2%
0.206

The study shows (from the previous statistical analysis for the two companies) the following: (using R^2)

A. Simple linear models

11.1.1. Linear function

The previous table shows that R^2 for (T) company = 68.1% (this means that 68.1% of all differences in dependent variable (total costs) are due to the independent variable (volume of production), and this percentage is more than R^2 in the (M) company =14% (A very small proportion in comparing with (T) company). The first result supports the prevailing assumption among accountants concerning the linearity of the cost function and how the volume of production is considered the main driver for all costs. In the second company (M), there are other variables with a greater impact on the cost function such as: achieving higher quality; change in cost object; diversity and complexity for the products; returns from technological changes; achieving economies of scale in the long time; and emergence of Activity Based Costing.

11.1.2. Quadratic and cubic functions

The previous table shows that R^2 is the same for (T) company (for two functions) =68.6% (this means that 68.6% of all differences in dependent variable (total costs) are due to independent variable (volume of production). On the other hand, R^2 is the same for (M) company (for two functions) but less for (T) company= 19.6% (this means that 19.6% of all differences in dependent variable (total costs) are due to independent variable (volume of production), and 80.4% due to other factors emergence in new manufacturing environment.

To sum up**:** the best model proves that the behavior of the cost function is quadratic or cubic for (T) or (M) company, and this result shows the unbecomingness in the prevailing assumption by accountants about the linearity of cost function (first class function).

B. Multiple linear models

The previous table shows that R^2 for (T) company is more for (M) company, it advances 89.8% (this means that 89.8% of all differences in dependent variable (total costs) are due to independent variables (volume of production) and the residual little percentage is due to other factors.

On the other hand, R^2 for (M) company=71.4% which means 71.4% of all differences in dependent variable (total costs) are due to independent variables (volume of production) and the residual percentage (28.6%) is due to other factors not included in the model and it is difficult to determine it.

C. Non-linear model (logarithmic model)

The previous table shows that R^2 for (T) company is more for (M) company, it represents 92.1% (this means that 92.1% of all differences in dependent variable (total costs) are due to the logarithm of the independent variables which determined in traditional environment.

On the other hand, R^2 for (M) company=67.2% (this means that 67.2% of all differences in dependent variable (total costs) are due to the logarithm of the independent variables and the residual percentage (32.8%) is due to other factors not included in the model and it is difficult to determine it.

To sum up**:** the best model to represent the cost function for (T) company is non-linear model (logarithmic model) (R^2 =92.1%), then comes the multiple linear model (R^2 =89.8%), indicating an assumption error in linear cost function under traditional production environment. In addition, the best model for (M) company is the multiple linear model (R^2 =71.2%), preceding the non-linear model (logarithmic model) (R^2 =67.2%).

ISBN: 978-1-61804-225-5

REFERENCES

[1] Ahmed Noor. (1999). Basic manufacturing cost accounting, faculty of commerce, Alex University, (In Arabic)

[2] Brimson, A. James. (1991). Activity Accounting an Activity-Based Costing Approach

[3] Cheolkyu Hong. (1998). "An analysis of modern costing systems in the context of the United Kingdom Telecommunications industry", PhD Thesis, the university of London

[4] Cooper, R. (1990). Cost classification in unit-based and activity-based manufacturing cost systems. *Journal of Cost Management, 4*(3), 4-14.

[5] Cooper, R., & Kaplan, R. S. (1987). How cost accounting systematically distorts product costs. *Accounting and management: Field study perspectives*, 204-228.

[6] Cooper, R., & Kaplan, R. S. (1991). Profit priorities from activity-based costing. *Harvard Business Review, 69*(3), 130-135.

[7] Cooper, R., & Kaplan, R. S. (1992). Activity-based systems: Measuring the costs of resource usage. *Accounting Horizons, 6*(3), 1-13.

[8] Heathfield, F. David and Soren Wibe. (1987). an introduction to Cost and Production Functions, Macmillan Education

[9] Horngren, charles T., AlnoorBhimani, George Foster and Srikant M. Datar. (1998). Management and Cost Accounting, Prentice Hall Europe

[10] Ibrahim Hammouda. (1995)." Study cost behavior in Egyptian insurance companies",Scientific Journal for Commerce and Financ***e***, , faculty of commerce, Alex. University, Vol.II, pp.267-307

[11] Kaplan, R. S. (1983). Measuring manufacturing performance: a new challenge for managerial accounting research. *Accounting Review*, 686-705.

[12] Kaplan, R.S., (1988). "Accounting Lag: The Obsolescence of Cost Accounting Systems", California Management Review, Vol. XXVIII, No. 2, PP. 174-199.

[13] Kaplan, S. Robert and A. Anthony Atkinson. (1998). Advanced Management Accounting, Second Edition, Prentice-Hall

[14] Miller, J. G., & Vollmann, T. E. (1985). The hidden factory. *Harvard Business Review, 63*(5), 142-150.

[15] Philip Fred Kelly. (1995). "A model for the use of cost information in AMT environment", PhD Thesis, the university of Huddersfield

[16] Rayburn, L. Gagle. (1996). Cost Accounting Issuing A Cost Management Approach, Sixth, Edition

[17] Samir Helal and A. Kotab. (2001). Basic cost accounting, faculty of commerce, Tanta University, (In Arabic)

[18] Shank, J. K., & Govindarajan, V. (1988). The perils of cost allocation based on production volumes. *Accounting Horizons, 2*(4), 71-79.

Authors Index

ISBN: 978-1-61804-225-5